

History of Space-Based Infrared Astronomy and the Air Force Infrared Celestial Backgrounds Program

S. D. Price

18 April 2008

Approved for Public Release: Distribution Unlimited



**AIR FORCE RESEARCH LABORATORY
Space Vehicles Directorate
29 Randolph Rd.
Hanscom AFB, MA 01731-3010**

This Technical Report has been reviewed and is approved for publication.

/ signed /

Robert A. Morris, Chief
Battlespace Environment Division

/ signed /

Stephan D. Price
Author

/ signed /

Paul Tracy, Acting Chief
Battlespace Surveillance Innovation Center

This report has been reviewed by the ESC Public Affairs Office (PA) and is releasable to the National Technical Information Service.

Qualified requestors may obtain additional copies from the Defense Technical Information Center (DTIC). All others should apply to the National Technical Information Service (NTIS).

If your address has changed, if you wish to be removed from the mailing list, or if the address is no longer employed by your organization, please notify AFRL/VSIM, 29 Randolph Rd., Hanscom AFB, MA 01731-3010. This will assist us in maintaining a current mailing list.

Do not return copies of this report unless contractual obligations or notices on a specific document require that it be returned.

REPORT DOCUMENTATION PAGE

Form Approved
OMB No. 0704-0188

The public reporting burden for this collection of information is estimated to average 1 hour per response, including the time for reviewing instructions, searching existing data sources, gathering and maintaining the data needed, and completing and reviewing the collection of information. Send comments regarding this burden estimate or any other aspect of this collection of information, including suggestions for reducing the burden, to Department of Defense, Washington Headquarters Services, Directorate for Information Operations and Reports (0704-0188), 1215 Jefferson Davis Highway, Suite 1204, Arlington, VA 22202-4302. Respondents should be aware that notwithstanding any other provision of law, no person shall be subject to any penalty for failing to comply with a collection of information if it does not display a currently valid OMB control number.

PLEASE DO NOT RETURN YOUR FORM TO THE ABOVE ADDRESS.

1. REPORT DATE (DD-MM-YYYY) 07-04-2008	2. REPORT TYPE Scientific Report - Final	3. DATES COVERED (From - To)		
4. TITLE AND SUBTITLE History of Space-Based Infrared Astronomy and the Air Force Infrared Celestial Backgrounds Program		5a. CONTRACT NUMBER		
		5b. GRANT NUMBER		
		5c. PROGRAM ELEMENT NUMBER 62601F		
6. AUTHOR(S) S. D. Price		5d. PROJECT NUMBER 621010		
		5e. TASK NUMBER SB		
		5f. WORK UNIT NUMBER ZZ		
7. PERFORMING ORGANIZATION NAME(S) AND ADDRESS(ES) Air Force Research Laboratory 29 Randolph Road Hanscom AFB, MA 01731-3010		8. PERFORMING ORGANIZATION REPORT NUMBER AFRL-RV-HA-TR-2008-1039		
9. SPONSORING/MONITORING AGENCY NAME(S) AND ADDRESS(ES)		10. SPONSOR/MONITOR'S ACRONYM(S) AFRL/RVBY		
		11. SPONSOR/MONITOR'S REPORT NUMBER(S)		
12. DISTRIBUTION/AVAILABILITY STATEMENT Approved for public release; distribution unlimite				
13. SUPPLEMENTARY NOTES				
14. ABSTRACT A retrospective is provided on space-based astronomy missions and the prominent role the US Defense Department (DoD), particularly the Air Force, played in early days of infrared astronomy and the technology development that was transitioned to the infrared astronomical community. The geophysics programs at the Air Force Cambridge Research Laboratories (AFCRL) and successor organizations (AFGL) at Hanscom Air Force Base are described in order to provide a context for the DoD infrared astronomy program. AFCRL and AFGL conducted the early mid-infrared probe-rocket based surveys as well as supporting related experiments under university contracts. The succession of subsequent orbital experiments is also described.				
15. SUBJECT TERMS Infrared observations; Space-based astronomy				
16. SECURITY CLASSIFICATION OF: a. REPORT Unclassified		17. LIMITATION OF ABSTRACT SAR	18. NUMBER OF PAGES	19a. NAME OF RESPONSIBLE PERSON Stephan D. Price
b. ABSTRACT Unclassified				19b. TELEPHONE NUMBER (Include area code) 781-377-4552
c. THIS PAGE Unclassified				

Reset

Standard Form 298 (Rev. 8/98)
Prescribed by ANSI Std. Z39.18

TABLE OF CONTENTS

1. THE LABORATORY FROM 1945 TO 2011	1
1.1. The Cambridge Research Center (1945 – 1960).....	4
1.2. Cambridge Research Laboratories (1960 – 1975)	8
1.3. Geophysics Laboratory (1976 – 1990)	12
1.4. Phillips Laboratory (1990 – 1997).....	14
1.5. Air Force Research Laboratory (1997 – 2011).....	16
1.6. External Support – Lifeblood of the Celestial Backgrounds Program	17
1.7. Astronomers Associated with the Laboratory’s Infrared Program	21
1.8. Personal Perspective	27
2. INFRARED ASTRONOMY: THE EARLY DAYS	33
2.1. Space Surveillance: Impetus to Infrared Stellar Astronomy.....	39
2.2. The First Near-Infrared Sky Surveys.....	45
2.3. The AFCRL Lunar and Planetary Research Branch.....	48
2.4. Additional References.....	57
2.5. Personal Recollections	58
3. INTO SPACE.....	67
3.1. LO-STAR (Stellar Radiation Sensor - SRS).....	70
3.2. Hedging Bets – ARPA funded University Efforts.....	74
3.3. HI STAR	75
3.4. The First Satellite-Based Infrared Surveys	82
3.5. HI HI STAR	83
3.6. HI STAR South.....	85
3.7. Personal Perspective – The HI STAR Era	90
4. A WEALTH OF DATA.....	97
4.1. Characteristics of the Data	97
4.2. AFCRL Source – What AFCRL Source?	107
4.3. Good to the Last Drop – of Information	111
4.4. Personal Perspective on the AFCRL/AFGL Survey.....	116
5. AIR FORCE BACKGROUND MEASUREMENT PROGRAM	119
5.1. Super HI STAR	119
5.2. The End of an Era – and the Beginning of Another	120
5.3. Earth Limb and Infrared Backgrounds Experiments	121
5.4. SPICE I	123
5.5. The BMP and MSMP Separation and Recovery Systems	125
5.6. SPICE 2.....	128
5.7. Far-infrared Sky Survey Experiment	131
5.8. Zodiacal Infrared Project	139
5.9. Earth Limb Clutter	146
5.10. Detector Non-Linear Responses	147
5.11. Classification Issues.....	151
5.12. Personal Perspective on the Background Measurements Program.....	153
6. FROM ROCKETS TO SATELLITES	157
6.1. The Infrared Astronomical Satellite (IRAS).....	160
6.1.1. IRAS Asteroids and Comets	168

6.1.2. IRAS Satellite Observations	169
6.2. Niche Experiments.....	171
6.2.1. Background Equatorial Astronomical Measurements (BEAM)	172
6.2.2. The Diffuse Infrared Galactic Background Experiment (DIGBE)	174
6.2.3 SPIRIT II.....	175
6.3. Shuttle-Based Experiments.....	175
6.3.1 The Spacelab 2 Infrared Telescope.....	175
6.3.2. Transitions.....	176
6.3.3. Shuttle-Based AFGL Background Experiments	176
6.4. The Cosmic Background Explorer.....	179
6.5. Personal Perspective	181
7. BACKGROUNDS AT HIGH RESOLUTION AND SENSITIVITY	187
7.1. The Large Aperture Infrared Telescope System.....	187
7.2. Celestial Background Characterization and Modeling	190
7.2.1. Resolution Enhancement of the IRAS Data.....	191
7.2.2. Infrared Galactic Point Source Model	197
7.2.3. Infrared Cirrus.....	202
7.2.4. Zodiacal Background	207
7.2.5. Asteroids, Moon and Planets	213
7.2.6. The Moon as an Absolute Calibration Source	214
8. FILLING THE GAPS IN THE INFRARED SURVEYS.....	217
8.1. The Japanese Infrared Telescope in Space (IRTS)	217
8.1.1. Galaxy Haloes and Low-Mass Stars	219
8.2. The Midcourse Space Experiment (MSX).....	219
8.2.1. The Spatial Infrared Imaging Telescope (SPIRIT III)	220
8.2.2. The Spacecraft	224
8.2.3. On Orbit	227
8.2.4. The MSX Galactic Plane Survey	229
8.2.5. A Survey of the Zodiacal Background and Regions Missed by IRAS	236
8.2.6. Raster Scan Maps of Galaxies and H II Regions	236
8.2.7. Targets of Opportunity.....	238
8.2.8. MSX Astronomy in the Post Cryogen Phase	240
8.3. Personal Perspective	241
9. NEW NEAR-INFRARED SURVEYS	243
9.1. The Near-infrared Camera and Multi-Object Spectrometer (NICMOS)	244
9.2. The Two-Micron All Sky Survey (2MASS).....	244
9.3. The Deep Near-infrared Survey of the Southern Sky (DENIS)	251
9.4. Deeper Near-Infrared Surveys	253
9.5. The Search for Near-Earth Objects.....	254
9.6. Personal Perspectives.....	260
10. SPACE-BASED INFRARED ASTRONOMICAL OBSERVATORIES	261
10.1. The Infrared Space Observatory (ISO)	262
10.1.1. Phillips Laboratory Connection	263
10.1.2. ISO Zodiacal Measurements	270
10.1.3. Brief Summary of Other ISO Results	271
10.2. SPITZER Space Telescope	271

10.3. Akari – ASTRO-F.....	277
10.4. Submillimeter Experiments	279
10.5. In the Queue.....	280
10.5.1. The Wide-Field Infrared Survey Explorer (WISE)	281
10.5.2. Stratospheric Observatory for Infrared Astronomy (SOFIA)	281
10.5.3 The Webb Telescope.....	282
10.6. Space Infrared Telescope for Cosmology and Astrophysics (SPICA)	282
10.7. Personal Perspective	283
REFERENCES	287
ACRONYMS AND ABBREVIATIONS	343

FIGURES

Figure 1. The Air Force Geophysics Laboratory complex in the late 1980s.....	2
Figure 2. An anonymous V-2 launch.....	5
Figure 3. The last AFGL Aerobee 350 rocket at the Smithsonian Air and Space Museum.....	7
Figure 4. The Multi-Spectral Measurements Program TEM-1 launch on 21 May 1980.....	13
Figure 5. The Far-infrared Sky Survey Experiment field team.....	27
Figure 6. Transmission characteristics of the atmosphere and filters used in the early radiometric subtractive filtering.....	36
Figure 7. The time variable infrared signature from a notional intercontinental ballistic missile.	40
Figure 8. The Air Force Maui Optical Station (AMOS) atop Mt. Haleakala, Hawaii at an altitude of 3054 meters.....	44
Figure 9. The AFCRL IR telescopes. At left is the ITTFL survey instrument supplied under the AFCRL contract.....	46
Figure 10. The ITTFL all-aluminum survey telescope newly installed atop Mt. John, NZ.....	47
Figure 11. The Two Micron Sky Survey Telescope in the Smithsonian Museum.....	48
Figure 12. Thermal emission from the 27 September 1996 eclipsed Moon.....	51
Figure 13. The atmospheric transparency at three different altitudes. (bottom) a mountain top observatory (e.g. Mona Kea), (middle) aircraft (e.g. the Stratospheric Observatory for Infrared Astronomy) and (top) balloon platforms.	69
Figure 14. The MAP II payload after recovery.....	72
Figure 15. Cross-sectional schematic of the HI STAR sensor.....	76
Figure 16. The HI STAR focal plane layout.....	77
Figure 17. A schematic of the HI STAR payload is at left and the payload section from the telemetry antenna to the nose cone separation line is shown above with the HI STAR sensor stowed and deployed (with cap on).	78
Figure 18. The HI STAR payload being mated to the Aerobee 170 before being mounted on the Nike booster in the tower.....	79
Figure 19. A daytime Aerobee 170 launch.....	80
Figure 20. The HI STAR survey pattern.....	81
Figure 21. The HI STAR South field team.....	86
Figure 22. The Nike booster on the launch rail.....	87
Figure 23. The HI STAR South Payload on top of the Aerobee 200 and Nike booster on the launcher.....	88
Figure 24. Launch of the HI STAR South at Woomera, Australia.....	89
Figure 25. The White Sands Army Base with the Organ Mountains in the background.....	91
Figure 26. The ELDO launch site at Woomera with an Europa vehicle on the pad.....	95
Figure 27. The 11 μ m sources measured by HI STAR and HI STAR South.....	97
Figure 28. Sample of data from the first HI STAR flight.....	98
Figure 29. An example of noisy data.....	99
Figure 30. The time history of the noise for the 11 μ m detectors during the first (left) and fourth (right) HI STAR experiments.....	100
Figure 31. Noise for the 11 μ m detectors second, fourth from the top and second from the bottom (left to right) during the fourth flight as a function of the angle between the sensor line-of-sight and the edge of the Earth.....	101

Figure 32. The point source rejection ratio for four AFCRL/AFGL sensors.	102
Figure 33. Definition of tangent height.....	103
Figure 34. Infrared signatures of dust particles from the second HI STAR experiment.	106
Figure 35. The 11 μ m scan across the Galactic plane at a longitude of 30 $^{\circ}$ on the first roll of the second HI STAR flight.	111
Figure 36. A scan along the Galactic plane by an 11 μ m detector from the first HI STAR flight plotted as a function of time.....	112
Figure 37. 11 μ m Galactic and Ecliptic plane crossings from the first HI STAR South flight.	113
Figure 38. The HI STAR South 11 μ m zodiacal radiances.	114
Figure 39. Infrared maps of the Cygnus region centered at 79 $^{\circ}$ Galactic longitude.....	115
Figure 40. The 10 μ m broad-band zodiacal radiance measured by ELE as a function of elongation.....	122
Figure 41. The SPICE sensor with the cover on is shown deployed during the horizontal test.	124
Figure 42. The SPICE/FIRSSE separation system is shown mated to the SPICE payload at the left and fully extended at right; all BMP experiments used a similar system.....	126
Figure 43. The not so soft SPICE I recovery.	127
Figure 44. The SPICE sensor in the clean room during field preparations.	128
Figure 45. The BMP payload configuration.	129
Figure 46. The mid-infrared Galactic center.....	130
Figure 47. The FIRSSE sensor.	132
Figure 48. Payload preparations for launch.	133
Figure 49. The payload in the tower.	134
Figure 50. Mating the payload to the rocket.	135
Figure 51. A view of the payload on the rocket with the gantry and preparation building rolled back.....	136
Figure 52. Just before launch. The separation system and rocket are being armed on the left.	137
Figure 53. Launch.	138
Figure 54. A successful soft recovery of the FIRSSE payload.	139
Figure 55. The ZIP payload on the ARIES motor.	140
Figure 56. The ZIP sensor is shown deployed in the cleanroom.	141
Figure 57. ZIP Zodiacial spectra.	142
Figure 58. The ZIP 2 11 μ m radiance measurements.	144
Figure 59. A comparison of the various infrared measurements of the zodiacal radiance along the ecliptic plane at \sim 12 μ m (left) and 25 μ m (right).	146
Figure 60. Polar Mesospheric Clouds observed by MSX.	147
Figure 61: Three examples of non-linear detector behavior.	148
Figure 62. The IRAS satellite. At top, the spacecraft undergoing laboratory preparations.....	161
Figure 63. The IRAS survey focal plane detector arrays.	162
Figure 64.: The IRAS infrared sky.	164
Figure 65. Celestial structure mapped by IRAS.	165
Figure 66. The zodiacal structure near the ecliptic plane observed at 25 μ m.....	166
Figure 67. The interstellar infrared ‘cirrus’ at the north (left) and south (right) celestial poles.	167

Figure 68. The BEAM experiment mated to the Castor-Lance rocket, which is mounted on the launch rail at the rocket range near Natal, Brazil.....	173
Figure 69. Liftoff of Shuttle Discovery at 11:31 GMT on 28 April 1991 from launch complex LC39A at Cape Canaveral carrying the AFGL CIRRIS IA and the Shuttle Kinetic Infrared Test experiments.....	177
Figure 70. CIRRIS 1A in Discovery Shuttle Bay.....	178
Figure 71. Three and a half years DIRBE near-infrared light curves for R Oct.....	181
Figure 72. An IRAS – MSX comparison in the Galactic plane at 355° longitude.....	187
Figure 73. IRAS background limited performance.....	192
Figure 74. High resolution IRAS images of M51, a large infrared bright galaxy with a small satellite galaxy.....	194
Figure 75. Enhancement of IRAS M31 observations.....	195
Figure 76. Cumulative source densities at ~28° longitude in the Galactic plane.....	196
Figure 77. The Milky Way according to the Spitzer infrared telescope facility.....	197
Figure 78. Distribution of mid-infrared point sources.....	201
Figure 79. The 100 μ m infrared cirrus.....	203
Figure 80. The supernova remnant centered on λ Orionis.....	206
Figure 81. The CBSD zodiacal model fit to an IRAS 12 μ m constant elongation scan (left) and pseudo DIRBE latitude scan (right).....	211
Figure 82. Residual plots between the DIRBE observations for day 4 of 1990 and the CB zodiacal model are shown for 4.9 μ m (top), 12 μ m (middle) and 25 μ m (bottom).....	212
Figure 83. The near-infrared extragalactic background.....	213
Figure 84. The SPIRIT III optics.....	221
Figure 85. The MSX focal plane layout.....	223
Figure 86. The MSX payload.....	225
Figure 87. The MSX payload on the Delta rocket at Vandenberg AFB, CA.....	226
Figure 88. The MSX astronomy experiments.....	228
Figure 89. MSX capabilities.....	229
Figure 90. The MSX Galactic Center.....	230
Figure 91. Infrared images of the Galactic plane between ~357° – 346° longitude.....	231
Figure 92. MSX images of two star forming region in the Galactic plane.....	232
Figure 93. The η Carina complex.....	233
Figure 94. Three regions in the northern Galactic plane.....	233
Figure 95. H II regions along the northern Galactic plane.....	234
Figure 96. A (Δl , Δb) \sim (6.5° \times 4.5°) MSX image of the Cygnus region centered at 79° longitude.....	235
Figure 97. Well resolved galaxies in Band A.....	236
Figure 98. MSX images of the Large Magellanic Cloud.....	237
Figure 99. MSX mid-infrared images of comet Hyakutake.....	238
Figure 100. MSX observations of comet Hale-Bopp.....	239
Figure 101. RSOs serendipitously observed by MSX.....	240
Figure 102. The 2MASS facilities.....	246
Figure 103. 2MASS imaging.....	246
Figure 104. 2MASS all sky images.....	247
Figure 105. Objects in the Galactic plane observed by 2MASS.....	248
Figure 106. 2MASS Atlas images of T (left) and L (right) sub-stellar brown dwarfs.....	249

Figure 107. The Galactic center in the near-infrared and combined with mid-infrared observations.	250
Figure 108. The modeled spectral irradiances of a near Earth object for two detection scenarios.	259
Figure 109. MSX raster scanned observations in the Galactic bulge (left) and an ISOCam image within the MSX field.	264
Figure 110. MSX and ISOGAL ($\Delta l, \Delta b$) $\sim 0.2^\circ \times 1^\circ$ infrared images centered at $(l, b) \sim (315^\circ, 0.0^\circ)$	265
Figure 111. The Galactic center at $\sim 8 \mu\text{m}$ from Spitzer (top), MSX (middle) and ISO (bottom).	266
Figure 112. A sample of ISO SWS spectra of the brightest infrared sources.....	267
Figure 113. Calibration results.....	269
Figure 114. A section of the southern infrared Galactic plane.	274
Figure 115. Selected images from the Spitzer Galactic plane surveys.	275
Figure 116. Spitzer spectra of SMC objects.	276
Figure 117. The $9 \mu\text{m}$ sky observed by Akari.	278
Figure 118: MSX raster image of the Galactic plane at 28° longitude.	284

Tables

Table 1. AFCRL/AFGL Experiments flown by the Infrared Celestial Backgrounds Group	18
Table 2. Space Experiments Funded or Supported by AFRL/AFGL	20
Table 3. Parameters of Photoconductors used for Infrared Astronomy.....	67
Table 4. 8 – 14 μ m Environmental Radiance	68
Table 5. SPIRIT III Spectral Band Parameters.....	222

Preface and Acknowledgements

Infrared Celestial Backgrounds, the name of the Department of Defense's infrared astronomy programs managed and conducted by the Air Force Laboratory from the mid-1960s to the end of the century, reflects the underlying theme of this history that highlights the Department of Defense's contributions, particularly those of the Air Force research contingent at Hanscom AFB, to infrared astronomy. My own career spans the *Infrared Celestial Backgrounds* program. Indeed, most of my 45 years in infrared astronomy has been supported by the Air Force, initially under contract to the International Telephone and Telegraph Federal Laboratories (ITTFL) in 1963 and, off and on, through 1967 where I worked with Freeman Hall to develop and use the near-infrared radiometer that replaced the one with which he conducted the first modern infrared sky survey. I also attended Ohio State University as Walt Mitchell and Phil Barnhart were completing the sub-contract effort funded by Eastman-Kodak under the Advanced Research Project Agency's Project Defender to observe bright infrared stars. I became a civilian employee of the Air Force Cambridge Research Laboratories (AFCRL) in 1969, just as the Optical Physics Laboratory began the AFCRL probe-rocket infrared sky survey program. This sky survey was not only at the forefront of infrared astronomy but was conducted on a scale usually beyond the capability of academia. Thus, I was fortunate to have begun my career at a time when infrared astronomy was a burgeoning new field and was not only able to do 'cutting-edge' research that was personally highly rewarding, but I also found the related practical Air Force space surveillance problems both interesting and challenging. Over the years, I participated in almost all of the Air Force infrared astronomy experiments, during which time I have had a number of memorable experiences, visited exotic places, and met many interesting people. This narrative is born, in part, from the urging of colleagues to write down the anecdotes with which I regaled them with about the places I have been, the interesting or unusual aspects of the research and the people that I have met.

I have preferentially used secondary references such as the books by DeVorkin (1986, 1992) and Doel (1992) and the reports by Liebowitz (1985, 1987, and 2002) for much of the background material before 1970. The research described in these historical accounts are based on primary archival material such as correspondence, notes, internal memoranda, interviews with and oral histories from the individuals involved; all of which are excellent examples of primary references. However, I do provide voluminous citations so that the reader may track down any of the historical tidbits that strike his/her interest. The most obscure book is often for sale on the internet, and the NASA astrophysics data service (<http://adswww.harvard.edu/>) has a huge on-line inventory of astronomical articles, which is continuously being updated with the older and the more obscure material. Almost all of the Air Force and other DoD technical reports cited herein may be obtained either from the Defense Technical Information Center (DTIC – <http://www.dtic.mil/dtic/search/tr/index.html>) or the National Technical Information Service (NTIS – <http://ntis.gov>); I provide the unique nine character DTIC number by which the cited reference may be found and, for NTIS, the NASA accession number. The extraordinary resources of the AFCRL library that included complete collections of all of the major and many of the more obscure science journals were of considerably help in tracing the early history (the library's *Philosophical Transactions of the Royal Society of London* collection is only one of five complete sets of this journal in the US). I was thus able to readily look up Herschel's 1800 *Philosophical Transactions* papers and the other references cited in Chapter 2 such as the *Scientific American* 1878 news article on Edison's proposal for an infrared sky survey.

As to what sort of history is in this report, Michael Hoskins, the editor of the *Journal of the History of Astronomy*, judged, in a 12 March 2008 e-mail, the style of portions of this report as “Whig history”, a pejorative term that denotes the chronicling of what was done and when. While this narrative isn’t as mechanical as Mr. Hoskins implied, it certainly is not as subjective and speculative as he defines the manner in which historians work: in his words “*Historians are like anthropologists who visit other cultures and immerse themselves in them in an attempt to portray them sympathetically to the outside world, the difference being that historians visit cultures in the past rather than elsewhere on the planet. An historian of astronomy tries to understand the challenges, interests, presuppositions etc of astronomers in times past.*”

In delving into the background material, I found that the Air Force’s infrared astronomy programs should properly be considered within a context of the vigorous upper atmospheric research conducted by the Air Force Cambridge Field Station after the Second World War. In the 1950s, the Air Force Cambridge Research Center (AFCRC) established programs in solar astronomy, the physics of space particles and fields, radio astronomy, cosmic ray physics, meteoritics and observational and laboratory astrophysics as part of this upper atmospheric research portfolio. Also, the probe-based infrared surveys were not the only infrared astronomy program within the Laboratories; the lunar and planetary physics program had begun in 1959 and this effort was more widely recognized initially; the Branch Chief, Jack Salisbury, having been interviewed by Walter Cronkite on television during the Apollo program. Therefore, I describe in the first Chapter how the upper atmospheric research led to the astronomy efforts that, in turn, were given a significant boost by the focus on space applications after the Russians launched Sputnik in October 1957.

Thus, many diverse threads are woven into the whole picture. I had long known that AFCRL had sponsored Freeman Hall’s infrared measurement but a number of other coincidental ties between the various AFCRL research areas and my own early career path came to light. For example, one of the infrared survey objectives was to measure the infrared zodiacal background from the thermal emission of dust in the solar system. So, I was surprised to discover that AFCRC/AFCRL had a program that lasted through the 1960s for *in situ* measurements of meteoritic dust particles that was conducted under the aegis of upper atmospheric research. Furthermore, since the laboratory equipment and techniques used by this program were instrumental to the success of our probe-rocket infrared surveys, I have given a bit more space to describing this research. Other intersections were peripheral, such as the AFCRL Astrophysics group having funded the shock tube work at Ohio State conducted by Paul Byard in the laboratory next to the one I was in when I was a graduate student. It also turned out that there were other connections between Ohio State and AFCRL. For example, the number of people who had studied molecular spectroscopy at OSU and later joined the AFCRL Optical Physics Lab was large enough they were locally known as the Ohio State mafia. This connection was strengthened by Laboratory sponsorship of the annual OSU Molecular Spectroscopy Conference. Also, the AFCRL radio astronomy group funded John Kraus for his early efforts on the OSU radio survey. Thus, I briefly mention the various cross-ties and the astronomy and astrophysics programs active at one time or another in the Laboratories.

Originally, I considered writing an encompassing history of the field since I knew many of the early contributors to modern infrared astronomy. However, it became evident that this would be a massive undertaking that would require several volumes. Using the subtext of the military contributions, particularly those of the Air Force Laboratory, I have focused on the history of mid-infrared (6 – 35 μm) astronomy and emphasized space based experiments.

Furthermore, I did not wish simply to create a dry narrative as to who did what and when much as I did for my 1988 *Publications of the Astronomical Society of the Pacific* article. And, frankly, I wanted to set the record straight by specifically giving not only appropriate credit to those who advanced the field with their pioneering efforts but also to provide a more balanced picture of the military's role than is usually acknowledged. For, as Martin Harwit (1981) noted in his book *Cosmic Discoveries*, "...a large portion of the major discoveries in astronomy have been made by people working outside the field and a significant fraction were made by military research." As examples, Harwit cites the AFCRL sponsorship that led to discovery of Galactic x-ray sources and the discovery of cosmic gamma rays by the Vela nuclear test monitoring satellites. It is not well known that the main research objective of the AFCRL Lunar and Planetary Physics Branch that sponsored the x-ray experiments was to study the infrared characteristics of solar system bodies and that the discovery of x-ray sources was, in the Branch's view, a by-product of the goal to measure x-ray fluorescence from the Moon.

The choice of focus turned out to be a good one. The early history in Chapter 2 contains material that is usually not found in other narratives, e.g. Allen (1974), while the review article *The Beginning of Modern Infrared Astronomy* by Low, Rieke and Gehrz (2007) is almost exclusively complementary to that in this report. Although I have relied on information in the Chapter by Harwit (2003) on *The Early Days of Infrared Space Astronomy* and the books by Davies, (1997) and Leverington (2000) on civilian space-based infrared astronomy experiments that were flown between the early 1980s and the late 1990s, I have added a significant amount of first hand material and a description of the DoD efforts, which these reference only touch upon or do not include. An exception to the complementary nature of the material is the description of *Infrared Detector Arrays for Astronomy* by Rieke (2007) that essentially duplicates portions of that given in Chapter 3. Furthermore, I published a condensed version of this history (Price, 2008) by excerpting and rearranging the salient information from Chapters 2 through 10. To preserve the flow of the present narrative, much of the text in this journal article has been preserved in the present report, rather than removing it to a reprint appendix. Thus, there are *verbatim* duplicate passages in both Price (2008) and this report.

While some have argued (or ignored) the point, I think that it is fair to say that by providing the results of the probe-rocket sky surveys that defined the large scale characteristics of the infrared celestial background to the civilian community, AFCRL and its immediate successor for the geophysics programs, the Air Force Geophysics Laboratory (AFGL), made significant, even critical, contributions to infrared astronomy. Equally important, the DoD transitioned the technology that was used to conduct the survey and Harwit has frequently acknowledged that this technology was critical for the success of civilian space-based infrared experiments. Indeed, the AFCRL experiment served as the proof-of-concept demonstration and validation called for in the National Academy of Sciences decadal study *Astronomy and Astrophysics for the 1970s* as a requisite stepping stone for a satellite program. However, the astronomical community did not universally accept the early probe-based survey contributions with good grace. A number of mid-1970s publications questioned contents of the survey catalogs; rightly so since the catalogs included a number of false entries that came about from our sponsor's directive to cover the maximum area of sky, which was done at the expense of reliability. This led Mather and Boslough (1996) to proclaim that it took a team of NASA sponsored astronomers to plan a survey correctly. Michael Rowan-Robinson (1993) agreed, stating that we, at AFCRL, did not take sufficient care in the conduct of the survey, which, as also noted by Dave Allen (1977), resulting in a large number of spurious source being included

in the preliminary lists. Such judgments marginalize the DoD contributions to infrared astronomy, but are also a part of the story and I try to objectively describe these issues in Chapters 3 through 5, which detail the AFCRL/AFGL survey experiments, as well as the problems encountered and how they affected the data. .

As I was involved in several of the early infrared astronomy efforts, this narrative naturally draws heavily my personal recollections. Thus, this history has some degree of subjectivity, as do most accounts that present the authors' assessment of events. Subjectivity can also be introduced by what material is to be included or discarded. For example, I provide more details on research conducted by the Air Force Laboratory than some of the contemporaneous civilian efforts. Also, more detailed information is given on experiments conducted before the mid-1990s, which is about the time that primary reference material shifted from the printed word to being web based. Thus, one can gain ready access to a wealth of details on the recent experiments from the web but this is harder to do for the older material. Furthermore, I have selectively highlighted the major discoveries and achievement of the various civilian experiments. I do, however, cite comprehensive reviews by others.

Memory is a fickle thing and, upon cross-checking many of the events that I described as I remembered them in my initial draft, I found that I had misdated and combined some different but related events. Therefore, I went to some lengths to verify the events and circumstances. For this I owe a large debt of gratitude to Dave Akerstrom, Phil Barnhart, Lou de Bottari, John Heintz, Mike Kiya, Ruth Liebowitz, Tom Murdock, Dave Pollack, John Salisbury, Howard Stears and Russ Walker for the discussions, information and corrections that they provided that filled in numerous missing details and corrected my memory lapses. I particularly note the contributions of John Dempsey who twice edited this report. Thanks to John, I smoothed out many of the transitions and double checked a number, and correct some, of the facts.

Since portions of this history are subjective and the content is influenced by my personal experience, the account is naturally colored by my own filter of biases and views. I have tried to provide an objective account of the topical research appropriate to each Chapter for either a defined period of time or for a series of experiments conducted under programs with common objectives. Thus, although the information is roughly arranged chronologically, some sections contain material that pertains to a coherent theme in which the timeline often overlaps events in other sections. For example, the common theme of rocket-based niche experiments in section 6.2 entirely overlaps the 10 year timeline of the shuttle-based experiments in the next section.

I also include a *Personal Recollections* or *Personal Perspectives* section at the end of some Chapters. The *Personal Recollections* recounts personal events contemporaneous with those in the Chapter and is rich in the anecdotes that I have been encouraged to write while my comments, observation and conclusions regarding the events described in the objective section of Chapters are in the *Personal Perspective* section. However, the personal sections are truly subjective and there is no loss of continuity in the main thread of the infrared astronomy research at AFCRL if the reader wishes to skip these sections.

To provide a context for the *Personal Recollections/Perspective* sections, I sketch my personal background prior to 1963 when I began my career in infrared astronomy in the following: I became interested in science while quite young, with an initial fascination with dinosaurs and other aspects of the distant past. I was struck by the fact that scientists were extraordinarily privileged because they were paid for doing what they wanted and enjoyed doing rather than merely working at a job. A scientist is what I wanted to be, but I also realized that I needed an education to become one and I was an indifferent student. My interest in science was

rekindled by the 1957 close approach of Mars to the Earth with the definite choice of astronomy as a career. However, my school grades were not very good until the last two years of high school when, in the 11th grade, my schoolwork and grades improved.

I was accepted to UCLA in 1959 for my undergraduate degree. Upon arriving at UCLA with the instructions on enrollment and course selection, I encountered the singular institution of ‘running for classes’, that is, standing in interminable lines with numerous others in an attempt to sign up for the desired courses. I was only able to enroll in about half the classes I wanted and had to scramble to get into alternatives for what was left for the remainder. With 22,000 students, UCLA was one of the larger campuses in the US at that time and the large campus and the cattle call for classes gave an impersonal face to the institution.

I enrolled in the interdepartmental Astronomy-Physics major, which had the virtue for me that an additional year of physics classes was substituted for the physical and organic chemistry classes that were normally required for a major in the physical sciences. This meant fewer laboratory classes to which I had an aversion, from the junior high school metal shop in which I melted the soldering iron, to the physics labs at UCLA. One worthwhile ‘lab’ class was typing, which I took as an alternative to yet another shop class in junior high school. The training paid off hugely with the advent of personal computers.

I had intended to take four years each of physics and mathematics and the maximum permitted of three years of undergraduate astronomy. However, my science and math grades during the first two years were mediocre. No course grade was lower than a C but few higher and, if it hadn’t been for the humanity classes, my grade point average would have been irrecoverable. I began to have serious doubts about being able to concentrate on any problem or topic well enough to develop reasonable study habits and without the necessary grades I would not be able to get into graduate school. I decided to put myself to the test during the Christmas vacation of my sophomore year. Up to this time I had done B/B- work in Ordinary Differential Equations and decided to study the course book by Coddington from cover to cover and to do every problem; the fact that the answers to every other problem were given in the back of the book was of considerable help. I steadily went through the book six hours a day during the entire two week vacation. I thought I had done rather well on the final exam several weeks later but was disappointed to receive a B in the course. I had found that the class lectures given by the instructor for the course, Dr. Biriuk, were clear and understandable and was pleased that he was scheduled to teach the Advanced Calculus course I had signed up for the next semester. Unfortunately, he had thrown out his back and a newly minted PhD took over the class. I did, however, run into Dr. Biriuk about a month after classes started the following semester and expressed my regret that he was not teaching the Advanced Calc course because the new guy had changed the content to emphasize theory rather than the practical applications that were specified in the university guidebook such as triple integrals, Gauss’ theorem, vector and tensor analysis, that were needed for advanced physics. Almost in passing, I also expressed disappointment in getting a B in the DiffE course because I felt that I had done very well on the final. It turns out that I had gotten an A in the class but the teaching assistant decided to give me a B. The good Doctor immediately took me to the Math department to change the grade. A similar situation occurred in my Thermodynamics class; the lab assistant arbitrarily raised the grade cut line so that I received the highest C in the class even though, numerically, it should have been the lowest B. The class professor also was also kind enough to change the grade upon my appeal. These, and other, arbitrary exercises of authority made me doubly cautious to remove personal opinions when judging an individual’s contribution or performance in the professional arena.

The UCLA astronomy department was undergoing a transition during my time there. George Abell, Lawrence Aller and Ray Weymann had been brought in to add an astrophysics research component to the existing meteoritics (Frederick Leonard) and the calculation of orbits of solar system bodies, spacecraft and binary stars (Robert Baker, Samuel Herrick, Maude Makemson, and Daniel Popper). Thus, my courses for the major were an interesting mix. The astronomy classes were mainly in the third and fourth year with the exception of Spherical Astronomy, which I took in sophomore year. The pocket calculator of the time, a slide rule, had insufficient accuracy for the problems and a six, or better yet eight, place logarithm tables were required. The professor, Maude Makemson, was old school and required that we add or subtract the logs left to right in order immediately estimate the magnitude of the answer and to catch errors mid-calculation. Robert Baker, a former student of Herrick's who purportedly had received the first US PhD in astrodynamics, taught Astrodynamics and Navigation which emphasized spacecraft orbits. The course text was the book on the subject that he wrote with Makemson. George Abell taught Introductory and Intermediate Astronomy with lessons gleaned from the final draft of his book on the subject while Lawrence Aller taught Introductory Astrophysics and the course text naturally was his book on the topic.

I graduated UCLA – barely, with a 2.4 grade point average thanks mainly to the non-science courses. However, I did well on my Graduate Record Examinations and was initially accepted into the Indiana University graduate school but Indiana ultimately rejected my application because of my final grade point average. I had also applied to the Ohio State University – but no reply meant no acceptance. Thus, it looked unlikely that I would be able to become a real astronomer with a PhD ‘union card’ that allows one to practice the arcane science in a manner recognized by one’s peers. I, therefore, scrambled to line up job interviews, three of them, my last semester at UCLA. One interview was with Aerojet Corp. in Azusa, California, the second with Martin Marietta in Denver and the third was with International Telephone and Telegraph Federal Labs (ITTFL) in Sylmar, California. Martin-Marietta flew me in for the interview but the position was in engineering and, given my difficulties with laboratory classes, there was no fit between my interests and education and their needs. The in-plant interview at the Aerojet Corp. was memorable. I was given a perfunctory interview with the assistant personnel manager and was then sent to be interviewed by a couple of first line managers, one of whom showed me into a huge room where he said I would be working if I took the job. The room was filled with rows upon rows of neatly aligned drafting tables throughout the area that were almost, but not quite, touching with a few cubicles in the corners for the management staff. It was a thoroughly depressing environment as later verified by a High School colleague who had briefly worked in this very room; I declined to further pursue this opportunity.

The last interview was with ITT Federal Labs in Sylmar, CA. I had a tie to ITTFL that provided an excellent entrée for that interview. ITTFL had sponsored the closest thing to a science club that we had in high school, the Future Engineers of America (FEA). Gerry Speen and Freeman Hall were the company representatives to our FEA group, whom we saw about once a month at our weekly meetings – Gerry more than Freeman. I interviewed both with Gerry and Freeman for a job. Gerry was very enthusiastic about the work his group was doing; but it was engineering and poor Gerry couldn’t understand why I didn’t share his enthusiasm. Freeman had completed the first infrared sky survey two years previously and offered me the opportunity to oversee the construction and use of a larger and more sensitive instrument. This was a far better offer, with the opportunity to do astronomy, than I ever expected without a graduate degree. Thus, began my career in infrared astronomy.

1. THE LABORATORY¹ FROM 1945 TO 2011

Prior to World War II, research in the physical sciences was funded, for the most part, by universities and augmented by grants, gifts from private donors, and endowments. Then the government invested heavily in military research and technical development during the War and continued significant post-war funding for radar, ballistic missile studies and environmental research, becoming the major financial resource for meteorology, the upper atmosphere research, geophysics, space research, and astronomy in the decade following the war. The influx of large amounts of government money, especially from the military, caused concern among many of the established astronomers and geophysicists that the government funding not only would erode the influence and control that they exercised in their respective disciplines but also dry up traditional sources of support (Doel, 1996; DeVorkin, 1999). The government largesse also changed the manner in which research was conducted from relatively small, long term and open-ended efforts by single individuals or small teams to large projects that usually had specified end products. Doel (1996) also noted that although disciplinary peers controlled funding allocations and priorities of a particular project, the project's longevity was somewhat uncertain as it depended on decisions by the funding agencies that were influenced by national policies and politics.

To meet the increasing research demands after the Second World War, the Department of Defense (DoD) turned to its few existing labs, such as the Naval Research Laboratory (NRL)², and created new military labs, the Army Air Force (AAF) Cambridge Field Station for example. Liebowitz (1987) noted that plans were laid out for Air Force research in a comprehensive report commissioned by General H.H. (Hap) Arnold, Commanding General of the Army Air Forces in November 1944. Gen. Arnold had tasked the Army Air Force Scientific Advisory Group led by Theodore von Kármán to study and recommend how the AAF should best prepare for the future. In the report, *Toward New Horizons*, Von Kármán recommended that existing Army Air Force developmental research facilities be expanded and new ones created under a budget that matched war time funding levels (Gorn (1994) provides a more accessible version of von Kármán's conclusions). Two AF basic research organizations were among the newly created labs; the Cambridge Field Station and the Applied Research Section at the Wright-Patterson AFB renamed the Flight (later Aeronautical then Aerospace) Research Laboratory.

In establishing the new Cambridge Field Station on 20 September 1945, the Army heavily recruited among the electronics engineers and scientists at the Massachusetts Institute of Technology (MIT) Radiation Laboratory and the Harvard Radio Research Laboratory who had worked on war-related radar and antenna research. The enticement to join the Field Station was that about half the military projects at these institutions were to be transferred into the fledgling organization. By the time the Air Force became a separate service in September 1947, the Field Station consisted of four electronic divisions.

King (1959) noted that the Army Air Force originally intended to recruit the scientists and engineers for employment either at Wright Field in Dayton, Ohio or the Watson Laboratory in Red Bank, New Jersey. This proved to be untenable as nearly all of those who expressed an

¹ The Laboratory collectively refers to the Air Force research organization initially based in Cambridge MA, then at Hanscom AFB.

² NRL is the oldest military laboratory, dating from about 1920, and was well positioned to take a lead in geophysics research at the end of the War. Amato (2001) described how NRL arose from a recommendation toward the end of World War I by the Navy scientific advisory board chaired by Thomas Edison to create a modern naval research facility for development and engineering.

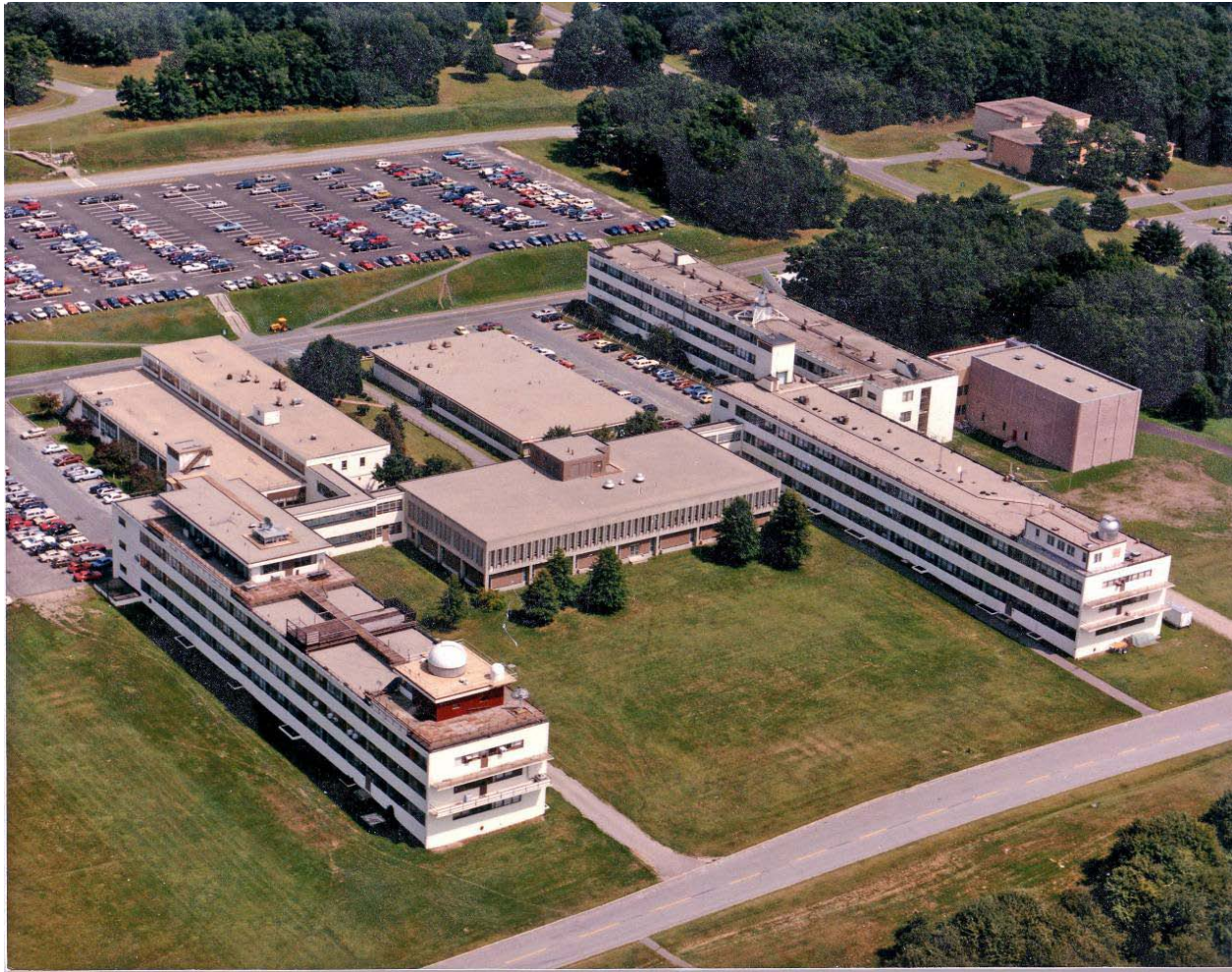


Figure 1. The Air Force Geophysics Laboratory complex in the late 1980s. The first two permanent buildings that were constructed at the site are at the left, the second two are at the right. The building between and at the upper center was originally a cafeteria and served as the infrared backgrounds experiments laboratory in the early 1980s; it is currently a conference center. The front office and the support functions are in the newer building in the middle of the complex. This building originally housed the computing facilities before those became decentralized. The small high bay building at the far right was intended to be used for on-site integration and testing of experiment payloads but that function was moved to Kirtland AFB within a few years after the picture was taken. The small building in the upper right corner is the library. John Howard, the first AFCRL Chief Scientist, used Lab discretionary funds to obtain Lord Rayleigh's laboratory notebooks as well as the original publications of Humphreys and historical documents from other 19th century scientists, all of which were housed in the library until being transferred to the Air Force Academy library in the winter of 2008.

interest in working for the new laboratory were not inclined to leave the Boston-Cambridge area. The Army Air Force consequently established a Field Station in Cambridge, Massachusetts under the jurisdiction of the Watson Laboratory for the new projects and employees with the expectation that the people would be moved at a later date. The other shoe fell on 3 May 1948 when the Air Material Command, to whom the Cambridge Field Station reported, confirmed plans to move the Field Station to Rome, New York. The workforce vigorously opposed the relocation and mounted a strong anti-move campaign that enlisted the support of local academics, contractors and Massachusetts politicians. In the political arena, the Massachusetts governor offered the Air Force land at the Bedford, MA airport for permanent laboratory

facilities as an incentive to keep the research organization in the state. The campaign was successful and the Field Station remained in Cambridge with the ‘less insipid’ name of Air Force Cambridge Research Laboratories (AFCRL). The research mission was then expanded to include geophysics in 1948 when the atmospheric sciences, meteorology and geophysics research at the Watson Lab was transferred to the Field Station to become the nucleus of six laboratories within a Geophysics Division; the antenna work already in the Boston area was put into the Electronic Research Division. In April 1951, the Field Station was assigned to the newly created Air Force Research Development Command (AFRDC), which was to organize and direct all in-house research at the Air Force laboratories. The AFCRL name was changed to the Air Force Cambridge Research Center (AFCRC) in June, at which time the organization was comprised of Geophysics and an Electronics Research Division. These two divisions were upgraded to Directorates in 1952.

The Air Force accepted the Commonwealth of Massachusetts’ offer of land at the Hanscom³ Field near Bedford, MA and construction on the first two permanent Air Force buildings began in October 1952. After an initial delay due to a freeze of military construction by the recently elected Eisenhower administration, the buildings were completed and occupied in 1954; the second two buildings of the initial main complex were completed in 1957 and were occupied by the Geophysics Research Division. Meanwhile, Hanscom became the official Headquarters for the Laboratory in June 1955. Figure 1 shows the complex as of the mid-1980s.

Most of the post-War basic and applied military research was either conducted in military laboratories or funded by them. However, from the beginning, the Air Force has grappled with what it wanted from its research institutions. This angst is reflected in the fact that the Air Force or the Department of Defense has appointed a committee every year or two to study how research should be organized, managed and/or conducted. In reviewing the studies prior to 1975, Sigethy (1980) unhappily concluded that the committee findings were based more on the preconceived views of panel members rather than on any formal or objective evaluation. As a result, although a variety of recommendations had been proposed no coherent view of the ‘proper’ organization has emerged. He stated that: *“Since most of these studies were only an accumulation of the opinions of the study group members, the membership of the group was an important variable in the final outcome of the reorganization. The studies produced in this period and, in general, in later periods are noteworthy by their dogmatic approach. There were no alternatives presented, little analysis and no recognition that other approaches might be reasonable or satisfactory. There was, however, a common thread throughout all the studies. The attitudes, perceptions, beliefs, motivations, habits and expectations of all the various study group members were essentially shared. As a result, there never was an analysis of the issues identified during this period. The Air Force had depended upon industry for its aircraft during World War II. It was natural for the Air Force to look to a source outside the Air Force for its research progress. The Air Force Advisors were university oriented so it logically followed that the universities were accepted as the primary outside source of scientific knowledge. Notably lacking in the study reports was a recommendation for strong in-house laboratories and in*

³ Laurence G. Hanscom, a newspaper reporter and an aviation enthusiast, was killed in a plane crash in 1941. The Massachusetts legislature established the Bedford Airport as a Commonwealth facility in May 1941 and a month later designated it as the Laurence G. Hanscom Field, Boston Auxiliary Airport at Bedford. The Commonwealth of Massachusetts transferred Hanscom Field legal operating rights to the Air Force on 7 May 1952. Hanscom Field was designated the Laurence G. Hanscom Air Force Base on 22 June 1974 and Hanscom AFB on 18 Jan 1977.

particular support for the existing in-house laboratory.” Or, paraphrasing Futrell (1971), the Air Force had decided that industry would be largely responsible for its new technology and that the role of the Air Force Laboratories was to stimulate and monitor such research.

Some organizational changes did define responsibilities. For example, after the Navy created the Office of Naval Research (ONR) in 1946 to oversee the increased funding to external organizations for basic and applied research after the War, the Air Force followed suit with its own Air Force Office of Scientific Research (AFOSR) in 1952 as the principal agency for basic research contracts to universities and non-government groups. However, at least up to 1975, AFCRL independently defined the basic and applied research to be conducted under its purview and the mix of in-house and contracted research, devoting as much as 70% of the research budget to in-house programs (Aviation Week, 1975).

The nature and structure of in-house research have changed considerably during the 65 years that the Hanscom contingent has existed. Broadly speaking, the organization and the character of the in-house Laboratory research may be divided into approximately 15-year periods that are composed of about a decade of relative stability followed by about five years or so of transition forced by external events and reorganizations of Air Force research priorities for its in-house efforts. The following five sections in this Chapter outline, in sequence, the organizational structure during these periods, and highlight the geophysics, space research and astronomy that were conducted. This introduction provides the background of the infrared astronomy programs and the general context for the details that are given in later chapters. Complementary historical material may be found in various technical reports: King (1959) provides a firsthand *History of the Air Force Cambridge Research Center 30 September 1945 to 30 June 1959* and Liebowitz (1985) presents an overview of the Laboratory’s Geophysics contributions to national defense. Liebowitz (1987) and Liebowitz and Kindler (1995) collectively chronicle the significant events and accomplishments of the Laboratory from 1945 to 1995. Details of the status of the research and accomplishments may be gleaned from the approximately bi-annual Laboratory reports on research; the first was published in 1961 and the tenth and last one in June 1987.



1.1. The Cambridge Research Center (1945 – 1960)

This initial period was one of growth, definition of the research mission and development of a well defined Laboratory organization. It spans the time from the formation of the Cambridge Field Station in 1945 to the creation of the Air Force Cambridge Research Laboratories in 1960. Fortunately, King (1959) provides a detailed history of the laboratory organization and management for this period as well as a summary of technical programs. King’s account emphasizes the research that led to the Nation’s first air defense warning system (and Lincoln Laboratory) as well as the first air traffic control system. Since

King provides briefer summaries of the geophysics programs, the initial military requirements with respect to geophysics are expanded upon in this section. The wide range of research is reflected in the AFCRC shield *circa* 1958 shown above. The three white stars in the upper left represent the AFCRC electronics, geophysics and human applications missions. The central cloud with two lightning bolts denotes the geophysics research, and the three concentric radar rings with a sweep line symbolizes the electronics component.

The military strongly supported geophysical research after World War II as it required this information for operations. For example, knowledge of the density, temperature and composition of the upper atmosphere was needed in order to understand how these factors influenced ballistic missile performance. Conditions in the ionospheric regions of the upper atmosphere affected radio communications and a link between solar activity and ionospheric disturbances was strongly suspected before the war. Also, it was speculated that solar ultraviolet radiation maintained the ionosphere but direct measurements of the solar ultraviolet flux were needed to quantify this connection. How the Sun affects the ionosphere and, in turn, how the disturbed ionosphere perturbs radio propagation was, and still is, of high military importance.

The post-War military emphasis on upper atmospheric research came with a new tool – rocket probes. A civilian V-2 panel was established in February 1946 to organize and direct the upper atmospheric experiments that were flown on captured German V-2 rockets; although the panel was ‘civilian-dominated’, the panel members had been engaged in war-time research either while serving in the military or allied with one of the military sponsored laboratories. These experiments were ‘free rides’ on the Army tests, from which the military expected to gain experience in missile operations, tracking and guidance and control, all of which supported the tactical ballistic missile program Project Hermes. The broad range of experiments included

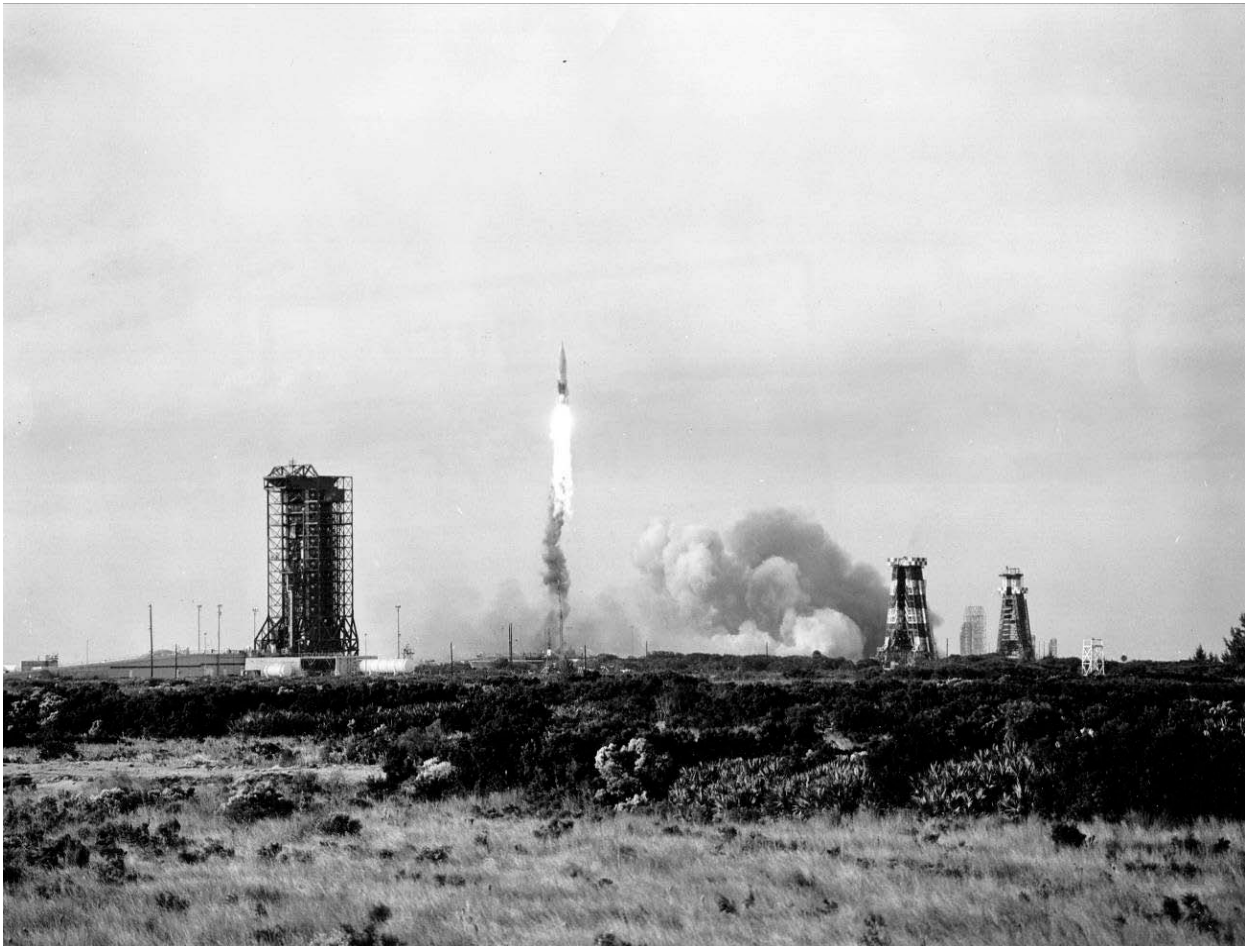


Figure 2. An anonymous V-2 launch. The White Sands Missile Range V-2 launch complex 33 was designated an Historical Landmark by the State of New Mexico in 1983 and, in 1985, a National Historical Landmark by the National Park Service.

studies of the radio propagation in the ionosphere, atmospheric composition, pressure, temperature and density, cosmic rays, meteoritics, atmospheric absorption in the ultraviolet and ultraviolet energy distribution of the Sun. The Naval Research Lab and Applied Physics Lab (APL) had a leadership role on the panel with support from General Electric Corp., the Project Hermes contractor; other organizations, including several universities, also participated. DeVorkin (1992) superbly chronicles the history of the US rocket-based upper atmospheric research conducted under the aegis of the panel from the initial post-War V-2 flights to the International Geophysics Year in 1957. The panel disbanded in 1961, having undergone several name changes during its 15 years of existence.

Both the Naval Research Lab and the Applied Physics Lab existed at the end of the War and both organizations had research groups that were adapted to conduct upper atmosphere experiments. In contrast, the newly formed Cambridge Field Station had to catch up. Marcus O'Day, Chief of the Cambridge Field Station's Navigation Laboratory, joined the V-2 panel a few months after it was formed and remained a member through the 1950s. On 21 November 1946, he supervised the successful launch of the first Air Force V-2 (#15) from Holloman AFB, NM. Since, the core professional staff of O'Day's Navigation Lab originally was composed almost entirely of PhD physicists recruited from wartime radar groups at Harvard and MIT, the disciplines of these scientists reflected the Navigation Branch's initial emphasis on electronics and radar research and, consequently, the first Air Force V-2 flights concentrated on ionospheric radio propagation and whatever enhanced the Branch's expertise in electronic detection systems. An anonymous AFCRC V-2 launch is shown in Figure 2.

The addition of 'upper air' to the Air Force research mission was complemented by the Air Force's decision to relocate the Watson Laboratory's Geophysical Research Division to the Field Station in November 1948. Since O'Day coordinated the early Air Force work on the properties of the upper atmosphere, his branch was designated the Upper Air Laboratory in March of 1949 to reflect the importance of this research.

The V-2 experiments extended to higher altitudes the in-situ measurements of the density, temperature and constituents of the upper atmosphere, cosmic rays and solar ultraviolet radiation that were conducted from balloons prior to the war. The ultraviolet transparency of the atmosphere is a direct measure of the ozone absorption profile as a function of altitude, which may be derived by measuring the ultraviolet spectrum of the Sun as it varied with altitude. DeVorkin (1992) noted that James Van Allen suggested a straightforward military payoff for this research: "*Since ozone was a primary indicator of height, studying its distribution would also suggest how it could be used to guide a missile.*" Richard Tousey's group at the Naval Research Lab flew a spectrometer mounted in the V-2 tailfin on the 10 October 1946 flight to obtain the first ultraviolet spectra of the Sun (Baum et al., 1946). However, the University of Colorado group achieved the 'holy grail' of the first far ultraviolet detection of Solar L α (Rense, 1953) on an 11 December 1952. O'Day had funded the University's Physics Department to develop a coronagraph and pointing control mechanism for the payload. The result was a major improvement in attitude control that was a key to the success of this spectrographic observation.

The 69th and last V-2 flew in September 1952. Of the various replacement options, the Aerobee emerged as the workhorse for upper atmospheric and astronomical research; Rense's L α experiment was flown on an Aerobee. The Navy had sponsored James Van Allen at APL to contract with Aerojet Engineering Corp in Pasadena and the Douglas Aircraft Company to develop an inexpensive liquid fueled rocket capable of lifting 100 lbs. to 100 miles altitude. Aerojet, a 1942 industrial spin-off of von Kármán and colleagues at the Caltech Guggenheim



Figure 3. The last AFGL Aerobee 350 rocket at the Smithsonian Air and Space Museum.

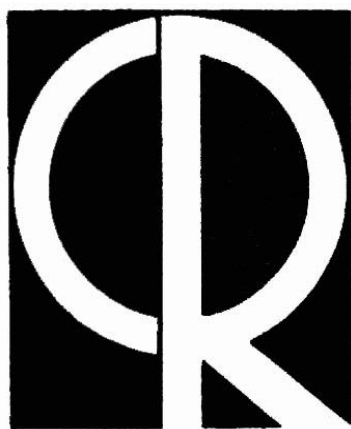
in density and height of the atmosphere that were being measured on rocket and balloon flights. At mid-century, an authoritative value for the variation in the solar constant was several percent (Doel, 1996). Thus, definitive measurements were needed to explore the Earth – Sun links to weather and, in this context, the first successful AFCRL Aerobee-based in-house experiment on 26 May 1950 was devoted to measuring the solar constant.

Marcus O'Day expanded the upper air research on the Sun–Earth connection to include optical and radio observations from ground-based facilities. Liebowitz (2002) describes the six year effort by O'Day and Harvard's Donald Menzel and Walter Orr Roberts to create the Sacramento Peak Observatory. The facility arose from O'Day's desire for a site to support Holloman AFB launches while also having it well located for upper atmospheric measurements. Initially, a tracking station was installed at a location that overlooked Holloman AFB and White Sands Missile Range to observe Air Force launches. A solar patrol was added in 1949 with small portable instruments to monitor the Sun and issue radio communications forecasting alerts to provide the Holloman launch crew with information on unusual solar activity. This arrangement coordinated observations from Sacramento Peak and the rocket experiments with simultaneously measured atmospheric effects. The Sacramento Peak facility was designated the Upper Air Research Observatory in April 1951, then the Sacramento Peak Observatory in May 1956 by which time a larger, permanent solar coronagraph became fully operational. Monitoring the Sun is still a major research activity for Air Force Research Laboratory scientists.

The Upper Air Laboratory was disbanded in April 1953 and merged with other geophysics programs (Liebowitz, 2002). Marcus O'Day then became Superintendent of the newly created Advanced Research Laboratory in which he started a program in plasma physics. He retired several years later and died on 16 November 1961. A crater is named after him on the

far side of the Moon to honor his pioneering space efforts and, in memoriam, AFRCL established the Marcus O'Day award in 1962 for the best annual scientific publication.

There were frequent organizational restructuring during the first fifteen years as the mission objectives were continuously defined/refined. Initially, the AFCRC research budget grew in the early 1950's due to the Korean war and the increasing scientific and technical Soviet threat but funding pressures later in the decade led the Secretary of Defense to propose a 10% cut in the fiscal year (FY) 1957 military research budget with the consequent cancellation of 600 Air Force and Navy research projects (Rigden, 2007). In light of the bleak outlook for AFCRC, Milton Greenberg, the Geophysics Research Directorate director, proposed to make his Directorate a private corporation that would operate under contract to the Air Force. After the proposal was informally rejected in the summer of 1958, Greenberg, and his directors of the Management Requirements and Programs Divisions and the Thermal Radiation and Photochemistry Laboratories left AFCRC in October 1958 to found the Geophysics Corporation of America (Liebowitz, 1985). The business plan of the new company was to perform geophysical research under government contracts, many of which were, as they expected, with the Geophysics Directorate. However, there was no mass exodus of geophysicists to the new company and the laboratory maintained a strong program in basic and applied upper atmospheric research and geophysics. In terms of manpower, the workforce numbered over 4200 by 1954 and remained at this level through most of the 1950s. However, only about a third of these people worked in core electronics and geophysics research. Others were staffed to run the facilities and several development groups such as the Atomic Warfare Directorate and an Operational Applications Laboratory that did research on communications and human information processing. The workforce declined toward the end of the decade as changes in mission and reorganizations resulted in research areas being terminated or reassigned to other laboratories such as the National Aeronautics and Space Administration (NASA). The space age heralded the next major reorganization and invigorated research at the Laboratory.



1.2. Cambridge Research Laboratories (1960 – 1975)

The Air Force Cambridge Research Center was slated for significant manpower and funding cuts in 1957 under the Eisenhower administration's plans to cut the deficit. The Department of Defense shifted emphasis from basic and applied research to operations, development and system support. The Air Force also directed that more research, especially basic research, be contracted outside the labs. This all changed as the Air Force responded to the Sputnik launch in October 1957. On 15 January 1959, the Air Force Research Development Division was established within the Air Force Research Development

Command, a move that led to a series of reorganizations that separated laboratory research from system development. On 1 April 1961 the governing organization for research, the Air Force Research Division was reconstituted as the Office of Aerospace Research (OAR), a separate operating agency that reported directly to Headquarters, US Air Force. This organizational change brought increased funding and elevated the importance of basic and applied research.

AFCRC was reorganized into the Air Force Cambridge Research Laboratories (a recycling of the name as the facility was also so designated between 5 July 1949 and 28 June 1951) to accommodate the new Air Force emphasis on space research. The Air Base Wing was

established in 1960 to oversee base operations and AFCRL became a tenant organization as did the newly created Air Force Electronics Systems Division (ESD). In April 1961, ESD was designated as the responsible agency for development and integration of electronic command and control systems that formally had been in AFCRC. The AFCRL Electronics and Geophysics Directorates were abolished on 15 Apr 1963 and the fourteen groups therein were reorganized into nine Laboratories: a microwave physics and a solid state science laboratory derived from the AFCRC Electronics Research Division, a Data Sciences Laboratory and six geophysics laboratories with a total personnel complement of about 1100 people that included 680 professional researchers. Subsequently, programs in space physics and optical/infrared physics were added and further reorganization produced 10 Laboratories plus the Sacramento Peak Observatory. The in-house research funding for supporting studies by universities and research contractors came from the AFCRL core applied research budget, the AFOSR basic research budget and from various customers such as the Advanced Research Projects Agency (ARPA) and NASA. The increase in federal research and development funds after Sputnik meant that the military, especially the Air Force, remained a major contributor for geophysics, upper atmosphere and space physics basic research to universities in the 1960s.

From its beginning, AFCRC/AFCRL was active in space flight, conducting a number of rocket and satellite based experiments both in-house and under contract, flying a probe-rocket experiment at the rate of about one a week through the 1960s. Most of the rockets flights carried Upper Atmosphere Physics Laboratory experiments, and a fair number of these were devoted to ultraviolet measurements. However, the Space Physics Laboratory conducted most of the astronomy during the AFCRL years; the few exceptions were the Terrestrial Sciences Laboratory's lunar laser ranging program that obtained the first returns in September 1969 from corner cubes placed on the Moon by Apollo 11 astronauts and an infrared astronomy program in the Optical Physics Laboratory that began in the early 1960s. AFCRC scientists flew experimental packages on the first US satellite in 1958 and AFCRL even designed and built its own series of satellites in the mid-1960s. AFCRC's early interest in satellite-based astronomical applications led to a contract with Lyman Spitzer at Princeton University for a detailed design of a space telescope system. Spitzer (1960) presented his concept at a 30 December 1960 conference at Case Institute of Technology on *Astronomical Observations from Above the Atmosphere*. Arthur Code (1960) gave a passing reference to a satellite based infrared survey in his presentation at this conference, by which he meant systematic infrared spectral and photometric measurements of known objects.

The Space Physics Laboratory continued the cosmic ray, meteoritic and radio astronomy research that dated to the 1950s and initiated new programs in optical astrophysics and lunar and planetary studies. The natural and artificial sources of radio emission originating outside the atmosphere and the propagation of these signals through the atmosphere were measured. Originally, a radio capability was proposed for Sacramento Peak but interference from Holloman AFB precluded quality measurements there. Harvard subsequently established the facility at Fort Davis, Texas under Air Force sponsorship and AFCRC set up its own radio telescope flare patrol on Prospect Hill in Waltham, Massachusetts. AFCRC also built and operated 84' and 150' steerable radio telescopes at Sagamore Hill, in Hamilton, MA in the late 1950s. The 84' instrument was put into operation in November 1958 and received the first radio signals bounced off the Moon that were transmitted from Jodrell Bank, England, although these radio telescopes were mainly used to monitor the Sun. AFCRL also funded the initial Ohio State University (OSU) radio survey (e.g. Scheer and Kraus, 1967) and, on a larger scale, channeled ARPA funds

to Cornell University to construct the Arecibo radio telescope; the design of the original steerable feed for the telescope was based on early 1950s research conducted by AFCRC. Arecibo construction started in August 1960 and facility operations began in early 1964.

The Space Physics Laboratory also had an optical astrophysics program to study plasmas and how they interact with magnetic fields. This program provided the seed money in 1958 for the Cerro Tololo project (Doel, 1992) a collaborative effort with Yerkes Observatory for the site survey in the Chilean Andes for a 60" telescope. The National Science Foundation funded site development and shared the cost of the telescope with AFCRL. The telescope was completed in 1966 and Space Physics Laboratory astronomers sporadically observed there until the Air Force gave up its interest in 1969. Optical spectra of gaseous nebula were obtained with this telescope to probe plasma temperatures and densities that were not achievable in the laboratory. To provide a basis for quantitatively interpreting these astronomical observations, complementary laboratory research with plasmas generated by exploding wires and shock tubes investigated transition probabilities (*f* values) of elements. Knowing the elemental *f* values allows one to convert the measured luminosities of the spectral lines of a given element into the amount of this element in the source while the specific lines detected says something about the plasma conditions in the nebula. The optical astrophysics group had a 20-foot shock tube for these measurements operating on-site as early as 1963 (e.g. Wolnik et al., 1969) and funded the OSU shock tube experiments (e.g. Byard, Roll and Slettebak, 1963; Byard and Roll, 1965).

After Sputnik, the Space Physics Laboratory's cosmic ray and meteoritic research, which dated to post War V-2 upper atmospheric experiments, enjoyed renewed emphasis. The rocket based cosmic ray experiments sought to measure the primary particles that created the air shower of secondaries observed from the mountain top and balloon platforms. DeVorkin (1992) noted that the military justification for this research at the time was as a means for improving atomic weapons technology and to mitigate the potential hazard to man in high flying aircraft and, with an eye to the future, to satellite instrumentation. Not much will be said regarding the cosmic ray effort other than it was quite an active program within the Laboratory until it was terminated in the late 1970's: cosmic ray and energetic solar particle packages constituted more than half the Laboratories' satellite experiments during the first two decade of space flight (Liebowitz, 1995).

The study of meteors was an original major research objective of the V-2 panel. Fred Whipple (1943), a V-2 panel charter member, posited that the brightness and length of meteor trails were indicative of the upper atmospheric density, temperature and composition profiles. To calibrate the mass and velocity – luminosity relationship, an artificial meteor experiment was flown under the auspices of Caltech's Fritz Zwicky in which explosive charges ejected small, high velocity pellets from the first V-2 night launch from White Sands in 1947, but nothing was seen. Meteors as remote probes came into question as the V-2 measurements of the atmospheric density and pressure profiles increasingly diverged from what Whipple had calculated from meteor trails. Using data from better monitoring cameras, Whipple subsequently deduced that meteor composition wasn't as homogeneous as he originally thought (DeVorkin, 1992), thus compromising their value as remote atmospheric probes. However, meteors are source material for hypersonic ballistic studies and meteor trails produce radar returns; hence the continued military interest in understanding their interactions with the upper atmosphere. At Whipple's urging, AFCRC repeated the artificial meteor experiment successfully in October 1957 (Doel, 1992) in which a multistage rocket lofted a package that used a shaped charge to blast the artificial meteorites into space. Subsequent April 1961 and May 1962 experiments studied the interaction of artificial meteorites as they entered the atmosphere (McCrosky and Soberman,

1962). The Meteor Physics group also conducted *in situ* experiments of the exo-atmospheric dust environments; the first micrometeorite detection experiment was flown on an Aerobee rocket from Holloman AFB, NM on 16 July 1957 and the first US satellite, Explorer I launched on 31 January 1958, carried AFCRC microphone and wire grid micrometeorite detectors to register particle strikes (Dubin, 1960).

For the broad picture of space-based micro-meteoritic research from the mid-1950s to the late 1960s, Hodge's (1981) description of the early interplanetary dust measurements nicely complements that in the *Historical Perspective* chapter by Fechtig (2001). The early attempts to collect extraterrestrial dust from pans of water on rooftops, in fossilized rock strata, and in the deep sea indicated that a very large amount of dust was falling onto the Earth each year. This was at odds with the particle density inferred from the observed brightness of the zodiacal light, the sunlight that is reflected by the dust. Contamination of the samples was suspected but early aircraft, balloon and the AFCRC rocket and satellite experiments tended to corroborate the high particle density near the Earth. Such a high flux was worrisome for the planners of the early space missions as it posed a risk of serious damage to satellites and, eventually, to man in space. However, Soberman and Della Lucca (1961) soon found from their analysis of acoustic detector data returned by Midas II (1960 ζ1) that these devices systematically measured much larger particle fluxes than wire grid detectors. Thus, the early satellite results using acoustic detectors appeared to be biased by instrumental effects and, as noted by Fechtig (2001), within a few years these detectors and the results obtained with them were rejected as unreliable.

The infrared probe-rocket based sky survey was conducted as part of the celestial backgrounds program within the Infrared Physics Branch of the AFCRL Optical Physics Laboratory. The Branch was established in the April 1963 reorganization with Russ Walker as the Branch Chief. The program objective was to define the distribution of infrared brightness across the sky through ground and space-based measurements and modeling. Between 1965 and 1975, Branch personnel flew 17 rockets under Russ Walker's direction: 12 devoted to infrared astronomy, three to infrared horizon measurements and two shared experiments. The Branch also conducted research on the optical transmission and emission of the atmosphere. The chemical reaction parameters measured in the Branch's laboratory chambers were used to improve the first principles physics models in the Branch's optical propagation codes and to interpret the rocket-probe measurements of emission from the undisturbed upper atmosphere. Liebowitz (1990) chronicles the evolution of these atmospheric research models into propagation codes that have become standards used throughout both the Department of Defense and civilian communities and the spin-off of specific application codes for defense systems.

Both the research portfolio and the Laboratory organization came under scrutiny at the end of the decade. The external impetus for this major 'sea change' was section 203 of the FY70 Military Procurement Authorization Act, dubbed the Mansfield Amendment that mandated that all Department of Defense research must demonstrate relevance to military systems or operations. On the other hand, Sigethy (1980) posited that other factors likely had more of an impact among which was the changing face of Air Force research, as evinced by the abolition of the Air Force Office of Aerospace Research in July 1970 with subsequent unification of all research and development under the applications oriented AF Systems Command. Major work force reduction also ensued as laboratory slots were reassigned to other Air Force elements. This occurred in the context of the general public disenchantment with both science and the military at the time. Fosset (1975) concurs but pragmatically assigns the demise of basic research within the Air Force Laboratory to the 1975 reorganization that deactivated the Aerospace Research

Labs at Wright-Patterson AFB and redirected the AFCRL effort into exploratory research; thus, ended the distinction between the AF development and research Labs.

These structural changes played out over five years. In 1970, AFCRL had ~1257 people in 11 Laboratories when the manpower reductions began as research objectives were adjusted. By the time this phased reduction ended on 30 June 1974, five branches within the Laboratories had been abolished and ~15% of the workforce or about 200 positions were eliminated. On 22 November 1974, the Air Force announced an additional reduction of 200 positions as part of the Alignment and Reduction Action under which AFCRL's geophysics research was to be transferred to Kirtland AFB, in Albuquerque, New Mexico. The vacated space was to be filled with people and programs that were to be transferred from the Rome Development Center in New York. After considerable political lobbying, the reductions were deferred and on 31 July 1975, the Secretary of the Air Force announced that the geophysics research would remain at Hanscom AFB, at least for the time being, thereby obviating the need for the Rome Development Center programs and people to come to Hanscom.



1.3. Geophysics Laboratory (1976 – 1990)

On 1 January, 1976 the AFCRL Microwave Physics and Solid State Sciences Divisions, as well as the Laser Physics, Electromagnetic Environment and Ionospheric Radio Physics Branches were transferred to a newly created Rome Air Development Center Detachment at Hanscom AFB. This affected roughly a third of the AFCRL complement and what remained of AFCRL was designated the Air Force Geophysics Laboratory (AFGL) on 30 June 1976 with an effective date of 15 January 1976. To reflect the Geophysics focus of the new

Laboratory, the organizational shield was changed from the simple CR letters of Cambridge Research Laboratories to a stylized depiction of the Earth at summer solstice.

Meteoritics and stellar astrophysics research had been terminated shortly after the Mansfield Amendment but the radio astronomy, cosmic ray studies and the lunar and planetary research hung on until the 1976 reorganization. Thus, with the exception of the solar physics work most of the Space Physics astronomy efforts had ended by the time the AFGL was formed. However, solar ultraviolet measurements from sounding rockets and satellites continued for another five years.

The infrared survey experiment program also underwent significant changes mid-decade. Funding for the probe-rocket experiments dried up in 1975. Convinced that infrared astronomy had no future at AFGL, Russ Walker left to join NASA Ames Research Center in 1976 and Bob McClatchey, who led the atmospheric propagation modeling and code effort in the Branch, was appointed Branch Chief upon Russ's departure. While the Optical Physics Laboratory became the Optical Physics Division under the AFGL organization, the Infrared Physics Branch remained essentially the same. The Air Force Systems Division funded a new probe-based infrared Background Measurements Program shortly thereafter with Bert Schurin as the program manager. This series of probe-based experiments surveyed the infrared celestial sky with larger sensors, measured the zodiacal background and observed the quiescent thermosphere. Seven experiments were flown between August 1976 and January 1985, two on Aerobee 350s and the rest on the much larger ARIES guided sounding rocket (an ARIES launch is shown in Figure 4).



Figure 4. The Multi-Spectral Measurements Program TEM-2 launch on 21 May 1980. This ARIES rocket from the White Sands Missile Range was the 1000th sounding rocket flown by the Laboratory.

program and outside money was not forthcoming. However, the idea of such a multiple objective mission resonated with SDIO, which initiated the Midcourse Space Experiment (MSX) in 1988. SDIO also funded AFGL to develop models and codes to describe the infrared celestial background at any specified wavelengths, spatial resolutions and sensitivities for contemplated military space surveillance systems. A fair portion of this funding was allocated to university research to analyze the existing infrared data, including a two-decade long development of infrared stellar standards to calibrate military and civilian satellite sensors.

The decade of stability after AFGL was formed was again followed by five years of organizational turmoil. US industrial laboratories were shifting their research to produce short term payoffs with practical applications and transfer of government laboratory technology into the commercial business sector became a highly valued metric. AFGL and the Astrodynamics and the Space Technologies Laboratories became part of the Air Force Space Technology Center (STC) when the latter was created at Kirtland AFB in October 1982. STC was assigned to Space

Burt Schurin took over as Branch Chief when McClatchey became Director of the Geophysics Laboratory's Atmospheric Division in 1981.

Two events then occurred that led to the termination of the infrared probe-rocket based astronomy experiments. First, the Strategic Defense Initiative Organization (SDIO) was formed in 1983/1984 and swept up a significant portion of the Air Force space related exploratory and developmental research funds. As these were the funds that supported the AFGL sounding rocket experiments, negotiations with Systems Division (SD) that were well under way for at least two additional flights were terminated. Then, the 1983 success of the much more sensitive NASA/Netherlands/UK Infrared Astronomical Satellite (IRAS) provided the definitive database on the infrared celestial background at the time. Consequently, the focus of the AFGL infrared celestial background research shifted from probe experiments to mining the existing data and developing satellite missions.

In 1981, AFGL funded the next logical step: a conceptual design study for an infrared satellite-based observatory and AFOSR added supporting analysis funds in 1984. At that time, AFOSR was contemplating supporting major 'flagship' research facilities for the Air Force but neither AFGL nor AFOSR budgets could sustain such a large and ambitious

Division in order to be answerable to the major user of its technologies. On March 9, 1989, the Air Force Geophysics Laboratory was re-designated the Geophysics Laboratory within STC. Later, to realize the economy of the reorganization, the Air Force Systems Command announced in November 1989 a 10% reduction in personnel, which included the Geophysics Laboratory workforce, over the ensuing three years. In this environment, the DoD Defense Science Board conducted yet another assessment of DoD research in 1986 and concluded that the military labs were in sad shape, recommending major changes in the DoD acquisition process and suggested that research facilities be combined (Day, 2000). Detailed studies of various consolidations options were conducted by the end of the decade, including the benefits of combining research across service boundaries and/or creating government owned contractor operated facilities to improve efficiency. The Air Force's preemptive response was to consolidate and reorganize its research with within five 'superlabs'. Thus, Phillips Lab was created.

1.4. Phillips Laboratory (1990 – 1997)



The DoD and the Air Force announced sweeping policy changes at the beginning of the decade that would significantly impact geophysics research. The Secretary of Defense issued the Defense Management Report on 11 January 1990 that specified how the DoD was to implement the Defense Science Board's recommendations for consolidating research within the various laboratories. The first step was to put a total in-position freeze on civilian hiring. In response, the Air Force considered

consolidating the Systems Command product centers and the laboratories that supported them. A proposal was put forward on 26 February 1990 to move the Geophysics Laboratory to Kirtland Air Force Base to join the Air Force research contingent already there. The cost of moving the Hanscom facilities were determined to be prohibitive, and no wholesale relocation took place.

The Geophysics Laboratory was downgraded to the Geophysics Directorate on 12 December 1990, a remote operating location of the newly established Phillips Laboratory headquartered at Kirtland AFB, NM. The creation of Phillips Laboratory as one of the four new Air Force superlabs imposed an additional management layer over the geophysics programs at Hanscom and research emphasis gradually shifted to engineering, development and testing. Then, funding for the Geophysics programs were zeroed out in the 1996 Air Force budget. Intensive lobbying by the Massachusetts congressional delegation, local firms that did business with the Directorate and by the Hanscom workforce did get most of the funding restored that September. However, the cut heralded a long decline in civilian staffing and core Air Force funding for AF geophysics research. The Aerospace Instrumentation Division at Hanscom was transferred to Kirtland as were several smaller groups. This loss of manpower coupled with 14 incentivized retirements and resignations between the first such opportunity in 1993 and the winter of 2008 eventually reduced the number of civilian positions at Hanscom by 75%.

Remarkably, the infrared astronomy effort remained robust despite all the changes and turmoil. The decline in the in-house funding that began in the mid-1980s with the end of the celestial background field experiments was compensated by customer funding from SDIO and NASA. SDIO sponsored the infrared astronomy group for background characterization studies and to direct the astronomy experiments on the Midcourse Space Experiment (MSX). Also, thanks in part to a collaboration with the Dutch, the infrared astronomy group had several experiments on the European Space Agency's (ESA) Infrared Satellite Observatory (ISO).

However, management oversight of the astronomy program did change quite a bit. In 1987, the eight people in the celestial backgrounds program had been formed into the Celestial Background Branch and the atmospheric propagation code work in the then defunct Infrared Physics Branch was transferred to the Infrared Technologies Division, which had been created from the Radiation Effects Branch after it was separated from the Optical Physics Division five years earlier. In 1990, the Infrared Technologies and Optical Physics Divisions were recombined and a single Background Branch was created from the Atmospheric and Celestial Backgrounds Branches in the two divisions; the commonality being that both groups flew rocket experiments.

The heritage of the atmospheric experiments dated back to shortly after World War II when, in November 1946, AFCRC began a long series of rocket flights to measure the electron concentration and energy distributions in the ionosphere (e.g. Lien, et al., 1953). This legacy was transitioned to the Radiation Effects Branch when Jim Ulwick, the principal investigator for many of these experiments, joined the Branch after the abolition of the Ionosphere Laboratory as part of the early-1970 reorganization. The Atmospheric Background Branch and its predecessors had conducted probe-based spectral and radiometric measurements of the aurorally disturbed atmosphere, most of which were flown from Fort Churchill, Canada or Poker Flats, Alaska. The Branch also used an instrumented KC-135 aircraft and Stair (1970) highlighted some early notable observations, such as measurements of the solar corona during the 7 March 1970 eclipse. Nuclear tests were observed by instruments on the aircraft. Tragically, on 13 June 1971, the KC-135 and four of the AFCRL Radiation Effects Branch scientists – John Cahill, Anthony Theriault, David Penny and Thomas Walters – were lost when the aircraft went down while returning from monitoring French nuclear tests in the South Pacific.

The Radiation Effects Branch also conducted laboratory studies of the reaction rates of the atmospheric molecules that produce airglow and auroral emissions to interpret aircraft, balloon and probe rocket-based observations of the aurorally excited atmosphere and infrared atmospheric background radiation produced by nuclear tests.

The rationale for combining the Backgrounds and Celestial Branches was that both groups flew rockets. The initial flight program of the atmospheric group had been a large scale measurement campaign (Infrared Chemistry Experiment Coordinated Auroral Program – ICECAP) that was conducted between 1972 and 1976 in which about a score of rockets were flown to probe the atmosphere. More than a dozen experiments obtained *in situ* measurements on the chemical emission in the disturbed atmosphere and several more passively observed the aurora. Besides observing the aurora, which was taken as the natural surrogate for a nuclear induced background, Bob O’Neil conducted five experiments between 1974 and 1979 that measured the chemical consequences of exciting the atmosphere with an electron gun to create artificial aurora (Fraser, Green and O’Neil, 1991); the final such experiment, EXCEDE III, was flown in 1990 (e.g. Rappaport et al., 1993). Infrared spectra of aurora were obtained with circular variable filters by the 1977 SPIRE (Stair et al., 1985) and the 1983 ELIAS (Caledonia et al., 1995) experiments, while interferometers were employed for the 1976 HIRIS (Stair et al. 1983) and the 1986 SPIRIT 1 (Adler-Golden, 1991) probe flights. These experiments complemented those of the infrared astronomy group that obtained analogous measurements on the quiescent atmosphere. The consolidated Backgrounds Branch assumed responsibility for the three remaining atmospheric backgrounds experiments: the SPIRIT II probe-rocket (Kemp, Larsen and Huppi, 1994) and the CIRRIS 1A Shuttle-based flight (Wise et al., 2001).



1.5. Air Force Research Laboratory (1997 – 2011)

The Air Force's Armstrong, Phillips, Rome and Wright superlabs were put into a single Air Force Research Laboratory (AFRL) on 31 October 1997 and the resulting entity assigned to Air Force Materials Command. This constituency is represented by four of the five stars to the left of the AFRL shield, the fifth denotes AFOSR. The central triangle represents the union of the aircraft, missile and spacecraft research within a single laboratory.

The independence of geophysics research within the Air Force was further eroded with the formation of AFRL. The Geophysics and Space Technologies Directorates were combined to form the Space Vehicles Directorate, headquartered at Kirtland AFB, with Ms. Christine Anderson as Director. Now all Air Force basic and applied research is conducted or sponsored by one of the 10 directorates within AFRL. Duffner (2000) uncritically described the formation of AFRL in a book: *Science and Technology The Making of the Air Force Research Laboratory*.

Corporate funding decisions shifted from Hanscom to Kirtland, which meant that the research emphasis favored technology development and flight demonstration of engineering concepts specified in the Directorate charter. Improvement of mechanical coolers for infrared focal planes is an example of technology development while the Directorate's TacSat program provides flight demonstrations to prove operational concepts. That this was an Air Force policy decision is evinced by the fact that during the formative year before the Research Laboratory was created, the soon to be AFRL commander categorically rejected Ms Anderson's request to alter the proposed name for her Directorate from Space Vehicles to Space Technology or simply Space to be more inclusive of the Hanscom work (Duffner, 2000). Furthermore, the Geophysics Directorate was renamed the Battlespace Environment (VSB) Division to reflect the application orientation of the new Directorate. Until this name change, the Directorate had enjoyed the wide-spread lingering name recognition of the Geophysics Laboratory, which gave researchers some organizational independence and ability to seek outside funds.

The geophysics funding line was subsumed under another program element after AFRL was established, disappearing from the Air Force research budget. The Air Force also deleted weather as a functional research area within the Laboratory. Although this move was directed at the Hanscom tropospheric weather programs, overzealous interpretation of the directive erroneously removed funding for the Space Physics 'space weather' programs, resulting in Hanscom being insolvent for the two year budget cycle. A Congressional add to the Air Force budget bailed out the Hanscom research site for the first year but the Directorate had to cover the second year with help from the Laboratory.

The two technical divisions in the Directorate, the Battlespace Environment (VSB) and the Spacecraft Technology (VSS) Divisions, were derived from the Phillips Laboratory's Geophysics and the Space Technologies Directorates, respectively, while a third Integrated Experiments (VSE) Division had its roots in AFGL's Aerospace Instrumentation Division. Under the Directorate's original organizational plans, the former AFGL Optical Physics Division was to be subsumed by the Spacecraft Technology Division at Kirtland. The management and infrastructure of the resulting hybrid division was to be located at Kirtland with the former Optical Physics Division Director, William Blumberg, serving as Division Technical Advisor and *in loco* representative of the Division Director. Although political pressure within the Air Force product divisions, the Hanscom research community, and the Massachusetts congressional

delegation failed to have the geophysics research at Hanscom AFB declared a separate AFRL directorate, it did result in cancelling the formation of the split division.

In March of 2000, a Space Weather Center of Excellence (CoE) was created at Hanscom that included the research in the former Space Physics and Ionospheric Physics Divisions. Another attempt was then made to subsume the optical physics programs piecemeal into the Spacecraft Technologies Division by creating a ‘Space Infrared Technologies Center of Excellence’, comprised of the Space Surveillance branch at Kirtland and the 15 people doing atmospheric and celestial backgrounds research at Hanscom. The remainder of the Backgrounds Branch would re-form into two new Branches within the Hanscom AFB based division.

The rationale for this CoE was a proposal for a dual use satellite to demonstrate infrared space surveillance and planetary defense – the detection and characterization of near Earth asteroids – that Mike Egan and I sent to Paul LeVan in the Kirtland Space Surveillance Branch in 1999. This proposal highlighted the Space Surveillance Branch’s potential contribution with regard to mechanical cryocoolers and high temperature mid-infrared focal planes. The Hanscom/Kirtland merged branch did not work out, principally because neither the VSS Division Chief nor his Branch Chief were able to integrate the backgrounds research conducted at Hanscom into the CoE and no one in the CoE took the initiative to advocate the space demonstration that was supposed to be the unifying focal point. For years later, the Hanscom people returned to the local administrative chain of command in 2004.

The infrared astronomy program is anticipated to continue until 2011 as external funding has been secured at least until that year. The 2011 horizon of this report, which was sent to the printers at the end of 2009, is set by the transfer of personnel to Kirtland AFB that year.

1.6. External Support – Lifeblood of the Celestial Backgrounds Program

Support from agencies outside the Air Force research laboratory has been essential for the celestial backgrounds program. Indeed, the AFCRL/AFGL probe-rocket based infrared survey programs and the longevity of the Celestial Background program critically depended on these outside resources. All but two of the 23 probe-rocket based experiments, MAP II and BEAM, that were conducted by the infrared astronomy group and listed in Table 1 were funded by external agencies. Maj. Bob Paulson from ARPA provided the funds for the HI STAR survey and his successor, Maj. Jim Justice, did the same for HI STAR South. Capt. Jenks, SAMSO, oversaw the modification and delivery of the Autonetics Stellar Radiation Sensor while Capt. Crabtree was in charge of the HI STAR construction. Capt Lyons followed Crabtree and was responsible for contract management for the HI HI STAR program.

Capt. Mike Kiya and Howard Stears joined the SAMSO infrared space surveillance program office in the mid-1970s just before the Background Measurement Program was initiated and provided management oversight for that program. Both had extensive backgrounds with cryogenic sensors and were well versed in infrared space applications, contributing to a number of programs over the years. Thus, we were able to discuss the issues, problems and objective of our research with a knowledgeable pair of Captains in the SAMSO program office. Mike Kiya’s long association with infrared sensors began in the mid-1960s when he was stationed at the Air Force Avionics Lab at the time they were developing the airborne sensors described in Chapter 3. He was assigned as the Air Force liaison officer to NASA Ames Research Center in 1977 where he made significant contributions to both IRAS and the Shuttle Infrared Telescope Facility (SIRTF) programs and helped Craig McCreight start the Ames detector program. After completing his military tour, Mike became an Ames civilian employee where, during the next

Table 1. AFCRL/AFGL Experiments flown by the Infrared Celestial Backgrounds Group

Experiment	Date	Pole star	RA	Dec	Alt (km)	Time (sec)
		Comments				
MAP-I	6 February 1970	---	---	---	144	240
MAP-II	27 July 1970	---	---	---	137	145
HI STAR using Aerobee 170 rockets						
A04.004-2	3 April 1971	α CrB	15 ^h 33 ^m	26° 49'	160	185
A04.004-4	29 June 1971	α Lyr	18 ^h 36 ^m	38° 45'	158	200
A04.004-5	29 October 1971	δ Tau	5 ^h 36 ^m	21° 13'	156	200
A04.004-6	18 January 1972	δ Per	3 ^m 52 ^m	31° 48'	161	200
A04.004-7	15 April 1972	α CVn	12 ^h 55 ^m	38° 28'	176	205
A04.004-8	18 August 1972	α And	0 ^h 7 ^m	28° 56'	171	250
A04.004-9	5 December 1972	α Ari	2 ^h 6 ^m	23° 55'	180	255
HI-STAR South – using Aerobee 200 rockets						
A05-391-1	4 September 1974	ϵ Sgr	18 ^h 23 ^m	-34° 24'	193	275
A05.391-2	11 September 1974	ACS failure – no data			---	
A05.391-3	17 September 1974	γ Gru	21 ^h 52 ^m	-37° 29'	191	280
Experiments on Aerobee 350 rockets						
A35.191-2	16 February 1974	HI HI STAR			111	~70
A35.191-1	3 December 1975	Super HI STAR ϵ UMa + β And			286	~350
A35.191-4	3 August 1976	Earth Limb Experiment – ELE			257	
Experiments on ARIES rockets						
SPICE 1	28 January 1979	Payload failure – no data			349	---
ZIP-I	18 August 1980	δ And	0 ^h 38 ^m	30° 45'	400	480
ZIP-II	31 July 1981	δ And	0 ^h 38 ^m	30° 45'	400	480
IRBS	4 February 1981	Separation failure – No data			387	---
FIRsse	22 January 1982	α Lyn	9 ^h 20 ^m	34° 28'	379	450
SPICE	14 September 1982	ϵ Cyg	20 ^h 45 ^m	33° 53'	364	455
ELC	26 October 1983	Some vis & IR zodiacal data			300	70#
SPIRIT II	29 March 1992	Aurora obs. from Poker Flats			400	
Castor – Lance from Barreira do Inferno rocket range, Brazil						
MAP	25 May 1973	Successful limb profile exp.			567	
BEAM	17 January 1985	Separation failure – no data			500	---
Orbital Experiments						
STS 39	28 April 1991	CIRRIS 1A (some IR Zod.)			260	~1 hr
STS 42	22 January 1992	Visual Zodiacal Experiment				~1 hr
MSX	26 April 1996	Astronomy: one mission goal			888	~250 hrs

Some of the reference material was taken <http://www.astronautix.com/>

seven years he was Lou Young's deputy manager on the SIRTF program and helped create the Large Deployable Reflector concept (Murphy et al., 1980; Swanson et al., 1983). Subsequently, he went to the SIRTF program office at NASA Hq. and, in the 1990s, became a consultant on DoD space Programs. Howard Stears had several consulting positions after leaving the Air Force. The one that intersects with this narrative was the Infrared Background Signature Survey

program mentioned in Chapter 6 that Howard directed as a consultant to the Ballistic Missile Defense Organization. AFGL had a role in analyzing the backgrounds data from this experiment, which was flown on the Shuttle mission STS-39 in 1992. Several company grade officers followed Mike and Howard but their contributions were mostly managerial.

Not in Table 1 are the two infrared horizon measurement experiments that were flown by the Infrared Physics Branch in 1966 and 1968 as these predate the first astronomy experiment. Of the atmospheric experiments only the Brazil MAP flight and the SPIRIT II and IRBS probes did not have astronomy as at least a secondary objective; the ELE, ELC and CIRRIS 1A mission profiles specifically included zodiacal background measurements.

Two years after the AFGL probe experiments ended, Barry Katz took over SATKA 32.1, the program that explored the phenomenology and satellite signature issues for the Strategic Defense Initiative (SDIO). Barry had an excellent grasp of the technical issues and decided within a year of taking the position that a technology demonstration satellite, which became the Midcourse Space Experiment (MSX), was required to provide real world measurements on the phenomenology pertinent to midcourse surveillance and the technology issues related to obtaining the data. The data from this satellite as well as the wealth of information from other resources were to provide the basis for a modeling effort for scene generation in which accurate encounter scenarios could be computationally generated for risk reduction in the design of testing of DoD systems. Barry understood the value of fully exploiting the MSX data and, in a rare decision for a DoD satellite program, provided adequate funds for the data reduction, analysis and modeling. Barry passed away due to complications from a heart transplant without seeing the fruits of his labors lift off from the launch pad in 1996.

Col. John Mill succeeded Barry Katz as the MSX program manager. Col. Mill was scientifically astute; he was an air weather office who had spent a tour of duty in that capacity at AFGL. John saw MSX through launch and mission operations before retiring. Col. Bruce Gilmain followed John as MSX program manager. Both John and Bruce had assured that adequate funding continued for the MSX data processing and reduction into early 2000s. Although an SDIO mission, MSX is listed in Table 1 because AFGL personnel played a major role in the system design, mission planning and execution and were responsible for a substantial portion of the data obtained by this satellite.

Concurrent with the MSX program we established a collegial working relationship with the infrared team at the Space Research of the Netherlands at Groningen. This resulted in our participation in the Short Wavelength Spectrometer (SWS) consortium for the Infrared Space Observatory (ISO) led by Thijs deGraauw. This provided access to ISO experiments through the time allocated to the instrument teams and a survey experiment directed by Alain Omont, Institut d'Astrophysique, Paris. Both experiments complemented the celestial data taken by MSX.

The MSX data was of sufficient quality that we approached NASA Hq. to solicit their interest and funding to produce research quality products from the observations. The case had been made to Michael Bicay before flight, but it was the video of the scan along the Galactic plane that was a persuading factor for Harley Thronson, Gunther Riegler and Ed Wieller after MSX was in orbit. NASA provided the funds to create the MSX images and catalogs and to host them at Infrared Processing and Analysis Center from where they are made available to the infrared astronomical community. NASA Hq. also funded us to analyze the MSX results and to process and analyze data from our ISO experiments. After this effort was completed in the mid-2000s, we were able to obtain a couple of small NASA grants to study the archived MSX data. Furthermore, NASA provided sustaining funds for our small celestial backgrounds team to do

Table 2. Space Experiments Funded or Supported by AFRL/AFGL

Experiment	Date	Comments	Alt (km)	Time (sec)
Cornell IR Probe-Rocket Celestial Experiments funded by AFCRL				
A04.004-3	2 December 1970	IR sky scan experiment	190	140
KP 3.39	17 July 1971	IR sky scan experiment	190	280
KP 3.40	18 July 1972	IR sky scan experiment	144	
Astrobee F	14 October 1975	IR zodiacal spectroscopy		
Caltech/ISAS Experiment on Terrier– Black Brant IX using AFGL (SCOOP) Optics				
36.163UR	28 May 1997	Near IR Telescope Exp: NITE	345	290
36.175UR	22 May 1998	CCD obs. of edge-on galaxies	337	
Orbital Experiments				
ISO	17 November 1995	European Space Agency IR Astronomy Experiment	1000 × 70,500	~2½ yr.

the 24 μm image processing for Sean Carey's Spitzer legacy program to survey the Galactic plane. This task was expanded to include a survey of the Cygnus X region and portions of the outer Galaxy. This legacy program plus some Spitzer grants independently obtained under the guest investigator program or teamed with Greg Sloan for spectral studies kept the celestial backgrounds program viable to the end of the decade.

Table 2 lists the astronomy experiments conducted by others in which the Laboratory played a meaningful role. ARPA funded through AFCRL contracts all or portions of the early 1970s Cornell University experiments flown by Jim Houck and colleagues that are the first four entries. Although AFGL did not provide financial support for or actively participate in the Caltech experiments (Bock et al., 1998), the fifth and sixth entries, these are listed because AFGL provided considerable capital equipment contribution in the form of the pressed sintered beryllium telescopes used on these experiments. Because AFGL personnel were less involved in the design and mission planning for ISO compared to MSX, ISO is relegated to Table 2.

While we may be generous in claiming supporting credits for some of the experiments in Table 2, we also acknowledge in later Chapters the major space-based infrared astronomy experiments in which we were not involved. We had little directly to do with IRAS, although the AFGL and IRAS programs influenced each other and AFCRL did extensively support preparation of the original proposal. Our only interaction with the Diffuse Infrared Background Experiment on the Cosmic Background Explorer was Tom Murdock's participation on the COBE science team. The Spacelab 2 experiment (Kent et al., 1992) was a NASA sponsored demonstration that infrared astronomy could be done from the Shuttle. The Infrared Telescope in Space heralded the Japanese entry into satellite based infrared astronomy while Akari is their most recent success. Similarly, although we had several experiments and a substantial amount of observing time on the Spitzer Space Telescope, it is not listed as we played no role in the design of the instrument or payload and only a user's participation in the execution of the mission.

Finally, an effort was begun in the late 1990s under the SDIO background characterization program to establish celestial references against which DoD sensors could be calibrated. The initial work was done under contract but AFRL took it on as an in-house task in the early 2000s. Mike Egan at National Geospatial-Intelligence Agency became interested in the calibration issue and funded us to the end of the decade to extend the wavelengths spanned by the standard stars and to establish the Moon as and disk resolved reference.

1.7. Astronomers Associated with the Laboratory's Infrared Program

This section highlights the people that were engaged in on-site infrared astronomy and concludes with an outline of the contractual efforts. The intent is to provide an overview of the astronomical program at Hanscom but especially to give the limelight to the individuals that were involved in the research.

Russ Walker initiated the infrared celestial background program in the early 1960s. Not only did the program address a defense need in surveillance but it also dovetailed nicely with his thesis research. Russ came to AFCRC as an Air Force officer in 1953 upon graduating from the Ohio State University with a Master's degree. After leaving the Air Force and a brief stint at Block Engineering, he returned to AFCRL, becoming the Chief of the Infrared Physics Branch in 1963. He closely directed the probe-rocket based infrared celestial survey experiments from the beginning of the program in 1968 until 1974. He left AFCRL in 1976 to join NASA Ames Research Center and work on the Infrared Astronomical Satellite. He is still active in the field, working at the Monterrey Institute for Research in Astronomy.

I doubled the number of astronomers on the program when I arrived in July 1969 and I have been doing infrared astronomy in the Laboratory ever since.

Lt. Thomas Murdock joined the AFCRL in 1972 after receiving his degree from the University of Minnesota under Ed Ney, a noted cosmic ray physicist who changed interests to infrared astronomy in the late 1960s. Ed advised Tom to look into doing his military service with the Air Force group near Boston that was flying infrared astronomy experiments. Since Tom's PhD research was on the infrared properties of Mercury and the Moon (Murdock, 1972; 1974), the AFCRL commander naturally sent him to see Jack Salisbury, Chief of the Lunar and Planetary Research Branch. Tom remembers a table tennis match on the observatory floor during working hours that tipped him off that the group may not have had a vigorous research program at the time and chose to join Russ' group. Tom served out his military obligation and went to work for a local research company for the mandatory year before being hired back as a civilian to become the principal investigator for the zodiacal experiments conducted under the Background Measurements Program. Tom left in the mid-1980s when the Large Aperture Infrared Telescope Satellite experiment proposed by AFGL failed to materialize. As a private contractor, he played a key role in the MSX program and became the principal investigator for the calibration and performance assessment team.

Lt. Robert Pelzmann, Jr. also came to AFCRL for his military service while finishing his PhD at Stanford University. He reduced the data from the Super HI STAR flight (Pelzmann, 1978a), which he leveraged upon completion of his military service to obtain a position with a NASA Ames contractor to support Henry Lum's bid for the IRAS data processing.

Paul LeVan was hired in 1982 after completing his degree at the University of California, at San Diego (UCSD). Barbara Jones, his thesis advisor, provided the entrée for our interview with Paul as she was the principal investigator on our UCSD contract to monitor the infrared fluxes of bright variable stars (Jones and Rodrigues-Espinosa, 1984). This was a follow-on effort to the UCSD portion of the systematic confirmation (or rejection) of sources in the AFCRL catalog by Rick Rudy, Tim Gosnell and Steve Willner (1979). Paul's most significant contribution was to construct one of the first infrared hyper-spectral camera that obtained low resolution 8 – 14 μm spectra over a cross dispersed spatial field in an effort to prove out spectral imaging capability for the Large Aperture Infrared Telescope concept. He used the camera at the University of Wyoming's Mt. Jelm observatory and published several papers on the results, most

of which are reproduced in the Phillips Lab technical report by Sloan, LeVan and Tandy (1993). Paul LeVan transferred to the Spacecraft Technologies Division of the Phillips Lab at Kirtland AFB in 1992 to pursue his interests in focal plane technology development. His assistance was critical in salvaging the 15 – 28 μ m band of the Short Wavelength Spectrometer on ISO.

I recruited Frank Clark, a University of Kentucky radio astronomy professor, after meeting him at the third IRAS conference in London in 1988. Frank spent a sabbatical at the Rijksuniversiteit in Groningen, Netherlands in the latter half of 1985 shortly after my five month stay there. Frank had published several articles interpreting the IRAS data both before and after joining AFGL and was the MSX program representative to monitor the data processing algorithm development for Lincoln Laboratory's Space Based Visible sensor on the satellite. He moved on to non-astronomical interests in 1995 but left a legacy as a Palace Knight mentor. Under this program, the Air Force paid qualified graduate students to attend graduate school. In exchange, the student entered into a non-binding agreement to work for one of the Air Force Laboratories upon graduation. Frank Clark recruited Russ Shipman, a University of Wyoming graduate student, while Mike Egan, from the Rensselaer Polytechnic Institute, independently applied to the program and was accepted. The Air Force also had a graduate school fellowship program with no such employment obligation in which Bruce Pirger enrolled in 1992. That summer Bruce worked with Paul LeVan on the AFGL spectrometer but subsequently dropped out of Caltech to take a position in the Cornell Astronomy Department's focal plane laboratory.

Russ Shipman and Mike Egan began working at the Geophysics Directorate in 1993; Mike having finished his degree and Russ to work on his thesis with Frank Clark as his on-site advisor. Both Russ and Mike contributed to the MSX data processing and their reduction and analyses were the basis for a number of publications. Russ also worked on the ISO Short Wavelength Spectrometer observations obtained by the AFGL dedicated time experiments. That led him to take a position at the Space Research Organization of the Netherlands (SRON) in Groningen in 2000 to work on the Short Wavelength Spectrometer Pipeline processing and to teach. Mike Egan became the Technical Advisor in the Hanscom component of the Kirtland AFB based Space Infrared Technologies Center of Excellence in 2000. Mike also left a few years later to pursue his career in another component of the DoD.

Kathleen Kraemer came to us as a National Research Council post-doctoral fellow from Boston University and did so well that she was hired to fill the position left vacant by Mike Egan's departure. Kathleen played a major role in completing the analysis and publishing the MSX observations and ISO Short Wavelength Spectrometer measurements. She also obtained guest investigator observation time on NASA's Spitzer Infrared Space Telescope, collaborated with Greg Sloan in analyzing instrument time spectroscopic observations and with Sean Carey in reducing the 24 μ m survey of the Galactic plane data and creating images.

During the first dozen years or so of the probe-rocket based experiments, our efforts were concentrated on preparing and flying the experiments and the subsequent data reduction to create the catalogs and maps that were the objectives of the program. This left little time for more than cursory analyses of the data. However, beginning in 1982, we were fortunately able to regularly augment the in-house analysis with post-doctoral fellows and summer faculty. The premier academic program was the National Research Council's Post-Doctoral Fellowship, which was run by the NRC under contract with the AFOSR. Nominally, the NRC post-doc position lasted two years and came in two varieties: a regular post-doc was offered to recent PhDs and a senior post-doc to established faculty researchers. Dissatisfaction arose in the Laboratory in the late 1980s over the NRC rejection of some candidates that the Laboratory mentors rated highly,

apparently a consequence of the NRC independent ranking of the candidates that did not factor in the research and mission objectives of the Laboratory. In response, AFOSR created a supplemental program – the Geophysics Scholars.

Steve Little, Bentley College, arrived as our first NRC senior post-doc in 1984. He was doing near-infrared photometry of H II regions and, with his wife Irene Marenin, analyzing stellar spectra. Steve was principal author of our penultimate paper on the rocket-based survey infrared maps of the Galactic plane (Little and Price, 1985). Irene Marenin, from Wellesley College, was our next NRC senior post-doc. Starting in 1986, she spent two very productive years analyzing infrared stellar spectra, concentrating on the IRAS Low Resolution Spectrometer (LRS) data that had then recently become available (Little-Marenin, 1988). Linda French, also from Wellesley College, followed Irene for a year in 1988 and studied Trojan asteroids.

A four year hiatus followed during which no post-docs were assigned to the infrared astronomy program, and then a number of astronomers were accepted in the early 1990s. After getting their degrees from Boston University, Tom Kuchar joined us in 1992 as a Geophysics Scholar and Randy Phelps as an NRC post-doc in 1993. Greg Sloan arrived in 1993 from the University of Wyoming as a Geophysics Scholar to pursue further work on the IRAS LRS spectra (e.g. Sloan and Price, 1995). Greg had previously worked with Paul LeVan on the AFGL array spectrometer, publishing several joint papers and basing his degree on the results obtained with that instrument. Tom Heasley spent the 1995 academic year as an NRC senior post-doc with an office at Boston University studying super-resolution techniques as applied to stellar clusters. Sean Carey, with his Rensselaer Polytechnic Institute graduate school ties with Mike Egan, opted for an NRC post-doc at the Laboratory in 1995. After the nominal two years, he continued as a Geophysics Scholar for another year. Brian Kane, from Boston University, had the NRC post-doc position with us that immediately preceded that of Kathleen Kraemer.

We needed a cadre of people for the MSX data reduction and analysis in the mid-1990s and Sean Carey, who began working on this effort as a Geophysics Scholar, was subsequently hired by the Institute for Scientific Research of Boston College (BC) as an on-site contractor. Tom Kuchar joined the effort as a BC contractors as did Don Mizuno, another Rensselaer graduate. The government and in-house contractor team of astronomers reduced the MSX data and created the catalogs and images that a common reference in infrared astronomical literature. The group also published over a score of articles based on the MSX data.

Greg Sloan returned as an on-site BC contractor for about a year in 2000 to support our ISO Short Wavelength Spectrometer analysis. He then took a position at Cornell University to work with the Spitzer Space Telescope Infrared Spectrometer team. Sean Carey also left late in 2001 for a position at the Spitzer Science Center. However, our continued collaboration with Greg was quite productive, resulting in papers on a rationalized SWS spectral database (Sloan et al., 2003), a classification scheme for the spectra in the database (Kraemer et al., 2002) as well as several articles that further analyzed these results. Charles Engelke joined the effort in 2002 as a part time on-site employee of Boston College. His first task was to analyze the spectra obtained by ISO camera's circular variable filter in a similar manner as to what was done for the SWS (Engelke, Kraemer and Price, 2005). He then made significant contributions to our effort to improve the absolute calibration of infrared standard stars (Price et al., 2004) in collaboration with Tom Murdock and Charles Paxson, both of whom were at Frontier Technologies Inc. To complete the ISO spectroscopic analysis, Tracy Hodge, from Salem State College, spent the summer of 2002 at AFRL in the AFOSR Summer Faculty Program working to put the ISO photometer spectra onto the AFRL infrared classification scheme. She finished a year and a half

later and published the results (Hodge et al., 2004a, b). Having Helen Walker of the Appleton Rutherford Lab visit us under the AFOSR Window on Science Program the summer that Tracy was here was of considerable help. Helen worked with the ISO photometer consortium and was intimately familiar with the spectrometer data and reduction procedures.

Funding for MSX data processing and analysis began winding down in 2001. We then assumed responsibility for the pipeline processing and automated imaging task for the Solar Mass Ejection Imagers (SMEI) on the Coriolis Satellite the following year to fill in the shortfall in keeping the on-site contract astronomers employed. This funding was ramped down after a couple of years, becoming essentially a maintenance effort by 2005. Fortunately, interest had been rekindled in another aspect of the MSX data, the photometric and radiometric properties of satellites measured during the MSX mission. Concurrently, thanks to Kathleen Kraemer's initiative and our continued collaboration with Sean Carey and Greg Sloan, we obtained NASA funding for Spitzer experiments and subsequent data processing and analysis.

Paul Noah joined the Boston College astronomers in the summer of 2006, providing on-site support to the program for about a year. Paul has worked off-and-on for the previous decade at a local contractor on the infrared celestial backgrounds characterization effort.

The Lab's infrared astronomy program was extensively supported by off-site contracts. A notable early example was the contracts that the AFCRL Optical Physics Laboratory gave Freeman Hall, at ITTFL, between 1960 and 1967 to obtain infrared radiometry of satellites and conduct an infrared sky survey. When the rocket-based survey effort began in 1968, AFCRL provided ARPA funds to four university efforts to complement the survey program. Frank Low and collaborators (e.g. Low and Aumann, 1970) made far-infrared observations of astronomical sources from the NASA Lear Jet under a Rice University contract; George Aumann based his PhD thesis on these observations. Frank Low was also principal investigator on the University of Arizona contract under which he attempted a ground-based mid-infrared survey (Low, 1973) and searched for sources detected on the AFCRL rocket-based survey (e.g. Low et al., 1976). Gerry Neugebauer (1972) at Caltech attempted a ground-based 5 μ m survey with limited results and then changed his effort to monitoring bright infrared variable stars. Jim Houck and his Cornell team flew rocket-based mid- to far-infrared astronomical experiments, which provided material for three PhD theses: Judy Pipher (1971), Tom Soifer (1972) and Dan Briotta (1976). Finally, Larry Mertz (1973) at the Smithsonian Astrophysical Observatory was funded to construct an infrared Fourier spectrometer and obtain the spectra of bright infrared sources. The spectrometer was built and some data were taken, but no publications came of the effort.

The release of *The AFCRL Infrared Sky Survey catalog* (Walker and Price, 1975) incited a feeding frenzy of follow-up observations and some doubts about the quality of the catalog were expressed in the literature when some sources could not be found. We had the Universities of Minnesota, Wyoming, and California at San Diego systematically look at every source in the AFCRL catalog to determine whether it was real or spurious and, if real, to confirm the photometry. The sky was divided into thirds and the same twenty minute interval in each hour of right ascension was allocated to each University. In addition to the aforementioned UCSD article, Grasdalen et al. (1983) and Ney and Merrill (1980) reported on the Universities of Wyoming and Minnesota results, respectively.

AFOSR began funding several contracts on our behalf in 1985 to support the concept design phase of the Large Aperture Infrared Telescope System (LAIRTS). AFOSR did the contractual paperwork while Tom Murdock provided technical direction. Several contracts were given for the systems design concept analysis for the telescope and focal planes. AFOSR also

provided continuing contracts to universities for cosmology studies under the aegis of what might be uniquely done with a satellite-based large infrared telescope, a very hot topic at the time. Using LAIRTS as a rationale, Henry Radoski, the AFOSR program manager, provided new contracts to Trinh Thuan (1988) at the University of Virginia for imaging and spectroscopic analysis of galaxies and Dennis Hegyi at the University of Michigan to measure the optical cosmic diffuse background. Thuan's effort was an extension of earlier research done in collaboration with Eric Jensen who had worked at AFGL under Radoski's AFOSR program (Jensen and Thuan, 1982). Similarly Radoski renewed Hegyi's 1980 AFOSR contract to use a CCD to detect faint objects (Hegyi, 1985). Bentley (1989), Eastern Montana College, was given a new contract to look into the possibility of observing galaxies in the early universe while George Smoot, University of California, investigated the cosmological Sunyaev-Zel'dovich effect, an energy increase in the cosmic background photons as they scatter from electrons in structures such as clusters of galaxies. Shorthill (1990), Utah University, studied the utility of solar system objects to calibrate space-based infrared sensors and the University of Wyoming received two contracts, one with Earl Spillar and the other had Harley Thronson as principal investigators, to study bright infrared sources observed on previous space-based experiments.

The AFOSR program burned brightly for about a year or so, and then faded as the scope of a flagship project proved to be too large. After the initial science contracts ran their course in 1988–1989, AFOSR provided new contracts at our direction to develop innovative technology for infrared astronomy under a much smaller program. Except for a follow-on contract to Thuan (1995), all of the original contracts, were allowed to lapse as their research objectives were incompatible with the new direction.

The new AFOSR program included the AFGL array spectrometer effort led by Paul LeVan and the contract to Mel Dyck and John Benson at the University of Wyoming to develop infrared interferometric techniques to measure the angular diameters of red giant stars (e.g. Benson, Turner and Dyck, 1989). Marsha Lebofsky (1989), University of Arizona, was funded to develop and test hardware for a 2 μm sky survey on the Kitt Peak transit telescope after which AFOSR and AFGL supported Susan Kleinmann (1994), University of Massachusetts, to prototype and demonstrate the feasibility of a Two Micron All Sky Survey.

In the mid-1980s, SDIO had funded AFGL to create first principles models and predictive codes to accurately describe the infrared celestial background to the derived requirements of 2" spatial resolution to a 10 μm brightness of 11th magnitude. The spatial resolution requirement was much higher than what was then available from sky surveys. Therefore, one of the first background efforts was to explore image enhancement procedures. We funded Do Kester and Romke Bontekoe (Bontekoe et al., 1991) at the SRON in Groningen to improve the resolution of the data taken by IRAS. Paul LeVan and I worked with the scientists at Mission Research Corp. and others to explore various super-resolution techniques (Gonsalves et al., 1987). MRC also sub-contracted with Ron Canterna, Gary Grasdalen and some of their University of Wyoming graduate students to support the image enhancement effort. The results were of good quality but, unfortunately, appeared only as a handful of American Astronomical Society Abstracts and the MRC final report (Kennealy et al., 1994).

Models were developed under the SDIO backgrounds characterization effort for the separate celestial background components and MRC was funded to integrate these models into a Celestial Background Scene Descriptor (CBSD – Kennealy et al., 1993) that could create an image for any direction and size of field in the sky in user specified spectral bands and spatial resolution. We adopted the Galactic model of infrared point sources created by Martin Cohen

and colleagues (Wainscoat et al., 1992) and funded Martin for upgrades and to validate the model against additional observations. After expanding the database of infrared measurements of asteroids (Tedesco et al., 1992, 2002), Ed Tedesco created the statistical asteroid model (Tedesco, Cellino, Zappalá, 2005) that is used in the CBSD. A number of people worked on the zodiacal component. Lee J. Rickard and Sally Stemwedel from NRL attempted, with limited success, to rectify the AFGL zodiacal measurements (Rickard, Stemwedel and Price, 1990). This analysis was followed by a more comprehensive one by Tom Murdock and his team (Burdick et al., 1994), also with limited success; the reasons why no closure was reached on these analyses was due to the non-linear behavior of the infrared detectors used to make the measurements, as explained in Chapter 5. Paul Noah, at MRC, coded the zodiacal model he and I developed with contributions from Mike Cobb, then at MRC, Frank Clark and others.

The extended and structured emission in the sky was the most intractable component of the background to model. We had several organizations work on this problem, including the University of Arizona (Low, Sykes and Cutri, 1991). Mark Sykes' ribbon model for the zodiacal dust bands was initially included in the zodiacal model but the cometary dust trails were never properly accounted for. The diffuse structured Galactic emission, loosely called infrared cirrus, was also never adequately modeled.

Beginning in 1987/88, SDIO funded AFGL to support defining the experiment and system requirements for MSX and the subsequent mission planning, execution, data reduction, and analysis of the celestial background experiments. The MSX Celestial Background team consisted of me, as Principal Investigator, Ed Tedesco (MRC), Martin Cohen (Univ. California, Berkeley), Russ Walker (Jamieson Science and Engineering), Mehrdad Moshir (Infrared Processing and Analysis Center/IPAC), Fred Witteborn (NASA Ames Research Center), Dick Henry (Johns Hopkins) and Larry Paxton (Applied Physics Lab) as co-Investigators. Mike Egan, Russ Shipman and Jayant Murthy (Johns Hopkins) were adjunct team members. Dick Henry, Larry Paxton and Jayant Murthy are ultraviolet astronomers and were included on the team in order to assure that the ultraviolet instruments on MSX were optimally used for astronomical observations. The Geophysics Directorate also funded John Lacy (1997) at the University of Texas in the early 1990s to obtain high resolution infrared spectra of bright stars to serve as benchmarks for the Short Wavelength Spectrometer on the Infrared Space Observatory.

The infrared astronomy experiments required a large crew for the laboratory preparations and the field expedition to launch the rockets and the size of the team increased as larger and more complex experiments were flown. However, mention is not given to the many skilled engineers and technicians that supported the experiment; such a list would be quite lengthy as the group photograph in Figure 5 of most, but not all, of the Far-infrared Sky Survey Experiment field team illustrates; another group photograph for our Australian experiments is shown in Figure 21 in Chapter 3.

The evolution of the celestial background program may be traced by the objectives for which contracts were given. In the early 1970s the contracts supported the in-house rocket survey program, followed later in the decade by contracts to systematically search and validate the catalog contents. In the 1980s, supporting efforts for a satellite based system were funded, first for LAIRTS, then for MSX. The celestial backgrounds program was expanded in the 1980s to include analysis of the space based observations and modeling of the various components of the infrared sky and then to analyze MSX and ISO data. The AFRL Celestial Backgrounds team dwindled through the first decade of the millennium as both internal and external support declined, becoming principally a calibration effort by the end of the decade.

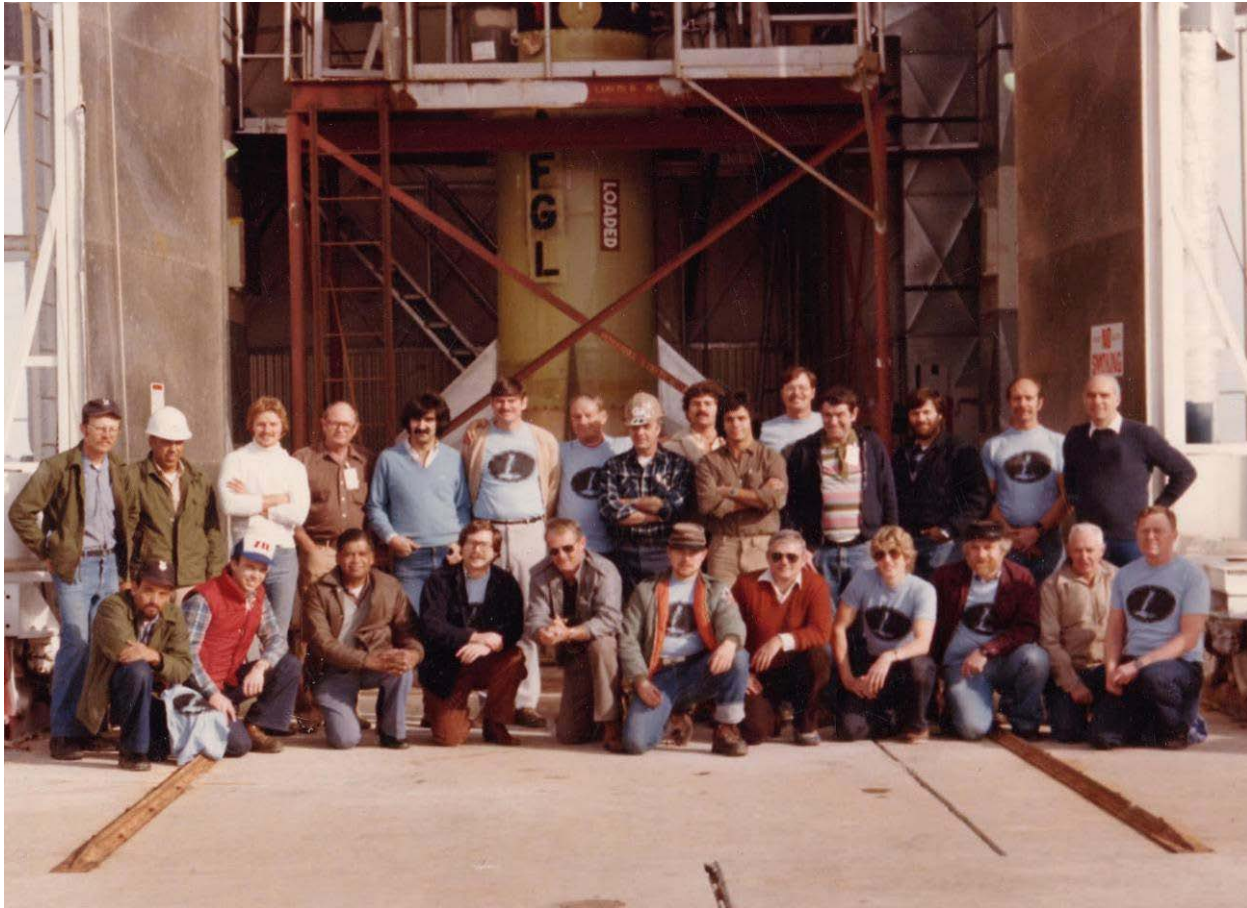


Figure 5. The Far-infrared Sky Survey Experiment field team. First row beginning at left: Navy support (?), Will Thorn (AFGL Aerospace Instrumentation Division - AI), Kandiah Shivanandan (NRL), Tom Murdock (AFGL/OP), Bob Scarborough (Space Vector – SVC, Vehicle), Glen Brown (AFGL/AI airman), Tom Campbell, Wentworth Institute of Technology (WIT), SVC ACS (?), Fred Devino (AFGL/AI), Gunner Briggs (Navy range), Frank Regan (AFGL contractor). Second row: Navy support (?), Chief Gonzales (Navy), SVC ACS (?), Joe Zinn (OSU telemetry), AI ? (SVC ACS), Steve Price (AFGL/OPI), Hal Geiss (SVC Vehicle), Ron Newcomb (SVC ACS), Chuck Galanis and Paul Cucchiaro (AFGL/OPI), Steve McIlhenny (SVC?), Pat Hurley (WIT), Chris Krebs (AFGL/AI), Dave Akerstrom (AFGL/OPI), and Eben Hiscok (AFGL/AI).

1.8. Personal Perspective

The only information I had about AFCRL before interviewing for a position there was that it funded the ITT survey and I had considered an article by Schurin and Ellis (1966), two Infrared Physics Branch molecular spectroscopists, for my thesis research. I was unaware of AFCRL's support for the OSU shock tube, radio astronomy, and molecular spectroscopy and remained so for some time after coming to AFCRL because of the consuming demands of the rocket experiments and, in part, because the AFCRL Laboratories operated rather independently and competitively with regard to each other. This independence limited inter-Laboratory communication and cooperation. The competition can be traced to how AFCRL was structured.

When the Office of Aerospace Research specifically delegated research leadership to the Laboratory Directors in 1962, the Laboratory Directors became Public Law 313 employees and had the equivalent rank to that of a flag officer (General). Then AFCRL was restructured in

1963, the Geophysics and Electronic Research Directorates were divided into nine Laboratories with roughly 100 people in each. Thus, Laboratory Directors had a considerable amount of independence commensurate with the responsibilities OAR gave to them, to structure the research portfolio within their Laboratories and to seek resources from external agencies. The Laboratory Directors and their senior managers tended to be competitive when it came to allocation of internal resources and in seeking customer funding; active cooperation across Laboratory organizational boundaries was rare. Thus, the distinctive research aspects of, say, the upper atmospheric chemistry studies conducted separately in the Space Physics and Optical Physics Laboratories were argued as reasons to isolate these efforts rather than pointing to the larger commonality for coordinating them. This attitude persisted long after resources began to dwindle and it would have been advantageous for the Labs to cooperate.

Laboratory program managers were so successful in obtaining funding from outside agencies that they were able to parlay customer support to stave off the two Air Force attempts to drastically curtail research after the 1974 reorganization. Unfortunately, despite these successes, the organization failed to coordinate a coherent and persuasive picture of the contribution and relevance of geophysics research to the Air Force mission and effectively communicate this to the Air Force decision makers. Numerous examples of relevance and contribution were readily available (e.g. Liebowitz, 1987). However, such arguments would have had to overcome the deeply entrenched mindset noted by Sigethy and Furtrell of the Air Force leadership that favored contracting out research and the long standing general low regard in which in-house scientists and their support staff were held. From the beginning, von Kármán questioned the quality of Air Force laboratory scientists, citing the Civil Service pay scale and the promotion and hiring system as detrimental to being able to hire and keep qualified scientists. Louis Ridenour, soon to become the first AF Chief Scientist, echoed this opinion regarding the poor quality of the AF scientist and both von Kármán and Ridenour recommended that basic research for the AF be conducted at universities rather than at in-house laboratories (e.g. Fosset, 1975).

Sigethy (1970) and Fosset (1975) note that between the 1949 Ridenour report and the mid-1970s, various study panels convened at one to two year intervals to advise the Air Force regarding the laboratory structure and mission. These panels were dominated by civilians from academic institutions (usually with a contingent from MIT) who, as Sigethy pointed out, introduced their own agenda into the panel findings. Foremost of these prejudices was that Air Force basic research should be conducted in civilian (their own) laboratories and a common ‘finding’ that was used to justify this conclusion was that the AF Labs and the scientists therein were not as capable as laboratories associated with academia. The continually cited poor quality of AF scientists and their research became a general belief within Air Force management, assuming the status of a “truism”. That this finding had no basis is evinced by the fact that the study panels rarely obtained firsthand knowledge of the quality of the research and the scientist in the Labs. The large majority of the panels and most notably the Blue Ribbon Defense Panel whose 1970 report led to the termination of basic research within the Air Force in-house labs did not trouble themselves to visit any of the Air Force Labs to assess the on-site situation. Thus, the labs and their existence were contrary to the advice and opinions of the research advisors from the academic community and, not having much experience with the technical and scientific results from the Air Force labs, the upper Air Force management uncritically accepted the study group results (Fossett, 1975).

The private sector strongly supported the business model in which the Labs were to fund the research while the universities and aerospace companies executed the effort. I was told by a

couple of high level aerospace company officials that we were violating fair trade practices when AFGL attempted to develop the Large Aperture Infrared Telescope System in the 1980s. Although this was a one-only sensor, the attitude seemed to be that we had unfair advantage as a government agency with a government funding line in pursuing a program that the aerospace industry felt rightfully should have been theirs as it involved advanced technology development that industry relied upon for a competitive edge. Conversely, the university attitude and that of the government civilian research centers such as NASA or NRC was that we had separate funding and therefore it was inappropriate for us to propose for some of the civilian programs as these funds were either internally directed or slated for universities. In either case the issue wasn't what concept could return the most science but allocation of resources.

That the negative attitude regarding Air Force Laboratory scientist and in-house research persisted for some time is implied in the 1989 study of the Air Force research organizations by the Air Force Chief Scientist, Dr. Robert Selden, who to his surprise, found that although that the Air Force Laboratories were not highly regarded within the DoD, they were much better than their reputation suggested (Day, 2000). In practical matters, Day also noted that the program managers in the Air Force product divisions looked to non-profit technical support contractors, such as the Aerospace Corp., for scientific and technical support rather than the Air Force Laboratories. Thus, the message of the quality of AFCRL research and its contributions to Air Force operations wasn't reaching the Air Force senior staff.

A consequence of this attitude was that Geophysics research has been attrited piecemeal over the years after 1974 by terminating programs, reducing the workforce, and reorganizations that reduced the authority and independence of the division chiefs. Of course, the handwriting was on the wall early on. In a rank conscious organization such as the Air Force, a Laboratory Director with a flag equivalent rank has to report to a General. Brig. Gen. Holzman commanded AFCRL from shortly after it was formed until October 1964, when he was succeeded by his vice-commander Col. Kiley. Brig. Gen. Kiley pinned on his star as he assumed command of AFCRL as did his successor, Brig. Gen. Long. After Brig. Gen. Long left in 1968, Colonels Flinders and Moran served as the AFCRL commanders the next six years, until AFCRL was organized in 1974. A Colonel may be assigned to a flag rank position but, unless he is promoted during his tenure, it was a sign that the Air Force intends to downgrade the organization. When the AFCRL Laboratories that conducted geophysics research were designated as Divisions within the Geophysics Laboratory, this *de facto* downgraded the position of Division Director. The Air Force replaced the Public Law 313 directors as they retired (or were reassigned to advisory roles) with individuals at lower rank.

The independence enjoyed by the AFCRL and AFGL leadership to set objectives and manage programs created an environment that produced innovative and high quality research, which was often judged to be world class by many outside both the Air Force and the study panels. This may have resulted in complacency that ill-served the organization. The Cambridge Field Station had been staffed by high quality engineers from Harvard's Radio Research Laboratory at and MIT's Radiation Laboratory, more from the latter than the former. Both institutions are prestigious and the people who took jobs at the Cambridge Field Station were highly regarded both by the Air Force, which is why they were recruited in the first place, and the local research community. Indeed, five of the first six Air Force Chief Scientists had worked at the MIT Radiation Lab sometime during the War (Day, 2000). Also, the fact that the Field Station workforce was able reverse the Air Force decision to move the Field Station to Rome, New York was another measure of their prestige and strong local academic ties. The ties to the

local academic community were further strengthened when Watson Lab's geophysics research moved to the Field Station. It is clear from the technical reports and Harvard monographs from the 1950s and 1960s that a revolving door existed between the geophysics research at Hanscom and Harvard University at the time. Also, several well respected German scientists, such as Heinz Fischer, the first Senior Scientist in the Optical Physics Laboratory, and Fred Voltz joined AFCRC under Project Paper Clip. Thus, AFCRC had the reputation of having top-notch people who conducted world class research, at least among the local academic community; this quality reputation was highlighted and enhanced by a series of 1959 newspaper articles by Ian Menzias, a Boston Globe reporter, on AFCRC research titled *Science City, Our Mysterious Neighbor*.

It was natural for AFCRL to proclaim the quality of its research as it was certainly at the 'cutting edge' in many fields. DeVorkin (1992) recognized Marcus O'Day's contributions to upper atmosphere research in his book and noted the key role that AFCRC scientists played in the wholesale revision of the standard atmosphere in mid-1950s that became the world-wide standard reference. Champion (1995) outlines subsequent AFCRL updates and extensions to the standard atmosphere while Doel (1996) extensively cited AFCRC contributions to geophysics and planetary sciences. Indeed the Laboratory's *Handbook of Geophysics*, the first of which was published in 1957 (Campens et al., 1957) and the third and last in 1985 (Jursa, 1985), were desktop references for many geophysicists and space scientists for over 35 years. Some of these early accomplishments by the Laboratory scientists are highlighted in the next chapter.

AFCRC also played a key role in developing the first air defense and air traffic control systems (Liebowitz, 1985; King 1959). However, there has been some revisionism in recently published accounts of this era to eliminate AFCRC's role. For example, Holbrow (2006) claims that the Air Force actively lobbied against the development of the air defense project, which required lobbying President Eisenhower by a senior MIT scientist to overcome. Johnson (2002) describes the senior Air Force staff's actions with regard to the radar early warning system (Project Lincoln) as prudent management that opposed Project Lincoln's request for emergency status that would give it priority for requisitioning scarce materials and resources. Holbrow also fails to credit the critical involvement of AFCRC with the Distant Early Warning radar system.

Although the air defense system was a joint service program, most of the support was provided by the Air Force with AFCRC responsible for its execution. John W. Marchetti, the AFCRC Technical Director and a staunch supporter of Project Lincoln not only provided AFCRC scientists to the program (up to a third of the government staff worked on the project at one time or another) but also diverted CRC funds to partially pay for the construction of Lincoln Laboratory. As a Major, Marchetti had served as the first Cambridge Field Station commander between September 1945 and September 1946. Upon leaving the service, he led the electronic research efforts at the Field Station for the next five years after which he became the Technical Director for all research at the Center.

When AFCRC abolished the Office of Technical Director in December 1953 because Mr. Marchetti spent a disproportionate amount of his time and effort advocating air defense research and development at the expense of the geophysics portfolio, he accused Air Force management of being against the air defense project and publicly and vigorously claimed that the military was interfering with decisions regarding the Center's research. Mr. Marchetti then displaced the Director of the Electronics Research Directorate, who promptly resigned. Considerable internal dissension ensued that, in short order, resulted in Marchetti's resignation. Marchetti then made numerous public allegations, especially to the national press, about how "...he was a martyr who had fought for the cause of civilian control of research at Cambridge and had been sacrificed by

a dominant military faction." (King, 1950). The press coverage eventually led to a 1954 Congressional Investigation that came to naught because, in part, a number of the AFCRC civilian scientists signed a statement that rejected Marchetti's allegations, asserting that there were no issues regarding military versus civilian control of research and that Mr. Marchetti's opinions were not representative of the scientist at the Center (King, 1959).

Unfortunately, AFCRL did itself a disservice by describing achievements with a good deal of hyperbole and taking more credit than was due at both an individual level and in corporate reviews on in-house research. Corporately, AFCRL public releases and internal management documents appear to take credit for all the research done either in-house or under contract, perhaps in an attempt to counter the 'received knowledge' regarding the poor quality of Air Force Laboratory scientists and research. Indeed, the only serious ethical complaint I heard after joining the organization was that some AFCRL contract managers and administrators required that their name be included on all contractor reports, publications and presentations under their purview even if they did nothing more than provide the contract funds. I later observed that this was, indeed, the case. While not rampant, the issue was serious enough that Dick Hendl, the Geophysics Lab. Chief Scientist (1985 – 1995), issued a directive as to who could, and should not, be listed on in-house and contractor reports.

The quasi bi-annual *AFCRL Reports on Progress* have the same tendency to hyperbole and assuming undue credit. The *AFCRL Reports on Progress* chronicled the breadth and scope of the research conducted by AFCRL and contained a treasure trove of the major and minor achievements. Unfortunately, these reports failed to separate the accomplishments of the in-house scientists from those of contractors. For example, the credit claimed in the 1963 *Report on Research* for the discovery of Galactic x-ray sources fails to mention that it was a contractual effort by Riccardo Giacconi at American Science and Engineering as described in Chapter 2. Of course, as the sponsoring agency AFCRL deserves all due credit for recognizing the value of the contracted research and for funding it but credit must be given to the scientists and their organization that actually performed the work. Similarly, the *AFCRL Reports on Progress* imply far more about AFCRL's role in establishing the Arecibo Radio Observatory and the Cerro Tololo Inter-American Observatories than what I described earlier in this chapter. This hyperbole required that I verify with independent sources the information that I extracted from these *Reports* in order to disentangle who deserved what credit and to identify the roles and responsibilities of the in-house scientists for research conducted within the laboratory, that performed under Laboratory contract and that resulting from a collaboration between the two.

Within a few years after I joined the Lab, AFCRL underwent a major reorganization following the Mansfield amendment. The period between 1972 and 1976 was uncertain and stressful on the workforce with the elimination of programs, such as optical astrophysics and the lunar and planetary research. The reorganization also produced fairly large reductions-in-force (RIFs) in 1972 and 1974. The 1974 RIF was accompanied by an Air Force announcement that the Geophysics programs would move to Kirtland AFB in November of 1974. The RIFs set off a scramble of 'bumping' as people with more years of seniority displaced newer hires in equivalent or lower grade positions or took unfilled slots, which left some AFCRL scientists stocking shelves in the base commissary. Ultimately, the Geophysics programs remained at Hanscom AFB. Rumor has it that Vice-President Nelson Rockefeller was influential in cancelling Rome Development Center's move from Rome, New York, to Hanscom. Since that move was an integral part of the overall realignment, the rationale for moving Geophysics to Kirtland was mooted. Most of the displaced scientists and technicians returned to the Lab.

Some have argued that the Mansfield Amendment was the single most significant event that led to the erosion of basic and applied research in the Air Force Labs. Indeed, AFCRL did downsize and terminate some of its programs by 1972. And even though additional programs were eliminated when the Geophysics Laboratory was formed in 1976 and the Air Force mandated that only 30% of laboratories' research funds be spent in-house, much of the short-fall was made up with outside funding. Thus, I place as a more definitive marker the downgrading of the Geophysics Laboratory to Directorate status and its concurrent designation as a remote operating location of Phillips Lab. Subordinating the Geophysics Directorate to the Phillips Lab management at Kirtland AFB in 1990 meant that decisions regarding geophysics research were made by a culture of development, test and engineering rather than scientific research. The shift to applications directed exploratory and developmental research reflected the changes in other government and industrial labs throughout the US at the time. However, putting the Hanscom research under Kirtland direction was an inefficient response as the professional culture as well as the mission objectives and environment were markedly different. In contrasting the AFRL and the AFCRL/AFGL cultures, I conclude that the independence of AFCRL/AFGL senior management, program managers, and individual scientists to set research goals and pursue external funding was most at odds with the Air Force leadership's concept of appropriate management and organizational command structure. A scientist could pursue his/her own research under AFCRL/AFGL, as long as he/she could persuade the AFCRL management or external sponsors to fund it. Little more than verbal coordination was needed with the Laboratory chain of command as to who was to be approached for outside funds. Indeed, a measure of one's performance within the organization at the time was how successful one was in obtaining outside funding, especially when the in-house funding began to decrease. The only restriction on the research was that its relevance to the military mission had to be shown and that it was not open ended, that is, products were produced on a reasonable schedule and that the effort would terminate when the final milestone was met.

Now, policy making and setting research objectives within AFRL are hierarchical with firm guidelines as to what research an individual scientist can pursue. The Directorate has six technical areas that encompass its mission and research programs have to address needs specified in one or more of the technical areas plans that define how the mission in a specific area is to be achieved. If a given research effort is not in the plans and the technical area leads do not alter the plans to include it, the Directorate policy is to terminate the research even if it is entirely customer funded, forcing some scientists in the Directorate to decline customer funding.

However, more value could have been had if management had made more of an effort to adapt the talents of the Hanscom people to fit the new direction. Under the evolutionary pressure to meet new Air Force objectives, some of the Hanscom people retired, most of those that remained adapted surprisingly well by structuring their programs to do good science while meeting the engineering oriented objectives, and a minority hunkered down until retirement.

An unstated condition for the Space Surveillance CoE Branch Chief was that the position had to be filled at Kirtland AFB and, as I was unwilling to move to Albuquerque, my position in the organization was undefined when the CoE was formed. Consequently, Col. Laura Kennedy, the Hanscom Division Chief, offered me a position in the front office and I accepted. Thus, freed of the administrative burdens of being a Branch Chief, I was able to complete the scientific analysis for many of projects that had been previously deferred owing to lack of time. Therefore, I was able to oversee the completion of the MSX data processing and analysis and publication of the astronomy results. We also took over the calibration effort begun by Martin Cohen.

2. INFRARED ASTRONOMY: THE EARLY DAYS

In *Countdown to the Invisible Universe*, Public Broadcasting's *Nova* Program on the Infrared Astronomical Satellite (IRAS) originally broadcast on 20 January 1987, Tom Chester condensed the history of infrared astronomy into the single (paraphrased) sentence: ... the two most significant events in infrared astronomy were Frank Low's invention of the infrared germanium bolometer (Low, 1961) and the Infrared Astronomical Satellite Dave Allen (1977) had a similar opinion about Frank Low's contribution, stating that "... *if I were asked to name the man who has done the most for infrared astronomy it would still be Frank Low...*" Low gave astronomers a sensitive but delicate device, a liquid helium cooled infrared bolometer, which detects the increase in temperature imparted by an absorbed photon. The blackened Low bolometer responds almost equally to radiation of all wavelengths, although it was used mostly for observations in the mid-infrared to the submillimeter. The doped germanium mid-infrared photoconductors preferred by some astronomers at the time and the Department of Defense exhibited large response variations that depended on where the star was on the surface of the detector and subtle non-linearities that compromised the precision of the early astronomical measurements. Although Low's bolometer had a much more uniform response, it was too slow and mechanically too delicate for space applications. Consequently, photodetectors have been universally used in space-based sensors. Additionally, Low was one of the first to optimize the telescope design and measurement techniques for mid-infrared ground-based observations to effectively cancel the huge thermal signal from the telescope and atmosphere in order to detect the very faint energy from the star. Low, Rieke and Gehrz (2007) provide a first person account of the contributions that Frank Low and his bolometer made to infrared astronomy in the 1960s and 1970s. While Frank Low deserves credit for his preeminent pioneering efforts in the field, he is but one of many who made meaningful contributions to infrared astronomy in the 1960s.

The Low bolometer and IRAS were preceded by over one and a half centuries of infrared detector development and applications to astronomy. Infrared astronomical histories usually begin with Sir William Herschel's 1800 discovery that a thermometer bulb registered a temperature rise when placed beyond the red end of the dispersed solar spectrum (Herschel, 1800a, b); Barr (1960) briefly noted that others had conducted analogous experiments during the previous 25 years but Herschel meticulously quantified his observations. Piazzi Smith (1858) is generally credited for the next astronomical achievement when he was just able to detect infrared radiation from the Moon in 1856. However, Macedonio Melloni actually was the first to measure heat from the Moon with a one meter diameter lens and a 'sensitive thermomultiplier'. Melloni's 1846 experiment was conducted within the context of his investigations into the nature of light and heat. In his last two papers Herschel (1800c, d) felt that he had compelling experimental evidence that light and heat rays were different and separable. Another component, chemically active rays, was discovered beyond the violet end of the spectrum about the same time as Herschel's investigations. Barr (1960) and Chang and Leonelli (2005a, b) explore the scientific debate that took place during the first half of the 19th century regarding the nature of light, heat and chemical rays: namely were infrared, visible and ultraviolet radiation a unified, continuous phenomenon or were they pluralistic, being composed of three distinct and parallel entities, illumination, radiant heat and chemical rays, respectively. Although some of the properties overlapped: chemical rays caused strong chemical changes in substances, such as silver iodide, chemical activity induced by illumination rays was weaker and of a different 'quality'. Originally of the pluralistic view, Melloni began a series of experiments around 1830

that led him to conclude that light and heat rays were different aspects of the same phenomenon. His observations removed the underpinning of the pluralistic theory; namely it was then ‘common knowledge’ that the Moon, unlike the Sun, radiated ‘cold light’ with no heat and therefore the illumination in the reflected sunlight from the Moon and heat had to have different qualities (Chang and Leonelli, 2005a). Thus, Melloni’s lunar observation was key to disproving the long standing convention that the Moon did not radiate heat.

Although John Tyndall, Edward James Stone and William Huggins made lunar thermal measurements during the 1860s (Becker, 1993; Brashear, 1991), Lord Rosse was the first to systematically study the radiant heat from the Moon. Rosse (1869, 1870, and 1873) quantitatively analyzed the disk integrated lunar thermal properties, observing the infrared emission through a lunation and during an eclipse. Sinton (1962a, 1986) described the pains that Rosse took in making his observations as accurate as possible. Rosse isolated the thermal emission by observing the Moon with and without a glass filter in the beam. All the radiation from the Moon gathered by his reflecting telescope impinged on the detector without the glass filter, while only the visible to near-infrared ($\lambda < \sim 2.5 \mu\text{m}$) sunlight reflected by the Moon got through the filter; the difference between the two was the thermal emission from the Moon. Rosse also presaged ‘sky chopping’ that was to become a standard infrared observing technique a century later. He found that the instability of his initial lunar measurements seemed to be correlated with the changing temperatures of the telescope and air. Consequently, he placed two identical thermopiles in the focal plane, one viewed the Moon while the other looked at the sky next to the Moon, and the signals negatively combined to cancel the emission common to the beams. Later, Boys (1890) used sky differencing to measure the thermal profile of the Moon at various stages with and without a water cell as the Moon transited across his detector.

The stellar observations obtained by Huggins (1869) and Stone (1870a, b) were described in qualitative terms: Arcturus radiated half again as much heat as Vega or equal to a candle at a distance of 10 feet, for example. Sensitivities were similarly expressed: Melloni’s thermopile could detect a man at 30’ while, circa 1901, Langley and Abbott’s improved bolometer could see a cow at a quarter of a mile (Hudson, 1969). Stone adopted a sky differencing procedure similar to Lord Rosse’s to improve detectability after he, Stone (1870a), noted that the amount of stellar heat he detected varied inversely with the humidity. Boys (1890) later tried but failed to detect several of the bright stars that had been observed by Higgins and Stone and concluded that these previous results were spurious. Boys (1895) is perhaps better known for measuring the gravitational constant to an accuracy that was not excelled for half a century.

Of particular interest was Thomas Edison’s foray into infrared astronomy. Edison had invented the ‘tasimeter’, a sensitive heat detection device, in the late 1870s, which partly satisfied Samuel Langley’s request to him for a more sensitive device than the bolometers then in use at the Allegheny Observatory. Edison accepted Henry Draper’s invitation to demonstrate the tasimeter by measuring the heat of the solar corona during the field expedition to Rawlings, Wyoming that Draper was organizing to observe the 29 July 1878 solar total eclipse. Three nights before the eclipse, Edison checked his equipment by observing Arcturus at about the same zenith angle as projected for the eclipsed Sun. Reportedly, Edison obtained five uniform deflections on the star compared to a zero response to a dark slide (Eddy, 1972). However, Edison’s eclipse measurements were plagued by difficulties and his report (Edison, 1878), which Draper read at the August 1878 *American Association for the Advancement of Science* meeting, described the instrument and measurement techniques at length but gave only a qualitative assessment of the results. In fact, Eddy (1972) noted that Edison never reduced his data being of

the opinion that the tasimeter was too sensitive to have produced good results. From published anecdotal information, Edison was purported to have estimated that the coronal heat was 15 times greater than that from Arcturus from which Eddy, by comparing the known fluxes from Arcturus and the corona, concluded that Edison had, indeed measured the corona. The press widely hailed Edison for his historical achievement although the astronomical community was aware that Luigi Magrini had observed heat from the solar corona 36 years earlier, during the 7 July 1842 total solar eclipse (Eddy, 1972). Enthused over the performance of his tasimeter at the eclipse expedition, Edison proposed in a *Scientific American* (1878) current events article to put it on a large telescope to explore blank areas of the sky. The purpose of this first ever proposed infrared sky survey was to detect unseen and unseeable stars by their invisible heat radiation. The specific objectives Edison offered were to observe stars with small visible brightness, sources too far away to be detected by ordinary means with a telescope and, since Edison believed that his tasimeter was more sensitive than photography, burnt out suns and dim planets.

Langley was one of the several astronomers who asked Edison for a tasimeter as it appeared to be about two orders of magnitude more sensitive than the devices that he was using in 1880. Despite numerous correspondences between the two, Edison never did comply with Langley's request, likely because the tasimeter proved to be unmanageable as an astronomical research tool. No less a personage than Lord Rosse experimented with it for several hours in October, 1878, commenting that the response was slow and a bit uncertain and that Edison's agent should return when the problems were worked out (Eddy, 1972). Therefore, Langley developed his own bolometer (Barr, 1963), borrowing some of the design concepts from Edison for his initial instrument (Brashear, 1990). Using this bolometer and subsequent improvements, he embarked on an extensive study of the Sun at the Allegheny Observatory. He obtained the first infrared grating spectrum of the Sun out to 5.3 μm and measured the positions of 750 spectral lines. Langley also had an abiding interest in determining the total energy received at the Earth from the Sun, the solar constant, and the constancy thereof. Such was Langley stature and his well deserved reputation for meticulous observing technique and data reduction that his estimate for the solar constant variation (Langley, 1904), as refined by Abbott (1930) – his associate at the Smithsonian Institution, held sway in scientific circles for 40 years. It is Langley's solar constant variation that is referenced by Doel (1996) and cited in Chapter 1. In order to derive the Solar constant, Langley and Very (1889) carefully charted the Earth's infrared atmospheric transmission, which led to their discovery of the 8 – 14 μm atmospheric window and, as a by-product, improved values for the temperature of the Moon (Sinton, 1986). Parenthetically, Langley was the first to fly an unmanned heavier than air craft and was conducting manned trials when word came from Kitty Hawk of the Wright brothers' success.

Nichols (1901) assessed the 19th century infrared stellar observations based on his August 1898 and 1900 comparative radiometric brightness measurements of Vega, Arcturus, Jupiter and Saturn using a more sensitive radiometer. Given his results and the sensitivity of his apparatus and observing procedures, Nichols concluded that the instruments used by Higgins, Stone and Boys were not sensitive enough to have detected heat from these stars. He also questioned Edison's Arcturus measurement, concluding that Edison would have needed a thousand times better sensitivity than Eddy ascribes to the tasimeter to get the purported result. Quantitatively, Eddy (1972) had estimated that the heat detectors in the late 1870s could sense a change of about 10^{-4} °F while Edison's tasimeter could measure temperature changes as small as 10^{-6} °F; this is contrasted to the 10^{-2} °F sensitivity that he estimated for Herschel's measurements and $\sim 10^{-3}$ °F for Melloni's experiments.

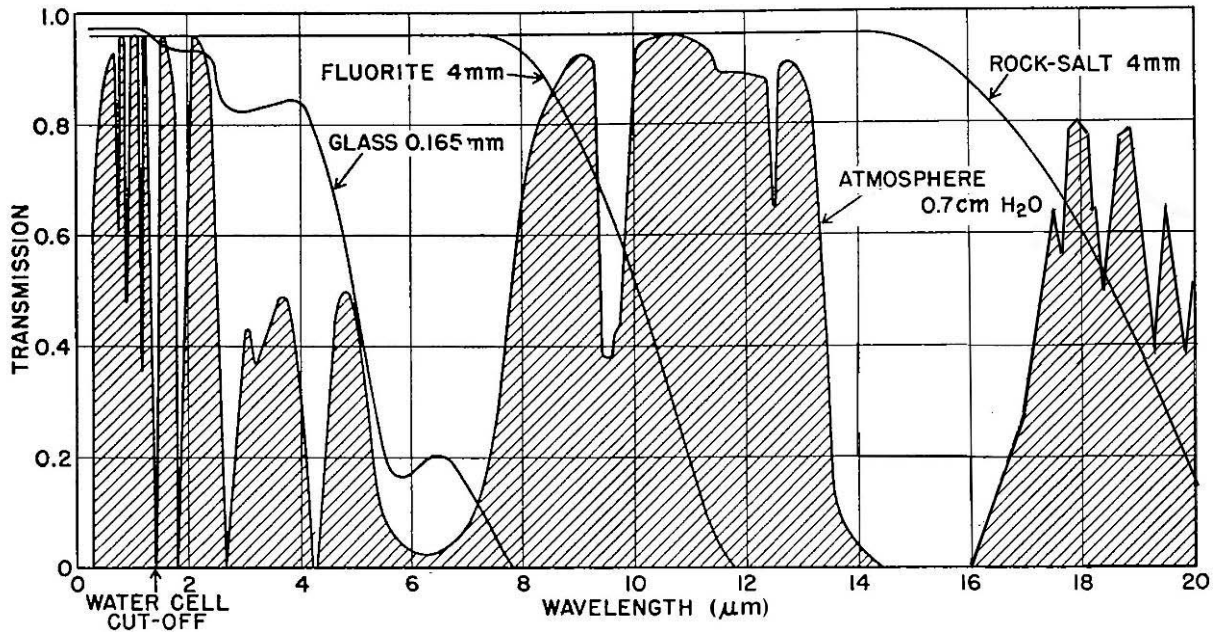


Figure 6. Transmission characteristics of the atmosphere and filters used in the early radiometric subtractive filtering. Shown are the water cell and glass filter as well the spectral transmissions of fluorite and rock-salt prisms used in spectral studies. This Figure is adapted from Pettit and Nicholson (1955) and modified by adding the 20 μm atmospheric window.

There is an ambiguity regarding the early radiant heat measurements; Barr (1960) noted that the word ‘infrared’ wasn’t coined until about 1880. Experiments that used glass prisms (Herschel), glass lenses (Melloni) or refractive telescopes (Edison) filtered out wavelengths longer than about 3 μm . Thus, the heat detected lies in the near-infrared. Water or glass cells used with reflective telescopes isolate wavelengths longer than about 1.4 and 3 μm , respectively; Figure 6 nicely illustrates this spectral division as well as the infrared spectral transmission of the atmosphere to 20 μm . Because the stellar spectral energy distributions steeply decline with wavelength, roughly half the radiant power for stars like the Sun lies at visible wavelengths and half between 0.75 to \sim 3 μm in the near-infrared, subtractive water or glass cell heat indices on stars were dominated by near-infrared radiation just beyond the spectral cutoff of the cell. On the other hand, analogous measurements on planets and the Moon with reflective telescopes, such as used by Rosse, isolated the longer mid-infrared wavelengths where the energy distributions from these bodies peak.

Coblentz (1915) obtained the broad band radiometry on 110 stars, then followed this study with more discriminating observations (Coblentz, 1922) to determine the energy distributions and estimated temperatures of stars as a function of spectral type by isolating broad spectral regions between the ultraviolet and 10 μm with subtractive filter measurements using yellow, red and clear glass filters as well as 1 cm thick cells of water, quartz and calcium fluoride (labeled fluorite in Figure 6). He determined that the energy distribution of red stars could be characterized by a blackbody equivalent temperature of about 3000K while that for blue stars was 10000K. Since the early detectors were exposed to the open air and subject to the vagaries of air currents, the sensitivity and reliability of the thermocouples in the 1920s were significantly improved by enclosing them in a vacuum cell (Brashear, 1992). Abbott (1929) thus measured the spectral energy distribution of 16 stars that spanned spectral types from B to M at nine

wavelengths between 0.44 and 2.2 μm with a Nichols radiometer and a well calibrated prism. He found, as expected, that the energy distribution of the hotter stars peaked in the blue and the peak shifted to the red for the later, cooler spectral types.

Pettit and Nicholson became the most prolific of the early infrared observers: measuring infrared radiation from stars, the Moon and the bright planets with a vacuum thermocouple on the Mt. Wilson Observatory telescopes. These studies included determining the heat indices of 124 stars and correlating the results with spectral type (Pettit and Nicholson, 1928). They found that their measured heat index and bolometric correction for stars were well correlated with temperature in the sense that cooler stars have a larger heat index and absolute bolometric magnitude. Kuiper (1938) used these observations to determine stellar bolometric corrections; the factor that converts the visual flux into the total flux from a star. Pettit and Nicholson (1933) also observed variable stars over their pulsation periods while Pettit (1961) summarized the thermocouple measurements that he and Nicholson made on the planets.

In 1927, Pettit and Nicholson (1927) conducted an infrared survey of sorts. They measured the heat index of nine optically faint red stars, which included a photographic search for cool stars, selected by Merrill and Humason (1927). They found nothing unusual except for a faint star near the Trifid nebula, which had a large heat index typical of long-period variable stars. Rust (1938) more or less repeated this experiment a decade later, obtaining spectral types for 23 stars that were found to have large photographic infrared indices and making radiometric measurements on three of the reddest objects. He found that these very red stars all had late spectral types and that there were no new types of objects with ‘excessively’ low temperature.

Emberson (1941) published the results of the Harvard College Observatory radiometric measurements program that began in the late 1930s. He found that the Harvard vacuum thermocouple magnitudes for his 82 stars differed systematically from those of Pettit and Nicholson with the Harvard radiometric magnitudes being fainter for the warmer stars while the cooler stars were brighter, likely reflective of the difference in transmission between the rock salt window used by Pettit and Nicholson and the fluoride window in the Harvard apparatus.

Infrared astronomy had progressed rather slowly during the century and a half after Herschel’s investigations owing to the limited capabilities of the bolometers or thermocouples in use. Thermocouples detected the changes in voltage across a bi-metallic junction when heated upon exposure to radiation while thermopiles are simply thermocouples connected in series for increased sensitivity. A bolometer, on the other hand, changes resistance when heated. Barr (1960) provides an excellent summary of the 19th century infrared detection devices and observing procedures that is complemented by the review of Arnquist (1959) while Allen (1975) describes their astronomical applications. The next major advance was the marked improvement in the performance of photodetectors. The photoconductive response of selenium had been discovered in 1873 (Lovell, 1968, 1969) and a few astronomers (e.g. Pfund, 1904; Stebbins, 1908) explored the material characteristics since the response of selenium extends into the very near infrared ($\sim 0.8 \mu\text{m}$). However, Minchin (1895) was the first to attempt to use a selenium cell to measure stars, with spurious results according to Nichols (1901). Selenium cells proved to be unreliable and other materials were sought. Case (1917) found that, among the numerous natural crystals he examined, Thallous Sulfide exhibited a photoconductive response ($\lambda < 1.3 \mu\text{m}$). Robert Cashman improved the manufacture of these cells in the 1930s (Lovell, 1971).

Because of the limited infrared response of selenium and Thallous Sulfide cells, infrared experimenters used thermopiles and bolometer for the next several decades (e.g. Pfund, 1916). It wasn’t until the late 1940s when astronomers gained access to lead sulphide (PbS) and lead salt

photodetectors that were at least 100 times more sensitive in the $1 - 5 \mu\text{m}$ region than previous devices (Sinton, 1986), that modern infrared astronomy began. Lovell (1968, 1969) traces the origin of the modern lead salt detectors from the early 1930s when Edgar Kutzscher in Germany, began his research on the devices. Kutzscher's team at the German Electroacoustic Company had improved lead sulfide detectors during the Second World War that were used to detect and track aircraft in the near-infrared. These facilities were captured by the Russians and provided the basis for the early detector development in the Soviet Union. Robert J. Cashman, at Northwestern University, turned his research from Thallous Sulfide to lead sulfide detectors in 1944 in support of the War effort. Because of the military application of this research, Cashman was unaware of Kutzscher's work until after the War when he was asked to evaluate one of the cells produced by Zeiss/Ikon.

A photoconductor relies on the inherent direct response to light of the material rather than indirectly sensing the thermal input from the observed photons. The electrons in a photoconductor are bound to the atoms in the in energy levels called the valence band. A conduction band lies at higher energy in which the electrons can move freely and there is an energy or band gap between the two. If an electron in the valence band absorbs a photon with energy greater than the band gap, it 'jumps' to the conduction band where it can be swept out and detected by applying a voltage across the detector. Since the photon energy is proportional to the inverse of its wavelength, the detector responds to wavelengths shorter than that equivalent to the band gap energy. The intrinsic response is defined by the intrinsic band-gap of the material, which is generally comparatively large, limiting the response to shorter wavelengths; intrinsic silicon responds to wavelengths less than $\sim 1.1 \mu\text{m}$, for example. The wavelength of the response may be increased by doping the material with appropriate impurities, which adds energy states in the band gap. Such *extrinsic* detectors are designated by the chemical symbol for basic material, a colon then that of the impurity, Ge:Hg or Si:As for example. Upon absorbing a photon, a valence electron may jump to an impurity state or conduction band, creating a 'hole' in the valence band, or one in an impurity state may transition to the conduction band; both holes and valence band electrons are swept out by the electric field. Hudson (1969) and Rieke (2007) provide excellent discussions on the workings of such detectors.

Gerard Kuiper found out about sensitive lead sulfide detectors in the fall of 1945 through interviews he conducted with German scientists as part of the US post-war assessment of the German technology. He also discovered that Cashman had led the American effort to make similar detectors. Believing that he had access to a capability unknown to other astronomers at the time (Doel, 1992), Kuiper teamed with Cashman to build an infrared spectrometer that responded to $\sim 5 \mu\text{m}$ with which he and his colleagues (e.g. Kuiper, Wilson and Cashman, 1947) used to obtain infrared spectra of stars and planets; Kuiper (1964) summarized the results from this 15 year long Lunar and Planetary Observatory program. Whitford (1948a, 1958), Washburn Observatory, also made early use of a Cashman lead-sulphide photocell to extend the interstellar extinction curve to $2.2 \mu\text{m}$. Other concurrent programs included Fellgett's (1951) observations on 51 stars in the near-infrared from which he derived visual – near-infrared color indices by differencing the stellar flux measured with and without a mica window in the beam. His results compared favorably with the earlier water absorption cell indices of Pettit and Nicholson. In France, a program was started in the early 1950s at the Haute Provence Observatory (Neant and Bigay, 1952) to measure the near-infrared color index of stars that culminated with the summary publication by Lunel (1960), which lists observations that are among the first to isolate the $2 - 2.4 \mu\text{m}$ spectral region with a spectral interference filter.

The pace of infrared observations picked up in the 1960s as detector development extended the accessible wavelengths to the mid-infrared. A note on nomenclature at this point. The various infrared wavelength regimes are determined by the phenomenology being measured and the type of (photo-) detector used for the measurement. Astronomical near-infrared (near-IR) traditionally has been taken to lie between 1.1 and 5.6 μm ; the short wavelength limit is nominally set by the 1.1 μm response cutoff of visible intrinsic silicon detectors and infrared photographic emulsions (the photographic infrared lies between 0.75 and 1.1 μm) while the long wavelength is set by the sensible cutoff of InSb arrays. The astronomical mid-infrared spans the wavelength range from about 6 to 35 μm and is the domain of extrinsic (blocked impurity band – BIB, also known as impurity band conduction – IBC) silicon photoconductors. Si:As BIBs are readily available and the most widely used for mid-infrared observations as the technology is mature and the detectors exhibit excellent response to $\sim 25 \mu\text{m}$; Si:Sb BIBs respond to 35 μm . The DoD has a different labeling system. Traditionally, the Short Wavelength Infrared (SWIR) lies between 1.1 to about 4 μm , while the Long Wavelength Infrared (LWIR) spans 6 to 35 μm . Between and overlapping the SWIR and LWIR are the mid-wave infrared (MWIR) and the mid-long wave infrared (MLWIR), the spectral limits of which are defined to suit the users' needs. Here, we use the SWIR and LWIR as defined and assume that MWIR lies between. We also ignore the sub-division of the longer LWIR wavelengths into long-long wave infrared (LLWIR) and very long wave infrared (VLWIR), as the boundaries of these relatively recent designations are arbitrary. Ge:Ga detectors are used for the far-infrared between 35 μm and 200 μm ; the response at wavelengths greater than the nominal 120 μm spectral cutoff of this material is achieved by putting mechanical stress on the detectors. The submillimeter is defined to be from about 100 – 200 μm to 1000 μm (1 mm) and bolometers are most commonly used in this regime. Standard astronomical infrared bands are tailored to match the atmospheric window regions centered at 1.2, 1.6, 2.2, 3.5, 4.8, 10 and 20 μm , the cross-hatched areas in Figure 6. The widely used Johnson (1966) photometric system labels these bands J, H, K, L, M, N and Q, respectively.

2.1. Space Surveillance: Impetus to Infrared Stellar Astronomy

Martin Harwit (1981, 2001, 2003) has commented on the prominent role of the military in developing the technology that has been and is being used for infrared astronomy. While Harwit mainly emphasizes the military contributions in monolithic mid-infrared detectors, focal plane arrays and cryogenic technology for space sensors that were transitioned to the infrared astronomical community, he also notes some of the in-house achievements of the military labs such as the mid-1960s pioneering space-based far-infrared astronomy experiments conducted by the Naval Research Laboratory and the first spaced-based infrared survey by AFCRL. Harwit (2001) quantitatively estimated that, between 1985 and 1992, the US military spent about twice as much on infrared space technology as did all the civilian scientific agencies over the entire world for all time. He then contrasted this with the less mature far-infrared and submillimeter technology in which the military has little interest and, consequently, the burden of technical development is borne by civilian agencies.

The early military interest in the infrared arose from the post World War II concerns regarding aircraft detection and ballistic missile defense. With the dawn of the space age, the space surveillance requirement included detecting a satellite against the celestial background. Little was known about the thermal properties of missiles or satellites in space at this time and even less about the stellar background against which these objects would be viewed. Figure 7 shows how the infrared signature of a missile changes during the trajectory.

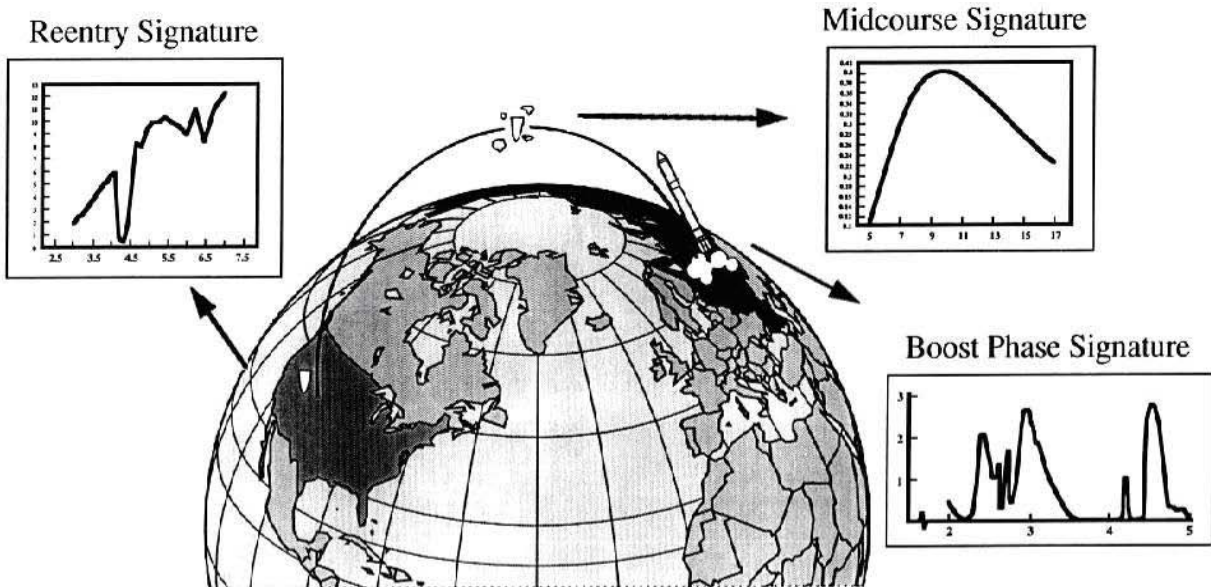


Figure 7. The time variable infrared signature from a notional intercontinental ballistic missile. During boost phase, the molecular bands in the exhaust are prominent; the midcourse phase is dominated by the cool passive emission from the object(s) while the heating upon reentry produces a very bright infrared signature (adapted from Jamieson, 1995).

Ballistic missile defense became an Army and Air Force requirement in 1946 to counter threats such as the V-2. Although the V-2 was a short range missile, Germany had plans to bring the war to the US, first from V-2's towed behind submarines in hermetically sealed containers, then with the A9/A10. This early intercontinental missile concept would have launched the A9 manned, winged glider atop the A10 rocket from Portugal in order to reach the US. The value of infrared for target detection was recognized early to counter the threat. According to Lovell (1968), Lawrence (Lou) Meuser, at the Air Force Avionics Lab in Dayton, Ohio, demonstrated infrared aircraft detection in 1951 using captured German PbS technology and parts that were assembled by Heinz Fischer in 1947. By 1948, a PbS detector was being tested in the guidance unit of the Dove air-to-air missile and not long afterward, the China Lake Naval Lab began developing the Sidewinder missile around an infrared detection system (Westrum, 1999). Max Nagel (Jamieson; 1995) traced the first application of infrared technology to ballistic missile defense to 1956, a reference to the April 1956 study by the Air Force Scientific Advisory Board and the Rand Corp. of the possibility of an infrared detection and early warning missile defense system from aircraft (Day, 2000). As shown in Figure 7, the missile payload gets very hot as re-enters the atmosphere, emitting copious amounts of infrared radiation.

The first successful Soviet intercontinental ballistic missile test in the fall of 1957 heightened the urgency for information in support of ballistic missile defense. Thus, AFCRC, among others, conducted a number of late 1950s experiments to measure the infrared emissions from the exhaust of rocket plumes. The signatures of several large rockets were observed with spectrometers and radiometers that were mounted on the missile itself and in cylinders that were released to fall through the plume. Optical and infrared sensors were also placed on re-entry vehicles to measure the thermal emission from the re-entry heating. The AFCRL Lunar and Planetary Branch looked into the inverse problem of how to mix the components of solid rocket fuel for pyrotechnic reentry decoys that would have desired spectral characteristics. This was

remote sensing in reverse: spoofing detection by generating spectral signatures instead of measuring and interpreting them.

The launch of Sputnik in October 1957 extended the need for defensive surveillance to satellites. Actually, observing Earth orbiting satellites, space surveillance in the military parlance, began somewhat before Sputnik when the Smithsonian Astrophysical Observatory fielded twelve 10" f/1 Baker-Nunn Schmidt tracking cameras (Whipple and Hynek, 1956) to track satellites (Campbell and Hynek, 1957, Hynek, Henize and Whipple, 1959). The Baker-Nunn system was later expanded into the Moonwatch program (Bakos and Campbell, 1960) that had, at its peak, ~150 volunteer teams of satellite observers around the world. The Baker-Nunn cameras continuously monitored the apparent positions of the satellites in order to derive orbits, although the rather crude photometry did allow a reasonable estimate of size and tumble rates. The Moonwatch program endured into the early 1970s (Cornell, 1975).

AFCRC's Project Harvest Moon (Champion, 1995) combined the Baker-Nunn camera measurements with radar observations to calculate accurate satellite orbits. The geophysics interest was to use the satellite drag derived from the time rate of change of the orbital elements to deduce the density of the highest layers of the atmosphere. Thus, there was a premium on the accuracy of orbit determination. As the number of satellites rapidly grew, Project Harvest Moon became an operational system: Project Space Track, created by ARPA as a joint Army-Navy-Air Force effort within the National Surveillance Control Center. Project Space Track was transferred, in due course, to Cheyenne Mountain, CO.

The US established its presence in space a few months after Sputnik with the Army's launch of Explorer I on 1 January 1958. A month later, the Department of Defense established the Advanced Research Projects Agency (ARPA) on 1 February 1958 with the charter to fund high risk/high payoff technology development and shortly thereafter, ARPA created Project Defender to conduct missile defense related research. It soon became apparent that detecting and tracking faint satellites against the background of stars might be problematic. There are roughly a quarter of a million stars brighter than 8.5 visible magnitude, which is about 10 times fainter than what the human eye can see, and the large majority of these stars are closely packed along the Galactic plane. ARPA, under Project Defender, funded much of the early research into how to detect, identify and track a faint target against such a background. As described in Eastman-Kodak monthly progress reports and various trip reports that Phil Barnhart very kindly made available, the Eastman-Kodak/Ohio State program provides an example of how an effort that originally was directed toward developing routines to detect a satellite against the visible stellar background evolved into pioneering research in infrared astronomy.

The Redstone Arsenal in Huntsville, Alabama contracted with Eastman-Kodak in the fall of 1959 to evaluate the magnitude of the stellar interference in detecting satellites and to develop solutions. Initially, moving target identification was favored in which the motion of the satellite is used to distinguish it from the fixed stars. To examine the added value of spectral discrimination for target identification, the spectral energy distributions for several stars were estimated by assuming that the stars radiated like a blackbody with temperatures equal to their effective temperatures, T_{eff} , which were defined by the spectral types of the stars. So, three pieces of astronomical information were needed to predict stellar brightness at any wavelength: the spectral type of the star, the relationship between the effective temperatures and spectral type and the brightness of the star at the standard visual wavelength. Eastman-Kodak thus calculated the visual to 3 μm flux in four spectral bands for the 20 brightest stars; similar calculations had been done independently by others (e.g. Larmour, 1952; Ramsey, 1961). Although simplistic,

these assumptions were consistent with the stellar infrared radiometric data obtained during the previous half century. However, to further the effort, Eastman-Kodak proposed to enlist academic support for the astronomy and William Haynie, the Eastman-Kodak lead investigator, contacted Allen J. Hynek at the Smithsonian Astrophysical Observatory in this regard because of Hynek's surveillance experience. Smithsonian couldn't commit to the effort and Hynek suggested contacting astronomers at either the Ohio State or Indiana University for astronomical background material; Ohio State accepted.

Because radars were range limited by their physical horizon and nuclear effects in the 1960s, the proposed radar-based defensive systems had to intercept reentry vehicles as they reentered the atmosphere after the decoys were stripped off (Jamieson, 1995). Therefore, the Eastman-Kodak effort became part of a larger anti-missile defense study being conducted for the Redstone Arsenal under which Hughes Aircraft Co. and North American Aviation's Autonetics Division in Southern California were funded to look at infrared decoy discrimination prior to reentry. Infrared offers an advantage over the visible in discriminating a target from background sources, if only that advantage could be realized. A (sub)orbital object absorbs solar energy and upwelling heat from the Earth and warms to temperatures comparable to that of the Earth. The object subsequently radiates away the absorbed energy in the infrared, as does the Earth. The result is that, in terms of radiated *vs.* reflected power, the thermal flux from an orbiting satellite is about as bright as the reflected sunlight. The infrared emission of ordinary stars, on the other hand, is about 10,000 times dimmer than the visible radiation, which means that the confusion in detecting a satellite against the infrared stellar background is correspondingly reduced. Redstone directed Eastman-Kodak to place more emphasis on the mid-infrared, which they initially did by extrapolating the spectra for the 20 brightest stars to the 8 – 13 μm region.

The questions that then needed to be addressed were: were the blackbody extrapolations adequate? If not, what were the infrared spectral characteristics of the known stars? Analogously; were the infrared measurements of the satellites commensurate with predictions? Finally, did the infrared sky hold surprises? In other words, were there populations of bright infrared sources that we didn't know about that were numerous enough to compromise the infrared advantage for satellite detection? The Pettit and Nicholson (1927) and Rust (1938) studies had indicated that there were no new classes of very low temperatures objects, but these investigations were small and quite limited.

To address the first question, Eastman-Kodak requested that Walt Mitchell and Phil Barnhart, an OSU professor and research associate, respectively, analyze the published infrared data. Plans were also laid for a 2.0 – 2.4 μm (X) and 3.3 – 4.2 μm (Y) measurement program using a newly constructed radiometer with cooled PbS and plumbide detectors at the OSU Perkins 69" telescope. These detectors were 'home-grown' for, as Lovell (1968) noted, Eastman-Kodak was a major manufacturer of lead salt detectors in the 1960s. The initial stellar observations were made in the summer of 1960 and, by October, OSU had obtained X band radiometry on 16 stars that revealed that the coolest stars exhibited small near-infrared flux excesses over blackbody predictions. The excesses were confirmed in the summer of 1961 with measurements on an additional 50 stars obtained on the Mt Wilson 60" and 100" telescopes (Barnhart and Haynie, 1964). Concurrently and independently, Freeman Hall (1961) used a 20" instrument to measure the 1 – 3 μm magnitudes for 40 of the reddest or brightest visible stars and planets. The flux scale of his observations was tied to a 500K blackbody at the telescope, thus becoming the first direct infrared stellar calibration. Hall also found that cool stars had somewhat more near-infrared emission than predicted from visible observations.

Harold Johnson at the University of Arizona was doing photometry at 2.2 μm (K) and 3.5 μm (L), respectively equivalent to the OSU X and Y, concurrently in the early 1960s. Johnson (1962) published his initial results on 52 stars and, in short order, extended the photometry for 16 of these stars to 5 μm (Johnson and Mitchell, 1963). These observations were a natural extension of Johnson's visible photometric studies that began in the 1950s at the Lowell Observatory. Under AFCRC sponsorship, Johnson had designed and built a visible photoelectric photometer with which to monitor the sunlight reflected by Uranus and Neptune in an attempt to measure the variability in the solar constant (Sinton, Johnson and Iriarte, 1959) and to study weather patterns on Mars and Jupiter as analogs for the Earth for developing predictive capabilities for Earth's weather (Doel, 1996, Jerzykiewicz and Serkowski, 1967). Also under this AFCRL *Study of Planetary Atmospheres* contract to the Lowell Observatory, Gifford (1956) reduced 15 years (1926 – 1941) of Lampland's unpublished thermocouple measurements on Mars at opposition and derived Martian surface profiles of the seasonal temperature distribution.

As informative as these measurements were, they said little about the 10 μm radiation, where the passive emission from a satellite in Earth orbit was expected to peak. Therefore, Eastman-Kodak constructed a photometer to accommodate a Ge:Cd detector in a liquid helium dewar for 7.5 – 13 μm measurements (Z band). And so began, as Barnhart and Mitchell (1966) described, a frustrating three years of trying to obtain measurements at this wavelength. The system was tried out during the summer of 1961 observing run at Mt. Wilson. After solving the initial mechanical problems of the detector leads breaking due to cold working as the dewar was cycled from room temperature to that of liquid helium and back again, the biggest difficulty became the very large spurious signal from the telescope and atmosphere. This signal arose from the manner in which the photometer modulated the background in an attempt to remove it. Consequently, the infrared observational program at Ohio State terminated in 1964 having obtained excellent data in the near-infrared X and Y bands but, unfortunately, poor 10 μm results. After writing a summary report on the observations as well as extrapolative modeling that could be used to predict the infrared brightness of an object (Barnhart and Mitchell, 1966), both Phil Barnhart and Walt Mitchell returned to their primary research interest of solar physics.

Although Sinton and Strong had obtained good quality 10 μm radiometry and spectra of Mars with a pneumatic Golay cell on the 200" Hale telescope in 1954 (Sinton and Strong, 1960a) and analogous observations of Venus during 1952 – 1954 (Sinton and Strong, 1960b), the cell wasn't sensitive enough to measure the fainter stars. The Eastman-Kodak/Ohio State attempts at 10 μm stellar photometry failed but Wildey and Murray (1964), at Caltech, had better success using the OSU chopping scheme, reporting 10 μm fluxes and visual to infrared color indices for 25 stars that spanned a large effective temperature range. In the same *Astrophysical Journal* issue, Low and Johnson (1964) listed 10 μm photometry on 15 stars and inter-compared their results with the stars in common with Wildey and Murray. In the Soviet Union, V.I. Moroz (1964, 1965a, b) led an early 1960s effort that produced moderate resolution ($\lambda/\Delta\lambda \sim 500$) near-infrared spectra of planets and stars (Moroz, 1966); Moroz et al. (1968) and Moroz, Davydov and Zhegulëv (1969) published the first Russian 10 μm measurements. Ed Ney's University of Minnesota group also began a productive infrared astronomy program in the late 1960s. At longer wavelengths, Johnson, Low and Steinmetz (1965) and Low (1966) reported 20 μm measurements of very bright stars while Low, Rieke and Armstrong (1973) attempted 34 μm measurements but the atmospheric transmission at 34 μm is poor and ground-based photometry at this wavelength was not pursued. Thus, by the early 1970s mid-infrared astronomy had become routine at several institutions, as Low, Rieke and Gehrz (2007) highlight.



Figure 8. The Air Force Maui Optical Station (AMOS) atop Mt. Haleakala, Hawaii at an altitude of 3054 meters. In the image on the left, the 3.67 m Advanced Electro-Optical System (AEOS) at the right is the largest optical telescope designed to track satellites (Mayo, 1999) and is currently used for most of the infrared imaging, photometry and spectroscopy (Witte, Landee and Musial, 1999). The telescope housing collapses as shown to avoid the problems associated with rotating a massive dome at the 15°/sec needed to track satellites. Dual 1.2 m telescopes in the dome on the back of the building roof at left are mounted on opposite sides of a single polar axis and are aligned to a common declination so that they can track and observe the same object; the larger dome houses a 1.6 m telescope (Lambert, 1999). Both these facilities have been used for infrared observations (Chapman, 1981). The three grey domes enclose a 0.4 m and two 1 m Ground-based Electro-Optical Deep Space Surveillance system (GEODSS) telescopes. The newest facility, the 1.8 m PanSTARRS-1 telescope, shown on the right is outside the left hand image in front of the AEOS. Information and image are taken from <http://www.maui.afmc.af.mil/gallery.html>.

Freeman Hall was one of the first to systematically address the question of what a satellite looked like in the infrared. The 4 November 1957 issue of *Aviation Week* (1958) announced the first reported infrared detection of a satellite in which an anomalously high near-infrared flux from Sputnik I was claimed to have been observed. The subsequent 1 – 3 μm measurements of Sputnik II by Moss and Brown (1958) with an uncooled PbS cell were entirely consistent with the observed flux being due to reflected sunlight. Hall and Stanley (1962), at the International Telephone and Telegraph Federal Laboratories (ITTFL) in Sylmar CA, settled the flux discrepancy issue with infrared radiometry of satellites using the 20" telescope. Hall and Stanley cooled their detectors with dry ice and the system was configured to either operate in the PbS region or at 2 – 6 μm with an InSb detector. Five satellites (Discoverer VIII, Sputnik III & IV, Midas II and Echo I) were looked at with successful PbS measurements on Midas II and Echo I and on the thermal emission from Echo I with the InSb cell with nominal results.

The DoD also built and operated a small number of ground-based observatories specifically for observing satellites. Lambert and Kissell (2000) all too briefly review the early history of the ground-based facilities that measured the visible and infrared photometric and spectral characteristics of satellites. A site at Sulphur Grove, Ohio and another at Cloudcroft, New Mexico were developed in the early 1960s by the Air Force Avionics Laboratory at Wright-Patterson AFB. The Sulphur Grove facility was used during most of the decade for visible photometry and imaging with a vidicon camera, but the site was closed early in the 1970s. Construction of the larger four-axis 48" (1.22 m) Cloudcroft telescope began in 1960 and it became operational in 1964. This observatory obtained optical measurements through the

decade and Lou Meuser attempted infrared measurements there in the early 1970s using a Baird Atomic Inc radiometer with an infrared linear array, reporting 2 – 14 μm signals on satellites and stars as early as 1972. The effort terminated in 1975 owing to the unreliability of the radiometer. Photometry, radiometry and imaging of satellites shifted to the ARPA site on Maui. A modern image of the facility is shown in Figure 8.

The ARPA (now Air Force) Maui Optical Station (AMOS) was developed for visible and infrared observations. Walt Mitchell (OSU) attended a 5 April 1962 meeting at Harvard University during which ARPA solicited interest from the astronomers present in using the infrared telescopes being built by Aerojet-General Corp under a University of Michigan contract. Two 36" telescopes were undergoing laboratory testing at the time, after which they were to be placed at the summit of Mt. Haleakala on the Hawaiian island of Maui. The telescopes were to be used to study missile re-entry but ARPA wanted to know what could be done to facilitate wider, civilian use of the instruments. These telescopes were installed in 1963 although 1965 was officially the first year of operation; the remainder of the facility was completed in 1969. Infrared observations became routine at AMOS in the early 1970s but it appears that the astronomers who attended the Harvard meeting did not pursue the ARPA offer.

2.2. The First Near-Infrared Sky Surveys

The early infrared photometry by Ohio State, Freeman Hall and the Univ. of Arizona indicated that although blackbody extrapolations from visible data under-predicted the infrared indices for the coolest stars, the excesses weren't very large. Furthermore, the initial 10 μm stellar photometry published by Wildey and Murray (1964) and Low and Johnson (1964) was entirely consistent with this conclusion. The feeling that little was new in the infrared was strong enough that discordant results (e.g. Johnson, 1965) were initially interpreted as being due to causes other than the intrinsic characteristics of the stars. An unbiased sky survey was needed to confirm that there were, indeed, no surprises in the infrared.

The telescope with which Freeman Hall obtained his stellar and satellite radiometry had a rapid response and a large $1/4^\circ \times 1/4^\circ$ instantaneous field of view that was swept 5° in declination by a scanning Newtonian secondary mirror. These were ideal properties for a sky survey, which Hall (1964) conducted in the summer of 1962. This survey covered $\sim 18\%$ of the sky in a 1.3 – 3 μm band and smaller areas at 5 and 10 μm . The survey sensitivity was relatively low, so only a score or so sources were positively detected in the near-infrared with the PbS cell while only Venus and Mars were detected at longer wavelengths.

Since AFCRL had funded Freeman Hall's efforts, the survey instrument reverted to the Infrared Physics Branch at the end of the contract. Russ Walker modified the ITTFL instrument to improve the sensitivity and added a second small telescope with the standard U, B, V bands plus filters in the four near-infrared atmospheric windows to measure the atmospheric extinction along the line of sight of the survey instrument as well as to obtain multicolor measurements on the brightest objects (Figure 9). Augason and Spinrad (1965) referenced this effort in their early 1960s survey of infrared astronomy and a description of it is given in the *July 1963 – June 1965 AFCRL Report on Research* but no results were published.

As a young Air Force officer, Russ was first stationed at AFCRC in 1953 after obtaining a Masters degree from the Ohio State University. Upon completing his military service, he worked for a while in industry, then returned to become the Infrared Physics Branch Chief in the Optical Physics Laboratory in the early 1960s. One of his first research topics was to estimate the near-infrared celestial background that a space-based sensor would see. He estimated the

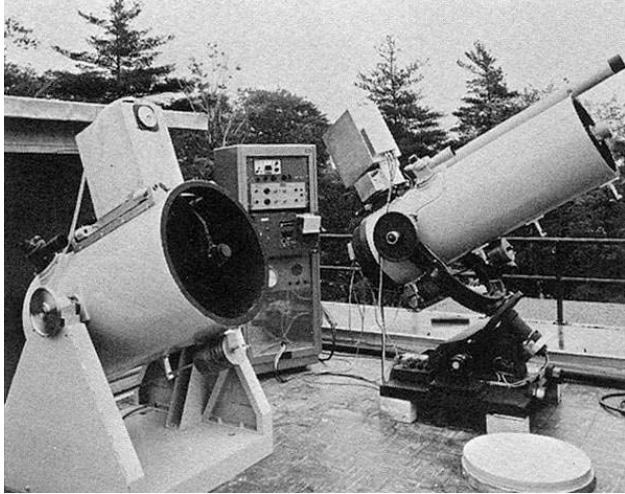


Figure 9. The AFCRL IR telescopes. At left is the ITTFL survey instrument supplied under the AFCRL contract. The telescope at right monitors atmospheric extinction simultaneously in U, B, V and four near-infrared wavelengths (Augason and Spinrad, 1965).

photometry on a number of bright stars and planets. A notable aspect of this research was that, like Freeman Hall, Russ put his infrared photometry on an absolute flux scale by referencing his observations to a blackbody at the telescope. Thus, by direct reference, he absolutely calibrated the zero magnitude irradiances of his photometric system.

Meanwhile, Hall set out to construct a more sensitive instrument with higher spatial resolution that could resolve the extended near-infrared sources that he believed were indicated in his survey. He adapted the Univ. Arizona design for an all aluminum infrared telescope by scaling the blueprints for the 60" mirror a centimeter to an inch, producing a 24" f/2 primary. Construction of the instrument began in the summer of 1963 under company Industrial Research and Development (IR&D)⁴ funds. The 30 element linear array of 1'×1' PbS detectors was filtered for an effective wavelength of 2.2 μm and cooled to ~ 35 C below ambient temperature by a Peltier thermo-electric cooler. The array spanned $1/2^\circ$ in declination and surveyed the sky at the sidereal rate with the telescope pointing near the meridian. An eight bladed opaque chopper modulated the field and the resulting signals synchronously rectified. After several stops and starts the instrument was completed in 1965 and a near-infrared survey of the northern Galactic plane began that summer. Freeman reported initial measurements of several extended sources such as the Crab nebula (Hall, 1966) but left ITTFL shortly thereafter to pursue his doctorate on the influence of cirrus clouds on the 8 – 14 μm radiance of the sky (e.g. Hall, 1967; 1968a, b).

In the summer of 1965, Freeman learned that Robert Leighton and Gary Neugebauer at Caltech also had begun a 2.2 μm survey of the sky visible from Mt. Wilson but in two infrared colors rather than one and with markedly better sensitivity than the ITT instrument. A *Sky and Telescope* article by Frank Bateson (1962) on what was then the world's southern most observatory led Freeman to decide that the most productive thing to do was to complement the

cumulative source counts as a function of infrared flux and the distribution of diffuse infrared radiation from the stars and zodiacal background (Walker, 1962). Subsequently, Walker (1964) assembled a visible to near-infrared photometric database, which he reduced to a common system, and derived the first major revision of the bolometric correction since the seminal paper by Kuiper (1938). Walker and D'Agati (1964) published these results as well as the predicted spectral energy distributions for a number of bright stars to 10 μm . Walker (1969) did his PhD research at Harvard University, with Carl Sagan as his thesis advisor, on the topic of *Infrared Photometry of Stars and Planets* for which he built and used several ultraviolet to the near-infrared (2.2 μm) photometers to obtain multi-color

⁴ At the time, government industrial research and development contracts had a provision that permitted the company to include a small percentage (~2%) in the negotiated contract amount for internal research and development. This IR&D research was supposed to be exploratory, the purpose of which was to encourage a healthy research component to the company business.



Figure 10. The ITTFL all-aluminum survey telescope newly installed atop Mt. John, NZ.

with the contract. Price (1968a) provides details of the ITT survey while Price (1968b) gave a more accessible but briefer account of the results. The single survey observation of note was the realization of one of Hall's objectives: the firm detection of an extended infrared source, which turned out to be a small, heavily reddened cluster of stars in Ara (Westerlund, 1968) discovered a few years earlier by Westerlund (1961). Borgman, Koornneef and Slingerland (1970) followed up with near-infrared photometry on the individual stars in the cluster and found it to be one of the most highly reddened objects in the Galaxy, lying behind 13 magnitudes of extinction. A near-infrared image of this object, Westerlund 1, is shown in Figure 105.

Pursuing the legacy of Hall's 1962 survey, Neugebauer and Leighton (1968b) embarked on a program for a much more sensitive near-infrared survey. Originally, a searchlight mirror was considered for the survey as such a mirror was readily available, large, lightweight and inexpensive. The concept had a precedent in the unsuccessful attempts by Whitford (1948b) to use such a mirror to survey the Sagittarius region at $2\text{ }\mu\text{m}$ and to measure the near-infrared radiation from the Galactic center; Becklin and Neugebauer (1965) first detected $2.2\text{ }\mu\text{m}$ emission from the Galactic nucleus using the $200''$ telescope.

However, Leighton (1998) soon rejected the idea of a searchlight mirror for the survey because of severe distortions. Instead, the Caltech team roughly figured a $62''$ aluminum mirror blank on a lathe and then applied the final figure by allowing epoxy to dry on the blank as it was spun at a rate sufficient to produce the desired $f/1$ focal ratio parabolic curvature. The epoxy surface was then aluminized. Two columns of $3'\times 10'$ PbS $2.2\text{ }\mu\text{m}$ detectors covered $40'$ in declination while a single $3'\times 20'$ intrinsic silicon I band ($0.9\text{ }\mu\text{m}$) detector spanned the central $20'$. The two PbS detectors in a row were electronically coupled and their signals negatively combined to eliminate the sky emission common to both beams. The telescope was scanned in right ascension between $\pm 30^{\text{m}}$ hour angle of the meridian then reset $15'$ northward. The scan rate was doubled for $\delta > 56^{\circ}$. The TMSS system is shown in Figure 11.

The TMSS began in January 1965 and was completed in the spring of 1968, covering three-quarters of the sky, the area within $-33^{\circ} < \delta < +82^{\circ}$, at least twice. Although the 5612 sources in the TMSS survey catalog have $K < 3.0$, the survey actually detected about 20,000 objects above a flux limit some four times lower. Several constraints set the higher catalog limit, one of which was confusion. According to Neugebauer and Leighton's standards, too many

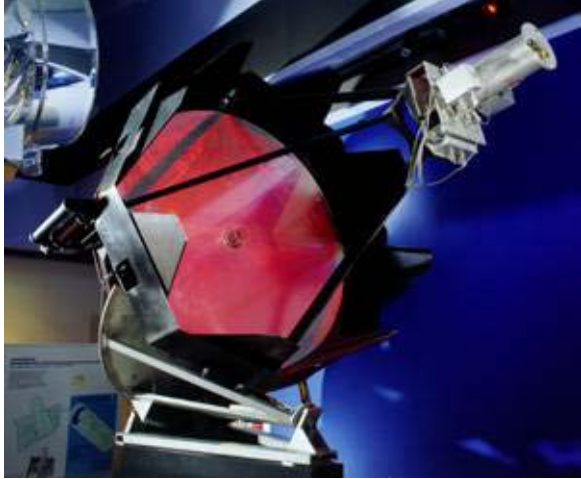


Figure 11. The Two Micron Sky Survey Telescope in the Smithsonian Museum. The detectors are at the prime focus of the (red) 62" primary mirror. The silver cylinder is the liquid nitrogen Dewar.

specifically δ between -33° and -47° . Even though these low declinations required observing through as much as five air masses from Mount Wilson, the results were still more sensitive than the ITT survey. However, these data were not of the high quality that Neugebauer and Leighton demanded of the TMSS and thus were not published; Martin Cohen (private communication) carefully vetted the limited distribution catalog to combine the numerous duplicate entries.

2.3. The AFCRL Lunar and Planetary Research Branch

The space race began in earnest after the October 1957 Sputnik launch and manned exploration of the Moon was soon established as a goal with the Air Force considering a manned lunar base (Brown, 1960). Many ambitious planners also had Mars penciled in as the next destination after the Moon. However, the exact nature of the lunar surface was a matter of conjecture at the time. Some believed that the surface had only a thin layer of dust while others (Gold, 1956) thought that the dust layer was thick enough to engulf any spacecraft that attempted to land; Salisbury and Van Tassel (1962) discussed this topic in detail. Early on, Salisbury et al. (1963) resolved how far a landing craft would sink into the lunar dust by measuring a high vacuum adhesion for silicate particles and correctly predicting the bearing strength of the lunar surface, although not everyone was convinced (Gold, 1965). The lunar surface properties also could be inferred by remote infrared observations. For example, the composition of the surface may be deduced from the infrared spectral signature indicative of its various mineral components while the relative strengths of these features are influenced by the size distribution of the lunar regolith (surface layer) and the packing of the particles. How hot the Moon gets during the daytime and how fast it cools with the onset of night or in eclipse also tells us something about the lunar surface; a rocky surface cools more slowly than a dusty one. In 1960, AFCRL established the Lunar-Planetary Exploration Branch within the Space Physics Laboratory, with Charles Campens as Chief and Dr. John Salisbury as the single person workforce, to investigate the infrared properties of the Moon and planets. John Salisbury had joined AFCRC in July 1959 to fulfill his ROTC military obligation after obtaining his degree from Yale University. He

sources along the Galactic plane were confused at fainter levels when more than one source appeared on the two electronically coupled $3' \times 10'$ PbS detectors at a given time.

The TMSS did discover a new class of objects, a population of very red stars that are bright at $2.2 \mu\text{m}$ but quite faint in the visible. Unlike the objects in Rust's study that were red due to molecular absorption in the visible, the TMSS stars are intrinsically cool, $\sim 1000\text{K}$. Neugebauer, Martz and Leighton (1965) gave a survey pre-release announcement of two of the brightest and most extreme sources, currently designated as variable stars IK Tau and V1489 Cyg, while Ulrich et al. (1966, 1967) provided information on 14 fainter very red, cool objects.

Caltech also mapped areas below the TMSS declination limit in 1967 through 1969,

subsequently became the Branch Chief in 1961. The Branch's charter to assess the Moon as a manned station is evident by the fact that the second published Technical report from the group was titled *Location of a Lunar Base* (Salisbury and Campens, 1961; the first Technical Report was a brief 1960 review of what was then known about the Moon).

Salisbury and his Branch also periodically compiled summaries of the research in the literature that they judged of value to their efforts. The first bibliography of published lunar and planetary research plus a synopsis of the articles was collected by Salisbury, Van Tassel and Adler (1961) and comprised a mere 28 pages. By the time Salisbury (1968), as editor, published the 3rd Supplement in 1968, the bibliography had grown to a book sized 304 pages. These annotated compilations were deemed important enough to the planetary research community that Salisbury and his team subsequently published them quarterly in *Icarus* beginning in 1970 with Volume 12 and continuing until Volume 22 in 1973.

Quantitative thermal measurements of the Moon date to Lord Rosse's fairly accurate disk integrated temperature profile during a lunation. Subsequently, the infrared fluxes during a lunation were occasionally updated over the next century using gradually improving detectors (e.g. Pettit, 1935). However, thermal measurements of the resolved disk of the eclipsing Moon in the first half of the 20th century were particularly interesting as the infrared changes in flux could be continuously monitored over a period of hours instead of weeks for a lunation. Pettit and Nicholson (1930) published thermal profiles across the full Moon and cooling curves near the limb during the 14 June 1927 eclipse. Pettit (1940) confirmed these earlier results by measuring the thermal profile near the sub-solar point for the 27 October 1939 eclipse. The measurements revealed a rapid decrease in the lunar brightness temperature with the onset of eclipse, from ~371K in full sunlight to ~200K shortly after the beginning of totality. The brightness temperature declined much more gradually during totality, from ~ 200K to ~175K with temperatures at the limb about 10K cooler. Paul Epstein (1928), a Caltech theoretical physicist, used Petit and Nicholson's observations to deduce that the lunar surface did not consist of bare rock but was covered by a thin insulating layer of dust. Doel (1996) noted that this was the first quantitative analysis of conditions on another planet. Subsequently, Wesselink (1948) published the first definitive theoretical analysis of these infrared eclipse observations and concluded that the lunar surface was either porous or, like Epstein, covered in dust.

By the mid-1960s, modelers had a few other observations to match. These included the Pettit and Nicholson (1930) and Sinton (1959) midnight point observations, the Strong and Sinton (Sinton, 1962a) temperature profiles for seven lunar regions during the first half of the 29 July 1953 eclipse and the Geoffrion, Korner and Sinton (1960) isothermal (equal temperature) maps of the Moon for various lunar phases between new crescent to old from raster drift scans across the Moon with a pyrometer on the Lowell Observatory 42" telescope. Ryadov, Furashov and Sharonov (1964) later made 8 – 13 μm observations between full Moon and 150° phase angle. In 1962, Murray and Wildey (1964) obtained 8 – 14 μm night side brightness temperatures of the Moon, which they (Wildey, Murray and Westphal, 1967) extended and refined in 1964. Low (1965) made analogous measurements at 20 μm .

As noted, since the heating and cooling cycle of an area on the Moon takes a few hours during an eclipse, infrared eclipse measurements can follow most of a complete thermal cycle in just one night's observing. Such cooling curves were measured for several lunar features during eclipses in the early 1960s. For example, Shorthill, Borough and Conley (1960) used a thermistor bolometer with a 5 – 40 μm system response to scan across the Moon during the 13 March 1960 eclipse. They measured a brightness temperature of <200K for the eclipsed lunar

disc but found that certain features, such as the crater Tycho, stood out with a 50K brightness temperature contrast over its immediate surroundings. The Aristarchus and Copernicus craters also displayed similar enhanced emission. Sinton (1960, 1962b) and Saari and Shorthill (1963) confirmed the 50K difference between Tycho and its surroundings at the beginning of the 5 September 1960 eclipse and Saari and Shorthill (1963, 1967b) derived temperature contour maps for several craters the day before, during and after this eclipse and determined eclipse cooling curves for the craters. These observations simply scanned across the Moon and, thus, were only able to sample a limited area of the lunar surface. Then, Saari, Shorthill and Deaton (1966) obtained the first global infrared maps of the eclipsed Moon by raster scanning the entire Moon during the 19 December 1964 eclipse with a 10" beam using a Ge:Hg photoconductor with a 10 – 12 μm filter; a single image took 16 minutes to complete. These images revealed a large number of hot spots that they labeled as thermal anomalies on the lunar surface that were appreciably warmer than their surroundings. Ultimately, Shorthill and Saari (1965a, b) tallied a total of about 1000 hot spots, which Shorthill (1973) defined as insolated areas that are >5K above their surroundings. The preliminary classification of Saari and Shorthill (1967b) associated about 85% of the hot spots with bright craters while another 9% corresponded to smaller isolated visible bright regions. Saari and Shorthill (1966) also converted their infrared images of areas selected as possible lunar landing sites in the lunar equatorial regions into a set of isothermal maps, then synthesized isothermal and isophotal (equal brightness) visible and infrared atlases of the Moon throughout a lunation (Shorthill and Saari, 1965b; Saari and Shorthill, 1967a). Both NASA and the Air Force supported these efforts.

This was the general state of infrared lunar measurements when the Lunar-Planetary Research Branch initiated a multi-faceted research program to study conditions on solar system bodies. Laboratory vacuum chambers were built to measure the spectra of candidate materials under simulated lunar temperature and vacuum conditions. The laboratory infrared spectra of the various materials thought likely to be found on the surfaces of the Moon, Mars and asteroids were assembled into a spectral library, which then could be compared with ground-based and balloon-borne infrared observations of these objects to infer their surface compositions.

Initially, the laboratory results were used to support analyses of lunar observations obtained by other researchers who were often financially supported by AFOSR and/or AFCRL. By the mid-1960s, however, the Branch had constructed its own facilities to observe the thermal characteristics of the Moon. Subsequently, Hunt, Salisbury and Vincent (1968) mapped about 70% of the Moon during the 13 April 1968 eclipse at 10 μm searching for lunar activity that they believed would show up as changes in the relative brightnesses of the thermal anomalies, especially the weaker ones, since the Saari, Shorthill and Deaton 19 December 1964 eclipse map, but found none. These observations were made with one of the first 60 cm Boller & Chivans telescopes built (serial number 2), which the Branch sited in Concord, MA. Salisbury (Smith and Salisbury, 1962) had considered, and then rejected, Cloudcroft as a site for this telescope. This interim infrared lunar observatory operated from the end of 1966 until November 1968, when a comparable instrument was opened on a site atop Mauna Kea in Hawaii. Built with AFCRL funds, the Mauna Kea facility was jointly operated with the University of Hawaii.

The anomalously warm regions of the Moon seen in eclipse are surface areas that retain heat from absorbed sunlight longer than their surroundings. The temperature contrast could arise, for example, if the areas were rocky and the cooler surrounding areas were covered by a layer of dust. The cooling rates measured for these anomalies were limited on the short scale by how rapidly an image could be scanned and on the long term by the approximately two hour

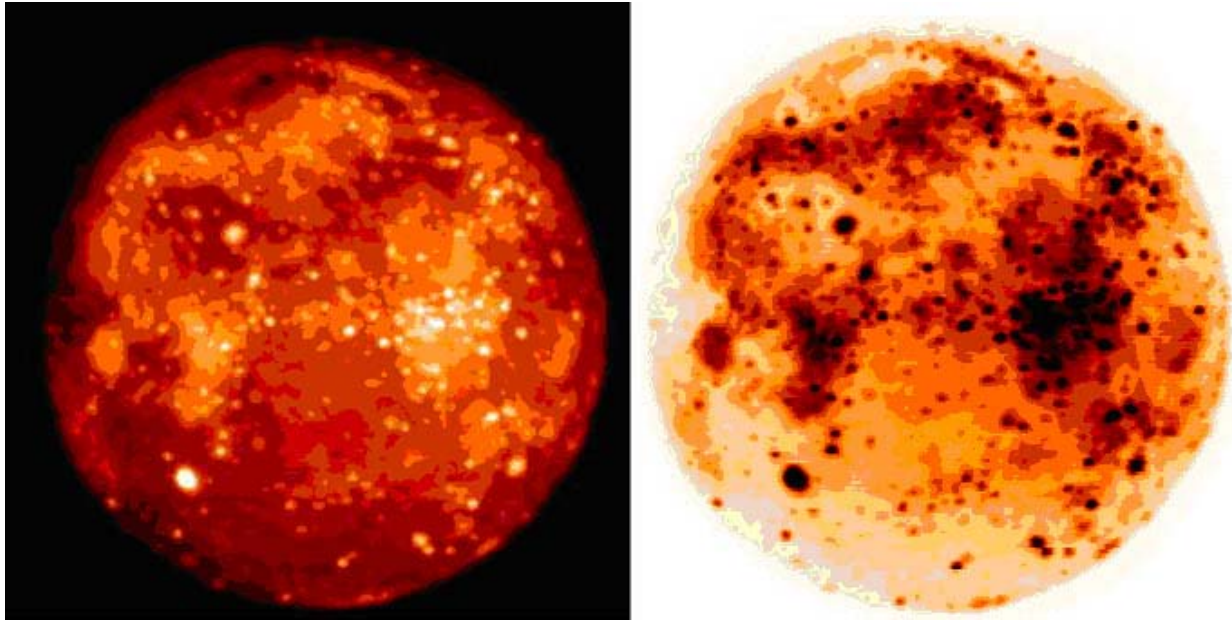


Figure 12. Thermal emission from the 27 September 1996 eclipsed Moon. At left is a Midcourse Space Experiment 4.3 μm image while the 8.3 μm data is shown on the right. Although the 8.3 μm flux is in soft saturation, hence the reverse contrast with dark being warm and light – cool, it better distinguishes differences at the lowest temperatures while differences at the higher temperatures are better defined in the 4.3 μm map. The thermal anomalies are evident: the crater Tycho is the brightest spot in the lower left.

duration of the eclipse. Price, Mizuno and Murdock (2003) improved the time resolution by imaging the Moon roughly every two minutes during the 27 September 1996 eclipse (Figure 12). The cooling profiles they obtained are in qualitative agreement with earlier measurement although the 4.3 μm brightness temperatures are about 20K higher. This discrepancy may be due to the lunar radiation efficiency (emissivity) at the short wavelength of the measurements or differing surface roughness within a region (Johnson, Vogler and Gardner, 1995).

Murray and Wildey (1964) found that thermal anomalies persisted for hours after sunset in the 8 – 14 μm band and that, in concordance with eclipse observations, Tycho and Copernicus were the most prominent hot spots. Later, Hunt and Salisbury (1967) tracked Tycho as it cooled for four days after sunset. Allen (1971a, b) subsequently observed the 10 and 20 μm cooling profiles on the night side of the Moon and was able to detect the thermal hot spots near the terminator for a couple of days after sunset. He further speculated that the anomalies retain heat because they are boulder strewn fields.

Winter (1971) reviewed how these observations were used to derive thermal characteristic of the lunar surface by fitting the parameters in the heat diffusion equation:

$$\rho(x)c(T) \frac{\partial T(x,t)}{\partial t} = \frac{\partial}{\partial x} \left[k(T) \frac{\partial T(x,t)}{\partial x} \right] \quad (1)$$

to match the cooling curves. $\rho(x)$ is the regolith density as a function of depth, x , and is usually assumed to be $\sim 1.3 \text{ g cm}^{-3}$ at the surface. $c(T)$ is the specific heat as a function of temperature, T ; $c(T)$ values for the Apollo 11 lunar soil sample were measured by Robie et al (1970). $k(T)$ is the thermal conductivity, generally assumed to be of the form $k(T) = A + BT^3$, where A is the solid body conduction and BT^3 the radiative transfer through the vacuum in the pore spaces of the soil.

The boundary conditions for this non-linear Equation are:

$$(A + BT^3) \frac{\partial T}{\partial x} = \varepsilon\sigma T^4 - F(T) \quad \text{as} \quad x \rightarrow 0 \quad (2)$$

and that the thermal gradient disappears at large depth. $F(T)$ is the flux into the surface due to insolation (the thermal input from the Sun) and ε is the average infrared emissivity, 0.93 to 1 in the lunar models, and σ is the Stefan-Boltzmann constant ($= 5.67 \times 10^{-8} \text{ W m}^{-2} \text{ K}^{-4}$). The non-linear partial differential Equation (1) does not have an analytic solution and must be solved by numerical techniques. The exception is the case of no thermal inertia in which the left hand side of Equation (2) is zero, an approximation realized on the sunlit surface of the Moon as the thermal inertia is less than 1% of the absorbed sunlight. Winter (1971), among others, noted that no single set of model parameters could reproduce both the thermal brightness temperatures of the Moon during a lunation and an eclipse. This is a consequence of the characteristic depth from which the emission arises; e.g. Wildey, Murray and Westphal (1967) noted that the eclipse emission comes from the top millimeter of the regolith while the nighttime emission is from a depth of a centimeter or so within granular material. Although selected representative locations on the Moon, such as the disk center, have been modeled through a lunation or eclipse as has the global low resolution distribution of temperature of the sunlit Moon, a disk resolved thermal model has yet to be developed that accounts for the thermal anomalies.

While the infrared broadband photometry of the Moon provides information on the physical characteristics of the regolith, such as what terrain might be dusty or rocky and by how much, additional information may be derived from the infrared emission spectra. Such spectra contain features indicative of the mineral composition, density, and particle size and packing. To explore these parameters, the Lunar and Planetary Research Branch created a spectral library from their laboratory measurements on likely lunar analog materials and used it to infer the mineral composition and surface properties of the Moon. The most prominent spectral features between 8 and 25 μm are the fundamental stretching and bending modes of various types of silicate molecules although grain size affects the exact wavelength of the peak and the shape and breadth of the features. The principle molecular vibration bands occur at what is classically labeled as the Christiansen frequencies of the minerals, where the maximum absorption or emission occurs at the wavelength at which particle scattering changes from being dominated by volume scattering to surface scattering (Hapke and Hale, 2000). The vibrational and electronic bands combine linearly in a coarse mineral mixture (Thomson and Salisbury 1993), which means that the surface composition and the relative amount of the various constituents may be inferred by additively combining the spectra of individual minerals from the spectral atlas in various proportions until a match is found with observations. However, other factors influence the spectrum. Van Tassel and Simon (1964) concluded from early laboratory measurements that the strength of the infrared spectral signatures depended on particle size in the sense that the signatures were weaker in fine powder compared to coarser material, becoming barely discernable when the particles are the size of sand grains. Hunt and Logan, (1972) extended and refined this analysis with detailed laboratory measurements on the effects that particle size has on the infrared spectrum for various silicate materials.

An observational database was needed with which to compare the laboratory spectra. Adel (1946) and Sinton and Strong (1960a) had published 8 – 14 μm spectra of the sunlit Moon while Murcay (1965) measured 8 – 14 μm spectra of the nearly full Moon on several nights in

the fall of 1964 that displayed subdued spectral structure. Hunt and Salisbury (1964) obtained 16 – 24 μm spectra at four locations on the sunlit Moon using a Golay cell in a spectrometer on the 42" Lowell Observatory telescope. The spectra did, indeed, differ between locations: the 19 – 23.5 μm emission from Serenitatis varied more steeply with wavelength than that from Copernicus. However, the atmospheric transmission impressed upon ground-based infrared spectroscopy dominated over the subtle mineral features in the lunar spectral energy distribution and one needed to get above the atmosphere to obtain uncontaminated measurements. Strong (1959) and deVaucouleurs (1959) had suggested that balloon-based astronomy could be a viable surrogate for that from satellites because, at altitude, a balloon platform is located above much of the atmosphere where the emission and absorption by atmospheric constituents are greatly reduced. Salisbury and Van Tassel (1962) also had pointed out that much of the thermal emission from the atmosphere that they believe had rendered ground-based determinations of brightness temperatures rather uncertain would be eliminated at balloon altitudes.

AFCRC/AFCRL had been involved in balloon research since shortly after the War and had actively advanced ballooning technology and applications. AFCRC/AFCRL and Holloman AFB combined have flown more than 2500 balloon experiments over the years and have set all the ballooning records for altitude, duration of flight and distance. A bizarre side note is that Air Force operations from Holloman AFB, New Mexico have been a major source for the UFO mythology. In the late 1940s, Watson Lab (soon to join the Cambridge Field Station) funded New York University for Project Mogul, a series of balloon flights that attempted to detect Soviet nuclear tests with acoustic sensors. The fourth flight in the series on 4 June 1947 and the first from Holloman AFB landed near Roswell, New Mexico. The recovery of the debris by a rancher plus later civilian observations of the recovery of the anthropomorphic dummies dropped from Holloman based balloon borne parachute tests under Project High Dive gave rise to the "Roswell incident." McAndrew (1995) has shown that this only became an incident in the 1970s with the publication of several lurid books about aliens, bodies and a crashed spaceship while he, McAndrew (1997), subsequently explained how the dummies and other balloon recovery incidents became the fodder for the Roswell UFO mythology. Ryan (1995), in his book: *The Pre-Astronauts: Manned Ballooning on the Threshold of Space*, tells the fascinating story of the manned balloon flights (Man High) in the early 1950s and the subsequent parachute tests with dummies (High Dive) and pilots (Excelsior) that culminated in Stargazer, a manned infrared astronomy flight. Additional information on Air Force ballooning may be found in the Holloman AFB Balloon Branch history (Anon., 1958).

While manned and unmanned balloons were used for cosmic ray research almost from the first ascent, David Simons (1958), an Air Force medical doctor who flew on a Project Man High experiment, pointed out the advantages of manned ballooning for near-infrared astronomy. Quantitative infrared astronomy from balloons had begun on 30 May 1954 when Audouin Dollfus rode a balloon to 7 km altitude in an attempt to measure water vapor on Mars with a lead sulfide cell on a 50 cm telescope. His rather clever detection scheme was thwarted by saturation of the 1.4 μm water band in the atmosphere above the balloon. He followed this feat in 1959 with near-infrared observations of Venus from 14 km altitude from which he derived the stratospheric water content, which he subtracted from subsequent mountain top measurements to calculate planetary values (Dollfus, 1964). Although these flights demonstrated that astronomy could be done from balloons, they returned limited quantitative results.

The DoD sponsored two manned astronomical balloon flights. On 28 November 1959, John Strong attempted to observe Mars and water vapor on Venus with a 16" Schmidt telescope

aboard the Navy sponsored Strato-Lab IV balloon flight (Ryan, 1995) but with limited results. Project Stargazer, proposed at the January 1958 AFCRC Balloon Conference, was a joint Air Force, Navy, Smithsonian Institution and MIT program (McAndrew, 1997) to do astronomy from manned balloon flights. Air Force Capt. Joseph Kittenger piloted the balloon while the Navy contributed an astronomer, William White, to make the observations. Project Stargazer flew on 13 December 1962 and obtained observations with a remotely controlled 12.5" telescope mounted on top of the gondola. A few months later, Stargazer II was in the final countdown on 20 April 1963 when a static discharge tripped the balloon release, ending the experiment. The single Stargazer flight was the seventh and final Air Force manned balloon flight and although labeled a "huge success" (Hynek and White, 1963, Ryan 1995), stabilization problems and the expense of mounting such efforts resulted in the program being canceled before the Lunar and Planetary Research Branch's manned infrared lunar experiment could be flown.

As would later be the case for space-based astronomy, balloon researchers soon preferred remote operations without the weight and safety burden of man and both the Navy and the Air Force flew unmanned astronomical balloon experiments throughout the 1960s. The Office of Naval Research, National Science Foundation, and NASA funded Princeton University to conduct the Stratoscope II flights that carried a 36" (0.9m) telescope; Stratoscope I was a late 1950s solar experiment. The first two Stratoscope II experiments were flown in 1963 and obtained near-infrared spectra of cool giant and supergiant stars (Woolf, Schwarzschild and Rose, 1964), the Moon, Jupiter, and Mars (Danielson, 1964). Woolf (1965), summarizes the results from both flights. Six more Stratoscope II flights obtained high resolution photographs of galaxies before the telescope was irreparably damaged.

The Lunar and Planetary Research Branch teamed with the Balloon Branch in a three-phased program to obtain infrared measurements from balloons, the most ambitious of which was Project Stargazer. About the same time as Stargazer, AFOSR funded John Strong, at the Johns Hopkins University, through an AFCRL contract to loft a modest sized instrument to an altitude of ~80,000' (24 km) on Project BalAst to measure water vapor, CO₂ and other gases in the atmosphere of Venus. Unfortunately, the instrument failed on the initial April 1962 attempt but a second, successful flight in February 1963 looked for the 1.3 μm band of H₂O and an October 1963 experiment extended the wavelength coverage to 3 μm to search for water ice (Bottema, Plummer and Strong, 1964). This was followed by Project Sky Top, which carried a near-infrared spectrometer to an altitude of ~100,000' (30 km) in January and February of 1963 to obtain thermal emission spectra of the Moon. AFCRL also provided ARPA funds to the University of Denver to fly an infrared spectrometer on an AFCRL balloon to measure the solar emission between 4 and 5 μm (Murcray, Murcray and Williams, 1964) as part of the long term AFCRL interest in determining the solar constant. At an altitude of 31 km, the observations were relatively free of atmospheric interference and the solar flux measured by this experiment was one of a limited number of high quality infrared observations used by Labs and Neckel (1968) to derive an absolute calibrated spectrum of the Sun.

Salisbury's group had contracted with Tufts University to construct a payload for their own in-house balloon-borne instruments to measure the infrared flux from the Moon and planets. Howell (1973), at Tufts University, described the first balloon package, which housed a 24" telescope. Van Tassel (1968) obtained the 9 to 22 μm lunar spectrum during the initial flight of this telescope in February 1966 but found no distinctive infrared spectral features that could be used for mineralogical identification. The 24" telescope and gondola package was flown 11 times between the first AFCRL launch in 1966 and the end of the decade when the lunar

measurements were terminated. Only a few experiments returned good data but, as Salisbury (23 October 2003 e-mail) pointed out, the expense of a balloon flight was quite modest and the payload was recovered. Thus, the ‘unsuccessful’ flights could appropriately be considered as engineering development tests to perfect the hardware and flight procedures.

Murcray, Murcray and Williams (1970) mated their spectrometer to the Tufts 24" telescope to obtain 7 – 13.5 μm spectra of six regions of the nearly full Moon on a 13 April 1968 AFCRL flight. They found that the observed spectral energy distribution in each region was broader than could be accounted for by a single temperature blackbody. In a companion paper, Salisbury et al. (1970) compared these results to the AFCRL spectral library but could not make conclusive matches. Vogler, Johnson and Shorthill (1991) attempted to correct the Murcray et al. results by their estimate of the residual atmospheric absorption above the balloon and found that the normalized emissivity varied from 105% at 7 μm to 90% at 13.5 μm . , Salisbury et al. (1995) then argued that the Vogler et al. analysis was flawed because only ozone absorption had to be corrected at the 32 km float altitude of this experiment. Furthermore, additional simulation chamber measurements showed that the vacuum environment enhances the mid-infrared emission near the Christiansen frequency, broadening the spectral energy distribution and shifting the peak to shorter wavelengths. Thus, Salisbury and his colleagues were finally able to match the observed balloon-borne lunar spectra and infer the lunar surface composition.

The Lunar and Planetary Research Branch also sponsored the initial steps into a new field of research: X-ray astronomy. In their extensive description of the AFCRL program of lunar measurements, Hunt and Salisbury (1969) mention in passing that AFCRL funded a rocket based experiment to detect X-ray fluorescence from the Moon. What followed was, as noted by Harwit (1981), an example of how military research has led to major astronomical discoveries. In 1959 John Salisbury discussed the idea of a rocket-based lunar X-ray fluorescence experiment with Riccardo Giacconi, American Science and Engineering Corp (AS&E) in Cambridge, MA. The first (unsuccessful) flight took place the following year. A second flight, on 18 June 1962, did not measure lunar fluorescence but did detect two objects, now designated Sco X-1 and Cyg X-1, outside the solar system (Giacconi, et al., 1962). Two more AFCRL sponsored experiments were flown in October 1962 and June 1963 that confirmed the discovery (Gursky, et al., 1963).

Giacconi (2005) apparently is of the opinion that the discovery of the X-ray sources was due as much to preparation as to serendipity. He states: *We were successful in interesting Dr. John Linday of the Goddard Space Flight Center ... in funding a small program to develop grazing incidence telescopes but not in interesting NASA Headquarters in funding rocket instrumentation to search the sky for X-ray stars. We therefore turned to the Air Force Cambridge Research Laboratories that had funded previous work by ASE in the classified domain. The Air Force was receptive to providing support to place a small aperture (1 cm^2) Geiger counter aboard a Nike-Asp rocket. The flight attempted in 1960 failed because of rocket misfiring. In January 1961 we received a new contract to fly four Aerobee 150 rockets for our experiments to search for X-ray stars, as well as lunar X-rays. The larger rocket permitted the design of a much more sensitive instrument. ... An important feature of the experiment was the use of a large field of view, which increased the probability of both observing a source anywhere in the sky and receiving a sufficient number of X-ray photons to make the detection statistically significant. ... After another rocket systems failure in October 1961 we had a successful flight on June 18, 1962, when we discovered the first extrasolar X-ray source (Sco X01) as well as the extragalactic X-ray background.*" Note that Giacconi places the search for x-ray stars before measuring lunar x-ray fluorescence, the putative purpose of the experiments.

The Lunar and Planetary Research Branch funded AS&E for three more rocket experiments (Sodickson et al., 1968). The 26 May 1964 flight carried an x-ray package but the attitude control system failed. The 9 November 1965 Aerobee flight carried a Block Associates interferometer in an attempt to measure the 7 – 30 μm spectrum of the Moon at 40 cm^{-1} spectral resolution. The pointing system again malfunctioned and only two noisy spectra of the Moon were obtained. However, Baker, Steed and Stair (1981) noted that this experiment serendipitously obtained the first interferometric spectra of the Earth's limb in which the CO_2 15 μm and 9.6 μm ozone bands were observed in absorption when the instrument looked at the Earth and in emission when viewed at a tangent height of 55 km above the Earth's horizon. The third and final experiment on 26 November 1966 carried a telescope with a circular variable filter that obtained infrared spectra of the Moon but data reduction was complicated by instrument problems. After considerable processing, the end results were 4 – 13 μm spectra of the lunar Mare and highlands, which revealed little difference between the two.

With the manned landing on the Moon in July 1969, lunar studies went from remote sensing to hands-on geology (e.g. Logan et al., 1972). By this time, the primary military objective of the lunar research to characterize the environment that man and/or machines would encounter on the Moon was achieved. The 1967 – 1970 AFCRL Report on Research assessed the situation: “*...long before Surveyor 3 had sent back to earth the first lunar photos of a disturbed soil, or the Apollo 11 and 12 astronauts stepped upon the moon, AFCRL scientists had derived what proved to be a valid model of lunar surface material. They concluded that the surface would be covered by a very fine powder, that it would be relatively firm and that the lunar powder would tend to adhere to all surfaces with which it came in contact.*”

Infrared lunar observations ended in 1970 and the Branch was renamed Spectroscopic Studies to emphasize a new charter to determine the infrared spectral properties of the planets, particularly as to their suitability as infrared calibration sources. The Branch was transferred to the Terrestrial Sciences Laboratory shortly thereafter and was then assigned to the Optical Physics Laboratory in 1974. Planets had always been a branch interest, as Van Tassel and Salisbury (1964) had measured the laboratory infrared spectra of the materials likely to be found on the surface of Mars. Under the new research objectives, Logan, Balsamo and Hunt (1973) mapped the 10.5 – 12.5 μm Martian surface brightness on the final flight of the 24" balloon borne telescope in April 1971. The system was absolutely calibrated in flight by on-board direct comparisons with a blackbody and several surfaces of various infrared emissivities at fixed, known temperatures. These measurements were supported by a detailed analysis of the surface conditions (Balsamo and Salisbury, 1973) and composition of Mars (Hunt, Logan and Salisbury, 1973). Wright (1976) used these measurements, among others, to develop an empirical model for the absolute infrared flux emitted by Mars that was used to calibrate far-infrared sensors.

A literature search and assessment by Cecil et al. (1973) indicated that Venus and Jupiter might also be suitable as infrared calibrators. A 50" balloon telescope, built by Tufts, was flown in July 1974 to measure the absolute irradiances from these planets, from which Logan et al. (1974) derived disk integrated temperatures. However, the observed spectral content of the objects compromised their value for calibration. On the other hand, the suitability of asteroids as infrared calibrators has been discussed by Müller and Lagerros (2002) and Price (2005). Earlier, Chapman and Salisbury (1973) compared the AFCRL spectral library to the observed spectral reflectivities of asteroids in an attempt to identify the surface mineralogy and speculated upon the reasons why a better correspondence was not found. Price (2004) reviewed the more recent attempts at matching laboratory and asteroids spectra.

The Spectroscopic Studies Branch was formally disbanded on 30 June 1976. The people in the group were laid off under a reduction in force and I was asked to dispose of the residual equipment. The Mauna Kea telescope was transferred to the University of Hawaii while the mothballed 24" Boller and Chivans telescope at Hanscom was given to Phillips Academy, a preparatory school in Andover, MA. The two balloon-borne telescopes and platforms were offered to the Harvard/Smithsonian Astrophysical Observatory because Fazio et al. (1975) had a far-infrared balloon program in the mid-1970s. Giovanni Fazio expressed an interest but stipulated that AFGL also had to provide funds to fly these telescopes. Since lack of funds was the reason for giving the hardware away, I found a home for the telescopes with Mike Mumma at NASA Goddard Space Flight Center. Giovanni later admitted that the funding request was a bargaining ploy and that they would have been delighted to have the hardware. This was a pity as Mumma never used the instruments before they were surplused.

After leaving AFCRL, John Salisbury continued his distinguished career in infrared spectroscopy as it relates to planetary surfaces, including the Earth. He initially went to the Department of Energy, then the US Geological Survey and, finally, the Johns Hopkins University; he is currently a consultant. Graham Hunt went to the US Geological Survey where, unfortunately, his research in remote sensing of minerals associated with ore deposits was cut short by cancer. Lloyd Logan had a successful career at Perkin-Elmer, ending up as a senior manager. Peter Dybwad started his own company that manufactures easily transported Fourier Transform infrared spectrometers. Jack Salisbury (23 October 2003 e-mail) kindly supplied the information regarding the fate of the people in the Lunar-Planetary Branch.

The atlas of mineral spectra is perhaps the best legacy of the Lunar and Planetary Research Branch. However, the Branch's balloon-borne experiments were unique as they are the only successful mid-infrared astronomical balloon-borne program in the literature except for the marginal quality spectra to 7 μm from the first Stratoscope II flight (Danielson et al., 1964). Martin Cohen (9 January 2009 e-mail) noted that Ed Ney had unsuccessfully attempted a 20 μm survey during two University of Minnesota balloon experiments in the late 1960s – early 1970s. Mid-infrared astronomical measurements from balloons are difficult for two reasons. First, despite the large reduction in atmospheric molecular band absorption and in the emission from the residual atmosphere above the balloon (see Figure 13), the mid-infrared thermal emission from the telescope is still substantial as the telescope equilibrates with the stratospheric temperature of 250 – 260K. Thus, the observations are limited to the brightest sources – the Moon and planets. More subtle is that when the measurements were made, lunar and planetary radiometry and spectroscopy did not excite much interest in the astronomical community.

2.4. Additional References

This brief history of infrared astronomy during the 25 years after World War II focuses on the various efforts to broadly characterize the infrared celestial background which led to the next major advance in infrared astronomy – the AFCRL mid-infrared probe-rocket survey in the early 1970s. Several very good historical accounts exist that fill in some of the gaps in this Chapter. The Low, Rieke and Gehrz (2007) article is an excellent complement in describing the prominent university based infrared programs in the 1960s and 1970s. Dave Allen's (1975) *INFRARED, The New Astronomy*, is an iconoclastic early history of infrared astronomy and is particularly useful in describing the detectors and observing techniques. Barnhart and Mitchell (1966) and Price (1988a) chronicle the often less well known 'firsts' in infrared stellar astronomy up to the mid-1960s and late 1980s, respectively. Sinton (1986) briefly highlighted selected

research between 1868 and 1960 with some details on how the early infrared astronomers separated the infrared from shorter wavelength radiation before the invention of interference filters. He further provides some details on the early efforts to define the infrared spectral transmission of the atmosphere and acknowledges the little heralded pioneers in the field such as Arthur Adel, who spent his career measuring the infrared atmospheric transmission/emission; he is credited with discovering the 20 μm atmospheric window (Adel, 1942). Particularly instructive for their historical context are the detailed assessments and conferences that review the then state-of-the-art in infrared astronomy. Augason and Spinrad (1965) appraised the technology extant in the mid-1960s for the NASA astronomy committee to “*...assess the possible applications of space techniques to this field.*” Conferences that discussed this emerging research field were: the June 1963 Liege conference on *Infrared Spectra of Astronomical Bodies*, the Goddard 1967 *Infrared Astronomy* conference (Brancazio and Cameron, 1968) and the 1967 conference *A Discussion on Infrared Astronomy* proceedings published in the 1969 *Philosophical Transactions* volume 264. Many of these meetings presentations described works in progress and, as such, contained detailed descriptions of instruments and observing procedures that are usually abbreviated in journal articles.

2.5. Personal Recollections

Freeman Hall hired me to work at ITTFL in June 1963. Freeman was an amateur astronomer who was able to carry his passion into the workplace although his primary interest, and PhD, was in atmospheric physics. Unfortunately, I had lost contact with him while I was at UCLA and, thereby, missed the opportunity to participate in his initial survey. However, I began working for him just as ITTFL approved his proposal to build a new, more sensitive radiometer with IR&D funds. My first task was to oversee the construction of the survey instrument. Freeman had been impressed by a *Sky and Telescope* article describing Harold Johnson’s all aluminum telescope that had been built specifically for infrared astronomy at the University of Arizona. Freeman obtained the blueprints for the 60" mirror from Johnson and scaled the design a centimeter to an inch. The second attempt at casting the mirror was successful with the minor voids in the blank being fixed by simply drilling out the blemishes and filling the voids by welding. The resulting 60 cm aluminum blank was much lighter than an equivalent sized glass mirror, which made the finished telescope much more portable, an objective of the program. The weight saving also permitted the use of a commercial 12" Newtonian mount for the telescope. The mirror was ground, polished and figured by Tinsley Corp., outside of San Francisco.

After joining ITT, I enrolled as a part time student in the Physics Masters degree program at Northridge State College in the fall of 1963 with the hope that I could eventually get into a PhD Astronomy program somewhere. However, toward the end of the fall, the assistant dean of the Ohio State graduate school called to inform me that OSU had, indeed, received my application but erroneously forwarded it to the Agronomy department for evaluation where it had languished in a drawer until being discovered months later and returned to admissions for proper routing. The admissions official indicated that it was too late for me to enter for the fall term and suggested that I probably wasn’t interested in OSU because of the delay. I said that I was, indeed, interested. The dean recommended that I contact Walt Mitchell, an OSU astronomy professor who was doing solar research at Mt. Wilson at the time, to arrange an interview. I explained the opportunity to Freeman and he generously offered to accompany me to the interview. We drove up the mountain on a drizzly morning to meet with Walt. The weather was damp and overcast with the first moisture the San Gabriel Mountains had received in some time,

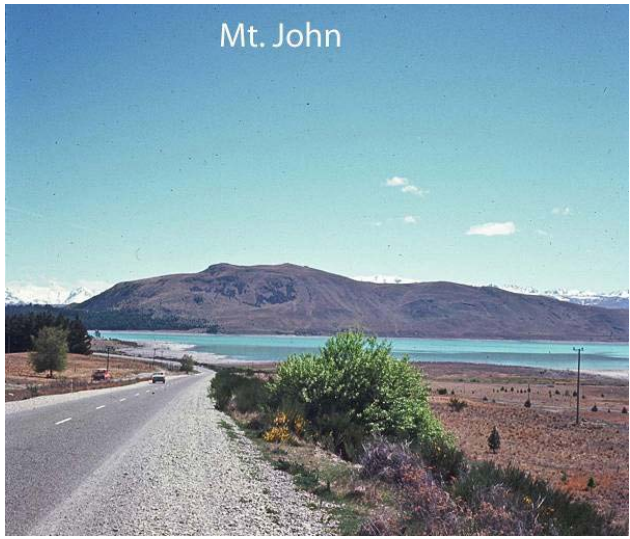
which allowed the observers time off so we were the only ones on the mountain. The facilities caretaker called us about an hour into the interview urgently asking for assistance. A small private plane had crashed into the trees at the top of the ridge and was ablaze, threatening to ignite the tinder dry forest. We hurried to the spot and I in my one and only suit straddled the headless body of the pilot to shovel dirt onto the burning plane.

Walt agreed to take me on as a graduate student and I was given a research assistantship to work on the ARPA funded Eastman-Kodak sub-contract to OSU to measure the infrared properties of astronomical objects. Stellar observations at 2.2 and 3.5 μm already had been obtained by this time and the unsuccessful effort to observe at 10 μm was underway.

I left for OSU shortly after Christmas to start the January 1964 winter quarter, thus, missing the introductory classes for two of the requisite yearlong courses. The department permitted me to take the second quarter of statistical astronomy on the premise that if I passed it was assumed I had to be proficient in the material for the first course. The OSU Astronomy department provided a rather good graduate education at that time with two years of interdisciplinary graduate courses being required to qualify for a degree. I took molecular spectroscopy from K. Narahari Rao, stellar atmospheres and classification from Phillip Keenan, and radio astronomy from John Kraus and Dr. H.C. Ko; all of whom were noted for some aspect of their field: Rao in molecular spectroscopy, Keenan for the Morgan-Keenan two-dimensional spectral classification scheme and Kraus and Ko for the first sensitive large area radio surveys.

The course requirements also included a year each of graduate instruction in physics and mathematics, and I greatly benefited from both. A senior professor taught the first two trimesters of the math course, which were among the best math courses that I have taken. He taught matrices in a clear fashion using examples from quantum mechanics and general relativity for tensor analysis. Unfortunately, an individual who seemed not to find reward in teaching replaced him for the third quarter. We were supposed to cover matrix theory and differential equations and their duality through quantum mechanics but spent all but the last week on the matrices. The final was an open book, take home exam worth the equivalent of four tests. The problems seemed strangely familiar; then I realized that they were taken from Coddington's *Differential Equations*, the same book from which I had attempted to solve every problem. I found the book in the library and checked it out: after all, the test was open book and open resource and the answers to every other problem were in the back of the book. I was able to solve all but one problem. I got through the first half of that problem before I got bogged down. Fortunately, this was one of the problems that had an answer in the back of the book and I worked the problems backward from the answer. I wasn't quite able to quite meet where my development from the beginning left off and had five points taken off for the disjoint.

Meanwhile, the ITT survey telescope had been completed and I returned in the summer of 1965 to begin surveying the northern Galactic plane, which was high in the sky, from an observatory platform atop the company's roof. A portable radio kept me company through the night with which I regularly pulled in the classical music station in San Francisco, listened to plays broadcast by the local PBS Station and kept up to date with on the scene reporting from the Watts riots. We detected a number of objects in the northern Galactic plane, all of them known and none were extended. However, during that summer, Freeman learned that Robert Leighton and Gerry Neugebauer were mapping all the sky available from Mt. Wilson in the near-infrared. Freeman and I paid Gerry Neugebauer a visit during which he showed us a room full of stacks of eight channel medical strip charts that comprised the raw data from the survey. The survey was well underway at this time and it was evident from our discussion that the larger, more sensitive



Caltech instrument well outperformed the ITT telescope. Since the ITT system was more portable, Freeman decided that the best return for the investment would be to complement the Caltech survey with southern hemisphere coverage. Bateson (1962) had published a *Sky and Telescope* article on the Mt. John observatory in New Zealand, the southernmost observing site in the world at that time. The observatory was a joint endeavor between the Universities of Canterbury and Pennsylvania. Freeman decided this was the place to go and set about modifying the AFCRL contract to cover a foreign field expedition.

I returned to OSU to obtain a Masters degree and came back to ITTFL after marrying Virginia (Ginny) Ann Terpary in June 1966 to prepare the survey radiometer to be shipped to Mt. John. It took the summer to obtain the necessary country clearances, then to pack and ship. The equipment was sent by sea, which took another six weeks. In the meantime, we visited the New Zealand consulate in Los Angeles to obtain visas since we would be staying longer than the six months permitted by the government for entering the country on simply a passport. The consul gave us a perfunctory briefing about his country and, after learning of Ginny's undergraduate major, spent the remainder of the hour talking to Ginny about her academic opportunities in New Zealand. Ginny had majored in Biology and did so well that she was permitted to take graduate courses in Botany and Plant Pathology. Since the New Zealand economy was, and is, primarily agrarian, the consul was most enthusiastic as to what Ginny could do in the country.

We arrived in Christchurch late in the New Zealand spring of 1966. Ginny enrolled as an agricultural microbiology graduate student in the Lincoln College, University of Canterbury and I went to Mt. John to set up the telescope and dome (Figure 10). Mt. John is located in the middle of the New Zealand's 'outback' between the Southern Alps to the west and the lower Two Thumb range that ribbed the east coast of the Southern Island. The site was almost due east of Mt. Cook, the mountain on which Sir Edmond Hillary honed his early climbing skills. On many clear evenings I watched Venus set behind the Southern Alps, flashing green just before it disappeared. Interestingly, I did not see the green flash for the setting sun. The survey was conducted just before solar maximum and enhanced airglow often made the sky milky and the Aurora Australis was frequently visible as muted pearly

searchlights but, unfortunately, no curtains of color. Stepping outside the cramped dome that contained the survey instrument to admire the grandeur of the southern Milky Way or searching the aurora for a hint of color, you could feel that you were the only one around for miles. That is, until a cough a





Lake Tekapo - Village and Hydro plant

Observatory Bamberg photographic cameras for discovering and monitoring variable stars, a semi-autonomous weather station and a 16" conventional telescope on loan to the Observatory from Frank Bateson, an amateur variable star observer who ran the facilities. Bateson had conducted the sight surveys that selected Mt. John for the observatory site and was instrumental in interesting the University of Pennsylvania in participating in the site development.

The weather was not good at Mt. John in 1966/67, especially when strong weather fronts moved through, which made the whistle of the wind around the observer's quarters a frequent companion. The wind was especially strong on the spring day in 1967 that the University of Canterbury held an open house. The anemometer was pegged at the 120 miles per hour maximum on the dial and one could barely walk between the buildings. One of the professors had brought his wife and three year old son to the open house. The wind lifted the poor youngster off his feet and he was prevented from being blown away only by the tight grip by his parents, one on either of his hands.

Since the survey could operate in somewhat marginal conditions, I was able to work a third of the nights. However, only about 25% of the nights were really of decent to good photometric quality. The weather was somewhat better in the winter and since Mt. John was at 45° southern latitude, the winter nights were long. Thus, because I was able to take data well

few feet away reminded you that sheep had the run of the place.

Mt. John was situated next to the glacial fed Lake Tekapo and the ground up rock in the water colored the lake a powder blue. The local economy of the small Lake Tekapo village was essentially that provided by the surrounding sheep stations and the Tekapo dam and the hydro-plant at its outlet. There was a small motel and pub that served as the watering hole for the area, a place where I spent some amount of time. The tourist attraction was a tiny stone church with windows that looked out over the lake.

Mt. John had a set of Remeis



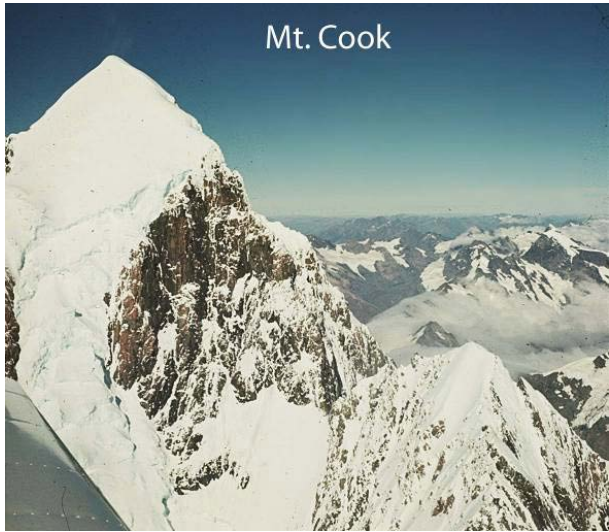
into twilight, I could observe for up to 14 hours in the winter. While waiting out the clouds, I looked up the site survey records and the logs from the previous four-year period of Mt. John operations and found that this dismal record was the norm (see also Hearnshaw, 1992). To be fair, Bateson (1962) had noted that meteorological records and the prevailing weather patterns over New Zealand did not meet the original goal of 200 clear nights a year for choosing a site. However, the 25%



Pennsylvania during the 1966/67 academic year. He was trying to obtain photometry on eclipsing binaries that had periods of about a day, or multiples thereof. New Zealand is roughly on the International Date Line and, therefore, is five to eight hours from the US and 12 hours from Europe. Thus, the site provided critical complementary phase information on these eclipsing stars. Bill held the distinction of being the first OSU astronomy department PhD graduate and he became associate dean of the OSU graduate school upon his return from New Zealand. Bill also taught me cribbage to while away the time waiting for the clouds to clear and to make it interesting he suggested playing for a penny a point. Needless to say, he cleaned my clock.

I had a routine under which I would spend 10 days at Mt. John and come back to Christchurch for four. Ginny and I had rented half a house in a suburb of Christchurch from a Canadian. Since insulation and central heating were innovative ideas to the country in the mid-1960s, I could see daylight from the couch in the living room through a crack between the wall boards. Although the winters were not excessively harsh, a few days were below freezing, we would often wake up in the winter with frost on the inside of the bedroom windows from the moisture in our breath. The landlord said that he used space heaters the first year he was in the country to keep his house toasty warm with the result that the electric utility sent an investigative team to find out what was wrong with the wiring of his house since his first months' bills were astronomically high. Besides an electric space heater, we also had small coal fireplaces in the bedroom and living room and we soon found out why using cheaper soft coal was a bad idea. Another thing that took some getting used to was that the soap was made from sheep fat renderings, which caused the flat have an aroma of sheep fat on damp days.

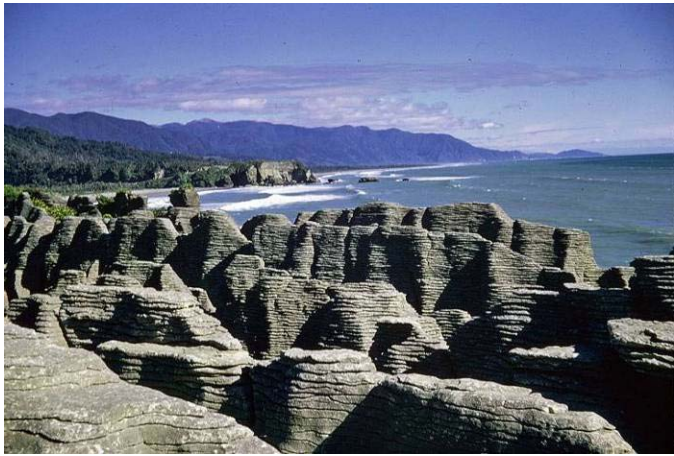
New Zealand is a beautiful country with a wide range of terrain and climates packed into an area smaller than California. It has the Southern Alps, fjords, glaciers and volcanic regions as well as exotic flora and fauna. And, overall, the people were genuinely friendly. However, there were puzzlements. For example, I was forced to pay import duty on a small number of transistors and other electronic component I had ITT ship to me to repair a problem with the radiometer and no amount of arguing would dissuade the customs official. On the other hand, the Home Office extended my visa without a problem, readily accepting my explanation that I was employed in the US, paid in the US and that I was not taking an employment opportunity away from a New Zealander by working for a New Zealand company. Indeed, Ginny and I subsisted entirely on the contract per diem for the field expedition as my salary was directly



We did some sightseeing the four consecutive days I took off every two weeks but it was limited owing to the demands of Ginny's graduate work. One of Ginny's classmates was a private pilot and we arranged to have him fly us around the South Island for a weekend if we paid for the gas. We set out from the Christchurch airport Saturday morning, flew over Lake Tekapo and around 12,419 ft high Mt. Cook at an altitude a little above the Piper Cherokee's 10,000 foot ceiling. We flew to the Queenstown airport and had lunch in this resort town. Because of an advancing weather front, the pilot decided to fly over the Eyre Mountains to our final destination, Lake Te Anau, instead of the usual, longer route through the mountain passes. The leading edge of the front had moved in by the time we reached altitude and the mountain range. The plane bucked in the strong frontal winds as we flew between the lower edge of the broken cloud deck at ~10,000' and the peaks of the razorback ridges at 8,500 to 9,000'. The nose of the plane kicked up as we caught the updraft from a ridge and the engine wound up toward stall while the pilot fought frantically to trim the plane, steer and reduce the engine revs. Just as the pilot stabilized the plane we would hit a downdraft and the pilot again fought to maintain equilibrium. With only a thousand feet between the bottom of the clouds, which also was the plane's altitude limit, and the tops of the ridges, I thought sure the plane would stall out and auger in before the pilot could recover. I just hoped that we would hit on the down-slope side of the ridge. That way we might have a chance over a head-on impact with the upslope. I figured as long as we were going in, I might as well take a couple of pictures since I was in the front seat with the pilot while Ginny and a friend of the pilot were in the back. Ginny later said that she was sure we were going to crash because the pilot had streams of sweat coursing down his neck.

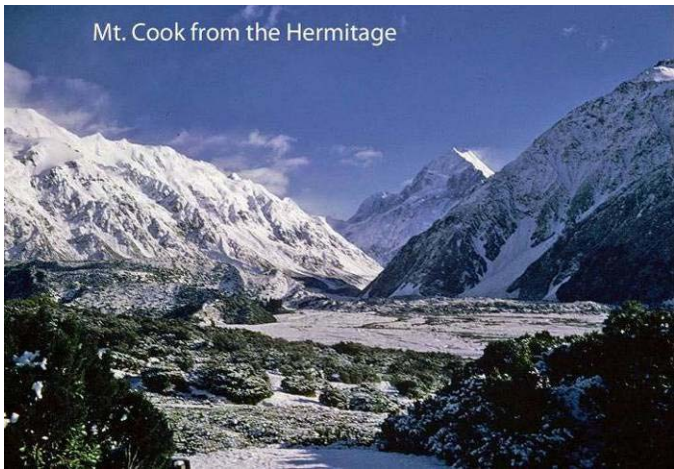


deposited into a US bank account, rather than bringing it into the country, in order to avoid possible tax claims by the New Zealand government, which would have amounted to 50% of my income. Every once in a while, the ITTFL comptroller would try to clear my outstanding travel advance that I had used to get set up in the country by withholding the per diem. On a couple of occasions, I had to get John Camus (a cousin of Albert) to straighten out these arbitrary bureaucratic decisions, which took about a week to ten days. John became the ITT section chief after Freeman Hall left to join the Douglas Advanced Research Laboratories in 1966.



smoothly as possible; the experience left me as uneasy flyer ever since. I read in Monday's Christchurch paper that the Otter pilot ran off the Dunedin runway upon landing later on Saturday and broke his leg; either the weather or the Scotch had gotten to him.

The ITT contract provided for two contingency trips in case we needed a technician for instrument troubleshooting and repair. Fortunately, Bill Protheroe was kind enough and knowledgeable enough to correct the few problems that arose. I had hoped that I could use the funds saved to extend the survey beyond the nominal one year. Ginny had completed her course work and had started her Masters research on improving the tolerance of clover for the acidy soil in the New Zealand tussock country. Unfortunately, ITT had just brought in Harold Gineen as president to make the company more profitable and the first thing he did was raise the indirect costs to exorbitant levels and making the charges retroactive to the beginning of the fiscal year. The company was forced to reduce the rate but only after my reserve was wiped out and the contract was put in the red. I was told to pack up and leave the country within a week. Fortunately, I was able to appeal to the good nature of the appropriate New Zealand officials to get the equipment packed and on the boat within the allotted time. This was quite an achievement as the Kiwis are rather laid back and have an attitude of 'she'll be right, mate,' to admonish one not to worry, if something doesn't get done today, it will tomorrow or some time.



grandeur of Mt. Cook centered in the window. We returned to Christchurch just in time to catch the overnight ferry to Wellington to join a bus tour of the North Island that we booked for the week before I left for the US.

was talking to the field manager about the conditions. A rather obese individual who was seated at the table drinking Scotch was making fun of us for being afraid of a little rough air. This fellow was a local cargo pilot who had come through the pass an hour earlier in a deHaviland Otter, a 1930s generation cloth covered plane. The next day, our pilot offered to show us some more of the sights during our return flight to Christchurch but I declined, wanting to get back to Christchurch as fast and as

Before I left New Zealand, we decided to take a couple of weeks to see as much of the country as we could. We had leased a car so Ginny could drive the 10 miles or so from the house to Lincoln College. So, we drove around the South Island, visiting the West Coast, stopping at the pancake rocks at Punakaiki and trekking up the Fox glacier. We stayed at the Hermitage hotel the second night of the trip, arriving after dark on a stormy evening. Opening the room curtains the next morning, we were greeted by



We caught the tour bus in Wellington the next morning. The tour hit all the major tourist spots on the North Island: Lake Taupo, the thermal areas at Rotorua, a boat drift through the glowworm caves at Waitomo, up 90 mile beach (actually only 67 miles long) above Auckland to the most northerly point on the island then down to the Bay of Islands.

We had to take a motor launch to the Whairangi fishing lodge in the Bay of Islands. The

lodge was in a deep natural harbor with a very narrow inlet flanked by volcanic teeth. As we got off the boat, Ginny failed to grip the camera, which fell overboard into about eight feet of water. I changed into swimming trunks and went diving for it in the bitterly cold sea water, much to the amusement of the Kiwis on the tour with further bizarre American antics. I immediately put the camera into fresh water hoping to save the film, but the pictures, alas, were ruined.

We spent the last night in Russell, a sport fishing resort town and wound up in Auckland the next day. I saw Ginny off to Christchurch that afternoon to finish her Master's degree and I returned to the States. John Camus sent me to see Russ Walker to present the New Zealand results to him and to solicit additional sponsorship. Russ was not interested in further funding ITTFL, so I probed for possible job opportunities, which were not available. I wrapped things up at ITT and returned to OSU late in the fall quarter to prepare for general exams.

I took general exams in the winter quarter of 1968, passed and advanced to the two hour oral portion. I thought I had done well enough on the oral exam but became seriously concerned when the committee caucus stretched to well over an hour. When it broke up I was told that I had, indeed, passed with little discussion but that the committee spent most of the time arguing whether the New Zealand survey results were sufficient for my thesis. The committee decided this research was inadequate and lacked sufficient area coverage or sensitivity to produce original enough results for a thesis. In hindsight, this was an appropriate position given the much better quality of the data from the unpublished southern extension to the Caltech survey. However, it did leave me in need of a thesis topic. An opportunity briefly arose early in 1968 when Gerry Neugebauer contacted Walt Mitchell, my thesis advisor at the time, to inquire if I would be interested in taking the TMSS instrument to Cerro Tololo, Chile to survey the southern hemisphere. I readily agreed. However, nothing came of this and I had to seek another topic.

I settled on developing a spectrophotometric scheme to classify stars using the strength of their infrared molecular features. Not coincidentally, the idea was similar to what Bob Wing had done for his thesis in the visible and very near-infrared and I changed thesis advisor from Walt Mitchell to Bob Wing. Since the features that I was interested in were in the near-infrared (1 – 5 μ m), I planned to resurrect the Eastman-Kodak/OSU instrument for the measurements, which would be supported by modeling and analysis. I unsuccessfully tried to get the photometer working for a couple of months before I found out that the best detectors and the photometer upgrades had been returned to Eastman-Kodak. So, I had to revamp the thesis to one that relied heavily on models with comparisons to the very meager available data, mostly the balloon-borne near-infrared spectra published by the Princeton group (Woolf, Schwarzschild and Rose; 1964). Without observational confirmation, the classification scheme I developed was merely a proposal, although some support for it came when Baldwin, Frogel and Persson (1973) proved out the suggestions at the long wavelength side of the 2.2 μ m atmospheric window.

Looking toward the future, I attended the December 1968 meeting of the American Astronomical Society at Austin Texas that featured an infrared astronomy session in hopes that Russ Walker would be there and I could set up a job interview with him. At that time, it was proving difficult to obtain academic positions by the traditional route in which one's thesis advisor used his/her contacts to line-up interviews for likely positions. Being a poor grad student, I didn't have the air fare to go the meeting. Fortunately, Brother Frank Dam agreed to fly us to Austin if we paid for the gas and plane rental. Frank was a Jesuit with an order based in Dayton and a fellow grad student who had a private pilot license and access to a Piper Cherokee. Prof. George Collins decided to go with us and kicked in half the cost from the money he received from the department to attend the meeting. Frank, another grad student and I flew to the OSU airport where we picked up George and off we went. The weather was good but with a enough of a headwind that it took over ten hours to get to Austin, where we wound up circling the Austin VORTEC transmitter in darkening skies trying to spot the airport. After about 10 minutes Frank located the airport and headed for it. He was so tired from 10+ hours of flying that he came in high. Although the tower waved him off, he came in anyway and we fortunately stopped short of the end of the runway. This was not a very comfortable trip for me given my experiences in New Zealand; and George decided to take a commercial flight back to Columbus.

Russ had just started the probe-rocket based sky survey program at AFCRL. Frank Low and Gerry Neugebauer were aware of this effort and, Frank at least, knew that ARPA was funding it. Russ, Frank, Gerry and I went to lunch during the meeting at which time Frank and Gerry discussed their proposals with Russ for ground-based mid-infrared surveys. I was included because Russ had asked me to join AFCRL to support the rocket-based survey, and I agreed. Both Frank and Gerry argued that the ground based surveys would be a backup in case the rocket survey was not successful. Frank was on record as questioning the technical maturity of space instrumentation for rocket-borne infrared observations (see his comments after Harwit's presentation in Brancazio and Cameron; 1968). He was also of the firm and correct opinion that significant improvements could be realized at that time in the sensitivity of ground-based infrared measurements with careful attention to telescopes and observing procedures.

I returned from the meeting a lot faster with a quartering tail wind and a job offer at AFCRL. The necessary paperwork was filled out, processed and I was asked to start in the spring of 1969. However, I was still trying to define what was acceptable for my thesis research and delayed reporting until July. Several of the faculty gave me the same admonition as they had when I left for New Zealand: that I would never finish if I left before completing my degree. They further argued that delaying the research for the degree could cause me to run afoul of the new department policy that a graduate student had seven years after passing the general exams to complete the degree, otherwise he/she would have to retake the exams to demonstrate currency in the field. This policy was instituted, in part, to coerce Ken Kissell into finishing. Ken, a 1950s contemporary of Bill Protheroe, worked for the Air Force Aerospace Lab in Dayton and had obtained a lot of very good data, but was taking time in writing up the results, finishing in 1969 (Kissell, 1969). I was able to complete my degree in December of 1970 (Price, 1970).

On July 4, 1969 we loaded up a U-Haul trailer, having put the baby grand piano into storage, and set off for Boston, arriving two days later. I called Russ to tell him we were in and he and his wife, Drizz, put us up for a couple of weeks until we found an apartment. I started working in Russ' Infrared Physics Branch in the Optical Physics Division of the Air Force Cambridge Research Laboratories on 7 July 1969.

3. INTO SPACE

Origins of space-based infrared astronomy can be traced to the technology development under ARPA's Project Defender and Project Order 1366, the Army Ballistic Missile Defense Agency and the Air Force efforts that began in the mid-1950s. A critical late 1950s advance was the reduction of noise inherent to the detector-preamplifier circuit to the point where background noise from self-emission limited the performance of photo-conducting detectors (Jamieson, 1984). Such a device could then be sufficiently cooled that background photon noise from the sensor components surrounding the detector limited performance. Background noise is due to random fluctuations in the photon stream intercepted by the detector and is called Poisson noise after Siméon Denis Poisson, the 18th century French mathematician who determined that the statistical uncertainty or noise in counting N events, such as photons, was the square root of N. This is known as background limited infrared performance or BLIP. Further increases in detector sensitivity could be realized by reducing the extraneous photon background from the detector surroundings with field stops to restrict the detector's field of view to just the measured area and cooling the detector cavity, the field stops and detector. Swift (1962) discusses these gains and, at the end of his article, is the first to suggest that a cooled sensor operated above the atmosphere could be orders of magnitude more sensitive than a ground-based instrument.

The Department of Defense preferentially chose to use photoconducting detectors because they had faster response and were more sensitive than the thermocouples and pneumatic Golay cells in early use. Also, compared to the Frank Low (1961) bolometer, the best infrared device in the 1960s, photo-detectors were much more robust and could more easily be configured into arrays. Since a bolometer measures the small increase in temperature of a 'blackened' detector produced when it absorbs a photon, the temperature change and, hence, sensitivity is inversely proportional to the mass of the detector. Also, the detector must be thermally isolated from its surroundings, which means these components must also have low mass. The small mass of the components makes the bolometer a delicate device.

Table 3. Parameters of Photoconductors used for Infrared Astronomy

Detector	Energy (meV)	λ_c (μm)	Typical Temp. (K)	Detector	Energy (meV)	λ_c (μm)	Typical Temp. (K)
PbS	440	2.8	77-300	Si (PV) CCD	1100	1.125	215-300
InSb	200	6.25	12-77	Si:Ga	72	17	6-10
				Si:As	54	23	4.2-10
Ge:Hg	91	13.6	25-60	Si:P	45	28	4.2-10
Ge:Cd	55	22.5	6-10	Si:Sb	43	29	4.2-8
Ge:Be	24	52	2-4.2				
Ge:Ga	11	113	2-4.2	HgCdTe*	480	3	77
Stressed Ge:Ga	6.2	200	1-3	HgCdTe (PV)	88	14	35-90

* Back illuminated array on a sapphire substrate; PV = photovoltaic

Table 3 lists the properties of some of the detectors used for infrared astronomy that are referenced in this report. The first column designates the material, the second the band gap energy in milli-electron volts, the third lists the cutoff wavelength of the response of the material [$\lambda_c = 1240 \mu\text{m}/E(\text{meV})$] and the last column contains the typical range of operating temperatures for the detector. A general correlation is evident in that the smaller the band gap energy, the

longer the wavelength of the response and the lower the operating temperature. The band gap in blocked impurity band (BIB) silicon detectors is decreased by about 20% with a corresponding increase in wavelength. BIBs also eliminate a number of nasty non-linear effects that are discussed in Chapter 5. As noted in the Table, mechanical stressing Ge:Ga detectors reduces the band gap and extends their far-infrared response. The lead salt detectors are polycrystalline films while the other detectors in the Table are single crystals. The Ge:xx and Si:xx are extrinsic detectors whereas the PbS, InSb and HgCdTe are intrinsic detectors.

Table 4 quantifies the increase in performance that is realized by cooling the sensor and elevating the observing platform. The left hand columns of Table 4 show that the 8 – 14 μm background radiance, which is proportional to the number of photons on the detector, is reduced by about 10^5 by cooling the detector surroundings from room temperature to that of liquid nitrogen; the corresponding reduction in noise is a factor of ~ 300 . The atmospheric background is reduced with altitude as shown in the right hand columns of the table. The altitudes for the first three entries are typical for a mountain top observatory, high altitude aircraft and balloon platforms; the zodiacal background sets the ultimate limit at satellite altitudes.

Table 4. 8 – 14 μm Environmental Radiance

Temperature (K)	Radiance ^a	Photons ^b	Altitude (km)	Radiance ^a	Photons ^b
300	5.5×10^{-3}	3×10^{17}		10^{-3}	5×10^{16}
200	6×10^{-4}	3.5×10^{16}		10^{-4}	5×10^{15}
77	5×10^{-8}	3×10^{12}		10^{-5}	5×10^{14}
35	2×10^{-15}	1.5×10^5	space	2×10^{-10}	10^{10}

^a $\text{w cm}^{-2} \text{sr}^{-1}$

^b $\text{photons sec}^{-1} \text{cm}^{-2} \text{sr}^{-1}$

Placing an infrared sensor in orbit eliminates both the background from atmospheric emission and the molecular absorptions that restrict ground-based observations to atmospheric windows. Figure 13 shows the atmospheric transparency at three altitudes. The principal mid-infrared molecular absorbers are H_2O , CO_2 and O_3 and ground-based observations are confined to the atmospheric windows between these bands. The CO_2 bands remain opaque for aircraft platforms, while the other absorptions are significantly reduced at balloon altitudes, in which case OH emission becomes important. Also, as previously noted, the sensitivity of balloon-borne mid-infrared measurements is limited by the thermal emission from the telescope, not the atmosphere. Since a space-based system is above the atmosphere, the telescope can be cooled to the point that self-emission no longer limits the sensitivity. Under these conditions, the sensitivity of a modest sized instrument out-performs the largest ground based telescopes.

Furthermore, unlike in the visible, the infrared flux from an Earth orbiting satellite only weakly depends on solar illumination and phase angle. Specifically, the temperature of an Earth orbiting satellite equilibrates with the near-Earth radiative environment and the resulting passive emission peaks at 10 – 15 μm . Reducing the satellite's reflectivity in an attempt to mask its visible signature increases the LWIR thermal emission, as do internal heat sources such as power dissipated in the satellite electronics. It is difficult to actively reduce the infrared signature of the satellite as that requires insulation coupled with radiative or active cooling; and even then the gains are rather modest. For example, an object in an equatorial orbit with little or no internal heat sources will cool from a sunlit equilibrium temperature of $\sim 280\text{K}$ to about 200K while it is in eclipse, which reduces the 9 – 14 μm satellite irradiance by a factor 6 and that in a 17 – 25 μm spectral band by only a factor of four. Thus, an Earth satellite in eclipse is bright in the mid-

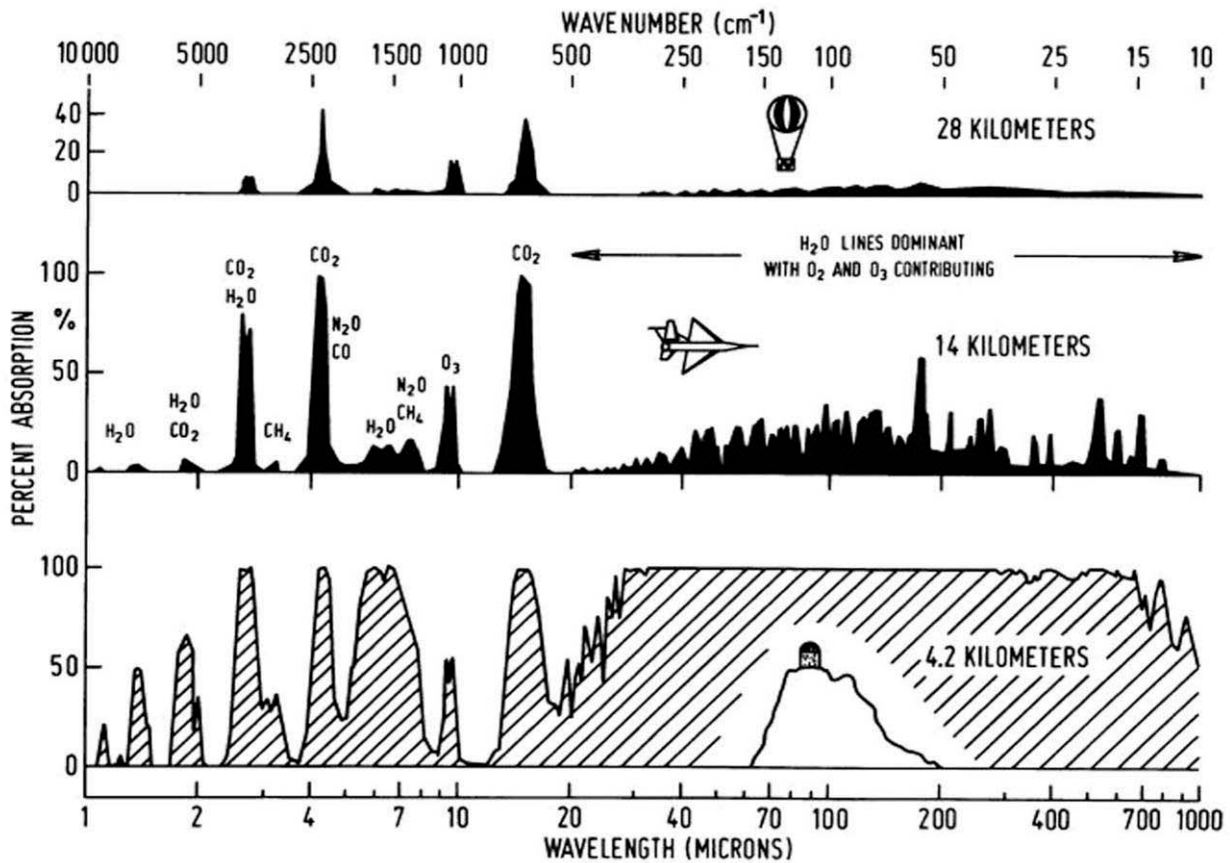


Figure 13. The atmospheric transparency at three different altitudes. (bottom) a mountain top observatory (e.g. Mona Kea), (middle) aircraft (e.g. the Stratospheric Observatory for Infrared Astronomy) and (top) balloon platforms. The major atmospheric absorption species are labeled. (Adapted from Harwit, 2003).

infrared (6 – 30 μm) but it is optically faint in the absence of sunlight. The result is that the infrared satellite signature is relatively insensitive to solar illumination conditions compared to the on – off visible signature as the target enters eclipse.

However, cryogenically cooled sensors are needed to realize the space-based infrared advantage and at least three aerospace companies were actively developing this technology in the 1960s. Lou Meuser, of the Air Force Avionics Lab, sponsored the early efforts in the Electro Optical Laboratory of the Autonetics Division of North American Aviation (later Rockwell Corp.) between 1962 and 1965. Initially, Autonetics developed aircraft based instruments, the first of which was a 25 cm steel sensor flown on a U-2 aircraft, for above-the-horizon observations of bright targets. More than 80 flights were conducted with these instruments between the 1966 program inception and 1972. Hughes also had an Airborne Infrared Measurement System in the mid-1960 and Aerojet Corp. in Azusa, CA built airborne cryogenically cooled infrared sensors, one of which was a forward looking infrared sensor (FLIR), dubbed the Model C19, that they advanced as a demonstration of technical capability.

These aircraft-borne instruments paved the way for space flights of cryogenic sensors. Hughes Aircraft Co. (HAC) in Culver City, California, built the Far-InfraRed Search/Track (FIRST) in the mid-1960s, one of several sensors for target signature measurements. FIRST was followed by other sensors based on the Hughes 6" (16 cm), helium cooled, beryllium, doubly folded Gregorian telescope design. These sensors had a variety of colorful acronyms: HI STAR,

FAIR (Fly Along Infrared), SCOOP and SOFT (Signature Of Fragmented Tanks), which became DOT (Discrimination Optical Testbed). FAIR was piggy-backed aboard other missions from the Western Test range, the first in 1970, and successfully demonstrated long range detection that measured infrared target signatures (Jamieson, 1995) while the five DOT tests were flown between 1975 and 1982; the single SCOOP Aerobee 350 flight failed. Collectively, these sensors flew about a dozen times between the late 1960s and the mid-1970s. Toward the end of the 1960s, the Autonetics group built a cryogenic bench test liquid helium cooled sensor with 4" optics, the AFIRST (Advanced FIRST), then a modified AFIRST, which was flown in 1969 by the Army to measure target signatures. Thus, a fair amount of sensor development had been done before AFCRL began the sky survey.

3.1. LO-STAR (Stellar Radiation Sensor - SRS)

Little was known about the mid-infrared background in the 1960s that a space-based surveillance system would see, let alone how these backgrounds would affect the proposed system's ability to detect and track a target. ARPA had funded the Eastman-Kodak/Ohio State effort to evaluate the infrared stellar background under Project Defender, and the Air Force sponsored the infrared surveys of Freeman Hall. However, these early efforts had little success in the mid-infrared ($\sim 10 \mu\text{m}$) and the stellar photometry by Caltech and the Universities of Arizona and Minnesota only indirectly addressed these questions. Although ARPA transferred the various Project Defender programs to the newly created US Army Ballistic Missile Defense Agency (ABMDA) in 1967 to have them concentrate their efforts toward developing infrared technology to measure the signature of re-entry vehicles late in their mid-course trajectory just before and during atmospheric re-entry, ARPA also continued the technology push for infrared applications in space under the newly created Project Order 1366. Meanwhile, the Air Force was also engaged in an ambitious program complementary to Project Order 1366 to develop the technology for infrared space surveillance and ballistic missile defense. Late in the 1960s, ARPA provided funds to the Air Force Space and Missiles Systems Organization (SAMSO) at the Los Angeles Air Force Station to develop sensors to survey the sky from sounding rockets flown by Russ Walker's Infrared Physics Branch in the AFCRL Optical Physics Laboratory.

Russ Walker and his team had experience with probe-rocket based infrared experiments, having flown an Aerobee 150 in the mid-1960s to measure the Earth's infrared horizon (Walker, Cunniff and D'Agati, 1966) and an upgrade of this experiment, the Minute of Arc Probe (MAP), from Fort Churchill in August 1968 to measure the $15.5 \mu\text{m}$ vertical profiles of atmospheric CO_2 , ozone at $9.6 \mu\text{m}$ and water vapor at $6.3 \mu\text{m}$. In 1968, Maj. Bob Paulson, at ARPA, funded Walker's group to conduct an LWIR survey of the sky. To accommodate ARPA's desire for proof-of-concept flights, Russ added a payload section above the MAP radiometer to carry the Autonetics Stellar Radiation Sensor (SRS), a modified AFIRST instrument (Figure 14). The SRS was a small Cassegrain telescope with a 4" (10 cm) diameter aluminum primary mirror with $\sim 58 \text{ cm}^2$ of clear aperture. A single linear array of six Ge:Hg detectors spanned a $\sim 1^\circ$ cross-scan field, and each detector subtended 1.5×3.1 microradians (μrad), or $5' \times 10'$. The detectors were filtered for an effective wavelength of $\sim 12 \mu\text{m}$ with a bandwidth of $\sim 2.4 \mu\text{m}$ and the entire sensor was cooled with liquid neon. Two successful flights of this experiment were conducted in 1970 that provided important technical 'lessons learned' for the actual background survey flights.

MAP I was flown on 6 February 1970 from Launch Complex 32 at the White Sands Missile Range on the Aerobee 150 M-1 motor with a VAM booster. The combined payload

weighed 174 kg and was lifted to a peak altitude of 131 km, which afforded 240 seconds of data acquisition. The MAP II experiment was flown on 26 July 1970 on an Aerobee 170 motor with a Nike booster. A faulty g-switch shut down the burn 5 seconds early on this flight, lowering the peak altitude to \sim 125 km, 50 km below anticipated. Afterward, the final MAP experiment was flown on a Castor Lance from the Brazilian Lancamento De Barreira do Inferno range in May 1973. Without the SRS and a recovery system, this experiment reached an altitude of 569 km.

On both LO-STAR⁵ experiments, the SRS was deployed to a zenith angle of \sim 46°, the payload was spun up to an angular rate of 8.85 °/sec, and then stopped for a background measurement after a 390° azimuth scan was completed. The SRS was then stepped 1° and the payload spun up again. For MAP II, 4° steps were used in order to span a wider range of deployment angles. Being a prototype, the SRS had its problems, most notably holding a vacuum. In the field, such leaks were ‘fixed’ with Glyptol, a red sealant, which earned the telescope the soubrette ‘the Glyptol special.’ Twice for each experiment we had to return from the field and send the sensor back to Rockwell to be reworked (third attempt was twice the charm). Lou DeBottari (private communication), the Rockwell senior SRS program manager, believes that “*... the damned Lockheed radiometer ... vented helium into the nosecone causing the SRS sensor to lose vacuum ...*”; the problem was solved by purging the payload with dry nitrogen. However, we did notice an uncanny timing: that when Lou arrived in the field, the sensor would spring a leak. Needless to say Lou was ragged about this.

MAP I scanned perpendicular to the winter Galactic plane and passed through the Draco – Ursa Majoris region in which Feldman, McNutt and Shivanandan (1968) had reported seeing very bright IR sources, which we failed to confirm. While a dozen or so of the detected point sources were tentatively associated with celestial objects, only the purported observation of the Orion nebula was reasonably secure (Walker and Price, 1970). However, the SRS did obtain an empirical upper limit to the LWIR cosmic background (Walker, 1971). The diffuse background flux was determined by measuring the impedance of one of the detectors, which was calibrated against an infrared emitting diode inside the sensor. Since the cosmic background was the difference between the observed value and extraneous sources of radiation, Russ developed a side-lobe model for the sensor and determined the model parameters from the background measurements as the SRS was deployed to the initial zenith angle. This was the first definitive quantification of the problem that off-axis radiation presents to an infrared sensor in space.

The LO STAR demonstration flights were invaluable for defining the technical problems that had to be addressed in order to successfully conduct an infrared survey with a cryogenically cooled telescope on probe-rockets. For example, the payload was supposed to capture and maintain the roll axis to within 1° of vertical. The star mappers indicated that the tip-off was more likely 5° and that the rotation pole may have wandered during the scan. The star mappers were small visible telescopes with a phototube that observes stellar transits through a focal plane mask shaped like the capital letter ‘M’ with a vertical slit in the middle. The roll rate of the payload may be derived from the stellar transit times between slits and the pattern of the relative spacing of the transits between the successive slits gives information on the tip-off angle of the pole of rotation from zenith; see Price et al. (1978) for details. Since the tip-off with respect to

⁵ Although Autonetics (a name derived by combining the Autonavigation and Cybernetics divisions) labeled their instrument the Stellar Radiation Sensor, the program was designated LO-STAR. The designation XX-STAR derives from the D* (D star) figure of performance for detectors; the larger the value, the better the performance. Hence, the LO-STAR program had an instrument of modest sensitivity; the HI-STAR instruments had much improved performance and the HI HI STAR was to be the most sensitive of all.



Figure 14. The MAP II payload after recovery. The MAP sensor is at the right in the payload. In the middle is one of the small optical telescopes (star mappers) used to determine the pointing of the payload. The SRS is at the upper left and, as may be seen, was not fully stowed for recovery. A jackscrew in the payload removed the SRS cover at altitude, then a one-axis gimbal in the payload deployed the sensor to a set of pre-programmed zenith angles and the payload was rotated to sweep the sensor field-of-view across the sky.

the plane defined by the center slit of the star mapper is reasonably well determined, but not in the orthogonal direction, the MAP experiments used three star mappers separated by $\sim 120^\circ$ in azimuth to try to improve the knowledge in tip-off angle. However, observations from the three star mappers were inconsistent and the attitude solution had a larger error than desired. The lesson learned, and already incorporated into the HI STAR payload design, was to use a star-tracker co-aligned to the roll axis of the payload to capture that axis to a star near zenith.

Another issue was the correlated noise, especially on MAP II, that was most likely due to contaminant particles from the payload; the near-field out-of-focus signals from particles are characterized by the double peaked signatures caused by the central observation (e.g. Figure 34). Particulate contamination from the payload also had been recognized as a source of the optical interference observed on several probe-rocket measurements flown in the late 1960s. Because the contaminating particles are typically quite small, the particle size and distance from the telescope could be estimated from the size of the out-of-focus image of the particle, the brightness of the image and the optical prescription of the telescope. Thus, Tousey and Koomen (1967) estimated particle sizes of between 10 and 330 μm and distances out to 500 meters for contaminants that were photographed during their rocket-borne coronagraph experiments; their

later flights used two coronagraphs to try to triangulate the distance to the particles. Because the derived distances were rather far, Tousey and Koomen initially inferred that the particles were interplanetary dust rather than being associated with the payload. However, this was soon contradicted by Evans and Dunkelman (1969), who observed similar particulate contamination on their daytime photographs of the Cygnus region from a 10 December 1967 rocket from which they deduced that the particle distances were within ~ 3 meters of the payload.

Payload design features and meticulous cleaning procedures developed by the AFCRL Meteor Physics group and the micrometric team at the NASA Ames Research Center (ARC) were successfully adopted by the HI STAR program. The AFCRL Meteor Physics group had an active probe-rocket program of micrometeorite sample and return experiments. Hemenway and Soberman (1962) described the most ambitious of these experiments, dubbed the Venus fly-trap because panels on the payload opened above the atmosphere to expose the collectors and closed before reentry; Soberman and Hemenway (1965) presented the results from the June 1961 flight of this experiment. AFCRL collection packages were also flown from several foreign ranges: four in June 1968 from the Karuna range in Sweden attempted to capture particles from the Areitids and Zeta Perseid meteor streams while four August 1968 flights from range near Natal, Brazil targeted the Perseid meteor shower. Ft. Churchill, Canada experiments attempted to capture the micrometeorites in noctilucent clouds (Carnevalle et al., 1970) that, at the time, were thought to be the nucleation sites for the formation of the ice crystals in the cloud. Skrivanek, Chrest and Carnevalle (1969) and Skrivanek, Carnevalle and Sarkesian (1970) summarized the results of these dust collections and found that, generally, the particle counts far exceeded those of other observers. In all likelihood, this was due to contamination introduced in the preparation of experiment packages, a problem that was recognized in the late 1960s.

NASA Ames Research Center also conducted probe-rocket based meteoritic collection experiments during the 1960s, often on the same flights as AFCRL packages. Farlow, Blanchard and Ferry (1966), Blanchard, Ferry and Farlow (1968) and Farlow (1968) summarize the NASA Ames results while Farlow, Blanchard and Ferry (1970) describe an unusual collaboration in which they were guest experimenters on the Air Force's Air Launched Air Recovery Rocket in November 1966 launched from a F 4C aircraft over White Sands.

Both the NASA and AFCRL groups recognized that the procedures used to prepare the collection packages could contaminate the experiments and both instituted preventive measures. Blanchard and Farlow (1966) describe the meticulous precautions they used for controlling contamination during the design, construction, testing and launch of their experiments while Blanchard, Farlow and Ferry (1967) assessed the effectiveness of these procedures. Many of the design and fabrication guidelines described in these publications, such as eliminating sharp corners, nooks and crannies where particulates could accumulate and the easy assembly and disassembly for cleaning, were subsequently incorporated in the AFCRL rocket-borne infrared sky survey experiments. Payload components were cleaned and assembled in a laminar flow clean room under Class 100 clean room conditions, then double bagged to maintain the cleanliness. The infrared survey program inherited the clean room facilities used by the Meteor Physics Branch after that Branch was disbanded in 1970. The 'lessons-learned' from the micrometeorite collection experiments with regard to payload preparation were critical to the success of the AFCRL infrared probe-rocket borne experiments, with only a small portion of a single experiment suffering interference as explained in Chapter 4.

3.2. Hedging Bets – ARPA funded University Efforts

Martin Harwit (2003) provides a firsthand account of his early days of infrared space astronomy that began in 1963 as a collaboration between his Cornell team and Doug McNutt and Kandiah Shivanadan from NRL. This collaboration flew the first infrared astronomy probe-rocket experiment in October 1965 (Harwit et al., 1966). The two groups then engaged in a friendly competition with the Cornell team being first off the mark with a flight on 29 February 1968. NRL followed shortly thereafter with a 28 March 1968 launch. The Cornell team observed far-infrared emission from the night sky above 120 km, which they thought to have confirmed on a December 1969 experiment (Houck and Harwit, 1969). Then, Feldman et al. (1968) detected bright discrete objects in the direction of Ursa Major during the NRL March 1968 flight. Rumor had it that, because of their experience, ARPA originally offered the HI STAR program to the NRL group but they declined as they were far too busy with the far-infrared experiments and they didn't want the added burden of security restrictions that the program brought with it. Russ Walker did note in a 13 October 1970 memorandum for the record that ARPA had initially planned to fund Doug McNutt at NRL for moderate spectral resolution measurements of the atmosphere with a helium cooled Ebert-Fastie spectrometer from an Aerobee 150 to be flown from White Sands. However, this flight did not take place.

ARPA funded Cornell University through AFCRL for further probe-rocket infrared astronomy experiments that, given the experience of the Cornell team, were a logical backup in case the HI STAR flights proved to be less than expected. The initial Cornell experiment was flown on an AFCRL Aerobee 170 in December 1970 to observe the Galactic plane but the successful HI STAR experiments began shortly thereafter and the need for a backup capability became less important. However, since the Cornell instrument could measure the flux from large extended sources that the HI STAR sensor electronics attenuated, ARPA and AFCRL sponsored refurbishing the payload and telescope for additional experiments, which were flown in July of 1971 (Houck et al., 1971) and 1972 (Houck, et al, 1972) on Kitt Peak National Observatory Aerobee rockets. Soifer, Pipher and Houck (1971) present the observations on H II regions from the first two flights while Houck et al. (1974) collect all the results of the Cornell flights into a single report.

The high pass filter in the HI STAR signal processing electronics that removed the off-axis Earth radiation also filtered out the large scale diffuse emission such as the $5 \mu\text{m} < \lambda < 23 \mu\text{m}$ zodiacal dust radiance reported by Soifer, Houck and Harwit (1971) at a fairly large ($\sim 110^\circ$) solar elongation. Therefore, AFCRL funded a fourth Cornell flight for follow-up spectrophotometry on the zodiacal background. This October 1975 experiment appears to have been contaminated with effluvia from the Astrobee-F rocket (Briotta, Pipher and Houck, 1976) with the consequence that the single useable spectrum was indicative rather than definitive. Indeed, extraneous signals plagued most of the Cornell experiments as well as those flown by NRL.

AFCRL also contracted with Frank Low and Gerry Neugebauer for celestial background studies. Gerry and Frank had argued that systematic rocket-based surveys were untried and risky and that it would be prudent to have a ground-based effort as a backup to address the ARPA objectives. Frank pointed out that considerable improvement in ground-based capabilities were in the offing through careful design of the telescope and measurement procedures. Caltech was given a contract in December 1969 to modify the TMSS 62" telescope for a $5 \mu\text{m}$ ground-based survey while the University of Arizona was contracted in the fall of 1969 for Frank Low to begin a 5 and $10 \mu\text{m}$ survey with their 28" (71 cm) telescope.

Frank Low had a dual appointment with the Univ. of Arizona and Rice University at that time and AFCRL funded Low to mount one of his liquid helium cooled bolometers to the 30 cm Rice University Flying Infrared Telescope and use it on the NASA Lear jet (Low, Aumann and Gillespie, 1970) to obtain the far-infrared airborne measurements. Although some initial results were obtained under this contract (Low and Aumann, 1970 and Harper and Low, 1971), the remaining analyses were done at the Univ. of Arizona (Rieke and Low, 1972a, b) and later under NASA funding. The Lear jet was taken out of service when NASA's Kuiper Airborne Observatory, a 91.5 cm Cassegrain telescope on a C141A was commissioned in February 1974 (Gillespie, 1981).

By the end of 1971, it was evident that the HI STAR survey was out performing the university efforts and both the Caltech and Univ. Arizona contract objectives were changed. Initially, Neugebauer proposed to duplicate the TMSS telescope and take it to Cerro Tololo to complete 2.2 μm sky coverage. We scraped together sufficient funds to build a second instrument and for one year of operations, promising our best effort for the rest of what was needed. Caltech had to have all the money up front and, regrettably, the proposal fell through. Instead, Caltech conducted one of the first systematic time series observations of variable stars at 2.2, 4.8, and 10 μm . Since Frank Low and Gerry Neugebauer were given interim HI STAR catalogs as they became available, Neugebauer also obtained infrared photometry on AFCRL sources that were associated with TMSS objects to examine the consistency of the AFGL 11 μm fluxes with the ground-based observations.

The University of Arizona covered about 700 deg^2 of the sky at 5 μm and 1900 deg^2 at 10 μm before calling a halt to the effort. Low (1973) lists the 44 'good quality' signals detected by this survey among which was one real source, AFGL 490, that was detected before it was picked up by HI STAR. Low also performed one of the first direct mid-infrared stellar calibrations under the AFCRL contract and searched for unidentified AFCRL sources.



3.3. HI STAR

In 1969, the Air Force Space and Missiles Systems Organization (SAMSO) funded Hughes and Aerojet to build the HI STAR instruments. Aerojet had developed the Model C19 laboratory demonstration instrument and Hughes Aircraft Co. was constructing the FIRST and FAIR sensors for the Air Force. The instruments proposed by both companies had about the dimensions and predicted performance specified by ARPA for the HI STAR survey. However, problems at Aerojet developed early; a presentation at the second

technical meeting devoted over an hour to 'proving' that the sensor performance requirements were needlessly severe for the surveillance mission, based on TMSS results. By the third technical meeting, it was clear that Aerojet could not meet the performance requirements and Capt. William Crabtree, SAMSO, terminated the contract for lack of performance. The funds recovered from the contract were given to Hughes to build a second HI STAR instrument. Capt. Crabtree was then able to keep the Hughes program on schedule and within reasonable cost.

The size, weight and optical design of the HI STAR instruments were a compromise between various performance parameters such as sensitivity, scan rate and spatial resolution. The effective telescope collecting area is limited by the size and weight of the instrument that

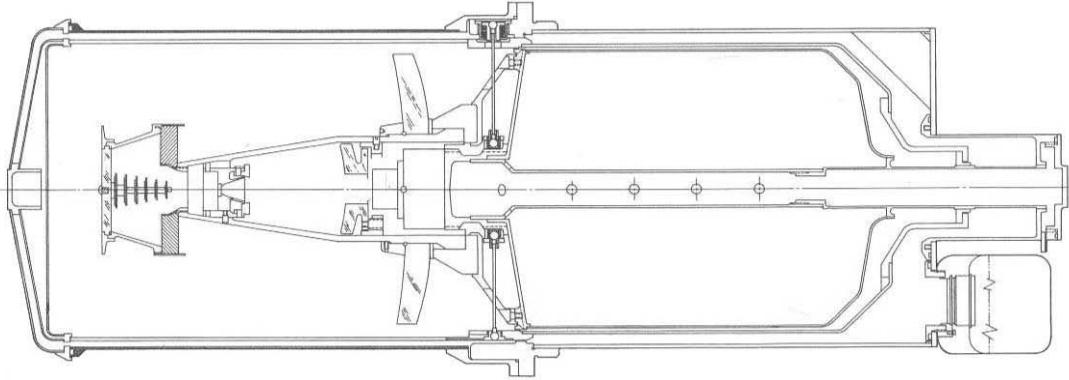


Figure 15. Cross-sectional schematic of the HI STAR sensor. The optics are to the left and the super-critical helium cryotank is to the right. The cavity housing the optics and cryotank is evacuated and the system behaves like a thermos. The doubly folded Gregorian f/3 optical system has a 16.5 cm diameter primary mirror and an effective collecting area of about 125 cm².

may be flown. The Hughes HI STAR sensor, shown in cross-section in Figure 15, consisted of beryllium four-mirror doubly folded Gregorian optics with a 16.5 cm diameter primary mirror. Such short, compact lightweight optics, the telescope length was only about 1½ times the diameter of the primary mirror, has a relatively large central obscuration and, consequently, a limited effective collecting area; the A_c was ~ 125 cm².

Ideally, one would like to conduct as sensitive a survey as possible over all the sky in multiple infrared spectral bands but practical considerations require compromises. The limiting irradiance of a scanning instrument is approximately given by:

$$B = \frac{4}{\pi} \frac{FS}{DD^* \varepsilon \Delta \lambda} \left(\frac{\Omega}{nT} \right)^{1/2} = \frac{S \text{NEP}}{A_c \Delta \lambda} \left(\frac{\omega}{\alpha} \right)^{1/2} \text{ W cm}^{-2} \mu\text{m}^{-1} \quad (3)$$

where:

- F = the focal ratio (focal length divided by the diameter, D , of the primary mirror) of the system; F is typically 3 to 3.5 for survey systems.
- S = the minimum signal-to-noise ratio (SNR) for a signal to be considered a potential real source; often S is chosen to be about three.
- ε = the optical efficiency of the system, which includes obscuration of the secondary mirror and the transmission/reflection of the optical system and spectral filters.
- D^* = detectivity, a measure of the inherent detector sensitivity in units of cm Hz^½ W⁻¹.
- $\Delta\lambda$ = the spectral bandpass of the filter
- Ω = the solid angle of the sky swept out in time T
- n = the number of detectors in the array
- NEP = the noise equivalent power of the detector in units of W Hz^{-½} and equals $\sqrt{A_{\text{det}}}/D^*$
- A_c = effective collecting area of the system $\sim \varepsilon \pi (1/2 D)^2$
- ω = scan rate
- α = the in-scan angle subtended by the detector

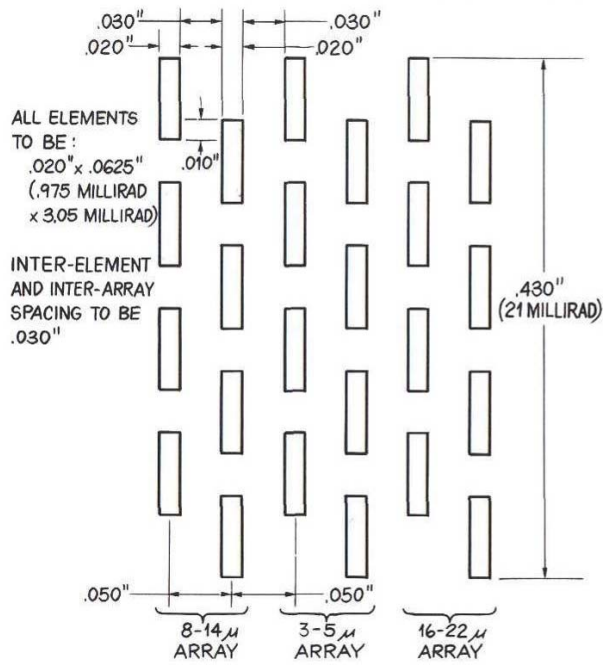


Figure 16. The HI STAR focal plane layout. All the AFCRL/AFGL survey experiments were configured similarly. The detector height to width ratio varied from 2:1 for HI STAR South to 6:1 for HI HI STAR. However, adjacent detectors overlapped by the diameter of the optical blur in all cases, so the entire energy from a transiting star was detected.

Thus, from Equation (3) the sensors should have been able to detect stars brighter than $\sim 4 \times 10^{-16}$ W cm⁻² at 11 μ m or roughly [11] ~ 0 magnitude at a signal-to-noise of about 3 or greater.

Three 8 element focal plane arrays spanned 1.2° in the cross-scan direction. The 8 Ge:Cd detectors were filtered for the 16 – 22 μ m region while the two Ge:Hg arrays had spectral band-passes of 3 – 5 μ m and 8 – 14 μ m. The Ge:Hg response cuts off at ~ 13.5 μ m but such detectors are intrinsically more sensitive than Ge:Cd detectors in the 4 and 11 μ m bands. The detectors were arranged as shown in Figure 16 such that a point source sequentially tracks across each filter at a given row of detectors. The entire system was cooled with super-critical helium, a state in which the liquid and gaseous helium are in equilibrium, which is achieved at a temperature of 5.5 Kelvin and at about three atmospheres of pressure. The temperature is low enough for optimum detector performance and the super-critical state assures good thermal contact with the tie points for the focal plane and telescope optics.

Four magnesium payload castings were made and three HI STAR payloads were ready by the time the sensors were delivered to provide rapid turn-around to meet the ambitious flight schedule. Unlike the LO-STAR flights, which took three field trips for each launch, HI STAR experiments went smoothly and each launch required only a single three-week field expedition.

The area of sky that can be surveyed during an experiment is set by rocket performance given the payload weight, which limits the time of data acquisition, the scan rate and the cross-scan extend of the focal plane and viewing constraints. The maximum permissible telemetry rate restricts the number of detectors in the focal plane, the scan rate and the detector resolution.

Thus, optimizing a single survey performance parameter has consequences for the other parameters. Since the sensor size is defined by the payload configuration and rocket performance, the best detectors are highly desirable as the sensitivity varies more slowly, as the square root, with the scan rate and in-scan resolution. The typical D* for extrinsic germanium detectors was $\sim 10^{14}$ cm Hz^{1/2} W⁻¹ or $\sim 10^{15}$ W Hz^{1/2} NEP under the low background conditions in space. To address the sponsor's objective to survey as much total sky as possible, the sensor electronics had a 280 Hz bandwidth that was matched to the 37.5°/sec scan rate necessary to cover the 20 – 35% of the sky available within 200+ seconds of experiment time afforded by the Aerobee 170 rockets.

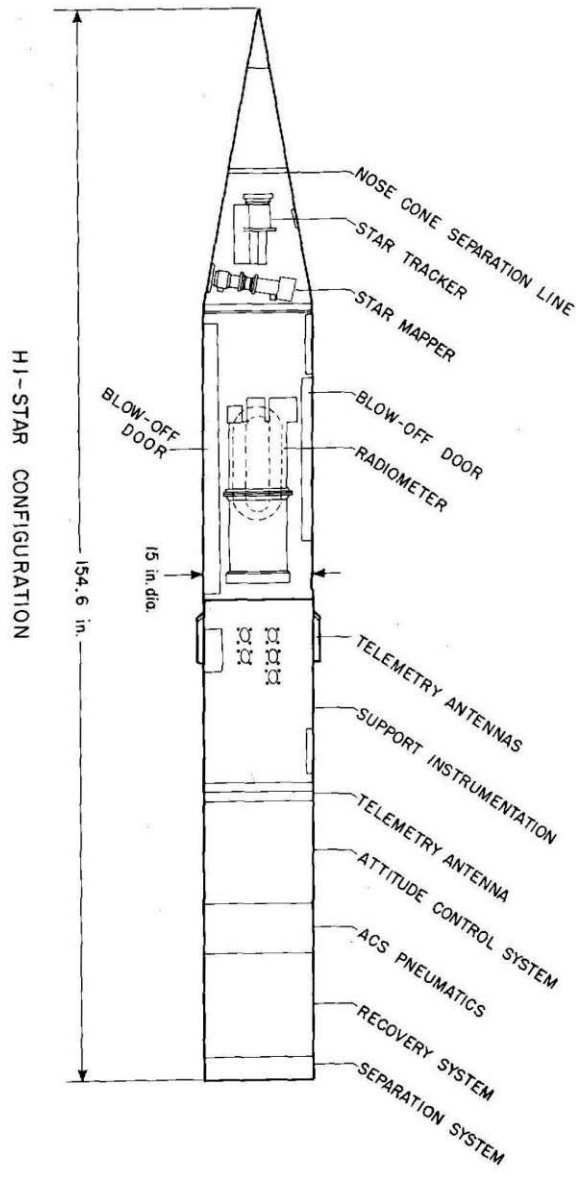


Figure 17. A schematic of the HI STAR payload is at left and the payload section from the telemetry antenna to the nose cone separation line is shown above with the HI STAR sensor stowed and deployed (with cap on).

A field trip had four critical milestones on a tight schedule to launch. First, a functional test was done a few days after we and the hardware arrived at White Sands to assure everything was in working order, which was not as trivial as it might sound. Initially, we shipped the hardware to El Paso as American Airlines cargo but soon changed to air-cushioned moving vans. Not only did the handling by American Airlines destroy the accelerometers glued to the payload, it tore them off. That nothing was seriously damaged was a testament to the rugged design and construction of the payload by the Wentworth Institute of Technology. This wasn't the only American Airlines incident. On one occasion, the vacuum diffusion pumps were delivered upside down, leaking pump oil. Even worse, after we sent the field equipment off to Logan Airport, the Coast Guard called to inform us that they fished one of our boxes out of Boston Harbor; the launch console in its shipping crate had been found floating next to the USS Constitution. Needless to say, the functional check after unpacking was an important first test.



Figure 18. The HI STAR payload being mated to the Aerobee 170 before being mounted on the Nike booster in the tower. Note the plastic bagging around the payload for contamination control.

After we arrived in the field and checked out the hardware, the sensor was pumped and cooled for the horizontal test, which was run at the end of the week in which everything was electrically connected and a simulated flight was conducted with the cold sensor, including sensor stepping (with the cap on).

The LO-STAR experiments had highlighted the necessity of actively capturing the pitch and yaw axes of the payload for accurate pointing knowledge. An ITT Fine Guidance Error Sensor (star tracker), made at the same Sylmar plant where I had worked, was co-aligned with the longitudinal, or roll, axis of the payload. Thus, after a successful horizontal test, the sensor was warmed and then the payload spin-balanced to reduce the cross moments for which the attitude control system would have to compensate. As shown in Figure 17, the HI STAR sensor was mounted on a one axis gimbal in the payload, nominally perpendicular to the roll axis, which deployed the telescope during the experiment. After the payload was cleaned, a theodolite was used to determine the gimbal readout and azimuth deviation as a function of deployment angle under class 100 clean room conditions; a picture of this procedure for the SPICE sensor is shown in Figure 44. Then, the sensor was cleaned again and vacuum pumped. The sensor housing was double bagged to preserve cleanliness and the payload was assembled, then mated to the rocket, as shown in Figure 18.

The assembly was mounted onto the Nike booster, which had already been placed in the launch tower. The sensor was pumped and cooled in preparation for the t - 3 day vertical test, which is a full up flight simulation in the tower without sensor deployment. The final three days were enough to warm the sensor, pump for a day and cool it for launch.

The HI STAR experiments were flown on Nike boosted Aerobee 170 rockets out of the White Sands Missile Range 350 tower at launch complex 36 (Figure 19). AFCRL purchased a lot of nine rockets, seven for the HI STAR series, one for MAP II and another for the first



Figure 19. A daytime Aerobee 170 launch. The Nike booster and the Aerobee sustainer are ignited at the same time and separate plumes for the two may be seen.

Cornell flight. The Aerobee numbering system indicates the performance: an Aerobee 150 could fly a 150 pound payload to an altitude of 150 miles (or 150 kg to 150 km), a 170 was capable of lifting 170 pounds to 170 miles and so forth for the Aerobee 200 and Aerobee 350. The AFCRL/AFGL payloads were much heavier than nominal, reducing the peak altitudes. For example, the Aerobee 170s lifted the ~450 pounds HI STAR payloads, to ~100 miles altitude.

Fifty-two seconds after launch and two seconds after the rocket burned out, the range commanded the vehicle to close the liquid fuel and oxidizer line check valves as a contamination control measure. The payload coasted until the aerodynamic drag was low enough for it to be stabilized by the attitude control system, which used dry nitrogen gas filtered through Millipore filters to prevent contamination. The nose cone and doors were then ejected and the 1.5 revolutions per second vehicle spin plus the residual atmosphere carried these items away and below the vehicle. The vehicle was then despun with yoyo weights and the payload separated

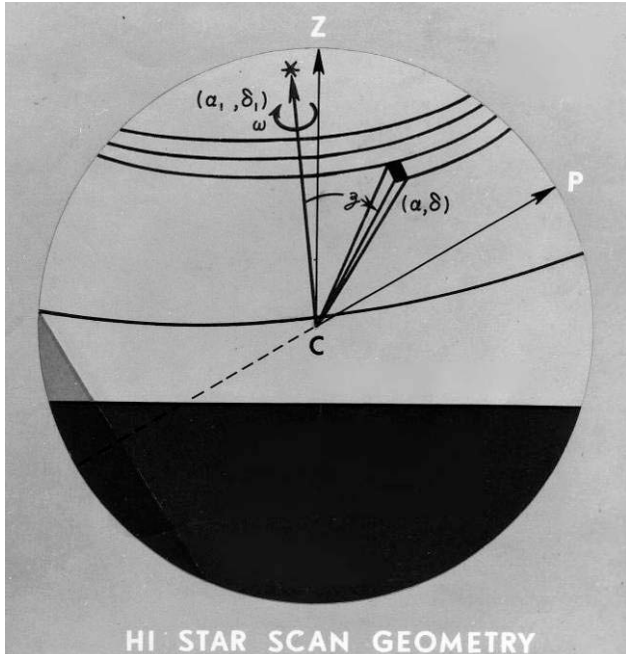


Figure 20. The HI STAR survey pattern. The payload at C rotates at a roll rate ω about the pole star with equatorial coordinates (α_1, δ_1) near zenith, Z, and the sensor is deployed to a zenith angle, ζ . The portion of the sky obscured by the hard Earth at peak altitude is in black at the bottom of the figure. The lighter cap opposite the celestial pole, P, defines the declinations that are not available to the survey from the White Sands Missile Range given the maximum deployment angle shown.

with the geometry shown in Figure 20. The payload was spun up to a $\sim 60^\circ/\text{sec}$ rotation rate (the designed linear rate of $37.5^\circ/\text{sec}$ times the cosecant of the zenith angle). The sensor was stepped down in 1.1° zenith angle increments as the roll angle passed through north. This assured contiguous coverage by overlapping the 1.2° cross-scan extent of the focal plane arrays on successive scans. Position and coverage problems during stepping were compensated by the high degree of overlap in this region from the different experiments. The scan rate was decreased by $\sim 20\%$ twice during the experiment to account for changes in the cosecant zenith angle distortion during which time an internal shutter was closed and internal diodes were powered to track the response of the sensor. The sensor was remarkably stable: sensor temperatures for all flights were the same, as were the diode amplitudes and sensor responses to them. Twenty-five to 35 scans were executed, depending on the anticipated rocket performance.

About 200 seconds of data were acquired on the ~ 25 rolls that were available on the first three flights, each of which covered about 15% of the sky. A somewhat lighter payload and fly-away tower shoes (lugs) increased the peak altitude by about three miles for the fourth flight. A further 10% performance improvement for the fifth through seventh flight was realized by sizing the motor nozzle for the flight profile with the HI STAR payload weight. About 20% of the sky was covered on the 35 rolls executed on these last flights. In total, more than 75% of the sky was surveyed on the seven HI STAR experiments.

from the rocket at a velocity of 1–2 m/sec by a ring of springs on the mating fixture attached to the rocket that were released by a Marmon clamp.

Next, the attitude control system captured the payload and pointed the star tracker at the pole star selected for the experiment; the choice of pole star dictated the area of sky to be surveyed. The launch was timed such that the star tracker locked onto the pole star that was generally within 6° of zenith. Once the star was acquired, the star tracker signals to the attitude control system held the roll axis of the payload inertially fixed to the star. Because of the spin-balancing, the payload rotated as a free body with little attitude correction. The analytic polynomial solutions to the roll positions derived from the stellar transits measured by the star mapper were accurate to the order of an arc minute for all experiments (Price et al., 1978).

The jackscrew tied to the sensor cap and payload insured a positive vacuum seal for ground preparations and the vibrations of launch then withdrew the cap and the sensor was deployed 143° to a zenith angle of 37° , after which a series of scans were executed

The sensor was stepped down in 1.1° zenith angle increments as the roll angle passed through north. This assured contiguous coverage by overlapping the 1.2° cross-scan extent of the focal plane arrays on successive scans. Position and coverage problems during stepping were compensated by the high degree of overlap in this region from the different experiments. The scan rate was decreased by $\sim 20\%$ twice during the experiment to account for changes in the cosecant zenith angle distortion during which time an internal shutter was closed and internal diodes were powered to track the response of the sensor. The sensor was remarkably stable: sensor temperatures for all flights were the same, as were the diode amplitudes and sensor responses to them. Twenty-five to 35 scans were executed, depending on the anticipated rocket performance.

About 200 seconds of data were acquired on the ~ 25 rolls that were available on the first three flights, each of which covered about 15% of the sky. A somewhat lighter payload and fly-away tower shoes (lugs) increased the peak altitude by about three miles for the fourth flight. A further 10% performance improvement for the fifth through seventh flight was realized by sizing the motor nozzle for the flight profile with the HI STAR payload weight. About 20% of the sky was covered on the 35 rolls executed on these last flights. In total, more than 75% of the sky was surveyed on the seven HI STAR experiments.

All seven HI-STAR experiments were successful. The first experiment was flown on 3 April 1971 and the series concluded 20 months later on 5 December 1972, a rather remarkable pace that required a flight every three to four months. This was a tightly coordinated program as the field expedition averaged about three weeks and, at best, we had one and a half payload teams working on the program.

3.4. The First Satellite-Based Infrared Surveys

In the late 1960s, ARPA and the Air Force SAMSO had very ambitious goals for space-based infrared surveillance and a succession of Air Force company grade officers pushed the technology and flight tests. At ARPA, Maj. Bob Paulson provided Project 1366 funds to SAMSO for the Autonetics Stellar Radiation Sensor and the Hughes HI STAR telescopes and to AFCRL to fly them. At SAMSO, Capt. Ted Jenks directed the Autonetics SRS effort while Capt. Bill Crabtree did the same for the Hughes HI STAR sensors. The SRS and HI STAR provided the technical demonstration for the first proposed operational infrared surveillance system, the Deep Space Surveillance System (DSSS), which was to fly by the end of the 1970's. However, a satellite demonstration was needed and SAMSO took the initial steps in 1971 by flying two celestial mapping satellites. The Autonetics Celestial InfraRed Mapper (CIRM) was an analog of the SRS except that it had a two color infrared focal plane and was cooled by a large super-critical helium cryostat. This experiment was launched on 6 June 1971 and surveyed 38% of the sky during its brief 138 minute mission. Unfortunately, cross-talk from the attitude control system into the sensor electronics limited the observations to the very brightest infrared sources. The Hughes HI STAR class Celestial Mapping Program (CMP) instrument was inserted into a sun-synchronous 793 km altitude circular orbit on 17 October 1971 on what was planned to be a long duration experiment as the sensor was cooled by a closed cycle Vuilleumier cooler. However, two problems arose that compromised performance and lifetime. A higher priority experiment on the payload required that the satellite be oriented such that the CMP sensor scanned parallel to the Earth's horizon rather than through the zenith as preferred. The photon background from off-axis Earth radiation in that configuration reduced sensitivity. The high priority package was to operate for the first several weeks and then emphasis was to shift to CMP and zenith scans. Unfortunately, the cryocooler flex lines across the scan gimbal began to leak after two weeks in orbit and CMP only obtained three orbits of data early in the mission. Although SAMSO considered CIRM and CMP as failures and the problems with the CMP cryocooler put a taint on mechanical low temperature coolers that lasted for decades, CMP did obtain redundant coverage in two infrared spectral bands on about as much sky (82%) as HI STAR and HI STAR South combined and demonstrated the feasibility of infrared space-based surveillance from an orbital platform. Holman, Smith and Autio (1976) also used the CMP data to demonstrate that particle radiation was not an insurmountable barrier to space-based infrared astronomy missions (see also McCarthy and Autio, 1978). They extracted the particle hits on the CMP detectors and found excellent agreement between the observed event rates and those predicted by NASA models, a crucial validation of the NASA models.

Independently, a different SAMSO program office began a near-infrared survey from orbit at about the same time. Steve Maran, Goddard Space Flight Center, and his Aerospace Corp collaborators (Maran et al., 1976) derived 2.7 μm light curves of variable stars from high time resolution observations between 1971 and 1975. Sweeny, et al., (1977, 1978) then compiled the satellite measurements into the Infrared Equatorial Catalog (EIC), an incomplete list of sources within 10° of the Celestial Equator. The initial catalog contained 2.7 μm fluxes

for 896 objects that were extracted from more than 40,000 individual measurements (Heinsheimer, et al., 1978): the faintest sources listed have a magnitude of [2.7] \sim 4, about the same sensitivity as the TMSS. Apparently a second catalog of 1278 sources over 57.5% of the sky inside the survey limits was compiled (Nagy, Maran et al., 1979; Nagy, Sweeney et al., 1979b) but not published. Ultimately, Sweeney and Richardson (1995) published a complete catalog with 2.7 μ m measurements on 7,220 stars extracted from the entire area within 10° of the celestial equator. Each source was observed at least twice.

The sensitivity of these satellite data was much less than what SAMSO projected for the system and a Background Measurement Satellite/Earth Limb Measurements Satellite (BMS/ELMS) and a Target Measurement Satellite (TMS) were to be flown mid-decade as an orbital validation of the DSSS concept. Two sensors on BMS/ELMS were to obtain definitive background measurements, one looking upward to survey the celestial background and the other to measure above-the-horizon radiance profiles in the Earth limb, while the TMS would demonstrate infrared target detection, acquisition and track against the backgrounds.

SAMSO issued a competitive proposal request in 1970 for the BMS/ELMS sensors. Honeywell Corp. responded with an off-axis Earth Limb Sensor (ELS) that was tailored to measure the atmospheric emissions above the edge of the Earth. Rockwell and Perkin-Elmer proposed conventional on-axis telescopes with Perkin-Elmer going so far as to build a 35 cm beryllium optical system (Figure 47) as a demonstration of their capability. Hughes had a hybrid design with a bar across the middle and down the barrel of the telescope. The bar housed the secondary mirror and re-imaging optics and served as an internal baffle: looking up it was an on-axis system with a large obscuration, looking into the Earth limb it was a quasi off-axis design. A fifth company noted that much of the size and weight of space-based cryogenic sensors was taken up by vacuum shell that was required for ground operations but not needed in space. Since the BMS sensors were to be cooled with a mechanical cryocooler, the company proposed to fold the optics and baffles into a compact package and launch them warm. Once in orbit the plan was to fire titanium balls into the fold points to pop the optics and baffles into proper position. Needless to say, this proposal was rejected outright.



3.5. HI HI STAR

The required BMS sensor performance was well over an order of magnitude better than the HI STAR instruments and SAMSO took an intermediate step by having Hughes Aircraft Co. and Rockwell International Corp. build full scale HI HI STAR sensors under the program direction of Capt. Jack Lyons. The instrumental performance on AFCRL Aerobee 350 sounding rocket flights was to be the basis for down-selecting the contractor to build the sensor to fly on the BMS along with the Honeywell Earth Limb Sensor.

Rockwell made an early major breakthrough on the HI HI STAR sensor by developing sensitive extrinsic silicon detectors for low background applications. Although the extrinsic photoconductive response of doped silicon was known since the early 1950s, their infrared properties were not well studied until the seminal paper by Soref (1967), who found that these detectors were sensitive, had a fast response and, compared to germanium detectors, they could be made at

lower cost with good reproducibility and could more readily be fabricated in large arrays. Extrinsic silicon detectors have much higher quantum efficiencies than germanium detectors, which are relatively transparent to the infrared photons that they are trying to detect. Jamieson (1984) pointed out that the dopant materials could be inserted into the silicon lattice in much higher concentration than in germanium, resulting in much shorter absorption lengths, higher quantum efficiency and, of particular interest to the military, smaller detector volumes that translate into less vulnerability to ionizing radiation. SAMSO accepted Rockwell's offer to substitute the new Si:As arrays into the HI HI STAR sensor.

Rockwell also implemented another focal plane development – trans-impedance amplifiers. The electrical resistance of a detector is increased by orders of magnitude when cooled under low background conditions. This increased resistance coupled to the stray capacitance in the detector pre-amplifier circuit reduces the detector response time (the inverse of the resistance times capacitance defines the frequency above which signal information is attenuated). To compensate for this, HI STAR amplified the high frequency signals in the on-board processing electronics while the HI STAR South signal bandwidth was reduced by increasing the in-scan width of the detectors. Trans-impedance amplifiers have a feedback circuit that reduces the resistance–capacitance product and thus increases the high frequency response of the system.

The 35 cm diameter aluminum primary mirror in the HI HI STAR doubly folded Gregorian telescope was coated with kanogen and super-polished. The stray light rejection was further improved with careful baffle design and empirical fine tuning. The barrel housing the secondary mirror was cantilevered rather than having spider vanes and both it and the inside of the heat shield were tooled as baffles (see Figure 44); the effective baffle angle, the angle from the optical axis at which the primary mirror just cannot be seen external to the sensor, was about 20°. Glints and preferred reflection paths were found by optically ray tracing with a helium-neon laser and corrected. To maintain cleanliness and the low scattering of the super-polished mirror, the sensor was outgassed each time it was cooled by several cycles of purging with dry nitrogen after which the sensor was vacuum pumped. The off-axis performance was tested in the Aerospace Mark I Environmental Chamber (Mattey, Dawbarn and Menzel, 1991) at the Arnold Engineering and Development Center (AEDC) and confirmed to be comparable to off-axis systems at angles larger than the baffle angle. The off-axis performance of the Rockwell HI HI STAR is labeled as SPICE in Figure 32.

The penalty for this high level of performance in a very compact volume was a very large secondary housing that obscured half the area of the primary mirror, resulting in an effective collecting area of $\sim 500 \text{ cm}^2$ or about four times larger than the HI STAR sensor. The three-color focal plane had bandpass filters centered at 4, 11 and 21 μm and the 18 detectors in each array spanned 2.5° in cross-scan. The detector dimensions were 0.5 by 3 mrad (1.7' by 10') and adjacent detectors in an array overlapped by the optical blur to ensure that all the energy from a star was detected no matter where it transited the focal plane.

The sensor was fixed looking aft within the 22" envelope of the payload, which matched the diameter of the Aerobee 350 rocket. The sensor cover was opened when a sufficient time had elapsed after separation from the sustainer and the payload was oriented to a position in the winter Galactic plane. The entire payload was then slued to scan the sensor across the sky.

HI HI STAR flew on 16 February 1974 but, unfortunately, a valve in the rocket fuel line had been installed backward, which reduced the efficiency of the rocket burn and the payload apogee to $\sim 110 \text{ km}$. Consequently, the payload re-entered the atmosphere early, after collecting

only about 70 seconds of data. The (still open) sensor cover was ripped off but, fortuitously, the payload was balanced about a minor axis and it spun in on its side like a maple leaf, markedly slowing the descent. A barometer switch deployed the parachute at 12,000', as designed, jamming it into the nose cone. However, the decent was slowed enough that the payload timer ultimately separated the nose cone, thus deploying the parachute about 1000' above the ground. We watched all this somewhat incredulously on telemetry. A couple of the crew set off for the base clinic where they had the devil of a time convincing the medics that they had a legitimate reason for requisitioning a couple of gallons of anhydrous (200 proof) ethanol that was needed to maintain a clean sensor environment while the optics were defrosted. However, enough data had been taken during this brief mission to confirm that the sensor performance was reasonably close to that specified, thanks to the more sensitive detectors and superior off-axis rejection.



3.6. HI STAR South

As AFCRL was finishing the HI STAR flights toward the end of 1971, Russ Walker successfully lobbied Maj. Jim Justice, who succeeded Maj. Bob Paulson at ARPA, to extend the sky coverage by funding southern hemisphere flights with modified HI STAR sensors. Flying the experiments from the Woomera, Australia rocket range provided coverage complementary to the HI STAR flights as the 65° latitude difference between Woomera and White Sands meant that in addition to mapping new areas in the southern sky, we also would be able to fill in the 'polar' holes left by the northern hemisphere experiments and add much needed redundancy.

The sensors were modified during refurbishment to incorporate the new more sensitive extrinsic silicon detectors: Si:As for the 11 and 20 μm bands and a Si:P array was substituted for the HI STAR 4.2 μm array for 24 – 30 μm measurements. Although 4.2 μm photometry provided valuable near-infrared color discrimination and the high degree of correlation with the TMSS catalog was used to update the aspect solution, the longer wavelengths added important information on the spectral energy distributions of the coolest sources and covered a spectral region not accessible from the ground. The in-scan width of the detectors was increased by 50%, further improving the sensitivity by decreasing the electronic bandwidth. The primary mirror was given a super-polished finish to reduce the photon noise from the off-axis Earth.

The sensor, payload, rockets and assorted hardware were airlifted to Woomera, Australia in late July 1974 and we arrived in early August for the seven week field expedition. We were given space in the satellite launch facility of European Launcher Development Organisation (ELDO) for payload preparation (Figure 26). Logistics forced us to fill the sensor in the preparation area, and then truck it to the Launch Area 8 site some five to seven miles away, where it was mated to the rocket while horizontal. The sensor was designed to be filled and maintained vertically and the consequences of not doing so were a higher thermal input and helium boil-off rate that reduced the hold time. We worked out the bugs for this procedure on the vertical test for the first flight and launch preparations went smoothly afterward.



Figure 21. The HI STAR South field team. Back row left to right, ACS person, two rocket support people, Jack Griffin, Russ Walker, Pete Tandy and Tom Murdock, all from AFCRL, a rocket support person, Roy Walters (AFCRL), two Woomera range support people, Steve Price (AFCRL). Front row, Tom Campbell (WIT), Lenny Scatch and Dick Buck (OSU), Ed LeBlanc (WIT), rocket support, unknown. Wentworth Institute of Technology (WIT) built the payload; Aerojet Corp built the rocket and attitude control system and Oklahoma State University (OSU) was responsible for the telemetry.

The HI STAR South experiments were flown on Nike boosted Aerobee 200 rockets, which lofted the payloads to a peak altitude of \sim 190 km. The resulting data acquisition time of \sim 275 seconds translated into about 10 more rolls than on the HI STAR experiments even though the HI STAR South flights had to punch through 4000' more lower atmosphere, the elevation difference between Woomera and White Sands. The sensor was deployed to an initial zenith angle of 80° and then stepped up 1.1° after a 360° roll. This was the reverse of the HI STAR stepping direction and was done to reduce the off-axis loading from the Earth as the altitude of the rocket at the start of the first roll was greater than for the last one.

Since the range support we would receive was uncertain, we shipped an HP9700 desktop calculator that I had programmed to do the wind weighting with a program supplied by our Aerospace Instrumentation Division. I had modified it to use an exponential rather than a linear segmented atmospheric density. However, the Australian range management required that the wind weighting be done by personnel at range headquarters, more than 200 km from the launch site, which meant that my wind weighting calculation would serve as backup.

The range wind weighting computer went down several hours before the first flight and they agreed to go with my predictions. The vehicle landed some 80 kilometers off course; WNW instead of the almost due North that I had predicted. I couldn't understand how I could



Figure 22. The Nike booster on the launch rail. The rail shoe is the attachment below and at the top of the white "Air Force" booster, which fits over a rail flange and holds the booster to the rail. During launch the shoe slides up the rail flange, which guides the motion of the vehicle.

have been so far off and carefully scrutinized the wind weighting program. I discovered a small programming error that could account for a few degrees in azimuth but nothing that would lead to such a large discrepancy. When I mentioned my error at lunch the next day, everyone jumped on the existence of the error and ignored that it mattered little to the predicted impact point. The reason was that the range was so unhappy with the discrepancy that they threatened to cancel the remaining flights and I had provided the reason not to do so. We were emphatically told that range personnel would do the wind weighting from then on and that I could support their calculations, if I wished. Whatever it took to finish the series of flights was OK by me.

I took a closer look at the problem. The rockets were flown from the portable Nike launch rail that NASA left for us from a previous field expedition. As seen in Figure 22, the shoes that hold the Nike booster to the rail fit around the edge of the rail. Gravity held the (brown) Aerobee 200 rocket in position to an extension of the launch rail when horizontal and on the booster when vertical. A white foam rubber pad, seen near the bottom set of umbilical connections in Figure 23, cushioned the booster on the extension. Not only was the payload and rocket much heavier than the launch rail was designed to handle but the front shoe on the booster came free of the rail after only a few feet of travel, while the rocket, itself, was unconstrained.

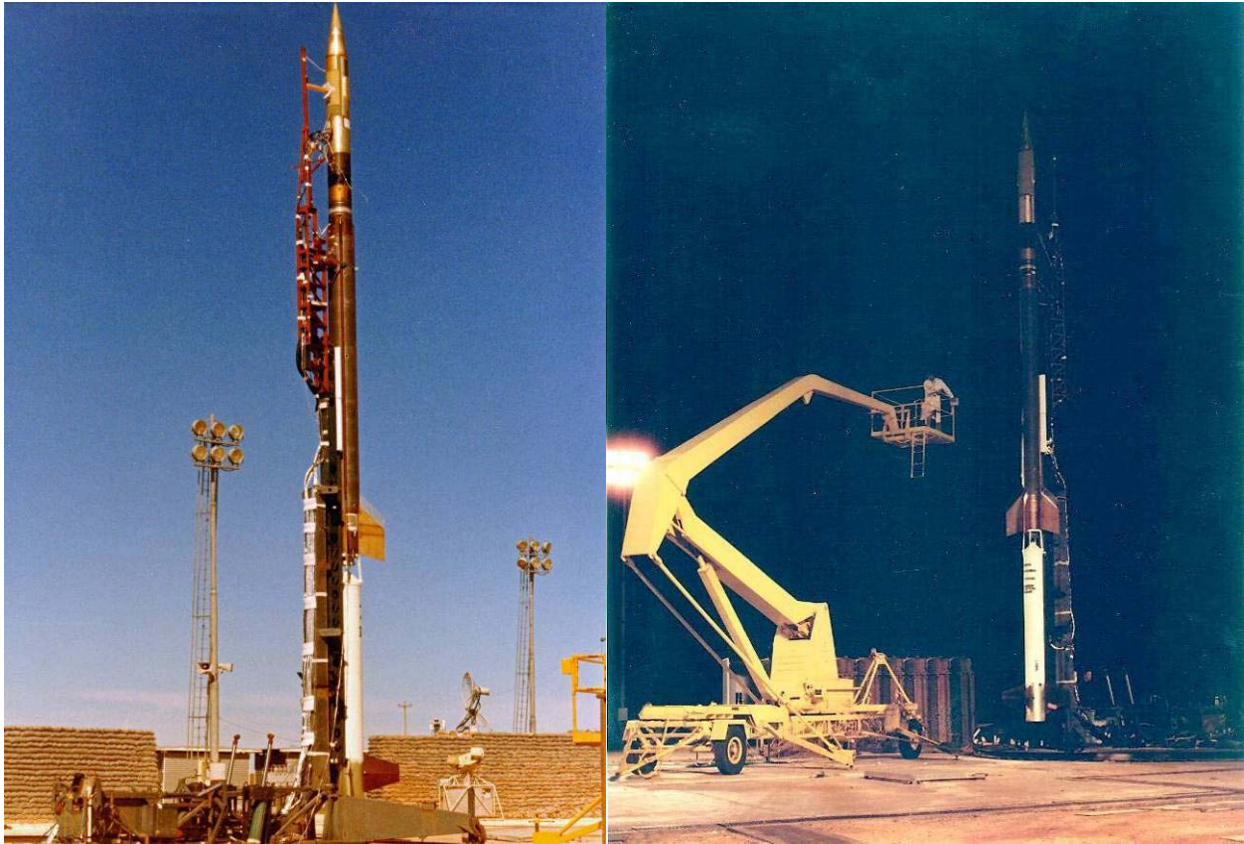


Figure 23. The HI STAR South Payload on top of the Aerobee 200 and Nike booster on the launcher. The rudimentary launch facilities required us to use a cherry picker for final preparations.

The weight of the configuration flexed the rail at launch, which flipped the rocket slightly, a motion that determined the track of the unguided vehicle far more than the winds.

The range wind weighting also was problematic. Mid-level winds were measured by range headquarters radar some ~200 km distant using balloons released a few hours before launch while the upper level winds were measured 10 hours earlier. However, the most grievous problem was the on-site measurements of the lower winds. Helium filled balloons were weighted to give a known rate of ascent, which defines the vertical position of the balloon as a function of time. After release, the azimuth and elevations of the balloons were measured with a theodolite at prescribed time intervals, which gives altitude and the down and cross range position at the specified times. A reasonable system – if the measurements made by the two range technicians doing the observations weren't, as I observed, compromised by liquid refreshment.

After four weeks of field preparation, three experiments were flown between 4 and 17 September, 1974. The first flight (launch is shown in Figure 24) was completely successful except for the impact discrepancy. One side of the ACS 200 Hz power supply inverter failed on the second flight. The sensor was deployed and stepped through the program but no data were collected as the ACS roll program was not executed. The parachute did deploy on the timer and the payload was recovered in good condition. On the third experiment, the sensor stepping hung up a third of the way into data acquisition, which meant that the sky was surveyed only over a deployment angle of about 10°. The parachute also failed to deploy properly and the sensor and payload were heavily damaged on impact.



Figure 24. Launch of the HI STAR South at Woomera, Australia. The white debris is from the Styrofoam support for the booster on the rail extension.

The HI STAR South flights mapped ~35% of the sky, thus increasing the total area surveyed by the combined HI STAR series to ~90% at 11 and 20 μm (Figure 27). Galactic longitudes between 280° and 317° were covered on the first flight and the remainder of the fourth quadrant would have been surveyed on the third flight if sensor stepping hadn't failed.

Unfortunately, the factor of four increase in sensitivity expected from extrinsic silicon detectors and the decrease in bandwidth wasn't realized; the HI STAR South experiments were about as sensitive as the best HI STAR measurements. The decrease was likely caused by a light leak through the labyrinth baffle between the optics and focal plane.

In total, the HI STAR/HI STAR South experiments had an 85% success rate if the third HI STAR South flight is counted as a 50% successful.

3.7. Personal Perspective – The HI STAR Era

My first government business trip (temporary duty or TDY) was to attend a conference on spacecraft contamination in Vail, Colorado in the fall of 1969. I got three things from the trip. First, contamination from spacecraft outgassing was a serious problem. Phenolics and other oil based substances could leave deposits on an optical system that would turn dark when exposed to sunlight and this residue was very difficult to remove. Second, the thermals on the eastern slopes of the Rockies could produce incredibly severe turbulence. Third, New England was very beautiful during the peak in the fall color. The flight from Logan airport took off eastward over the sea, banked north then west, taking the plane over southern New Hampshire. The riot of fall colors was something that I had not seen before, having grown up in Southern California. The New Zealand larch turned a brilliant yellow in the fall, but the larch groves were a monotone of color.

However, I spent most of my first three years of business travel at the White Sands Missile Range and I enjoyed the many trips there. The White Sands Missile Range is a high desert site at about 4000' elevation that covers much of the Tularosa basin between the Sacramento Mountains on the east and a western range consisting of (going north) the Organ Mountains and Elephant Butte. As may be seen in Figure 25, the Organ Mountains fancifully resemble the pipes of an organ, hence the name. The area was rich in tourist attractions and we spent a fair amount of our free time sight-seeing.

We visited the gypsum deposits on the eastern edge of the range that make up the White Sands monument. Russ and I also dropped by the AFCRL's Sacramento Peak solar observatory in the Sacramento Mountains and wangled a tour. On the way, we went by the Cloudcroft Observatory but couldn't raise anybody to show us around. We were more successful with a nighttime visit to Northwestern University's Corralitos Observatory. The observatory's 24" Cassegrain telescope was housed in a small dome on the lower eastern slopes of the Organ Mountains, just this side of the pass that runs through leftmost notch in the peaks in Figure 25. J. Allen Hynek, the facility's director, was there when we visited and he showed us around. The observatory had a lunar transient phenomena program at the time that used an image orthicon tube looking for gaseous emissions vented from the lunar subsurface or flashes from meteor strikes. Try as I have, I cannot find any connection between the Corralitos Observatory and the optical space surveillance community even though Hynek emphasized the satellite surveillance capabilities of the instrument, showing us several satellites moving through the image orthicon's field and spent most of the time talking to us about this rather than the lunar monitoring. As



Figure 25. The White Sands Army Base with the Organ Mountains in the background. The missile park is in the foreground and displays some of the various types of rockets that have been flown from the range. (This image is courtesy of <http://www.wsrmr-history.org/index.htm>.)

mentioned in Chapter 2, Hynek had been a prominent player in the Moonwatch program and Lincoln Laboratory chose the image orthicon concept for their GEODSS facility.

We also visited the cliff dwelling ruins in the high plateau about 100 miles northwest of Las Cruces. We passed several old gold mines in the mountains on the way and were able to persuade the people who wanted to stop and explore them not to as it was too dangerous. Besides a number of abandoned gold mines, White Sands Missile Range has its own treasure story. The range was obliged to grant access to Victorio Peak at the edge of the Jornada del Muerto desert in 1972 at the petition of F. Lee Bailey. Bailey had obtained a court order to permit his consortium access to the range to search for Doc Noss' lost gold. In 1937, Doc Noss discovered a shaft near the top of Victorio Peak that led to a treasure of jewels, coins, gold bars and valuable artifacts whose modern worth is estimated at least 2 billion dollars. He removed some of the gold over several years but collapsed the shaft while attempting to widen it with dynamite. Noss was shot and killed in 1948 during an argument with a man who was trying to 'fence' the gold for Noss. Access to the area was shut off during the 1955 expansion of the White Sands Missile Range as the newly acquired area included Victorio Peak. Legal battles ensued by Noss' heirs for access to Victorio Peak to hunt for the treasure. The saga of F. Lee Bailey's legal machinations that resulted in a one week access being granted in 1972 was a major story in the El Paso newspaper at the time, which is how I became aware of it. The Bailey expedition found nothing. There is an abundance of evidence that the treasure existed. However, speculation is that the treasure was removed by Army personnel and either given to the Treasury and/or found its way into private pockets. (More on this story may be found at <http://www.legendsofamerica.com/HC-Treasures5.html>.)

The longest sight-seeing trip was to the Carlsbad Caverns in the Guadalupe Mountains about 150 miles from El Paso. The drive was about three hours each way but the Caverns were

well worth it; we got to see the bats flying out at twilight. For the shorter trips, there was a park closer to our motel near the top of the pass over the mountains just north of El Paso, which had hiking trails and caves to explore. When we were on the 1974 HI HI STAR field expedition, the desert sky was clear enough near the top of this pass that comet Kahoutek was quite impressive from that vantage.

We fell into the habit of having a late afternoon/early evening dinner at the La Posta restaurant in Mesilla before the launch. Mesilla is noted as the town where William Bonnie, aka Billy the Kid, hung out. La Posta, the town and its surroundings of cotton and chili fields were a bit run down at this time, although La Posta served some of the best Mexican food that I have tasted, especially the salsa. The restaurant had a neon sign for the bar over one of the doors; you opened it and found yourself on the street opposite the only liquor store in town. The restaurant provided set-ups for the beer or wine that you purchased (something we seldom did since we had a full night ahead). Since then, La Posta has been remodeled and the homes surrounding the Mesilla town square have been converted into upscale tourista shops. The liquor store is gone and La Posta now serves drinks. Wistful remembrances perhaps but some of the colorful ambiance is missing from both the up-scale town and the restaurant. After dining at La Posta, we would drive through Las Cruces to I-10 to begin the long climb up the western side of the pass on US 72/80 and through the Organ Mountains. As we crested the pass through the mountains, we would often see the shadow of the Earth from the setting Sun in the atmosphere, astronomers call it the girdle of Venus. The shadow would visibly climb during the time it took us to drive out to the launch site.

The Missile Range had its own biota but most of the animals kept out of sight so that when we did see them, it was under unusual circumstances. We watched a pair of large golden eagles construct an outsized nest atop one of the telephone poles on the road from El Paso to the Range during several field trips. Chicks came in due course, fledged and abandoned the nest. One would occasionally see an Oryx, an African antelope with spiral horns. The Oryx had been imported for hunting, and thrived on the range because the environment was similar to their home and hunting on the range is strictly regulated. Mule deer were also plentiful, but they mostly came out at night posing a hazard for drivers. Then, in the spring of 1972, the Tularosa basin received quite a bit of rain, turning the flat area around the range's small air strip into a shallow lake. The rains also flooded the tarantula holes, driving them above ground in droves and scores of the spiders were on the road during the drive out to the payload preparation area. The rattlesnakes had the same problem and came onto the roads to dry out and warm up.

With regard to the conduct of the experiments, I was impressed with Russ' meticulous attention to detail and risk avoidance during the HI STAR program. Any problem, no matter how small, that arose in the laboratory had to be fixed before we went into the field. Problems in the field had to be resolved before we went on to the next major functional check before launch. And when Russ did gamble, it was with a high degree of certainty. For instance, we had fairly strong westerly winds on our last HI STAR experiment; strong enough that range safety recommended a no-go several hours before launch. Russ noted that the predicted trajectory consistently displayed little East – West dispersion, the narrow dimension of the range, but did vary by 10 – 15 miles in the predicted downrange impact point, well within the range boundaries. Range safety had an instant impact predictor that plotted the impact location if thrust to the rocket was shut down at the current instant of time during the flight. If the predicted location fell outside boundaries defined by range safety, which were several miles inside the physical boundaries of the range, range safety would terminate the flight. Russ took a chance and

launched the rocket. I was at the preparation area about a mile to the south of the launch tower and could see that the tower was canted to the east as far as it would go; since an unguided rocket flies like an arrow into the wind, the tower has to be tilted in the direction that the wind is blowing to compensate for it during powered flight. The rocket snapped northward as soon as it left the tower and flew down the middle of the range, just as Russ had anticipated. Other experimenters weren't as cautious. NASA had so many flights terminated because the principal investigators launched against range safety's recommendation, that Goddard Space Flight Center assumed launch decision responsibility, calculating the wind weighting in Greenbelt and forwarding the decision to the blockhouse.

The 'firmed' schedule for the Australian expedition had us departing late in the spring of 1974. I gambled and purchased airline tickets for my wife and daughter to go to New Zealand, counting on me being able to piggy-back the trip to Australia. Hah! I learned my lesson not to count on any field expedition schedule. So, I canceled the airlines reservations, losing \$50 a ticket, bought a Datsun 260Z 2+2 and scheduled a June vacation in Canada to break the car in. We had twice previously visited Canada, once a dash up and back to Cap Chat, Quebec for the 10 July 1972 total solar eclipse and another time a group of us went to the Trois Rivières area for a sugar house party arranged by a relative of George Vanasse, one of the senior scientists in the branch. However, I had finished the catalog before I could go on vacation. I completed the processing that June and left to tour the Maritime Provinces. On the tour, we had lunch overlooking the harbor at Moncton, New Brunswick, which is noted for the tidal bore. Since we were there near low tide, several hours before the bore was due, we missed the daily, several foot wall of water coming in with the tide. The large tidal variation in the harbor was evident, however, in the difference as to where the boat rode at anchor when we were there at low tide and the high water mark. We then went to the northernmost spot on Cape Breton. The village, Meat Cove, was so small that we drove through without noticing it. The road went from paved to gravel to dirt and we wound up in someone's backyard where the woman hanging wash stared curiously at us. We also visited St. John and Prince Edward Island to complete our tour.

We left for Australia in August, 1974; I watched the newscast of President Nixon boarding the presidential helicopter for the last time after resigning from office from my hotel room during our one night layover in Honolulu. We arrived at Woomera after a night in Sydney and the weekend in Adelaide. On the flight to Adelaide, we spent a couple of hours on the plane waiting to take-off from the Sydney airport because one of the unions was on strike. The Ansett stewardess (motto – chance it with Ansett) snippily explained that we had no right to complain about the delay because her union was due to strike in a couple of months.

Upon arriving at Woomera, we were lectured on the range regulations and assigned accommodations, which consisted of a single bed, a small wardrobe and a bench attached to the wall that served as a desk. We were given bed linen and a towel but discovered that wash cloths had to be purchased at the small stores that were only open during the day and Thursday evening.

Our daily schedule was restricted by the operating hours of the mess hall. It closed at seven and we had to return well ahead of that hour to be able to get a meal. You were out of luck if you were late because, unless it was Thursday, there was no other place on the base where you could eat. There was a roadhouse just outside the base limits, but getting back onto the base was a hassle. The mess hall would provide a box dinner, if requested beforehand, but only times we knew we would be working late were launch nights. My overall impression was that the range was struggling financially and that our expedition was a welcome source of income. Thus, we

had to stay at the barracks and eat in the mess hall rather than make use of the numerous small empty houses at the base where we might be able to prepare some of our own meals.

There were limited things to do during off-hours. On Wednesdays, vintage English movies were shown in the pub, Thursday had evening shopping and, on an occasional Saturday afternoon, amateur Australian rules football. Otherwise it was socializing and playing snooker at the pub next to the mess hall. One outing was for an authentic Australian barbecue when one of the range people invited us to his house for a cookout on the 'barbi'. This was on a Thursday evening so we could go to the butcher's to buy our steak, or whatever. Rather than the open American barbecue grill, the fellow had sheet metal over a gas fire, which he greased-up by tossing a couple of sheep sausages on top to cook. Tom Murdock and I agreed that we should let the others go first to cook off the sheep fat. Just as we judged the grill was right, our host noticed that it was dry and, commenting that he had to fix that, tossed a couple of more sausages on – aargh! I can only stand mutton in a very spicy curry and lamb prepared with lots of garlic. Even then, I find the cooking aroma off-putting. (The New Zealand and Australian detergents are made from sheep renderings and the washing reeked of sheep fat when it was humid.)

We discovered that the US Air Force had a 'commissary' liquor store on the range with limited operating times, one to two hours for one to two days a week. The Air Force personnel at Woomera supported the *Joint Defense Facility Nurrungar*, which was a communications ground station for U.S. Defense Support Program satellites (the facility was closed in 1999). Since we were on Air Force travel orders to a military base, we were allowed to purchase from the store. This was a really good deal as we didn't have to pay the state or federal tax. Since the store was open a limited time during working hours, we would place our order with a designated buyer for the group, who would return with a trunk full of booze.

We all found our own recreation to pursue in the evenings. Dick Buck, a telemetry engineer from Oklahoma State University (first row center in Figure 21), had purchased a raw opal. He glued it to a pencil eraser and spent nights in his room sipping Scotch and grinding the opal into shape on a piece of sand paper. Dick's room was across the hall from mine and many was the night I fell asleep to the skritch, skritch of Dick grinding away on his opal. He finished shaping and polishing the stone by the time we left but poor Dick had to pay import duty on the gem because, though his original purchase price was well below the allowable limit, customs said that the value that he added while out of the country made the stone subject to duty.

Business at the Woomera range was in decline when we were there and it showed. We were assigned the European Launcher Development Organisation's launch complex 6A for our field preparations; this facility is shown under construction in Figure 26. This site had a large vehicle assembly building, home to a contingent of sulfur crested cockatoos at the time, that we didn't use, and the checkout and launch facilities under the concrete vehicle rollout track, which we did. The old launch fixture at the end of the rollout platform overhung the top of a scarp of a small valley that debouched into a dry lake. (The locals told tales of the first satellite launch attempt of the Europa, shown on the launch stand in Figure 26, which consisted of a British Blue Streak rocket, a French Coralis second stage and a German Aatris third stage, that broke into three pieces along national lines a few seconds after launch. However, a satellite was launched successfully from Woomera on 28 October 1971, only three years before our field expedition.)

The year before we arrived was a wet one for the outback and, consequently, there were much more vegetation and wildlife than usual; certainly much more green vegetation than is shown in Figure 26. Lake Hart, the dry lake at the end of the defile where the preparation area was located, had water that we could see off in the distance that seemed to retreat as the days



Figure 26. The ELDO launch site at Woomera with an Europa vehicle on the pad. The roll-away vehicle assembly building is the tall structure in the background. The paved access road goes in front the vehicle assembly building and circles under the concrete roll-out platform. Our preparation area, unfinished in this picture, was beneath the roll-out platform forward of the access road. The launch complex in the far background was dismantled and the dirt roads were overgrown by 1974. The image was taken from <http://homepage.powerup.com.au/~woomera/eldo.htm>.

went by. A few of us decided to walk out to the ‘shore’ during the few hours we had off one day. We hiked down to the dry lake where we noticed a series of evenly spaced kangaroo tracks running in a straight line past where we were that disappeared in the distance. “Let’s follow the tracks.” So, we set off trailing the kangaroo and eventually passed a sign cautioning that the lake was a target range and not to pick up ordinance. After a quarter mile or so, I noticed that I was starting to sink into the lake surface. Tom poked a stick that he had brought along into the ground and it went as far as he would push it. Since I was the heaviest of our little expedition, I decided prudence was the better part of being stupid and turned back. The others went on for a ways, but turned back before discovering where the kangaroo went. We found out later that this was a bottomless lake and that things, such as unspent ammunition, would sink out of sight after lying on the surface for a while.

The road to the ELDO site went in front of the vehicle assembly building, circled 180°, dropping through a cut in the terrain to pass underneath the roll-out platform between the vehicle assembly building and the launch stand. Our preparation area was at this lower level. The 2 kilo-Watt electric motor we had brought to convert the Australian 50 Hz current into the 60 Hz ac that our equipment ran on was placed outside next to the preparation building so that the walls would damp out its loud high pitched whine. Just as we turned the corner and started our decent into the cut one morning, we found a kangaroo, a big blue, hopping down the road in front of us. (Blue kangaroos are really a nice shade of deep mahogany.) We slowed down to match his speed. The closer we got to the generator, the louder its whine and the more nervous the kangaroo became, hopping a bit from side to side. We had him boxed, so we thought, we were behind him, the generator was in front and the sides of the cut on either side of the road were 10'

high or more. All of a sudden, the kangaroo was gone in an eye blink. He had jumped over the side of the cut far enough away that we didn't see where he landed.

The Australian outback had many other exotic animals, at least to us. Driving back to the barracks one evening, we came upon a couple of emus running parallel to the road, one on either side; the locals depict an emu as a snake in a haystack on sticks. We slowed down behind them to match their speed. The emus and we went down the road together at 30+ mph for some distance before they ran off. The emus would, as if on cue, occasionally and simultaneously cross in front of us, keeping one on either side of the road.

On my one sightseeing trip while at Woomera, we stopped to watch a mother emu cross the road with half dozen or so chicks in single file. A 'sleepy' lizard was also next where we stopped. This rather large (about 10" long) lizard put on an aggressive display as we approached: opening its yellow mouth wide and thrusting out its purple tongue. The locals said that the sleepy has a tenacious bite and that it is virtually impossible to pry its mouth open if it bites you. So tenacious, that they say that if it bites the tire of your car you will hear the thump, thump for miles as it spins around, mouth clamped on the tire.

Australia is synonymous with opals and the range had a little shop run by Opal Marie, who had a daytime job on base, so her shop hours were limited. She also had an opal claim in Andamooka, a mining town 100 km or so north of Woomera and an hour plus drive from the barracks. I visited Andamooka on one of the 1½ days that I had off in the six weeks that we were on the range. Opal Marie had said that we could dig around her claim and keep anything we found. The government required that every claim be worked on-site for a certain period of time, a week each year I think, for the claim holder to keep title. Marie recently had the overburden of her claim dug out and I watched several of the guys dig into the Earth frantically searching for opals and concluded that the old overburden was on top and that Marie's generosity was a clever way of getting some of the spent earth shoveled off. I wandered off to sight see, being careful not to step off the paths between claims (trespassing a claim was a shooting offense, I was told). I wound up visiting the 'mayor of Andamooka,' an old fellow who resided on his claim the year around. He had hit the lottery in the 50s and saw no reason to work, beyond what the government required to keep his claim. An old car in front of his tiny dwelling was up on blocks and chock full of magazines and books – his library. He was kindly disposed to us Yanks as he had recently doubled the area of his dwelling using the wood and waterproof covering our Aerojet rocket crew had given him from the crates that the Astrobee 200's were shipped in. He invited me in, and gave me a water glass of port that he called plonk; British slang for cheap booze. This he poured from a gallon jug that he kept in his refrigerator next to a raw leg of lamb. The gallon jug was filled from a 55 gallon drum on his porch that he had delivered in on a regular basis. We chatted and nibbled on the fresh water shrimp that one of his mates brought by until our unsuccessful opal miners showed up to dicker with him to buy the plotch or opal matrix he had on hand. This was one of the more interesting highlights of the trip.

It must be said that the dedication and professionalism of the experiment team, some of whom are shown in Figures 5 and 21, produced a remarkably high 80% success rate over the years: 20 successes out of 25 flights. Most of the team seemed to have received personal reward in a successful experiment and worked hard to ensure success, devoting extra hours or weekend days, if necessary, to provide the time needed to correct problems that arose (during the previous test, for example) to maintain the schedule for the next major test.

4. A WEALTH OF DATA

The nine HI STAR/HI STAR South experiments surveyed approximately 90% of the sky at 11 and 20 μm to a flux of $\sim 10^{-15} \text{ W/cm}^2$ although some sources were detected up to four times fainter. Because of the change of the filter for the southern hemisphere flights smaller areas were covered at 4 μm (~75%) and 27 μm (35%). The area covered by the experiments and the distribution of the 1151 11 μm sources in the AFGL catalog are shown in Figure 27.

4.1. Characteristics of the Data

Under the best conditions, such as the ~0.8 seconds of data shown in Figure 28 that were taken at a time when the system noise was near minimum, the noise equivalent irradiance was $\sim 3 \times 10^{-16} \text{ W cm}^{-2}$ or about 3 higher than the sensitivity predicted by Equation (3). Unfortunately, the noise changed during an experiment, as may be seen by comparing Figures 28 and 29 of data taken on the same flight: Figure 29 is late in the experiment from the next to the last roll and has a high noise level. The variable noise in the constant signal-to-noise ratio selection criterion used to extract potential sources meant that the minimum brightness of the extracted sources changed during the experiment, rendering the flux limit at which a source catalog is complete somewhat problematic. Also, reliability is best assured by redundant observations and although the areas covered by the individual HI STAR experiments did overlap, a fairly large area (20 – 25%) of the sky was covered only once and a goodly portion of this area had elevated noise.

The display format for the raw data is arranged in triplets of the output from the three colors in a single row of detectors (Figure 16) with the rows ordered by increasing zenith angle, top to bottom. Thus, a single source appears as a grouped triplet such as the bright stellar source

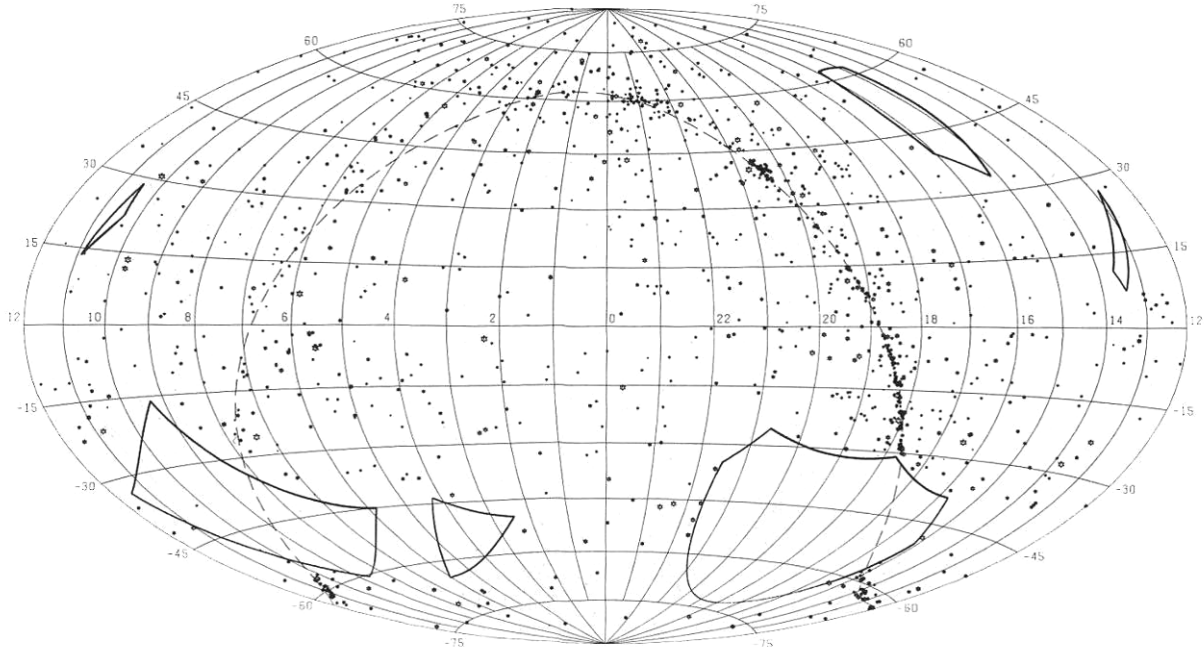


Figure 27. The 11 μm sources measured by HI STAR and HI STAR South. This Aitoff equal-area projection is in equatorial coordinates with the dotted line tracing the Galactic plane. The thick solid lines define the boundaries to the survey.

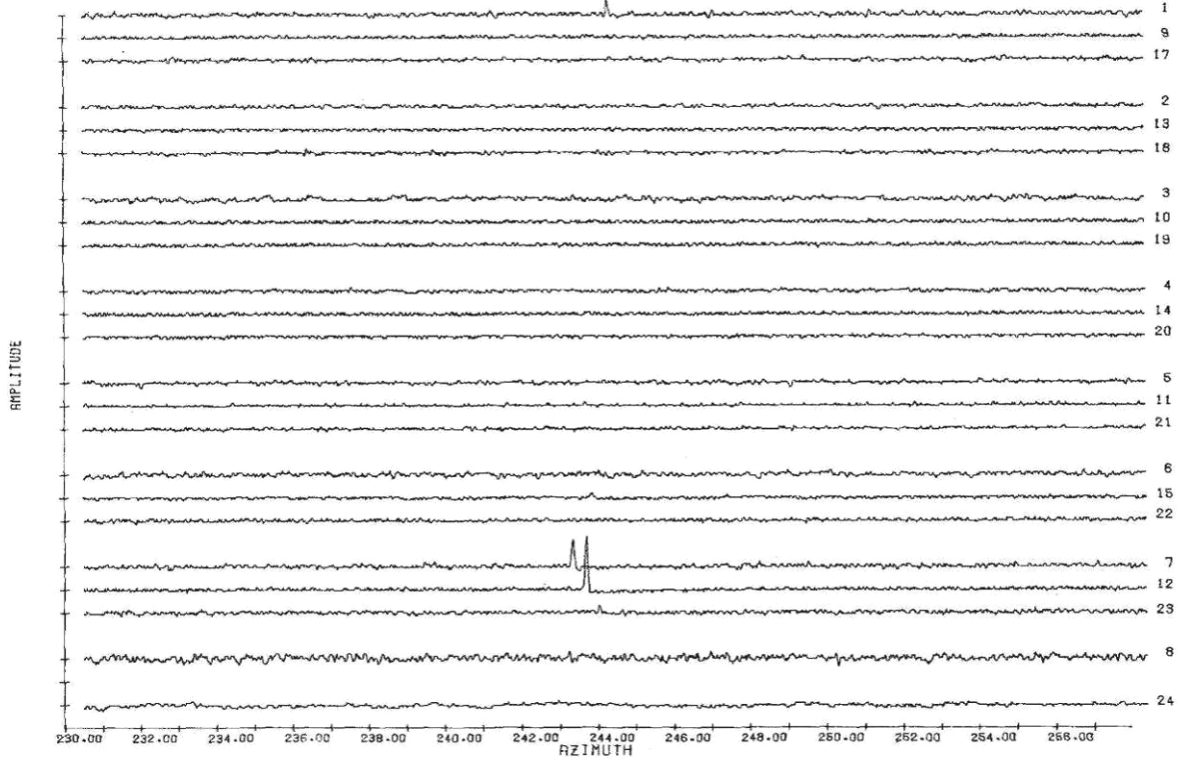


Figure 28. Sample of data from the first HI STAR flight. The system noise shown is the best achieved by the HI STAR experiments.

in Figure 28 that is readily visible on the next to the last row of the focal plane. The azimuth axis is the position of the focal plane center reference and, therefore, the stellar signals are displaced by the offsets of the three bands. That the star is relatively warm is inferred from the fact that the $4.2\text{ }\mu\text{m}$ signal is strongest, while the $11\text{ }\mu\text{m}$ and $20\text{ }\mu\text{m}$ signals are successively weaker. The numbers at the right label the detector that generated each scan in the plot: detectors 1 – 8 for $11\text{ }\mu\text{m}$, 9 – 16 for $4.2\text{ }\mu\text{m}$ and 17 – 24 are $20\text{ }\mu\text{m}$. For reasons we never discovered, detector 16 at the bottom of the $4.2\text{ }\mu\text{m}$ array of the HI STAR 1 sensor became excessively noisy only when the cover was removed in flight (e.g. Figure 34) and is, therefore, not plotted in most of the Figures. The source on detector 1 in the middle of the plot proved to be spurious.

The excess noise in Figure 29 is Poisson noise from the Earth's flux that gets through the sensor baffles and field stops to impinge onto the detectors. Since the Earth's radiation peaks in the mid-infrared, the noise is much larger in the 11 and $20\text{ }\mu\text{m}$ arrays than in the $4\text{ }\mu\text{m}$ MWIR band. The noise for the eight $11\text{ }\mu\text{m}$ detectors as a function of time is plotted for the first and fourth HI STAR flight in Figure 30 in which sensor stepping is noted by the 0° azimuth due North tick marks at the top of the plot. Since the latitude of the HI STAR experiments was close to $\sim +32.5^\circ$, the pole star for the first experiment, α CrB, $(\alpha, \delta) \sim (15^\text{h} 33^\text{m}, 26^\circ 49')$, tipped the rotation axis of the payload south (azimuth $\sim 180^\circ$) by about 6° from local zenith. Thus, the angle between the line of sight of the sensor and that the edge of the Earth changes by $\sim 12^\circ$ during a roll, producing the obvious cyclic variation in noise in the left hand plot. As may be seen from Figures 28 and 29, the detectors at the bottom of a given band that have lines of sight closest to the Earth are noisier than those higher in the focal plane. The pole star for the fourth flight, δ Per, $(\alpha, \delta) \sim (3^\text{h} 52^\text{m}, 31^\circ 48')$, placed the rotation axis of the payload within 1° of local

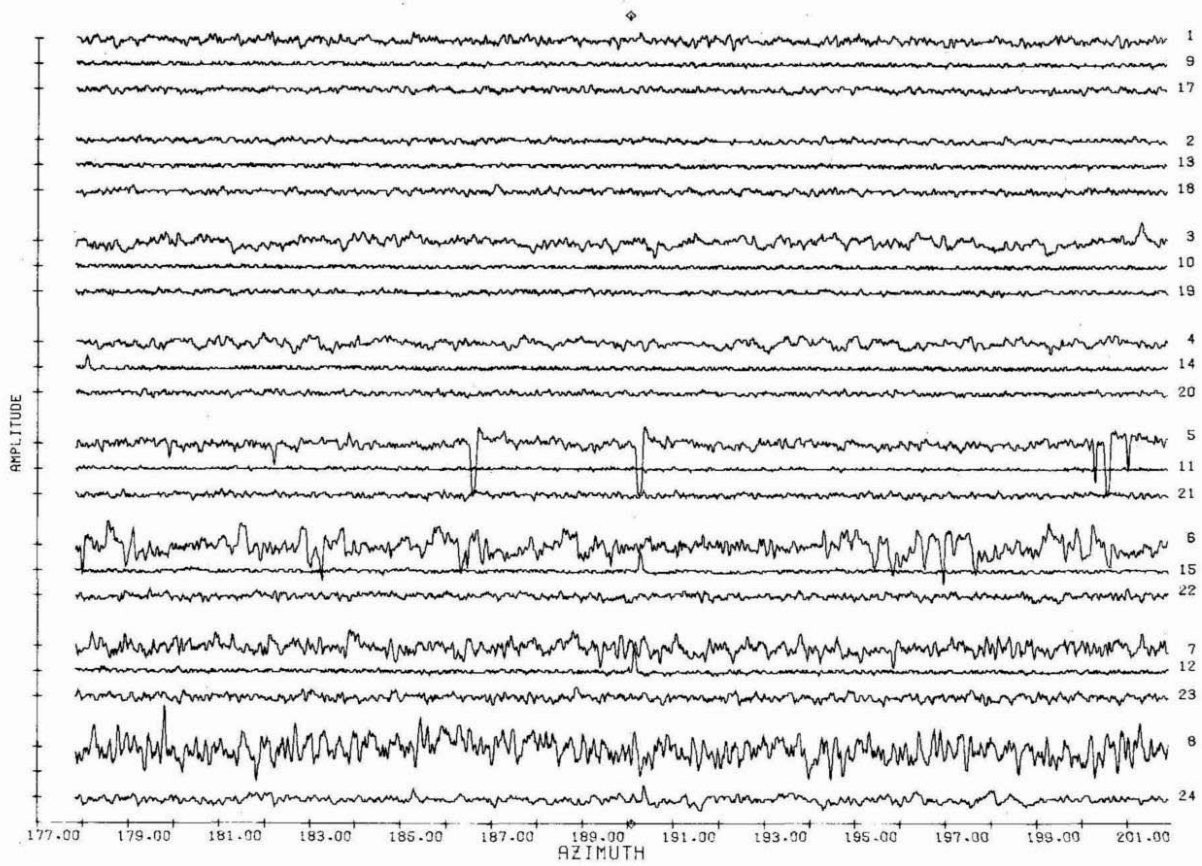


Figure 29. An example of noisy data. The source transiting detectors 12 and 15 is real while the bright, spurious 20 μm source on detector 24 is marked by diamond on the x-axis is not.

zenith. Consequently, the noise variations in the right hand plot are considerably damped, becoming only barely discernable at the end of the mission when the sensor steps closest to the Earth. The elevated noise during the initial several rolls is due to thermal flux from the payload above the sensor detected through the side-lobe response of the instrument.

The dependence of the noise on the flux from the Earth is more clearly seen in Figure 31 which plots the noise for the detectors second from the top and bottom of the 11 μm array plus one from the middle during the fourth flight as a function of the angle between the sensor line of sight and the edge of the Earth. This angle is the first order parameter for the amount of flux from the Earth entering the front of the sensor; the 30° minimum off-axis angle shown in these plots was typical for the HI STAR and HI STAR South experiments. The detectors at the bottom of the array are photon noise limited during the entire mission while those from the middle to the top appear to achieve maximum sensitivity for about a third of the experiment. The upturn in noise for angles greater than 50° is caused by the off-axis flux from the payload. The measured noise that is plotted is the root sum square of the minimum detector noise, nominally the 5 – 6 mV displayed on these plots, with the photon noise.

Both the HI STAR point source response as a function of flux and the noise response as a function of background radiance were calibrated in the 7V chamber at the Air Force Arnold Engineering and Development Center (AEDC) from which Price and Walker (1978) found that the responsivities from the point source and noise calibrations agreed to within the measurement

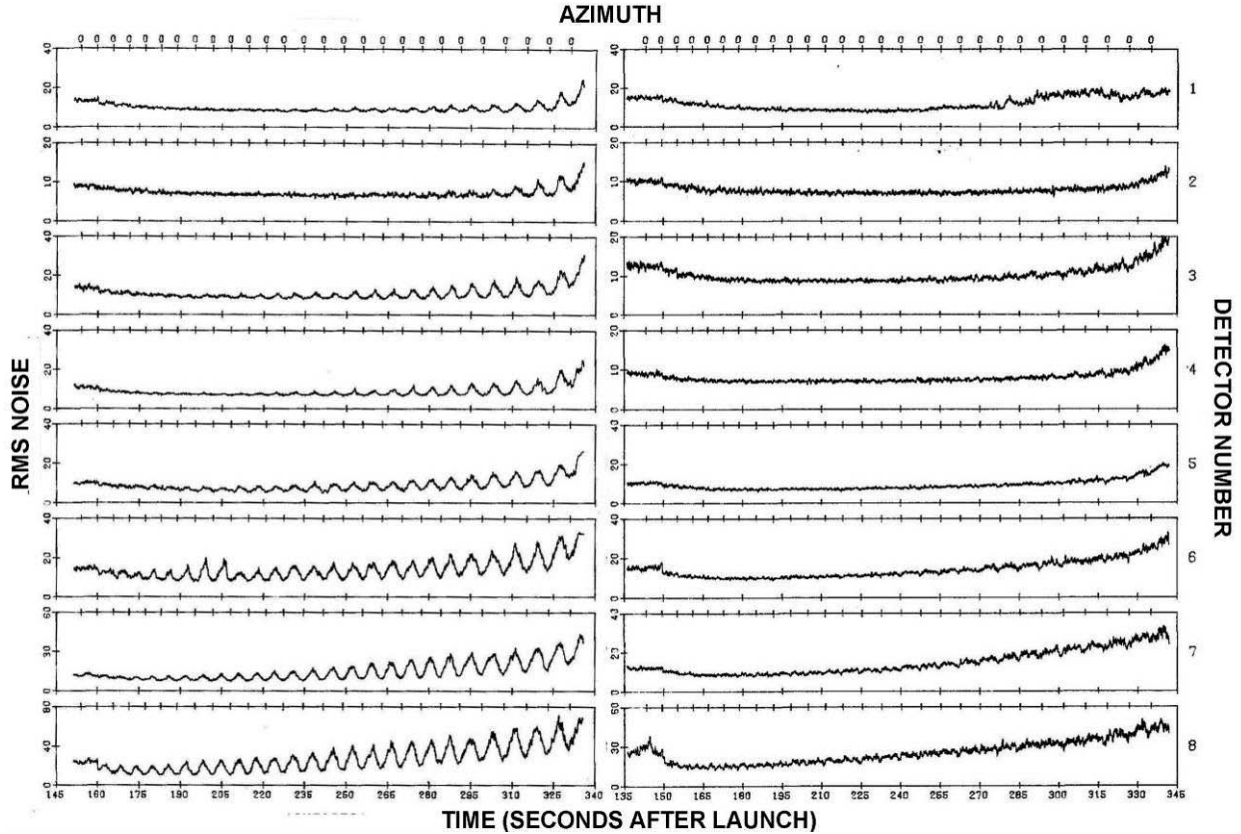


Figure 30. The time history of the noise for the 11 μm detectors during the first (left) and fourth (right) HI STAR experiments. Time from launch is at the bottom and North (0° azimuth) is denoted by the tick marks at the top. The cyclic pattern in the left hand plot is created by the pole of rotation being tipped about 6° south ($\sim 180^\circ$ azimuth), which causes the line of sight with respect to the Earth's edge to vary by $\sim 12^\circ$ during a roll. The rotation pole is tipped by only $\sim 1^\circ$ in the plot on the right. Despite the different behavior with time for the two experiments, the noise averaged over a given roll is about the same.

errors. The photon noise as a function of off-axis angle as shown in Figure 31 was inverted using the 7V chamber calibration to estimate the HI STAR point source rejection ratio of the sensor for angles greater than 30° , to which was added a model prediction at smaller angles to produce the curve shown in Figure 32. The radiance through the off-axis response is estimated at $\sim 4 \times 10^{-9} \text{ W cm}^{-2} \text{ sr}^{-1}$ at 30° from the Earth. This is about 10 times the noise equivalent radiance and provides a photon background noise of about 3.5 higher than the system noise; the off-axis radiance for the end detectors was about four times higher and the noise was twice as great. No excess noise was observed in the 11 μm band for the two HI STAR South experiments although variations of a factor of two, at most, were observed in the 20 and 27 μm detectors.

The non-rejected Earth radiation (NRER) seen by a sensor is given by:

$$NRER = \text{Const} \int_{\text{hemisphere}} PSRR(\theta, \phi) H(\theta, \phi) 2 \sin \theta \cos \theta d\theta d\phi \quad (4)$$

$PSRR$ is the point source rejection ratio as a function of off-axis angle, θ , and azimuthal angle, ϕ , about the sensor line of sight. For a rotationally symmetric response, the $PSRR$ consists of three components:

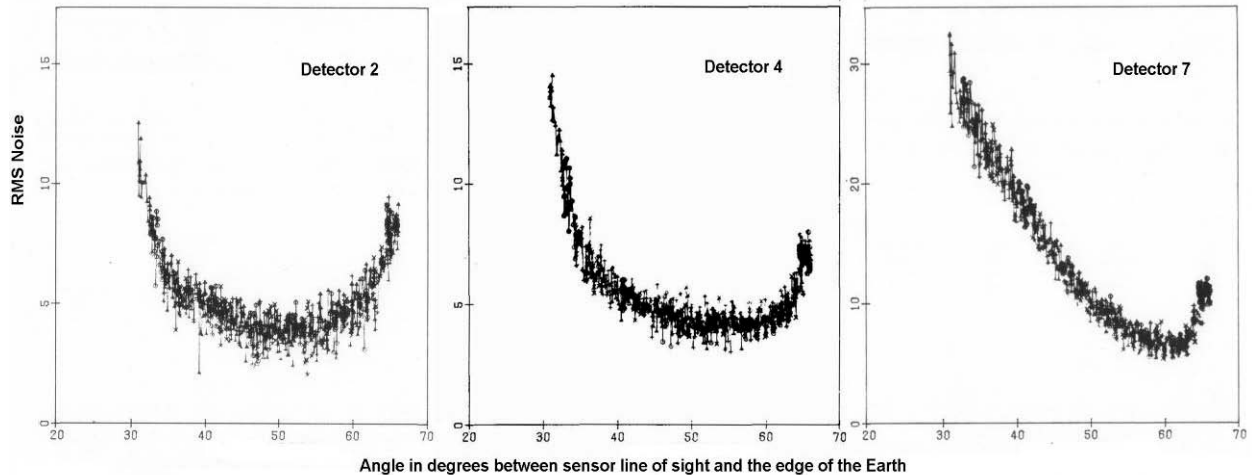


Figure 31. Noise for the 11 μm detectors second, fourth from the top and second from the bottom (left to right) during the fourth flight as a function of the angle between the sensor line-of-sight and the edge of the Earth. The noise floor, 4 – 5 mV on this scale, corresponds to a radiance of $\sim 2 \times 10^{-10} \text{ W cm}^{-2} \text{ sr}^{-1}$.

$$PSRR = A\theta^{-3} + BRDF(1^\circ)\theta^{-n} \times F(\theta) + k \cos \theta \quad (5)$$

The $A\theta^{-3}$ diffraction contribution dominates within the focal plane area and assumes this analytic form as the result of averaging the intensity distribution of the diffraction pattern at large angles. The second term is an empirical function for direct scattering from the primary mirror. The Bidirectional Reflectance Distribution Function (BRDF) is the angular distribution of the scattered light from the mirror illuminated at the incident off-axis angle θ . The exponent, n , is roughly 2 with larger values claimed for super-polished mirrors. $F(\theta)$ is the fraction of the primary mirror that is illuminated. It is a quasi-linear function of θ between full and a quarter illumination, then decreases more steeply with increasing angle reaching zero at the baffle angle, $\tan^{-1}(W/L)$, and beyond; L is the baffle length, W is the diameter of the mirror plus the distance between the mirror edge and the baffle.

Mirror scattering dominates the sensor side-lobe response when the primary mirror is directly illuminated by an off-axis source. Thus, lengthening the baffle reduces the baffle angle and improves the intermediate off-axis rejection. Also, the rather modest scattering properties of HI STAR polished beryllium mirrors, with a $BRDF(1^\circ) \sim 10^{-2}$, could be improved by coating the mirror with electroplated gold or electroless nickel as this surface can take a smoother polish. Several sensor manufacturers developed ‘super-polish’ processes for coated metal mirrors that produce surfaces comparable to the smoothest fused-silica mirrors, some 10 to 100 times better than uncoated mirrors. The super-polished nickel finishes are generally used as they have somewhat lower scatter than the gold coatings. The HI STAR South and HI HI STAR mirrors were electrolessly coated with kanogen, a nickel-phosphorus alloy, and super-polished. The HI STAR South point source rejection curve in Figure 30 was scaled to be 10 better than HI STAR, a modest extrapolation of the improvement in scattering by the super-polish. Unfortunately, it was soon discovered that nickel coated mirrors developed a blue haze that degraded the super-polish and scattering properties if exposed to laboratory air for even a modest length of time. Champetier and Giguere (1982) found that the blue haze was created by chemical reactions between the nickel in the plating and contaminants in (sub)urban air and, if left unattended for long periods of time, the corrosive reactions could permanently damage the coating. They

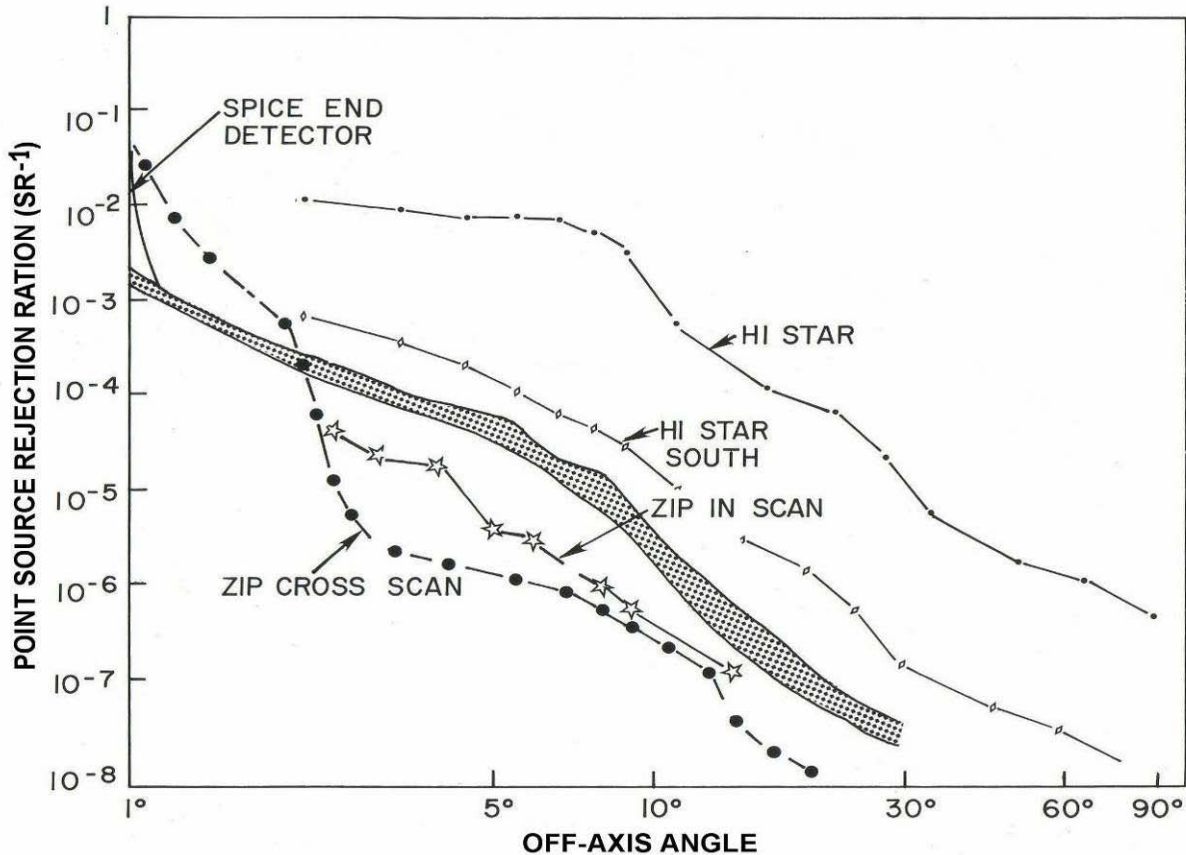


Figure 32. The point source rejection ratio for four AFCRL/AFGL sensors. The ratio is the measured radiance at the focal plane divided by the incident irradiance on the entrance aperture from a point source at a specified off-axis angle; thus, the units are sr^{-1} . The HI STAR South curve is scaled from HI STAR values by assuming it equals 10^{-3} at 1° off-axis. The SPICE and ZIP curves are the best laboratory measurements.

further established that the degradation could be slowed or halted by regular cleaning. We usually cleaned the primary mirrors of the sensors just before going into the field and sometimes as part of the field preparation. Having controlled the deleterious effects of blue haze, we found that particulate contamination on the mirrors then became the dominant source of scattering.

The third term in Equation (5) is the baffle cavity scattering function, which is assumed to be proportional to the amount of radiation entering the baffle, hence the $\cos \theta$ term, that is diffusely scattered and diluted by the factor k . In the simplest form, k is a constant on the order of 10^{-6} but as may be seen for the ZIP and SPICE sensors in Figure 32, some companies claim a relatively steep θ dependence of k . The inside baffle surfaces of almost all infrared sensors are coated or anodized to absorb the impinging radiation, thus reducing the magnitude of k .

Scattering measurements from test samples of the baffle surfaces indicate that there is higher scattering at small angles with respect to the baffle surface. In other words, scattering down the baffle barrel is larger than at angles more nearly normal to the baffle. Circular vanes (Figure 47) are inserted or the baffle surface is grooved (Figure 44) to intercept these 'grazing' rays. The edges of the vanes have to be rounded as knife-edged vanes would introduce diffraction effects.

Optimizing sensor design for off-axis rejection been an active area of research since the 1970s as reflected by the twice yearly conferences on this topic held by the *Society of Photo-optical Instrumentation Engineers (SPIE)* in the references). Sophisticated predictive modeling and codes, supported by laboratory measurements, have been developed for system design

studies. However, the optimal performance predicted by laboratory measurements and the stray-light rejection codes were never achieved in flight. Don Smith (1988) found, as expected, that the stray light observed during the HIRIS probe-rocket borne aurora experiment (Stair et al., 1983) was impressed with the signature of the upwelling infrared Earth radiation. He also estimated that the in-flight off-axis performances of this and other AFCRL/AFGL experiments were 20 to 40 times poorer than predicted and that the degradation had to occur before flight (Smith; private communication). Brown and Smith (1990) then analyzed the infrared spectral reflectance of several black coatings commonly used on baffles and found that the specular reflectance averaged 5 – 10% while the diffuse component was generally less than one percent. However, a spectral signature characteristic of the primer and paint used in the coating was seen for both. Surprisingly, they also found the baffle coating signature in the stray light spectrum from the SPIRIT I experiment (Smith et al., 1991), indicating that a measurable fraction of the off-axis radiation from the Earth was reflected from the baffles even though the off-axis angle was less than the baffle angle and scattering off the primary mirror was supposed to dominate. Thus, stray light is a difficult problem for infrared sensors even today (see Figure 117).

How close the sensor came to the Earth during the rocket surveys was a performance consideration in the design of the experiment as it impacted the area of sky to be covered. After HI STAR, the off-axis rejection of the sensors and the background noise was reduced by altering the experiment profiles to increase the angles to the Earth. Although the off-axis problem is eliminated by keeping the sensor line of sight far from the Earth, the DoD was interested in the sensor performance looking close to the Earth. For a surveillance system in an orbit that is depicted by the blue circle at the confluence of the lines in Figure 33 to view a ballistic missile in the green trajectory curve, it must look at tangent heights below local horizontal (the line tangent to the blue circle) to detect the missile even though the missile's peak altitude exceeds that of the surveillance system. The closer to the Earth (smaller tangent heights) the system can look, the earlier the missile can be detected and the longer it can be tracked; Jamieson (1995) noted that the original surveillance system goal was to operate within a degree or so of the edge of the Earth. However, the closer the system looks to the edge of the Earth, the more stringent the off-axis rejection requirements and one degree from the Earth is very stringent, indeed.

There is also a space surveillance advantage to looking below the spacecraft altitude and as close to the edge of the Earth as performance constraints allow. A surveillance sensor detects much more of the population of objects in low Earth orbit at altitudes less than that of the sensor when looking sideways through the field. A surveillance sensor samples the population of low altitude Earth orbiting satellites twice over the same range of altitudes between the tangent height defined by the below horizontal look angle and the altitude of the sensor: on the near side of the

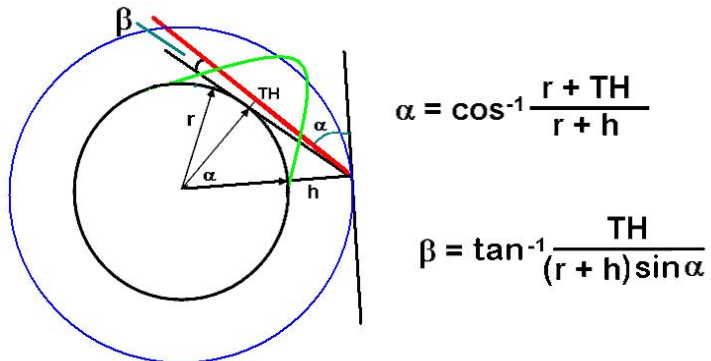


Figure 33. Definition of tangent height. The black circle depicts the Earth with radius r and the sensor is in an orbit, the blue circle, at an altitude of h . The tangent height, TH , is the altitude of the closest point that the sensor line of sight comes to the surface of the Earth. Beta is the angle between the edge of the Earth and the sensor line of sight while α is the angle between the line of sight and local horizontal and is usually either known or defined.

tangent height and again on the far side. Also, the closer to the Earth's horizon the sensor acquires a satellite, the longer it can track the object. However, viewing near the Earth means that the sensor will be degraded by the increase the photon noise from the stray radiation of the bright Earth that enters through the side-lobe response of the sensor, which reduces sensitivity and dynamic range. The sensor cannot operate in certain areas of the sky where this degradation becomes severe and this restricts the volume of space and look directions that may be covered.

The large range of HI STAR deployment angles that were influenced by background noise was unanticipated. However, in fairness to Hughes, who made the sensors, the requirement at the time was that the sensor was not to be background limited when looking at a tangent height of 100 nautical miles (~ 185 km), a condition that was never met for the HI STAR experiments. The maximum tangent height is the payload altitude (Figure 33) and, from Table 1, the peak altitudes for all the HI STAR flights were less than 100 nautical miles; the HI STAR South experiments were barely higher. Thus, the off-axis performance requirement, other than doing the best possible, didn't apply for these experiments.

The variable background noise from the non-rejected Earth radiation caused the flux of a potential source that just exceeded the signal-to-noise selection criteria to vary by up to a factor of 6 during an experiment. This presented the greatest problem in compiling a complete and reliable catalog. Initially, potential signals greater than three times the time dependent noise above a running average were selected. This produced far too many false sources, especially in the regions with elevated noise. Guided by the fact that there were (real) large-scale undulating signals in the data, a zero sum high pass digital filter sized to a point source was added to reduce the low frequency noise and then, in tandem, a matched filter shaped like a point source response was applied to try to improve the source discrimination and quantification. Developing, testing and applying the processing procedures to the data and digesting the results in order to modify and improve the algorithms were laborious and time consuming. The programs were coded in FORTRAN on punch cards and initially run on the AFCRL IBM 7090/4 mainframe computer. Processing a single experiment took all night using the full capacity of the machine. The computer capability just kept pace with the processing requirements as improvements were added. Initially, it took a couple of hours to calculate the mean level and noise for the 23 active HI STAR detectors (channel 16 was inoperative for the first six flights) then to project the average and extract potential sources. The simple zero sum filter added little computational burden but the matched filter required a lot of memory and computational time, which the CDC 6600, the next AFCRL mainframe computer, provided. Adding the cross-correlation coefficient parameter for point sources further impacted processing time. The final processing runs took about four hours for each flight, which were usually done at night when the CDC machine could be entirely devoted to the problem. Processing the data from last experiment, the only one to use the slightly less sensitive second HI STAR sensor, took 10 hours over two nights as the data had to be pre-conditioned to remove the correlated noise created by cross-talk from the payload electronics. All this effort was expended for what is now a very modest 75 Mbytes of data. We had a single programmer/analyst (me), who was in the field at least a month out of every three. As additional flight data became available, the requirement for confirming observations of a source in a region surveyed more than once was made both more stringent and sophisticated by calculating the signal-to-noise of a source on a given experiment for confirming flights and applying the redundancy criterion if the predicted signal-to-noise exceeded the selection criterion of three. This was quite a detailed bookkeeping task as the specific detector and predicted time of observation on the confirming experiment had to be identified.

Catalog reliability was best assured by redundant observations and approximately 75% of the sky surveyed by the HI STAR flights was covered more than once with about half being covered at least three times. Unfortunately, a goodly portion of the rest of the survey area that was covered only once had elevated noise. This is why the University of Arizona and Caltech were asked to do follow-up observations to confirm sources. Although there were a fairly large number of spurious sources in the HI STAR preliminary lists, the improved processing identified and rejected the majority of these from the final catalogs. Of the 118 sources in the preliminary catalog that Low (1973) searched for but did not find only 20 made it into the AFCRL catalog.

False sources were created by a variety of effects. As may be seen from Figure 29, the detectors spiked at very high photon backgrounds. Most of these spikes are negative, but some are positive, thus creating spurious sources. Contamination is another source of spurious signals. The HI STAR experiments were flown from White Sands Missile Range, a dusty location as anyone who has visited the range can attest, and exposed surfaces accumulate a dust layer within a few days. Holdale and Smith (1968) had found that the surface winds and the dryness of the region surrounding White Sands Missile Range combined to loft a considerable amount of dust into the air and that this dust is mainly confined to the surface boundary layer in the Tularosa basin. The HI STAR program successfully adapted payload design and cleaning techniques developed by the interplanetary dust collection experiments described in the previous Chapter.

The AFCRL/AFGL probe-based infrared survey experiments could readily detect thermal emission from particulate contamination in the field-of-view. Therefore, the payloads were designed to be easily cleaned: areas that could not be cleaned, such as the electronic decks, were hermetically sealed and the air vented through Millipore filters during rocket ascent. The entire payload and telescope exterior was cleaned in a laminar flow cleanroom using a Freon wash and an ultraviolet light to detect particles. Dust doesn't fluoresce under ultraviolet light but organic particles, such as dead skin and dandruff, do. The logic was that if the payload has been cleaned of all organic particles from the local vegetation and human handling, it was likely that the dust was also eliminated. After the final cleaning, the payload was sealed in double static free plastic bags; the removal of which was the last payload operation before launch. Cunniff (1978) and Price, Cunniff and Walker (1978) provide more details on the payload design and cleaning procedures, which proved to be quite successful with only a small portion of the second HI STAR experiment having any indication of dust contamination. Such contamination was easily recognized by their double peaked signatures that correlated across the focal plane as shown in Figure 34. The particulates are visible at 11 and 20 μm but not at 4.2 μm as would be expected from a cool ($\sim 270\text{K}$) particle in thermal radiative equilibrium near the Earth. The central obscuration of the HI STAR telescope creates an annular, near-field, out-of-focus image, which produces the characteristic double peaked signal as the sensor scans past the particle. The particle distance may be estimated from the optical prescription and the angular distance between the peaks; the color temperature is derived from the observed 11 to 20 μm flux ratio and the size from the inferred distance and blackbody flux at the calculated color temperature.

Outgassing from the payload and water vapor could freeze out onto the very cold optical surfaces. Solvents of low molecular weight as well as the phenolics and oils in electronic components were known to outgas on satellite missions while water vapor is a difficult to eliminate atmospheric constituent and just a few molecular monolayers of ice dramatically increases the optical surface scattering, seriously degrading the off-axis performance of the instrument (Viehmann and Eubanks, 1972). Therefore, after bagging, the payloads were purged with water free dry nitrogen generated by passing liquid nitrogen boil-off through a filter.

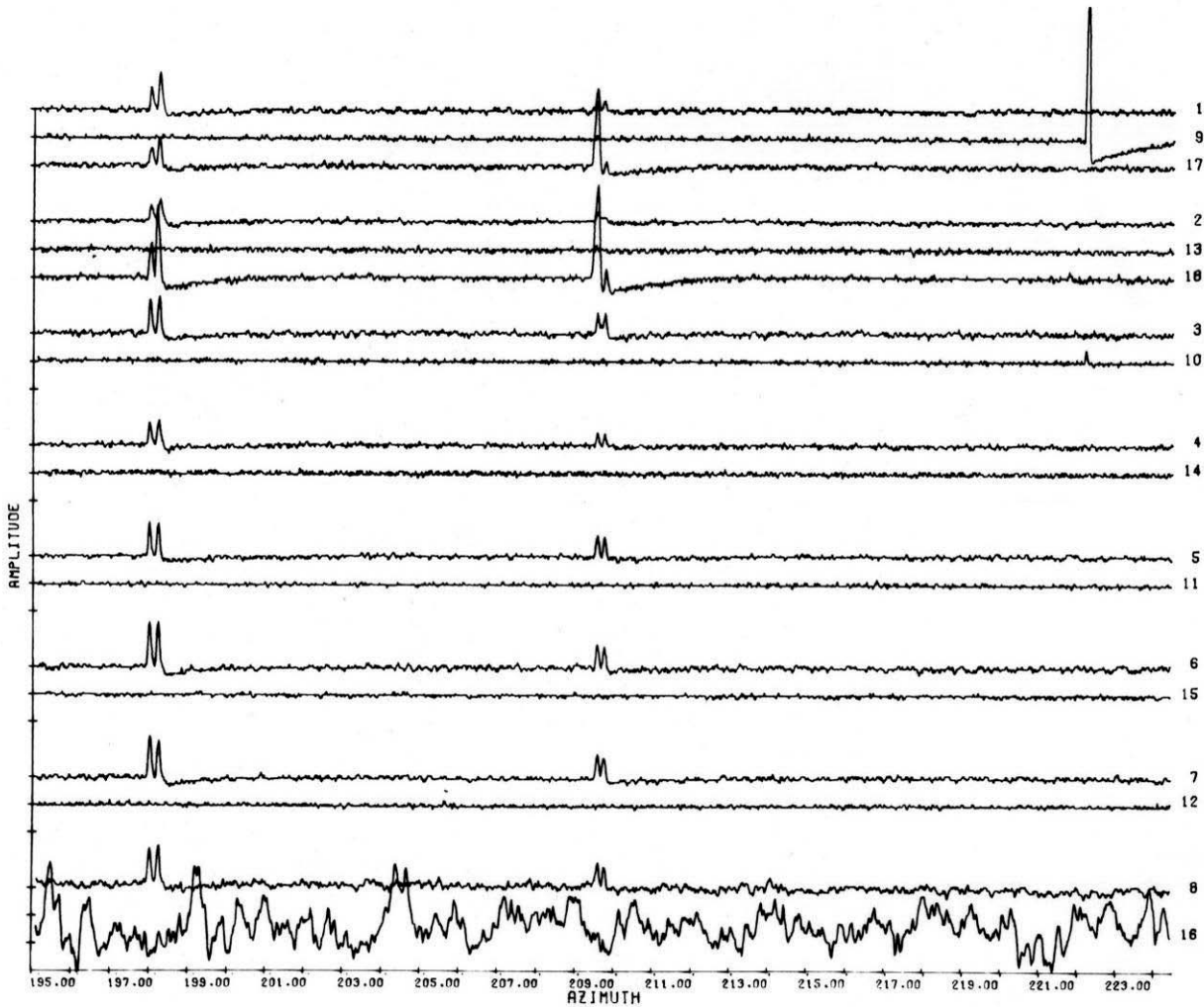


Figure 34. Infrared signatures of dust particles from the second HI STAR experiment. The lower six 20 μm detectors were inoperative on this flight and are absent in the plot. The centrally obscured optics creates double peaked signature. An energetic particle interaction with detector 9 may be seen in the upper right. Such a signature is representative of the detector and electronic system response.

Energetic particles, such as cosmic rays, an example of which is shown on detector 9 in the upper right in Figure 34, were another source of spurious signals. The interaction was very fast, essentially a “delta” input function, and the resulting signal was representative of the detector and signal processing electronics system response. The effect of the high pass filter in the signal processing electronic is evident as the negative excursion with the slow recovery tail after the spike. The time-to-peak for particle interactions of reasonably strong signals was about half that for real sources and this distinction was used to eliminate these events. However, it was difficult to discriminate against the lower amplitude events; the spurious source on detector 1 in Figure 28 is likely such a low amplitude energetic particle interaction.

Real moving objects such as asteroids and satellites were the bane of the survey because of the limited redundancy and great care was taken to account for them. Fortunately, the 22 HI STAR detections of 17 asteroids were bright enough that they could be readily identified by associating their observed positions with the predictions in the annual Russian Ephemeris of Small Planets. Identifying satellites was more complicated.

Satellite ephemerides were calculated in sensor coordinates by a program jointly developed by AFCRL and the North American Aerospace Defense Command's (NORAD) Analysis group. The program sought an iterated solution that matched the predicted satellite position with the sensor line of sight. The standard orbit propagator was used with the NORAD element-sets for the experiment epoch to determine the satellite positions. The satellites were pre-filtered to limit consideration to only the 8 – 15% of the population above the sensor horizon at the mid-point of the experiment. This criterion assumed no rejected satellite would enter the field swept out by the sensor since the survey data were obtained within less than three minutes of the mid-time of the experiment and the maximum zenith angle was usually $< 80^\circ$. The payload trajectory and sensor azimuth solutions expressed as time dependent polynomials were provided as input to the program as was elevation angle for each roll. The roll solution was inverted to derive the time that the satellite would be at the predicted azimuth; this time is then used to update the position of both the satellite and payload. Usually two or three iterations were all that were needed to converge to the solution. Satellite track errors were expressed in time and solutions found in increments of 5 seconds between track errors of ± 15 seconds. About two-thirds of the input list of satellites was then eliminated by requiring the objects to have elevations within 2° of the nominal deployment angle and at a time within the ± 15 second track error. The list of sources observed by the survey experiments was then compared to the predicted crossings and a subjective judgment was made as to whether a match existed if 1) the observed detection did not correspond to a known celestial object, 2) it was not observed on an overlapping scan, 3) that the source was not extended as might be expected for particulate contamination, 4) the observed position matched the predicted one within 0.2° and the track error is < 3 seconds. Interestingly, because of the manner in which the survey was conducted, about half the objects were detected on two or more scans.

Seven high confidence satellite observations were found on the first five HI STAR experiments and the list expanded to about 30 objects with probable associations from all seven of the HI STAR experiments; a total of ~ 60 satellites were seen on all of the AFCRL/AFGL celestial survey experiments flown between 1971 and the early 1980s. About half of the satellites were measured in two mid-infrared bands and, thus, a color temperature could be derived. The color temperature distribution peaked sharply at 280K, as might be expected, but the temperature extremes in the distribution were ~ 200 K and 395K. Because of the limited sensitivity, the detected objects were relatively nearby, ranging from about 500 km to 5000 km.

4.2. AFCRL Source – What AFCRL Source?

We distributed progressive survey results within the DoD community and infrared astronomers under DoD contract as soon as they were available⁶. The reliability of the preliminary catalogs improved as more experiments added redundancy and the data processing evolved. The initial catalog from the first three experiments listed 1,412 sources while the five flight catalog, which had the widest 'private' distribution, contained 2,066 sources.

⁶ The DoD sponsored a regular series of topical meetings at which early results and progress of the AFCRL/AFGL backgrounds efforts were reported, including the HI STAR preliminary catalogs. The Office of Naval Research in Pasadena began sponsoring the joint-service classified symposia in August 1949, the forerunner of the Infrared Information Symposium (IRIS) meetings that were devoted to the military applications of infrared technology. The first IRIS proceedings were published in 1956. The name of the symposia became the Midcourse Measurements Meeting (MMM) about the time ARPA Project 1366 came into existence and then the Strategic Signatures Symposium (S³) in 1974. The meetings are currently known as MD-SEA.

ARPA required that the final HI STAR report and catalog be finished before we went to Australia for the HI STAR South experiments. The catalog was reasonably complete in spring of 1974 and when it came out in 1975; the *AFCRL Infrared Sky Survey* catalog (Walker and Price, 1975) contained 3198 objects. Although we did some additional tweaking before publication, there was insufficient time to digest and account for the confirmation searches by the University of Arizona, and others. However, sources in the preliminary lists were removed as the area surveyed increased and the added redundancy was used in compiling the Catalog; Low et al. (1976) acknowledged the deletion of spurious sources in the preliminary lists from the catalog.

Pressure began to mount from the infrared astronomy community for access to the survey results after articles began to appear in the literature in 1972 – 1973 based on preliminary information from the five experiment version of the catalog. Then, a figurative feeding frenzy was set off in the infrared astronomical community with the July 1975 publication of the AFCRL catalog. Appetites had been whetted by the first assessments of the preliminary lists by the University of Arizona that appeared in abstracts at American Astronomical Society meetings (Kurtz et al., 1973; Kleinman and Lebofsky, 1975; Lebofsky, Kleinmann and Rieke, 1975). Also, articles began to appear in the literature on objects in the preliminary lists that had unusual infrared properties: Humphreys et al. (1973) proposed that TMSS+10420 could be similar to the bright super-massive super-giant star η Carina based in large part to its very bright 20 μ m HI STAR flux; Cohen (1973) confirmed the existence of a bright AFCRL infrared source near the Rosette Nebula as did Cohen and Barlow (1973) for two symmetric (bi-polar) nebulae; Wynn-Williams and Becklin (1974) used the catalog to assess infrared fluxes from H II regions while Strom et al. (1974) did the same for H II regions in external galaxies. Merrill and Soifer (1974) presented the spectrum of an obscured source in Cygnus (AFCRL 2591) that they obtained as part of a program of spectroscopy of AFCRL sources (Merrill, 1975), while Simon and Dyck noted strong 18 μ m absorption in this source and AFCRL 2205. Finally, Ney et al. (1975) found very strong infrared emission from CRL 2688 while Westbrook et al. (1975) noted that AFCRL 618 was a similar bright infrared object, but with emission lines of ionized gas. These papers cited private communication from Walker and Price as their information source and there was some sentiment in the community at that time that AFCRL was giving unfair privileged access to a few infrared astronomers. This was a valid criticism in the abstract but the preceding litany of papers by diverse authors from a variety of institutions show that few people were left out. I was told that a copy of the preliminary catalog simply appeared at the Infrared Telescope Facility (IRTF), source unknown, after it was published as part of a limited access report.

The catalog publication was soon followed by a number of articles that tallied the success or failure of ground-based confirmation of the AFCRL sources. Cohen (1975) attempted to find optical counterparts for ~700 unidentified AFCRL sources but, not surprisingly, could propose tentative optical identifications for only 6% of them. More appropriate mid-infrared searches were conducted by the University of Arizona (Lebofsky, Kleinmann and Rieke, 1975; Low et al., 1976; Lebofsky et al., 1976, 1978 and Kleinmann et al., 1979) and by Gehrz and Hackwell (1976) while near-infrared searches for southern hemisphere sources were done at 2.2 μ m by the Australian infrared group (Allen, Hyland and Longmore, 1976; Longmore, Hyland and Allen, 1976; and Allen et al., 1977) and by Persi and Ferrari-Toniolo (1984) at 3.6 μ m. These efforts found that the catalog had a fairly high false entry rate (~20%) although the exact number couldn't be ascertained because many of the sources that failed to be confirmed were extended H II regions (Kleinmann et al., 1979; Price, 1981; Price, Marcotte and Murdock, 1982) that, though very bright, could not easily be seen by ground-based instruments because of sky chopping.

The early studies selectively concentrated on objects with unusual HI STAR photometry such as sources detected at 11 μm and/or 20 μm without associations with known objects. Consequently, the success or failure to confirm these sources did not reflect the true reliability or completeness of the catalog as a whole. Therefore, we contracted with the Universities of Minnesota, Wyoming and California at San Diego to look at every source in the AFGL catalog of Price and Walker (1976) even if it had a plausible association. We divided the catalog entries into thirds by assigning the same 20^m right ascension interval every hour to each university. Gosnell, Hudson and Puetter (1979), Rudy, Gosnell and Willner (1979), Ney and Merrill (1980) and Grasdalen et al. (1983) published their findings, the combined results of which indicated that the AFGL catalog had about a 90% confirmation rate for the mid-infrared objects.

NASA had a keen interest in the technical maturity demonstrated by the AFCRL/AFGL survey. The Infrared and Space Astronomy Panels of the National Academy of Sciences (1973) decadal study for the 1970s gave a priority recommendation that NASA fly a satellite to survey the infrared sky and another for a space-based infrared observatory. Preparatory to these satellites, the Panels recommended that probe-based technology demonstration experiments be flown and time and money would be saved if the HI STAR experiments could substitute for these NASA proof-of-concept flights. The 1974 National Academy of Sciences (1975) Space Sciences Board reiterated the need for a demonstration of cryogenically cooled infrared sensors in space (Harwit, 2003). The board would support an infrared survey satellite but only on the condition that the technological maturity could be demonstrated. In response, NASA requested that Mike Hauser from Goddard Space Flight Center lead an IRAS feasibility study (Hauser et al., 1976) to assess the technology inherent in the AFCRL experiments.

From their assessment of the reliability and completeness of the AFCRL catalog, the IRAS feasibility study concluded “*... that the source definition procedure may have been efficient in locating real sources but did not constitute a highly efficient filter against spurious signals.*” The study was especially concerned that the AFCRL survey did not have a self confirming strategy to scan a given area of the sky two or more times on a single experiment. However, there were some in the community that assigned the AFCRL catalog problems to the ignorance of those of us at AFCRL who conducted the experiment and reduced the data. For example, Mather and Boslough (1996) interpreted the feasibility study’s finding to mean that we, at AFCRL, “*... were unaware of techniques that would have helped ... avoid cataloging erroneous signals. ...*” but that the astronomers on the study team knew how to do it: “*...the IRAS scientists who had anticipated every problem ...*”

The IRAS feasibility report was not as harsh, stating that: “*These problems are of equal concern to Price and Walker, who have, in fact, identified and analyzed most of them. They are also in the process of preparing a revised catalog which will discuss much of what is presented here, and in which source identification procedures will be improved.*” Indeed, the feasibility study was conducted in the winter of 1976, just after we had completed the AFGL catalog (Price and Walker, 1976). The added redundancy from the HI STAR SOUTH flights, coupled with refinements in the source selection criteria, significantly improved source reliability by eliminating approximately a thousand spurious AFCRL sources from the AFGL catalog. Of the 25 ‘unconfirmed’ AFCRL sources compiled by Frank Low as a case study in the draft IRAS feasibility report, 75% were rejected from the AFGL catalog and two of the remaining six are well known extended infrared sources that Low couldn’t detect from the ground. Although most of the rejected sources were spurious, those that were deemed likely real were put into the Supplemental Catalog (Price, 1977). These improvements were in place when the IRAS

feasibility study was conducted and not, as Mather and Boslough (1996) imply, as a result of advice from the IRAS astronomers.

Some found the problems with catalog reliability provocative and expressed themselves on the issue (Allen, 1977; for example). Others were dismissive of the survey accomplishments. Rowan-Robinson (1993) wrote “*Between 1971 and 1974, Steve Price and Russ Walker, working at the US Air Force Geophysics Laboratory, carried out a rocket survey of the sky at wavelengths of 4, 11, 20 and 27 microns. Unfortunately, they did not take the careful approach of the 2-Micron survey and published a preliminary catalogue which contained many spurious sources. My research assistant Stella Harris and I found that the genuine sources could almost all be characterized as normal stars, stars surrounded by a cloud of dust (or circumstellar dust shells) or star forming clouds.*” Dave Allen (1977) concluded that a good third of the AFCRL catalog was spurious and, in agreement with Rowan-Robinson, that the survey produced nothing new. Whether we found hitherto before unknown objects may be argued *ad infinitum* based on one’s definition of new and/or discovery. For example, in their preface to the *Proceedings of the Toruń Workshop on Post-AGB Objects*, Szczerba and Górný (2000) credits the AFCRL surveys with discovering the prototypical proto-planetary sources AFGL 618 and 2688, which represent stages in the post Asymptotic Giant Branch evolution that were not previously recognized. Although others may argue that sources such as the red rectangle were known from optical studies, these were not identified as a distinct stage of stellar evolution until attention was focused on them when the AFCRL survey found them to be intrinsically very bright in the infrared (e.g. Cohen et al., 1975; Westbrook et al, 1975). The fact that the AFCRL surveys were the first to measure the large scale infrared emission along the Galactic plane and zodiacal background was not widely credited.

Finally, there was the universal lack of understanding as to what our sponsors wanted from the survey. Mather and Boslough (1996) speculated the Air Force wanted an infrared catalog “so its weapons would not shoot down galaxies, stars and other sources of infrared radiation”, a flippant remark belied by the fact that the late 1970s Anti-Satellite program tests specifically targeted bright infrared celestial sources to ‘shoot down’. The fact was that almost nothing was known about the mid-infrared background before the HI STAR survey and the seven HI STAR experiments covered the maximum sky available as quickly as possible to observe the most stressing scenarios in order to meet an ambitious surveillance system design schedule. Thus, the premium was to quickly cover the sky, even at the expense of reliability, to make sure that there were no surprises. Harwit (2003) quoted Russ Walker’s assessment: “*The Air Force was interested in assessing the “worst case” scenario that the sky could produce in the mid-infrared. The basic parameters of any sky survey are (1) sky coverage, (2) completeness, and (3) reliability. Conducting a survey requires tradeoffs to be made between these parameters. With our limited resources we chose to go for maximum sky coverage (thus, little or no re-scan overlap), and emphasize completeness at the expense of reliability. These choices (in the interests of our sponsor) caused no end of grief with the astronomical community. There were many objects we reported that could not be confirmed from the ground. Most turned out to be of an extended nature and were lost to telescopes with small fields and chopping secondary mirrors. However, to be fair, there were some that were spurious, the price paid for choosing completeness at the expense of reliability. In our defense, we did discover many new and interesting sources (e.g., the red rectangle) and set the stage for a satellite to do the job properly.*”

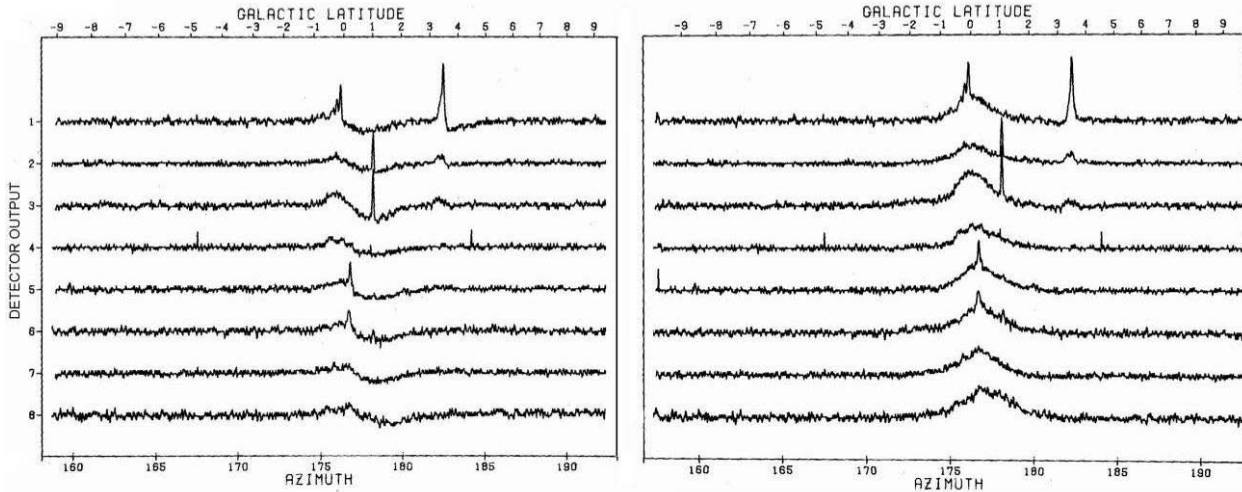


Figure 35. The $11\text{ }\mu\text{m}$ scan across the Galactic plane at a longitude of 30° on the first roll of the second HI STAR flight. Extended emission from the plane created the undulation in the center of the image on the left. The pole star, α Lyr at $(l, b) \sim (67^\circ, 19^\circ)$, was specifically chosen because it was near the plane so that the scans were nearly perpendicular to it. AB Aql is the peak on detector 1 at 0° latitude and the giant H II region W40 is the extended source at $+3.5^\circ$ latitude. The low frequency attenuation in the data has been restored in the plot on the right by applying the inverse z-transform of the electronic high pass filter.

Thus, the conduct of the AFCRL/AFGL survey was driven by ARPA and Air Force requirements, not those of astronomers and, ultimately, the issues regarding the AFCRL survey were about astronomers' opinion of the catalog contents and access to the material rather than questions of technical maturity. By the time of the IRAS feasibility study, AFCRL had flown 11 cryogenically cooled infrared experiments, eight of which were fully successful, two partially successful and only one an outright failure: the Army and Air Force about a dozen similar sized instruments and the Air Force had successfully operated the IRM sensor and CMP instrument in orbit. The principal remaining issue was to contain superfluid helium for far-infrared sensors.

4.3. Good to the Last Drop – of Information

The HI STAR experiments established that the celestial background contained no show stoppers that would seriously compromise the performance of an infrared surveillance system and demonstrated infrared space surveillance by detecting and identifying Earth orbiting satellites. The HI STAR experiments also obtained unique measurements of the atmospheric shock produced by the re-entering Aerobee 170 sustainer at $90 - 120$ km altitudes. These signals were broad, extending some tens of degrees and attenuated by the high pass filter in the signal processing electronics resulting in a characteristic undulating signature. A similar signal was seen as the second flight crossed the Galactic plane; the $11\text{ }\mu\text{m}$ data from which are shown on the left hand plot in Figure 35. We had seen highly attenuated Galactic plane signals on the first flight owing to the oblique angle at which the rolls cut the plane. Thus, we specifically selected the pole star of the second flight to be close to the Galactic plane and the experiment profile to extend the maximum deployment angle to order to reach the Galactic center, even though we suspected that this would enhance the noise for the 11 and $20\text{ }\mu\text{m}$ observations of the center. Since the HI STAR and HI STAR South experiments had obtained unique information on the extended infrared contents of the sky in addition to the various catalogs, we set about to wrest as much information from the database as possible.

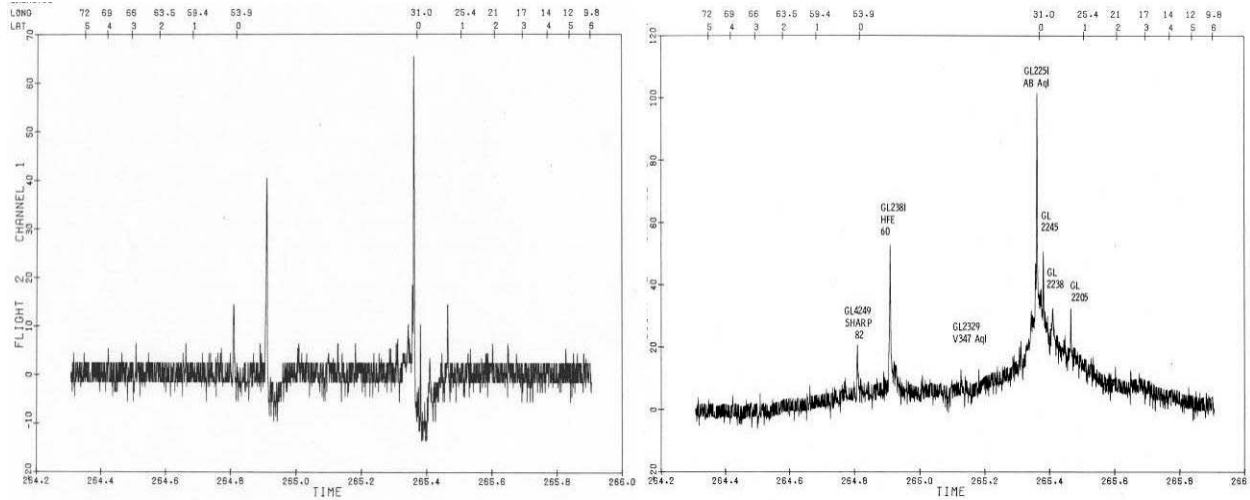


Figure 36. A scan along the Galactic plane by an 11 μm detector from the first HI STAR flight plotted as a function of time. The original data are on the left and the restored results are on the right. The latitude and longitude of the points where the scan crosses specific latitudes is denoted at the top of the plot.

The response of the signal processing electronics was shaped by the filters in the amplifiers: a low pass filter was incorporated to enhance the signal to noise of point sources and a high pass filter to eliminate the extraneous background such as that from the non-rejected Earth radiation. Without this high pass filter, the sensor would have been saturated much of the time. The two cascaded high pass filters in the signal processing electronics have a digital equivalent called a z-transform. By inverting the z-transform and deriving the corresponding recursive digital operation it represented (Shanks, 1967), we had a means of correcting for the attenuation of the high pass filtering and recovering low frequency information, the broad, extended signals, from the data. The attenuated low frequencies of the data in the left hand plot of Figure 35 were restored with this technique, as shown in the plot at the right. Price (1978a) and Price and Marcotte (1980) provide the details of the restoration procedure.

This was a powerful technique for recovering highly attenuated signals, as may be seen in Figures 36 and 37. Data from an 11 μm detector from the first HI STAR experiment is shown in Figure 36 before and after processing. The 1.6 sec long scan traverses the Galactic plane at a pronounced oblique angle, initially it crosses the plane at 54° longitude, dipping to between 0° and -1° latitude until it crosses again at 31° longitude at about the same location as in Figure 35. Diffuse emission from the Galactic plane was recovered over a ~30° longitude range. Figure 37 shows an 11 μm measurements of the zodiacal emission observed on the first HI STAR South flight and the restoration. The feature had a very large amplitude and angular extent and the extended signals from both the zodiacal dust and the Galactic plane are highly attenuated in the original data. As the characteristic frequency of the observed zodiacal crossing is ~1 Hz, the filtering in the on-board signal processor attenuated the electronic signal from the source by more than a factor of 100; it is barely visible in the raw data in the left plot of Figure 37.

The results of the restoration processing for the HI STAR and HI STAR South experiments were combined to create the first large scale, low resolution (~1°) mid-infrared maps of the zodiacal dust cloud (Price, Murdock and Marcotte, 1980) and the Galactic plane (Price, 1981); the Cornell flights had only sampled relatively small areas of these phenomena. Further processing created intermediate resolution (~1/2°) maps of Cygnus X (Price, Marcotte and Murdock, 1982; see Figure 39) and the W3, W4 and W5 H II regions (Thronson and Price, 1982).

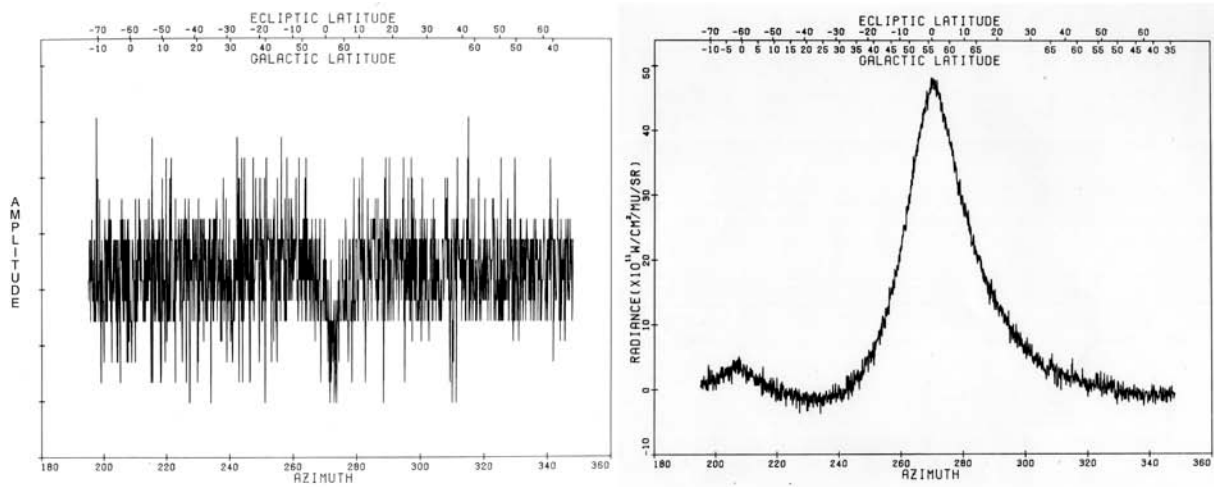


Figure 37. 11 μ m Galactic and Ecliptic plane crossings from the first HI STAR South flight. The amplitude scale on the left has been expanded until the telemetry bit-change is evident; the signatures of the extended sources in these data are barely noticeable. The restored profiles of the Galactic and ecliptic planes are shown on the right. The zodiacal profile spans $\sim 80^\circ$ in scan azimuth.

A very broad and attenuated signal was evident in a general southerly direction on all the HI STAR flights when the payload was between altitudes of ~ 125 and 85 km. The phenomenon was very bright, particularly in the $3 - 5 \mu\text{m}$ band. We restored the low frequency information with the inversion routine despite the data being heavily filtered. This phenomenon likely was due to the shocked wake from the Aerobee motor as it hypersonically re-entered the atmosphere. Having separated from the payload at about $1-2$ m/sec, the Aerobee was several hundred meters below and slightly to the south of the payload. The shock excites the atmospheric molecules but quantum mechanical considerations do not permit the major constituent of the atmosphere, N_2 , to radiate away the energy. However, the N_2 collisionally excites CO_2 , which does radiate. The $\text{CO}_2 4.3 \mu\text{m}$ band is within the HI STAR $3 - 5 \mu\text{m}$ filter, which is why the observations at this wavelength were so bright. Although the HI STAR $8 - 14 \mu\text{m}$ and $16 - 24 \mu\text{m}$ spectral bandpasses were chosen to avoid the $15 \mu\text{m}$ CO_2 band, the emission from the shock was broad enough that the spectral wings of the band are detected in these filters but with lower intensities.

The order in which the results were obtained generally reflects the tractability of the data restoration. The large and bright observations of the reentry wake and the zodiacal cloud were done first because the detector to detector discrepancies in the restored output had far too high a spatial frequency to be real and could be heavily smoothed. As with any inversion process, the restoration is sensitive to noise in the data and initial conditions adopted for the inverse filter. Also, a value for the constant component of the background has to be assumed since the high pass electronic filter completely removes this information. Very extended sources also will have undulations arising from a small amount of low frequency noise that is restored along with the attenuated signal. The saving grace is that the large correlation lengths in the restored signal permit a fair amount of smoothing as depicted in Figure 38 for the zodiacal data. The restored $11 \mu\text{m}$ ecliptic plane radiances are shown on the left after an initial smoothing and the line is an analytic fit to the mean values through the data. Additional smoothing reduces the $10 - 20\%$ scatter in the data to produce the contour plot on the right. The highly smoothed contour plot still contains a trace of low frequency noise which shows up as the vertically correlated wiggles in the outermost contours.

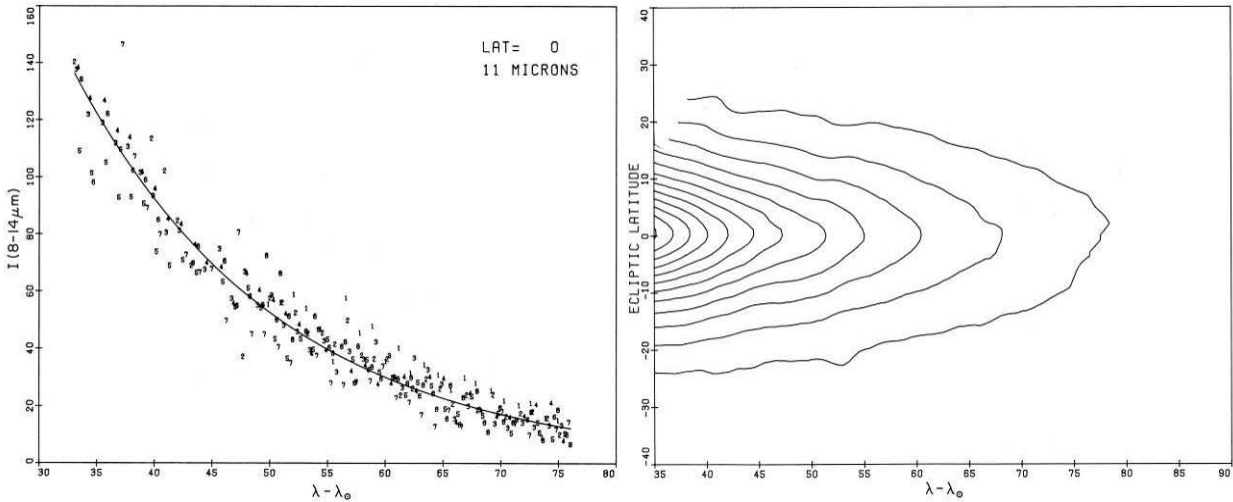


Figure 38. The HI STAR South 11 μm zodiacal radiances. The restored radiances along the ecliptic plane are plotted on the left. The highly smoothed contour plot is on the right.

The low resolution Galactic plane maps were published next as a fair degree of smoothing was used to remove detector to detector discrepancies while the best resolution maps were done last as they had to rationalize the detector to detector variations with a minimum of smoothing. This was difficult to do when the real data had scale lengths approaching that of the higher frequency noise such as in the oblique crossing of the Galactic plane in Figure 36.

However, we were able to obtain good quality restorations from the HI STAR data as shown by the 11 μm map of the Cygnus X region at the top of Figure 39. This image is compared to a well calibrated higher resolution 8.3 μm map from the Midcourse Space Experiment on the bottom. JPL created the HI STAR image as part of the IRAS data processing development. The scaling of this image makes the baseline errors from the restoration more evident than in the Price, Marcotte and Murdock (1982) contour maps. The radiance sensitivities in the two images isn't that much different in terms of $\text{W cm}^{-2} \text{beam}^{-1}$ as the more sensitive MSX observation have about a 300 times smaller beam (as may be seen from the image of NML Cyg, the quasi-point source below the center of the images).

The HI STAR/HI STAR South experiments were an outstanding success. They demonstrated that space-based surveillance was possible and that the space-based cryogenic sensor technology was mature. While issues arose over the reliability of the initial catalogs and whether or not the experiments made new discoveries, the program did achieve a number of firsts. These experiments were the first to conduct a large scale survey of the mid-infrared celestial background. Besides the stellar content of the sky, the sensors obtained the first infrared measurements of asteroids from space and the first good quality infrared observations of Earth orbiting satellites. The Galactic plane maps created by the low frequency restoration revealed the true extend and mid-infrared brightness of H II regions, which explained the difficulty that ground, based equipment had in confirming these sources. Also, the diffuse emission centered on the plane was found to be too large to be due to stellar sources alone, which led Price (1981) concluded that about half the emission had to arise from interstellar dust. Finally, the initial HI STAR South experiment was the first to map the large scale zodiacal emission and collectively, the results from the survey flights produced the first mid-infrared maps of the emission along the Galactic plane.

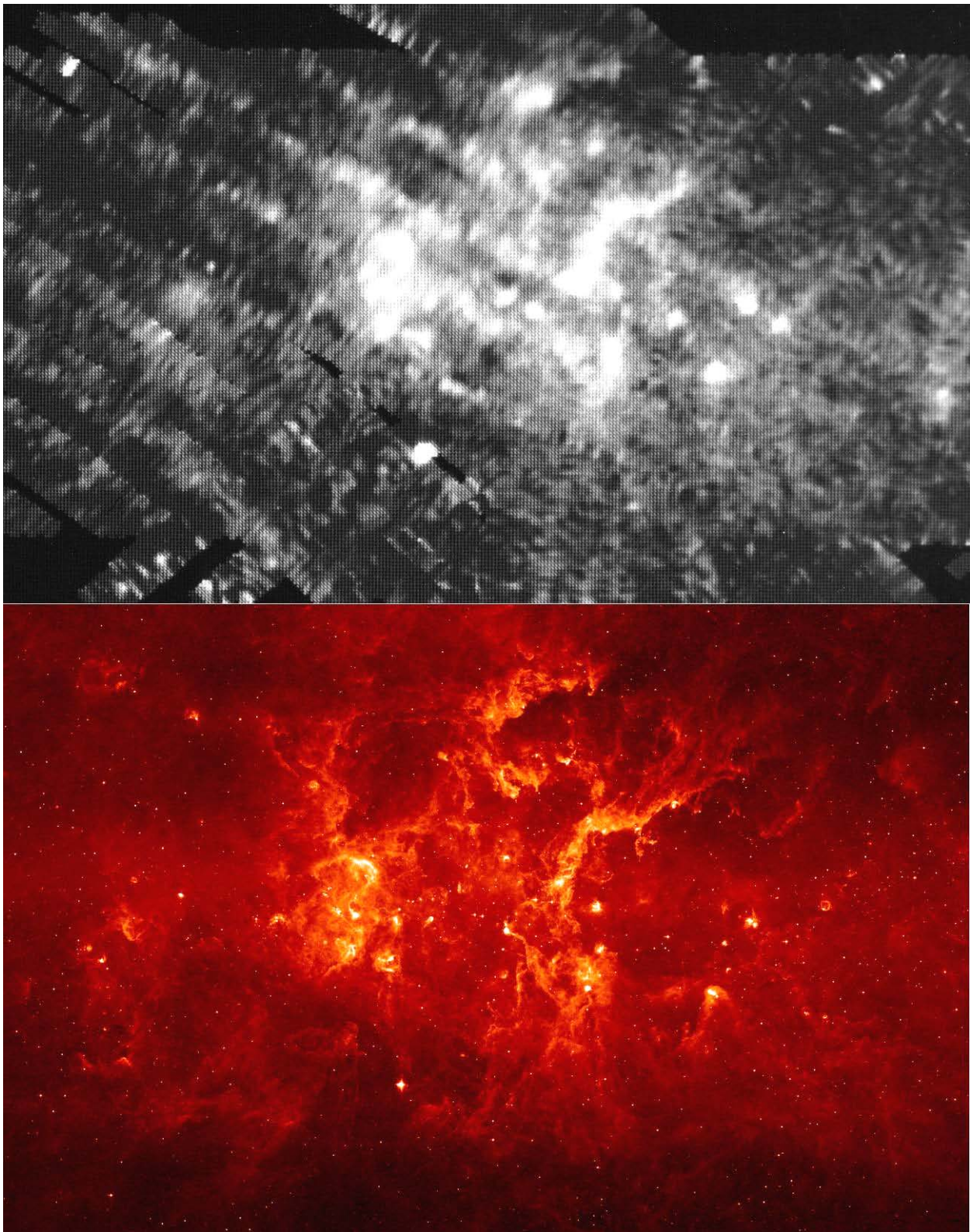


Figure 39. Infrared maps of the Cygnus region centered at 79° Galactic longitude. JPL processed the $11\text{ }\mu\text{m}$ HI STAR image at the top. A noisy detector causes the strips that are offset by $\sim 1^\circ$ on successive scans. The higher resolution Midcourse Space Experiment $8\text{ }\mu\text{m}$ image at bottom is aligned to the HI STAR map and spans about 13.8° in longitude and 9° in latitude.

4.4. Personal Perspective on the AFCRL/AFGL Survey

I was responsible for the HI STAR data from acquisition through processing and analysis. The data processing part I understood, but matching telemetry requirements between what was transmitted and received was new to me. The HI STAR telemetry rate was 855 Kbs (kilobits per second), just under the 1 Mbs that the White Sands Missile Range advertised as their capacity at the time. However, the Range Control Center (RCC), from whom we had requested telemetry support, was unable to lock onto the telemetry from our first HI STAR horizontal test and I was dispatched to see the folks at the New Mexico State University (NMSU) Physical Sciences Lab (PSL) antenna site some 5 – 7 miles downrange of the launch complex with the backup pulse code modulation (PCM) unit to try to find out why. PSL had a 15' antenna and would receive and record flight telemetry, if funded to do so. The facilities were good but occasionally had trouble with reception near peak altitude. However, the large range dish at the top of the Sacramento Mountains, to the east of the missile range, had no trouble receiving data throughout the flight. (The RCC also was where range safety personnel did the instant impact predictions that were used to decide whether to terminate the flight; the predictive wind weighting for the go – no go decision was done in the blockhouse.)

The carrier frequency band of the telemetry was modulated such that a ‘1’ bit was at one edge of the band and a ‘0’ bit at the other. The PCM unit coded the data in a non-return to zero format in which the 1-bit did not have to be reset to 0 if the next bit was also 1. On the average, such a scheme has half the transitions as one in which each 1-bit was reset. This reduced our telemetry bandwidth requirements by half; that is, our 855 Kbps telemetry should easily be decoded by a system that used a half megahertz filter. The PSL folks patiently explained all this to me after verifying that they had no problem reading the telemetry from the spare PCM unit.

I relayed this information to the Range Control Center people, who insisted that there was nothing wrong with their system. After much testing and retesting, they successfully decoded the telemetry from our t – 3 day vertical. However, we fortunately had the Physical Sciences Lab support our launches as a backup as the range was unable to decode data from the fifth experiment due to bandwidth problems. It turned out that the RCC did, indeed, have the proper filters and that the bandwidth used by the Sacramento Peak receiving station was adequate. The problem was the filter used in the relay network that was used to transmit the telemetry from Sacramento Peak to the Range Control Center was set at the lower bandwidth normally used for everyday operations and range telemetry people seldom thought about checking this link.

I usually stayed an extra day after the launch to ensure that the PSL data tapes, digitized from the telemetry analog tape, were packed and placed with the rest of the field hardware to be shipped to AFCRL. The first experiments needed five seven-track 1600 bits/inch tapes for the flight data. This was reduced to two nine-track 6250 bits/inch tapes, when that standard became available, although the range continued to provide five tapes at the lower density.

Because we were processing the HI STAR data, SAMSO initially requested AFCRL to reduce the CIRM and CMP data. My singular puzzle is what if we had accepted the CMP processing task? It would have been difficult to do and success was hardly assured, especially with the demanding deadlines imposed by SAMSO. Russ Walker had presented the situation to me that SAMSO had requested AFCRL to do the CIRM and CMP processing and I was free to accept it if I was interested but there was no offer of internal support; I had the impression that I would be on my own. The daunting aspects of the problem were the potential volume of data and, more importantly, determining the aspect in which the satellite position was a critical input.

Today, the aspect solution is trivial but I did not know how to do it in 1971 and I turned to Robert McInerny and Ed Robinson, our data processing/analysis people, to assess the program requirements and AFCRL's ability to meet them. They decided that given the volume of data, that the lack of partitioned processing for classified data at the central computer site would interfere too much with normal AFCRL computer operations. Classified processing would have required several hours each day to set up the CDC 6600 main frame computer for each run, then to purge the computer and reconfigure it for normal unclassified operations afterward. This was an inordinate amount of time considering the processing demands of others at AFCRL. It may have been that the inexperience of the computer center analysts with processing large volumes of satellite data led the central site managers to decline the task rather than the classification issue, which I regarded was a work around. It turned out that the limited CMP lifetime produced only three orbits of data whose total volume was about three times that of the HI STAR and HI STAR South experiments combined. Having the CMP data in hand before publishing the AFCRL catalog would have given us critical redundant information to make the catalog highly reliable without compromising classified information from that mission.

Also, I was already maxed out as the sole analyst on the HI STAR project as well as for processing the measurements. Not only were we in the field an average of three out of every fourteen weeks, but another week every quarter was taken up with HI HI STAR technical meetings. Ultimately, Barry Grish and Ted Lynch at the Riverside Research Corp. in New York City reduced CIRM and CMP data, producing a CMP catalog that contained ~255 LWIR sources with high quality detections extracted from the survey (Heintz, 1972). Note that the position errors that, according to Mather and Boslough (1996), Frank Low supposedly found in the CMP map were not in the CMP source list. Because AFCRL declined to do the CIRM/CMP processing, IBM was selected to do the BMS satellite data processing (Winter and Smith, 1977) rather than AFCRL as originally planned.

I was taken aback by the very negative attitude with which some infrared astronomers received our catalogs. For example, Russ Walker (12 June 2002 e-mail) was very aggressively questioned at the July 1975 Snowmass, CO. infrared panel meeting of the Space Science Board chaired by Gerry Neugebauer as to why the survey wasn't conducted properly and why Russ did it the way he did. What is the right way to conduct a survey from a rocket with limited time for rescan? Well, Frank Low told me at a 26 January 1976 IRAS feasibility study working session at AFGL that he would set the sensor at a single deployment and scan the sky at the same zenith angle for the entire experiment. Given this criterion, it is puzzling as to why it was incumbent on AFCRL to take these steps and not others, such as Cornell University, whose experiments had little redundancy and confirmation. However, we actually unintentionally did as Low suggested, repeatedly scanning the same swath of sky on the third HI STAR South flight; the sensor gimbal hung up after about 10 steps and the same zenith angle, within a few arc minutes, was scanned for the remaining 20+ rolls. We found no improvement in reliability beyond seeing a source twice and it is questionable as to whether this added redundancy was worth the experiment not being able to survey the southern Galactic plane on that flight.

We could have limited the deployment to zenith angles between 45° and 65° for, as may be seen in Figure 31, the noise is at a minimum in this region, varying by less than a factor of two. Also, there would have been sufficient observing time on a single flight to cover most if not all the area between these angles twice. However, the quantification of the off-axis noise necessary to set such deployment limits was part of the redundancy calculations to determine whether a source had sufficient signal to noise to be seen on a confirming flight and the results in

Figures 30 and 31 were not derived until well after the experiments had been completed. Alternatively, the areas covered on the three experiments flown in 1971 could have been resurveyed by flights in the second year. However, these options would have excluded observations of some of the more interesting sources and precluded mapping of the Galactic center. In hindsight, the only thing I would have changed would have been to execute $\sim 390^\circ$ rolls so as to not miss portions of the sky when the sensor was stepped. None the less, our strategy for completeness worked reasonably well when the data from all flights were incorporated into the catalog. Problems encountered during the flights provided important lessons learned for future missions, such contamination and off-axis rejection and defined the procedures necessary to mitigate or eliminate them.

Also, it should be noted that the strongest and most puzzling signals, at least initially, occurred late in the flight on rolls contaminated by off-axis radiation from the Earth and, given the program objective to characterize all the available background, we needed to keep the same experimental geometry to see if the signals would repeat. They did. Although the signal was never suspected to be astronomical, they were created by the re-entry wake emission from the rocket sustainer, it was necessary to understand the source.

Many early publications in the astronomical literature emphasized the spurious sources, although some of the initial exploratory articles expressly recognize AFCRL for the interesting objects that were reported. It seems to me that many of those who had searched for AFCRL sources were unhappy with wasting their time on spurious objects, which led to the complaints regarding completeness and the claim that we did not properly conduct the survey. The proper conduct of the survey would have resulted in far fewer sources, spurious and otherwise but it probably would have obviated the need for the IRAS feasibility study. Indeed, Russ Walker had his name removed an author of the IRAS feasibility study after the initial May 1976 draft because he believed that the report was not balanced. He felt that, in assessing the technology, the draft report had devoted insufficient space to the positive aspects of the HI STAR survey that demonstrated the maturity of the technology. The final text was not as critical of the AFCRL effort as the draft.

However, underlying all this, I sensed a frustration by some who felt that they could have done better than we if only they were given the technology and resources that we had (e.g. Allen, 1977). Thus, not only we were intruding on their field of research, but doing so with an ‘unfair’ advantage by using equipment that was not universally available.

The Air Force Celestial Backgrounds program continued to influence infrared astronomy for a number of decades after the AFCRL/AFGL experiments were completed with in-house research and supporting infrared astronomical research contracts. The program also provided the occasional next advance in the field. These occasional advances may also have been source of dissatisfaction for those with a ‘not invented here’ attitude. In other words, if it wasn’t done by NASA or at an academic institution it wasn’t done at all, or at least properly. This usually is manifested by not ascribing professional credit to DoD efforts or even acknowledging the existence of such programs. Fortunately, the influence of personalities and “turf” wars have declined as the field matured over the years.

5. AIR FORCE BACKGROUND MEASUREMENT PROGRAM

After a couple of years of development, SAMSO decided to remove the celestial sensor from the BMS payload and to replace the ELS with a second generation instrument, the Earth Limb Measurement Sensor (ELMS) and renamed the result Earth Limb Measurement Satellite (also ELMS). SAMSO directed that ELS was to be completed and retrofitted for an Aerobee 350, which AFCRL would fly as the Earth Limb Experiment (ELE) to provide lessons learned that were to be incorporated into ELMS.

The sensor performance requirements were quite different for observing against the celestial background compared to detecting targets through the foreground emission from the limb of the Earth, although Hughes claimed their design could operate in both regimes. As seen in Figure 33, the closer to the Earth the system can look, the earlier the missile can be detected and the longer it can be tracked. However, the closer the system looks to the edge of the Earth, the more stringent the off-axis rejection requirements, and the original surveillance system requirement to operate within a degree of the Earth's edge (Jamieson, 1995) was very demanding. The baffle angle is the key parameter for off-axis performance since scattering of Earth radiation from the primary mirror is the single largest contributor to stray Earth light at the focal plane. Thus, the longer the baffle tube is compared to diameter of the mirror, the better the near-field off-axis rejection. The unobscured off-axis optics of the Earth Limb Sensor allowed for a long baffle and a small baffle angle but at the expense of a smaller collecting area for a given sensor volume. ELS also improved off-axis performance with super-polished mirrors, internal baffles and Lyot stops that supposedly produced an off-axis rejection superior to that of the on-axis optics of the HI HI STAR sensors.

Originally, AFCRL was to fly the two HI HI STAR sensors and the ELS on Aerobee 350s in 1973 – 1974 but only the Rockwell sensor came even close to meeting the schedule. SAMSO then decided not to fly the Hughes HI HI STAR instrument and, since the Honeywell ELS delivery was two years in the future, Russ Walker negotiated a substitute experiment, Super HI STAR, for the Aerobee 350 that was originally assigned to the Hughes sensor.



5.1. Super HI STAR

This experiment used the remaining HI STAR South instrument and payload in an attempt to measure the absolute infrared zodiacal radiance and to demonstrate that an infrared sensor in space could coherently co-add data from a redundantly scanned area of sky to improve sensitivity. However, by the time of the 13 December 1975 flight Russ Walker was so deeply involved in the NASA Infrared Astronomical Satellite (IRAS) program that he didn't go into the field.

A star tracker was substituted for the star mapper in the HI STAR payload in order to lock two axes of the payload to ϵ UMa and β And, which are $\sim 90^\circ$ apart. The HI STAR South focal plane and field stops were rotated by 90° so that a $1.2^\circ \times 10^\circ$ swath of sky was covered by scanning the gimbal 10° up and down. An initial calibration sequence centered the scan on β And while the attitude control system rotated the payload 1.35° back and forth at a rate of $0.44^\circ/\text{sec}$ during the gimbal scan, thus scanning β And several times across each detector. The scans were interrupted for ~ 30 seconds near the 286 km peak altitude

and again before the sensor was stowed for re-entry. The internal shutter was cycled open and closed at a rate of 1 Hz during these stares in an attempt to chop the absolute zodiacal radiance.

Pelzmann (1978a) described the numerous problems that plagued this experiment.

Although correlated noise, among other difficulties, compromised the co-addition, data processing did improve the signal-to-noise on β And with about a 70% efficiency from the \sqrt{N} ideal. Besides β And, only one possible source was extracted, a tentative 20 μm measurement of NGC 389 + 393, a spiral and elliptical galaxy close enough together to be scanned by a single detector. Unfortunately, a piece of payload debris at one end of the scan field interfered with the observations, especially during the stare and chop segments, rendering the absolute zodiacal radiance measurements useless. Finally, recovery failed and the payload and sensor were lost.

5.2. The End of an Era – and the Beginning of Another

AFCRL was in turmoil in the mid-1970s as AFCRL programs terminated and the workforce was reduced, culminating in the geophysics programs being reconstituted into the Air Force Geophysics Laboratory (AFGL) in 1976. Plans were made, and then rescinded, to move the geophysics programs to Kirtland AFB in New Mexico. Seeing no future for infrared astronomy in AFGL, Russ Walker left early in 1976 for NASA Ames Research Center (ARC) to work on IRAS and Burt Schurin, an atmospheric spectroscopist who was the principal investigator for the ELS experiment, became the new program manager. He, Tom Murdock and I began discussions with Maj. Kurt Curtis, Capt. Mike Kiya and Capt. Howard Stears at SAMSO for a follow-on background measurements program.

The Air Force's Deep Space Surveillance (DSSS) Program also came under scrutiny at this time. Various reviews were held of space based infrared technology and the DSSS program in the mid-1970s that ultimately concluded that the technology was not sufficiently mature to proceed with an operational system. Other factors also were involved as Mike Kiya noted (12 December 2003 e-mail): "*The major factor in these programs being killed was the '73 ABM treaty which shifted emphasis from midcourse missile surveillance to space surveillance*". The BMS was also cancelled and a conceptual design for hybrid sensor experimental satellite (HYSAT) was initiated in 1975. The Earth Limb Measurement Satellite (ELMS) survived until the mid-1970s when it fell victim to cost overruns and schedule slips. Subsequent studies for an operational system to replace DSSS were completed in 1978 and produced the Space Based Surveillance System (SBSS) concept.

With the demise of the DSSS and the BMS, we negotiated with SAMSO for what support we could provide for the SBSS. SAMSO initially committed to the ELE probe flight with the Honeywell ELS sensor to obtain infrared upper atmospheric measurements. After the ELMS satellite was cancelled, SAMSO directed that the sensor be modified for a probe-rocket experiment, which we would also fly, the modified instrument being labeled as the Infrared Backgrounds Sensor (IRBS). However, SAMSO decided to rely on implementing the HYSAT concept for the more complete background information that they needed. Hughes was given a contract in 1976 for their HYSAT concept, which was renamed the Space Infrared Experiment (SIRE); the system subsequently was configured for the Shuttle (Ferdman and McCarthy, 1981).

Although the SAMSO program office would rely on SIRE for the requisite background information, we, at AFGL, viewed SIRE as an uncertain quantity with an ambitious schedule, and counter-proposed a series of probe flights in addition to the ELE and the IRBS atmospheric experiments to measure the absolute zodiacal radiance and to survey the celestial background to

HI HI STAR sensitivities for SIRE risk reduction. These experiments were constituted into a new Background Measurement Program (BMP) under which we proposed to build two absolute radiometers to measure the zodiacal background and to refurbish the HI HI STAR sensor. To save program costs, the zodiacal experiments were initially to be flown on Castor-Lance rockets that AFGL had in inventory. The HI HI STAR and IRBS were to fly on an ARIES, which had been developed a few years earlier by Space Vector Corp. from the second stage of the Minute Man I under NRL sponsorship. The first ARIES flew in 1973 and it was qualified at White Sands Missile Range in 1974. The ARIES could loft our anticipated ~700 kg (1500 lb) payloads to an altitude of approximately 360 km (225 miles), which permitted about 450 seconds of data acquisition. Thus, the ARIES gave us a capability to match the SIRE performance except for the redundancy permitted by the time in orbit.

The SAMSO program management disagreed, preferring to rely on SIRE for the data. We won approval for the expanded program from higher levels within the Air Force and then had to smooth the ruffled feathers at SAMSO caused by this back channeling. Fortunately, Mike Kiya and Howard Stears are consummate professionals and continued to support the scientific and technical objectives of the program.

5.3. Earth Limb and Infrared Backgrounds Experiments



We still had the unfinished business of flying ELE to complete our obligation for the Aerobee 350 based measurements. An outstanding issue at the time was the absolute radiance of the zodiacal background because it provided the ultimate limiting background photon noise for infrared space-based surveillance systems. The predicted radiances depended on the model assumptions, with the published values of Frazier (1977a, b) and Röser and Staude (1978) differing by at least a factor of four. Such divergence translates into a factor of two in background limited system sensitivity. Soifer, Houck and Harwit (1971) had the only published infrared measurement at the time as the HI STAR South

data were yet to be reduced. Regrettably, Briotta, Pipher and Houck (1976) deemed their spectrophotometry to be so uncertain that they did not publish their results. The situation was fluid enough at the time that the Hughes phenomenologist, Pete Jericke, was able to present zodiacal backgrounds at various SIRE meetings that seemed to be tailored to prevent limiting SIRE's performance. Frazier (1977b) pointed out that some of Jericke's zodiacal radiance estimates were well over a factor of 10 lower than those of others. Because of this uncertainty, SAMSO agreed to divide the ELE timeline, observing the upper atmosphere during the first half of the experiment and the zodiacal background the second half.

The ELS off-axis telescope had a clear aperture collecting area of about 324 cm^2 . Having been made circa 1970/1971, the two Santa Barbara Research Center focal planes in the sensor consisted of doped germanium photo-conductors. One focal plane had a small array of detectors with $\sim 4 \mu\text{m}$ bandpasses while the other was located at the focus of a grating spectrometer that, in conjunction with interference filters, divided the 5 to $15 \mu\text{m}$ spectral range into $0.4 \mu\text{m}$ intervals. Unfortunately, in a measure of false economy, SAMSO decided not to include MOSFET protection in the detector circuits and, as a consequence, half of the detectors were blown by the time of the flight. Thus, it was decided not to open the sensor to repair some internal problems and for final cleaning of the optics for fear of losing more detectors.

Originally built for satellites, ELS and IRBS were plumbed for a mechanical cryocooler. Thus, both sensors had to be retrofitted to accommodate helium tanks and both suffered cryogen plumbing problems. The ELS internal heat exchanger was difficult to align properly, which caused the secondary mirror to run 20K warmer than planned during flight with the subsequent loss of the long wavelength data; IRBS suffered from leaks.

ELS was an absolute radiometer that measured the constant and slowly varying flux from the background. A cold chopper placed at the first field stop of the telescope modulated the radiation at 45 Hz producing periodic detector signals that were synchronously rectified on-board. In this scheme, a detector alternately viewed the outside radiation, then the cold reference blade that, ostensibly, had no flux. The signal was band pass filtered to reduce noise, resulting in a smoothed 45 Hz periodic output with positive and negative peaks. Another circuit detected the phase of the chopper blade, that is, its position as a function of time, and this information was used to detect the times the signal passes through zero volts to synchronously rectify or invert the negative portion of the signal. The rectified signal was further smoothed, sampled and sent to the ground. This produced an absolute measurement of the background taken in a very narrow electronic bandpass. The chopper drive had two coils: a small magnet on one of the chopper tines drove the chopper blades by electromagnetic induction from the first coil while the second coil picked up the tine motion, also by magnetic induction. The drive coil failed during a cold test in the laboratory and, to avoid the perils of another sensor disassembly, a fix was achieved

by driving the blades with the pickup coil for a number of cycles, then using it to detect the motion of the blades, the information from which was used to adjust the drive to keep the chopper in resonance. The fix worked but the launch loads on the 3 August 1976 flight were high enough that this feedback process took half the flight to re-establish resonant motion. Data was lost until the chopper recovered at $t+265$ seconds. Fortunately this was in time to obtain all the zodiacal data.

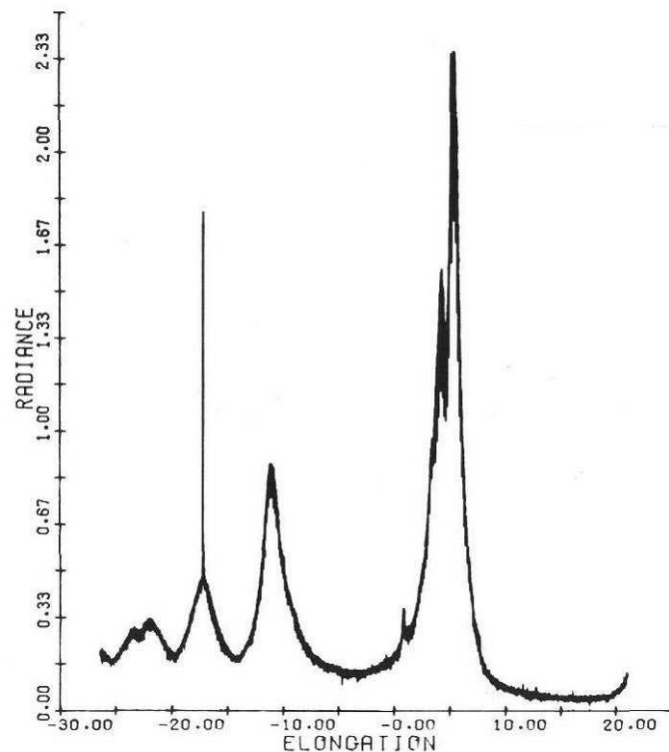
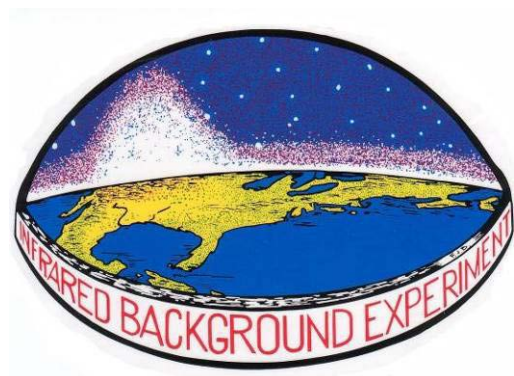


Figure 40. The $10 \mu\text{m}$ broad-band zodiacal radiance measured by ELE as a function of elongation. The discontinuity at $+4^\circ$ elongation, elongations east of the Sun are positive, is an attitude adjustment to maintain the line of sight greater than 3° from the Sun. The large spike at -17° is the near-field ($1/3^\circ$) off-axis detection of Mercury. AFGL 1283 is the smaller peak at $+1^\circ$.

The experiment profile took advantage the $\sim 10^\circ$ sensor baffle angle and the ELS superior small angle stray light rejection to measure the zodiacal background near the Sun. Sawtooth scans centered on the ecliptic plane beginning 26° west of the Sun were executed with increasing amplitude while scanning toward, then past, the Sun. An Adcole Sun sensor and a star mapper provided pointing information. Figure 40 shows the broad ($\Delta\lambda \sim 4 \mu\text{m}$) $10 \mu\text{m}$ band radiometric data as a function of solar elongation. The excellent near-field off-

axis performance of the sensor was qualitatively verified by the fact that the maximum observed radiance came from the ecliptic plane crossing near the Sun rather than the closest approach to the Sun at 3° north ecliptic latitude.

We decided not to recover the ELS because the sensor had so many problems and IRBS, a purportedly better sensor, was being constructed. Not including the parachute recovery system lightened the payload, which increased the peak altitude and data acquisition time.

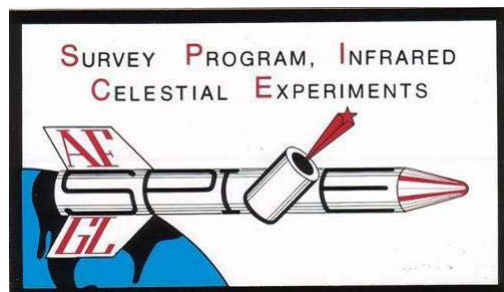


scrubbing the launch. I discussed the problem with Bert Schurin, the BMP program manager, and Tom Murdock, the IRBS test director. Tom and I proposed, and Burt agreed, to advance the launch time as much as possible.

IRBS was to measure the molecular emissions in the upper atmosphere through the terminator, the boundary between the sunlit atmospheric layers and those in the dark. A considerable amount chemical activity was known to occur during terminator crossing, and a lot more was suspected, as the energy input from the Sun was turned off. Since there was a fair amount of leeway in the exact geometry that would provide measurements on the night side, the daylight side as well as the terminator, the launch time could be moved forward by an amount only limited by the fixed maneuvers already programmed into the attitude control system.

I sat down in the area usually reserved for the White Sands wind weighting crew (as a guided rocket, the ARIES didn't need wind weighting) with my hand-held Texas Instrument programmable calculator and came up with a recommendation to advance the launch by more than an hour and a half, much to the relief of the Honeywell engineers. Fortunately, the range was able to accommodate the new launch time. Col. D'Arcy, the AFGL vice-commander and the only official above Branch Chief to attend one of our launches, reportedly commented about how casual we were about flying these experiments as he saw us wait to the last several hours to set the exact launch time. Little did he know how frantic the situation really was.

The IRBS payload did not separate from the rocket motor and since the sensor looked out the back end of the payload, it took no data. The ~700kg of added weight of the motor was too much for the recovery parachute and the payload and sensor were destroyed upon impact.



5.4. SPICE I

In the summer of 1976, Rockwell began repairing the damage sustained in the 1973 HI HI STAR flight and to reconfigure the sensor to accommodate a payload design that may be described as a scaled up HI STAR (see Figures 41, 44 and 45). Rockwell modified the external plumbing to fill the cryotank and built a

new cover and sensor front end to mate with the cover removal mechanism in the payload. New 8 – 14 μm and 16 – 22 μm arrays were built and a Si:Sb 24 – 32 μm detector array was substituted for the 3 – 5 μm HI HI STAR array. The 18 somewhat wider 2.5' \times 10.5' detectors in each SPICE focal plane array spanned the 2.5° cross-scan field. These were the first detectors with transparent contacts in which the bias is applied parallel to the incident radiation. Since the top surface of the detector is biased, it has to be transparent to the incident infrared radiation – hence the name. Arrington et al. (1976) had shown that the response over the surfaces of detectors in which the bias was applied to the sides or perpendicular to the incident radiation was quite irregular and that the variation depended on the area of the surface that was illuminated. Transparent contacts reduced, but not quite eliminated, these response variations.

SPICE I, the first of the BMP experiments, was flown on 27 January 1979. Castor, a Gemini, was chosen for the pole star in order to fill in much of the sky not covered by HI STAR and HI STAR SOUTH experiments. The 38" (0.95 m) payload easily accommodated the SPICE and FIRSSE (Section 5.7) sensors and was sized to the 38" Minute Man I third stage that was originally mounted atop the 44" (1.1 m) second stage (the ARIES) and we could use the readily available standard Minute Man I interstage. Because buffeting and high reentry heating were

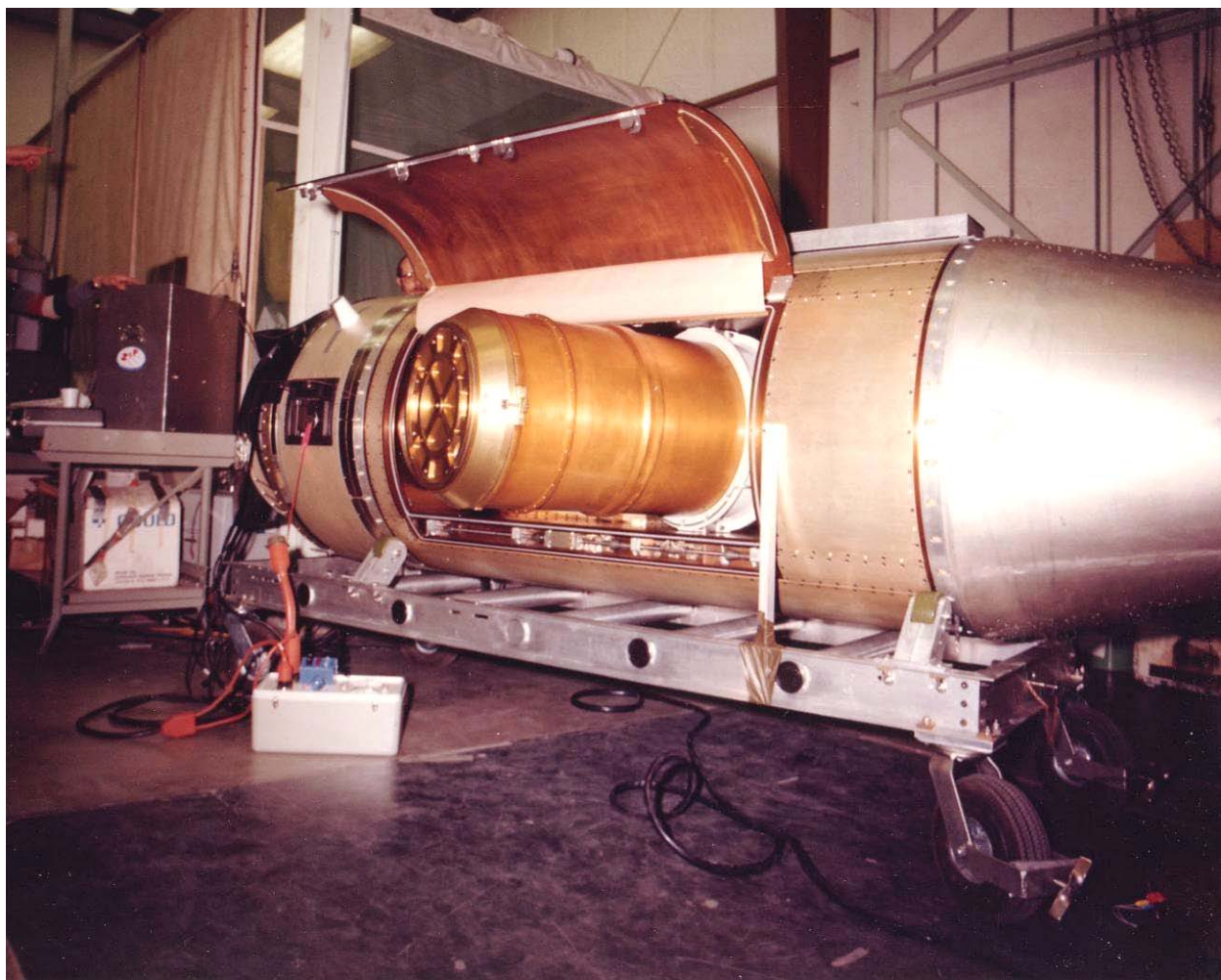


Figure 41. The SPICE sensor with the cover on is shown deployed during the horizontal test. The payload door may be seen above the sensor.

expected in recovering the payload from the anticipated 350+ km peak altitude, a single resealable payload door was built that would open to deploy the sensor, and then close for recovery (Figure 41). Unfortunately, the volume of air in the payload sensor cavity was too great to be evacuated rapidly through the large dual Millipore filters and the resulting internal overpressure caused the door to hang up. Consequently, the sensor jammed into the closed door when deployed by the payload timer. Everything else worked well on the flight except that the sensor did not fully stow and the cover wedged onto the edge of the vacuum housing. The cold sensor was again open to the atmosphere but sustained relatively minor damage.

Our SAMSO sponsors were none too pleased with the payload door failure and directed Aerospace Corp. to conduct a thorough review of the payload design before we could refl y it. We supported that review and fixed the problem by putting $\frac{1}{2}$ psi pop-off valves into the payload to vent both the electronic section and the sensor payload cavity as the rocket ascended. These valves would open to allow air inside the payload to escape as long as the pressure inside the payload exceeded that outside by one-half pound per square inch. As the rocket and payload reached the more tenuous atmosphere, more of the venting was through the Millipore filters. It was anticipated that the air vented by the pop-off valves would be carried behind the payload during ascent and that the valves would seat before the rocket left the atmosphere. This sequence would ensure that the cleanliness of the payload was preserved.

Aerospace Corp. engineers identified several other less serious issues, such as the star mapper door that had torn off during recovery with only minor and repairable damage. We worked out an accommodation in which Aerospace would work with us to solve the design problems and that they would send an Aerospace engineer to AFGL to look over our shoulder as we did the rework. Then, rather than having to prove to Aerospace engineers that we did it right, we had one of their own confirm it.

5.5. The BMP and MSMP Separation and Recovery Systems

Separating the payload from the spent ARIES motor was a serious contamination concern as, unlike the liquid fueled Aerobees, there were no valves to shut down the burn. Pressure monitors in the combustion chambers on early ARIES flights indicated that although thrust dropped markedly at the t+62 seconds nominal burnout, it did not disappear but slowly tailed off as the residual solid fuel and the butyl rubber liner continued to smolder and burn. Briotta, Pipher and Houck (1976) had suggested that post burnout particulate contamination from their solid Astrobee motor caused the rapid, large amplitude fluctuations that compromised their infrared zodiacal measurements. Our concern was heightened when Anderson, et al. (1979a, b) reported an anomalous ultraviolet spectral signature and a discontinuity in the background measured during their ARIES based experiment. We speculated that the chuffing motor had overcome the modest ~ 1 m/sec velocity that their spring loaded separation system imparted to the payload and that the motor had actually struck the payload causing the discontinuity. Furthermore, the products of the residual smoldering ARIES motor innards were the source of the anomalous ultraviolet signature that they observed. Price et al. (1980) deduced this based on results from the AFGL Multi-Spectral Measurements Program (MSMP) TEM-1 (TEM – Target Engine Module) experiment, which had been flown on an ARIES in 1977; the TEM-2 launch is shown in Figure 4. An attitude control problem left the measurement module tumbling and a vidicon camera observed the motor as the sensor module slued across the sky. As it looked in the general direction of the spent motor, the near-infrared circular variable filter spectrometer detected a strong localized HCl signal, a known and prominent combustion product of the

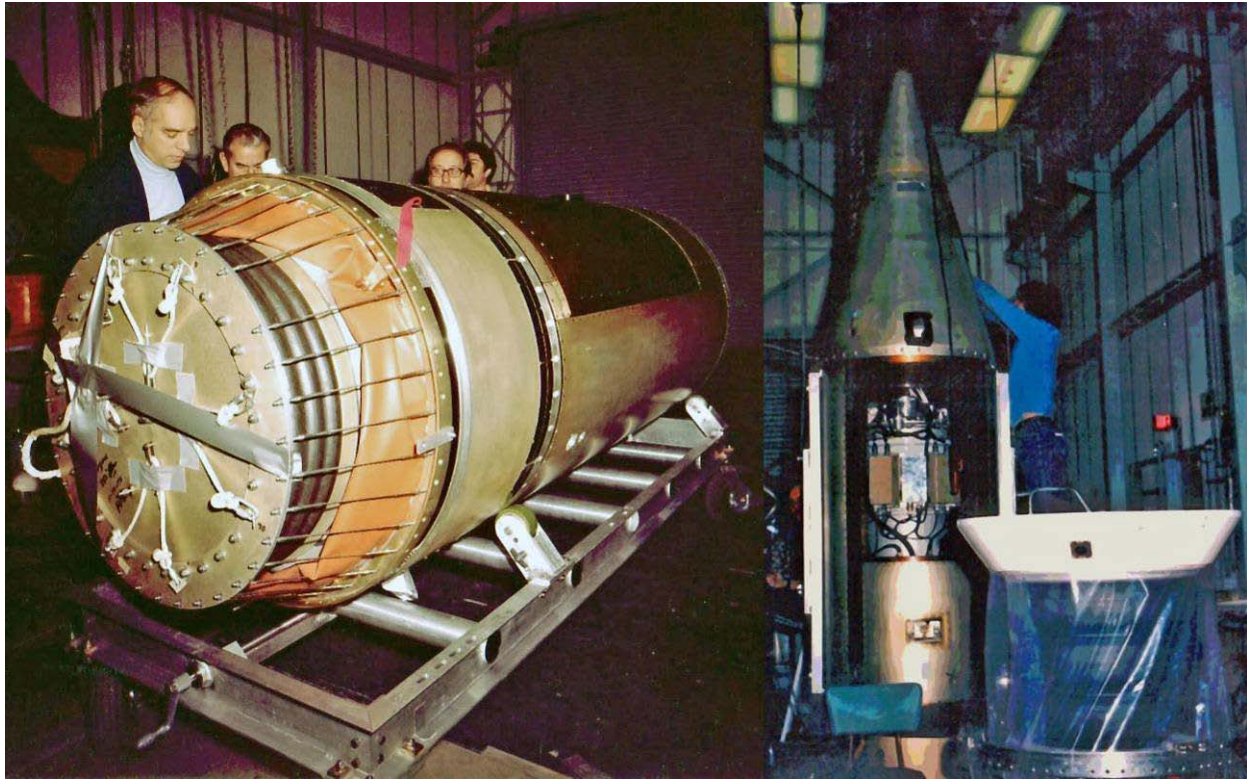


Figure 42. The SPICE/FIRSSE separation system is shown mated to the SPICE payload at the left and fully extended at right; all BMP experiments used a similar system. The airbag is the black pleated ‘rings’. The orange neoprene shroud shown on the left is cleaned on the inside before mating it to the payload. The entire separation system fits into the ARIES interstage, which is mated to the thin beveled back rim of the payload. The FIRSSE separation system is shown fully extended in the right image. The dish, barely visible on the left under the neoprene and clearly seen on the right, pushes against the bottom of the payload during separation.

smoldering rocket fuel. Price et al. suggested that the ultraviolet excess seen by Anderson et al. came from CO and CO₂ molecules that are known constituents of the ARIES motor effluvia.

To explore this problem, the AFGL Aerospace Instrumentation Division flew a television camera on a Black Brant VC solid rocket from White Sands Missile Range in August 1979 with dramatic results (McKenna, 1981). The camera looked out the back of a payload and saw first light as the spring loaded separation system pushed the motor and payload apart. The motor was seen to recede from the camera, slowly come to a stop, then advance toward the camera, ultimately passing the payload before half the time above the atmosphere had elapsed. Furthermore, others also had observed that residual thrust from a spent Black-Brant solid motor could cause the rocket to overtake the payload (e.g. Gush, 1981).

Thus, we needed a much more robust separation system than springs. The solution was a pneumatic system of narrow ‘tires’ fused together with sealed sides, as shown in Figure 42. The separation system was contained within and anchored to the ARIES transition stage and attached to the payload by a Marmon clamp. The payloads weighed about as much as the spent motor, the worst case separation scenario as this balance resulted in the smallest separation velocity. None the less, the system was able to achieve about 8 – 9 m/sec separation velocity. We also delayed separation until ~15 seconds after burnout to provide time for the exhaust pressure to decline to a fraction of a psi, as verified by a pressure monitor in the motor. The payload was separated from



Figure 43. The not so soft SPICE I recovery. The payload impact was much harder than anticipated with the standard recovery pack used on this mission. Despite the appearance, the internal damage was limited.

the motor at about $t + 75$ seconds and at $t + 127$ seconds, a cold nitrogen gas system in the ARIES tumbled the rocket so that it had no net forward thrust. Was this enough?

Radar track showed that the ARIES motor made up about half the separation velocity by the time it was tumbled. However, some environmental contamination was apparent in the data from the first zodiacal experiment that we inferred was due to effluvia from the tumbling motor that was spewed into the field-of-view when the nozzle was pointed upward since it occurred at roughly the same azimuth on each roll. We subsequently increased time to separation by another 5 seconds and tumbled the rocket in such a fashion that the nozzle never pointed upward.

MSMP and BMP shared another payload issue; the parachute initially used for recovery was inadequate for the payload weights. The largest parachute in the standard recovery pack at the time had a 20' canopy, which resulted in too high a descent speed and the consequent force of impact with the ground was hard enough to damage the SPICE I payload, as seen in Figure 43. MSMP funded the successful qualification of a 28' recovery parachute while the BMP developed the common separation system. The x-shaped parachute worked well (Figure 54) and there was no recovery damage on any of the remaining BMP and MSMP flights.

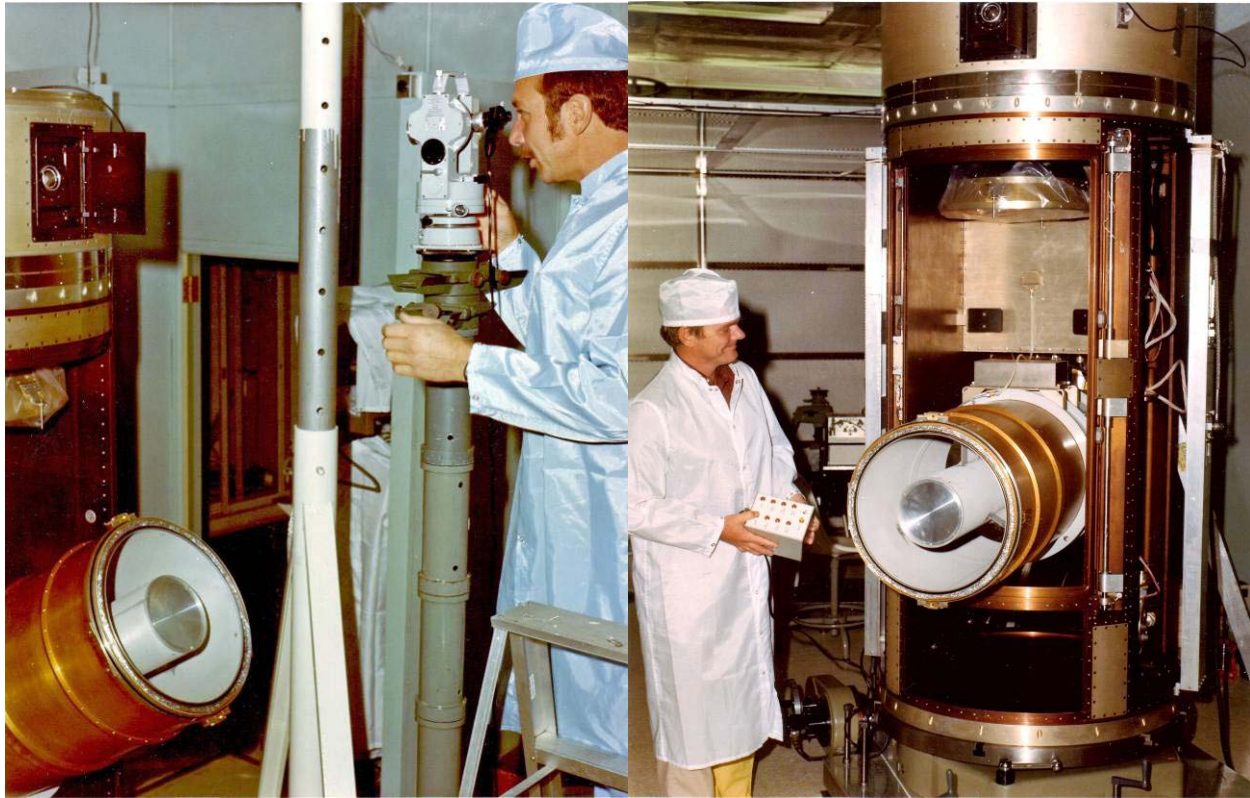


Figure 44. The SPICE sensor in the clean room during field preparations. Dave Akerstrom, laboratory chief engineer for SPICE, is calibrating the deployment positions on the left. The sensor deployment angle and the azimuth bias are referenced to the center slit of the star mapper at the top of the payload, as a function of the digital readout of the encoder on the deployment gimbal. Tom Campbell, from Wentworth Institute of Technology, is shown on the right stepping the sensor through the deployment program. The sensor is at maximum deployment in this image and the SPICE primary mirror is just visible. The baffle surface are grooved then anodized with an infrared absorbing material that looks grey in these images. The center tube houses the secondary mirror and is configured as part of the baffle in order to improve the off-axis rejection.



5.6. SPICE 2

The refurbished Rockwell SPICE sensor was successfully flown on 14 September 1982 from White Sands with the configuration shown in Figure 45. The experimental profile had the payload being flipped 180° after separation while the payload door was opened and the sensor was deployed to a zenith angle of 40°. After the payload was inverted and stabilized, the star tracker locked onto the pole star, ϵ Cyg for this experiment. The payload was spun up and executed a 382.5° azimuth roll

after which the sensor was stepped 4° in deployment angle while the roll rate was adjusted to maintain a linear scan rate of 15°/sec across the focal plane. The step and roll rate change were completed within the extra 22.5° at the end of each roll so that, unlike previous experiments, a complete 360° almucanter (small circle on the sky) was surveyed on each roll. The sensor was stepped down 12 times by 4°, reaching a maximum deployment of 85° near the apogee. The sensor was then stepped up such that the deployment angles were interleaved with those

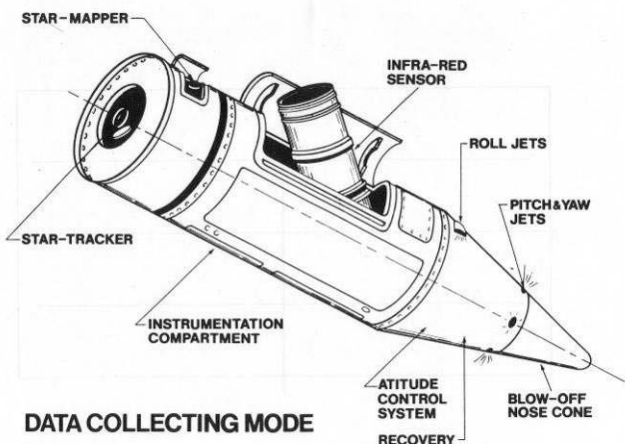


Figure 45. The BMP payload configuration. The star tracker looks out the separation plane of the payload and the recovery parachute is in the nose section, the reverse of HI STAR. As for HI STAR, the sensor cover is removed by a jack screw in the payload and the instrument is deployed on a one axis gimbal. The payload door was opened to allow the sensor to deploy then closed after the sensor was stowed.

Our AF Space Division⁷ sponsors required that SPICE include a secondary experiment to observe an Earth satellite in which they were interested. This was the inverse of the problem that we usually tackled of identifying serendipitously observed satellites after the fact, which is much easier than trying to measure a specific target on a given experiment. Once September 1982 had been set by the pace of payload preparations and the approximate sidereal time of launch was established by the choice of pole star, dynamicists at Aerospace Corp. set the time of launch such that the sensor field of view would sweep over a high value target. Neither the range nor I liked the fact that the exact launch time was at the end of our half hour launch window since range safety had to block US Highway 70/82 for the maximum 1½ hours allowed by agreement with the state of New Mexico. The launch occurred on time and sure enough a strong signal characteristic of a satellite was seen with the distinctive cool three color signature within about 1½ seconds of the predicted time. The Aerospace people were jubilant and immediately set about to call a high ranking general in Washington with the news. I urged caution as the 1½ seconds was in scan time not satellite track, which placed the object 22° off in azimuth angle, far too large to be the desired satellite. The call was made anyway, waking the general in the wee hours of the morning. Subsequently, there was some explaining to do as to why the predictions were wrong. The programmer had failed to convert all the angles into consistent units and

executed during the first half of the experiment. Thus, a third of the sky was surveyed with about 40% redundancy (plus the areas covered while stepping).

Having the sensor's line-of-sight come closest to the edge of the Earth near apogee, when the depression angle to the Earth, $\alpha + \beta$ in Figure 33, was at a maximum of 25°, minimized the off-axis radiation from the Earth during the experiment. Thus, the edge of the Earth came no closer than 25° to the sensor line-of-sight. This and the very good off-axis rejection capabilities of the SPICE sensor meant that background photon noise was not a problem for this experiment. However, a low amplitude direct extended signal from the Earth was seen when the sensor step was reversed near apogee. Figure 44 shows the SPICE sensor deployed for calibration and testing while in the field clean room.

⁷ The Space and Missile Systems Organization (SAMSO) at the Los Angeles Air Force Station in El Segundo, CA was formed in 1967 when the divisions responsible for the development of ballistic missiles in San Bernardino (originally created in 1954) and satellite systems (1957) were merged. On 1 October 1979 SAMSO was divided into a Ballistic Systems Division (BSD) and a Space Division (SD). SD became Space Systems Division (SSD) on 15 March 1989. The Ballistic Missile Organization, the successor to BSD, was again put under SSD jurisdiction and, on 1 July 1992, the merged group was redesignated the Space and Missile Systems Center (SMC).

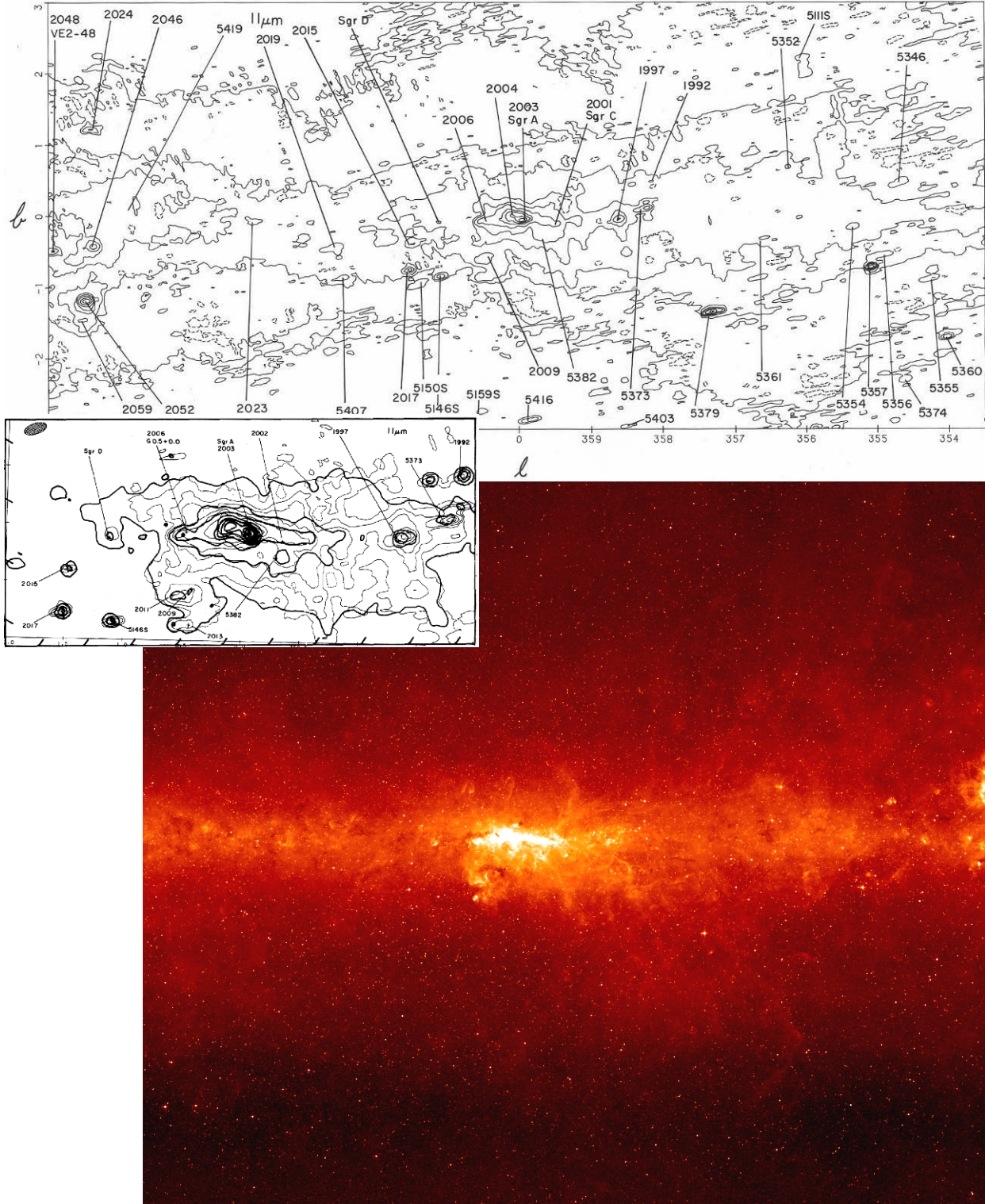


Figure 46. The mid-infrared Galactic center. The $(\Delta l, \Delta b) \sim (\pm 6.5^\circ, \pm 3^\circ)$ contour plot at the top is the $11 \mu\text{m}$ restored image from SPICE II with a beam size of $\sim 2.5 \text{ mas}$; the insert at middle left overlays the IRAS $12 \mu\text{m}$ contours (heavy lines) onto the center of the SPICE map (light lines). The $8.3 \mu\text{m}$ Midcourse Space Experiment image at bottom spans 10° in latitude and longitudes between $353^\circ > l < 5^\circ$ and is aligned so that the latitudes correspond with the upper contour plot. The MSX image was obtained at much higher resolution ($\sim 1 \times 10^{-8} \text{ sr beam}$). The IRAS overlay was kindly supplied by George Aumann.

interpreted radians as degrees for the launch time calculations, analogous to the English/metric mix-up that doomed the Mars Climate Orbiter in 1999. The object we actually observed was a rocket body, which was of little interest.

Since the SPICE pole star, ϵ Cyg, was near the Galactic plane at $(l, b) \sim (76^\circ, -5.7^\circ)$, the scans were almost perpendicular to the plane. The SPICE low frequency signals were restored to create infrared Galactic plane maps that covered longitudes between -6° and $+37^\circ$ but at higher resolution and sensitivity than HI STAR, as shown in the top contour plot of Figure 46. Little and Price (1985) published the maps for the region within 2° of the Galactic center; the $11\ \mu\text{m}$ map was the cover illustration of the *Astronomical Journal* in which the article appeared. George Aumann provided the insert that overlays that cover illustration with the Infrared Astronomy Satellite (IRAS – next Chapter) $12\ \mu\text{m}$ contour map of the Galactic center in heavy lines. Although the SPICE beams size, the cross hatched oval in the upper left of the insert, was about five times larger than that of IRAS, the center maps were of comparable resolution.



5.7. Far-infrared Sky Survey Experiment

Although the NRL far-infrared experiments ended with their last flight in 1968 (Feldman, McNutt and Shivanandan, 1969), NRL was still interested in such experiments. Kadiah (Kandi) Shivanandan⁸ called us toward the end of the HI STAR program to explore the possibility of putting far-infrared detectors in the sensor. Reluctantly, we had to decline the suggestion as the HI STAR sensor could not be easily modified to accommodate the superfluid helium required for such an

experiment. NRL again proposed a far-infrared collaboration five years later. As before, we couldn't modify an existing sensor but suggested building a new one. The Perkin-Elmer Mark VII optics (right hand image in Figure 47) were available, which NRL purchased. We proposed to our Space Division sponsors to build a backup capability for the SPICE experiment, a Far-infrared Sky Survey Experiment (FIRSSE), around the Mark VII optics and an NRL funded focal plane. Space Division supported the construction and integration of the sensor and a second SPICE payload in which either the SPICE or FIRSSE sensors would fit. We agreed to incorporate the same three mid-infrared focal plane arrays and spectral bandpasses as SPICE in the FIRSSE telescope in addition to the two new far-infrared bands.

A space-based far-infrared experiment, or at least one high in the atmosphere, is required as the atmosphere is essentially opaque at wavelengths between $\sim 35\ \mu\text{m}$ and $120\ \mu\text{m}$ (see Figure 13). The 1970s National Academy of Sciences (1973) astronomy decadal report rated the construction of a high angular resolution stratospheric observatory for $100\ \mu\text{m}$ observations as a top priority as the next logical step after the 12" telescope on the NASA Lear Jet that Aumann and Low (1970) used to obtain the first good quality far-infrared measurements of the Galactic center. The mid-1970s inauguration of the Kuiper Airborne Observatory, a 36" (0.91 m) telescope on a modified C-141 transport aircraft was the realization of that recommendation. The National Academy study also gave a high priority to a moderate sensitivity $100\ \mu\text{m}$ balloon-

⁸ Shivanandan (2008) had been peripherally involved in an early AFCRL sponsored rocket experiment. While an MIT graduate student he had worked at AS&E supporting the calibration of Giacconi's x-ray experiments described in Chapter 2.

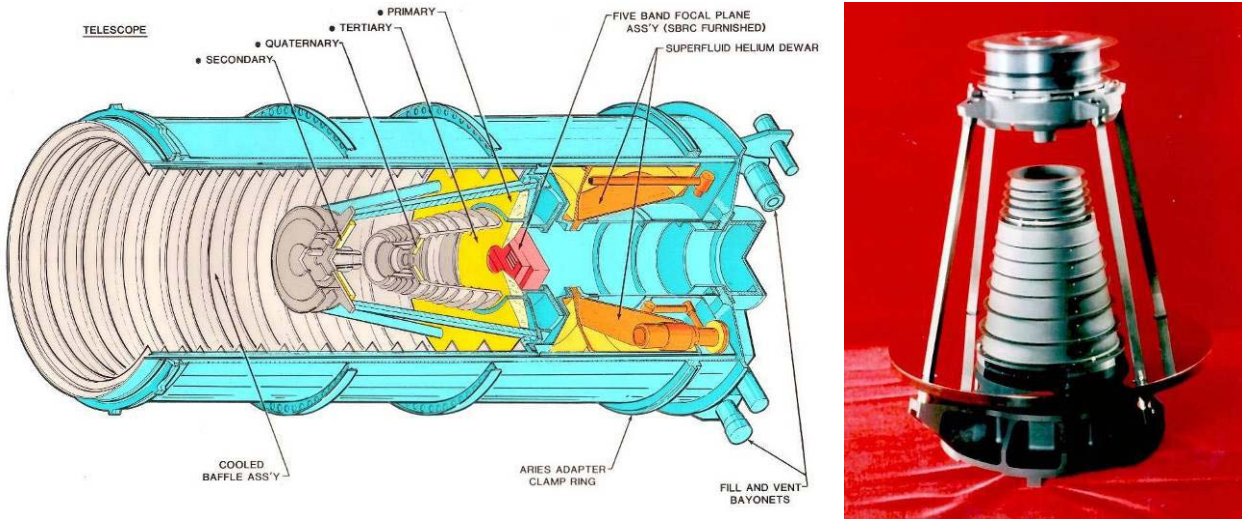


Figure 47. The FIRSSE sensor. An isometric cutaway drawing of the sensor is shown at the left and a picture of the Perkin-Elmer Mark VII optics is at the right.

borne sky survey to extend the initial results obtained by Hoffman et al. (1967), who had mapped half the sky during two balloon flights but only detected the Moon. A more successful survey of the Galactic center by Hoffman, Frederick and Emery (1969 and 1971a) and the Galactic plane (Hoffman, Frederick and Emery, 1971b) soon followed. However, the contemporaneous far-infrared surveys by Friedlander and Joseph (1970), Friedlander, Goebel and Joseph (1974) and Furness, Jennings and Moorwood (1972) produced mixed results. The various balloon programs active at the time are described in the February 1974 NASA Ames Research Center Symposium *Telescope Systems for Balloon-Borne Research* and in the reviews of Hoffman (1977) and Okuda (1981). Ultimately, a systematic moderate sensitivity all-sky far-infrared balloon-based survey never materialized.

The decadal study also gave the same moderate priority to a more sensitive 100 μm survey from rocket-borne instruments as it did for a mid-infrared satellite survey. Harwit (2003) describes the first far-infrared probe-rocket based experiments conducted by the Cornell University and the Naval Research Laboratory. The subsequent AFCRL supported Cornell probe-rocket flights also had a far-infrared component. FIRSSE was to improve upon the resolution, sensitivity and the area covered by these early experiments.

Since NRL had purchased the telescope and the focal plane, they received the choice focal plane real estate at the center of the array for the long wavelength detectors. The 2.2° circular focal surface of the Mark VII optics was slightly curved and the larger far-infrared detectors would accommodate the astigmatism from fitting a flat detector array into the curved focal surface. The 15 detectors in the three FIRSSE far-infrared arrays spanned the full 2.2° in the cross-scan direction while the 13 element 11 and 21 μm arrays covered ~1.8° on either side of the far-infrared arrays. The 30 – 50 μm array incorporated 4'×12' Ge:Be detectors while an array of 5.3'×12' Ge:Ga detectors covered the 50 to 100 μm spectral region; the 27 μm Si:Sb array was considered a far-infrared band for this sensor. Shivanandan et al. (1978), Price, Murdock and Shivanandan (1981) and Price, Shivanandan and Murdock (1983) provide details of the FIRSSE hardware, experiment and performance.

Ball Bros. Space Division in Boulder, Co. built the sensor around the MARK VII optics and the Santa Barbara Research Corp. focal plane. Dick Herring, the Ball vice-president, had



Figure 48. Payload preparations for launch. The ensuing series of images follow the sequence of launch preparations using a montage of photographs from the SPICE and FIRSSE experiments. Above left, the cleaned and bagged payload has been loaded on a cart on a pickup truck to be taken to Launch Complex 36 at the White Sands Missile Range. It is shown here as it is being lifted off the truck. The right hand picture shows the payload being hoisted into the roll away launch preparation building.

spent a year with the far-infrared team at Groningen, Netherlands and helped develop their concept for an infrared satellite that was subsequently combined into the Infrared Astronomical Satellite. In addition to Herring's far-infrared experience, his division had a group of talented cryogenic engineers one of whom, Jim Lester, led the FIRSSE effort.

Ball Bros. was also the major supplier of star trackers after ITT got out of the business in the mid-1970s; they even inherited Dick Gotschall from ITT, whom I had known when I worked there in the mid-1960s. We had exhausted our original supply of the three ITT trackers after twelve flights during which a HI STAR South and the Super HI STAR payloads were destroyed. Consequently we also contracted with Ball to build the BMP star trackers. Thus, meetings at Ball served the dual purpose of assessing progress on both the sensor and the star trackers. The regular monitoring proved to be valuable as initially progress with the star trackers was very slow, but the bills were mounting. We were able to nip a costly overrun in the bud.

The AFCRL/AFGL mid-infrared sensors were cooled with super-critical helium, a liquid-gas transition phase of helium with good thermal contact properties. It is formed by pressurizing the cryostat to three atmospheres at very low temperatures. Super-critical helium has an equilibrium temperature of about 5.5K in space, making it easily possible to cool the focal planes to about 7K. However, the sensitivity of the far-infrared germanium detectors is poor at 7K, which precluded the HISTAR instruments from being used for far-infrared observations. The detector sensitivity is improved if the array is cooled to fluid or, better yet, superfluid helium

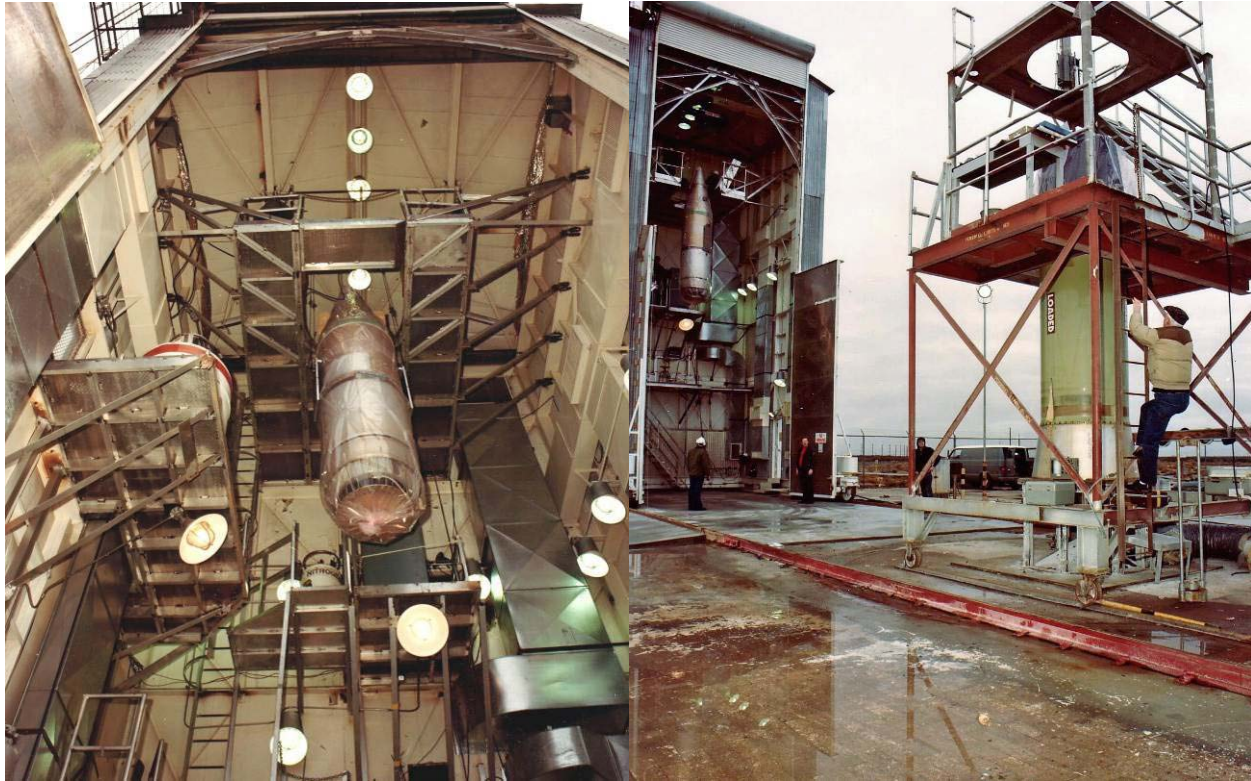


Figure 49. The payload in the tower. The bagged payload is waiting to be mated to the rocket at left. The final touches are put on the ARIES in the motor gantry while the payload is suspended in the launch preparation building on the right. Gunnery Officer (Gunny) Briggs is climbing the ladder.

temperatures. To achieve these temperatures, the FIRSSE tank was vacuum pumped, reducing the vapor pressure by boiling off the liquid helium and decreasing the helium temperature. The helium can be stabilized at its 4.2K boiling point but it is much better if the cryotank contains superfluid helium at or below its 2.2K phase transition temperature. The heat capacity of the phase transition keeps the temperature of the fluid at that point for a long time.

However, liquid and superfluid helium has some counter-intuitive properties, one of which is that it flows toward heat and, if not contained, will flow out the vent line, drastically reducing the lifetime of the mission as happened on some of the very early probe experiments. Thus, the invention of sintered nickel and ceramic porous plugs in the 1970s to contain superfluid helium made FIRSSE and IRAS possible. The FIRSSE sintered nickel porous plug separated the liquid and gaseous helium, retaining the former and allowing the latter to pass through. The helium gas vented by the cryotank was sent through a series of heat exchangers to cool the FIRSSE heat shield, which extended the cryogenic hold time of the sensor. Because the best performance of the far-infrared detectors required very low optics temperatures, thermal straps made of 0.99999 pure aluminum tied the optics directly to the cryotank to eliminate photon background from these components. The thermal straps to the secondary mirror were laid down on the backside of the four secondary support struts that are visible in Figure 47. Similar straps were used on the focal plane, the support structure and the inner radiation shield.

Filling the FIRSSE dewar was rather complex compared to the steps needed to fill a super-critical helium cryostat. For the latter, the dewar is filled, the vent line is closed and the liquid helium is heated until the super-critical helium was formed. A relief valve in the vent line

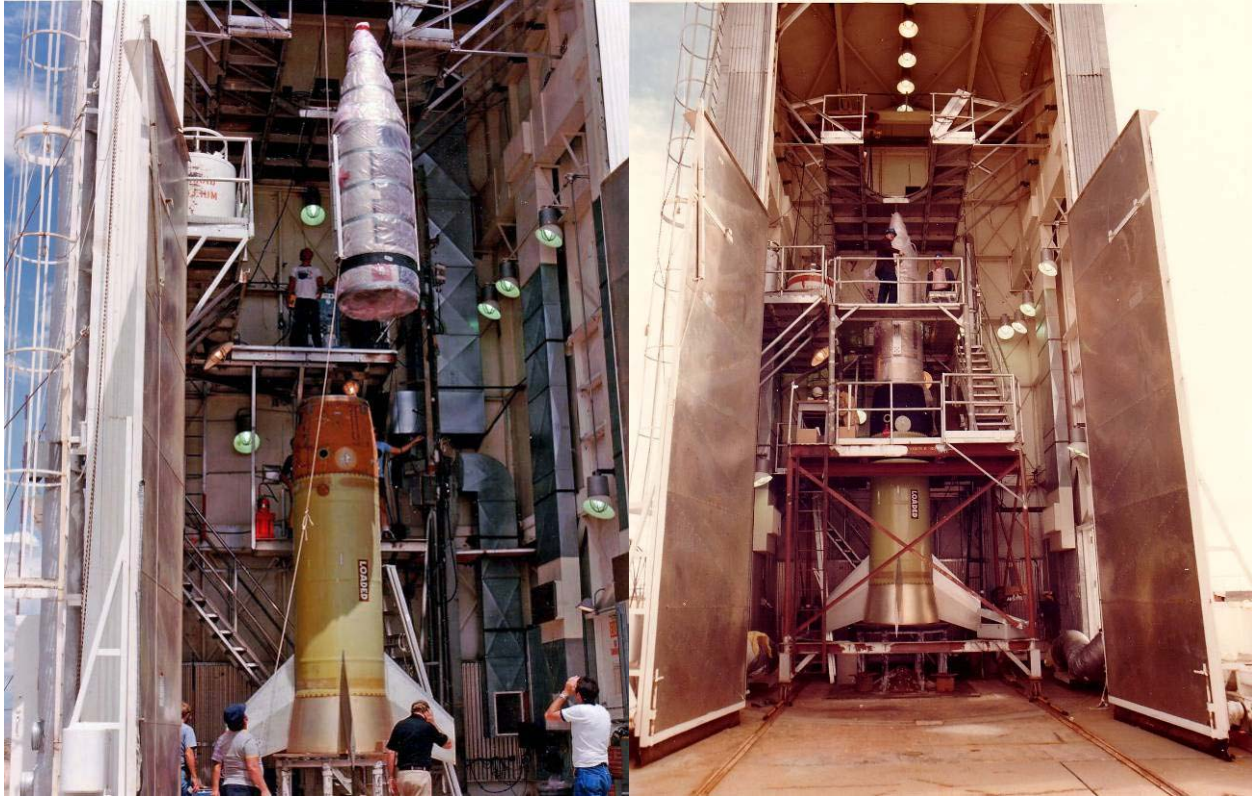


Figure 50. Mating the payload to the rocket. The preparation building is rolled into place over the ARIES to mate the payload to the rocket as shown in the picture on the left. The ARIES motor and payload have been mated in the picture on the right. The large white cylinder with the orange band is a 500 liter liquid helium dewar used to fill the sensor. The solid motor is 44" in diameter and the Minute Man second to third stage transition stage, best seen in the left hand Figure, accommodates the 38" diameter payload.

maintained the three atmospheres pressure necessary for super-critical helium. To fill the full 17 liter FIRSSE dewar capacity, an elaborate scheme was devised in which the supply dewar and the FIRSSE cryotank were pumped to form super-fluid in both. This reduced the fluid in the tank by a couple liters and replacing this ullage was highly desirable as it increases the hold time, the time that the sensor vent line could be closed while still maintaining the operating temperature. Therefore, superfluid helium from the supply dewar was transferred to the FIRSSE cryotank to fill the ullage. This was all new to us, so every time we filled the FIRSSE tank was a learning experience. Fortunately, we perfected the technique on the last fill, just in time for launch, almost completely filling the dewar with super-fluid.

Figures 48 through 54 show the launch preparations for the celestial experiments with a combination of SPICE and FIRSSE photographs.

FIRSSE flew on 22 January 1982. Given the time of year, the pole star, α Lyn, was chosen to survey the second and third quadrants of the Galactic plane between longitudes $\sim 130^\circ$ and $\sim 245^\circ$, which complemented the area that SPICE II was to cover later that year. The profile was similar to that of SPICE: the sensor initially deployed to a zenith angle of 41° and the payload was rotated 382.5° at a rate sufficient to produce a $15^\circ/\text{sec}$ effective linear scan rate across the focal plane. The sensor was stepped 3.14° in zenith angle after each roll was completed. Because the FIRSSE off-axis performance was inferior to that of SPICE, the



Figure 51. A view of the payload on the rocket with the gantry and preparation building rolled back. The assembled experiment seen from the preparation building is on the right during t-3 hour check.

maximum deployment zenith angle was a more conservative 75° . The maximum deployment occurred on the 11th roll around the peak altitude; the sensor was then stepped up 1.5° and the deployment angles on subsequent rolls were decreased by 3.14° . Thus, ~20% redundant coverage was obtained in the long wavelength bands with about 10% at the shorter wavelengths.

FIRsse was a qualified success with two sensor problems that seriously compromised the value of the observations. Most important to our sponsors was that the bias on the 11 μm array was shorted when the focal plane was installed in the sensor. Although one might see how such a problem could arise in the rat's nest of cables from the focal plane to the signal processing electronics through the heat sinks where the failure occurred, the loss of the array for flight was due to inadequate testing of the completed instrument. We monitored the 11 μm response to internal stimulators, but the devices were tailored for the far-infrared channels and we thought that the small 11 μm response we observed indicated a working array. The response was actually due to cross-talk from the longer wavelength detectors through the shorted bias.

The second problem was that the focal plane temperatures were not stable during the experiment, which degraded the sensitivity of the Ge:Ga detectors for about a third of the flight and induced spiking in the Ge:Be array. Both problems compromised the rescan confirmation. The cause of variation of the focal plane temperatures fell into the 'why didn't we think of this before flight' category. The focal plane and optics were thermally tied to opposite sides of the same inner cold ring of the dewar. The rather large, >10 Watt, thermal input into the sensor from the Earth and payload during the experiment was mostly absorbed by the baffles, which are cooled by the venting helium, but a large fraction was intercepted by the back of the secondary mirror, which is tied directly to the tank through the optics. The very low heat capacity of the cryotank at the operating temperature meant that any heat on the tank is immediately conducted to the cryogen. The thermal input from the optics onto the cryotank ring drove the super-fluid helium away from the area (or vaporized it), which allowed the ring and hence the focal planes to warm up to as high as 5K. The ring and focal planes would cool as the super-fluid surged back resulting in a fluctuating focal plane temperature. The problem could have been easily fixed by attaching the optics to a part of the tank far away from the focal plane attach points. However,

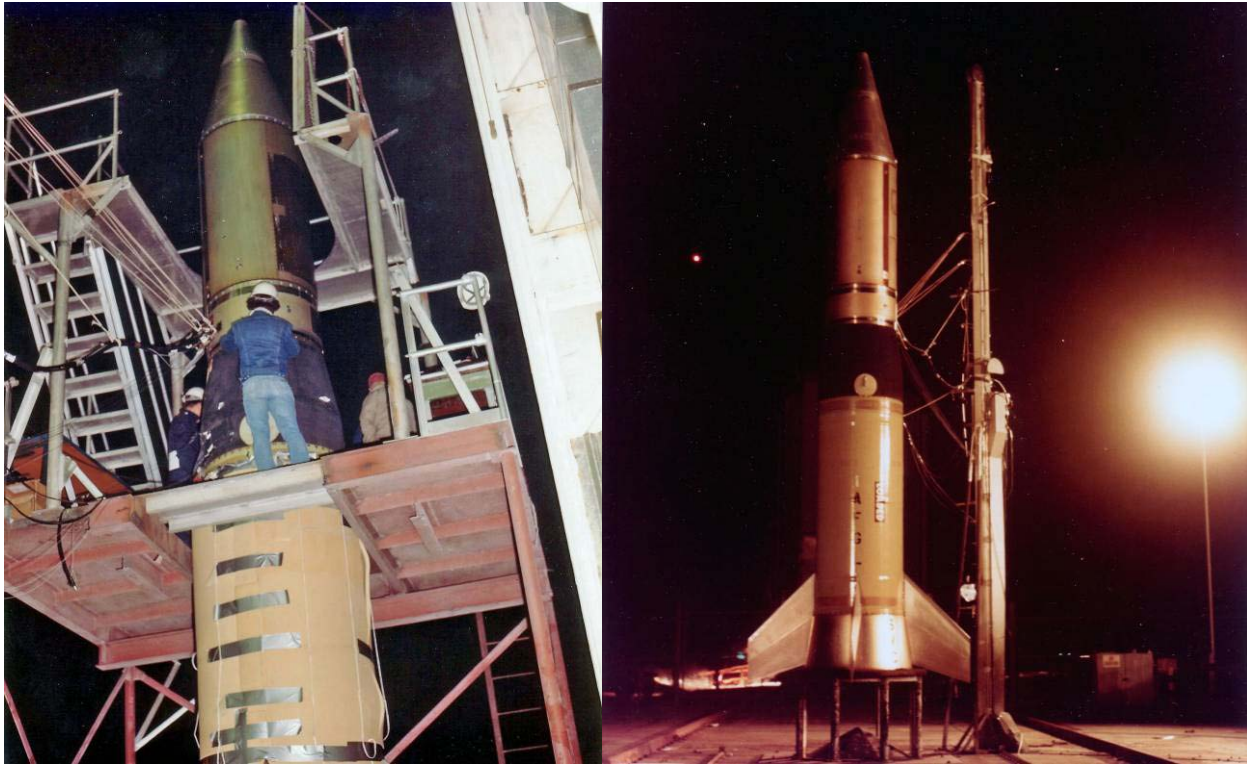


Figure 52. Just before launch. The separation system and rocket are being armed on the left. The rocket on the pad during final countdown to launch is shown at the right.

the loss of the 11 μm channel was a ‘fatal’ flaw that led Space Division not to support a FIRSSE reflight.

Details of the FIRSSE hardware, experiment and performance are given by Price, Shivanandan and Murdock (1983) while Price et al. (1983) published the scientific results in the form of a list of the bright 90 μm sources detected by FIRSSE with corresponding 50 μm fluxes, when available. Since most of the sources were H II regions for which the peak flux occurs in the far-infrared, Price et al. (1983) also estimated total luminosities from the FIRSSE measurements. LeVan and Price (1984) published the 27 μm to 90 μm FIRSSE and SPICE observations of the asteroids, the most significant finding from which was that the large asteroids exhibited a wavelength dependent emissivity with the value in the far-infrared being less than that in the mid-infrared. The SPICE point source detections and the 20- and 27 μm FIRSSE measurements were combined with the AFGL Catalog to create *The Revised AFGL Infrared Sky Survey Catalog* (Price and Murdock, 1983) of 2970 infrared sources. Since the SPICE and FIRSSE system noise was much more uniform and the sensitivities were at least ten times better than those of the HI STAR/HI STAR South experiments, the uniformity in the SPICE and FIRSSE signal-to-noise improved the catalog completeness and the better sensitivity increased reliability. The reliability was further improved by incorporating the results of the follow-up confirmation studies by the Universities of Wyoming, Minnesota and California, San Diego into the revised catalog.

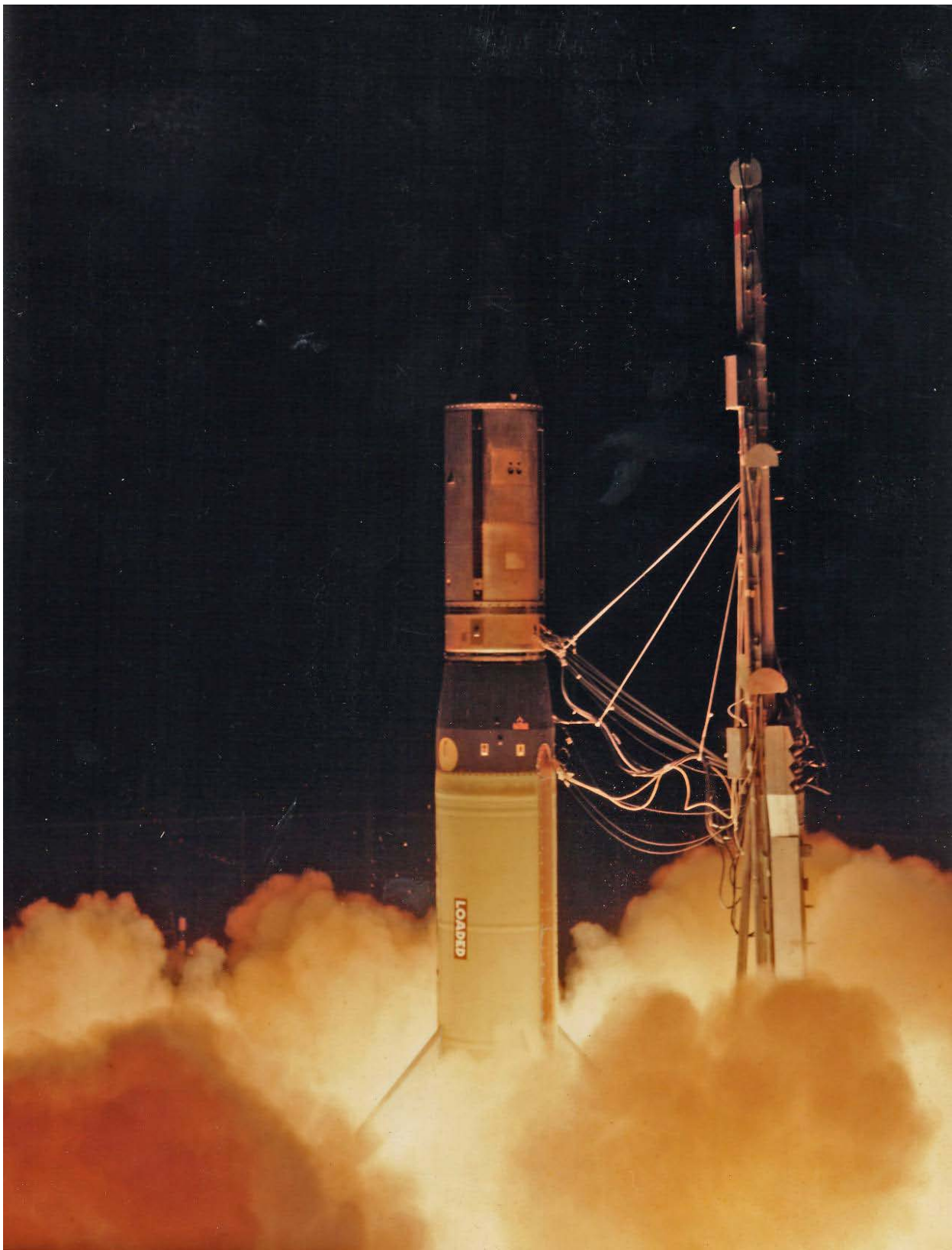
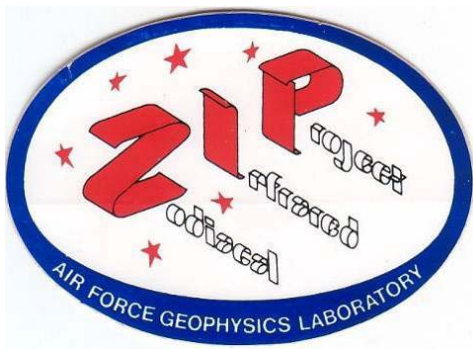


Figure 53. Launch.



Figure 54. A successful soft recovery of the FIRSSE payload. Tom Murdock is in the red parka and Dave Akerstrom is in the black hat.

5.8. Zodiacal Infrared Project



The Zodiacal Infrared Program (ZIP) experiment was largely Tom Murdock's creation. Tom had come to AFCRL in 1972 as an Air Force first lieutenant to complete his military obligation after obtaining his PhD from the University of Minnesota with Ed Ney as his thesis advisor. Tom proved to be a good addition to the infrared celestial background team. Using the methodology he established in his thesis, he predicted the

asteroid contribution to the infrared content of the sky (Murdock, 1973). Tom also had a facility with hardware and provided field support for the HISTAR South experiments. Subsequently, he was the lead scientist for the preparation and launch of the ELS, although Bert Schurin remained principal investigator. Thus, he was a natural choice to lead the zodiacal background measurement effort.

Initially, Russ Walker had proposed that the zodiacal observations critical to surveillance system design could be obtained by a series of Super HI STAR experiments in which the sensor was pointed in various directions in the sky while the internal shutter chopped the signal. Tom successfully argued for a dedicated experiment using a specially constructed sensor to survey the absolute infrared spectral radiance over a large range of solar elongations in spectral bands tailored to observe the defining characteristics of the background.

AFGL proposed to fly ZIP on the Castor-Lances it had in storage to save costs but few missile ranges could accommodate the rocket because of its large impact dispersion (a circle in which the payload would land with a 95% probability based on past experience). AFCRL had flown a Castor-Lance from the range near Natal, Brazil, but it was deemed unlikely that we could seal the payload well enough for the requisite water recovery. However, our Aerospace Instrumentation Division launch team thought that an agreement could be worked out with the Woomera, Australia range management to fly the Castor-Lance from there even though the dispersion just scraped the range boundaries. To place this in context, the dispersion was larger than the error between the predicted and actual impact point for the first HI STAR South launch, which came down within 30 or so miles of a small settlement. The range had us target a nominally unpopulated impact point and supposedly saw to it that the area was truly evacuated. Although the range was sparsely populated and the people were warned to evacuate or take cover for the launch, few did.

Carson Alexiou Corp. began design and construction of the ZIP sensors in September 1976. Tom left the military shortly thereafter and worked for a year for a local contractor before we could hire him back as a civilian (the government required that people leaving the military at

that time had to wait a year before being hired into the civil service). The sensor was designed to fit into the 22" diameter payload that was built to easily mate to the 17" diameter Lance motor. Putting a larger diameter payload on a smaller motor is called a 'hammer head' and the mismatch in the diameters cannot be too large as it leads to drag and flight stability problems. It was subsequently decided after construction of the 22" diameter payload and the sensor that fit into it had begun that many problems would be avoided by flying ZIP on the ARIES from the White Sands Missile Range. The end result was rather ungainly configuration in which an additional transition stage was added to the normal 44" to 38" ARIES transition stage, as seen in Figure 55.

Murdock et al. (1980) describe the rather complex off-axis optical design of the ZIP telescope, which was relatively compact and tailored for the superior off-axis performance required for absolute



Figure 55. The ZIP payload on the ARIES motor.

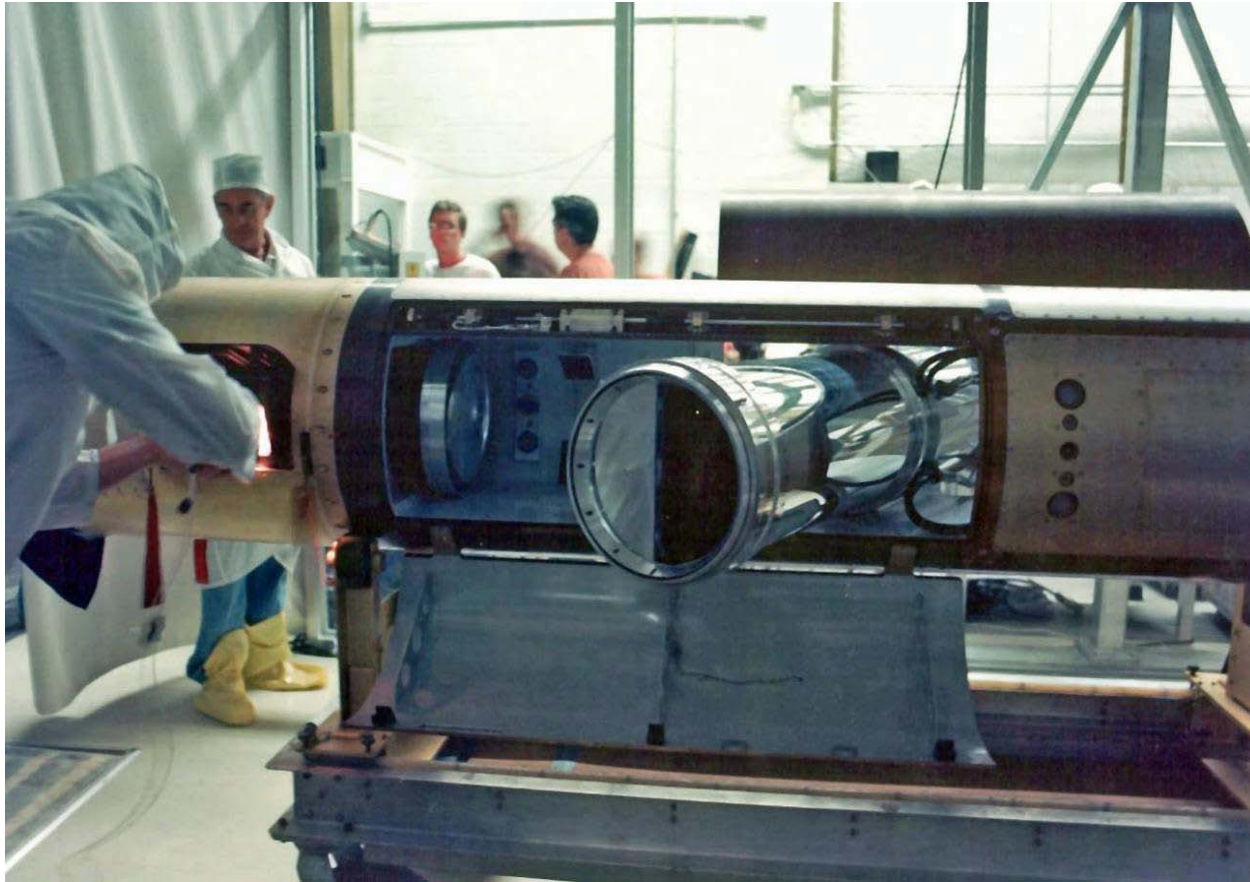


Figure 56. The ZIP sensor is shown deployed in the cleanroom. The 'D' shaped aperture is visible, as are the front and rear doors that were opened to accommodate the length of the sensor when deployed.

radiometric measurements from a probe-rocket platform. Rather than being circular, the primary mirror was 'D' shaped with rounded corners to decrease the baffle angle and maximize the collecting area of the primary mirror while keeping the sensor volume to a minimum. This design permitted the relay optics to be folded into the other half of the sensor cylinder (see Figure 56). The off-axis performance was measured to be quite good (Wong, Wang and Murdock, 1980; Murdock and Price, 1985) with a baffle angle of $< 5^\circ$ and a superior far-field rejection ratio as may be seen in Figure 32.

The telescope had a clear aperture area of 81 cm^2 , two-thirds that of the HI STAR South sensors. However, the solid angle subtended by the 5' (cross-scan) by 15' (in-scan) detectors was ~ 1.5 larger so the ZIP telescope had about same radiance response since the sensitivity to extended sources is a function of the inherent sensitivity of the detectors and the étendue, French for extent, which is defined as the collecting area times the detector solid angle. The 15 color focal plane spanned 2 to $30 \mu\text{m}$ with spectral bandpasses of $\Delta\lambda \sim 1.5$ to $4 \mu\text{m}$. The spectral range encompassed the transition from thermal emission to reflected sunlight from the zodiacal dust and the mid-infrared spectral resolution was sufficient to measure broad, solid state spectral emission features in the zodiacal dust, such that from silicates that were indicated by the Cornell zodiacal experiment (Briotta, 1976; Briotta, Pipher and Houck, 1976). The focal plane was a matrix of 4×4 modules with two detectors under the same filter in each module while one of the corner modules had blank reference detectors. Four detectors in different filter bands were

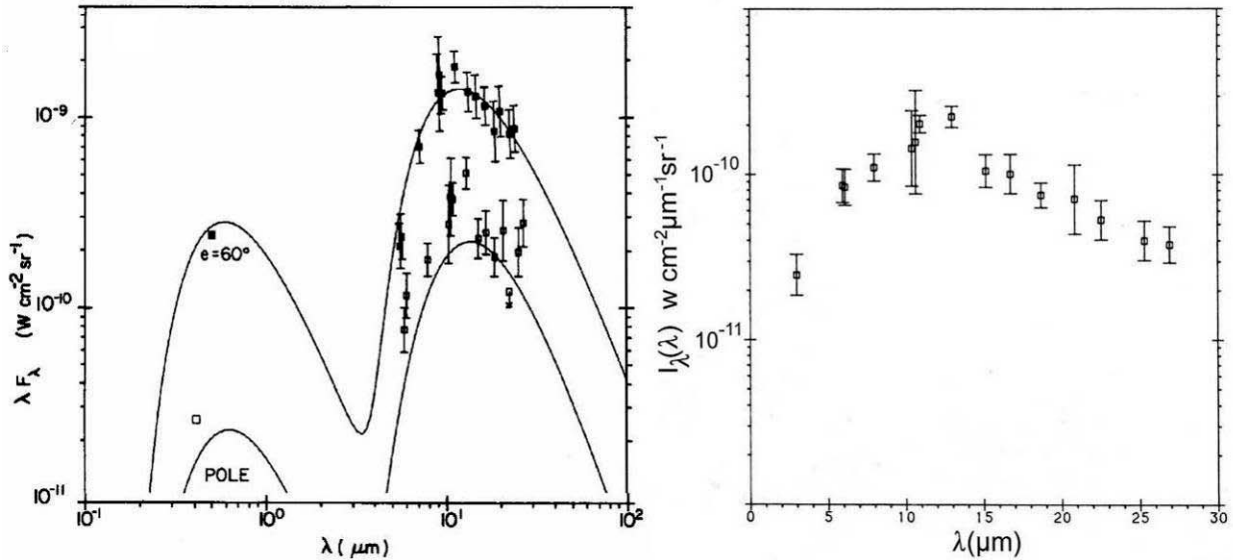


Figure 57. ZIP Zodiacal spectra. The left hand Figure is adopted from Murdock and Price (1985) and shows the ZIP spectra in the ecliptic plane (top) at a 60° elongation and the north ecliptic pole (bottom) with a simple model as the solid lines. While the spectrum at $\epsilon = 60^\circ$ is in good agreement with the model that at the north ecliptic pole is not. A $10 - 13 \mu\text{m}$ excess emission is indicated in these data and in the ZIP 1 spectra in the ecliptic plane at an $\epsilon = 45.5^\circ$ in the right hand plot. Note that the abscissa scales are different.

aligned in a row with an inter-row spacing of about $7'$. Murdock and Price (1985) show a layout of this porous focal plane; porous because a star could transit the focal plane without being detected. Fourteen modules had Si:As detectors with transparent contacts while the remaining two had Si:Sb detectors that covered $22 - 30 \mu\text{m}$. The detectors were chopped at a frequency of 100 times a second by a cold reference blade. The chopped signal was sent to the ground at ~ 1000 samples/sec and was digitally rectified at the Laboratory rather than on-board. A reference signal was also telemetered that measured the phase of the chopper blades.

Two ZIP experiments were flown from White Sands, one on 18 August 1980 and the other on 31 July 1981, and both used the same pole star, δ And. The first experiment was entirely at night, whereas the timing of the second had the payload ascending from shadow into sunlight at $t + 160$ seconds and back into shadow at $t+350$ seconds at an altitude of about 250 km. The sensor was initially deployed to a zenith angle of about 40° for both experiments and the payload rotated to scan the sensor at a linear rate of 7.5° across the sky. For ZIP 1, the sensor was stepped by 4° after each 365° roll until a maximum deployment angle of 80° was reached, after which the sensor stepped up, repeating the area covered by the previous two rolls. ZIP 2 stepped by 7.5° for six rolls to a maximum deployment of 85° . The sensor was then stepped up to repeat the geometry of the previous three scans.

Murdock and Price (1985) published the ZIP results; examples of ZIP 1 and ZIP 2 spectra is shown in the left hand plot of Figure 57 in which the data is given at a 60° elongation in the ecliptic plane (top spectrum) and at the north ecliptic pole (bottom spectrum). The spectrum on the right is derived from the ZIP ecliptic plane crossing at 45.5° elongation. It may be noted from the plots that the high radiance spectra in the plane have an excess that is most prominent in the $13 \mu\text{m}$ channel and that the lower radiance spectrum at the pole is somewhat discordant, as are spectra at large elongations. The inconsistencies must be due to uncompensated biases in the data since they are larger than the $\sim 30\%$ formal uncertainties assigned to the measurements that

are depicted by the error bars. Because of the unknown biases, we never trusted the spectra enough to attempt a mineralogical analysis of the excess. The same comment applies to ZIP spectra of the Galactic plane extracted by Rickard, Stemwedel and Price (1990). However, in the perfect 20–20 vision of hindsight, it appears that we were overly cautious in not further pursuing the analysis of the ZIP ecliptic plane spectra as these are in good quantitative agreement with the independent measurements of Reach et al. (1996; 2003).

The 11 μm radiance *vs.* time measured on ZIP 2 is displayed in Figure 58; the raw data is shown at top and that after editing and correction for various artifacts at the bottom. Burdick et al. (1994) described in detail the various processing steps used to create Figure 58 and added two more, an estimate of the off-axis contamination from the Earth and the change in response of the ZIP 2 detectors due to warming of the focal plane from the thermal input from the Sun.

Some artifacts in Figure 58 are easily identified as obvious optical contaminants associated with the hardware. For ZIP 1, we deduced that the contamination was due to effluvia from the motor. The fix, described in the separation system section, appears to have been successful as no such contamination showed up on the second flight or on the celestial survey experiments. The spikes denoted by asterisks in the top of Figure 58 are either signals from a detached piece of the ZIP 2 payload (Murdock and Price, 1985) or sunlight reflected from droplets or frozen particles of nitrogen that condensed from the attitude control gas (Price, 1988b). The attitude control system vents gas through control jets, located as shown in Figure 45, to move and control the position of the payload. Both MSMP and ZIP 1 used argon while all the other BMP experiments used nitrogen. Argon has a higher specific impulse than nitrogen so less of it may be used to achieve the same results. Both argon and nitrogen are advantageous as they have no dipole moment and, consequently, no strong infrared emissions. However, the ACS gas is cooled when ejected from the nozzles into space and, if the gas expands rapidly enough, it may condense into droplets or even freeze. The expansion ratio of the ACS jets can be sized to decrease condensation but not eliminate it without significantly reducing effectiveness. Since Kolb et al. (1983) observed ultraviolet and visible sunlight reflected from the plume of argon gas ejected by the MSMP ACS jets, which Kolb et al. (1985) attempted to remove from the measurements, Price (1988b) reasoned that sunlight reflected by the ACS gas plume was the best explanation for the observed geometry and the spectral characteristics of the ZIP 2 contamination. The contamination was observed 5 to 7 seconds after the sensor was stepped, when the sensor line of sight looked in the direction of the gas plume expelled by the ACS during sensor stepping to change the roll rate but only on the seven rolls executed while the payload was in sunlight. It was not visible during the four rolls in the Earth's shadow. Furthermore, the spectral energy distribution of the artifacts was characteristic of a source much warmer than the Earth, such as sunlight. The only puzzle is that no upwelling infrared Earth radiation was seen reflected by the particles when the payload was in shadow. It should have been at least as bright at that from the Sun at wavelengths greater than about 8 μm .

Radiance from the residual atmosphere above the payload and a time dependent background that was ascribed to payload outgassing were also removed. However, the origin of these artifacts was uncertain and the methods used to correct them were open to interpretation, which made the uncertainty analysis difficult. The atmospheric emission appears below 240 km altitude and is manifested by the up-turn in radiance at the very end of the ELS and ZIP data. Since the last two ZIP rolls repeat the zodiacal geometry of previous rolls taken at much higher altitude that were, presumably, free of this interference, the radiance difference between these rolls is the atmospheric contamination. Symmetry arguments were used to extend the correction

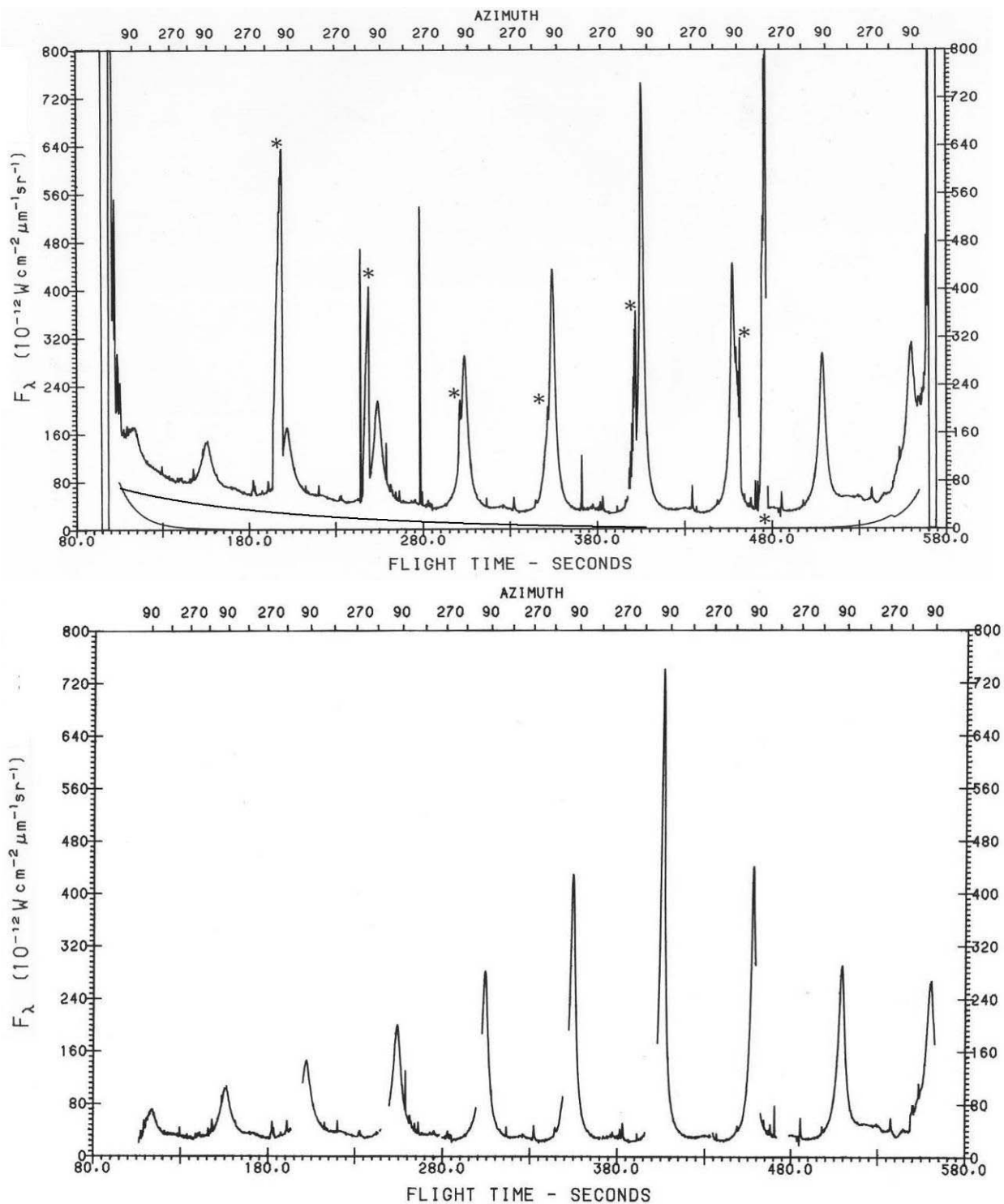


Figure 58. The ZIP 2 11 μm radiance measurements. The extraneous signals in the raw data in the top plot are also typical of the ZIP 1 and ELC (Section 5.9) observations. The curve with the long decay time is the effects of the purported payload outgassing while the shorter curves at the beginning and end are off-axis Earth radiation plus emission from the residual atmosphere. The asterisks denote optical contamination that has been interactively removed. The data after removing extraneous sources of interference are shown at the bottom.

to the first roll. The up-turn in the ELS and ZIP filters that contain the $\sim 5.5 \mu\text{m}$ atmospheric NO molecular band is much more pronounced, in agreement with expectations; Matsumoto, Akiba and Murakami (1988) clearly see NO emission above their experiment at an altitude of 300 km. On the other hand, the scale heights derived from the ZIP data for the purported atmospheric emission are about twice as large as atmospheric emission models predict.

More problematic was ascribing the origin of the background with the long time constant at the beginning of the experiment in Figure 58. Price (1988b) speculated that this effect was either due to outgassing from the payload or dielectric relaxation after the detectors were saturated by being exposed to very high backgrounds during cover removal and sensor deployment. Since the payload outgassing correction was subtractive but that for dielectric relaxation was multiplicative, the choice of phenomenon had a profound influence on the final results. We chose a subtractive correction derived by fitting a low order analytic curve that flattened the radiance profiles such that the minimum zodiacal radiance measured for each scan ‘made sense’. Support for outgassing as the cause came from Army infrared experiments that detected elevated radiances that seemed to be due to payload outgassing based on the fact that the attitude control system gas appeared to ‘punch holes’ in this background. Also such interference appears to have been the bane of most, if not all, of the Japanese infrared probe-rocket experiments (e.g. Matsuura, et al., 1994). It was also known that the attitude control system gas could create an elevated pressure in the vicinity of the payload if expelled rapidly enough. This happened on the second HI STAR South flight when the power inverter on the attitude control system failed, opening all the control valves and venting the gas rapidly enough that the pressure gauge in the sensor cap measured a perceptible gaseous environment. For the BMP experiments, about half of the ACS gas was expelled in the maneuver to invert the payloads to the initial position to acquire the pole star. These facts argue that the time-decreasing extraneous background is near field contamination, the radiance of which we estimated and subtracted from the bottom plot in Figure 58.

Don Smith (1989) searched the data from several rocket-based infrared atmospheric experiments for extraneous signals above 100 km tangent height and concluded that the data were contaminated with off-axis Earth radiation. Smith estimated that the in-flight off-axis rejection of the sensors that he examined had been degraded by a factor of 35 compared to pristine conditions in the laboratory. This finding was consistent with the degradation of the ZIP 2 telescope measured by Wong, Wang and Murdock (1980) after the instrument was stored for a period of time. However, Smith’s interpretation that the excess that we label as ‘atmospheric contamination’ on the ZIP experiments was due to off-axis from the Earth is highly problematic as the ZIP lines of sight were always much greater than the baffle angle. Even if we assume that the ZIP off-axis rejection was degraded by a factor of 40, the off-axis contribution from the Earth would be a few percent of the minimum measured zodiacal background (Burdick et al., 1994).

The $11 \mu\text{m}$ profiles in Figures 38, 40 and 58 were the first large scale sampling of the thermal emission from the zodiacal cloud and initially defined the overall geometry of this background. Although the absolute radiances were correct within the estimated errors, the major scientific payoff, absolute spectral radiances from the zodiacal dust cloud, remained tantalizingly elusive. This was despite over a decade of trying to extract the information with a reliable error analysis and small enough uncertainties that definitive conclusions could be drawn (Murdock and Price, 1985; Rickard, Stemwedel and Price, 1991; Burdick et al., 1994).

The zodiacal radiances measured in the broad $11 \mu\text{m}$ and $25 \mu\text{m}$ bands by ZIP and ELS are compared to other observations in Figure 59 along with a physical model described by Noah

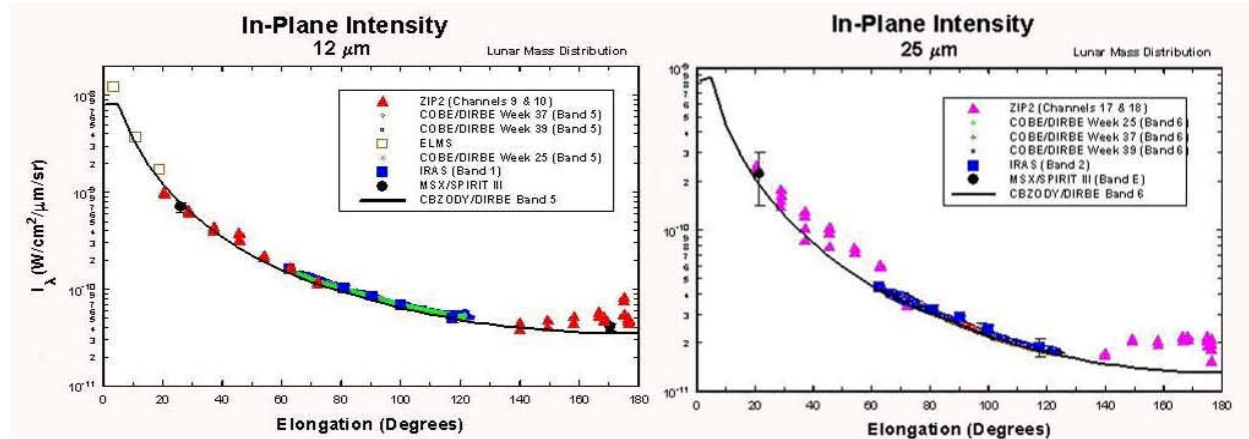


Figure 59. A comparison of the various infrared measurements of the zodiacal radiance along the ecliptic plane at $\sim 12 \mu\text{m}$ (left) and $25 \mu\text{m}$ (right).

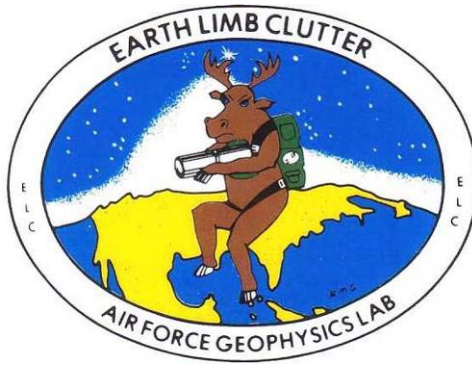
and Noah (2001a). Generally the agreement is reasonable on this logarithmic scale although the longer wavelength ZIP 2 results tend to be higher than other experiments.

5.9. Earth Limb Clutter

In 1981, we negotiated with Space Division for additional BMP flights to investigate one of the remaining surveillance system uncertainties: the amount of structure, if any, in the emission of the quiescent atmosphere. The photon noise from atmospheric emission and the off-axis radiation from the Earth limit the sensitivity of the system and reduce the dynamic range when a sensor looks into the Earth limb. These problems can be overcome, but another arises, namely

that the structure in the atmospheric emission can create a form of clutter noise to compromise system performance. At the time, AFGL Radiation Effects Branch was conducting experiments such as the spring 1986 flight of the Spectral Infrared Interferometric Telescope (SPIRIT 1; Smith et al., 1991), to measure the aurorally disturbed atmosphere. Aurorae and other unusual atmospheric structures, such as the polar mesospheric clouds shown in Figure 60, were known to be a source of clutter noise for a system but it was not uncertain as to whether the unperturbed or quiescent atmosphere also had structure. We proposed to modify the ZIP I sensor to find out.

The last BMP flight, the Earth Limb Clutter (ELC) experiment was flown in October 1983. The significant modifications to the ZIP 1 sensor for the ELC experiment were to reduce the detector instantaneous fields-of-view to 1×1 mrad and to use a new set of 5 to $30 \mu\text{m}$ filters; the four corner focal plane detector modules had filters centered on the $15 \mu\text{m}$ CO_2 band in order to measure small scale structure in the emission from this important atmospheric constituent. The experimental profile had the sensor deployed to 90° , perpendicular to the longitudinal axis of the payload, throughout the experiment while the attitude control system maneuvered the payload to perform the observations. An initial 60 second, 430° roll scanned the sky at a 90° local zenith angle. Then, a sequence of maneuvers was executed in which the sensor alternatively stared at a fixed point in the atmosphere or executed several $\sim 12^\circ$ long back-and-forth scans at various tangent heights looking either north or at the terminator crossing. Toward



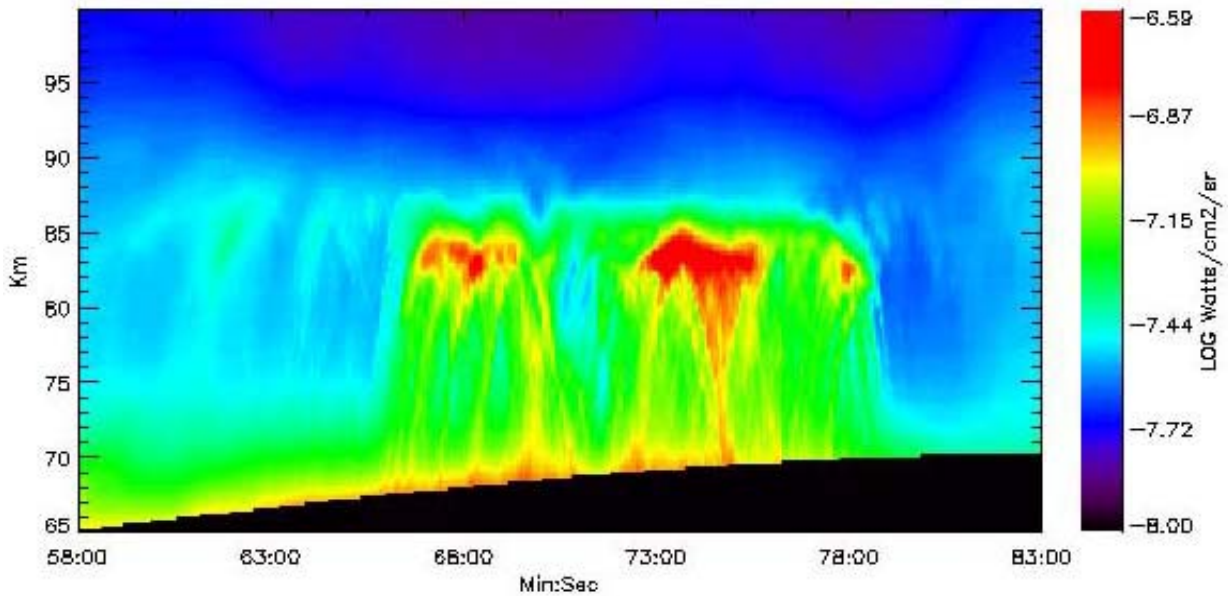


Figure 60. Polar Mesospheric Clouds observed by MSX. These thin, high altitude clouds form in the Polar Regions during the summer and are also called noctilucent clouds when observed in the visible. The sensor is saturated in the black region at the bottom of the image, which is $\sim 2^\circ$ above the edge of the Earth. The height of the image is 1° ; the tangent height is designated on the y-axis. The Figure is adapted from O’Neil, et al. (2008).

the end of the experiment the payload was rotated to lie on its side to observe a ‘half slice’ of atmosphere as the payload fell through it.

ELC also obtained zodiacal measurements simultaneously in the visible with the star mapper and in the infrared from the sensor during the initial roll. The roll covered 430° in azimuth and scanned nearly perpendicular to the ecliptic plane, coming within 19° from the Sun. Since the ELC detector solid angles were ~ 5 times smaller than those used in ZIP and the chopping frequency was about 4 times higher, the ELC radiance sensitivity was about 10 times less than for the ZIP experiments. The same extraneous interferences observed on the initial rolls of the ZIP flights (top plot of Figure 58) were also seen. Cobb, Burdick and Murdock (1993) attempted to calibrate the ELC response on the long scan against the IRAS measurement at the South Ecliptic Pole and found that, for the most part, the ELC $11\text{ }\mu\text{m}$ and $26\text{ }\mu\text{m}$ results made sense, but the values at other wavelengths are discrepant by up to a factor two.

5.10. Detector Non-Linear Responses

Monolithic (single crystal) extrinsic photoconductors, such as the ones used on the AFCRL/AFGL experiments, exhibit a variety of non-linear effects when operated under low background conditions. Except for SPICE and ZIP, the AFCRL/AFGL experiments had transverse biased detectors that, as discussed by Arrington et al. (1976), were subject to non-uniformity of response over their surfaces. Sayre et al. (1976) also found that the spectral response, and hence the total response, of such a detector depended on how its surface area was masked. This is most certainly the explanation as to why the amplitude and shape of the point source signals measured by Super HI STAR were different between the up and down scans (Figure 2 in Pelzmann, 1978a).

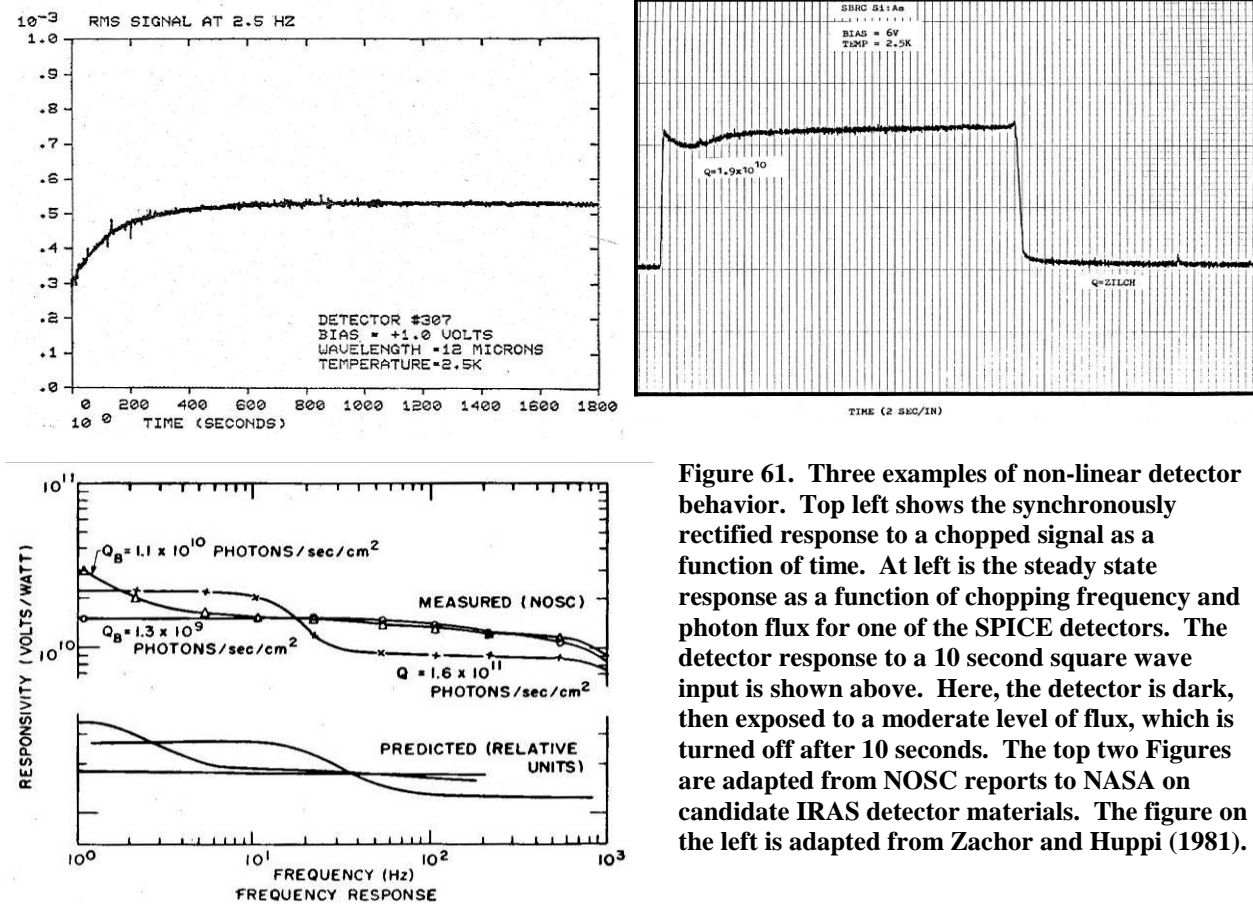


Figure 61. Three examples of non-linear detector behavior. Top left shows the synchronously rectified response to a chopped signal as a function of time. At left is the steady state response as a function of chopping frequency and photon flux for one of the SPICE detectors. The detector response to a 10 second square wave input is shown above. Here, the detector is dark, then exposed to a moderate level of flux, which is turned off after 10 seconds. The top two Figures are adapted from NOSC reports to NASA on candidate IRAS detector materials. The figure on the left is adapted from Zachor and Huppi (1981).

More serious was that the monolithic detector response is non-linear with multiple time constants in which the gain and time constants depend on the background flux on the detector. The general characteristics of these effects are displayed in Figure 61 while additional examples may be found in Arrington and Eisenmann (1977). The top left plot in Figure 61 shows the rectified signal from a constant flux modulated at 2.5 Hz from the moment of exposure in which the rectified signal increases with time to an asymptotic value almost twice as large as the initial response. The top right plot displays the time history of the response to a sudden change in the input flux level. Instead of a linear flat response, the actual output jumps to an initial value, called the photoconductive gain, after which a 'hook' in the response with time is often observed. The response then slowly increases, asymptotically approaching a steady state gain that depends on the bias and absolute flux level. Finally, the frequency response for a typical SPICE detector is shown in the lower left. The SPICE detector bias was set to be as high as possible for the maximum photoconductive gain, which resulted in a steady state gain several times larger than the instantaneous gain. IRAS applied a smaller detector bias, which reduced the detector non-linearities to a steady state value of only about 25% above the photoconductive gain (*IRAS Explanatory Supplement*, 1986) but at the cost of lower responsivity and sensitivity.

The response peculiarities shown in Figure 61 arise from dielectric relaxation within the material, recombination trapping, charge carrier sweep out, contact effects and how the bias and ground contacts are made with the detector. Dielectric relaxation results in a high responsivity at

low frequency and a low responsivity at high frequency, as shown for the SPICE detector. The frequencies at which the transition between the different response characteristics occur is related to the electrical conductivity of the detector that, in turn, depends on the bias voltage, the background photon flux and the detector operating temperature. Blouke et al. (1972) made an early attempt to characterize these effects with a simple transfer function with three (background dependent) characteristic time constants that were empirically determined by fitting the response vs. frequency measurements. Zachor and Huppi (1981) and Zachor et al. (1982) attempted a system identification analysis to derive analytic expression for the time and frequency non-linear response for the SPICE detectors, with limited success. Sclar (1983) describes the general behavior of extrinsic photoconductors, reviews the various detector effects and provides a simple empirical formula to describe the non-linearities. These attempts to analytically represent the response were doomed to failure because, as shown in the upper right plot in the Figure, the response to increasing flux is different than that for decreasing flux; specifically, removing the flux results in an instantaneous decline that is followed by a long decay in the signal without the hook response. As Fouks (1993) noted, this means that the system transfer functions of the detector response as a function of time or frequency and the resulting analytic expressions derived to represent them are different for increasing flux as compared to decreasing flux onto the detector. Fouks constructed a detailed analytic model for the detector response to a step or off – on function. This model is not exact as it was obtained by assuming that a number of ‘second order’ expressions may be neglected (Fouks, 1993) and, consequently, is an approximation to the true detector response. Coulais and Abergel (2000) translated the Fouks steady state model into a dynamic one with incremental steps. Over the years a rich literature has been published that describes, analyzes and models these effects but, as Dutch Stapelbroek (private communication) from the Rockwell Detector Lab. observed, there are so many variables to the problem that the solution has to be tailored for the specific detector and application.

The photometry in the survey catalogs is little affected by these non-linearities as the high pass filter used for the celestial survey experiments to remove the extended background also eliminated the low frequency gain effects. Since the linear scan rates across the focal planes were held roughly constant, the frequency content of the point source measurements remained about the same for a given experiment. Under a given set of operating conditions, the sensor responses were remarkably repeatable. For example, the HI STAR and, separately, the HI STAR South, detector responses to the internal stimulators varied by less than 2% during an experiment and from flight to flight. These stimulators were exercised when the roll rate was changed and the shutter closed. Price (1978b) and Price and Walker (1978) had also shown that the external sensor calibrations were quite consistent. The in-flight calibration of the survey instruments against stars had a standard deviation of $\sim 10\%$ and agreed well with AEDC ground chamber measurements. The questions, therefore, were what was the influence of the non-linear effects on the low frequency restoration of the zodiacal measurements and the maps of the Galactic plane and how much does the steady-state gain differ from the (point source) photoconductive gain upon which the AFCRL/AFGL survey instruments were calibrated?

Price (1981) conservatively estimated that the HI STAR + HI STAR South Galactic plane radiance maps were accurate to within a factor of two. Subsequently, Price, Marcotte and Murdock (1982) reduced the uncertainty and recommended that their previously published zodiacal dust cloud radiances be decreased by a factor of two, which was the difference between the restored HI STAR South radiances and the ZIP measurements. In retrospect, the non-linear distortions in the Galactic plane measurements were either removed as low frequency noise, as

would have happened to the low frequency tails quantified by Deul and Walker (1989) for the IRAS detectors, if they existed in the AFCRL/AFGL data, or absorbed in the error budget, as the restored radiances compare favorably with more recent independent distortion free measurements (Freudenreich, 1996, Price, et al., 2001).

The ELS, ZIP and ELC zodiacal observations were absolute measurements obtained by chopping the radiation on the detector then rectifying the signal. Thus, the signals were restricted to a narrow electronic bandpass centered on the chopping frequency and it would be reasonable to expect not to have to worry about the messy time response variations. This, unfortunately, was not the case. As may be seen for the SPICE detector, the responsivity decreases with increasing flux at the 45 and 100 Hz chop frequencies of ELS and ZIP, respectively, albeit at a focal plane photon flux of two to three orders of magnitude greater than what these sensors would see from the zodiacal background. However, such an effect may explain why the 45 Hz responsivity of some of the ELS detectors decreased by up to a factor of three when looking at a constant radiance for 20 minutes in the laboratory (Murdock, 1977), as shown in the upper left of Figure 61.

On the other hand, the ZIP detectors were saturated when the cover was removed and the sensor deployed. Since the change in responsivity is strongly influenced by the flux levels incident on the detectors immediately before the measurements, this saturation may explain the time dependent decay in the top plot of Figure 59. We assumed that this decay was an additive environmental background rather than a multiplicative response change. Likely both effects are present but there was inadequate information to separate them.

Not only does the overall detector responsivity depend on its operating temperature (e.g. Sargent, 1997) but, as Boisvert et al. (1992) has shown, the responsivity at longer wavelength changes more than that at shorter wavelengths. Except for the FIRSSE and ZIP 2 experiments, the focal plane temperatures were stable throughout the flight. Although the FIRSSE focal plane thermal excursions caused problems with the Ge:Ga and Ge:Be detectors, the silicon detectors were little affected as the temperature did not exceed 5K. However, when the ZIP 2 payload was sunlit, the focal plane temperature increased as the sensor stepped closer to the Sun, reaching a maximum of ~10K at which time the Si:Sb detectors exceeded their operating limit and turned off. The focal plane temperature declined as the sensor subsequently stepped away from the Sun. The response variations due to temperature changes were estimated from the differences between the measurements on the redundant rolls that covered the same zodiacal background obtained at different temperatures with one set in sunlight and the other in the Earth shadow. Burdick et al. (1994) attempted to account for this variation in their reprocessing of the data.

As Jamieson (1995) pointed out, a hardware fix for these problems was in the works. Beginning about 1980, the DoD funded a concerted development effort to harden infrared detectors to high energy radiation so that they could operate in an elevated gamma ray or enhanced particle environment from the Van Allen belts and the South Atlantic Anomaly. The detectors were made thinner and thinner to reduce their capture cross-section and, concurrently, doped more and more heavily to keep the infrared absorption and response of the material high. In this process, engineers at Rockwell developed blocked impurity band (BIB) conduction in Si:As detectors in 1979 (Stetson et al., 1986). Fortunately, not only are the aforementioned non-linearities considerably reduced in BIB detectors but the long wavelength responses of the detector were extended by 20 – 30%, a salubrious by-product for infrared astronomy. However, the non-linear responsivities still plague the Ge:Ga detectors that are still used in the far-infrared on current space missions, complicating the data processing for Spitzer and Akari.

5.11. Classification Issues

The classification guidelines that governed the early 1970 AFCRL background experiments were ambiguous except to state that enough information could not be revealed to enable the calculation of the inherent sensor performance. The classification guide⁹ allowed some of the experiment details to be presented, such as the spectral region, the scan geometry and the data processing algorithms but was vague regarding the measurements. We interpreted the guide to mean that nothing was to be revealed that would indicate the performance capability of the instrument, such as the details of the spectral response of the filters and the signal-to-noise of the observations. The IRAS feasibility study specifically pointed to these issues as hampering an independent assessment of the AFCRL catalog because the signal-to-noise of each observation was not given nor were the details of the area surveyed on each flight. This information was protected by the manner in which we provided the data and the variable signal-to-noise during the experiments despite the careful analysis of Grasdalen et al. (1983) in which they derived the 4, 11, and 20 μm magnitudes to which the catalog is complete.

The ambiguous classification of the background measurements was removed in the guide that covered the BMP program¹⁰, which specified that data from the BMP experiments were to be classified. However, the rationale for the SAMSO classification guidelines was not universally held. Captains Stears and Kiya felt as we did, that you should not and could not classify nature. Indeed, Mike Kiya had some heated discussions with Major Curtis, the SAMSO program manager, on this topic but to no avail.

SAMSO indicated that it had choices with regard to restricting information on the performance capabilities of the sensors. Either the hardware could be classified, which would be expensive, or the measurements taken with the sensors were to be classified. SAMSO emphatically chose the latter, less expensive alternative. Col. R.G. Dingman, Assistant Program Director, Space Defense System Programs, stated the SAMSO position in a 1 December 1978 letter to us that *“The present guidelines serve to protect the very significant investment this country has made to date in LWIR technology. ... By openly publishing the IRB data and analysis we are, in fact, presenting the specific operating requirements and inferring the capabilities of future military hardware.”* (IRB was the initial name for the BMP.)

The security restrictions upset some in the civilian community; the key issue seemed to be access to extrinsic silicon detectors. For example at the IRAS community meeting held on the second evening of the June 1976 *Infrared and Submillimeter Astronomy Symposium* in Philadelphia, Susan Kleinmann expressed a concern that the program not be delayed because the proposed detectors for IRAS might be embargoed by the DoD. A prominent Dutch astronomer sitting in the front row responded by getting down on his hands and knees and pounding the floor while loudly proclaiming that IRAS hardware and technology was not and could not be classified by international agreement. Dave Allen (1977) focused his frustrations on the accessibility of the technology, petulantly writing: *“Developments now occur in military laboratories whence they are inclined to leak only when some ageing General has been persuaded that further developments have made them obsolete or that the enemy already has one. One of the most*

⁹ SAMSO Security Classification Guide Advanced Surveillance Technology PE 63424F Project A issued by SAMSO dated December 1972 and modified by change letters #1 of 11 June 1973 and #2 of 15 January 1974

¹⁰ Space Defense System Program (SDSP) Security Classification Guide, dated March 1979 plus letter change #2 dated 29 September 1980

infuriating things to an infrared astronomer is to know that a detector far better than he has access to is orbiting the Earth attached to a large optical telescope looking downward!"

The detector issue was confounding to the DoD as well. Early in the IRAS program, Dr. Eisenmann at Naval Oceans Systems Center (NOSC – the organization responsible for testing focal plane technology for the DoD at the time) requested guidance on how to handle the detectors that NASA was sending him to test. NASA specified that the detectors and results be treated as unclassified, which was a problem because Eisenmann was well aware that some of these devices, such as the Rockwell SPICE detectors, were taken from the same boule and wafer as those used in classified DoD programs. Drs. Eisenmann, Walker (AFGL) and Shivanandan (NRL), Mr. Brockway (Office of the Under-Secretary of Defense for Research and Engineering – OUSDRE) and representatives from NASA met in Washington DC and decided that NASA would have access to discrete extrinsic silicon detector technology for the IRAS focal plane only. Even then, the issue wasn't that simple. In early 1978, I forwarded Frank Low's requested that we provide him samples of the SPICE detectors for him to test on behalf of SIRTF to Jim Higgens, our AFGL liaison with SAMSO, since SPICE hardware was covered by the SAMSO security guide. Although Low had a security clearance, he was unable to obtain the detectors because, as Jim Higgens stated in his letter to Major Curtis (SAMSO) dated 2 March 1978, he could not comply with the AF security guidelines in force at the time regarding the physical security of the detectors. Thus, NASA's successful negotiations with the Air Force provided US astronomers with unclassified but conditional access to the detectors a short time later¹¹.

This background is lost to some of the IRAS participants. George Rieke (2006) stated that in regard to the IRAS mid-infrared detectors that "...*the potential military contribution has been overestimated*," likely a reference to the fact that JPL had to rework the inoperative focal plane delivered by Rockwell, a major DoD systems company. The fact was that the doped silicon detectors chosen by IRAS for their sensitivity were developed by the military and access to them was restricted at the time, with IRAS the singular exception. Otherwise, IRAS would have had to use the commercially available extrinsic Germanium detectors that, besides exhibiting all the non-linear effects discussed above, had much lower quantum efficiencies and, hence, were correspondingly less sensitive than the extrinsic silicon detectors.

Also, few in the civilian community that we dealt with either understood or appreciated the restrictions that classification placed upon us and the labyrinthine procedures needed to change those restrictions. Or they felt that the restrictions only applied those in the DoD and not to them. For example, Frank Low offered to publish the CMP catalog results under his name if only we at AFGL would get the data unclassified. We actually indirectly provided the rationale for declassifying the CMP data in several letters to SAMSO that corrected numerical mistakes in their draft classification guide and explained why it made sense to set a brightness measurement level above which the natural backgrounds would be unclassified. Col R.G. Dingman, SAMSO, responding to a formal 12 October 1978 NASA letter of request, submitted a recommendation through appropriate Air Force channels to declassify the CMP report that listed the LWIR measurements, but with qualifications. A 29 September 1980 letter change #2 from Mr. E. Yokum, the SAMSO Security Chief, directed revision of the security guide such that the CMP measurements brighter than $10^{-16} \text{ W cm}^{-2} \mu\text{m}^{-1}$, the value we had originally suggested, were unclassified. As far as I know the CMP data were never published in the open literature; the only reference I could find as to their use was Pelzmann (1978b) who describes the algorithms

¹¹ Letters to Mr. Myron W. Krueger, NASA, Hq dated 6 Mar 1978 from R.N. Williams, Rear Admiral, US Navy, and from BG D.A Vogt, Military Assistant , Strategic and Space Systems dated 25 Jan 1980.

that he (Pelzmann, 1978c) applied to the CMP data as a demonstration of the NASA ARC capability to process satellite-based infrared survey data and to estimate the magnitude of the IRAS processing task. These effort occurred before the data were formally declassified.

Illogically, the same change letter maintained the classification of the BMP calibrated data at any flux level. The guide did except data obtained by the two far-infrared FIRSSE bands as the Air Force had no interest in these wavelengths and permitted the shorter wavelength observations to be included for those sources detected in the far-infrared. In practical terms, the guide permitted us to publish the far-infrared catalog of Price, Murdock and Shivanandan (1983), the analysis of the brightest far-infrared sources by Price et al. (1983) and the FIRSSE far-infrared measurements of asteroids (LeVan and Price, 1984); all other BMP measurements were classified. The single concession in the guide was the adjective ‘calibrated.’ We could process the data in telemetry counts in an unclassified environment at considerable less hassle but the results became classified when the calibration was applied. Classification of the BMP observations was also an access issue for people within the Air Force and NASA. For example, Howard Stears, who was then at USAF Headquarters, invited us to present the BMP results to the April 1981 SPIE *Infrared Astronomy – Scientific/Military Thrusts & Instrumentation* meeting that he co-chaired with Nancy Boggess from NASA Headquarters. We described the SPICE and FIRSSE experiments, which were yet to be flown. Howard was disappointed that we did not present some ZIP I results from the experiment that was flown the previous summer, as the zodiacal background was an important topic for IRAS. I pointed out that BMP results were still classified, which he found just as illogical as he did when he was at SAMSO.

We began petitioning Space Division in October of 1982 to change the classification guide to allow us to publish the astronomy results since the Infrared Astronomical Satellite was in orbit and its performance far surpassed that of the BMP experiments. It took until summer of the following year before Maj. Gen. Randolph, Vice Commander Space Division, signed out the official change letter dated 12 August 1983 that allowing us to publish. In anticipation of the approval we submitted the *Revised AFGL Catalog* (Price and Murdock, 1983) for internal editing on 14 June 1983 knowing that formal approval would be forthcoming before publication. This change guide also declassified the previously classified BMP reports. Abiding by the classification guidelines was (and is) an obligation we had because we were employed by the DoD, which gave us access to cutting-edge technology with which to do our experiments.

5.12. Personal Perspective on the Background Measurements Program

The problems with the HI STAR data and the effort to restore the low frequency information convinced me that I had to thoroughly understand how the instrument distorted information in the process of converting the incoming photons into recorded electronic signals to properly reduce and analyze the data. This required understanding the sensor with a detailed knowledge of the instrument transfer function that could only be gained from the data and the in-flight calibration with help from ground characterization. The sensor performance projected during various design reviews were mere idealizations and verification of, or improvement upon, the manufacturer’s performance claims was essential. Furthermore, a full explanation of how the data was reduced is needed since a number of ‘discoveries’ have been traced to instrument or processing artifacts. Above all else, the derived results had to make physical sense.

Since data processing has been facilitated over the years by a number of generic routines that have been coded and made generally available such as those in *Numerical Recipes* (Press et al, 2007) and the open source Image Reduction and Analysis Facility (IRAF), algorithms, routine

processing may now be taken from these resources rather than having to be coded for each experiment. Also, data processing architectures such as the interface description language (IDL) make concatenating standard routines straightforward. However, a thorough understanding of the sensor performance is still needed to select the most appropriate routines for the processing and, above all else, the derived results have to make physical sense. The ZIP and ELC processing demonstrated the pitfalls of applying standard routines in an uninformed fashion.

At the time of the ZIP flights, Len Marcotte, our single government in-house analyst who helped to reduce and process the celestial survey data, was working full time on deconvolving the celestial data to produce the large scale Galactic plane and Zodiacal maps. Thus, we needed to augment our data processing capability for the ZIP experiments. The central computer site had several contracts with local institutions that could be tapped to support data processing and analysis, which most AFGL experimental programs did. A Boston College contractor determined the payload position and pointing for ZIP and ELC and another group reduced data. The premium for the contractors was to obtain results quickly, which kept the costs down, and standard routines were applied with little or no validation of the results. For example, sixth and seventh order polynomials were derived for the altitude, latitude and longitude solutions, a bit of overkill as we had previously found that a fourth order was adequate to accurately represent the trajectory. Inexplicably, the Boston College analyst used one polynomial solution for the ascent and a different one for the descent with unrealistic discontinuities in position, velocity and acceleration at apogee.

More problematic was how the ZIP and ELC sensor data was processed. Rather than synchronously rectifying the data using the phase signal from the chopper monitor channel, which would have required some algorithm development and coding, the contractor took the expedient of applying a quadrature demodulation routine, a standard numerical analysis technique when phase information is absent. However, the procedure introduces a small bias in the rectified signal by including the noise power that lies within the narrow bandwidth centered on the chop frequency, which is eliminated by destructive interference when the noise is synchronously rectified. Although a small contribution to the minimum signal measured during the experiment, the bias was known to exist, its magnitude could be estimated and a correction applied to the results. It took a step-by-step written description to convince the contractor analyst that the bias did indeed exist in the asynchronously demodulated data.

Archiving the step-by-step development that detailed this analysis proved to be useful as it was resurrected almost decade later for the Space Dynamics Laboratory's (SDL) calibration of the SPIRIT III non-linear response. SDL had developed a clever laboratory calibration scheme in which they flooded the focal plane with various known radiance levels that spanned the dynamic range of the instrument while adding a small modulated beam of constant known flux to this background radiance. SDL used quadrature demodulation to rectify the chopped signal while cancelling the background. Since the modulated flux was kept constant for all background levels, the measured decrease of the rectified signal with increasing background calibrated the non-linear response, *but* only after SDL properly included a noise bias estimate.

The contractor who reduced the ZIP and ELC data also seemed to be unfamiliar with the phenomenology being measured and made use of standard data processing resources without trying to make physical sense of the results. Because of the experiment profile, ELC did away with the star tracker and substituted rate integrating gyroscopes for accurate positions. The ELC pointing solutions were derived by turning the numerical crank on the attitude quaternions using the calibration values supplied by the gyroscope manufacturer. The rate integrating gyro

solutions were reinitialized with episodic reference to stellar observations by the star mapper to correct the accumulated errors in the aspect solution. The result was segmented position solutions with physically unreasonable instantaneous position jumps between the segments. Even with this artifice, the positional errors were large enough as to compromise the interpretation of the atmospheric measurements.

After our Space Division BMP managers expressed dismay over our lack of progress on the ELC analysis at a meeting in Los Angeles nine months after the flight, Len Marcotte and I tackled the ELC aspect problem to try to resolve the major stumbling block in the analysis: accurate positions. The star mapper had detected stars during the initial 430° long roll but only episodically during the back-and-forth scans after that. We, therefore, derived independent star mapper position solutions for the initial long roll and the short above the horizon scans. These solutions were independent because we had no way of connecting them without using the quaternion solution that we were trying to calibrate. Using the star mapper derived solutions as truth revealed several discrepancies in the quaternion solution; the most significant was the presence of at least one error in the calibration parameters programmed into the attitude control computer, which was quite serious as that computer directed the payload maneuvers. When the rate integrating gyros were calibrated on the ground, they were subject to torque from gravitational acceleration that is absent during the flight. A correction factor was calculated for this torque and programmed into the attitude control system but, as it turned out, with the incorrect sign; instead of cancelling the torque term, the on-board computer doubled the error. We discovered this by comparing the gyro positions during the short scans, which said that the same field-of-regard was repeatedly scanned, with the star mapper solutions, which clearly showed that the field-of-regard systematically shifted westward with time. Agreement was achieved by subtracting twice the torque parameter programmed into the system.

Also, it was found that one of the attitude control system roll jets had developed a small leak that accelerated the payload about the roll axis contrary to what was assumed. Since ZIP 2 and ELC used the same payload and attitude control system, we were able to back-track to find that the leak first manifested itself in the middle of the ZIP 2 experiment. Ordinarily, the payload was accelerated to the programmed rate then the limits, or dead band, to which the roll rate was constrained were relaxed to permit the payload to freely rotate. The leak pushed the roll rate to the dead band limit, which meant that free body rotation no longer applied. Accounting for these problems improved the aspect solution considerably, although a complete and consistent quaternion attitude solution was never achieved and some segmentation was still required. The scans and stares into the Earth limb for which star mapper data were not available were updated using the 15 μm CO₂ measurements for horizon sensing. After a considerable processing, a negative result was derived for the basic experiment objective: no structure or clutter was measured in the quiescent Earth Limb.

With regard to the technical developments of the program, it has always been a puzzle to me as to why Rockwell apparently failed to capitalize on their technical advances. SAMSO had accepted the Hughes proposal to retrofit their HI HI STAR instrument for SIRE even though Hughes had failed to deliver an instrument for us to fly. The internal cryogen lines of the Hughes sensor were made of the wrong grade of aluminum and leaked like a sieve because cracks were created at every bend. Thus, the internal plumbing had to be replaced as well as most of the optics, a much bigger and more expensive set of tasks than refurbishing the Rockwell instrument that had relatively minor damage from the HI HI STAR recovery. The reasons, according to Mike Kiya (12 December 2003 e-mail) and Howard Stears (15 December 2003 e-

mail), were that the Hughes proposal was technically superior to that from Rockwell and Hughes had demonstrated space-borne cryocoolers experience with CMP. Rockwell did not play to their strength in that their Seal Beach division submitted the HYSAT proposal, whereas the Anaheim group, having built the HI HI STAR instrument, was much more experienced with space qualified sensors. The recollection of John Heintz (27 August 2009 e-mail), a senior Hughes program manager at the time, is consistent with this: namely, that the Hughes HYSAT LIWR utility study that demonstrated the value of space based LWIR and the CMP success was the justification to get SIRE into the SAMSO budget and to expedite the SIRE competition. .

Rockwell also made significant technical advances in developing infrared detectors but seemed not to capitalize on them. The rapid spread of extrinsic silicon detector technology was understandable as Soref (1968) originally investigated the material and Rockwell engineers presented enough information at a SPIE meeting on Infrared Devices in Hawaii about their BIB detector development to allow others to follow their trail. However, Rockwell management failed to capitalize on the company's advantages in detectors during the brief windows of opportunity. As Dave Pollock (6 March 2002 e-mail) puts it "*While* " Rockwell "*had some great scientists and engineers they never seem to be well applied to the tasks to be accomplished.*" Dave Pollack and Lou DeBottari, two senior Rockwell engineers who worked on cryogenic cooled sensors, also indicated that Rockwell seldom coordinated well across division lines when proposing and executing the major infrared programs, whereas the Hughes corporate culture was such that successfully completing the job transcended division boundaries.

Although the BMP and MSMP shared the cost of development of the separation and recovery systems, they were distinctly different programs at AFGL with separate SAMSO/SD program managers. Capt. Kiya and Stears were very supportive and had a genuine interest in the success of the BMP flights. They were also technically quite knowledgeable and we could discuss with them, or argue as the case may be, the merits of what we proposed to do. Maj. Weppner, the MSMP program manager, was more of a manager and did not see much distinction between AFGL programs. Indeed, one day he called me into his office as I walked by on one of my SAMSO visits to query me about the progress Al McIntyre, the MSMP program manager, was making resolving the latest MSMP problem. Maj. Weppner was quite dissatisfied with my answer that I didn't know because MSMP was a different program run by a different Branch on different floors. In his eyes, we were all AFGL PIs and should know what going on.

On the other hand, Maj. Weppner did have his hands full with Al McIntyre who was a superb spin meister. For example, Al had initially estimated the success of the November 1977 TEM-1 flight at much less than 50%. The success grew as the pointing knowledge improved and the sources of measured emissions, such as the ARIES exhaust, could be identified. Al's final assessment was that the experiment was almost a complete success, despite not accomplishing the basic mission of measuring the TEM rocket plume. Naturally, such flexibility comes in for some ribbing. On TEM-2, the separation system was pressurized in the gantry during the t-3 day live test of the experiment but the timer was delayed by several minutes so as to not separate during this flight simulation. Unfortunately, someone forgot to shut off the timer, the Marmon clamp was released in due course and the airbag separation system kicked the MSMP payload up by 4" – 6". By great good fortune, no one was on the ARIES scaffold at the separation level when this happened. Given Al's propensity for hyperbole as to the success of the first MSMP experiment, we dubbed this event as the lowest altitude MSMP flight. True to form, Al calculated an 86% success because this was a successful field test of the separation system. Al did go on to fly a successful TEM-2 (see Figure 4) in 1980 and TEM-3 in 1982.

6. FROM ROCKETS TO SATELLITES

Soifer and Pipher (1978) reviewed the improving infrared astronomical instrumentation and observing techniques during the 1970s. With these advances came a corresponding increase in the observational database both in terms of the number of sources observed in the infrared and in the accuracy and finesse of the measurements. The general progress may be seen by contrasting the initial assessments of the field by Webbink and Jeffers (1969) and Neugebauer, Becklin and Hyland (1971) with those later in the decade: Stein (1975), Allen (1975, 1977) and Beckman and Moorwood (1979). Each review reflects the authors' view of what were the important milestones and I highlight mine in this section.

First, a basis was needed to determine what was normal and what was unusual. Thus, systematic studies of the infrared characteristics of known astronomical sources were carried out to ascertain their infrared properties. By the end of the 1960s, Johnson and his colleagues established the broad-band radiometric properties of stars as a function of their spectral type and luminosity class. Ed Ney's group at the University of Minnesota, primarily Bob Gehrz, Mike Merrill and John Hackwell, with lesser contributions by Dave Allen and Martin Cohen, refined the infrared characterization of stars begun by Johnson et al. with intermediate band photometry. They also measured rarer objects such as Wolf-Rayet stars. Infrared observations of H II emission regions, reflection and planetary nebula and galaxies also appeared the literature.

Of course, the reddest and most unusual sources in the TMSS and the AFCRL/AFGL catalogs came in for scrutiny, both to determine their individual infrared characteristics and to look for similarities among the sources in order to categorize them. Red stars dominate the bright near-infrared sky with more than two-thirds of the TMSS sources being cool M, S or C stars with the mode in the spectral type distribution at M5; half the objects are M3 – M 7 giant stars ($T_{\text{eff}} \sim 3500 \pm 200\text{K}$). The survey observation of the heavily reddened cluster in Ara by Price (1968) highlighted the relative transparency of the interstellar dust in the infrared. Since many of the reddest TMSS objects, sources with $I-K > 3.6$ – the difference in the $0.9 \mu\text{m}$ TMSS I band and $2.2 \mu\text{m}$ K band magnitudes – tend to be intrinsically very bright late spectral type giant and supergiant stars that are reddened by interstellar extinction, these objects are valuable near-infrared probes of Galactic structure (Mikami and Ishida, 1981). Although the preferential detection of cooler objects by the TMSS was anticipated, if not their actual numbers, it was the reddest sources ($I-K \sim 7.5$) that indicated something previously unobserved, stars within circumstellar dust shells. Among the brightest AFCRL/AFGL mid-infrared sources were even redder classical Mira variable stars with circumstellar shells and pre-planetary and bipolar nebulae. The mid-infrared catalog also contains a proportionally larger fraction of very red, dusty carbon stars compared to the TMSS results.

Infrared emission from dust was found to be ubiquitous: surrounding stars, in H II regions and other locations of on-going or recent star formation such as molecular clouds and active galaxies as well as in planetary nebulae and interstellar dust. And, the dust has different mineralogies. Woolf and Ney (1969) noted the spectral signature of silicate material in their infrared spectroscopy of the dust in the circumstellar shells of cool oxygen-rich stars. Subsequently, Maas, Ney and Woolf (1970) drew attention to the similarity in the emission spectra of the dust in comet Bennet with that in the μ Cep circumstellar dust and the absorption feature in the Orion Trapezium region. Forrest, Gillett and Stein (1975) concluded that emission by silicate dust was common in the circumstellar shells of oxygen rich, cool Mira variable stars. Carbon dust was also found: Treffers and Cohen (1971) detected the spectral signature of silicate

carbide in the shells of two very bright carbon stars while Forrest, Gillett and Stein (1975) observed a cool continuum beneath the silicate carbide feature that they attribute to graphite in a number of cool carbon variable stars. The emission features arise from circumstellar shells created by mass loss from the stars in which dust grains form in the gas flowing out of the stellar atmospheres at appropriate distances from the stars. The dust is heated by the stellar visible and ultraviolet radiation it absorbs and then radiates this absorbed energy in the infrared. If the mass losing star is oxygen rich, its circumstellar dust shell will have silicate features while carbon stars produce carbon rich dust shells.

The infrared spectra of planetary nebulae obtained by Gillett, Forrest and Merrill (1973) showed prominent mid-infrared lines from ionized Ne, Ar and S as well as fainter elemental lines, at least in the very bright mid-infrared source NGC 7027. The authors speculated that the 11.3 μm feature they detected may have been due to carbonate dust. However, this was but one of several ‘unidentified features’ found in this source; others are at 3.3, 3.4, 6.2 and 7.7 μm . Léger and Puget (1984) advanced the now widely accepted identification of polycyclic aromatic hydrocarbons (PAHs), very small grains of connected carbon ‘benzene’ rings with hydrogen atoms attached; Allamandola, Tielens and Barker (1985) called it ‘auto exhaust’. The excitation mechanism for these features is the same non-equilibrium process that Sellgren (1984) proposed to explain the very high, $\sim 1000\text{K}$, near-infrared continuum color temperature observed in reflection nebula in which very small grains absorb an ultraviolet photon, which warms the grain to a relatively high temperature because of the small number of internal energy states. The resulting near-infrared continuum is at a higher temperature than expected from thermal equilibrium. For the polycyclic aromatic hydrocarbons, the energy is partitioned among the vibration and rotation states and is re-emitted at the characteristic wavelengths of the unidentified features. When the Kuiper Airborne Observatory was put into service in February, 1974 (Gillespie, 1981), astronomers had an accessible platform above much of the atmospheric interference from which to obtain high quality mid-infrared spectra of these features.

An area not adequately covered in the aforementioned review articles was infrared measurements of airless solar system bodies. Allen (1970) presented an infrared method for determining asteroid sizes and used it to derive the diameter of 3 Vesta. The planetary community was initially skeptical of Allen’s results as they were $\sim 50\%$ larger than previous direct optical size measurements. However, direct measurements were difficult to make and soon additional infrared observations were found to support the larger asteroid diameters. Infrared diameters provided a powerful tool for resolving the ambiguity that arises when a visible measurement is used to estimate size; based on simple visible photometry one cannot distinguish between a small, bright object and a large dark one – the visible albedo (total fraction of incident sunlight reflected by the object) of asteroids varies by as much as a factor of 25. Allen’s determination was based upon a model of the thermal emission from the asteroid in which the asteroid diameter and albedo were derived from visible and infrared observations by fixing other parameters using reasonable assumptions about the physical properties of the asteroid. Jones and Morrison (1974) added their own refinements, while Lebofsky et al. (1986) created the “Standard Thermal Model” against which other modeling results are usually compared. The radiometric diameters of more than 200 asteroids had been estimated from infrared photometry by the end of the decade (e.g. Morrison, 1977).

Murdock (1974) published a superb set of infrared phase curves for Mercury, vastly improving on the work of Pettit and Nicholson (1936) four decades earlier. Pettit and Nicholson crudely measured Mercury’s radiometric phase curve by subtractive filtering through a cover

glass, a water cell and fluorite (Figure 6 shows the wavelength regions isolated by these filters). Murdock's measurements in 10 bands between 2.3 μm and 18 μm were of such quality and sampling density that the phase curves were well defined by the measurements themselves. The wavelength range was easily sufficient to separate the reflected near-infrared sunlight and the thermal emission from the day lit side and dark side of the planet. Murdock also measured the lunar phase curve and noted differences between Mercury and the Moon both in their respective phase curves and their reflected visible to near-infrared colors.

Thus, ground-based infrared observations provided insight into the physical processes for a wide variety of objects but the information available was incomplete on several accounts. For example, star forming regions in molecular clouds and H II regions were found to be intrinsically and apparently the brightest mid-infrared sources but the small fields of view required by ground-based systems seriously underestimated the flux. However, the instantaneous field of view of the AFCRL/AFGL survey detectors was large enough to measure the entire mid-infrared luminosity of these extended objects. Although the HI STAR/HI STAR South results created a small cottage industry of follow-up observation, characterization and discovery (pre-planetary nebulae: e.g. AFGL 2688, AFGL 618, and AFGL 2591) during the latter half of the 1970s, the TMSS and the HI STAR had a survey wavelength – sensitivity bias. For example, galaxies were found to be very luminous in the infrared, with the fluxes of many of the brightest peaking in the far infrared. The HI STAR survey tentatively detected only a single galaxy, M82, while HI STAR South, SPICE and FIRSSE detected a half dozen more, primarily due to the addition of the 27 μm band. What was needed was a survey to moderate sensitivity over a broad range of wavelengths that would observe a large enough sample of different types objects that meaningful statistical deductions could be made about their various observed properties, that is, the sample is large enough to classify the objects with criteria such as spectral energy distributions or color, luminosity, space distribution and the relationship of one distinctive group with another.

The value of such a survey was recognized by various science policy assessments. The National Academy of Sciences' Survey Committee's review of the status of astronomical facilities and research recommended investments for the 1970s that was published in the National Academy of Sciences (1973) decadal study for *Astronomy and Astrophysics for the 1970s*. Russ Walker was a member of the disciplinary panel that produced an *Infrared Astronomy* section for the report that contained a roadmap for developing infrared satellites, but placed such facilities as a third priority behind large aircraft and ground-based instruments, a balloon-borne 100 μm survey and high resolution spatial interferometer. One recommendation was to fly a small infrared astronomical satellite to survey the sky for which the subcommittee projected a two year development time at an estimated cost of \$20M. A second recommendation was to fly an Orbiting Astronomical Observatory class satellite with a cooled observatory style telescope at a projected developmental cost of \sim \$100M. Lyman Spitzer, Jr. (see Spitzer, 1960) is credited as a prime mover behind the Orbiting Astronomical Observatory concept, a series of fairly large astronomical spacecraft flown by NASA beginning in 1966. Within a year or so of the report, the observatory recommendation evolved into the Shuttle (later Space) Infrared Telescope Facility (SIRTF). The separate Space Astronomy panel gave a high priority to an infrared all sky survey from a small satellite and, recognizing the limited lifetime of expendable cryogens, concluded that several such satellites were needed to cover the sky with the ultimate goal being an infrared Large Space Telescope cooled with closed cycle refrigeration. Both the Infrared and Space Astronomy panels emphasized the need for significant technological development in order to build such instruments and both panels expressed concern regarding

environmental contamination due to particulates and airglow. Thus, the stage was set for a space-based all sky survey at much higher sensitivity and spatial resolution than the AFCRL/AFGL experiments.



6.1. The Infrared Astronomical Satellite (IRAS)

In late 1971, Gerry Neugebauer and others at Caltech requested that JPL study the mission requirements for a far-infrared satellite-based survey of the sky. The result was an unsuccessful May 1972 proposal to NASA for an Infrared Astronomical Satellite (Smith and Squibb, 1984). Two years later, NASA Headquarters issued Announcements of Opportunity 6 and 7 for an Explorer class astronomy mission on 15 July 1974. The response was overwhelming with 121 proposals submitted. Among the 13 infrared proposals, the top

ranked were those by teams led by AFCRL, Cornell University and Goddard Space Flight Center. Independently, Dutch scientists had begun to develop an infrared satellite concept in 1972 with Ball Brothers Research Corp. A 1974 design study based upon the experience gained from the Dutch far-infrared balloon program (e.g. Olthof and van Duinen, 1973) and through it their association with Ball Bros. Research Corp. (Greeb and True, 1973) led to a proposal for an infrared satellite mission to the Netherlands Agency for Aerospace Programs (NIVR) as a follow-on to their successful ultraviolet Astronomical Netherlands Satellite (ANS). The cost and scope of the proposal exceeded what NIVR could support so, in September 1974, the Dutch brought their proposal to NASA for consideration as a joint mission. NASA agreed and, in 1975, formed a Joint Mission Definition Study Team with Russ Walker as Chairman. This team was composed of six members from Walker's original consortium, three others from competing proposals and nine European members. The Netherlands formally approved the joint project in December 1976 followed by NASA in January 1977. With formal approval of the IRAS Project, NASA reconstituted the Mission Definition Study Team as the Joint IRAS Scientific Working Group with Gerry Neugebauer and Reindeer van Duinen as the US and European co-chairmen, respectively. The Science Working Group was expanded to 12 US and 16 European members during the mission and Harm Habing replaced van Duinen as the European co-chair.

The Dutch built, integrated and tested the spacecraft, which was modeled on the ANS satellite, and managed mission operations while NASA provided the telescope, the Delta 3910 launch vehicle, the data reduction and processing and distribution of the products. The Netherlands forged a separate agreement with the British under which the Appleton Rutherford Laboratory supplied the ground station to receive the telemetry data from the two on-board tape recorders, operations and a preliminary data analysis facility with which to obtain rapid assessment of the health and status of the satellite and survey.

Martin Harwit (2003) provided some of the background on IRAS' inception in his review of early infrared space astronomy. Particularly informative are the direct quotes that he includes from some of the principals in the IRAS program. Michael Rowan-Robinson (1993) shared his first hand personal observations with numerous anecdotes of some not so well known aspects of the IRAS development and early operations while the book by Mather and Boslough (1996) is, perhaps, the most informative. Mather was a member of the IRAS Mission Definition Study team and he describes the interaction between US, Dutch and British members of the team with NASA as they tried to accommodate a cosmic background experiment.

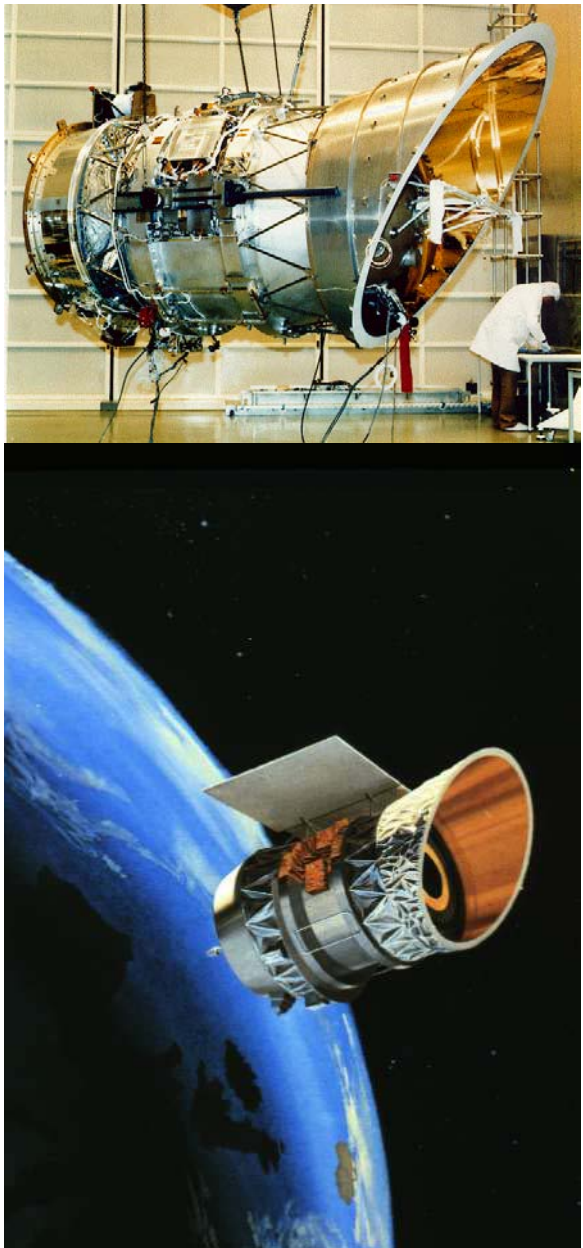


Figure 62. The IRAS satellite. At top, the spacecraft undergoing laboratory preparations. An artist's conception of the satellite in orbit is at the bottom.

bands. The large $3' \times 5'$ Ge:Ga detectors at either end of the focal plane span the longest wavelengths (100 μm). The other arrays are ordered down the focal plane (in-scan direction) as follows: 60 μm ($1.5' \times 4.7'$ – Ge:Ga), 25 μm ($0.75' \times 4.6'$ – Si:Sb) and 12 μm ($0.75' \times 4.6'$ – Si:As). The detectors are staggered and sized to provide the best positional information for a transiting source. In an attempt to improve sensitivity and uniformity of response over the detector aperture, each detector was housed in an integrating cavity and the focal plane apertures had field lenses that imaged the primary objective. The integrating cavity permitted smaller detectors to

Because superfluid helium was to be used, IRAS required much more technology development than anticipated from the baseline of the largest space-proven infrared sensor at the time, the Rockwell HI HI STAR. Conrad and Irace (1983), Leverington (2000) and Mike Kiya (private communication), among others, enumerated the numerous unexpected hardware problems that arose.

A 700 liter dewar of 1.8 K super-fluid helium (78 kg) to cool the IRAS telescope to <5 K and the focal planes to <2.6 K for a period of (initially) 15 months. This is in contrast to the 17 liter FIRSSE super-fluid dewar that lasted only for hours. Ball Bros. Corp., the prime contractor and system integrator for the telescope, selected Perkin Elmer for the optics. The IRAS Ritchey-Chretien beryllium two-mirror $f/9.6$ telescope had a 60 cm diameter primary, 70% larger than the 35 cm Mark VII beryllium optics they had previously built; the only comparably sized set of beryllium optics at the time was the AFCRL 60 cm balloon-borne telescope flown by Jack Salisbury's group. Some minor problems arose with the IRAS primary mirror during construction. It had to be masked down to 57 cm to eliminate a turned down edge, and an accident during polishing left a scratch on the primary that, although cosmetically unappealing, did not compromise the optical performance.

The focal plane design and mission operations were a compromise between the NASA objectives to conduct a sensitive mid-to far-infrared all sky survey and the Dutch desire for observatory style observations. The survey focal plane, shown in Figure 63, had two arrays of detectors in each of four spectral

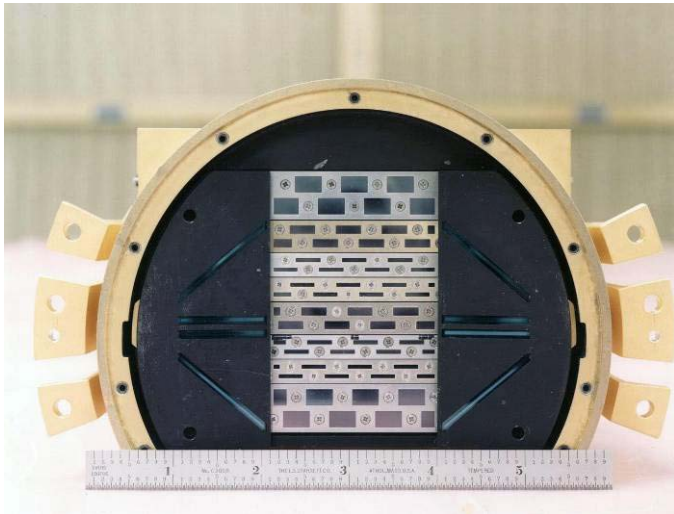


Figure 63. The IRAS survey focal plane detector arrays. The 100 μm arrays are at the ends of the focal plane. Inside these from top to bottom are the 60, 25 and 12 μm arrays followed by another bank of arrays in the same order. The long, narrow slits are apertures for the near-infrared aspect detectors.

higher temperature (~77K) than MOSFETs, which presented the problem of how to heat the devices while isolating the resulting radiation from the 1.6K detectors. The ingenious solution that Frank Low devised was to suspend them on very thin monofilaments in their own light tight enclosures and to have them self heat as they powered up. The JFETs also had lower noise, thus improving the sensitivity of the system. There were further detector problems that required replacement of the 100 μm detectors. The bias on one of the 25 μm modules shorted out and the operability of this module was restored by reworking the electronics and reversing the bias and ground. Conrad and Irace (1984) describe this fix and explain why two of the 25 μm detectors were rendered non-functional to keep the rest of the module operating.

Several problems also arose during dewar construction. One was that an inspector dropped his mitering pin into the multi-layer insulation when he measured the tolerances at the top of the cryostat mouth: MLI or super insulation is composed of thin layers of Mylar with a highly reflective coating. Concerned that the pin could create a thermal short, the engineers x-rayed the telescope to find the pin but were surprised to discover a number of pins. Apparently, the seamstresses who stitched together the 57 layers in the MLI blankets had left some of their needles behind. To the best of Mike Kiya's recollection, the needles flew with the telescope.

Some of the cryogenic valves leaked under certain conditions and the overall reliability of the valves was questioned. Pressure surges in the tank could be quite high and during one of the superfluid helium top-offs in the laboratory the surges burst the pressure disks in the tank. The combination of thermal problems and the cryogenic difficulties ultimately reduced the original 460 day expected lifetime to 221 days.

These and some equally or more serious difficulties were described by Smith and Squibb (1984) while Conrad and Irace (1984) highlighted the technical challenges faced by the IRAS developers. Major subsystems, such as the focal plane assembly and the cryostat, were redesigned and reworked, all of which took time and cost money. By the time IRAS was

be used than ones that would have to cover the full aperture, which improved sensitivity. However, the detector response as a function of position within the aperture was still far from uniform.

The survey focal plane assembly had numerous problems. The MOSFETs used to pre-amplify the detector signals were carefully chosen for optimum performance but, inexplicably, about two-thirds of them had electrostatic damage when the arrays were checked at Ames after delivery. As noted in Chapter 5, the contemporaneous Honeywell ELS focal plane had the same problem, which was due to improper handling and the decision not to incorporate MOSFET protection in the preamplifier circuits. JPL rebuilt the IRAS focal planes using more resistant thermally isolated JFETs built by Frank Low. JFETs operate at a

launched on 25 January 1983, almost exactly two years after the original launch date, the initial \$37M (Leverington, 2000) to \$52M (Smith and Squibb, 1984) cost estimate, commensurate with the inflation adjusted \$20M estimated by the 1970s decadal studies, had increased to about \$110M (Smith and Squibb, 1984). The European contribution was another \$52M.

In light of the technical problems, IRAS was an outstanding success. The satellite was inserted into a dawn–dusk Sun synchronous orbit at an altitude of \sim 900 km and, after a two week check-out, began survey operations on 10 February 1983. The mission lasted 300 days, ending on 22 November when the cryogen ran out. The satellite, telescope, mission operations, survey strategy and data reduction procedures are detailed in the IRAS Explanatory Supplement (*Infrared Astronomical Satellite*, 1987); a synopsis is given here. The telescope generally surveyed the sky with two scan segments per orbit at constant elongations: one segment from the meridian between the Sun through the North Ecliptic Pole to the meridian through the South Ecliptic Pole, the other from south to north. The $3.85'/\text{sec}$ linear scan rate along a segment was slightly faster than the orbital rate. Successive scans were nominally offset by $\frac{1}{4}^\circ$ in sun-centered elongation, or half the cross-scan extent of the focal plane. Thus, the survey had a high degree of redundancy. A ‘real’ source was detected twice in a given spectral band on a single scan, once in each of the two focal plane modules in that band. The source was scanned again within a matter of hours on the $\frac{1}{4}^\circ$ overlap on successive scans that defined single survey coverage. It took four orbits to cover the $\sim 1^\circ$ daily orbital precession, so two sectors on each side of the sky were covered at the same time. This scheme produced two almost complete semi-independent surveys of the entire sky in about six months; semi-independent because the effects of the South Atlantic Anomaly (SAA) and interference from the Moon were partially correlated.

About two-thirds of the mission was devoted to the survey, which included part of a third survey, filling in holes left by avoiding the Moon, the South Atlantic Anomaly and satellite eclipse and to compensate for minor malfunctions. The remainder of the mission time was spent on observatory style observations with the Dutch Chopped Photometric Channel and Additional Observations in which the survey array was raster scanned back and forth across a given position at selected rates and scan leg offsets. Calibration observations were obtained in this mode.

The Dutch contributed three focal plane devices, the entrance apertures of which are not shown but were located below the ruler in Figure 63. A single $5 - 8 \mu\text{m}$ detector had an aperture sized to the diffraction blur of the telescope to measure the source density statistics. Sources were extracted from the detector data stream by the on-board signal processing, counted and the result sent to the ground. Unfortunately, this device did not function properly. The chopped photometric channels obtained absolute 50 and $100 \mu\text{m}$ photometry through diffraction sized apertures at higher spatial resolution ($\sim 1.5'$) than the analogous survey detectors. A cold internal chopper blade modulated the signal and provided an absolute reference. About 1500 observations were made with this device (Wesselius et al., 1985) that included several hundred small galaxies (van Driel et al., 1993). However, the most productive instrument was the Low Resolution Spectrometer (LRS), an objective prism spectrometer with a $6'$ in-scan by $15'$ cross-scan aperture mask with three detectors that spanned a third of the mask for $7.7 - 13.4 \mu\text{m}$ spectra plus two detectors that covered half the mask for 11.0 to $22.6 \mu\text{m}$ spectra.

The Low Resolution Spectrometer (LRS) conducted a $7.7 - 22.6 \mu\text{m}$ spectral survey of the bright infrared sources. The IRAS Explanatory Supplement describes the spectrometer and observing strategy while Wesselius, Kester and Roelfsema (1993) provide additional details. To increase the dynamic range, the LRS was oriented to scan a spectrum decreasing in wavelength and the anticipated steep rise in signal for stars was attenuated by a high pass filter in the signal

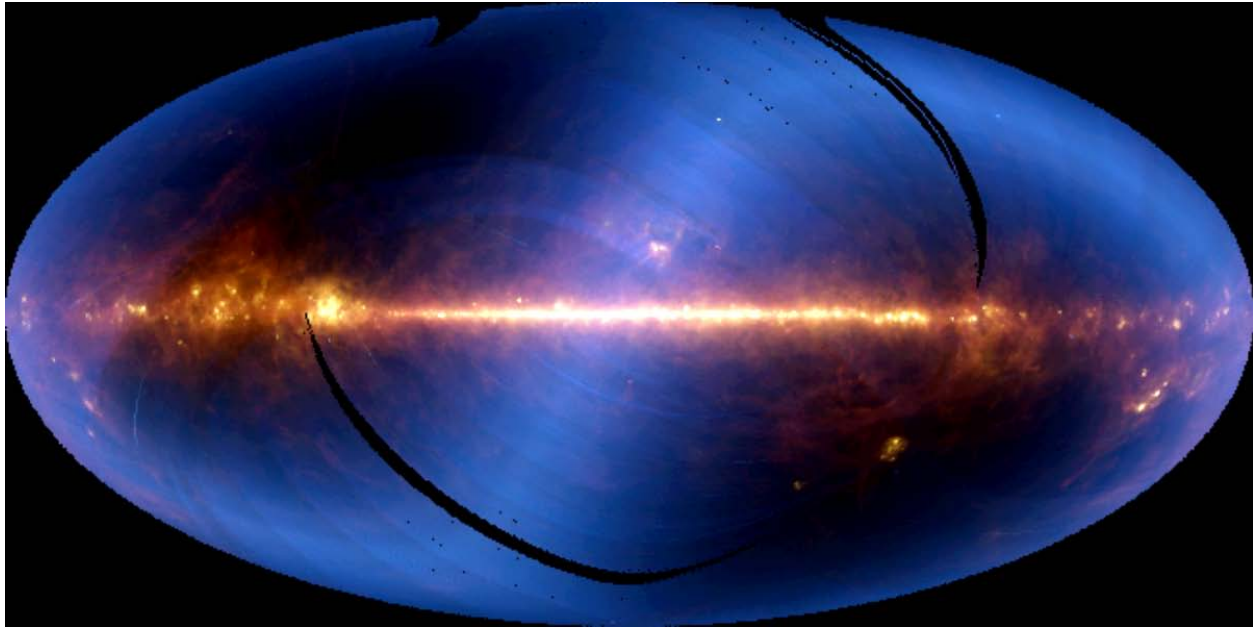


Figure 64.: The IRAS infrared sky. The IRAS observations are averaged into $1/2^\circ$ bins in this Aitoff all-sky projection in Galactic coordinates. The Galactic plane runs horizontally across the image with the Galactic center in the center. The image is color coded so that the $12\text{ }\mu\text{m}$ observations are in blue, $60\text{ }\mu\text{m}$ in green and $100\text{ }\mu\text{m}$ in red. Thus, the color is an indicator of the relative temperature: blue is warm and red is cold. The ecliptic plane is highlighted by the blue sinusoid from the relatively warm zodiacal dust emission. The interstellar emission associated with the Galactic plane is cooler and is dominantly in red. The two black arcs are areas that were not redundantly surveyed. (This Figure and Figures 62, 63 and 67 are from the Infrared Processing and Analysis Center, Caltech/JPL. IPAC is NASA's Infrared Astrophysics Data Center.)

processing electronics. Thus, the data were processed in a similar fashion as described in Chapter 4 for reconstituting extended sources to extract the final spectra. Olnon et al. (1986) assembled the initial results into a spectral atlas while subsequent processing by Kwok, Volk and Bidelman (1997) extracted complete or partial spectra for 11,224 of the brightest mid-infrared objects. These spectra have become a rich resource for studying the physical properties of cool sources and a number of discoveries have been made with them. For example, a very small number of carbon stars were found to have silicate dust shells (Little-Marenin, 1986; Willems and de Jong, 1986). This highly unusual circumstance is either due to a circumstellar shell created by an oxygen-rich binary companion to the carbon star or the carbon star was newly transformed and the observed shell is a remnant created during its previous incarnation as an oxygen-rich star.

Initial IRAS results were published in the 1 March 1984 *Astrophysical Journal Letters*, roughly concurrent with the Neugebauer et al. (1984) summary in *Science*. Subsequent developments were presented in the proceedings of the three annual IRAS workshops that began in 1985 (Israel, 1986; Preite Martinez, 1987, Lawrence, 1988). Beichman (1987, 1988) and Soifer, Houck and Neugebauer (1987) reviewed the significant initial IRAS results. The following are my highlights.

As may be seen from Figures 64 through 67, dust emission dominates the infrared sky. The relatively warm ($\sim 260\text{K}$) zodiacal dust is observed over the entire sky but the emission is strongest along the ecliptic plane, the “S” shape in Figure 64. Emission from the cooler interstellar dust along the Galactic plane lies in the mid-plane of the Figure. Both the zodiacal

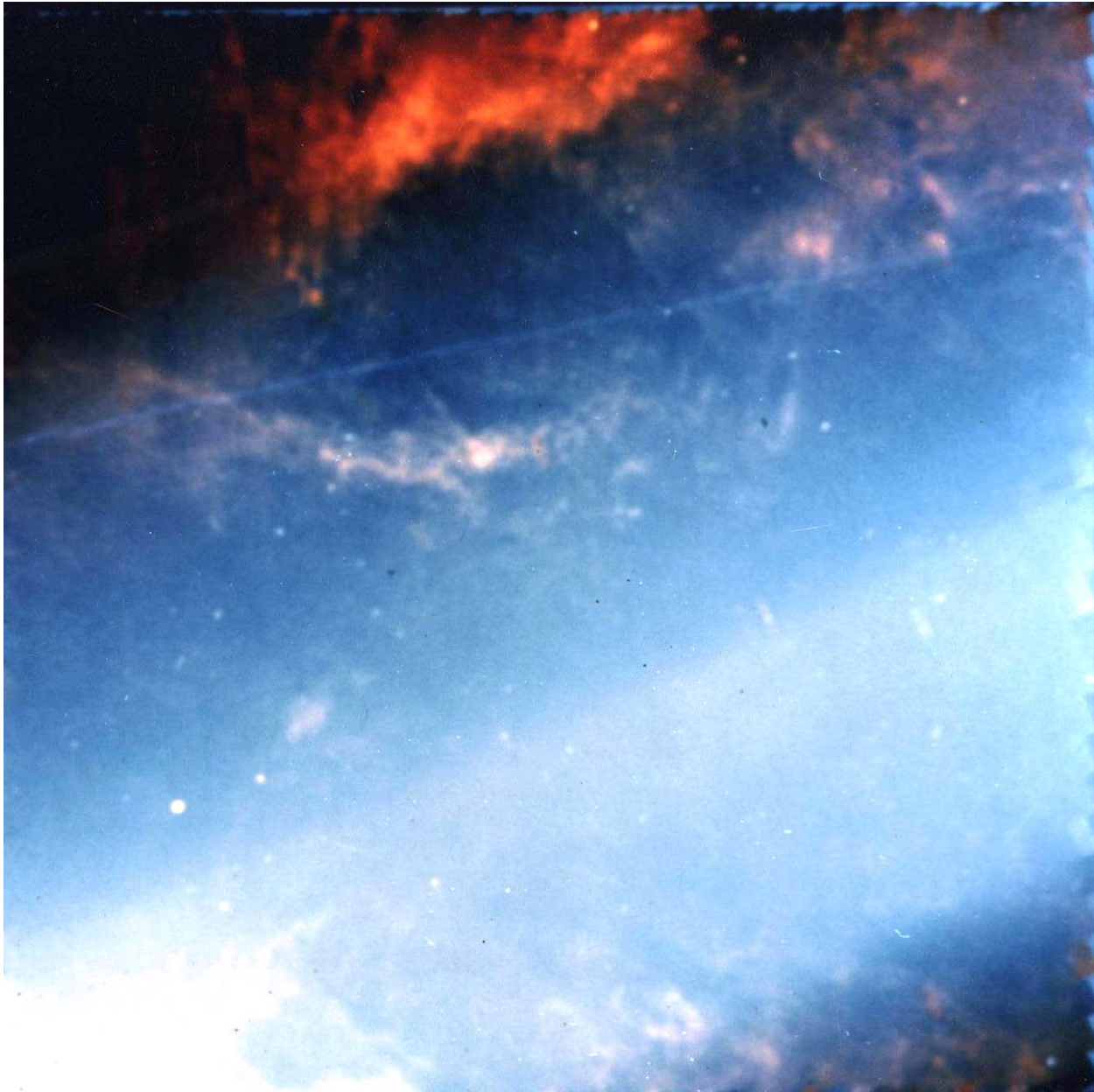


Figure 65. Celestial structure mapped by IRAS. This false color map plots the 12 μm fluxes as blue and 100 μm as red. The comet Temple 2 dust trail streaks across the top half of the image while the diagonal broad light blue bar is the very bright mid-infrared emission from the zodiacal dust along the ecliptic plane; the pronounced edges to this feature highlight the inner zodiacal dust bands. The more complex structure is the emission from interstellar dust, which is cool and, therefore, dominantly red away from the ecliptic plane.

and interstellar dust have coherent small scale structure. IRAS found two new features in the zodiacal cloud, bands of enhanced emission that circle the sky roughly parallel to the ecliptic plane and cometary dust trails, both of which are evident in Figure 65. The dust bands are a $\sim 5\%$ enhancement over the smooth emission near the plane, creating the visible edge to the ecliptic plane in the Figure; the dust trail in the orbit of the short period comet Temple 2 is the diagonal line across the upper third of Figure 65. The structures are more clearly seen in the global maps shown in Figure 66 in which the larger scale zodiacal emission has been filtered out. Sykes

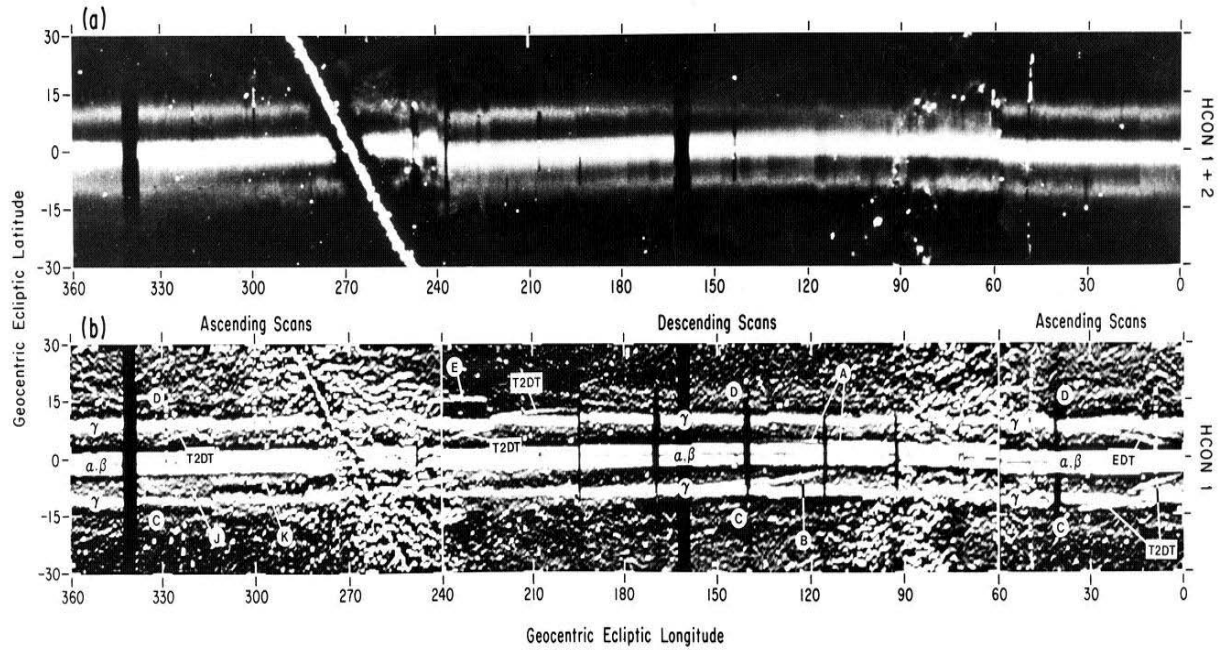


Figure 66. The zodiacal structure near the ecliptic plane observed at 25 μm . The data have been high pass filtered in latitude to enhance the smaller scale structure. (a) An average of the first two surveys (HCONs). (b) The map of the ecliptic plane from only the first survey, which shows finer detail. The well defined dust bands are labeled α , β and γ . T2DT and EDT are the Temple 2 and Encke comet dust trails. A – E denotes possible cometary dust trails while F - N letters label possible dust band segments; GC is Galactic cirrus from interstellar dust. The diagonal feature is the Galactic plane. Figure is adapted from Sykes (1988)

(1988) extracted seven band pairs from the IRAS data and labeled the most prominent bands as α , β and γ . These bands were originally associated with the Themis, Koronis, and Eos asteroid families respectively, while Reach, Franz and Wieland (1997) correlated Sykes' M/N band pair with the Maria family and tentatively associated the J/K bands with the Eunomia family.

Recently, Nesvorný et al. (2003) advanced plausible arguments to re-assign the β band to the Karin family and the γ band to the Veritas family while Nesvorný et al. (2008) proposed the Beagle grouping, a recent Koronis subfamily, for the origins of the α Band. Nesvorný, Vokrouhlický and Bottke (2006) also proposed associations of the fainter bands as due to recent breakups, such as the E/F pair that might have been created by the Datura asteroid cluster.

IRAS detected bright patches of infrared emission from interstellar material at higher Galactic latitudes that Low et al. (1984) dubbed ‘infrared cirrus’ because of its wispy appearance. Interstellar clouds create the filamentary structures seen in Figure 64 near the Galactic plane, while Figure 67 shows the infrared cirrus emission at the north and south celestial pole where the density of the interstellar medium is nominally low. The emission from the interstellar dust is higher than what expected for large grains in equilibrium with the interstellar radiation field. The 60 μm to 100 μm color temperature discrepancy is not severe according to Beichman (1987), only a factor of two deficit in the interstellar radiation field. However, equilibrium arguments break down completely for the characteristic 12 – 25 μm temperatures of \sim 500K. Non-equilibrium heating of small grains by the interstellar radiation field was suggested, analogous to what Sellgren, (1984) proposed to explain the near-infrared emission from reflection nebulae. Emission from polycyclic aromatic hydrocarbons has been invoked by

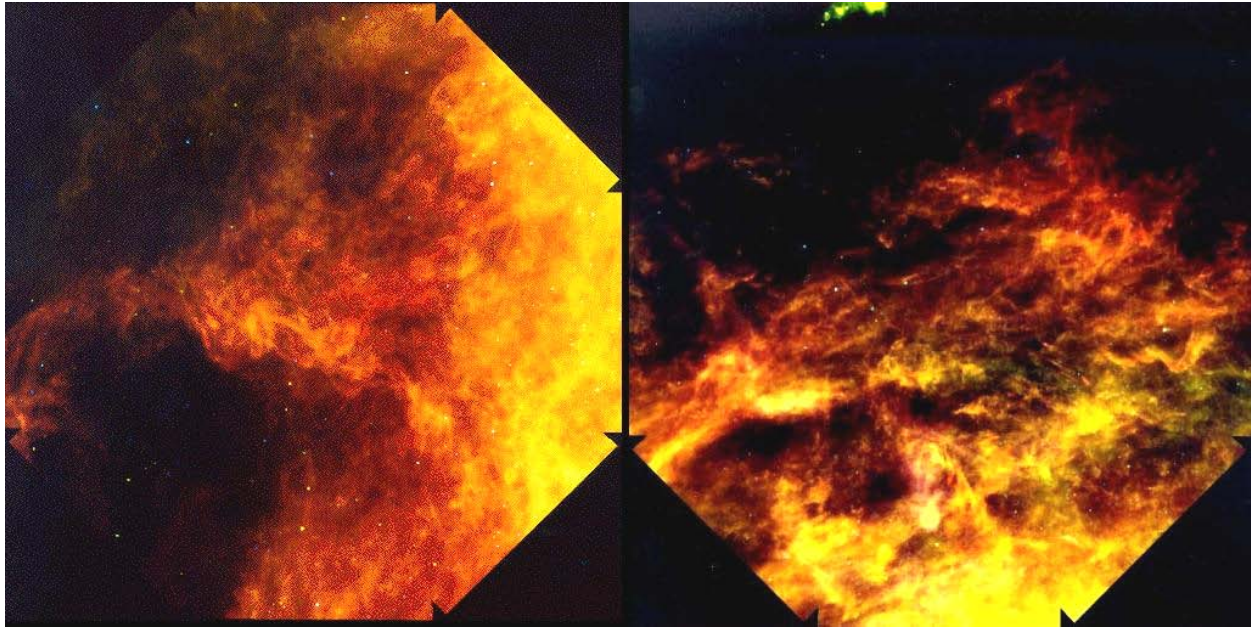


Figure 67. The interstellar infrared ‘cirrus’ at the north (left) and south (right) celestial poles. Each image is about 30° across. The IRAS $12\ \mu\text{m}$ band is color coded blue, $60\ \mu\text{m}$ green and $100\ \mu\text{m}$ red. The cool temperature of the dust is highlighted by the yellow to red colors.

Léger and Puget (1984) to explain the excess mid-infrared emission but spectral confirmation has been difficult because of the low surface brightness of the high latitude cirrus. Both mechanisms appear to be important in the interstellar medium near the Galactic plane (see Flagey et al. 2006).

To assess what was unusual in the IRAS database, an analysis of the IRAS photometric characteristics of normal stars was needed. Waters, Coté and Aumann (1987) calculated the IRAS infrared to visible color indices of ordinary stars using IRAS photometry while Cohen et al. (1987) improved the analysis by including interstellar extinction and more photometric resources for the fainter and rarer objects. Infrared excesses in what were supposed to be normal stars led to the discovery of disks of debris around ordinary stars. Aumann et al. (1984) found excess far-infrared emission around Vega (α Lyr), a somewhat vexing result as this star has been used the fundamental calibration source for two centuries (Hearnshaw, 1996). Detections of disks around three cooler main sequence stars soon followed (Gillett, 1986); the disk around β Pictoris has been extensively studied over the years as it is relatively close and is spatially resolved. Collectively, these disks around main sequence stars are thought to be examples of proto-planetary systems or failed planetary systems.

The extensive IRAS database promised to be a resource for astronomical research for many years. To realize this potential, NASA established the Infrared Processing and Analysis Center (IPAC) on the Caltech campus in 1986 to provide processing and analysis tools for the astronomical community to use IRAS data with an eye to future support for of NASA-sponsored infrared missions. The initial products IPAC produced were: a six volume *Point Source Catalog* of $\sim 246,000$ sources detected during the survey and a 7th volume of $\sim 17,000$ sources with small scale structure; plus a catalog of more than 12,000 galaxies and quasars associated with IRAS sources (Lonsdale et al, 1985). This was followed by a catalog of resolved galaxies (Rice et al., 1988), a high resolution image gallery of large galaxies (Rice, 1993) and an all-sky atlas of images, the Infrared Sky Survey Atlas (Wheelock et al., 1994), from which many of the images

in this section are taken. Documentation that provides detailed descriptions of the satellite, the mission and data process as well as access to the data products is available at the JPL web site: <http://irsa.ipac.caltech.edu/IRASdocs/iras.html>. The IPAC support for IRAS data now spans more than 20 years, so the above thumbnail sketch is far from complete. Unfortunately, no comprehensive description of the program has been written; the IRAS mission and the myriad results require a book in itself.

6.1.1. IRAS Asteroids and Comets

Community interest in the potential wealth of information that IRAS could provide on asteroids was articulated in a series of workshops prior to and during the early phase of the survey. In response, the IRAS program established an asteroid advisory group shortly before launch to provide guidance in developing an IRAS data processing subsystem to extract potential asteroid observations. Independently, the preliminary analysis facility at Appleton Laboratory in the UK incorporated a fast moving object detection capability. This facility processed the data in near real time to monitor the data quality and the progress of the survey and the fast moving object search subsystem extracted the bright moving objects, such as comets Encke and Temple 2, from the data stream by examining pairs of bright sources that failed to confirm on overlapping scans (e.g. Green et al., 1985).

The IRAS survey was not structured be able to associate multiple observations with a given non-inertial object and to derive an orbit from them. Instead, the asteroid subsystem had to do after the fact identifications by positional coincidence with predictions based on the orbital elements of the known asteroids. Thus, the number of asteroids associated with IRAS observations would grow as additional objects were discovered and orbital elements determined.

Although the asteroid processing fell victim to budget problems in 1984 and there were insufficient funds to fully document and validate the results, the initial observations were compiled into the 1986 *IRAS Asteroid and Comet Survey—Preprint Version 1*. This preprint reported associations with 1811 asteroids, 1790 of which were observed more than once. The preprint also included 47 LRS spectra on 31 asteroids. Subsequently, Cohen and Walker (2002) surveyed the LRS database and extracted more than 500 LRS spectra on 245 asteroids.

Since NASA declined to further fund the asteroid effort, concerns arose that the asteroid data analysis software and database would be lost as the IRAS processing was transferred from the JPL IBM 3030 to the IPAC Cyber mainframe computer. As Tedesco et al. (1992) described, AFGL stepped in to fund porting the asteroid subsystem and update the IRAS sightings with the larger asteroid orbital element set then available. Tedesco et al. (1992) compared the IRAS potential asteroid database against the 7311 known asteroids with good orbits as of December 1990, which was more than double the 3458 objects used for the preprint catalog, to create the IRAS minor planets survey (IMPS) catalog. The more stringent IMPS positional matching criteria rejected 210 of the preprint associations, leaving 1580 asteroids in common to both catalogs. The next iteration (Tedesco, Egan and Price, 2002) found 2228 asteroids associated with two or more IRAS sightings, an increase of 432 multiply observed asteroids over IMPS, among the 26,791 numbered asteroids cataloged by the Minor Planet Center as of July 2001. These were tabulated into the supplemental infrared minor planet survey (SIMPS) catalog.

Since Tedesco et al. did not catalog comets, AFGL supported Mark Sykes and Russ Walker to extract and analyze the comet observations. Sykes (1988) and Sykes and Walker (1992) examined the 1836 12 μm , 25 μm and 60 μm Sky Flux Plates, 246 IRAS additional observation images and the zodiacal history file and extracted a number of features of possible

cometary origin. The observations were then compared to the orbital projections of known short- and long-period comets, to 36 asteroids with comet-like orbits and to 58 meteor streams. The dusty comae of seven short period comets were identified while Walker, in his preprint chapter, associated as many as 25 comets with point detection in the IRAS database. The IRAS images revealed a new feature: dust trails in the orbit of the comets (Sykes et al., 1986: Figures 65 and 66). Eight trails were associated with known short-period comets but no trails could be associated with meteor streams or comet-like asteroids. Subsequently, Nakamura et al. (2000) did report on a quantitative visible measurement for the Temple-Tuttle dust trail that gives rise to the Leonid meteor showers. Sykes and Walker (1992) determined that dust trails of the eight known short period comets responsible for producing them were preferentially detected when the comets were near perihelion. Using the much more sensitive Spitzer telescope, Reach, Kelley and Sykes (2007) found debris trails associated with an additional 22 short period comets for a detection rate of 80% (27 of 34) of all the short period comets surveyed by IRAS and Spitzer. The trails extended from a few degrees in length to several tens of degrees in the case of Temple 2 but were narrow, with a width near the IRAS resolution. Sykes et al (1986) concluded that for the dust trails to be narrow the dispersion velocities of the ejected cometary particles must be low and that these long and narrow quasi-linear linear dust trails are vastly more extensive in the LWIR than indicated by visual observations.

6.1.2. IRAS Satellite Observations

Space-based infrared sensors are efficient surveillance systems and, as previously noted, the AFCRL HI STAR rocket-probe celestial surveys obtained good quality infrared measurements of satellites. These observations demonstrated that the infrared color temperature could be used to statistically determine whether an RSO was active or not and that the surface composition of a satellite could profoundly influence its infrared signature. IRAS was an even more capable surveillance instrument, as Russ Walker out pointed in his presentation to Lt Col Brian Bell and Col R. Mercer (OUSDR&E) in January 1981. As Walker presented it, IRAS could detect a softball sized satellite at the distance of Los Angeles to New York, which corresponds to a 1 m² target in geosynchronous orbit. However, the opportunity to extract satellites (resident space objects, RSOs in surveillance parlance) from the IRAS data stream was not pursued as a consequence of this meeting due, in part, to the fact that RSO detections would be rejected in the processing pipeline unless special software was written. Also, the initial NASA and the Air Force agreement specified that such information would not be sought. However, once information exists in an open forum, it cannot be suppressed.

In September 1983, a Space Division captain and his Aerospace advisors, Art Morris and Gary Mueller, met with members of the IRAS program at JPL to discuss extracting RSO signatures from the data. Rowen-Robinson (1993), who was not present at this meeting, none-the-less observed that; John Fowler was “*...a strong individual who could not be intimidated by NASA management. At one time the US military began to take an interest in IRAS because the telescope would get sightings of all the satellites in higher orbits than IRAS, including some that they perhaps did not know about. John was asked to write some software which would recognize satellite crossings in the data, so that this information could be passed on to the military. He simply refused point blank to do so. I believe this task was eventually carried out by other less robust souls some years after the mission, as part of the Star Wars programme.*” As with many speculative statements, this one is both incorrect and incomplete. Art Morris’ recollection of that meeting was that some of the JPL people were brusquely uncooperative, invoking international

agreements rather than principle as the reason for not cooperating with the Air Force. Rowan-Robinson also was mistaken about the IRAS capabilities; the survey strategy made it unlikely that the telescope would see objects at altitudes below \sim 2000 km. Furthermore, it was members of the astronomical community associated with the IRAS program that were soon extracting RSO signatures and publishing the results; the so-called Star Wars involvement came much later.

Control of the satellite information was lost when the IRAS data were made public. Anz-Meador et al. (1986) were the first to report finding (three) objects in orbit while purportedly searching for space debris in the IRAS source reject file. Anz-Meador et al. searched only a small fraction (\sim 3%) of the source reject file, specifically the 100 or so hours of data taken when the IRAS scan looked almost radially away from the Earth. They selected only scans along a great circle, or nearly so, because that greatly simplified calculating the encounter geometry

Dow et al. (1990) avoided the messy orbital calculations by systematically examining the 1836 12, 25 and 60 μ m IRAS sky flux plates for signals indicative of satellites crossing the focal plane and extracted the sightings of 466 objects. The out-of-focus signatures of 12 objects marked them as possible near field contaminants while the remaining 454 far-field sources were considered as potential satellite observations. The apparent motion of the satellite across the focal plane caused the object to appear at two inertial locations in the same color images due to the offset of the detector modules (see Figure 63); an example such an offset from MSX is shown in Figure 101. The satellite displacements in the Sky Flux images provide a limited track that was used to estimate the range and inclination of the satellite; the resulting range estimates were between 4000 and 70,000 km. Dow (1992) also inferred the physical characteristics for 45 bright objects that had 12 and 25 μ m measurements at signal-to-noise ratios of at least 40. Dow et al. concluded that there may be thousands of much fainter objects in the IRAS data base, in agreement with the fact that roughly 3000 transient objects were removed from the final IRAS Sky Survey Atlas (ISSA) images.

Contrary to Rowan-Robinson's conjecture, it was the European Space Research and Technology Center (ESTEC) that systematically mined the IRAS database for satellite signatures. Walsh, Wesselius and Olthof (1989) did a feasibility study on extracting space debris from the IRAS data that led to a 1989 ESTEC contract to the Space Research of the Netherlands (SRON) in Groningen. SRON was to develop software to extract satellites and debris signatures by their geometric track across the IRAS focal plane and derive their radiometric properties, then to apply the routine to the entire IRAS survey to extract debris signatures

Wesselius et al. (1990) outlined the SRON procedures used to identify their first RSO in the IRAS database, the 66-53J Transtage, while de Jonge et al. (1992) provided a more complete description of the processing for three other large objects. SRON calculated the lines of sight between these objects and IRAS every 30 seconds for the entire IRAS mission and then examined IRAS signals at the times of possible coincidence to look for characteristic satellite tracks. RSOs tracks are distinctly different than those from stars in that an inertial source tracks across the focal plane without cross-scan motion with a specific time offset defined by the \sim 0.25° between the two detector modules in the same LWIR band and the 3.85'/sec survey scan rate. RSOs will have a cross-scan component and the time between detections by successive detectors will, generally, be less than for an inertial source.

Initially, the encounter geometries for the four satellites were calculated and the data from the IRAS detectors were plotted for several seconds around that time. The signals were visually correlated for reasonable straight line tracks that could be associated with the objects. Color temperatures and effective emitting areas were derived for the objects from the IRAS 12 –

25 μm measurements. The speed at which the object transited the focal plane was calculated and the track angle determined by the pattern of detectors in the focal plane that observed the objects. Orbita were determined from the observations assuming that they were circular.

Wesselius et al. (1992) described the final SRON catalog of reasonable quality IRAS satellite observations and their derived characteristics of temperature, size, and orbit. The visibility of the observations was enhanced by a zero sum filter with a width matched to the width of a point source. Peaks 3.5 or more times the local noise were extracted and the time, inertial position and the detector on which the peak occurred were recorded. Pairs of peaks in adjacent 12/25 μm modules were coupled and a confirming signal was searched for in a third module along the track line defined by the first two peaks. The sighting was saved as a potential satellite if the confirming peak was found and the transit speed across the focal plane was between 3.1'/sec and 25'/sec. The fluxes extracted at the same wavelength also had to agree within a factor of 5. These criteria were rather weak and the reliability of the \sim 200,000 potential sightings in the resulting database was low. SRON estimated that only \sim 5% of these sightings were expected to be real. Wesselius et al. (1992) also included a LRS spectrum of one bright object that displayed a featureless blackbody spectrum with a temperature of about 300K.

Gaposchkin and Bergemann (1995) obtained definitive results by correlating a high confidence subset of \sim 136,000 sightings in the SRON potential RSO list with predicted encounter geometries based on the 1983 satellite ephemerides with respect to the IRAS lines of sight during the mission. They found 2047 matches on 465 satellites, a 1.5% return. Their matching criteria required that the computed and observed positions be within 0.6° and that the angular velocities had to agree to within 0.5'/sec. The 465 RSOs were two-thirds of the 700 objects in the official satellite list above 1000 km altitude at the time. Most of the observed RSOs were in geosynchronous orbit and roughly a third (162) were rocket bodies. On the average, IRAS observed a given satellite 4 to 5 times during the 10 month mission.

Gaposchkin and Bergemann reduced the dispersion in the measured satellite flux by carefully screening the observations to eliminate the fluxes for objects that were not completely on a detector, thus reducing the bias in the band averaged flux. They also color corrected the photometry, which the SRON analyses did not. The resulting satellite detections were collected and physical properties, such as temperatures and emissivities were derived, from which they drew inferences about various classes of RSOs based on the infrared signatures. Lane, Baldassini and Gaposchkin (1995) did a metric analysis of the IRAS RSO detections but could only come to some general conclusions owing to the porosity of the focal planes to RSO transits.

6.2. Niche Experiments

The fate of the AFGL probe experiments and IRAS were inextricably entwined even though the two programs had limited interaction. At 50 times better sensitivity and 8 times smaller beam size, the successful IRAS mission undercut the rationale for the AFGL celestial and zodiacal survey experiments. However, the success of IRAS did get the BMP astronomy data de-classified and published. Thus, the 14 September 1982 SPICE 2 flight heralded the end of the AFGL rocket-based infrared astronomy experiments. The IRAS success meant that probe-rocket based sky surveys were not viable and we had to find a unique niche if we wanted to continue to fly experiments. We negotiated with Space Division in December of 1982 for a follow-on series of probe flights that included a dedicated SPICE experiment to measure a high priority target tentatively from the rocket range on Kauai, Hawaii. I went to Kauai to discuss

what it would take to fly an ARIES from the site with the range people but was not received with much enthusiasm. However, consideration for this experiment ended on 15 March 1983 while still in the planning stage. Probably not coincidentally President Reagan announced the formation of the Strategic Defense Initiative Organization (SDIO) in his “star wars” speech on 23 March 1983. Subsequent discussions with Space Division regarding a second ELC experiment against the disturbed atmosphere were cancelled in December 1983. We then submitted the ELC II proposals to SDIO, which had swept up the technology development funds in the services at the beginning of the 1984 fiscal year. Any further astronomy experiments had to be conducted with funds eeked out of our internal budget.

6.2.1. Background Equatorial Astronomical Measurements (BEAM)



We had one last astronomy experiment. After the SCOOP contract had terminated at the end of 1980, SAMSO offered us the residual FAIR and SCOOP hardware: a complete FAIR sensor, most of a SCOOP sensor, pieces of a second SCOOP and some additional optical components. Since we had a complete HI STAR payload and the Castor-Lance that was originally slated for ZIP, we had the makings of an experiment that would be inexpensive enough to be funded from the Laboratory budget. However, SPICE and FIRSSE were more sensitive and IRAS more sensitive still, so the experiment had to address issues the other programs could not.

Laboratory funds were appropriated in the fall of 1982 to build the Background Equatorial Astronomical Measurement (BEAM) payload around the HI STAR casting and to contract for a new focal plane. An in-house effort built the signal processing electronics and replaced the barrel of the FAIR telescope to accommodate the HI STAR cover design and cover removal mechanism. The principal changes to the new Santa Barbara Research Corp. focal plane for the refurbished FAIR sensor were to incorporate the $6 - 9 \mu\text{m}$ band that was being considered for space surveillance applications instead of the $8 - 14 \mu\text{m}$ band. Thus, this experiment would return real background data in the proposed system band and provide a short wavelength measurement for BMP and IRAS sources. Parenthetically, because this spectral band contains the strongest PAH features, cameras on the Infrared Space Observatory, Akari and Spitzer chose spectral bandpasses very similar to BEAM’s as the principal band for imaging.

The practical reason for the decision to fly the experiment from the range near Natal, Brazil was that the Castor-Lance dispersion made a land range problematic. The Barreira do Inferno rocket range would accept a Castor-Lance as the impact point would be in the Atlantic Ocean and it also had the advantage of being near the equator. Thus, the experiment would be thrown away, something we were unwilling to do with the SPICE or FIRSSE sensor until IRAS was successful. The Castor-Lance was anticipated to loft the 200kg HI STAR payload, minus the recovery pack, to an altitude in excess of 500 km. This provided enough time to cover the available sky twice, providing the minimum amount of critical redundancy.

The BEAM experiment could fill the remaining gaps in the *Revised AFGL Catalog* sky coverage with the appropriate choice of the pole star. The scan profile deployed the sensor to the minimum 40° zenith angle, then stepped it down by an angle slightly less than the cross scan field of view to a maximum deployment angle of about 85° , which would occur at peak altitude and maximum depression angle of the Earth. Subsequent sensor steps would decrease the

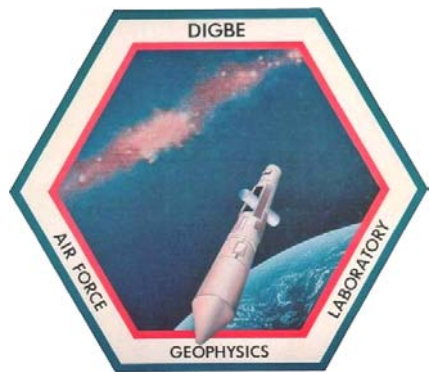


Figure 68. The BEAM experiment mated to the Castor-Lance rocket, which is mounted on the launch rail at the rocket range near Natal, Brazil. Dave Akerstrom is leaning against the launcher and scales the size of the assembly in this photograph.

deployment. Approximately 25% of the sky would be rapidly covered twice within about 10 minutes. This also meant that all the satellites above the horizon bright enough would be seen, many of them multiple times. Hopefully, we could extract valuable enough information from these observations to interest the Air Force to repeat the SPICE attempt to observe a specific object.

BEAM was launched on 17 January 1985 but, unfortunately, the experiment failed because the transition stage between the two motors did not separate. The Lance motor ignition blew the Castor and transition stage away but the resulting g-forces damaged the payload electronics to the extent that the experiment programming was not executed. The official explanation for the failure was that the launch ignition flames burned through the umbilical containing the arming switches, which was not sheathed in fire proof material as it was required to be, and shorted the separation circuit to the safe position. As may be seen in Figure 68, the umbilicals come down the back of the launch rail. This explanation is at odds with the speculation in the field that the squib holes in the separation system were too deep and that, when fired, they failed to set off the prima-cord to separate the Castor from the Lance.

6.2.2. The Diffuse Infrared Galactic Background Experiment (DIGBE)



First comes the experiment concept, then the logo, and then, with luck, the experiment. The Diffuse Infrared Background Experiment (DIGBE) began in 1987 with a contract to Rockwell International Corp. for an infrared solid state photomultiplier (SSPM) photon counting focal plane. The idea was to put this device in ZIP and substitute a circular variable filter for the chopper at the first focus to obtain low resolution spectra of the diffuse emission along the Galactic plane. Despite the modest ZIP effective collecting area, the large detectors and photon counting meant that this experiment should have had background-limited sensitivity.

The experiment concept was unique as it covered spectral regions that could not be easily observed from the ground. If non-equilibrium heating of PAH molecules caused the large $12\text{ }\mu\text{m}$ excess observed by IRAS, the spectral features in this emission should be observable along the Galactic plane where the infrared emission from the interstellar dust is most intense. Even then the surface brightness of the emission was low but the proposed background limited DIGBE spectrometer with large instantaneous fields-of-view could observe these purported spectral features. The Galactic plane was too broad for IRAS LRS spectra so the only information then available on the emission were balloon-borne photometric observations in filters centered on the near-infrared features and the ZIP photometric spectra in the first quadrant extracted by Rickard, Stemwedel and Price (1990).

Lou DeBottari offered the detectors at cost in order to get a flight demonstration of this new and innovative Rockwell technology. However, Lou retired before the contract could be signed and his replacement wanted full fee. This was far too expensive for our limited resources and the program was cancelled by the end of the decade.



6.2.3 SPIRIT II

The AFGL Infrared Technologies and Optical Physics Divisions were re-combined in 1990 and we inherited two experiments in the subsequent merger of the Atmospheric and Celestial Background Branches, one of which was the Spatial Spectral Rocketborne Interferometer Telescope II (SPIRIT II). This Ballistic Missile Defense Organization (BMDO as SDIO was renamed in the late 1980s) sponsored experiment was designed to measure the structure in the infrared emission from the aurorally disturbed atmosphere between tangent heights of 60 to 170 km. The off-axis telescope had an elliptical primary with a 40 cm major axis and a six color

infrared radiometer with pixels sized to the optical blur of the telescope. The radiometer shared the focal plane field with an interferometer spectrometer. The Talos boosted Aries I motor lofted the payload to a 330 km altitude from the Poker Flats, Alaska rocket range into a bright aurora in March 1992. Kemp, Larson and Huppi (1994) describe the instrument and provide an overview of the mission results in terms of sensor performance. Because of pointing uncertainties, among many other problems, little information of value was extracted from this experiment.

6.3. Shuttle-Based Experiments

In the late 1970s, the major infrared space-based experiments such as the Air Force SIRE and NASA's Shuttle (later Space) Infrared Telescope Facility (SIRTF) were mandated to fly on the Shuttle. This was a reasonable choice in one respect – expendable cryogens had to be used because mechanical cryocoolers at that time were massive and their technical risk was high. Thus, having a Shuttle based sensor, or sortie mission for the initial SIRTF concept, permitted the telescope to be recovered, the focal plane instruments to be swapped out and the cryogen recharged for another flight. However, contamination was recognized as a problem with the seminal theoretical analysis of Simpson and Witteborn (1977) but experimental confirmation was needed. The DoD flew the first infrared contamination monitoring experiment in late June 1982, the Cryogenic InfraRed Radiance Instrumentation for Shuttle (CIRRIS 1). CIRRIS 1 mated the HIRIS interferometer that had been flown from Poker Flats in 1976 and 1977 (Stair et al., 1983) to a set of ZIP fore-optics; Ahmadjian et al. (1981) described the CIRRIS 1 sensor and the various experiments that were to be conducted, including the science objective of measuring the spectral detail of the infrared emissions in the upper atmosphere. The cover failed to open during the flight and no data was taken.

6.3.1 The Spacelab 2 Infrared Telescope

NASA's infrared contamination experiment was the Spacelab 2 Infrared Telescope (Koch et al., 1982), a small 15 cm f/4 Herschel telescope attached to a 250 liter dewar of superfluid helium. The 10 detector focal plane contained four Si:Ga detectors; one for star sensing in a 2 – 3 μm band, two for molecular contamination in 4.5 – 9.5 and 6.1 – 7.1 μm bands and one as the analog of the 8.5 – 14 μm astronomical N band. Three 18 – 30 μm Si:Sb and three 70 – 120 μm Ge:Ga detectors were filtered to duplicate the IRAS 25 and 100 μm bands. A cold shutter provided the reference for the absolute photometry. Each $0.6^\circ \times 1^\circ$ detector was masked by an

opaque strip down the middle to provide discrimination against radiation hits and contamination. The mask also provided characteristic on-off-on signatures for point like sources that were used for confirmation as was association of detections on different orbits.

The telescope was flown in July/August 1985. The telescope scanned the sky at a rate of 6°/sec, sweeping out a 90° arc perpendicular to the shuttle's orbital motion. Thus, ~60% of the sky was surveyed on each orbit and the coverage was increased to 90% by rolling the Shuttle 30° about the velocity vector. The mission objectives were to monitor the infrared contamination environment surrounding the Shuttle, to assess the technology issues related to handling 250 liters of superfluid helium and the porous plug phase separator on the Shuttle as a path finder for SIRTF and to map the diffuse emission from the celestial foreground that would have to be subtracted to derive the cosmic background.

A small piece of torn insulation contaminated most of the measurements, but useful results were obtained. Besides observing a much higher than anticipated foreground from Shuttle contaminants (Koch et al., 1987) that led to the cancellation of a proposed second flight, the experiment successfully tested handling of superfluid helium in orbit. Since weight wasn't an issue, a modified commercial helium storage dewar was flown to reduce costs. The dewar was connected to a rotary joint to permit the sensor to scan across the sky (Davies, 1997). Also, despite the contamination, Koch et al. (1988) was able to extract 2.4 and 7 μm maps of the first quadrant of the Galactic plane while Kent et al. (1992) published improved 2.4 μm maps.

6.3.2. Transitions

The January 1986 Challenger disaster had a profound effect on major space-based programs. The US military had decided not to use the Shuttle for polar orbits in the mid-1980s and NASA had to follow suit as the Air Force stopped work on the Vandenberg AFB Shuttle launch facilities. George Rieke (2006) described the many incarnations of the Shuttle (later Space) Infrared Telescope Facility, which required a redesign from being a Shuttle based sensor, as the name change implies while the Cosmic Background Explored (COBE) also had to be redesigned for a dedicated launch vehicle (Mather and Boslough, 1996). Another astronomy casualty was the German Infrared Laboratory (GIRL). GIRL was a half meter superfluid helium cooled telescope designed to obtain 2.5 – 200 μm images, spectra and polarimetry of the atmosphere and astronomical sources from a German built Shuttle pallet (Lemke et al., 1985). The program began in 1977 but was cancelled in 1986 after Messerschmitt-Boelkow-Blohm (MBB), later Deutsche Aerospace AG (DASA) had built a significant amount of hardware. The major Air Force programs were not directly affected as both SIRE and the AFGL entry, LAIRTS, had been canceled by the time of the Challenger disaster.



6.3.3. Shuttle-Based AFGL Background Experiments

The Shuttle schedule slip due to the Challenger disaster delayed the launch of the AFGL/BMSO Cryogenic Infrared Radiance Instrumentation for Shuttle (CIRRIS-1A) experiment, the most sophisticated experiment that we inherited in the merger of the Celestial and Atmospheric Backgrounds Branches. The off-axis CIRRIS 1A sensor had a 12" (30.5 cm) diameter D-shaped primary, an infrared radiometer with both fixed and selectable bandpass filters and a 2.5 – 25 μm Michelson interferometer with

1 cm^{-1} spectral resolution. This resolution was easily sufficient to resolve the molecular emission lines in the atmosphere. The interferometer and radiometer fields of view were co-aligned with 161 cm^2 collecting area for the interferometer and 182 cm^2 for the radiometer. CIRRIS 1A was a much more capable replacement mission for the failed 1982 CIRRIS 1. Originally, this experiment was manifested to fly in the late 1980s but the delay in the launch schedule allowed enough time to substitute blocked impurity band detectors were in the focal plane which markedly reduced but did not quite eliminate the non-linear response that caused ghost features in the interferometer spectra.

The sensor was flown on Shuttle Discovery mission STS-39 on 28 April 1991 into a 260 km altitude orbit; the launch is shown in Figure 69. The 57° orbital inclination was the maximum that the Shuttle could achieve from Cape Canaveral and was chosen so that CIRRIS 1A could observe as close to the poles as possible. The CIRRIS 1A operations began about a day after launch, which allowed time for the Shuttle to outgas and the particulate environment to clean up. A scheduling conflict was resolved that permitted a little more than 30 hours of data to be taken during the first four days of the mission before the cryogen ran out. Eighteen hours of the data were considered to be of very high quality. Fortuitously, moderate intensity auroral



Figure 69. Liftoff of Shuttle Discovery at 11:31 GMT on 28 April 1991 from launch complex LC39A at Cape Canaveral carrying the AFGL CIRRIS IA and the Shuttle Kinetic Infrared Test experiments.



Figure 70. CIRRIS 1A in Discovery Shuttle Bay. The University of Arizona ultraviolet experiment is the horn in the foreground atop the labels. The UV, the IBSS infrared sensor and a visible sensor were on the SPAS II Pallet, a free flying platform during the mission.

gases were measured in the stratosphere at 14 km. These included carbon tetrafluoride, carbon tetrachloride, the chloro-fluorocarbons CFC 11 and 12, and HNO_3 . The Shuttle-induced optical contamination was also observed by the experiment both with well resolved spectra and good quality radiometry (Wheeler et al., 1992; Dean et al., 1994).

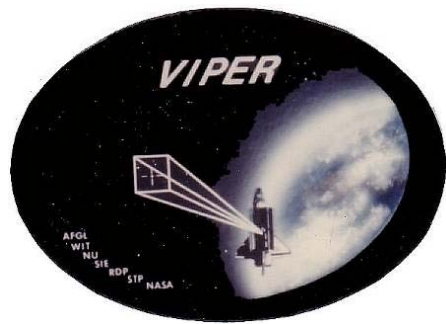
Wise et al. (2001) also mentioned CIRRIS 1A celestial observations, specifically infrared radiometry on α Boo, α Sco and α Cen, primarily for calibration cross-checks. A zodiacal experiment was also conducted. Unfortunately, the experimental profile was set before the measurement geometry was discussed with the AFGL infrared astronomers. Thus, the recommendation that the scan be altered such that the closest approach to the Sun was not in the ecliptic plane could not be implemented. Despite approximately a year's effort, we could not disentangle zodiacal emission from off-axis radiation from the Sun.

STS-39 also carried an SDIO experiment with a multi-sensor suite to measure rocket engine plumes, propellant and gas releases as well as the Earth and Earth limb backgrounds on the Shuttle Pallet Satellite (SPAS II). SDIO had purchased the SPAS II, which originally had been the GIRL pallet, and funded MBB to build the Infrared Background Signature Survey (IBSS) sensor because of their experience in developing the various GIRL engineering models (Seidel and Passvogel, 1994). IBSS was a 5 cm off-axis Herschelian telescope with a radiometer and an Ebert-Fastie grating spectrometer in a 300 liter supercritical helium cryostat. The spectrometer covered wavelengths from 2.5 to 22.5 μm (Lange et al., 1990) while the 9 filters in the radiometer were centered on the atmospheric absorption bands and window regions between 2.5 and 7.5 μm . The pallet was released from the shuttle bay for a week of measurements and then recovered. Howard Stears was the system engineer on IBSS and one of two flight directors during the mission. In addition to IBSS, the pallet in the foreground of Figure 70 also carried ultraviolet and visible sensors for which AFGL played a leading role in the Earth background observations.

activity occurred during much of the mission. The CIRRIS 1A observations remain as the highest resolution and sensitivity spectral data to date on the upper atmosphere.

CIRRIS 1A, shown in the shuttle bay in Figure 70, conducted the first global survey of the infrared emission from the mesosphere and lower thermosphere and made a number of discoveries and significant observations. John Wise and the CIRRIS 1A team (Wise et al., 2001) provide a comprehensive overview of the CIRRIS 1A experiment as well as a detailed summary of the scientific and technical results from the CIRRIS 1A articles published prior to 2001. The briefest summary of the highlights include: a new class of non-local thermodynamic equilibrium emission from the highly rotationally excited diatomic molecules OH, NO and NO^+ at altitudes of 50 – 80 km and above 140 that were observed both in the day and at night. Trace greenhouse

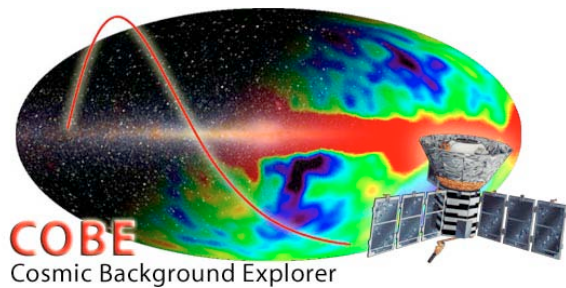
Ahmadjian et al., (1992) reported the results from an AFGL/Goddard Space Flight Center get-away-special Spacecraft Kinetic Infrared Test experiment on STS-39 to measure the infrared Shuttle glow. The experiment detected the infrared glow from NO, NO⁺, OH, and CO during quiescent conditions. However, the glow intensified by factors of 10 to 100 when the orbiter fired its thrusters, with significant changes in the relative spectral flux. The experiment was reflown on STS-62 in March 1994 in conjunction with the Experimental Investigation of Spacecraft Glow package that extended the spectral range from the UV to the MWIR. Swenson et al. (1995) found that the glow was extinguished when N₂ was released into the ram direction and reappeared after the release stopped; the intensity of the glow was found to scale as the atomic oxygen density above 200 km. The effect of the temperature of the surface and type of paint were also investigated.



of the reflected zodiacal light. Light scattered by the small particles thought to comprise the bulk of the zodiacal dust should be reddened but the existing measurements were contradictory on this. VIPER was flown of Shuttle mission STS-42 on 22 January 1992 but instrument problems and optical contamination compromised the results.

Paul LeVan was the principal Investigator on the VIIsual Photometric ExpeRiment (VIPER). This get-away-special experiment was designed to obtain photometry on the zodiacal background in well quantified standard B, V and R photometric bands. Models of the reflected zodiacal light and thermal emission did not agree with visual and infrared measurements in the sense that model parameters adjusted to fit the measured infrared flux predicted more visual radiance than observed. Another issue was the color

6.4. The Cosmic Background Explorer



As Harwit (2003) indicated, two incompatible objectives arose during the IRAS Mission Definition Study: one was for a complete sky survey at reasonable spatial resolution to enumerate the discrete sources and the other was for a low resolution survey of the diffuse cosmic background. IRAS would do the survey and a

separate mission, the Cosmic Background Explorer (COBE), was proposed for the other.

Two different historical perspectives on COBE are available. One, *Wrinkles in Time* by George Smoot and Keay Davidson (1994), emphasizes Smoot's role with COBE's Diffuse Microwave Radiometer within the context of the cosmic background research that he and his University of California group had been engaged in for the previous two decades. The title of Mather and Boslough's 1996 book *The Very First Light: The True Inside Story of the Scientific Journey Back to the Dawn of the Universe* indicates that the record had to be set straight as to the events that produced COBE. This narrative is much more informative with a description of contemporaneous research and how the program made the successful transition from the shuttle to free-flying satellite. Originally, COBE was to be launched on a Delta vehicle (a Delta is shown in Figure 87) but it was redesigned when NASA mandated that the Shuttle would be its main launch vehicle. Having grown to 4.5 m in diameter given the ample room of the Shuttle bay, COBE had to be scaled back to 2.5 m with a concomitant 50% mass reduction to fit on the

Delta rocket. The book is also generous with credit although, as previously noted, it does have its own misstatements and misattributions. Mather and Smoot shared the 2006 Nobel Prize in Physics for their cosmic background discoveries, particularly for the COBE contributions.

Boggess et al. (1992) provide an overview of the COBE instrumentation, mission and initial results. COBE was launched into a 900 km altitude sun-synchronous orbit on 18 November 1989, carrying a Diffuse Infrared Background Experiment (DIRBE), a Far-Infrared Absolute Spectrometer (FIRAS) and the Diffuse Microwave Radiometer (DMR). The DIRBE and FIRAS instruments were cooled inside a 650 liter superfluid helium dewar while the three DMR instrument, which required no cooling, was mounted outside the dewar. The cryogen ran out after 10 months of operation, exceeding the minimum six month mission requirement. FIRAS stopped operating with the depletion of the cryogen while the four DIRBE near-infrared bands continued to take data for another three years at reduced sensitivity. Since the DMR did not require cooling, this instrument was operated for four years.

With respect to the cosmic background, the FIRAS measurement of the 3 K background was, perhaps, the most widely heralded COBE accomplishment. Fixsen et al. (1996) presents the final analysis from the mission: a background temperature of 2.728 ± 0.004 . The ~ 1 part in 10^3 dipole variation in temperature provides the direction in which the Sun is moving with respect to the cosmic background to an accuracy of $18'$.

The DIRBE instrument returned data of most interest to our mid-infrared focus. The DIRBE radiometer was an off-axis Gregorian telescope with a 19 cm diameter primary mirror. The 10 spectral bands included the astronomical J, K, L and M bands centered at 1.25, 2.2, 3.5 and 4.9 μm respectively, analogs to the IRAS 12, 25, 60 and 100 μm bands and bands at 140 and 240 μm . Dichroic filters co-aligned all the $0.7^\circ \times 0.7^\circ$ detectors to the same field. A cold tuning fork chopper modulated the field at 32 Hz and the signals were synchronously rectified on board and averaged to a rate of 8 samples per second; the result was telemetered to the ground. The COBE payload was spun once every 75 seconds about an axis maintained at a constant 94° solar elongation. The DIRBE optical axis was tilted by 30° from the payload spin axis, so it swept the sky between elongations of 64° and 124° . This produced uneven coverage with areas at the extremes in elongations of the circular scan overlapping while the center of the circle had a single orbit fill factor of about 20%. Unaliased coverage of the $\sim 50\%$ of the sky within the scan limits took more than a day to obtain. Depending on location, a given area of sky was measured anywhere between 100 and ~ 1900 times during the 10 month cold mission.

Hauser et al. (1998) extracted values for the extragalactic background at 140 μm and 240 μm DIRBE observations and upper limits at the shorter wavelengths. However, an accurate zodiacal model is required to subtract from the observations for this analysis. DIRBE improved upon the IRAS maps of the zodiacal background in several ways. Being an absolute radiometer with blocked impurity band mid-infrared detectors, the DIRBE measurements were mostly free of the non-linearities that plagued the IRAS observations. Also, the DIRBE extended the wavelength range into the near-infrared, thus spanning the transition from reflected sunlight to thermal emission. Kelsall et al. (1998) represented the DIRBE zodiacal observations in terms of a surface brightness model in which 45 free parameters were determined by a non-linear least squares fit to 87,000 observations. The average error in the fit was 2% although Kelsall et al. noted that biases were present. Wright (1998) developed a model, revised by Georjian, Wright and Chary (2000), with a different geometric representation of the zodiacal cloud that fitted 30 plus parameters to 10^5 observations under the weak (they claim) condition that the 25 μm residuals must be zero in the northern Galactic polar cap. Cambrésy et al. (2001) commented (as

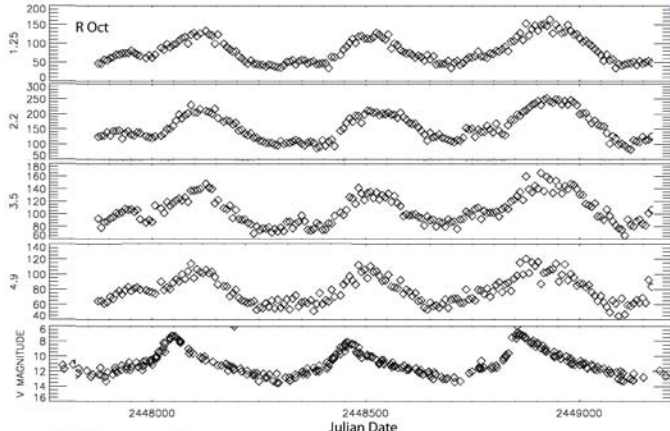


Figure 71. Three and a half years DIRBE near-infrared light curves for R Oct. The peak in the visible light curve precedes that in the near-infrared by a fifth of a period.

the Galactic plane at the fainter levels. However, it was the only large scale survey of the celestial sphere between 2.2 and 8 μm . The DIRBE stellar measurements not only filled in this wavelength gap but also densely monitored the infrared variability of sources. The Smith et al. (2002) paper on the infrared variability of bright Mira variable stars measured by DIRBE alerted Mike Egan and me to the fact that the COBE web based data tools hosted by Goddard included a capability to extract photometry on a specified source. We discussed modifying the point source photometry tool with Dave Leisawitz but we didn't have the funds when Dave had the manpower and *vice versa*, so the idea languished. We discussed the idea with Beverly Smith, East Tennessee State Univ., and assisted her in a proposal to AFOSR, which didn't pan out. However, Smith was successful with a modified version to NASA under which she worked with the Goddard people to modify the photometry tool and used it to extract observations of bright evolved stars (Smith, 2003) away from the Galactic plane. Point sources were then systematically extracted regardless of confusion, which produced the DIRBE point source catalog (Smith, Price and Baker, 2004) containing photometry on 11,788 of the brightest near- and mid-infrared sources in the sky. Smith, Price and Moffet (2006) extracted infrared light curves from the data and determined phase lags with respect to the visible. Smith and Price (2009) extended the variability analysis to a three and a half year baseline as may be seen in Figure 71 by extracted photometry from the weekly averaged maps archived during cold era and the post cryogen mission.

6.5. Personal Perspective

The Air Force funded the Background Measurement Program as a risk reduction capability to the SIRE. Since there was a considerable amount of complementarities in hardware development and data processing between IRAS and the AFGL Background Measurement Program, especially the Far-Infrared Sky Survey Experiment, I wrote to Dr. Gerry Neugebauer, the IRAS project scientist, on 6 February 1978 suggesting that an exchange of information on the Background Measurements Program and IRAS such as progress reports on the hardware and flight data tapes for software development would benefit both programs. Some technical exchange had already taken place such as the IRAS feasibility study and testing of SPICE detector material on behalf of IRAS. Dr. Neugebauer declined this offer, replying in his 1 March

have many others) that parametric models are not unique and that artifacts remain after various models has been subtracted from the data. Thus, zodiacal models have to prove themselves against the yardstick of the DIRBE measurements.

Because DIRBE was optimized to measure the diffuse background, the detectors were large (0.5 deg.²) and the data processing was tailored to extract the low frequency components of the observations. DIRBE did measure stars, although at ~200 times lower sensitivity at 12 and 25 μm than IRAS and it was hopelessly confused along

1978 letter that “... *the aim of the IRAS policy is that no one, including IRAS team members, should be in a privileged position with respect to the data. Consequently, we are issuing frequent public bulletins giving objects of special interest and we have set up a publication system which does not give privileged access to anyone*” (underline is in the original). On the other hand, he did hope that we might provide “... *FIRSSE tapes to the IRAS project ... they would be extremely useful.*”

I believe that my interest in the IRAS mission data was misunderstood. I had no desire to ferret out some discovery through privileged access. Rather, I wanted to understand the distinctive aspects of the sensor performance since such was needed to intelligently use the IRAS data for Air Force purposes. For example, IRAS used detectors that we knew displayed non-linear behavior. Did this behavior create the zodiacal dust bands? Was it responsible for the difference in zodiacal background levels between IRAS and the AFGL experiments noted by Beichman (1987)? If so, how much of the problem was attributable to IRAS? The IRAS database was going to be mined for years to come and understanding the nature and limitation of the data were essential for us in addressing Air Force celestial background issues.

From its inception, IRAS was the logical successor to the AFGL rocket-borne infrared surveys and we committed appreciable effort to the initial phases of that program. Both Tom Murdock and I wrote sections of the initial IRAS proposal, and we assisted the team in the final proposal preparations on Russ Walker’s behalf. Thus, it was more than a bit disappointing to hear through the grapevine that we (among many others) were removed from the IRAS team when NASA accepted the proposal.

We, at AFGL, were directed by letter from HQ Air Force to provide whatever assistance and information that NASA required for the IRAS. To this end we cooperated fully with the IRAS feasibility study team, led by Mike Hauser, and exercised our data processing software to determine run times so that the IRAS processing group at JPL could size the magnitude of their task and, as noted in Chapter 4, provided data against which JPL could exercise their algorithm development. We isolated the unconfirmed sources specified by the feasibility study team; some of these results are shown in Figures 28 and 29. However, it is likely that the close similarity between the AFCRL/AFGL source extraction and quantification routines and those used by IRAS had more to do with the fact that these were ‘optimal’ established procedures, rather than the day I spent describing them in detail to the IRAS data processing team at JPL. Robert Pelzmann (1976, 1977a) also described the AFGL routines, incorporating many *verbatim* extracts from AFCRL and AFGL technical reports in NASA Ames Research Center internal reports that supported Henry Lum’s bid for the IRAS data processing task.

IRAS promised to be *the* infrared celestial database and it behooved us at AFGL to exercise the data for DoD infrared celestial background modeling. My overtures to collaborate with some of the IRAS team members after the appearance of the March 1984 announcement issue of the *Astrophysical Journal Letters* were futile. However, I did discuss the various aspects of the IRAS data in which I either had an interest or questions with Bouwewijn Baud and Joop Renes at the June 1984 Baltimore meeting of the American Astronomical Society. Renes was presenting a summary of work on *Processing of Compressed IRAS Data* at the meeting while Baud had a poster paper on *A Giant Asymmetric Dust Shell around Betelgeuse* using the compressed data. I had received several IRAS internal monographs written by Joop Renes and Douwe Beintema on collapsing the IRAS database by B-spline convolution (e.g. Renes, 1979; Beintema, 1979), which had been incorporated into the IRAS Preliminary Analysis Facility (Renes and Beintema, 1981). Renes worked for the Dutch National Aerospace Laboratory and,

with the successful implementation of the spline processing, went on to other things after the IRAS mission. Boudewijn Baud was at the Laboratory for Space Research (SRON) in Groningen, Netherlands, which had a complete set of the IRAS data as well as the condensed spline tapes. I was most interested in the spline data as that could be more easily used to address the detector non-linear response questions I had. I discussed these issues it with Boudewijn Baud and he indicated that it might be productive for me to spend some time at SRON.

We exchanged letters regarding research at SRON during which time I found that I could travel on permissive temporary duty (business travel) for up to 180 days; the permissive status in this case meant that I agreed to receive less than the full per diem reimbursement. I set about arranging a six month stay at SRON beginning in July of 1984. Boudewijn suggested that I defer the start of my stay to the beginning of the school year in September, but personal and profession (BEAM) commitments did not permit this. I arrived in Groningen in late July 1984, a bit to the surprise of the administrative staff at SRON. Little preparation had been made for my arrival, in part because Boudewijn had accepted an offer to work at Fokker and his attention was directed to wrapping up things at Groningen. I activated the Eurail pass that I bought in the US and spent the next two weeks touring Europe with my wife and daughter. Upon returning to Groningen, the immediate task was to settle in and find a place to stay.

I had heard about how bicycle oriented the Dutch were and took my 10 year old Raleigh over for transportation. What a hassle, but one worthwhile in the end. The SRON staff found an apartment advertised in the paper about 7 miles from the institute, a convenient commute by bike paths. However, it took a while to get used to the rules of the road. The Dutch commuting bicycles were tanks compared to the Raleigh and I had to watch my speed. None-the-less, I did bump into a couple of people: one was a youngster coming from a blind feeder path onto the main bicycle path without looking; the other was an older gentleman who decided to suddenly turn around without warning in the middle of the path. However, the absolute yield to the right remained a problem. I was used to absolute right of ways at intersections from New Zealand, but with regard to bicycles this extended to cars exiting parking lots and my close brushes were a concern for Douwe Beintema with whom I most frequently rode.

I would often ride around the area to sightsee on the weekends usually north of Groningen. As with most of the country, Groningen was surrounded by farms. Tooling down a country road in the fall, I would come across a huge pile of sugar beets next to, and sometimes into, the road. Sugar beet was a major local crop and processing plants in the eastern part of the city, the industrial section, created a miasma of earthy-sweet redolence in late September – early October when the wind was blowing in the right direction.

The land outside the city was low-lying generally at or below sea level and important structures such as historic churches or manor houses (small castles), called borgs, were located on slightly raised areas. The low lying topography created some unusual sights. Cycling with Douwe in the Drente province south-east of Groningen, I noticed a fellow wind-surfing above me on a grassy rise. Douwe explained that he was on a canal that was raised above the ground and used as a drainage channel for the area. Another interesting sight on that trip was a stand of the last remaining original hardwood in the country and the remnants of a peat bog that had long since been exhausted. Another time I was cycling into the institute the morning after a pretty intense North Sea storm. Most of the way was low-lying and awash except for the bicycle path, which was slightly elevated. One had the feeling of riding on the surface of the water.

Thijs deGraauw, the SRON director at the time, persuaded me that I should learn Dutch since I was staying in the country for a while. I counter-argued that I wasn't staying long enough

to justify paying the expense out of my pocket for the language course taught by the Rijksuniversiteit that hosted SRON. We compromised by splitting the cost. This was a late afternoon class held a couple of days a week and attended by a diverse group of people, most of who were immigrants there to learn to speak Dutch as a necessity of their employment. I made pretty good progress during the first five or six weeks after which I could carry on a pretty decent social conversation for a few minutes. However, I noticed that although I could initially engage the people at the institute, they would switch to English when they felt the conversation wasn't progressing fast enough. My ability hit a wall when the class got to helper verbs (have or be, for example). I just couldn't master the Dutch implementation.

I returned to the US in mid-December, a month before the end of my permissive TDY. The University and SRON closed for the two plus weeks of Christmas vacation and it made little sense to hang around only for the final two weeks of TDY. Owing to several factors, I didn't do much with the IRAS data, itself. However, my stay at SRON was quite productive. I learned a lot about the mission operations and the data characteristics from the SRON scientists who had spent time at the IRAS Preliminary Analysis Facility at the Appleton-Rutherford Lab in England and the full up processing facility at JPL. I also established a professional relationship with the SRON astronomers through which they supported the background characterization work at AFGL. This collaboration led to my being appointed to the Dutch-German Short Wavelength Spectrometer consortium as a co-Investigator. This spectrometer was one of the four focal plane instruments on the European Space Agency's Infrared Space Observatory. Shortly after returning from the Netherlands, I was off to Brazil for the BEAM expedition. The rocket, payload and our laboratory people were first to arrive in the field to unpack for BEAM and set up. I arrived a week later and encountered visa problems. We had obtained the six month multicolor Brazilian visa about three months earlier and I was told at the Rio de Janeiro airport that although the visa was supposed to be valid for six months it had to be used within a relatively short period of time after being issued! I provided the port of entry people with the contact information for our Brazilian Air Force liaison but it was several hours before I was cleared. I missed the flight to Natal and the next flight was in the early evening about 10 hours later. I lounged around the airport for a while then rented a cab for a couple of hours to tour the city, including to the top of Sugarloaf. I finally arrived at Natal and was relieved to rest up at last in the rather decent motel that our lab and payload crew were staying at on the beach a few miles from the range. The port city of Natal was about 10 – 15 miles north of the motel.



The Barreira do Inferno rocket range was named for the red cliffs that jut into the nearby Atlantic ocean. Loosely translated, the name means the gates of hell and was so called because the red in the cliffs were reminiscent of flames when viewed during the day from far enough at sea. The area around Natal and the range was labeled as jungle although the vegetation was much sparser than what one would see in the National Geographic. However, there were plenty of tropical aspects to the area. There were green frogs on the range the size of small dinner plates. Tropical produce and seafood were readily available and

the fruit selection at the hotel breakfast was always quite plentiful. On weekends, small cafes would be set up on the beach with portable stoves, card tables, chairs and beach umbrellas being hauled in by small trucks or Volkswagen buses. The principal menu item was fish and you were assured that the fish was swimming in the ocean less than an hour or so before it was served. We certainly dined well during the trip. For me the dinner highlights were carne del sol aged beef and the churrasco or Brazilian barbecue.

On my first day on the range, I completed the necessary access paperwork and Chuck Howard, our Aerospace Instrumentation Division point man, introduced me to the base commander. Chuck did a superb job in coordinating our requirements, which was no easy task as I had the impression that the base commander was not completely happy with the fact that we were being hosted on his range by the Air Force command based in San Jose, a completely different military organization than his.

The range upper management was sensitive regarding the launch of foreign rockets. Earlier in the year, a German experiment had gone seriously off course and landed within a few miles of one of Brazil's major hydroelectric facilities. So, our request to alter the normal due east flight profile to fly as near as possible to avoid the worst effects of the South Atlantic Anomaly was vigorously discussed. Finally, we reached an accommodation to set a NNE course and, at least this time, the rocket went where predicted.

Preparation for the launch went well until the $t - 3$ day test. As may be seen from Figure 68, the launcher is much larger, heavier and sturdier than the Nike launcher we had at Woomera. However, it is still an erectable standing structure and, as at Woomera, the cryogen fill for the sensor had to be done at the payload preparation area and then the payload carted to the launcher where it was mated to the rocket, the clean bags removed and the launcher erected. Since the sensor was horizontal during all this time, which increased the cryogen boil off rate, the premium was on doing these steps as quickly as possible. The $t - 3$ day test was a disaster of miscommunication between our team and the Brazilian support crew and confusion in the blockhouse. Next day's post mortem started off somewhat rancorously but soon settled down to making it clear as to who does what and when. I took over as the experiment representative in the blockhouse where my primary duty was to check off the items on the procedure checklists for preparing the rocket, payload and sensor as they were accomplished. My checklists were backups to the ones the preparation teams were executing and I would only be called upon if there were a serious problem that caused a delay. Fortunately, on launch night nothing was delayed long enough that an 'executive' decision was required.

Several hours before launch the blockhouse was full with the launch officer, me, the range commander, people doing wind weighting and others. As the countdown progressed I became more intent on ticking off the items on the checklists as they were announced. The pace of the tasks quickened as launch approached until about $t - \frac{1}{2}$ hour. I glanced up and was surprised to find the blockhouse empty except for the launch officer and me; everyone else had stepped outside to watch the launch. I did the same at $t - 0$ and watched the Castor motor burn for about 20 seconds before going to the next room in the blockhouse where we set up our telemetry ground station. As we counted out the flight time events, we noticed that separation was delayed and when it occurred something was wrong. We watched through the time by which the system was to have been despun without a decrease in roll rate. Furthermore, there were no sensor signals. Well before peak altitude it was depressingly obvious that the experiment had failed.

Thus, our series of infrared probe-rocket borne astronomy experiments ended on a down note. But this was not for lack of trying for just one more success. As previously mentioned our proposal for a SPICE flight from Kauai to measure a specified target and an ELC II experiment to try to observe structure in the disturbed atmosphere in addition to the visual – infrared zodiacal background were submitted to Space Division but were not funded; the last thing I did before going to Groningen was to rewrite the ELC proposal in the format specified by SDIO – but nothing came of this. Besides BEAM, internal AFGL funds supported the small shuttle based VIPER visual photometric experiment to measure the zodiacal background, which failed to return useful data. The DIGBE work began on a shoe-string internal budget in the mid-1980s but the experiment foundered when Rockwell decided not to provide the infrared photon counting focal plane at cost. After DIGBE, we revamped our approach and proposed small, relatively inexpensive rocket borne experiments to address a single question, such as the atmospheric vertical profile of atomic oxygen but also were unsuccessful. Our swan song with regard to probe-rocket flights was the marginally successful SPIRIT II experiment.

We also approached NASA. We proposed to refurbish the ZIP 1 sensor and fly it as a throw-away experiment from Kauai into the 11 July 1991 solar eclipse to measure the near- to mid-infrared emission from the zodiacal dust near the Sun. I talked briefly with the NASA discipline scientist to whom the proposal was sent at an Infrared panel meeting of the National Academy of Science study for the 1990 decadal report but he had no recollection of receiving it. Some Schafer Corp. managers heard of the proposal and liked the idea of putting ZIP on a satellite. They suggested we assemble such a proposal and submit it out of cycle. We did so but also to no avail. Perhaps our best thought out proposal to NASA was for a Near-infrared Astronomy Satellite. This was collaboration with the Smithsonian Astrophysical Observatory, as lead, and a number of other institutions including AFGL under which we were to supply the FIRSSE Perkin-Elmer optical system that was surplus after the FIRSSE flight. This proposal also was rejected but left a legacy as will be explained in Chapter 9.

Thus, by the mid-1980s we were truly out of the business of fielding our own celestial experiments. The laboratory field crew held on for the better part of another decade, in part supporting small instruments such as the AFGL imaging spectrometer and the atmospheric experiments that we had inherited in the merger of the Celestial and Atmospheric Branches. Future astronomy experiments would have to be on satellites flown by other agencies.

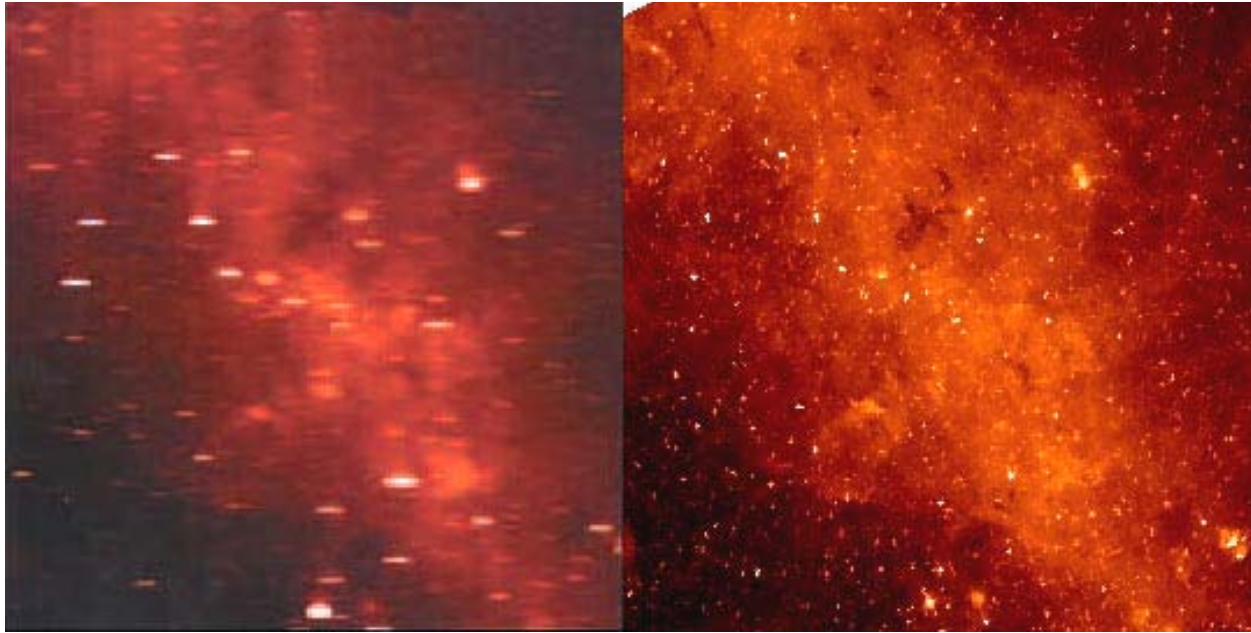


Figure 72. An IRAS – MSX comparison in the Galactic plane at 355° longitude.

7. BACKGROUNDS AT HIGH RESOLUTION AND SENSITIVITY

In the 1970s and early 1980s, performance studies for infrared surveillance systems to operate in the most stressing mission scenarios led to a definitive set of sensitivity and resolution requirements: a spatial resolution of $10 \mu\text{rad}$ ($\sim 2''$) and a knowledge of the sky to an irradiance of $4 \times 10^{-21} \text{ w cm}^{-2} \mu\text{m}^{-1}$ at $10 \mu\text{m}$ or [10] ~ 11 mag. Consequently, the contemplated systems designs tended to have apertures of ~ 1 m. The IRAS mid-infrared detectors subtended a solid angle ~ 3 arcmin 2 , or 3.7×10^{-7} sr and a detection limit of $\sim 2 \times 10^{-19} \text{ w cm}^{-2} \mu\text{m}^{-1}$, but the system requirements were about 100 times more stringent.

Figure 72 graphically demonstrates the ability that a higher spatial resolution system has to separate closely spaced objects and distinguish sources in regions of high source density and clutter. The IRAS $12 \mu\text{m}$ image on the left has the best resolution that can be achieved using linear procedures to create images from the survey data (Kennealy et al., 1994). The $8.3 \mu\text{m}$ MSX image on the right was extracted from a much larger panoramic image that has a resolution of about $45''$; the inherent MSX resolution was about half that. Not only are the stellar signatures smaller in the MSX image but the complexity of the extended structure is much better defined.

7.1. The Large Aperture Infrared Telescope System

At the end of the 1970s, Tom Murdock led an AFGL effort to define the design requirements for a sensor to acquire a missile in early midcourse, track it and quickly predict a trajectory and impact point. The SAMSO programs, particularly SIRE, were burdened by mission creep that seemed to have diluted the objectives for which they were originally created and by the consequent increased cost and weight. Furthermore, the SIRE aperture was a third of a meter and could not meet the recently defined performance requirements. We felt that we could build a meter class sensor in the Lab and, beginning in 1981, allocated in-house funds to a conceptual design of a Large Aperture Infrared Telescope System (LAIRTS). Space Division

was initially interested in LAIRTS for risk reduction as it would prototype the engineering required for sensor risk reduction. We also recognized that although IRAS and COBE were in the queue, LAIRTS could also serve as a pathfinder mission for NASA's SIRTF infrared observatory, which was well deferred at the time.

The Laboratory established the Infrared Backgrounds at High Spatial Resolution in-house work unit¹² with Tom Murdock as manager; the name reflects the principal system goal. The work unit objective was to develop the LAIRTS lightweight aluminum optics, to scope the on-board electronic processing necessary to handle the high data rate from the infrared mosaic focal planes that were in the early stages of development and to design the system pointing control. With regard to the last task, we explored the cost savings of using the Talon Gold pointing system, which had demonstrated more than sufficient pointing accuracy before it was shelved in 1985. The Defense Advanced Research Agency (DARPA) offered the platform because LAIRTS could be considered a replacement for the Talon Gold sensor that had not been funded. A concurrent AFGL Aerospace Instrumentation Division in-house work unit was created to develop and flight test a superfluid cryotank assembly for LAIRTS. FIRSSE had provided our first experience with superfluid helium but a much larger system was needed for the LAIRTS Shuttle flights. Analogously, the principal engineering objective of NASA's Spacelab 2 Infrared Telescope was to test the behavior of a large superfluid helium tank in the Shuttle environment.

Regan (1988) summarized the original LAIRTS concept: a diffraction limited (at 5 μm) four-mirror off-axis telescope with a mosaic array camera and an imaging spectrometer. The original design specified a ~80 cm by 56 cm elliptical primary mirror in a telescope that had to fit within a 39" (99 cm) diameter cylinder, be $\leq 96"$ (2.44 m) long and weigh less than 250 kg. Two focal plane instruments were baselined: a two-dimensional array camera with a 24 position filter wheel that covered the 5 – 25 μm spectral range and a 2 – 24 imaging spectrometer. A three mirror optical relay to the camera increased the plate scale so that the array covered a $1^\circ \times 1^\circ$ field of view. The imaging spectrometer was to have short and a long infrared component each of which used an etalon in the initial design for high spectral dispersion between 2 and 24 μm .

As Jamieson (1995) noted, the DoD began a concerted and well funded effort to improve extrinsic Silicon detector performance and to create two-dimensional infrared arrays. Given the early development status of the arrays, we needed experience with their use. A work unit was established in 1984 under the direction of Paul LeVan to build the read out electronics for the 58×62 pixels of a Si:Ga engineering array that the Army had lent to us. This camera was to be used to obtain 8 – 14 μm spectra of astronomical sources but we planned to incorporate a similar mosaic array into an imaging spectrometer camera to obtain spectra in one direction of the array over a linear field of view in the other (LeVan, 1990). Since two-dimensional arrays create large volumes of data, AFGL also funded the Oklahoma State University telemetry group who had supported most of our probe-rocket experiments to design a data storage system for the 128×128 arrays (Gwinn, 1985) contemplated for early LAIRTS operations.

A considerable amount of progress was made by the time of the May 1985 preliminary design review (PDR). Tom Murdock had twice briefed the DoD Space Experiments Review Board (SERB); the SERB provides the ride and mission operations for DoD space-based experiments at no cost to the Laboratory. Performance trade analyses by the Sensor Systems Group (SSG), who built the ZIP sensors, led to a 25% reduction of the size of the optics with a

¹² The Laboratory research management was structured at the time into large scale projects, which are divided into tasks that defined an area of research. A specific effort within a task was assigned an in-house work unit with formal reporting requirements on progress.

more circular 24" (61 cm) primary mirror. SSG also built a two-thirds scaled version of the LAIRTS primary to demonstrate the manufacturability of light weight aluminum mirrors. This 16"×13.75" (41 cm ×35cm) elliptical mirror had a 3" (7.6 cm) thick honeycombed substrate, which reduced the total weight of the mirror by 60%. Mastandrea, Benoit and Glasheen (1989) described tests of this mirror at cryogenic temperatures. Although SSG's manufacturing methods were successful, they did find that stresses between the electroless nickel plating and the aluminum substrate induced by cooling the mirror distorted the figure. Polishing and figuring the substrate after removing the nickel plating eliminated the problem.

Given FIRSSE's qualified success, we were interested in accelerating the development of the long-wavelength technology. Consequently, Kandi Shivanandan (1988) designed a high resolution ($1000 < \lambda/\Delta\lambda < 10000$) 50 to 200 μm Fabry-Perot spectrometer for LAIRTS under AFGL sponsorship; he presented the design of this spectrometer at the LAIRTS PDR. Since LAIRTS was to be shuttle-based, focal plane instruments could be switched between flights. In a similar study, Bob Gehrz, University of Minnesota, also presented a concept for a mid-infrared spectrometer at the PDR. This instrument design was conducted within the greater context of AFGL teaming on his proposal to build the SIRTF spectrometer in response to the NASA SIRTF instrument announcement of opportunity that had come out in May 1983, so many aspects of the design could be used for both SIRTF and LAIRTS. However, Jim Houck's Cornell University team won the SIRTF spectrometer bid in 1984.

In 1982, AFOSR let it be known that they were interested in supporting 'flagship' facilities, national scale experiments that would produce major breakthrough results. In March of that year, John Garing, the Optical Physics Division Director, and I presented the LAIRTS concept and expected scientific return to the AFOSR vice-commander, Col. Baker, who had been the AFGL commander between 1979 and 1981. AFOSR decided that LAIRTS fit their objectives and provided AFGL with a substantial amount of research funds, \$1M/yr, in 1984. The catch was that the money had to be managed directly by AFOSR and we could not use it for in-house support for the program. The AFOSR LAIRTS related funding supported two categories of contracts. One directly funded some aspect of the LAIRTS program; the others were contracts that Henry Radowski, the AFOSR program manager chose to renew using the development of mosaic array readouts for LAIRTS as a rationale. These contracts were to Trinh Thuan at the University of Virginia for imaging and spectroscopic analysis of galaxies and Dennis Hegyi at the University of Michigan to measure the optical cosmic diffuse background. Marcia Lebofsky (1989), University of Arizona, also built a focal plane package under an AFOSR contract for the Kitt Peak 72" transit telescope around a 32×32 element Rockwell near infrared CCD that was to be used for a 12 deg² survey to a 2.2 μm magnitude of 17.

AFOSR contracts for LAIRTS support also were given in consultation with AFGL. Kandi Shivanandan put a Si:Ga mosaic array into their Fabry-Perot interferometer to attempt observations on the UK Infrared Telescope Facility as a proof-of-concept for the LAIRTS spectrometer. AFOSR also provided a multiple objective contract to Richard Shorthill (1990; also Vogler, Johnson and Shorthill, 1991) at Utah University to improve thermal modeling of asteroids so that they could be used for calibration, to calibrate whole disk thermal emission from the Moon against laboratory standards and to transfer this calibration to Vega, Mars and Venus. Tom Murdock also had AFOSR provide a small contract to George Smoot at the University of California, Berkeley to build a He³ refrigerator cooled bolometer that might be used to detect small anisotropies in the cosmic background at mm wavelengths from ground-based telescopes

(Smoot, 1990) with an eye toward space applications on LAIRTS. Tom had met Smoot at the COBE Science Working Group meetings, which he had been attending since 1976.

At AFGL's behest, AFOSR subsequently issued several contracts to understand the brighter IRAS and AFCRL/AFGL sources. Susan Kleinmann (1988) at the University of Massachusetts analyzed the statistical properties of the sources measured by IRAS. At the University of Wyoming, Paul Johnson and Harley Thronson measured the brightness distribution and polarization of a number of the regions around sources with circumstellar dust while John Hackwell and Earl Spillar were to measure the brightness distribution at high spatial resolution of a selection of resolved AFGL and IRAS sources. Steve Little, from Bentley College, joined our AFGL group for a two year National Research Council senior post-doctoral fellowship in 1984. He teamed with the Wyoming group to obtain high resolution near-infrared maps of the giant H II region W51 (Little et al., 1989). These efforts also supported the high resolution investigations conducted under the AFGL backgrounds characterization program. Finally, Alan Bentley (1989) was given a small contract to model the background as a planning tool for scheduling the LAIRTS observations.

Tom Murdock (14 February 2002 and 19 October 2006 e-mails), recollected that the LAIRTS demise came when Col. Friel, the Space Technology Center commander to whom AFGL then reported, called a meeting with the AFGL commander, Col. Joseph Morgan III, Tom Murdock and Col Wormington, the Space Division manager for the Space Surveillance and Tracking System (SSTS) Special Programs Office; SSTS was the successor concept to the SBSS. Cols. Friel and Worthington concluded that LAIRTS should be terminated because it would not be able to provide the requisite data for the SSTS design decision deadline in 1986, missing the Preliminary Design Review date by eight months. Less than three weeks after the meeting, Space Division announced a three year slip in the SSTS schedule. Seeing no personal future with the Air Force, Tom Murdock resigned from AFGL in June 1985 to take a position with General Research Corp the day following that announcement.

With the end of the LAIRTS program, AFOSR reduced funding for the related university contracts by not renewing the initial efforts as they terminated. Emphasis for the remaining contracts was shifted to innovative astronomical techniques. These included Paul LeVan's imaging spectrometer effort at AFGL (Sloan, LeVan and Tandy, 1993). Mel Dyck and James Benson, University of Wyoming, received funds to develop an infrared speckle interferometer in order to measure the angular diameters of dust shells around red giant stars, the initial results from which were published by Benson, Turner and Dyck (1988). The contract objective of the University of Massachusetts was changed to support prototyping the Two Micron All Sky Survey effort (Kleinmann, 1992; Kleinmann et al., 1994).

7.2. Celestial Background Characterization and Modeling

Dr. Barry Katz came to SDIO in the mid-1980s from the Naval Weapons Lab to manage the Surveillance, Acquisition, Track and Kill Assessment SATKA S32.1 program. He became interested in creating a Strategic Scene Generator that would condense the acquired knowledge of the backgrounds into models and databases that could be used to generate realistic background scenes onto which threat scenarios could be overlain. This tool would be invaluable for design trade studies and risk mitigation for proposed space-based surveillance systems. Tom Murdock had met Barry after leaving AFGL and recommended that he contact AFGL for the celestial backgrounds modeling. Subsequently, the Strategic Defense Organization (SDIO) began funding AFGL in 1986 to create first principles physics-based models that would accurately

describe the characteristics of the Celestial Background in any user defined infrared spectral band at a user specified spatial resolution. These models were to be packaged into a Celestial Background Scene Descriptor (CBSD) that would paint realistic scenes from the background component models and databases.

The approach was to analyze and improve upon the existing data and to interpret the results into component codes such as models for 1) Galactic point sources, 2) discrete extended sources, 3) filigreed large scale emission 4) the zodiacal emission and 5) moving sources in the solar system. Once validated, the models were to be incorporated into the scene generation capability. But first one had to obtain the necessary data.

7.2.1. Resolution Enhancement of the IRAS Data

The IRAS performance was limited by the background as demonstrated in Figure 73 in which the logarithm of the flux of every 100th source in the *IRAS Point Source Catalog* is plotted as a function of the sine of Galactic (left) and ecliptic (right) latitudes; equal areas of sky are encompassed by the same interval in the sine of the latitude on such a plot. Photon background noise limited behavior of the IRAS 25 μm detectors is evident by the dependency of the minimum source flux on ecliptic latitude. Because sources are extracted at the same signal-to-noise ratio, the minimum source flux is higher in the ecliptic plane where the zodiacal background, and the attendant photon noise, is elevated. The minimum source flux decreases monotonically to the ecliptic poles as the background decreases.

The degradation in IRAS' ability to distinguish sources in regions of high source density is shown in the left plot in Figure 73 in which the logarithms of the fluxes for every 100th 12 μm source near the Galactic plane within 30° of the Galactic center are plotted at left. The source density is high in the inner Galactic plane and, as may be seen in Figures 64 through 67, there is also quite a lot of structured emission from the interstellar medium. The combination of high source density and structured emission created confusion and clutter noise for IRAS, which resulted in fainter sources not being detected. The nominal IRAS minimum 12 μm and 25 μm detectable flux of about 0.4 Jy was increased by up to a factor of 10 along the inner Galactic plane. The IRAS data processing team empirically determined that, for the 3.7×10^{-7} sr beam size of the 12 and 25 μm IRAS detectors, confusion set in at an area density of about 25 sources/deg².

The limits imposed by background photon noise may be improved by co-adding all the data obtained on a given area of sky. Kleinmann et al. (1986) did this for the 1813 pointed Additional Observations (AOs), the raster (back and forth) scans over the same approximately one square degree of sky. Kleinmann et al. extracted nearly 44,000 sources from the ~ 1100 deg² covered by these observations and compiled the results into an *IRAS Serendipitous Catalog*, which is on the average five times more sensitive than the IRAS survey. However, fields with 40 or more sources/deg² were still dominated by confusion. On a larger scale, Moshir et al. (1992) co-added the 8 to 12 overlapping survey observations to create the *IRAS Faint Source Survey*, which contains $\sim 173,000$ sources to approximately 3.5 times lower flux than the survey. Again, confusion limits the catalog to latitudes greater than 10° away from the Galactic plane.

Improving source detection in confused regions requires increasing the spatial resolution through image enhancement procedures. This problem is simply stated but its solutions are far from easy. The observed image on a two-dimensional (x,y) grid may be mathematically described by:

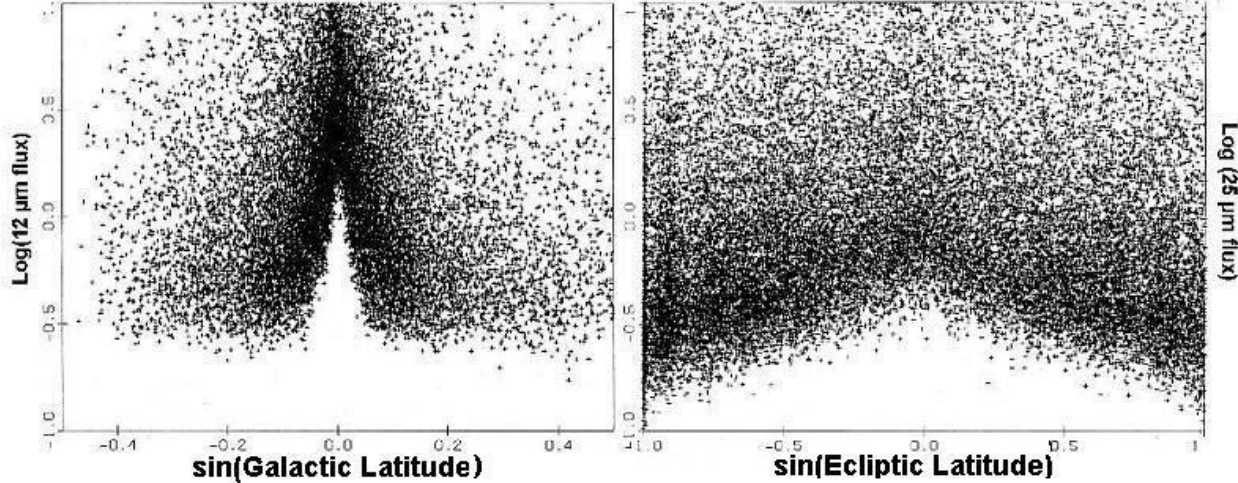


Figure 73. IRAS background limited performance. The flux for every 100th source in the *IRAS Point Source Catalog* is plotted as a function of the sine of the Galactic (left) and Ecliptic latitude (right). Vertical bands of equal width encompass the equal areas of sky. The image at left shows the sensitivity loss due to confusion and clutter along the Galactic plane. Photon noise from the zodiacal background in the right hand plot makes the minimum extracted source flux a function of ecliptic latitude.

$$D(x, y) = P(x, y) * I(x, y) + N(x, y) \quad (6)$$

where $D(x, y)$ is the observed image, which is formed by convolving (designated by $*$) the system response function, $P(x, y)$ with the true image, $I(x, y)$, to which the measurement noise, $N(x, y)$, is added. In the convolution operation, $P(x, y)$ is centered at every (x, y) grid position and the $P(x, y)I(x, y)$ product at each point is integrated over x and y . The simple solution divides out the response function by multiplying the equation by its inverse. Symbolically, in matrix notation:

$$I \sim (P^T P + \langle N^2 \rangle)^{-1} P^T D \quad (7)$$

the transpose of the response function, P^T , is the response function displaced both vertically and horizontally. The convolution in Equation (6) is a filter that smears out point sources and sharp edges and increases the overlapping of closely spaced sources. The inversion in Equation (7) is inherently unstable, in large part because the higher spatial frequency information is attenuated by the filter and the inevitable measurement noise is considerably enhanced by linear inversion. Thus, an iterative solution is required with some form of positivity constraint such that no part of the true image is negative. However, as Puettner, Gosnell and Yahil (2005) noted in their review article, the iterative procedures used to solve the equation are many and varied. At AFGL, Paul LeVan (1985) explored a maximum entropy metric, a popular approach at the time, to improve the inherent spatial resolution of the SPICE and FIRSSE measurements with an eye on applying it to AFGL array spectrometer data (e.g. Appendix I of Sloan, LeVan and Tandy, 1993).

As may be seen from Equations (6) and (7), the raw data and an accurate representation of the system point response function are needed to optimally enhance the spatial resolution of the IRAS data. Since the data were not generally available in 1985/1986, AFGL gave a contract to SRON in March 1986 through AFOSR (only AFOSR could provide AF research funds to European institutions) to address a number of IRAS data quality issues, one of which was to develop and apply image enhancement techniques to improve the sensitivity, resolution and

quality of the images created from the IRAS observations. Another SRON objective was to derive an improved global calibration and to remove artifacts, such as heavy striping, that were apparent in the initial IRAS Sky Flux images.

IPAC became interested in improving the resolution of the IRAS data and, in January 1987, began a series of high-resolution workshops, chaired by George Aumann, for interested parties. IPAC also made the requisite information for image restoration available to the community. We allocated some of our SDIO background characterization funds to a Mission Research Corp. (MRC) contract to support our image enhancement effort. MRC had submitted a strong proposal with Jack Kennealy as principal investigator. Kennealy, who had done image enhancement on defense reconnaissance satellite data, teamed with Bob Gonsalves, the Director of the Tufts Electro-Optics Technology Center, who could draw upon graduate students to support the effort. However, we first needed the data, which IPAC provided in the form of position tagged fluxes from each detector in a scan and the individual detector responses.

Several aspects of the IRAS data seriously complicated image enhancement. The data were not uniformly sampled. Although a given detector was sampled at a constant rate with uniform position increments, the offsets between the two columns in an array and between arrays in the same spectral band meant that the detector outputs were not in phase, that is, the samples for different detectors did not occur at the same in-scan positions. Also, the detectors were not uniformly spaced in cross-scan. More problematic, each detector had a different asymmetric point response function. The Rockwell IRAS detectors also produced tails to bright point source after they was scanned akin to that in the upper right plot of Figure 61; LeVan (1985) had noted a similar asymmetry for the Rockwell SPICE detectors. Gonsalves (Korte et al., 1989) and Silbermann (1989) independently found that the tails were well represented by a decrease proportional to the inverse of the time after the point source was scanned. Although Deul and Walker (1989) modeled the tail by the sum of two exponentials, this formulation is virtually the same as the inverse time function over several exponential time constants. Even more problematic was the fact that the cross-scan responses varied from detector to detector with many of the detectors exhibiting hot spots, as may be seen in Figure 74. However, the most serious problem was that the detector tracks over a given region of sky on overlapping survey scans were not parallel and usually crossed.

The first step in the MRC processing was to interpolate the data to the same in-scan grid. The background was then subtracted from each scan, a necessary step for the positivity constraint to work but also it effectively removed the tails. Bob Gonsalves gave Michel Marcuse, one of his Tufts graduate students, the Master's thesis problem of putting the data onto a uniform grid with a minimum of distortion. The minimum mean square error (MMSE) interpolation that Marcuse (1988) developed preserved the inherent spatial resolution of the data, as may be seen in the top rows of Figure 74 and 75, producing a much better image than the standard IPAC product at the time even without image enhancement.

The key to the MRC resolution enhancement technique was the Filtered Entropy Restoration (FIER) procedure developed by Huei-Mei Kao (1986) for her PhD thesis. Gonsalves and Kao (1986, 1987) described the technique, while Gonsalves, Korte and Kennealy (1987) and Gonsalves et al. (1990) discussed its application to the IRAS data. This approach had the advantage of rapidly converging, which was critical to being able to process a large amount of data on the work stations available at the time.

Participants in the high resolution workshop agreed to tackle a single object, M51, a large infrared bright galaxy with a nearby companion, in order to inter-compare results derived from

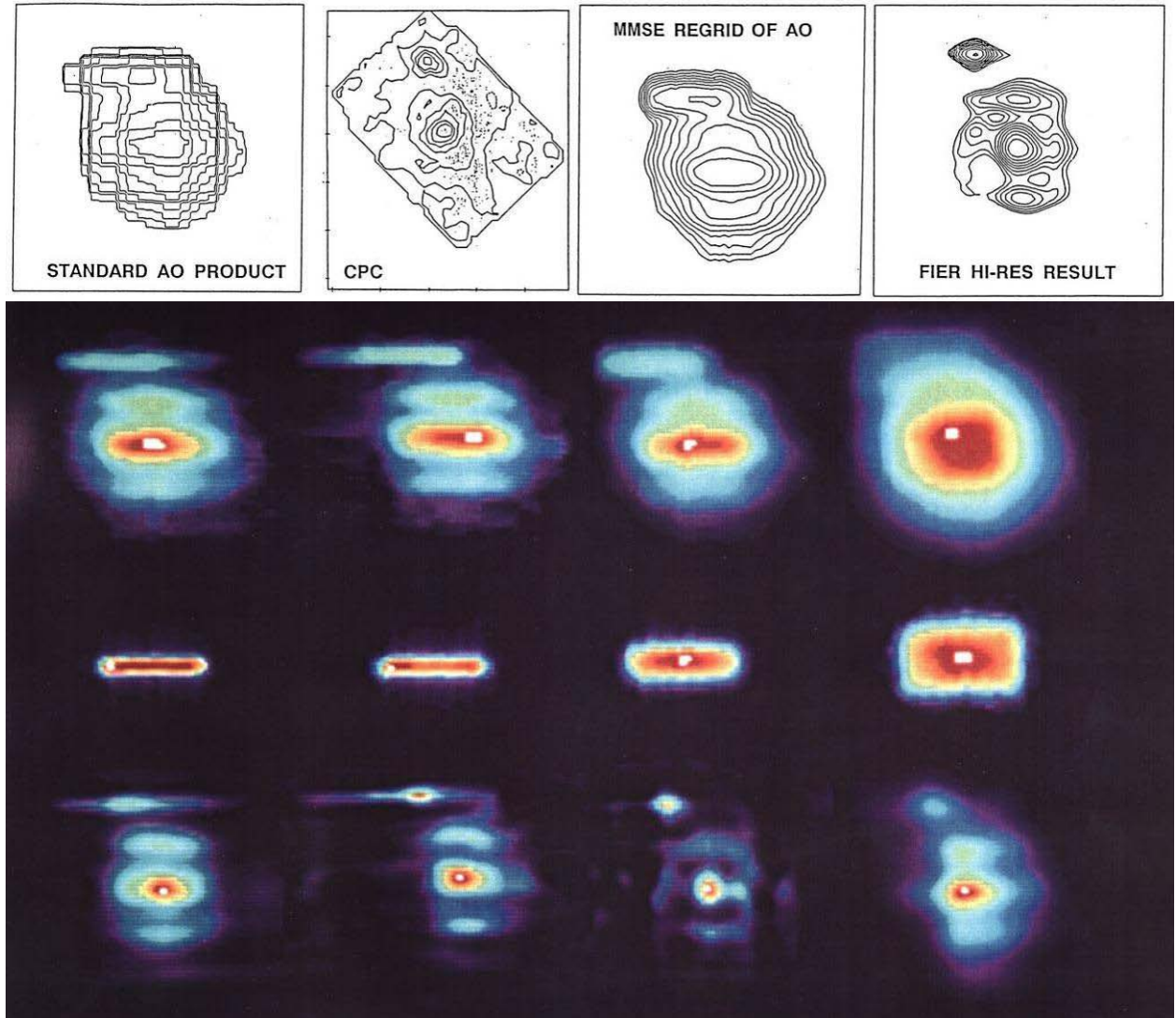


Figure 74. High resolution IRAS images of M51, a large infrared bright galaxy with a small satellite galaxy. Top row of plots show (left) the 60 μm image from the raster scanned Additional Observation (AO) of M51 with the standard IPAC imaging; (second from left) a 50 μm chopped photometric channel image at higher inherent resolution than the survey; (second from right) the minimum mean square error (MMSE) re-grid of the data; (right) the MRC filtered entropy restoration. The colored plots show the MMSE regrid (top row) for the 12, 25, 60 and 100 μm data from left to right, the point response functions used to deconvolve the data are in the middle row while the bottom shows the results of the deconvolution.

the different methods preferred by various groups. M51 had both an IRAS raster scanned AO, which simplified the data processing, as well as survey measurements. Gonsalves et al. (1987) published an early comparison of M51 deconvolutions using the maximum entropy method as implemented at AFGL and the MRC filtered entropy routine while Bonterkoe et al. (1991) presented their M51 results. The final MRC results (Korte et al., 1989) are shown in Figure 74 in which the top row of plots shows that the MMSE regrid routine, which is the step before the image restoration, produced a better 60 μm image than the IPAC standard imaging product. The 50 μm chopped photometric channel image has about three times better resolution than the survey detectors and is correspondingly better resolved than the MMSE image. The filtered

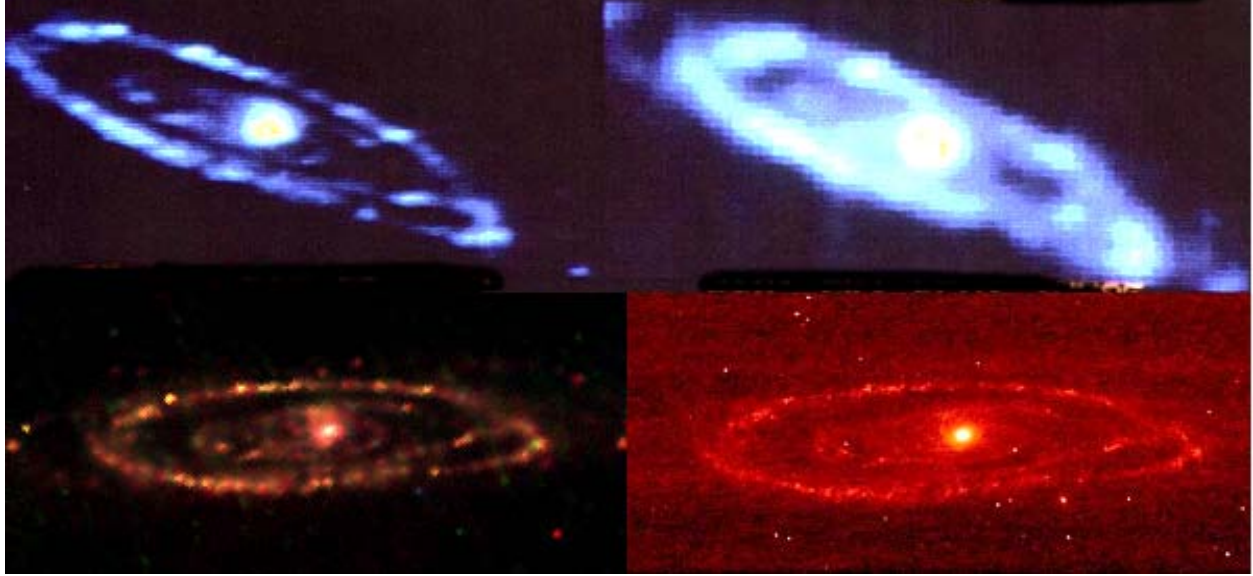


Figure 75. Enhancement of IRAS M31 observations. Top right panel shows the IRAS sky flux plate for this object, top left is the minimum mean square error re-grid. Bottom left is a maximum entropy deconvolution by Kester and Bontekoe. Bottom right is an 8.3 μm MSX image at an inherent resolution of about 20''.

entropy restoration provides even more detail. The minimum mean square error regrids of the data in the four IRAS bands are shown in the next panel (top row in color) and the point response function adopted for each band are in the next row. The filtered entropy results in the bottom row have improved spatial resolution with only a few deconvolution artifacts. An analogous comparison for M31, the Andromeda galaxy, is displayed in Figure 75.

Marcuse's formulation of the minimum mean square error interpolation assumed a triangular autocorrelation function (PP^T in Equation (7)), with a maximum value in the middle tapering linearly to zero at the edges of the detector aperture. Bob Gonsalves modified the procedure to account for the complex response function of each detector, which was provided by Mehrdad Moshir at IPAC, and to 'whiten' the result. Nominally, the result is a uniformly sampled image in which the 15 or so values of P and P^T needed in Equation (7) are reduced to a single response function, P_M , which is used to enhance the image. Gonsalves, Canterna and two of Canterna's graduate students, Rob Hermann and Leisa Townsley, drafted a paper: *A Mean Square Error Method for Iterative Image Restoration* that, unfortunately, was never published. However, good ideas are seldom lost and Pijpers (1999) developed and published the same formalism for single pass image enhancement.

In the end the different participants in the IPAC workshop preferred their own procedures to the exclusion of others. Aumann, Fowler and Melnyk (1990) chose a Maximum Correlation Method that they developed into the IPAC HIRES tool for IRAS data users to create enhanced resolution IRAS images upon request. Ron Canterna and Gary Grasdalen, at the University of Wyoming, preferred John Skilling's commercial Maximum Entropy Method version while Bontekoe and Kester, SRON, started a small business using their pyramid maximum entropy method (Bontekoe, Koper and Kester, 1994). Based on the successful initial effort, AFGL gave MRC a follow-on contract in 1990 to create high resolution 12 and 25 μm images of the IRAS confused regions using the filtered entropy approach and to catalog the sources extracted from them. The filtered entropy procedure was selected because it converged much more rapidly than the other methods, which was essential given the very large volume of data to be processed and

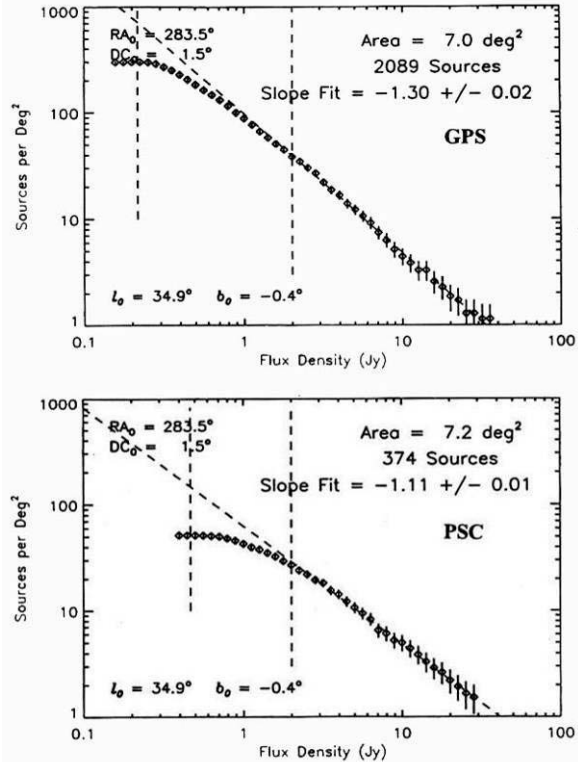


Figure 76. Cumulative source densities at $\sim 28^\circ$ longitude in the Galactic plane. MRC Galactic Supplement Catalog counts are at top, those from the IRAS Point Source Catalog are at the bottom.

within $\sim 5^\circ$ of the Galactic plane and in the Orion, Ophiuchus and Cygnus regions that were labeled as confused. The Wyoming team compared their results with the sources in the *IRAS Point Source Catalog* and ground-based 10 μm searches for verification. Since Wyoming used a different enhancement technique on a different dataset, they provided an independent assessment of the reliability and completeness of the MRC results. Kennealy et al. (1994) details the image enhancement procedures and summarizes the MRC and University of Wyoming results.

An impressive reduction in confusion noise was realized as may be seen in Figure 76, which compares the cumulative source counts per deg^2 from the high resolution work (top) with the *IRAS Point Source Catalog* (bottom) for same Galactic plane region. The dashed line at 2 Jy is the flux to which the *IRAS PSC* is complete in this region while the line to the left in each plot is the minimum source flux for the respective data processing. As may be seen, the high resolution processing extracted many more faint sources. At the June 1993 IPAC high resolution workshop, we confidently announced the imminent release of the supplemental catalog (Price et al., 1994) but, alas, Chapter 14 of the MRC report contained a number of caveats that noted errors in or desired improvements to the artifact and background removal, noise characterization and photometry. These were to be corrected in the second pass through the data.

We scrambled to re-process the data to account for the caveats. However, the principals involved, Jack Kennealy and Bob Gonsalves had moved on to other things, Bob Gonsalves to work on compensating for the Hubble Space Telescope being out-of-focus (e.g. Gonsalves and Nisenson, 1991). We decided to do the reprocessing at AFGL to correct what we then thought

the computational capabilities available in 1990. In contrast, Cao et al. (1997) used the Caltech super-computer with a modified version of the Aumann, Fowler and Melnyk (1990) algorithm to create a 60 and 100 μm high resolution atlas of the entire Galactic plane within $|b| < 4.7^\circ$.

MRC processed the region within $\pm 5^\circ$ latitude of the plane and $\pm 120^\circ$ longitude of the Galactic center, compiling the results into a 12 and 25 μm Galactic plane supplemental catalog. IPAC provided the data in the form of all the survey scans that crossed specified $6^\circ \times 6^\circ$ fields. The scans for a given field were sorted into quadrants 3.5° on a side and the data in a quadrant were divided roughly into ‘hour confirming’ scans. The hours confirmed scans were processed individually, allowing source extractions from two to three independent datasets for confirmation. As a quality check, MRC subcontracted with the University of Wyoming to deconvolve the smaller dataset of pointed observations in and near the Galactic plane with the maximum entropy processing and to extract the sources. The University of Wyoming processed the data from the roughly 300 raster scanned additional observations

was the most significant error – the incorrect assumption that the HCON scans were parallel. This assumption reduced the number of times that the matrices implicit in Equation (7) had to be calculated from once per output grid position to once per grid column. However, the assumption created spurious sources, eliminated real sources and distorted the photometry where the scans crossed. We recoded the imaging routine to calculate the matrices for each grid point using actual detector positions. Once we got into the codes we found a number of other conceptual and programming errors. MRC had calculated the overlap integrals, PP^T , using the detector response rather than its transpose, which exaggerated the detector asymmetries rather than compensating for them, thus introducing additional photometric error. Also, a natural consequence of Equation (7) is that some of the weights are negative and, after we reprocessed the data, we discovered that the MRC code had set all the negative interpolation weights to zero, increasing the uncertainty in the photometry. We ran out of time and money and had to abandon the effort without creating a Galactic Plane Supplemental Catalog. However, Pérault et al. (1996) did use the preliminary version of the supplemental catalog to successfully avoid bright infrared sources in the Galactic plane. Kerton and Martin (2000) subsequently created super-resolved imaging of the Galactic plane at 12 and 25 μm using the Cao et al. (1997) procedures.

7.2.2. Infrared Galactic Point Source Model

The Galaxy is a two-armed barred spiral; see Figure 77 for an infrared view. Other major features are a bulge, an inner bar, a thin exponential disk and an extended low density halo. These components are inferred from survey and deep observations at wavelengths ranging from the radio to the ultraviolet. The different wavelengths probe different constituents: the visible

through the near-infrared (0.3 – 3 μm) is dominated by stars, the radio wavelengths directly trace the distribution of gas while the mid-infrared preferentially detects dust heated by nearby stars such as in compact H II regions, reflection and planetary nebulae and stars with circumstellar dust shells. By analogy with other galaxies, these constituents can have markedly different geometries. Newly formed stars and H II regions have a patchy distribution resulting in an ultraviolet picture of a galaxy that either has an amorphous appearance or patchily traces the spiral arms. Young to middle aged stars define the grand spiral design apparent in visible images of galaxies while the older infrared bright stars have a smoother distribution with a low arm to inter-arm contrast.

We view the Galaxy from our vantage (or disadvantage for Galactic structure studies) slightly above the median plane about two-thirds the distance from the center to the luminous edge. Before the advent of infrared surveys, models of the stellar background were incomplete because interstellar extinction limits

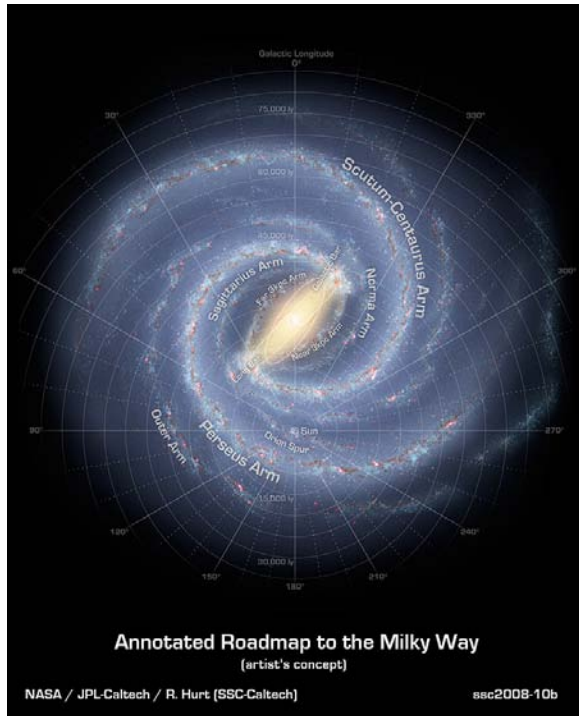


Figure 77. The Milky Way according to the Spitzer infrared telescope facility. Image courtesy of the Spitzer Science Center

visual investigations to high latitudes, the solar neighborhood and a handful of ‘window’ regions near the plane. Deriving the intrinsic properties of the bright beacons, such as giant and supergiant stars, is thus biased by being restricted to a small number of relatively nearby objects or to distant ones in extinction windows. From such limited observations deVaucouleurs and Pence (1978) deduced that our Galaxy is a mildly barred spiral and inferred some characteristic scale lengths. Bahcall and Soneira (1980a, 1984) created the first comprehensive modern era model of the visible stellar distribution in the Galaxy using visible source counts to enumerate the principal Galactic components. Mamon and Soneira (1982) then extrapolated the model into the near-infrared. Although extensively validated against visible observations (Bahcall and Soneira, 1980b, 1981, Bahcall et al., 1985), the model is degenerate near the galactic plane and has only a single luminosity function.

The stellar distribution in the Galaxy is best defined by a sensitive infrared sky survey, hence the interest in improving the resolution and sensitivity of the IRAS data. The infrared interstellar extinction is a small fraction of that in the visual. For example, the galactic center is virtually opaque in the visual with only one photon in $\sim 10^{11}$ reaching us while 10% of the 2.2 μm radiation gets through. Thus, it was not surprising that Eaton, Adams and Giles (1984) found that the Mamon and Soneira (1982) infrared extrapolation was inadequate near the Galactic plane. Also, the visible models could not account for the coarse structural details revealed by low spatial resolution infrared surveys of Hayakawa et al. (1979, 1981), Kent et al. (1992), Arendt et al. (1994), Freudenreich et al. (1994) and Freudenreich (1996). Although the infrared maps derived from these surveys measured the north-south asymmetry of the Galaxy and the size and shape of the bulge, and constrained the overall structure parameters, the resolution was too coarse to determine more than a single stellar population per wavelength regime. Walker and Price (1973) did fit a relatively simple model to the HI STAR observations (Walker, 1978) which only crudely separated populations based on the TMSS and 4.2 μm AFCRL surveys. Krassner (1979, 1981) modified this model to predict faint 2.2 μm source counts.

The initial more sensitive early 2.2 μm surveys ($K < 10$ mag) covered small areas and the modeling was directed toward separating field stars from those in H II regions (Elias, 1978b). The comparable sensitivity and resolution near-infrared Galactic plane surveys conducted in the 1980s by Kawara et al. (1982), Jones et al. (1984), Eaton, Adams and Giles (1984) and Ruelas-Mayorga (1991a) also covered rather limited areas; the most extensive of these surveys, the two micron Galactic survey (TMGS) of Garzón et al. (1993), encompassed 255 deg² of the sky with 15" detectors to a limiting magnitude of $K \sim 9.8$. The Deep Near-infrared Survey of the Southern Sky (DENIS) and the Two Micron Sky Survey (2MASS) considerably improved the situation by the turn of the century with 1.25, 1.65 and 2.17 μm all sky coverage to a sensitivity of $\sim 10^{-20} \text{ w cm}^{-2} \mu\text{m}^{-1}$ with 2" pixels. However, DENIS and 2MASS results became available well after the SDIO/BMDO sponsored background characterization program had ended.

Although the early near-infrared models of Elias (1971a), Jones et al. (1984) and Ruelas-Mayorga (1991b) matched the available near-infrared observations rather well, they failed in the LWIR near the Galactic plane (Garwood and Jones, 1987) because the prominent LWIR sources are too faint in the visible and near-infrared to have been included. Since distinctly different types of objects dominate the LWIR sky, the parameters of the CBSD Galactic point source model were tuned to the IRAS mid-infrared measurements and the subsequent deep near-infrared surveys were used to validate the model and to highlight discrepancies. Chester (1986) estimated that the bright beacons that dominate the 12 μm sky could be seen throughout the Galaxy at the [12] ~ 5 IRAS limiting magnitude. However, source confusion compromised

IRAS sensitivity along the Galactic plane, reducing the distance to which these bright beacons could be seen. Super-resolution reduced the confusion as indicated in Figure 76 and the analysis of Evans et al. (1989), University of Wyoming, who super-resolved AO Galactic plane fields at 22° and 29° longitude from which they concluded that the IRAS *Point Source Catalog* was reasonably complete to 2 Jy in these fields while their super-resolved images had a confusion flux limit of about 0.8 Jy.

Confusion also distorted the IRAS photometry. Although, the University of Wyoming image restoration processing was able to resolve many sources in the IRAS *Point Source Catalog*, the individual fluxes of the resolved sources near the Galactic plane seldom summed to the flux listed for the single IRAS source. Thus, the IRAS observations are degraded in precisely the region that contains the most information on the Galactic constituents and structure. This is particularly the case in and near the center where density gradients and relative contributions from the stellar constituents change rapidly.

The Evans et al. source counts the fields indicate the existence of a very thin (< 170 pc) disk population as well as a very red component, which was confirmed by Burnup and Canterna (1991), who found that the IRAS Galactic plane sources could be divided into three distinct components based on their [12]–[25] colors and latitudinal distribution: a ‘blue’ thick (< 460 pc scale height) disk component that had colors similar to oxygen and carbon-rich AGB stars with newly formed dust shells, a blue thin (< 140 pc) disk component and, at $l \sim 28^\circ$, a very thin (< 50 pc) and a very red ($T < 250$ K) component with colors similar to those of T Tauri stars, planetary and reflection nebulae. Hammersley et al. (1995) noted a similar population division at $2.2 \mu\text{m}$ with corresponding scale heights that they label as old and young exponential disk components. Walker and Cohen (1988) and Walker et al. (1989) more finely classified the different constituents of the mid-infrared background by their IRAS colors.

There have been numerous attempts to divine Galactic structure from infrared survey data. This is notoriously difficult as the observed quantities, the number of sources as a function of brightness in a given direction is a (triply) integrated quantity: over the brightness (luminosity) distribution of an individual Galactic constituent, over the density of constituents as a function of position and then with respect to distance along the line of sight. The diffuse observations obtained with large instantaneous fields of view, such as from DIRBE/COBE, introduce a fourth integral, the integrated irradiances of all the sources in the field of view. Inverting the integrals is inherently unstable and a variety of approaches are used to eliminate and/or invert the integrals to derive the space density of sources. A prominent background component with a narrow luminosity dispersion is frequently adopted to remove the integration over luminosity (Habing et al., 1985; Habing, 1988; Weinberg, 1992a,b; Allen, Kleinmann and Weinberg, 1993). With an assumed luminosity function, the various procedures used to invert the remaining integrals to obtain the spatial distribution of sources include harmonic analysis (Weinberg, 1992a) and Richardson-Lucy maximum entropy (Binney, Gerhard and Spergel, 1997) but the most common “inversion” technique is to assume a functional form for the Galactic constituents, exponential disk with exponential vertical distribution (a deVaucouleur’s spheroid and an elliptical bulge are also often added) then tune the model parameters to match the observations.

The two features that dominate large scale infrared maps are a radial exponentially decreasing disk that vanishes at a Galacto-centric distance of 12–14 kpc and a central bulge. The derived distance of the Sun from the Galactic center is between 7–8.5 kpc, while the exponential scale length of the disk inferred from observations varies from 2 to 6 kpc with the near-infrared yielding shorter values (1.8 – 3.0 kpc) than the longer wavelength IRAS data (3.5–5.7 kpc).

Thus, where the Galaxy ends depends on the wavelength of observation. On the other hand, Seiden, Schulman and Elmegreen (1984) argues that the disk need not be exponential; that stochastic star formation and the observed surface density of gas in the galaxy produces a $[1/R - \text{constant}]$ distribution where R is the Galacto-centric distance. Such a distribution mimics an exponential over much of the surface but has the consequence that the disk terminates when $1/R$ equals the constant. Habing (1988) found that his disk component cuts off 1 Kpc beyond the Sun in qualitative agreement with the $1/R$ distribution. The vertical density distribution is usually taken to be exponential although Freudenreich (1996) modeled the COBE/DIRBE disk observations with the $\text{sech}^2 z$ distribution that is characteristic of an infinitely large isothermal thin disk. This distribution was specifically rejected by Kent, Dame & Fazio (1991) as incompatible with their observations.

Hammersley et al. (1995), Cohen (1995), Freudenreich (1996) and Makiuti et al. (2002) placed the Sun 12–20 parsecs above the Galactic plane. Derivation of this geometric parameter shows how modeling assumptions influence the result. Unavane et al (1998) obtained the contrary result that the Sun was 14 parsecs *below* the median plane from the latitudinal distribution of stellar colors of DENIS sources toward the center of the Galaxy. This analysis was influenced by interstellar extinction, which they assumed to have a symmetric exponential vertical distribution about the plane. As Milne and Aller (1980) found, there is more absorbing dust above the plane than below, which qualitatively accounts for the Unavane et al. results.

Djorgovski and Sosin (1989) noted that the peak in the latitude distribution of IRAS red stars selected by the Habing (1988) color criteria had a roughly sinusoid deviation from the Galactic equator with the maximum amplitude of $\sim 1^\circ$ at about 90° and 270° longitude. The median in the distribution was offset by about 0.17° below the Galactic plane, the probable reflex of the height of the Sun above the plane. Freudenreich et al. (1995) confirmed this deviation in the COBE/DIRBE surface brightness distributions and found that the far-infrared radiances traced the velocity integrated H I maps, which suggests that the interstellar dust is displaced in the same way as neutral hydrogen. The old disk population that is tracked in the near-infrared was found to have the same displacement but at about half the amplitude, in general agreement with Djorgovski and Sosin. The similarity with the H I maps led Djorgovski and Sosin and Freudenreich et al. to interpret these observations as due to a warp to the plane. Hammersley et al. (1995) accounted for the asymmetry in the observed distribution of old disk stars by tilting the Galactic plane by 0.4° about a node at $\theta = 165^\circ$ and placing the Sun 15 pc above the plane. They further attributed the warp signature to structure or corrugations in the plane.

The nuclear bulge is a prominent inner Galaxy feature in near-infrared surveys. López-Corredoira et al. (1997) found a paucity of bright ($M_K < -8.5$) bulge giants compared to either the luminosity distribution observed by Eaton, Adams and Giles (1984) or that predicted by Wainscoat et al. (1992). Habing et al. (1986) noted that the vertical surface density of the coolest bulge giants and AGB/Long Period Variable (LPV) stars observed by IRAS declined more steeply (scale length ~ 1 Kpc) than in the visual or near-infrared (~ 2.7 Kpc). On the other hand, Weinberg (1992b) analyzed the space distribution of the IRAS 12 and 25 μm AGB variable stars and concluded that the mid-infrared bulge reported in the IRAS data did not exist but was a projection effect of the disk that apparently enhanced surface density toward the center. The degree of flattening of the bulge also is inconsistent. DeVaucouleurs and Pence (1978) derived a 0.6 visual axial ratio while that from diffuse 2.4 μm measurements varied from the 0.52 of Maihara et al. (1978) to 0.25 of Garwood and Jones (1985). Kent et al. (1991) noted that a simple ellipsoidal surface density did not apply and that the IRAS and COBE observations

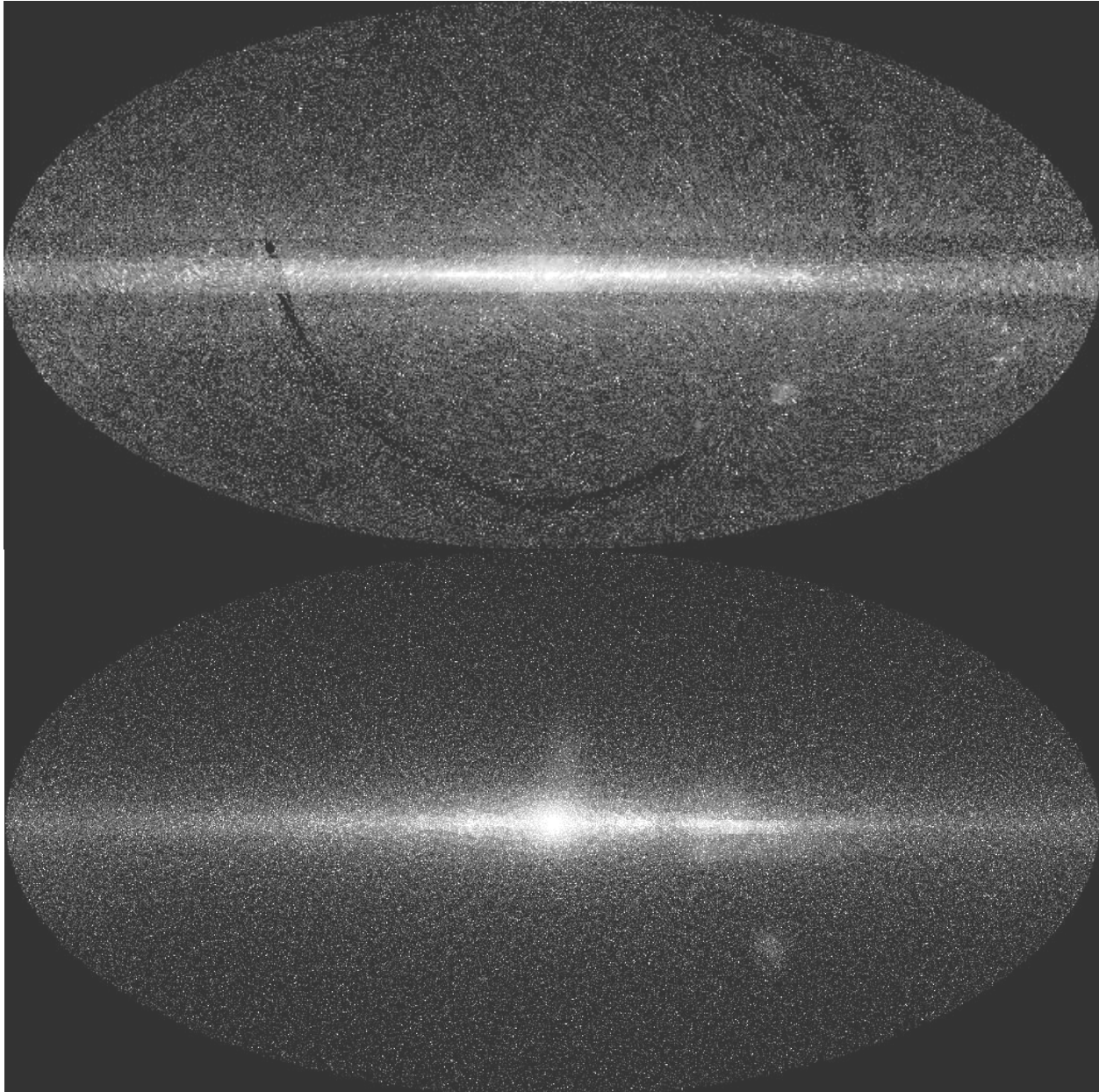


Figure 78. Distribution of mid-infrared point sources. The observed mid-infrared point sources brighter than $\sim 6^{\text{th}}$ magnitude are shown at the top. The IRAS $12 \mu\text{m}$ sources from the point source and faint source catalogs are plotted along with the Midcourse Space Experiment $8.3 \mu\text{m}$ observations to fill in the gaps and confusion along the plane. The Faint Source catalog lists sources at latitudes $|b| > 10^{\circ}$ while MSX only covers $|b| \sim 5^{\circ}$; hence the light and dark banding along the plane. The differences in sensitivity between the IRAS detectors give rise to the striping that is manifest as strings of sources along the scans. The $12 \mu\text{m}$ point sources to 7^{th} magnitude predicted by CBSD are shown in the bottom panel.

indicated that the contours are boxy; a result that Weiland et al. (1995) attribute to interstellar extinction. Weiland et al. deduced that the DIRBE near-infrared surface brightness of the bulge had the form of a flattened ellipse with minor-major ratio of ~ 0.6 . The bulge is not evident in the DIRBE $12 \mu\text{m}$ observations, supporting Weinberg's conclusion that it is a projection effect.

The 2.4 μm diffuse observations of Hayakawa et al. (1979; 1981) clearly show that the brightness of the inner Galaxy is asymmetric. The asymmetric emission ridge was initially suggested to be due to a ring of material at 3 kpc but Simonson and Mader (1973) argued that the feature was a dispersion ring of 0.3 ellipticity with the spiral arms merging with the ring at the extremities; the northern half is somewhat brighter as this end of the oval is tipped toward us by 30°. Weinberg (1992a) deduced that a bar, rather than a ring, is present in the inner Galaxy based on his analysis of IRAS sources, a conclusion Cole and Weinberg (2002) supported with COBE/DIRBE 2.2 μm observations. The only consistent conclusion of the various studies is that the bar is tipped toward us in the first quadrant (Weiland et al., 1994) although the derived angles vary from -36° with respect to the Sun-Center line of sight to -75°.

Wainscoat et al., (1992) created an infrared point sources model of the Galaxy, SKY, under NASA funding, the heritage of which dates to Walker and Price (1973). The SKY model structures the Galaxy with an exponential disk, bulge, spiral arms, a 4 Kpc molecular ring and the local spur, all of which are represented by analytic expressions. Each component has its own source population with an individual characteristic density and intrinsic brightness distribution. In addition to using individual luminosity functions in specified spectral bands as is normally done, the SKY luminosity function also can be defined by components with distinct absolute infrared spectra, permitting direct estimation of the point source background in a user defined spectral bandpass. SKY was originally developed to account for the IRAS observations but AFGL funded Cohen (1993) to extend the model, SKY3, to predict source counts in any infrared filter. The model has since evolved to include visible and ultraviolet wavelengths. Under SDIO funding, SKY4 accounted for the measured ultraviolet source counts, improved the geometric parameters of the major components of the Galaxy (Cohen, 1994) and shifted the Sun from the mid-plane of the Galaxy (Cohen, 1995). The current version, SKY5, updated the ultraviolet to 35 μm extinction and includes more recent absolute visual magnitudes based on Hipparcos measurements with the consequent adjustment of the stellar space densities.

The point source model is compared to the observed mid-infrared sources in Figure 78. The distribution of the 12 μm sources in the *IRAS Point and Faint Source Catalogs* plus the MSX 8.3 μm sources is shown in the top panel. The IRAS Faint Source and MSX surveys are reasonably complete to $\sim 6^{\text{th}}$ magnitude but do not have contiguous coverage. The IRAS *Faint Source Survey* is limited to $|b| > 10^{\circ}$ Galactic latitudes while MSX coverage is confined to $|b| < 5^{\circ}$, and the less sensitive IRAS *Point Source Survey* fills in the area between, hence the light-dark banding. The 12 μm CBSD point source model prediction (Noah and Noah, 2001b) to 7th magnitude is shown in the bottom panel. MRC modified the SKY5 model (CBSKY) to provide the imaging capability shown and added various components not in SKY5, such as the Large Magellanic Cloud in the center of the lower right quadrant, stars in the ρ Oph molecular cloud complex just above the Galactic center and the star forming regions to the right of the center. As may be seen, these features have counterparts in the map of observed mid-infrared sources. However, the bulge in the model is not reflected in the MSX data.

7.2.3. Infrared Cirrus

Spatially extended structure has been detected over the entire sky in the ultraviolet, visual and infrared. At intermediate to high galactic latitudes this background is due to the interstellar dust, which Low et al. (1984) called infrared cirrus because of its wispy and filamentary appearance. The infrared structure of this component has a wide range of scale lengths, from degrees along the filaments down to the 2' resolution of the IRAS images while structure exists

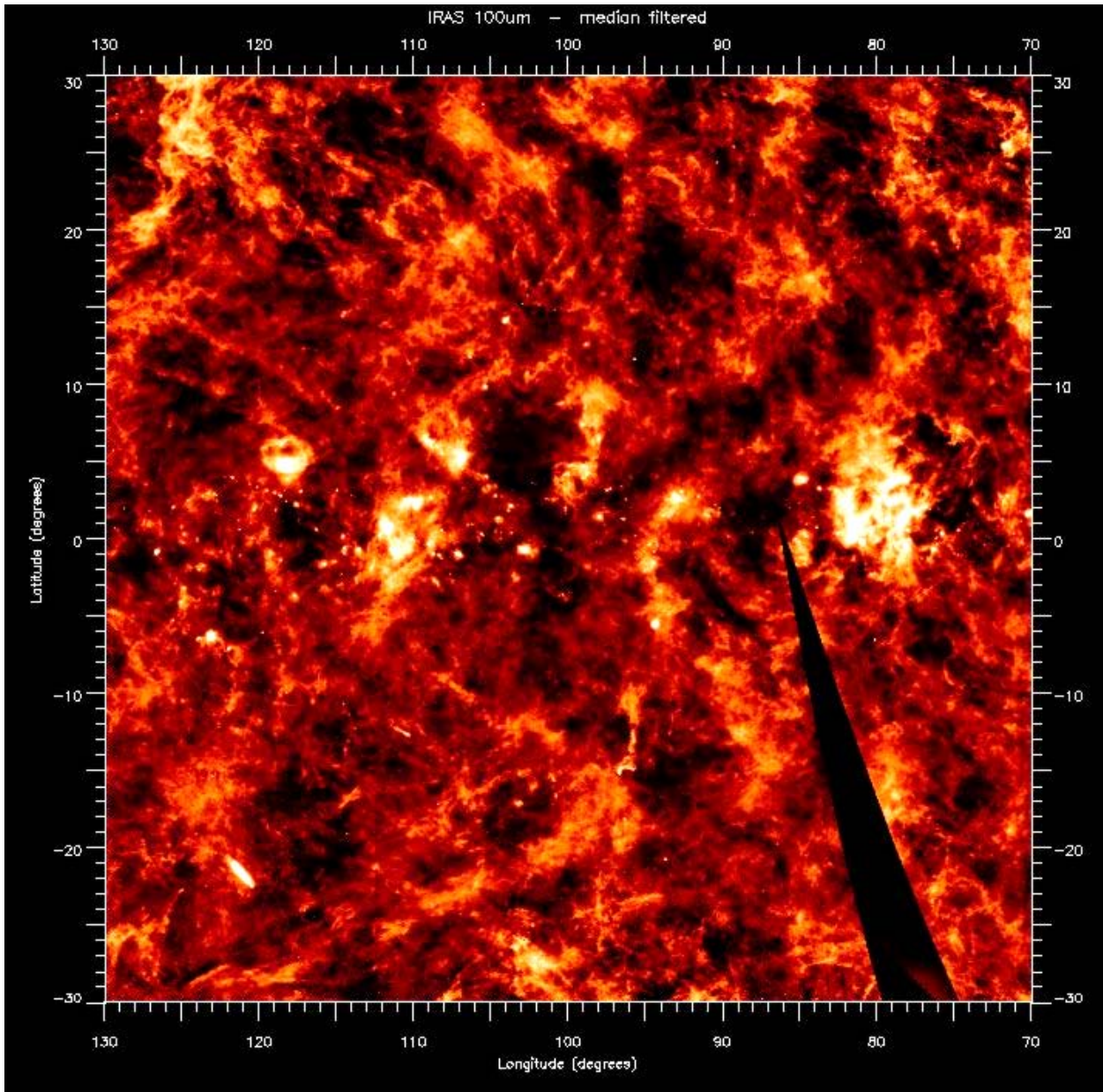


Figure 79. The 100 μm infrared cirrus. This map has been median filtered to remove the large scale emission and point sources. The area covers about one-twelfth of the sky and is centered on the Cygnus region. The dark slice at lower right was not redundantly covered by IRAS and the ellipse in the lower left corner is the Andromeda galaxy. This image is courtesy of William Waller, Colby College.

to the arc second scale on visual photographs. This phenomenon produces aspect-dependent clutter for a scanning system, which is illustrated by the fact a third of the objects in the IRAS point source catalog are now known to be dense condensations (knots) in this structured background that were scanned in an aspect that produced point-like signatures (Chester, 1986). False source detections in a staring system are evinced by their tendency to lie along filaments.

The initial approach to characterizing the infrared cirrus was to generate 100 μm maps covering the sky, such as shown in Figure 79, because the infrared cirrus is usually brightest and the contrast with other celestial components greatest at this wavelength, then to use the structural

content and spectra from the LRS to extrapolate to shorter wavelengths and higher spatial resolutions. Measured rather than modeled spectra were needed as the mid-infrared emission was found to far exceed that predicted from IRAS far-infrared color temperatures and the wispy structure did not exactly correlate at all wavelengths as the 12 μm background was proportionally most intense near stellar sources of heating.

Cox, Krugel and Mezger (1986) and Pajot et al. (1986) proposed that, on the Galactic scale, at least some of the excess mid-infrared emission arises from the non-equilibrium heating of small dust grains by the interstellar ultraviolet radiation field. Draine and Anderson (1985) had calculated that substantial amounts of continuum radiation shortward of 50 μm can be produced by temperature fluctuations in small interstellar graphite and silicate grains. These temperature fluctuations are large when the energy of the absorbed photon is comparable, or greater, than the average heat content of the grain. For the interstellar radiation field this will occur for grains with radii less than 0.03 μm (Desért, Boulanger and Shore, 1986).

On the other hand, Puget, Léger and Boulanger (1985) and Allamandola et al. (1985) suggested that a significant fraction of the interstellar mid-infrared radiation is band emission from polycyclic aromatic hydrocarbons (PAHs). Léger and Puget (1984) had pointed to the similarity between the PAH molecule coronene and the unidentified emission features detected at 3.3, 3.4, 6.2, 7.7, 8.6, and 11.3 μm in reflection nebulae and some H II regions. Allamandola et al. (1985) noted similar agreement between the band spectrum of chrysene and auto exhaust while Papoular et al. (1989) found that vitrinite, an organic component of coal, had a better spectral match to the infrared spectral bands. In support of the proposed identification, Léger and d'Hendecourt (1985) and Crawford et al. (1985) found a reasonable match between the absorption spectrum of singly ionized PAHs and the visual diffuse interstellar bands, and the former authors concluded that although only a small number PAHs are stable in the interstellar medium, they are the most abundant molecules after H₂ and CO. Alternatively, Duley and Williams (1986) argued that PAHs existed only in shock formation regions since chemical reactions with H and O will effectively destroy them in the interstellar clouds. Instead, they proposed that hydrogenated amorphous carbon dust would form in denser diffuse and dark clouds that could, in part, account for the cloud-to-cloud variation in the 12 to 100 μm measured intensity ratios as well as in different regions of infrared cirrus. Kwok (2008) reviewed the rich complexity of organic molecules in space of which PAHs are a component.

Thus, a decent signal-to-noise infrared cirrus spectrum was needed to unambiguously confirm the presence of these spectral features in the interstellar medium. To this end, AFGL funded SRON to extract and co-add LRS spectra of the brightest cirrus knots to create a mid-infrared cirrus spectrum. Unfortunately, this goal was defeated by the low surface brightness of the cirrus and the high pass filter in the LRS on-board signal processing electronics. Giard et al. (1989) and Ristorcelli et al. (1994) obtained crude estimates of the strength of the PAH emission by mapping the Galactic plane in filters centered on the 3.3 μm 6.2 μm PAH features and compared the results with IRAS and 2.2 μm maps. Although this analysis suggested the presence of PAHs, it was not definitive. Proof came when Mattila et al. (1996) found PAH features in their 5.8 – 11.6 μm ISOPhot spectrophotometry of three Galactic plane fields. They noted that although the features were prominent, no discernable continuum was seen; therefore, the absorbed energy was preferentially emitted in the bands. Boulanger et al. (2000) confirmed these results with more sensitive 5 – 16.5 μm ISO circular variable filter spectra and found infrared PAH bands in isolated higher latitude dust clouds that are bathed in a less intense local interstellar radiation field. Flagey et al. (2006) matched these observations with a three

component model with a continuum peaking at ~ 3 μm and a combination of PAH cations and neutral molecules. Since PAH features are present in the IRAS 12 μm band but are few and weak in the other bands, the observed emission from interstellar dust has a minimum at 25 μm .

To characterize the infrared appearance of the interstellar dust, AFGL had the University of Arizona analyze the emission mechanisms and to correlate the structure seen by IRAS with observations taken at higher resolution and/or sensitivities at other wavelengths. Since the excitation mechanism for the mid-infrared interstellar dust emission is the UV–visual interstellar radiation field, high latitude visible dust clouds can be correlated with bright mid-infrared cirrus (deVries and LePoole, 1985). The visible scale lengths of this dust have been measured to much smaller spatial extent than that of IRAS, so perhaps the statistical properties derived in the visible might be applied to longer wavelengths.

Low, Sykes and Cutri (1991) found that 100 μm cirrus emission generally clumped into large complexes that extend over tens of degrees of sky and that fainter structure filled the areas between the complexes. Thus, as seen in Figure 79, cirrus is present no matter where you look. The 100 μm emission was also found to correlate well with column density of atomic hydrogen, molecular CO gas and extinction and, in the absence of local heating, 12 μm emission. The 20–30K color temperatures of the Galactic cirrus that Paley et al. (1992) derived from the IRAS 60 and 100 μm fluxes is higher than expected from heating by the interstellar radiation field. However, the mid-infrared emission, especially at 12 μm , was orders of magnitude larger than predicted from the long wavelength fluxes and the color temperatures derived from them. Although Boulanger and Pérault (1988) found that the 12 μm and 100 μm emission were well correlated on the largest scales, the University of Arizona study noted that the 12 μm to 100 μm flux ratios varied up to a factor of 50 over a range of environments, which means that the emission at 100 μm cannot be a universally reliable tracer of the 12 μm emission.

Could the information in a cirrus field, such as shown in Figure 79, be condensed to a concise representation for background characterization? Low, Sykes and Cutri (1991) and Gautier et al. (1992) calculated power spectral densities for a number of bright infrared cirrus fields. The power spectral density is a measure of the brightness power as a function of spatial frequency that is, analytically, the square root of the modulus of the Fourier transform (the Fourier transform times its complex conjugate) of the image. Gautier et al. co-added data within 5' of cross-scan in six separate regions of the sky from 8° long 100 μm survey scans to increase the signal-to-noise. They then assumed circular symmetry to convert their one-dimensional results into two-dimensional power spectral densities and found that, to within the analysis uncertainties, their results were well fit by a power law with a single -3.0 exponent, a value that is consistent with the velocity dispersions for H II regions.

Sykes, Low and Cutri (1991) did a more extensive and detailed analysis. They found that, overall, the power spectral densities were symmetric in the full two-dimensional power spectral densities that they calculated for 24 fields at 100 μm and four 12 μm fields. This indicated that no large scale coherence was present in the structure. However, some short scale asymmetries were noted in about 20% of the fields. The best fits that they found to both the 12 and 100 μm power spectral densities had spectral exponents of -2.9 to -3.0, in agreement with the subsequent analysis of Gautier et al. The ~ -3.0 index also applied to the smaller scales obtained from the more sensitive one-dimensional raster scanned additional observations. Recently, Ingalls et al. (2004, 2006) and Kim et al. (2008) have found that the exponent at 8 and 25 μm steepens to -3.5 for scales smaller than $\sim 4'$, the IRAS limit, as the structure changes from being two-dimensional to three.)

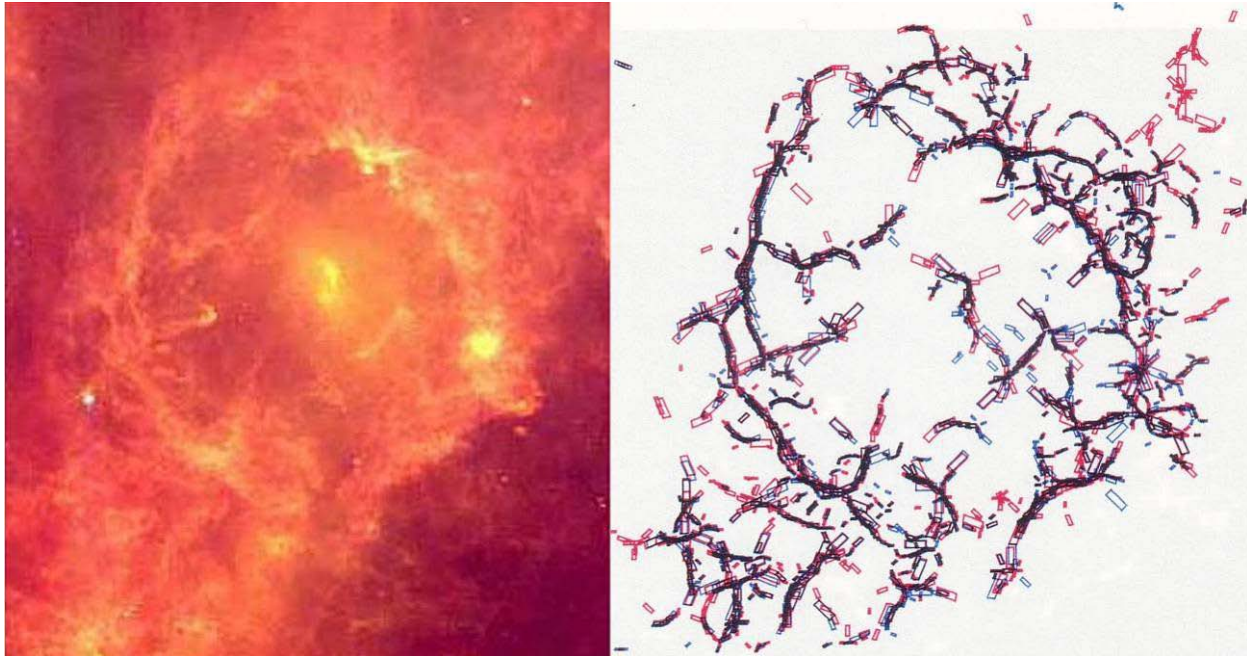


Figure 80. The structure centered on λ Orionis. The IRAS image (left) is color coded blue, green and red for 12 μm , 60 μm and 100 μm , respectively. At right are the scales 2 through 5 extractions of the 60 μm (blue) and 100 μm bar features from the image on the left; the scales as indicated by the size of the bar.

These studies indicated that a small number of parameters could succinctly express the structure of the infrared cirrus. Over most of the sky, the derived two-dimensional power spectral densities were found to be simply represented in terms of the inverse angular scale length, s , by $C s^{-3}$; the normalization constant, C , is proportional to the total power in a given field. Since the value of C is roughly the same in large fields such as those shown in Figure 79, only a small number of values needed to be calculated. The 12 μm exponent was found also to be -3 where the emission was strong enough for a determination to be made. However, the interstellar 12 to 100 μm intensity ratio varies quite a bit with position, which requires more values of the normalization constant to be determined. Assuming that the -3 exponent applies to smaller scale lengths, we can invert the power spectral density to obtain a two-dimensional intensity distribution down to the smallest scales set by the SDIO requirements. Unfortunately, since phase information is lost in the calculation, the shape and connectivity of structures, such as linear features or arcs, in the image is also lost as is the scan aspect character of the data. Thus, a synthetic image created from the power spectral density derived in this analysis would consist of circular or elliptical blobs, usually assumed to have a Gaussian shape, the number and brightness of which are set by C and the exponent, that are randomly distributed in the images. Thus, the reconstituted image may have general statistical similarities with the original image but look nothing like it.

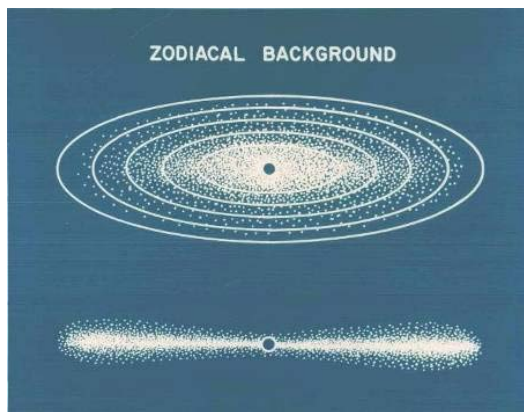
The $9^\circ \times 14^\circ$ MSX image of the Cygnus region in Figure 39 shows that there is a considerable amount of correlated structure in the extended infrared emission, at least at the lower Galactic latitudes. Not only are there linear correlations but circular and arcurate features abound, such as in the circular feature centered on λ Orionis shown on the left of Figure 80. Barry Katz, the SDIO program manager for the background characterization effort, funded Glenn Jones of the UK Defense Research Agency and Sally Watson (SD-Scicon) to explore a fractal based representation of the infrared cirrus (Watson and Jones, 1992) in which a wavelet process

operates on the image and extracts bars over a range of scales and orientations. The wavelet bar is convolved with image over a range of factors of two cascaded in scale, and local maxima are extracted from the filtered result. The 60 μm (blue) and 100 μm (red) bar features extracted from Figure 80 are shown on the right of the Figure; note that there is a trend for the 100 μm features to lie slightly further away from center of the ring than those at 60 μm .

Watson and Jones found that the infrared cirrus was fractal, a characteristic that could be used to compress the data while preserving connectivity. They created curves of the number of filtered features exceeding a given flux level as a function of flux that were reasonably straight lines; a single fractal scale factor was found that caused the lines to overlap. This scale factor could then be used to extract the distribution of bars to smaller spatial scales, which would be painted onto the picture with random orientation but with connectivity to the extracted features.

Although compressions of 250:1 could be realized, inverting the result at such large ratios produced unrealistic images. The best results were obtained by storing the position, scale, feature type (bar orientation) and intensity of 2–4 feature scales at a factor of 20 compression.

Jones provided the fractal algorithms that Watson developed under the SDIO effort to MRC as a tool for the background characterization effort. As promising as the results from this effort were, no further work was done after 1992.



7.2.4. Zodiacal Background

The zodiacal dust cloud has been observed since antiquity as the false dawn or the lingering twilight that persists especially after springtime sunset or before fall sunrise in the northern hemisphere. The small solar system dust particles that produce this phenomenon are thought to originate from asteroid collisions and comets. The diffuse radiance from thermal emission or sunlight reflected by the zodiacal dust provides the ultimate source of background photon noise for a telescope operating in

Earth orbit or, anywhere else within the inner solar system. This background is present in all viewing directions because, as indicated by the accompanying cartoon, the Earth is buried near the median plane of the dust cloud. The photon noise from this background is increased when looking closer to the sun where the zodiacal background is highest, which degrades system performance. The zodiacal minimum has been explored by experiments to observe the cosmic background: in the ultraviolet where the solar spectrum is much reduced (Henry, 1991), between 2 and 4 μm where both reflected sunlight plus the thermal emission from the cloud is at a minimum (Matsumoto Akiba and Murakami, 1988, Matsumoto et al. 1996, Kelsall et al., 1998) and in the far-infrared (Kelsall et al., 1998)

A physical model of the zodiacal background requires knowledge of the wavelength dependent reflectivity, absorptivity and emissivity of the dust grains as a function of particle size, how the particle size distribution varies with position in the dust cloud and the particle density as a function of distance from the Sun. The zodiacal brightness is thus modeled by a double integral. The particle size dependent visible reflectivity, including the phase function (Lamy and Perrin, 1986), or emissivity in the infrared, is integrated over the particle size distribution (Röser and Straude, 1978, Frazier, Boucher and Mueller, 1987). To derive the absorptivity, emissivity and reflectivity of the grains from first principles we need to know the dielectric constants for the

mineral and physical composition of the dust and a theory of how radiation interacts with the particles based on the heterogeneity and the shape of the dust as a function of particle size (e.g. Reach, 1988). The outer integral sums the contribution from the various elements along the line of sight and requires the geometry of the cloud.

The complexity and coupling of parameters in the integration is inevitably reduced by appealing to independent measurements and arguments of physical plausibility. For example, the Sun is the gravitational center of the solar system so the early zodiacal cloud models assumed azimuthal symmetry with respect to the sun. Dermott et al. (1992) later argued that Jupiter perturbs the cloud to offset the geometric center from the Sun and that this offset was detected by IRAS as a few percent deviation from symmetry; Kwon et al. (1991) also noted a large scale East-West asymmetry in their visible data. Other asymmetries are present. Visual observations by Maucherat, Llebaria and Gonin (1985), Misconi and Weinberg (1978), Leinert et al. (1980), Nikolsky et al. (1985) and IRAS infrared measurements (Hauser, 1988) indicate that the ecliptic is not the fundamental plane of the cloud. This introduces a low frequency yearly variation in the zodiacal background but, unfortunately, no consistent global representation has been defined. Taking the infrared and visual data separately, the cloud may not have a single plane of symmetry but one that is dominated by the gravitational influences of the Earth and Venus.

The simplest dynamical model of the dust cloud hypothesizes that the Poynting-Robertson force from solar radiation and corpuscular drag from the solar wind causes the dust particles to spiral inward from where they originated on time-scales of 10^{4-6} years (Wyatt and Whipple, 1950). For a time independent source of dust, this drag force preserves orbital inclination, reduces the orbital eccentricity and produces a steady-state radial dust density distribution proportional to the inverse of the heliocentric distance, independent of particle size and composition. However, particles from a given source will segregate by composition and size because they have different infall rates, and collisions and solar heat-induced structural changes are expected to cause dust populations to evolve with time. Although orbital dynamics calculations (Briggs, 1962) and perturbations (Leinert, 1975; Trulsen and Wiken, 1980) predict a density distribution that is an inverse power law in heliocentric distance, the specific power index is not universally agreed upon. Leinert et al. (1981), Röser and Straude (1978), Giese, Kneissel and Rittich (1986) and Kelsall et al. (1998), to name a few, use the -1.3 index derived from the optical data returned by the Helios satellite. Hahn et al. (2002) found a steeper -1.45 ± 0.05 exponent provided a better fit to their Clementine measurements close to the Sun. On the other hand, Deul and Wolstencroft (1988) obtained a -1.1 ± 0.1 index in their fit to the same IRAS data as did Good (1994) in deriving his value of -1.803 ± 0.014 . Murdock and Price (1985) state that a -1 exponent provides the best-fit power-law model for ZIP ecliptic plane observations, but that the fit is not satisfactory over the entire $22^\circ - 180^\circ$ range of elongations. Levasseur-Regourd and Dumont (1988) attempted to reconcile the $r^{-1.3}$ distribution from the Helios observations and the r^{-1} derived from the infrared by proposing a dust albedo that varies as $r^{-0.3}$.

Fitting the data to derive a mean particle size, reflectivity and/or emissivity can lead to large errors when extrapolating beyond the wavelength of observation; but it is done anyway to simplify the problem. The analytic expression currently used for the particle size distribution is a fit to the in-situ measurements of the mass distribution of dust particles collected/detected near the Earth by Grün et al. (1985). Adopting this distribution for the global background requires that the composition and shape of the dust particles as well as the size distribution remain the same throughout the dust cloud, assumptions which observations by Schuerman (1980) have called into question.

The zodiacal database to which the model parameters are tuned is voluminous but, until recently, with limited common overlap between visible and thermal infrared emission. Except for the Solar Mass Ejection Instruments (SMEI) observations (e.g. Buffington et al., 2009), the global visible zodiacal measurements are ground based and quite old with the two most widely cited databases dating to the 1960s: the Tenerife measurements that are rationalized and tabulated by Levasseur-Regourd and Dumont (1980) and the Haleakala observations (Weinberg and Mann, 1967; Misconi et al., 1990). Such ground-based observations are difficult to make because the diffuse zodiacal background must be extracted from the temporally and spatially variable atmospheric emission and transmission (e.g. Kwon, Hong and Weinberg, 1991). Also, the synthesis of visible observations by Leinert et al. (1998) has a minimum elongation of 15° because scattered sunlight in the upper atmosphere swamps observations closer to the Sun. James et al. (1997), Ishiguro et al. (1999) and Mukai et al. (2003) obtained more recent CCD observations of the zodiacal cloud, the Gegenschein and dust bands from Haleakala while a ‘tour de force’ analysis of diffuse sky measurements in H α and Mg I λ 5184 enabled Reynolds, Madsen and Moseley (2004) to derive the general motion of the zodiacal dust particles. Ipatov et al. (2008) attempted to match dynamic models of likely sources of zodiacal dust to the James et al. observations and concluded that at least half the particles are cometary dust.

A satellite provides atmosphere-free observations and of the various space probes the Helios 1 and 2 observations are generally taken as benchmarks. Although the observations were confined to specific latitudes well out of the ecliptic plane, they provide invaluable *in-situ* measurements of the visible zodiacal brightness between 0.3 and 1 AU (Leinert et al., 1981). Beyond the Earth, AFOSR funded Weinberg and his colleagues (Weinberg & Schuerman, 1981) to analyze the *in situ* visible measurements obtained by the Pioneer 10/11 probes between 1 and 2.5 AU. Subsequently, Hahn et al. (2002) combined mosaics of seven fields taken over a six week period in the visible between 3° and 30° solar elongations that were obtained with the Clementine navigational cameras when the Moon occulted the Sun as seen from the spacecraft to create intensity maps that provide an averaged view of the inner zodiacal cloud. On the larger scale, SMEI obtains an all sky image at elongations greater than 22° once every 103 minute orbit (Jackson et al., 2004) measuring the visible zodiacal light at a signal-to-noise of at least 50. As a multi-year mission, SMEI measures temporal variations with time scales up to a year.

Soifer, Houck and Harwit (1971) made the first infrared observations of the zodiacal emission in 1971 from a probe-rocket while the third HI STAR South experiment mapped the area $35^\circ < \varepsilon < 75^\circ$ in 1974 (Price, Murdock and Marcotte, 1980) and the 1976 ELS flight sampled the elongation range $3^\circ < \varepsilon < 25^\circ$ (Murdock, 1977). Murdock and Price (1985) discuss the two ZIP flights that observed between 22° from the sun to the anti-solar direction. Unfortunately, the background dependent non-linearities in the bulk detectors used on the AFCRL/AFGL flights rendered the data inconsistent and uncertain. Furthermore, we could not disentangle the solar off-axis contribution on the CIRRIS 1A experiment from the true near-Sun zodiacal radiance. Near-infrared observation close to the Sun ($\varepsilon < 4^\circ$) searched for burnout zones during solar eclipses from the ground (Petersen, 1967, 1969; MacQueen, 1968; Mankin, MacQueen and Lee, 1974; Lamy et al., 1992), from balloons (MacQueen, 1968; Maihara et al., 1985) or in the mid-infrared from aircraft (Lena et al., 1974) with contradictory results.

IRAS and COBE each spent 10 months mapping the infrared zodiacal background over all ecliptic latitudes and longitudes. However, these data are restricted to solar elongations between 60° and 124°, a relatively benign background for a surveillance system. The weighting of the dust density and the volume emissivity in the zodiacal brightness integral is such that

observations over this elongation range mainly probe aspects of the cloud near the Earth. For example, Reach (1991) concluded that at least 78% of the observed 12 μm radiance and 65% that at 25 μm comes from emission within 0.25 AU of the Earth. The IRAS and COBE longer wavelengths probe further into the solar system but at reduced contrast to other emission such as infrared cirrus. Price et al. (2003) published MSX infrared zodiacal observations that overlapped these NASA measurements and extended the elongation coverage closer to the Sun and in the anti-solar direction.

On the smaller scale, Sykes found as many as seven pairs of dust bands between 1° and 3° in width girdling the sky, bisected by the ecliptic plane. Within the 60°–124° IRAS and COBE elongation limits, these bands appear as a 1–6% brightness enhancement above the general zodiacal background (Figure 66). These bands arise from the debris from asteroid collisions (Sykes et al., 1989; Sykes 1990). Since the estimated lifetime is $\sim 10^6$ years for an average solar system dust particle, the dust lost to the cloud has to be replenished and Dermott and Nicholson (1989) and Sykes and Greenberg (1986) have argued that enough dust is injected into the cloud by the asteroid collisions that create dust bands to make up for the loss. However, Kresak (1980) and Sykes and Walker (1992) show that an appreciable fraction must also come from short period comets, a conclusion supported by Jenniskens (2008) in his review of dormant comets and meteor streams. Dynamic considerations predict that both the cometary and asteroid collisional debris will form shells similar to the dust bands as the orbital nodes of the particles precess due to perturbations. Collisions comminute the particles and Poynting-Robertson drag causes them to spiral inward toward the Sun. During all this, the orbital inclination is preserved with the result that sheets of material should form from these events in the zodiacal cloud which, in projection, should be observable as clutter. Additionally, it is possible that the Earth and Venus resonantly trap the particles in quasi-stable regions creating small scale density enhancements (Jackson and Zook, 1989). Reach (1991) and Dermott et al. (1994) detected such an enhancement in the IRAS data due to dust trapped trailing the Earth; Reach et al. (1995) confirmed this finding in the COBE data. However, dynamic modeling of the evolution of the zodiacal dust bands by Nesvorný et al. (2006) and Ipatove et al. (2008) have shown that dust band particles migrate inward to ~ 2 AU where the larger particles are scattered by the strong planetary secular resonances there and the bands lose coherence.

Kelsall et al. (1998) published a parametric model to account for the zodiacal emission measured by DIRBE. They adopted analytic expressions for the geometry of the cloud, then adjusted the 45 free geometric, reflective and emissive parameters in the model using a non-linear least squares fit to 87,000 observations; about an equal number of fixed model parameters were adopted *a priori*. The average error between the DIRBE measurements and the Kelsall et al. model was $\sim 2\%$. Subsequently, Georjian, Wright and Chary (2000) created their own model to account for what they perceive as deficiencies in the one developed by Kelsall et al.

Noah and Noah (2001a) describe the CBS model created under the SDIO background characterization program. The parameters of this model were originally adjusted to fit the IRAS data and a comparison between the model and an IRAS 12 μm ecliptic pole to ecliptic pole scan is shown in Figure 81. The model was intended to be an interpretive tool by explicitly including the dust mineralogy and attempting to tie the observations at different wavelengths together by deriving the best fitting mineral composition of the dust. Thus, rather than modifying one of the DIRBE driven models, we continued to refine the CBS zodiacal model against DIRBE data (Figures 81 and 82) and ISO, MSX and SMEI observations.

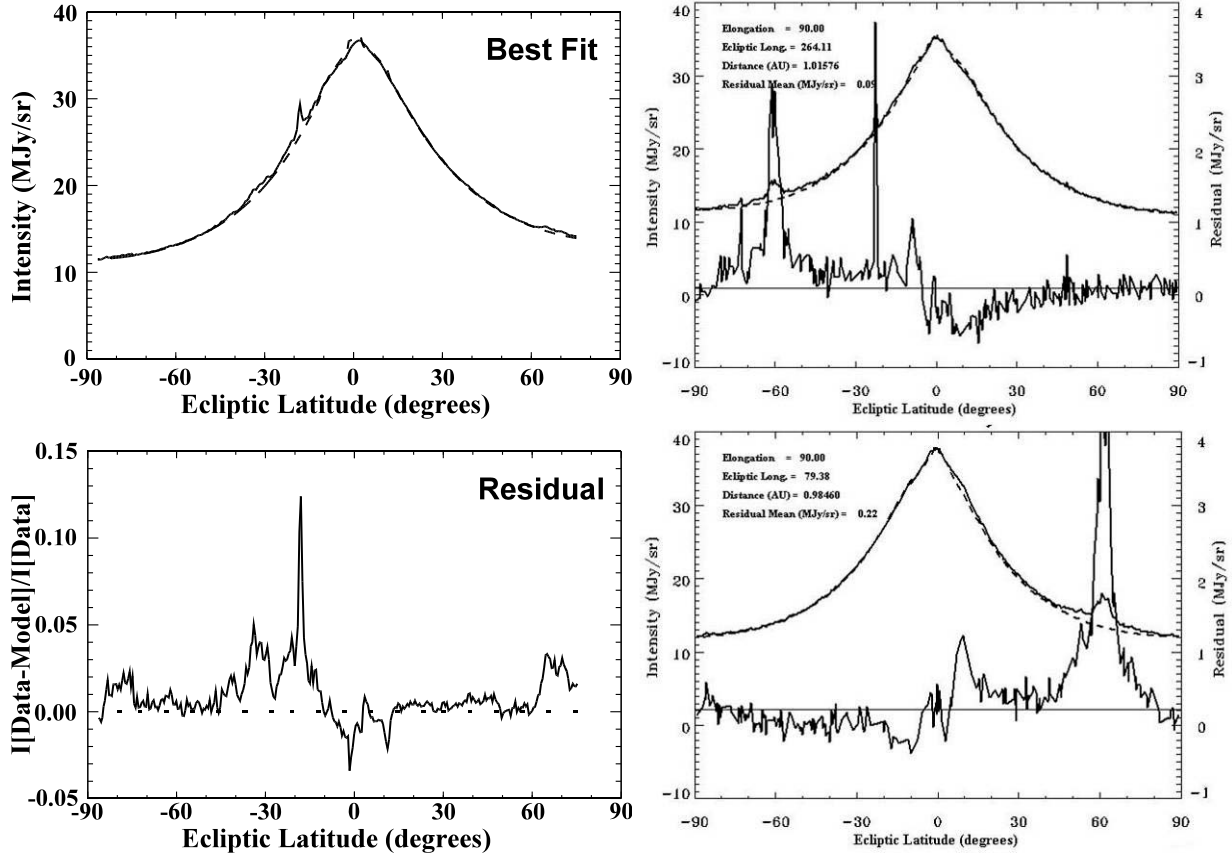


Figure 81. The CBSD zodiacal model fit to an IRAS 12 μm constant elongation scan (left) and pseudo DIRBE latitude scan (right). DIRBE did not scan along a constant elongation so the data points at 90° elongation for two days during the mission are shown. The average of the residuals between the data (solid lines) and the model (dashed lines) is of the order of 5%.

The CB Zodical model, CBZodi, assumes that the decrease in the zodiacal dust density is proportional to the inverse of the heliocentric distance ($1/r$) but with the center of the cloud offset slightly from the Sun (Dermott et al., 1992; Kelsall et al., 1998). The model assumes two planes of symmetry for the cloud, each with an individual inclination, longitude of the ascending node and, at 1.02 AU where the planes join, density normalization. Smoothing over the density normalizations produces a circumsolar ring at 1.02, just outside the orbit of the Earth (Jackson and Zook, 1989; Dermott et al., 1994; Reach et al., 1995) and small density enhancements in this ring leading and trailing the Earth are included to match the East – West asymmetry observed in the infrared. A third plane, with geometry dominated by Venus (Misconi and Weinberg; 1978), is a user option. A 4 AU boundary was adopted for the cloud as van Dijk, Bosma and Hovenier (1988) posited a finite dust cloud to reconcile a $1/r$ dust density variation with a steeper than $1/r^2$ decrease in zodiacal brightness that Schuerman (1980) found between 1 and 3 AU in the Pioneer 10 data. Hovenier and Bosma (1991) set the cloud limits between 2.8 to 3.7 AU based on the Toller and Weinberg (1985) improvements to the Pioneer zodiacal light photometry.

The volume emissivity was calculated using the methodology of Reach (1988) with a reasonable fit to the infrared photometry and spectroscopy found for a 70% to 30% mix of astronomical silicate and graphite (as defined by Reach), respectively. In the visible, the three term Henyey-Greenstein scattering function of Hong (1985), as modified by van Dijk, Bosma

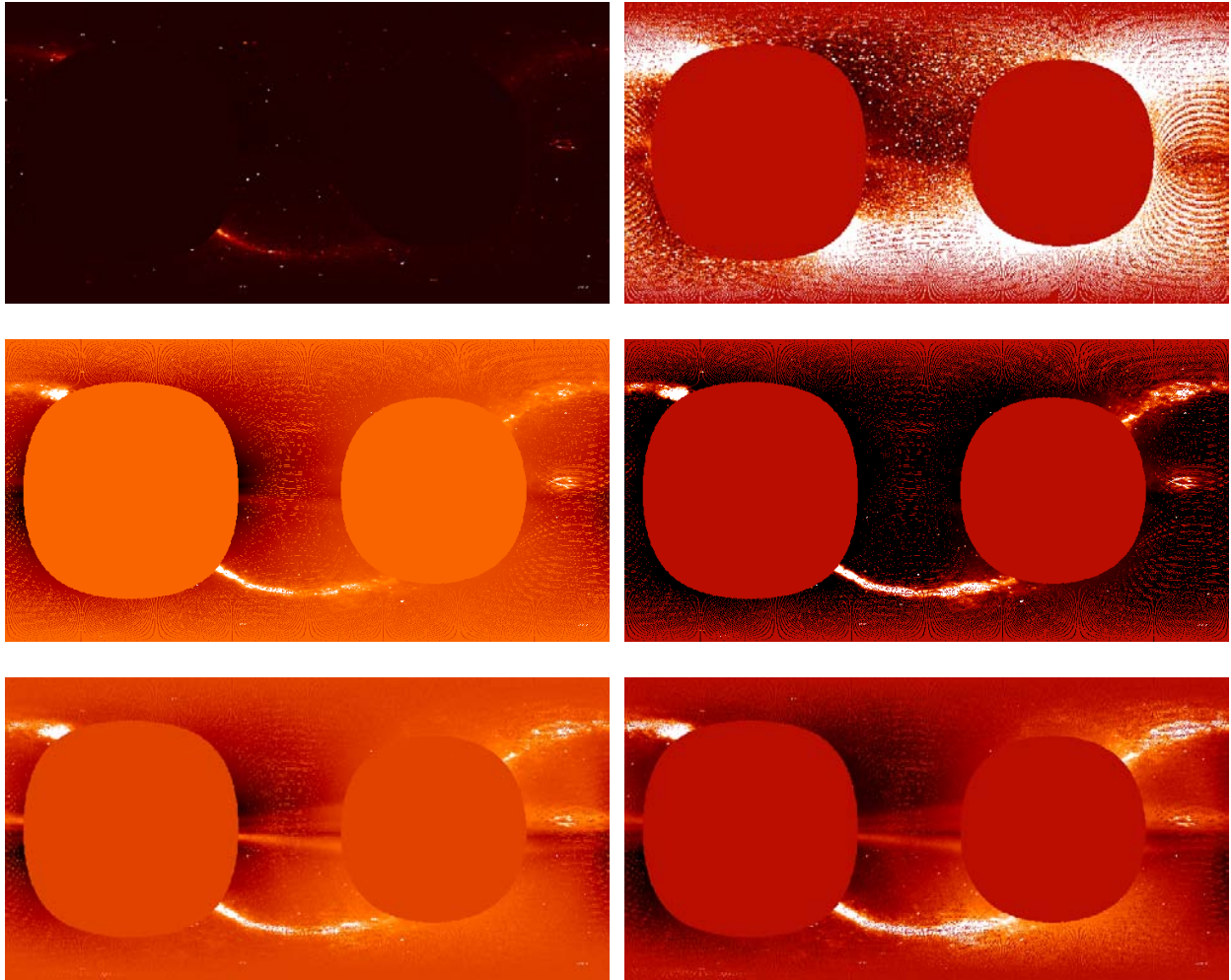


Figure 82. Residual plots between the DIRBE observations for day 4 of 1990 and the CB zodiacal model are shown for 4.9 μm (top), 12 μm (middle) and 25 μm (bottom). Radiance residuals are plotted on the left, percent differences are on the right. Radiance residuals greater than 5 MJy/sr are in white while black depicts residuals less than -5 MJy/sr. The largest inaccuracy is in modeling the dust bands. (Figure is adapted from Noah and Noah, 2001a). The Galactic plane is the white sinusoid.

and Hovenier (1988) for a finite dust cloud, is used. Hong fit the predicted in-plane integrated zodiacal brightness using the Henyey-Greenstein function to the Tenerife observations (Dumont and Sanchez, 1975) to derive the parameters. It was necessary to add a backscatter term to the model to account for the SMEI space based observations of the Gegenschein (Buffington et al., 2009).

The 4.9, 12 and 25 μm CBZodi model predictions are subtracted from the respective DIRBE observations in Figure 82. The largest positive residuals (color coded white) are from the Galactic plane while those at 4.9 μm are dominated by stars. Negative residuals are black and the two circular orange areas are regions without data. The largest modeling residual error is in the representation of the zodiacal dust bands. The CBSD model was tested against 38 days of DIRBE observations selected at various times during the mission and the mean of the normalized absolute values of the deviations between the model and the observations were found to be 10%, 8% and 11% at 4.8, 12 and 25 μm , respectively. Further adjustments of the model, particularly the band contribution, should reduce these averages.

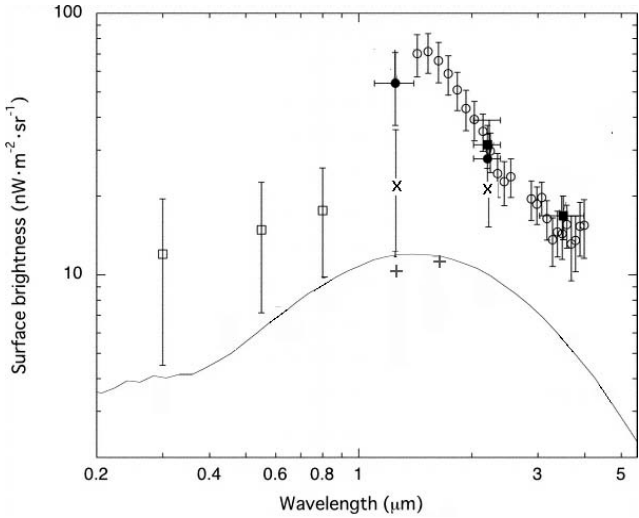


Figure 83. The near-infrared extragalactic background. The open circles are the IRTS near-infrared spectrum of the extragalactic background and the filled squares that overlay the IRTS data are the COBE observations. The open squares are the visible extragalactic background light observed by Bernstein, Freedman and Madore (2002) while the line is a model of the observed integrated background from known galaxies. The x's are the Levenson, Wright and Johnson (2007) DIRBE values. The plus signs are the NICMOS values (Thompson, 2008). The Levenson et al. analysis is consistent with visible results and are discordant with the IRTS excess. Figure is adapted from http://www.jaxa.jp/article/special/astro_f/3/index_e.html.

be removed by simply rescaling the zodiacal model by 23%. Levenson, Wright and Johnson (2007) confirmed that this is, indeed, the case with respect to the DIRBE observations (the x's in Figure 83) by subtracted the flux of 2MASS stars from the DIRBE fields that they analyzed and then removed the zodiacal foreground using the Georjian et al. (2000) model, which constrains the 25 μm residuals to be isotropic in the fields. Thompson (2008) derived the values from NICMOS observations on the Hubble Deep Field (+'s) in which he was able to separate the measured contribution from the zodiacal background and distant galaxies.

7.2.5. Asteroids, Moon and Planets

As moving objects, asteroids represent a source of false signals to the surveillance system. The SDIO/AFGL Background Characterization Program funded Ed Tedesco to update the IRAS asteroid catalog using the larger list of numbered asteroids available since the IRAS Asteroid and Comet preprint and to derive their physical properties, which were needed to predict their radiometric brightness as a function of time. The ultimate objective was to create a model that would predict the infrared irradiance in any specified spectral band for all the asteroids larger than 1 km in diameter. The deterministic part of this model estimated the irradiances of the known asteroids while a statistical component forecast the background for the objects as yet to be discovered.

The importance of an accurate zodiacal model was highlighted by the analyses of Matsumoto, Akiba and Murakami (1984, 1988) in deriving the near-infrared extragalactic background. Georjian, Wright and Chary (2000), Wright and Reese (2000) and Cambrésy et al. (2000) had also derived this background from DIRBE observations but the Matsumoto et al. (2005) Infrared Telescope in Space (IRTS) results in Figure 83 were at higher spectral resolution. The near-infrared extragalactic background in these articles was derived by carefully subtracting the Galactic and zodiacal foregrounds and accurate models are critical to such an analysis. For that, Matsumoto et al. modified the Kelsall et al. (1998) model for the IRTS spectral bands and subtracted the subsequent zodiacal predictions and those for a Galactic model from the IRTS spectrometry. But, as Dwek, Arndt and Krennrich (2005) noted, the excess in the near-infrared background derived by Matsumoto et al over the visible extragalactic light extrapolated into the near-infrared mimics the spectral shape of the zodiacal background itself and could

Tedesco et al. (2002) compiled the diameters and albedos in the Small IRAS Minor Planet Survey catalog (SIMPS) from which he calculated asteroid size–frequency distributions (Tedesco, Cellino and Zappalá, 2005). Analogous with the previous study of Cellino, Zappalá, and Farinella (1991), Tedesco divided the asteroid population into discrete groupings for each of nine zones in the Main Belt and the 15 Hirayama dynamical families. Each group has a characteristic albedo and size – frequency distribution, which he used to extrapolate the group population to a diameter of 1 km. The resulting statistical asteroid model sums the individual size distributions from which the albedo and size of an object in a given distribution is used to predict its infrared flux and the position at a given time. The orbital elements are either assigned deterministically to the asteroid if it is a known object or the mean elements of the distribution with each ‘unknown’ asteroid given a random epoch are used. This statistical asteroid model is the component of the Asteroid, Moons and Planets module in the CBSD; actual orbits may now be used in the module as orbits for nearly half a million asteroids are known.

Although AFGL supported Mark Sykes and Russ Walker to develop a model for comets and their trails, this effort was not completed and comets were not put into the CBSD. However, the planets and the four Galilean moons of Jupiter were (Kennealy et al., 1993). The planets were assumed to radiate as blackbodies at the equilibrium temperature produced by the solar input at their mean heliocentric distances. Slightly higher temperatures were adopted for Jupiter, Saturn and Pluto based on measurements reported in the literature. Since the Moon and most of the planets are resolved at the 2" finesse originally required by the CBSD, account is taken of their illuminated surfaces. The position of the object is calculated and the phase angle from the Earth is derived. The planets are assumed to be spherical and the illuminated surface visible from the Earth is assumed to scatter sunlight in proportion to the Bond albedo adopted for the object. Full disk thermal emission is adopted for planets with atmospheres, while the night sides of airless planets are assumed to have no emission.

7.2.6. The Moon as an Absolute Calibration Source

The Moon is well resolved at the 2" pixel size required by the SDIO background characterization effort. The lunar model in the CBSD simply provides disk-resolved images of the Clementine basedmap reflectivity for the visible portion of the Moon and a 90K dark side temperature. A more sophisticated model has been developed that may be used for calibration.

Because it is very bright, the Moon has been used to calibrate space-based sensors. Most of the effort dating to Lord Rosse’s work has been to accurately quantify the reflective and thermal emission properties of the Moon. It has only been relatively recently that attempts have been made to accurately describe these properties to an absolute scale. For example, the primary objective of the AFOSR sponsored contract to Shorthill (1990) was to establish the Moon as an infrared calibration source. Much later, Kieffer and Stone (2005) did provide analytic expressions for the calibrated visible to near-infrared irradiance of the Moon as a function of phase angle.

Kennely et al. (2010) coupled a unique database derived from Clementine space probe maps of the lunar surface with ground based imagery to produce resolved disk radiances that agree to <1% with an absolute calibration pedigree that is accurate to <5%. Clementine was born from a NASA and BMDO study that concluded that a small deep space mission could do good science while testing test advanced technology developments. As described by Nozette et al. (1994), the Clementine mission would test lightweight miniature sensors and components by obtaining imagery of the Moon and the near-Earth asteroid, Geographos. NASA provided

science support in return for access to data collected during the mission. The BMDO selected the Naval Research Laboratory (NRL) to be responsible for mission design, spacecraft engineering, manufacture and test, the launch vehicle integration and flight operations, while the Lawrence Livermore National Laboratory (LLNL) provided lightweight imaging cameras. Goddard Space Flight Center provided trajectory and planning for the lunar mission.

Clementine carried four sensors: a five color (0.415, 0.75, 0.90, 0.95, and 1.0 μm – Bands A through E, respectively) – an UV-Visible instrument, a 1 – 2.7 μm near infrared camera, a high resolution visible camera and an 8 – 9.5 LWIR μm camera. The UV-Vis and LWIR cameras have the best calibrations while the UV-Vis camera returned the highest quality data. The $4.2^\circ \times 5.6^\circ$ UV-Vis field-of-view was covered by a 384×288 element CCD array while the LWIR camera had 128×128 HgCdTe array.

The Clementine mission spent 71 days between 19 February and 3 May 1994 mapping the Moon from lunar orbit. McEwen (1996) and McEwen et al. (1998) describe the photometric model and the routines used to normalize the Clementine observations and to generate the basemap, the fundamental reference for the disk resolved lunar reflectance. The basemap is a global montage of the Clementine B (75 nm) filter images of the entire Moon normalized to nadir viewing (0° emittance angle, e), a 30° incident angle, i , and a 30° solar phase angle, α . The data comes in two element sizes, one at 2 km and the other at 200 m.

The reflectance scattering model we use is modified from Hillier et al. (1999):

$$R(i, e, \alpha) = \frac{\varpi}{4\pi} \frac{\mu_0}{\mu_0 + \mu} ([1 + B(\alpha)]P_{HG}(\alpha) + M(\mu_0, \mu))(1 + B_C(\alpha, h_C)) \times S(i, e, \alpha, \bar{\theta}) \quad (8)$$

Here, μ and μ_0 are the cosine projection of the surface element for the incident and scattered rays, ϖ is the single-scattering albedo while the singly scattered component, $[1 + B(\alpha)]P_{HG}(\alpha)[1 + B_C(\alpha, h)]$ is composed of a two term Henyey-Greenstein single particle scattering function times a shadowing opposition enhancement and a coherent backscatter term. M is a multiple scattering term while S is shadowing due to surface roughness.

Hillier et al. fit the reflectances for a number of locations in the lunar highlands and maria to derive the scattering parameters for these terrains in each of the Clementine UV-Vis filters. We employed more recent analytic representations for several of the scattering components and re-derive the parameters. The disk resolved absolute radiance from the Moon is calculated from Equation (8) for a specified i , e and α and scaled by the Sun – Moon – observer geometry. Hillier et al. assume, as do almost all modelers, that the Moon is spherical and that i and e are with respect to the surface plane perpendicular to the radius vector. We assume that these angles are with respect to the normal of the surface element, which is defined by the Clementine radar altimetry. Multiplying the reflectance by the solar flux puts the result on an absolute scale; after correcting for the factor of 0.52 that Hillier et al. (1999) noted was necessary in their Appendix C to bring the basemap reflectances into agreement with previous work.

The absolute calibration of the disk resolved radiance was verified by reference to an independent dataset, that obtained by the Robotic Lunar Observatory (ROLO) of the US Geological Survey (USGS). ROLO consists of two 20 cm telescopes co-aligned on the same telescope mount; one instrument images the Moon in 23 narrow visible spectral bands between 350 nm and 950 nm onto a 512×512 element CCD while the other telescope images the Moon in nine narrow near-infrared bands between 0.95 and 2.5 μm onto a 235×256 array. Kieffer and Anderson (1998) provide information on the observing program and the complexities of the modeling while Stone, Kieffer and Anderson (2002) described how a large number of multicolor

lunar images are obtained during the two week period between the first and third quarter of the Moon, which were calibrated against frequent observations of standard stars (primarily Vega) and rationalized to standard Sun – Moon and observer – Moon distances. Stone et al. estimated the absolute accuracy of the lunar measurements at 1.5% in the visible and 2.5% in the near-infrared. The absolute calibration is referenced to a Kurucz model atmosphere scaled to the Hayes (1985) absolute flux at 0.5555 μm . However, it now appears that Vega may undergo episodic brightness variations as large as 6% (Engelke, Price and Kraemer, 2010).

To validate the model parameters in Equation (8) and assess the accuracy of the results, we compared the photometric model predictions to ROLO data kindly made available to us by Tom Stone for the 11 sites that Kieffer and Stone (2005) used to derive their analytic expressions for the disk integrated lunar irradiance. The ROLO data includes the observed reflectivities for groups of ROLO pixels at each site along with the selenographic (sub-earth and sub-solar) coordinates for the time of observation. The phase angle and the incident and emergent angles are calculated from this information. The reflectances in all the ROLO photometric bands are calculated from the photometric model and compared to the observations. Although the two component maria and highlands model reproduced most of the ROLO data quite well, a third bright “crater” component was found to be necessary to account for the higher albedo reflectivities. Adjustment of the parameters in this three component model was made against three full disk ROLO calibrated images of the Moon at and within one day of being full. The agreement is quite good, <1% discrepancy after adjustments for systematic trends in the Clementine basemap: a small East-West linear trend in reflectivity and striping near the equator.

In the infrared, Pugascheva and Shevchenko (2001) derived analytic expressions for the low resolution 10 – 12 μm temperature distribution of the Moon from the isothermal contour maps derived by Saari and Shorthill (1967) and their own space-base observation. Pugascheva et al. (1999) applied this formulation to calibrate the infrared images from a geosynchronous satellite. Higher resolution and more accurate representation are obtained by solving for Equations (1) and (2) for each surface element. A reasonable approximation may be made by assuming that the lunar thermal inertia is negligible as less than 1% of the absorbed solar energy is conducted into the surface for a surface element in sunlight, (e.g. Sinton, 1962a). In this case the left hand side of Equation (2) is zero to good first order and the thermal energy balance equation may be expressed by:

$$T = \left[\frac{(1-r'_h)S}{\varepsilon\sigma R^2} \cos i' + \frac{6}{\sigma} \right]^{\frac{1}{4}} \quad (9)$$

Here, T is the temperature of the surface element, S is the total solar flux at 1 AU, R is the Moon’s heliocentric distance in AU, σ is the Stefan-Boltzmann constant, and r'_h is the hemispheric albedo defined by Hapke (2002), which is calculated using the direction cosine of the modified incident angle, i' , that account for the local vertical defined by the topography; the hemispheric albedo times the spectral solar flux is integrated over wavelength. The emissivity of the surface, ε , is usually assumed to be 0.9 to 0.97. The $6 \text{ (W/m}^2\text{)}/\sigma$ term was suggested by Racca (1995) to account for the flux from the subsurface of the Moon as it reproduces the 102K temperature of the lunar surface measured at lunar midnight. A full solution to Equations (1) and (2) is required with the small position dependent thermal inertia of the lunar surface in order to reproduce the images in Figure 12.

8. FILLING THE GAPS IN THE INFRARED SURVEYS

Japan's first infrared astronomy satellite, the Infrared Telescope in Space (IRTS), obtained near- and mid-infrared spectrophotometry and far-infrared and submillimeter photometry. The IRTS spectra overlapped that of the IRAS LRS although at coarser resolution and extended the wavelength range to $1.3\text{ }\mu\text{m}$. IRTS was one of several experiments on the Japanese Institute for Space and Astronomical Science (ISAS) Space Flight Unit, a multi-purpose free-flyer spacecraft, which was launched on ISAS HII rocket on 18 March 1995 into a circular orbit at 286 km altitude with a 28.5° inclination. IRTS covered about 7% of the sky in the 26 days of operation. Shuttle Endeavor on STS-72 recovered the payload in January 1996.

On the other hand, the astronomy experiments on the SDIO Midcourse Space Experiment (MSX) were designed to specifically address the gaps in the coverage of the inertial and zodiacal backgrounds of previous surveys owing to the loss in the IRAS sensitivity due to confusion along the Galactic plane and the restricted solar elongations of the surveys. Launched on 26 April 1996, MSX was a multi-objective experiment with 11 sensors that collectively spanned the spectral range from the ultraviolet ($\sim\text{Ly}\alpha$) to the LWIR ($25\text{ }\mu\text{m}$). This was the most complex DoD experimental mission ever flown and eight Principal Investigator (PI) teams were formed to encompass the widely diverse experimental objectives. The third of a meter clear aperture off-axis telescope had five line scanned infrared radiometer arrays while a Michelson interferometer provided low spatial resolution spectra. The MSX sensitivity and resolution were intermediate between those of IRAS and the Infrared Space Observatory (ISO) camera. Routine data collection began in mid-June and the infrared cryogenic phase of the mission ended on 22 February 1997 with the exhaustion of the solid hydrogen coolant. Although spacecraft power, tape recorder capacity and telemetry limited the duty cycle to about 10%, astronomical observations accounted for 40% of the measurements obtained during the cryogenic phase.

To be complete, very brief mention is made of the Wilkerson Microwave Anisotropy Probe (WMAP), the follow-on to COBE for high angular resolution submillimeter to millimeter cosmic background measurements. WMAP has back-to-back 1.4×1.6 meter diameter primary reflectors that provide differential photometry and polarimetry in five bands between 0.7 and 15 mm from passively cooled microwave radiometers at an angular resolution of about 0.23° , some 20 times better than the DMR and FIRAS on COBE. Page et al (2003) give a description of the satellite and radiometers. The satellite was launched in June 2001 and is providing results that continually improve the sensitivity. An excellent description of the history of cosmic background research with numerous first-hand vignettes may be found in Peebles, Page and Partridge (2009), the penultimate chapter of which places the WMAP results into context.

8.1. The Japanese Infrared Telescope in Space (IRTS)

In 1982, Hayakawa (1982) presented a concept for a Spacelab borne Japanese instrument: the Infrared Telescope in Space (IRTS). His proposal was forward looking as the Japanese space agency only begun flying infrared astronomy experiments on sounding rockets a few years earlier. Initially, the rocket experiments built on the balloon-based efforts by Okuda and his Kyoto University team and Hayakawa and his Nagoya University group. These small balloon-borne telescopes obtained low spatial resolution near-infrared maps of the Galactic plane in the narrow window between atmospheric OH emission lines at $2.3\text{ }\mu\text{m}$. As Okuda (1981) noted, these results, plus the HI STAR maps, provided the first global infrared picture of the Galaxy.

The first Japanese probe-rocket demonstration experiment that was flown in January 1977 by Hayakawa et al. (1978) looked for near-infrared flux in the Galactic anti-center direction. Not only was the atmospheric interference that plagued balloon experiments eliminated on this and subsequent flights, perhaps replaced by rocket/payload effluvia, but much broader spectral bands were used to increase the sensitivity. The Nagoya group (Noguchi et al., 1981) followed with an August 1978 flight that scanned 3° long latitude profiles of the Galactic plane at 29° longitude in spectral bands centered at 2.0, 2.8 and 4.5 μm . Subsequent experiments concentrated on the near and far-infrared diffuse cosmic background, starting with an early 1980s flight from which Matusumoto, Akiba and Murakami (1984) reported a bright isotropic 1 – 5 μm background. This experiment was reflown in January 1984 and obtained narrow band 1 – 5 μm spectrophotometry of the sky (Matsumoto, Akiba and Murakami, 1988). An overzealous data reduction and analysis led to an unrealistic measurement of the 2 μm cosmic background (Figure 83 has a set of updated measurements).

The Nagoya group teamed with Andrew Lange and Paul Richards at the University of California, Berkeley to fly sub-millimeter cosmic background experiments in September 1985 and February 1986 (Matsumoto et al., 1988). Matsuura et al. (1995) then extracted zodiacal background measurements made with a near-infrared grating spectrometer on February 1990 and 1992 flights. The latter experiment also included a far-infrared photometer with which Bock et al. (1993) measured [C II] 158 μm line emission. Noda et al. (1992) noted that these experiments were demonstration flights for IRTS using a 2/3 scaled version of the proposed orbital telescope; the IRTS telescope had been scaled down to 15 cm from the 20 cm March 1987 baseline. All told, the Japanese space agency has flown a dozen or so probe-rocket based infrared astronomy experiments over a twenty year period.

Murakami et al. (1994) describe the IRTS sensor and mission, a collaboration between the ISAS and NASA, while the four focal plane instruments are detailed in the *Astrophysical Journal* papers that follow that article. IRTS had a small, f/4 Ritchey-Chretien telescope with a 15 cm primary aperture, comparable in size to the HI STAR sensors. The four IRTS focal plane instruments consisted of near, mid- and far-infrared grating spectrometers and a four spectral band far-infrared/sub-millimeter photometer. The size and position of the detectors in the spectrometer focal planes set the spectral resolution and wavelength that were observed. The 32 $8.5' \times 8.5'$ InSb near-infrared spectrometer detectors covered 1.38 to 3.98 μm with a rather coarse wavelength resolution ($\Delta\lambda$) of $\sim 0.13 \mu\text{m}$ while the 4.5 – 11.7 μm mid-infrared spectrometer had a comparable Si:Bi detector array that had spectral bandwidths that varied from 0.23 μm to 0.36 μm . The four channel far-infrared grating spectrometer measured the 63.1 μm [O I] and the 158 μm [C II] lines with a spectral resolution, $\lambda/\Delta\lambda$, of about 400 while lower resolution ($\lambda/\Delta\lambda \sim 130$) channels measured the continuum on either side of the [C II] line. The far-infrared to sub-millimeter photometer had broad ($\lambda/\Delta\lambda \sim 3$) spectral bands at 150, 250, 400 and 700 μm . Collectively, the four focal plane instruments spanned the wavelengths from 1 to 1000 μm .

IRTS began scanning great circles on the sky on 29 March and covered $\sim 2700 \text{ deg}^2$ by the time the 90 liters of superfluid helium ran out 26 days later on 24 April. Murakami et al. (1996) gave an overview of the instrumentation and an as-run profile of the experiment.

Point sources were extracted from the near and mid-infrared spectrometer data. Le Bertre et al. (2003) obtained 14,223 good to high quality near-infrared point source detections while Le Bertre et al. (2001) found ~ 600 mid-infrared objects. The system had a point source detection limit of about [2.2] ~ 8 and [3.5] ~ 7 magnitude, although source confusion near the Galactic plane reduced the sensitivity by about a factor of 10. Le Bertre et al. (2001, 2003) analyzed

these observations to identify and characterize mass losing asymptotic giant stars whereas Matsuura et al (1999) studied the spectra, detecting water vapor absorption in early M-type stars.

Matsumoto et al. (1996) and Ootsubo et al. (1998, 2000) extracted diffuse near and mid-infrared zodiacal spectra, respectively, at high ecliptic latitudes. Chan et al. (1998) deconstructed the diffuse mid-infrared spectra taken in the Galactic bulge to infer that the emission arose from M and K giant stars plus an admixture of emission features from the interstellar medium. Chan et al.(2001) subsequently conducted a more extensive study of the IRTS mid-infrared spectra of the interstellar medium. At longer wavelengths, Makiuti et al. (2002) analyzed the distribution measured for the far-infrared [C II] emission and concluded that the emission line arises mainly in ionized regions, which was expected as this line is a major cooling mechanism in such regions. They also deduced that the Sun is about 20 parsecs above the Galactic plane from the observed asymmetric north-south distribution of the emission, a result that compares favorably with other good quality determinations.

8.1.1. Galaxy Haloes and Low-Mass Stars

Matsumoto continued his collaboration with Lange and Bock well into the 1990s. In the early 1990s, Andrew Lange and Jamie Bock (Bock et al., 1994), at Caltech, proposed a Near-infrared Faint-Object Telescope Experiment for a very sensitive large format InSb array with a cooled 50 cm diameter telescope to look for cool objects, such as brown dwarfs, highly red shifted sources and proto-galaxies. Andrew Lange contacted GL not long thereafter to inquire as to the possibility of financial support for such an experiment. Although we couldn't provide funds, we did make a substantial capital contribution in the form of the SCOOP surplus hardware: a complete sensor and most of a second telescope with some spare optical parts. Bock et al. (1998) describe the experimental configuration with the SCOOP optics and the initial attempt to measure the near-infrared halo around the edge on galaxy NGC 4565 from a Black Brant IX flown out of White Sands Missile Range on 28 May 1997. Although Uemizu et al. (1998) tried to make some sense of the measurements; the results were compromised by the sensor being out of focus. The focus was corrected for the 22 May 1998 reflight that observed NGC 5907 (Yost, et al., 2000) and Xu et al. (2002) estimated the 4 μ m surface brightness fluctuations from both sets of measurements. It is of note that Erik Jensen had studied the halo of NGC4565 while a post-doc at AFGL/Sac Peak (Jensen and Thuan, 1982) while Dave Barnaby, who was our BMP program manager as a Captain at SAMSO in the early 1980s, and Harley Thronson (1992) analyzed their near-infrared measurements of NGC 5907.



8.2. The Midcourse Space Experiment (MSX)

By the mid-1980s, the SIRE demonstration program was defunct and LAIRTS had been terminated. Thus, the DoD did not have a satellite-based technology demonstration when Barry Katz came to SDIO. Barry was aware of the AFGL LAIRTS study and saw the need for a phenomenology mission to support discrimination requirements combined with a technology demonstration to explore engineering issues regarding the long term operation of cooled infrared systems in space. At about this time, Space Division issued a request for proposals for a

Surveillance and Tracking Experiment Program based on SIRE performance (Mike Kiya, 6 January 2004 e-mail). Hughes and Rockwell responded in the summer of 1986 but the program did not proceed after proposal evaluation. Instead, Barry Katz funded Tom Murdock to lead an Aerospace, AFGL and ABMDA team to assemble the DoD targets and backgrounds requirements into a report that was submitted in the fall of 1987 as the basis for a new joint program. Subsequently, SDIO and the Air Force sponsored the 1987–1988 National Midcourse Sensor Study, which concluded that a meter class sensor was not required to meet the surveillance demands to detect, acquire and track exo-atmospheric targets (Stair, 1996). A smaller instrument could do the task and Barry Katz decided that SDIO would build a Midcourse Space Experiment (MSX) as the demonstration. A Science and Engineering Support Team (SEST) was formed toward the end of 1988 that included representatives of the principal engineering and background interests to determine the sensor performance requirements and the phenomenology pertinent to the midcourse target detection phase of space based surveillance.

At AT Stair's recommendation, Katz visited the Utah State University (USU) Space Dynamics Laboratory (SDL) and came away impressed with their experience with cryogenically cooled infrared sensors for space applications such as SPIRIT II that were of a size comparable to that contemplated for MSX. In the winter of 1988, Katz funded SDL to construct the Spatial Infrared Imaging Telescope (SPIRIT III) and the Johns Hopkins Applied Research Laboratory (APL) to build the payload.

The MSX PI team, half of whom had served on the SEST, was formed in early 1990 as a steering committee for the program. Eight MSX PIs, led by AT Stair, conducted a wide range of experiments that were divided by instrument and objective: the Early Midcourse (Glenn Light – Aerospace Corp.), Space Surveillance (Mike Gaposchkin – Lincoln Laboratory), and the Theater Missile (Wally Moore – ABMDA) teams observed man-made objects. Three other teams measured the natural backgrounds: the Terrestrial Backgrounds team (Jerry Romick – APL) observed the Earth's atmosphere with the ultraviolet – visible sensors while the Earthlimb team (Bob O'Neil – Geophysics Directorate) obtained infrared observations of the hard Earth and the atmosphere; the Celestial Backgrounds team (Steve Price – Geophysics Directorate) did astronomy. The two other teams explored technology issues associated with the spacecraft performance: the Contamination Control team (Manny Uy – APL) monitored the environment in the sensor and near the spacecraft and the Data Certification and Technology Transfer team (Tom Murdock – General Research Corp.) accurately quantified and monitored the performance of the various instruments. Mill et al. (1994) provides an overview of the MSX mission and a general outline of the hardware while Voss (1997) discussed the MSX technology transfer to the civilian community, sketching the multidiscipline scientific return expected from the mission and presented some initial results that prominently featured the astronomy observations.

8.2.1. The Spatial Infrared Imaging Telescope (SPIRIT III)

Ames and Burt (1993, 1994) describe the SPIRIT III design while Bartschi, Morse and Woolston (1996) gave details on the completed instrument. The aluminum primary mirror in the SPIRIT III off-axis telescope had a 35 cm circular aperture. Although the ZIP 'D' shaped mirror had more collecting area in a given sensor volume, Tom Murdock successfully argued for a circular aperture to assure that the sensor would have a well-defined and quantifiable point response function. This goal was compromised somewhat by a Lyot stop that was inserted to reduce the off-axis radiation for the experiments that viewed near the Earth. The Lyot stop also reduced the clear aperture collecting area by about 7% to 896 cm².

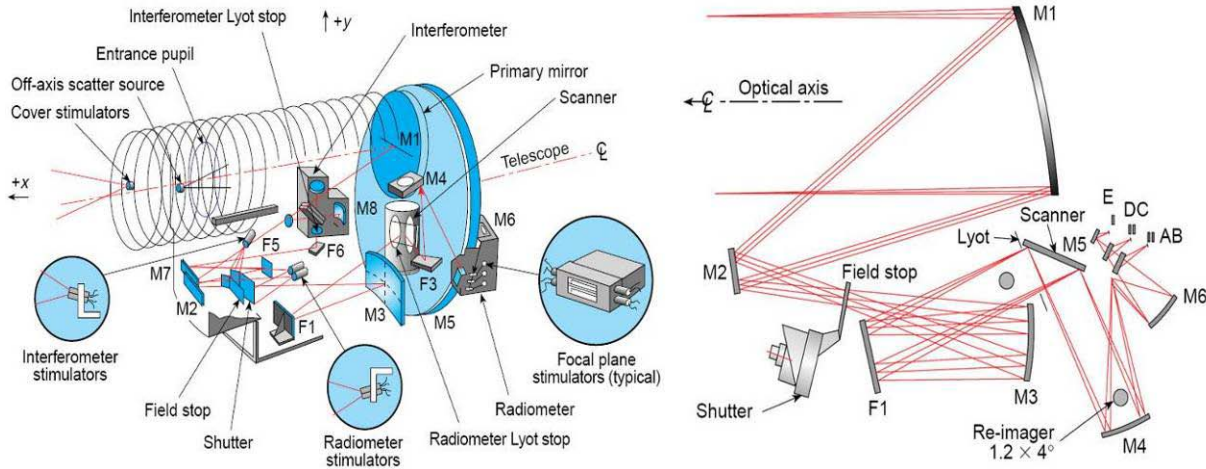


Figure 84. The SPIRIT III optics. The telescope components and the relative sizes of the mirrors are diagrammed on the left and a ray trace through the radiometer is shown on the right; the mirrors are labeled M and folding flats with F. Specific labeled features are: the shutter that blocked in-coming radiation to internally calibrate the focal planes; the Lyot stop that reduced the near-field off-axis diffraction from the primary mirror; and the scan mirror that swept the instantaneous field of the linear focal plane arrays across a 1° by 0.75° to 3° field-of-regard. Figure was adapted from Bartschi, Morse and Woolston (1996).

Besides two sets of internal stimulators that were used to track the radiometric response, several other devices were built into the optical bench to monitor or improve performance. A two-axis autocollimator was intended to measure SPIRIT III azimuth and elevation boresight movements relative to the spacecraft optical bench during the flight but proved to be unnecessary and was never used. Two contamination monitors were built into the sensor. A cryogenic thermal gravimetric quartz crystal microbalance placed next to the primary mirror measured and identified condensates. The vibration frequency of the microbalance indicated the amount of deposition while the manner in which the frequency changed as the device was warmed indicated the molecular species. An off-axis light source to monitor the scattering from particulates and condensed vapor contaminants from a one-inch diameter spot on the primary mirror at a single off-axis angle was to indicate when the primary mirror needed cleaning with a CO₂ laser, a popular idea in the late 1980s. The risks of the laser were deemed too great and the technical maturity was less than desired and the idea was abandoned before the Critical Design Review. Although the scatter monitor was retained, it was not used, as the information was provided by other means. The optical layout and a ray trace through the optics are shown in Figure 84.

Each of the five infrared, line-scanned, Si:As blocked impurity band focal plane arrays in the SPIRIT III radiometer had eight columns with 192 rows of 18.3" square detectors. Except for the 4.3 μm B Bands, the columns covered $\sim 1^\circ$ in cross-scan. Originally, Band B spanned the entire cross-scan field with a 6 – 8 μm filter, providing additional mid-infrared spectral selectivity and isolating the prominent PAH bands. The Band B filter was subsequently changed to compensate for the loss of 4.3 μm data when the Boost Surveillance and Tracking System was cancelled. Band B was divided in cross-scan by two slightly different filters centered on the atmospheric 4.3 μm CO₂ band; the central obscuration of the filter holder reduced the number of active B Bands detectors by $\sim 15\%$ to 76 in each subarray. Overall, less than 2% of the remaining focal plane detectors were non-responsive or rejected for various reasons. The system parameters are given in Table 5 in which the source detection limits in column 5 are robust estimates based on the log (number of sources) vs. log (flux) plots in Egan et al. (2003).

Table 5. SPIRIT III Spectral Band Parameters

Spectral Bands	Active Pixels in Array	λ_e (μm)	Isophotal $\Delta\lambda$ (μm)	Source Detection Limit		Ω_{prf} ($\times 10^{-8}$ sr)
				(W/cm 2)	Jy	
A	8 x 192	8.28	3.36	1.8×10^{-18}	0.16	1.06
B ₁	2 x 76	4.29	0.104	2×10^{-17}	30	1.4
B ₂	2 x 76	4.36	0.179	2.2×10^{-17}	12	1.4
C	4 x 192	12.13	1.72	4.4×10^{-18}	1.25	1.17
D	4 x 192	14.65	2.23	2.5×10^{-18}	0.8	1.13
E	2 x 192	21.34	6.24	1.1×10^{-17}	2.6	1.26

After a number of development and manufacturing difficulties, Aerojet Corp. delivered high quality Band A and B arrays. The Rockwell Band C, D and E arrays were also acceptable and the best were installed in the sensor. The Rockwell arrays began to fail because the gold substrate lines implanted in the focal planes were too thin and the preamplifier nano-wires that were welded to the lines pulled away as the sensor was thermally cycled during the ground tests. The failed arrays were replaced by backups that were about a factor two less sensitive in Bands C and D and four in Band E. This is the reason for the widely divergent sensitivities in Table 5.

The MSX spectral bands were not typical astronomical bands. Bands B and D were centered on the 4.3 and 15 μm CO₂ atmospheric molecular features, respectively, to probe the atmospheric distribution of this molecule. Being relatively free of molecular absorption, Bands A, C and E can see deeper into the atmosphere. Band A was the most sensitive and covered a spectral region not easily available from the ground but it is sufficiently similar to Akari, ISO and Spitzer camera bands to permit direct comparisons. Band C is a narrower analog of the IRAS 12 μm filter and COBE/DIRBE Band 5. Band E is an analog of the Spitzer 24 μm band and COBE/DIRBE band 6, both of which are commonly compared to the IRAS 25 μm band.

Bands A, D and E were co-aligned by means of dichroic filters as, separately, were Bands B and C with the two sets of co-aligned arrays being separated by about $1/4^\circ$. Half the columns in each array were offset by half a pixel row, resulting in $\sim 9''$ cross-scan sample spacing as shown in Figure 85. To reduce the telemetry rate, only half of the total number of columns were active, as specified in column 2 of Table 5. However, all Band A columns were active and at least one column on either side of the stagger was active in the other bands.

The diversity of the MSX experiments required that observations be made with a number of different strategies against a wide range of backgrounds, from looking at the hard Earth and Earth limb to deep space. To accommodate these varying conditions, SPIRIT III had two scan modes and a number of gain states. An internal scan mirror, so labeled in Figure 84, could either be fixed or scanned at a rate of 0.46 $^\circ$ /sec with amplitudes of 0.75 $^\circ$, 1.5 $^\circ$ or 3 $^\circ$. The mirror scan mode used the high 25 Mbps data rate and nearly all of the ~ 100 astronomy measurements taken by the Data Certification team used this mode. The 12 bit telemetry word provided a dynamic range of about 3000 in a given gain state when account is taken of the dark offset. Four gain states in the mirror fixed mode and three in mirror scan accommodated the large range of backgrounds with a total dynamic range of $\sim 2 \times 10^5$. All the celestial experiments used the more sensitive mirror fixed mode, which had five times longer integration time and a 5 Mbps data rate.

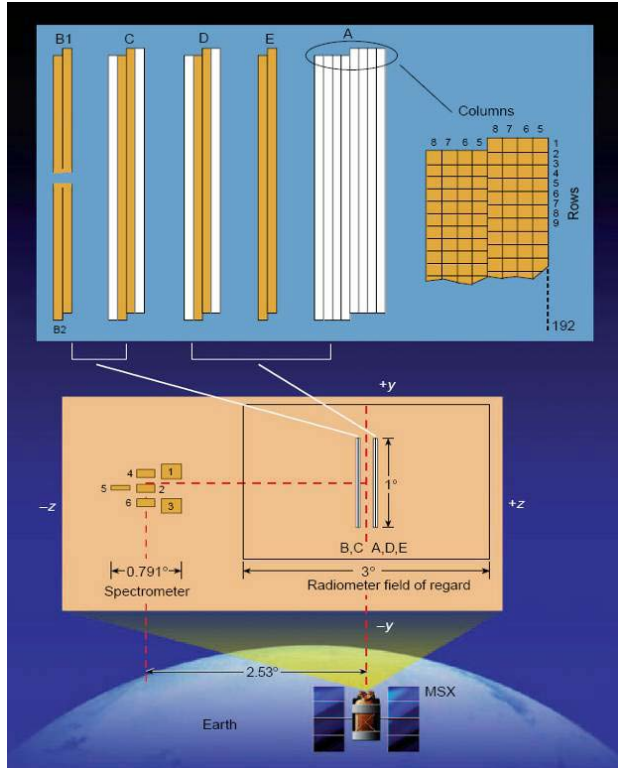


Figure 85. The MSX focal plane layout. Half of the focal plane columns are vertically offset by half a detector in each Band, which provided critical (Nyquist) cross-scan sampling. The interferometer detectors are offset from the radiometer arrays by $\sim 2.5^\circ$ in the scan direction. Adapted from Bartschi, Morse, and Woolston (1996).

astronomically usable detectors obtained 6 – 10 μm and 16 – 28 μm spectra. Resolutions of 2, 4 or 20 cm^{-1} were available by scanning the mirror at constant speed for 4, 1 and 0.4 seconds, respectively. A helium-neon laser timed the sampling with an electronic clock as backup. The backup was a wise precaution, as various problems required that almost all the interferometry to be conducted in the timed mode. Because of the problems, only two good quality astronomical spectral observations were obtained.

The SPIRIT III optical bench was cooled by a 944-liter solid hydrogen cryostat. Solid H_2 was chosen because it has much higher specific heat than helium, which translates into a much longer mission lifetime for a given volume of cryogen. The dewar was sized to meet the initial design goal of a two year mission lifetime with a 22 month requirement. As Tom Murdock (8 June 1999 e-mail) noted, this would span two fiscal years during which it was anticipated that sufficient funds would be obtained to support four, then two, dedicated target missions. Also, a two year mission allowed reasonable statistics to be gathered on the seasonal variation over the Northern Hemisphere. Ames and Burt (1993) initially estimated the SPIRIT III cryogenic lifetime at 20 months based on thermal analysis of the final sensor design, which they (Ames and Burt, 1994) subsequently revised to 18 months after taking into account additional the thermal loads such as from the auto-collimator and scattering monitor.

For the astronomical observations, the spacecraft motion scanned SPIRIT III across the sky at rates between 0.02 and 0.125 deg per sec. Over 80% of these measurements were taken in the highest gain but the gain was reduced by factor of four and the survey scan rate decreased for the last 20% of the observations to partially compensate for increasing noise toward the end of the mission when rising focal plane temperatures elevated the dark offset above mid-scale in the highest gain.

The SPIRIT III interferometer shared 24.7 cm of the primary aperture. A column of three $6.4' \times 9.5'$ detectors were located on the centerline of the interferometer, which was offset by $\sim 2.5^\circ$ from the radiometer, while three $13' \times 13'$ detectors were placed two on one side of the central column and one on the other as shown in Figure 85. The detectors and filter characteristics were tailored to observe spectral detail in the Earth's atmosphere. The center detector covered 3 – 5 μm while the other two detectors spanned the entire 2.7 to 26 μm interferometer spectral range; one of the latter channels had a notch filter that eliminated the CO_2 15 μm atmospheric band. The two large

During the November 1994 field preparation for launch, a catastrophic cryostat failure that, as Tom Murdock (27 July 1999 e-mail) noted “*...split the vent tube plumbing through the heat exchanger like a banana peel from end-to-end along the soldered seam of the two quasi-semi circle pieces*” and almost terminated the program. Schick and Bell (1997) attributed the failure to stress corrosion in the vent and fill port valves while the SPIRIT III Failure Review Team Final Report ascribed the failure to improper cryogen handling and top-off procedures. The Failure Review implied that if the stress corrosion cracks were the ultimate cause of the failure, such cracks were likely due to the stresses induced by improperly filling the cryostat. At first, the program replaced the valves with spares and repaired the damaged plumbing in an attempt to fly within six months, by April 1995. However, further problems led to a redesign of the valves and an additional year launch slip.

The launch delay afforded the opportunity to partially disassemble the sensor. The optics were returned to Sensor Systems Group (SSG) to be cleaned and repolished; the scan mirror was a loss and was replaced with the backup subassembly. The violence of the rupture had spewed the iron oxide (rust) in the vent line catalytic converter everywhere within the vacuum vessel. Molecular hydrogen has two states in roughly equal proportions at room temperature, a higher energy ortho state in which the spins of the two protons are aligned parallel and a lower energy para state in which the spins are in opposite directions. The ortho states are converted to para as the gas is cooled and frozen. The iron oxide catalyst converts the low energy para state into the higher ortho state and the latent heat from the transition is used to cool the sensor. Other refurbishments included inserting a sapphire blocker into the Band B filter stacks that greatly improved the spectral purity (out of spectral band rejection) of the observations. Regrettably, there was neither sufficient time or funds to replace the degraded Rockwell arrays.

Unfortunately, the uncertainty as to the true cause, and fix, of the cryostat failure led to the conservative program management decision not to fill the tank ullage during preparation for the April 1996 launch, which resulted in the cryotank itself not being completely filled. Schick and Bell estimated that the incomplete fill of the tank reduced the cryogen life by four months and that more than two months of mission time were lost due to degraded performance of the insulation around the cryostat from the failure. None of these estimates factored in the roughly three times larger than anticipated parasitic thermal load from the front end of the sensor that came to light in March 1996 during the only complete cold cycle cryogen system fill after the rebuild. This test was conducted to prove that the hold time in the H₂ tank was sufficient to move from the preparation building to the launch complex. The tank warmed up past the freezing point in three days, much shorter than the estimated ten days.

8.2.2. The Spacecraft

The 2.7 ton, 1.5×1.5×5.1 meter MSX spacecraft, shown in Figure 86, supported four sets of electro-optical sensors. As the primary mission instrument, SPIRIT III is mounted at the center of the spacecraft. The four APL ultraviolet-visible imaging telescopes and the five ultraviolet to far red hyperspectral imagers collectively referred to as UVISI, are attached to the sides of the spacecraft. The 15 cm Space Based Visible (SBV) surveillance telescope that SSG built for Lincoln Laboratory (Harrison and Chow, 1996) is on the back left side of the payload in the upper right of Figure 86. All the sensors are referenced to the spacecraft optical bench.

The MSX payload, shown on the Delta rocket in Figure 87, was launched on 24 April, 1996 into a ~900 km polar orbit that precessed at ~15° a year. Thus, the downward looking observations would probe seasonal variations on the Earth under different sunlit conditions from

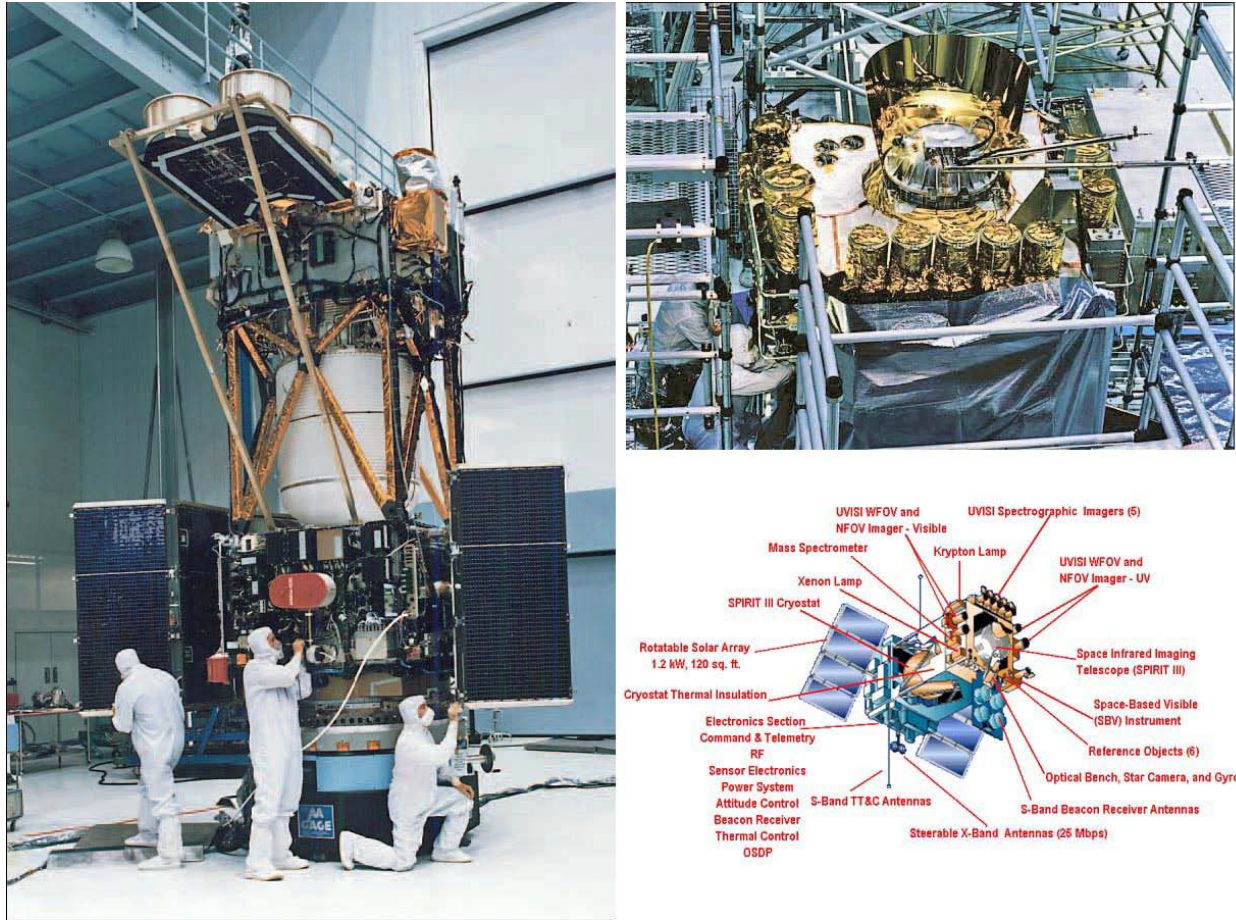


Figure 86. The MSX payload. The assembled payload without the thermal blankets and reflective covering is shown at left. The SPIRIT III cryotank is the white cylinder and the beacons used to track cooperative targets are on long struts. The payload front end is shown in the upper right in which the SPIRIT III solid argon cooled cover and Sun/Earth shade are prominent features in the center. The APL ultraviolet – visible imagers and spectral imagers are arrayed around the sides of the payload and the Lincoln Laboratory Space Based Visible Sensor is on the left. The payload components are labeled in the lower right.

dawn–dusk to noon–midnight over the 18 month cryogen lifetime estimated by Ames and Burt (1994). Phase 1 of the mission ended on 20 February 1997 and was devoted almost exclusively to SPIRIT III observations. The crystal quartz monitors then assayed the cryo-deposition on the mirror as the sensor warmed up. During the following half year, Phase 2 emphasized astronomy and atmospheric measurements with the UVISI sensors. The final phase began in October 1997, when the SBV became an Advanced Concept Technology Demonstration for the US Space Surveillance Network (Stokes et al., 1998), terminating operations after 11 years in mid-2008. The spacecraft and its resources were sized for the 36 minute dedicated target mission. This observation was recorded at the high 25 Mbps data rate and the spacecraft was slued at the highest tracking rates. Spacecraft passes over the John Hopkins APL X-band ground station in Columbia Maryland were usually long enough to downlink the contents of one full tape recorder per day. The spacecraft had two tape recorders that could redundantly record the high priority target events or, as was usually the case, used in tandem with one recorder being downlinked while the other recorded the measurements for the day. Power and telemetry downlink time limited the spacecraft to a ~10% duty cycle, or two to five observations each day.



Figure 87. The MSX payload on the Delta rocket at Vandenberg AFB, CA. The Delta sports the maximum complement of nine strap-on booster motors.

8.2.3. On Orbit

SPIRIT III wasn't as sensitive as anticipated owing to elevated noise from higher than expected focal plane temperatures. The SPIRIT III optical bench was thermally tied to the top of the cryotank by means of shrink fitted fixtures as were the focal plane straps. SDL had estimated that the focal plane temperature would be $\sim 10\text{K}$ at the beginning of the mission since they had added more copper straps between the dewar cold finger and the focal planes than the original design called for. During flight, however, the solid H_2 quickly shrank away from the tank top where all the heat from the sensor was dumped, the consequence of which increased the focal plane operating temperatures. Also, the coupling between the four thermal links on the top of the tank and between the cryogen and tank walls was not as good as expected. The tank was packed with aluminum foam to conduct the heat from the optics and focal plane tie points on the tank walls to the frozen H_2 , but either the foam was not as efficient as anticipated or the press fit between the foam and the tank walls did not have as good a thermal contact as expected. Thus, the cause of the elevated focal plane temperatures was analogous to the reason for the large FIRSSE focal plane temperature excursions in which all the thermal input from the optics and focal plane were deposited at a few closely spaced points on the cryotank, driving the cryogen away from those locations and elevating the temperatures.

For whatever reason, the beginning of the mission SPIRIT III focal plane temperatures were $\sim 11.2\text{ K}$, about 1 K higher than expected, and the subsequent temperature rise was faster than anticipated. The detector responses and dark offsets dynamically responded to the focal plane temperature variations. Remarkably, thanks in large part to Ray Russell (Aerospace Corp.) of the Data Certification team, the SDL ground chamber characterization of the sensor response as a function of all conceivable parameters and the on-orbit performance assessment experiments executed for the SDL and Data Certification teams provided excellent first order normalizations to correct for these changes. That is, all changes except the average factor of two loss in overall sensitivity due to increased noise from the higher temperatures. Price et al. (2004a, b) meticulously processed the 220+ MSX calibration observations against standard stars and confirmed that the response as a function of temperature normalizations derived by SDL in their preflight calibrations were accurate to within 1 – 2%, except for Band E where discrepancies as large 10% were found. Price et al. (2001) also described further refinements that were derived from the astronomy experiments that, when implemented, produced research quality products.

To assess the scattering properties of the mirror, the Data Certification team took a set of measurements approximately every two months in which the same sun-centered elongations were scanned over a three day period as the Moon transited the region. The astronomical payoff was a set of sensitive infrared ecliptic plane profiles at $\sim 90^\circ$ and 180° elongation. The practical consideration was to use the Moon as a very bright quasi-point source to derive the scattering properties of the primary mirror as the mission progressed. The unpublished results were subsequently verified by O'Neil, Gibson and Richards (2006) who deconvolved the non-rejected Earth radiation from their MSX Earthlimb observations to derive the mirror scattering function.

While the observations against the Moon provided a direct measure of the total scattering from the mirrors, the cryogenic quartz crystal microbalance proved to be an effective monitor of molecular deposition on the mirror. Since the microbalance was located next to the primary mirror and had to be heated in order to identify the species, this was done only twice during the cryogen phase of the mission. Once was to identify the gradual buildup of a film while the SPIRIT III cold cover was in place. The culprit was oxygen that was migrating from the baffles to the colder optics (Wood et al., 1998). A second assay after the cover was ejected found that a

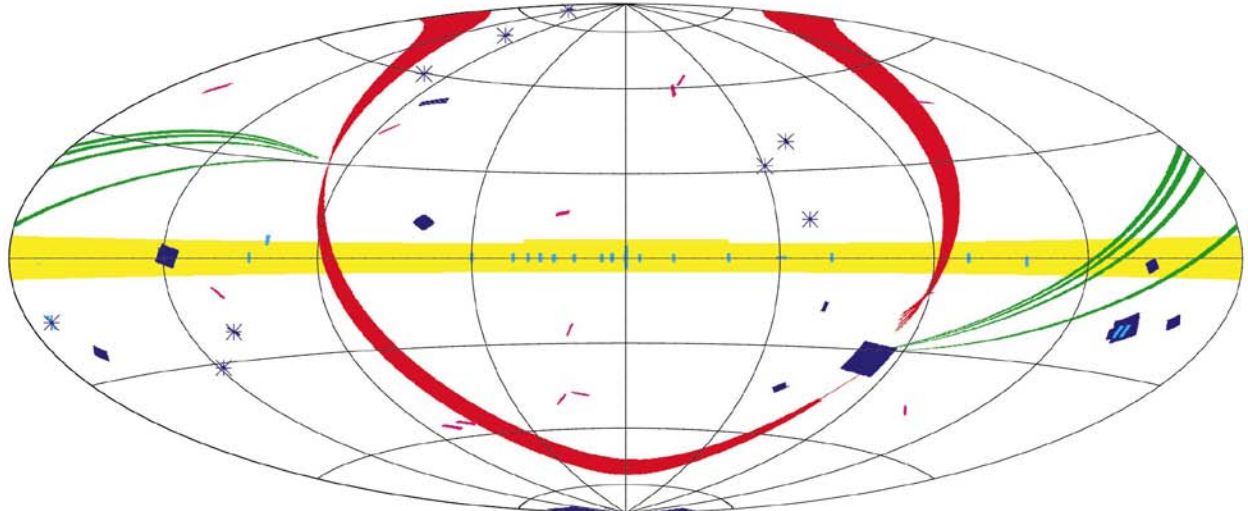


Figure 88. The MSX astronomy experiments. This Galactic Aitoff projection has the 10° wide Galactic plane survey depicted by the yellow horizontal band. The red band covers the areas of sky missed by IRAS, which simultaneously sampled the zodiacal background to 180° sun-centered longitudes. The green arcs represent the five zodiacal scans at sun-centered longitudes between 25° and 30° . The blue patches are surveys of areas of extended emission such as the Large and Small Magellanic Clouds, the Orion and Rosette nebulas and resolved external galaxies. The smaller markings and asterisks are raster scans of specific objects.

72 \AA thick layer of argon had been deposited during release of the argon cooled cover. The microbalance also indicated that water vapor from the multi-layer insulation was the principal outgassed component as the sensor warmed up after the cryogen ran out (Uy et al., 2000).

Two-thirds of the Phase 1 observation time was allocated to the Earthlimb, Celestial and the Data Certification experiments. Roughly 100 hours of observing time were given to the Celestial measurements while another 35–40 hours were devoted to astronomical calibration measurements conducted by the Data Certification Team. The SPIRIT III was designed to have a fairly large area scan rate (1 deg^2 in 8 seconds in the mirror fixed mode). Thus, surveys of regions of extended emission and/or high source density were preferentially selected to take advantage of the MSX survey rate, resolution and sensitivity. As shown in Figure 88, approximately 10% of the sky was covered by the astronomy experiments.

The PIs were requested to provide mission operations with a short list of measurements that were to be executed early in the mission in order to obtain initial high value results and to provide an early sample of data with which each team could tune their data processing routines. Underlying the request for early sampling was the uncertainty in the cryogen lifetime. We chose the Small Magellanic Cloud (SMC) for the initial astronomy measurement as it is small enough to be completely mapped on a single $3^\circ \times 3^\circ$ raster scanned observation by both SPIRIT III and the ultraviolet small field imager. The SMC was measured about three weeks after launch, followed by a long scan along the Galactic plane through the first and fourth quadrants a week later and then a raster scan of the Galactic center the day after that.

There was a fair amount of latency in spacecraft operations with only limited ability for real time commanding and data transfer. Experiment commands were up-linked to the spacecraft one to three days before execution. Normally, down-linking the data from the spacecraft, processing it through the APL mission operations center and out the Phillips Laboratory MSX Data Analysis Center took on the average of a week to ten days.

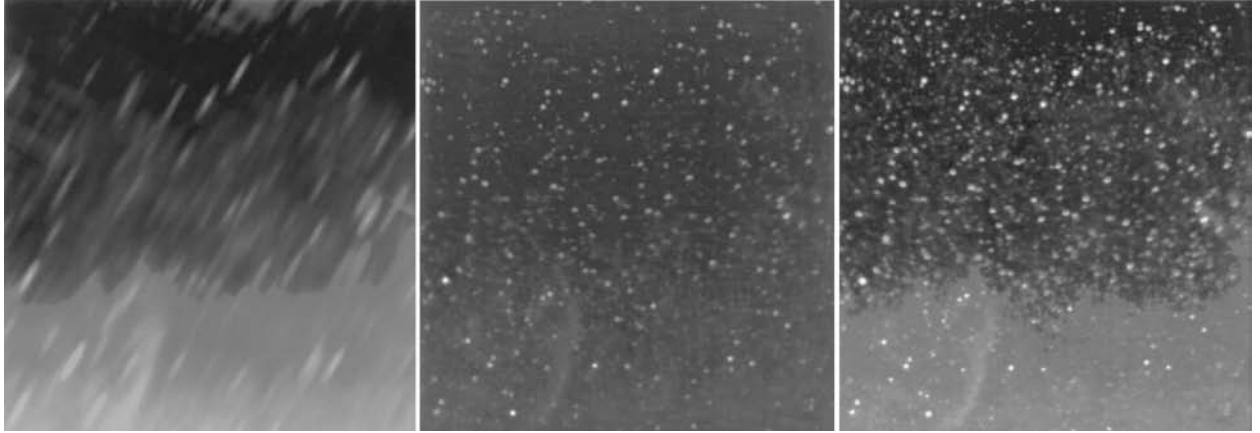


Figure 89. MSX capabilities. A $1^\circ \times 1^\circ$ IRAS 12 μm MMSE image 1.5° above the Galactic center is at left, the 8.3 μm full resolution Galactic plane survey image is in the center while the five times more sensitive raster scan image is on the right; the wisp at the bottom toward the left is more clearly seen in the center of the multicolor image at the lower left of Figure 90. The confusion in the IRAS image is evident as closely spaced sources are merged. These sources are well resolved in the MSX images.

8.2.4. The MSX Galactic Plane Survey

The Galactic plane was mapped to take advantage of the higher resolution of SPIRIT III to improve on the confusion that plagued IRAS: Figures 72 and 89 graphically depict the MSX resolution improvement over IRAS in reducing confusion. The left image in Figure 89 is a MMSE regrid of the IRAS survey data in a $1^\circ \times 1^\circ$ region centered at 1.5° in latitude above the Galactic center. An MSX Band A image of this region created from the four survey scans is shown in the center while the five times more sensitive Band A raster scanned image is at right.

The MSX Galactic plane survey covered a 10° wide band centered on the plane with $1^\circ \times 182^\circ$ ($\Delta b \times \Delta l$) constant latitude scans with up to four-fold redundancy. The small vertical green lines along the plane in Figure 88 denote $1^\circ \times 3^\circ$ raster scans that mapped selected locations at greater sensitivity to probe Galactic structure more deeply. (Only fields in the first quadrant were usable, the others had an incorrect gains setting or, later, elevated noise.) Price et al. (2001) describes the survey and the creation of $1.5^\circ \times 1.5^\circ$ full resolution images in each MSX spectral band as well as the $10^\circ \times 10^\circ$ lower resolution panoramic maps; a number of images from the Galactic plane survey are shown in this section. Figure 46 is a $(\Delta l, \Delta b) \sim 12^\circ \times 10^\circ$ Band A panorama of the Galactic center region in which the glow from the diffuse emission and density of point sources in the 40" pixels may be seen to extend to the latitude limits of the image. We chose a $\pm 5^\circ$ latitude limit for the MSX survey based on the HI STAR maps of Price (1981), which indicated a $\sim 3^\circ$ width at half maximum for the 4 μm emission along the Galactic plane at longitudes $|l| < 30^\circ$. A sensitive survey should extend to three scale heights, hence the 5° limit. Unfortunately, the small spectral bandwidth and étendue of the MSX 4 μm Bands meant that the radiance sensitivity was too low to produce good quality images. Although more recent Galactic plane surveys by ISOGAL (Omont et al, 2003) and the Spitzer GLIMPSE (Benjamin et al., 2003) and MIPSGAL (Carey et al., 2009) were more sensitive and had higher resolution than MSX, they were restricted, for the most part, to within 1° of the plane and 60° of the center. The extent of the diffuse emission along portions of the Galactic plane and interesting sources at the larger latitudes makes the $\pm 5^\circ$ limits a reasonable and productive choice for MSX.

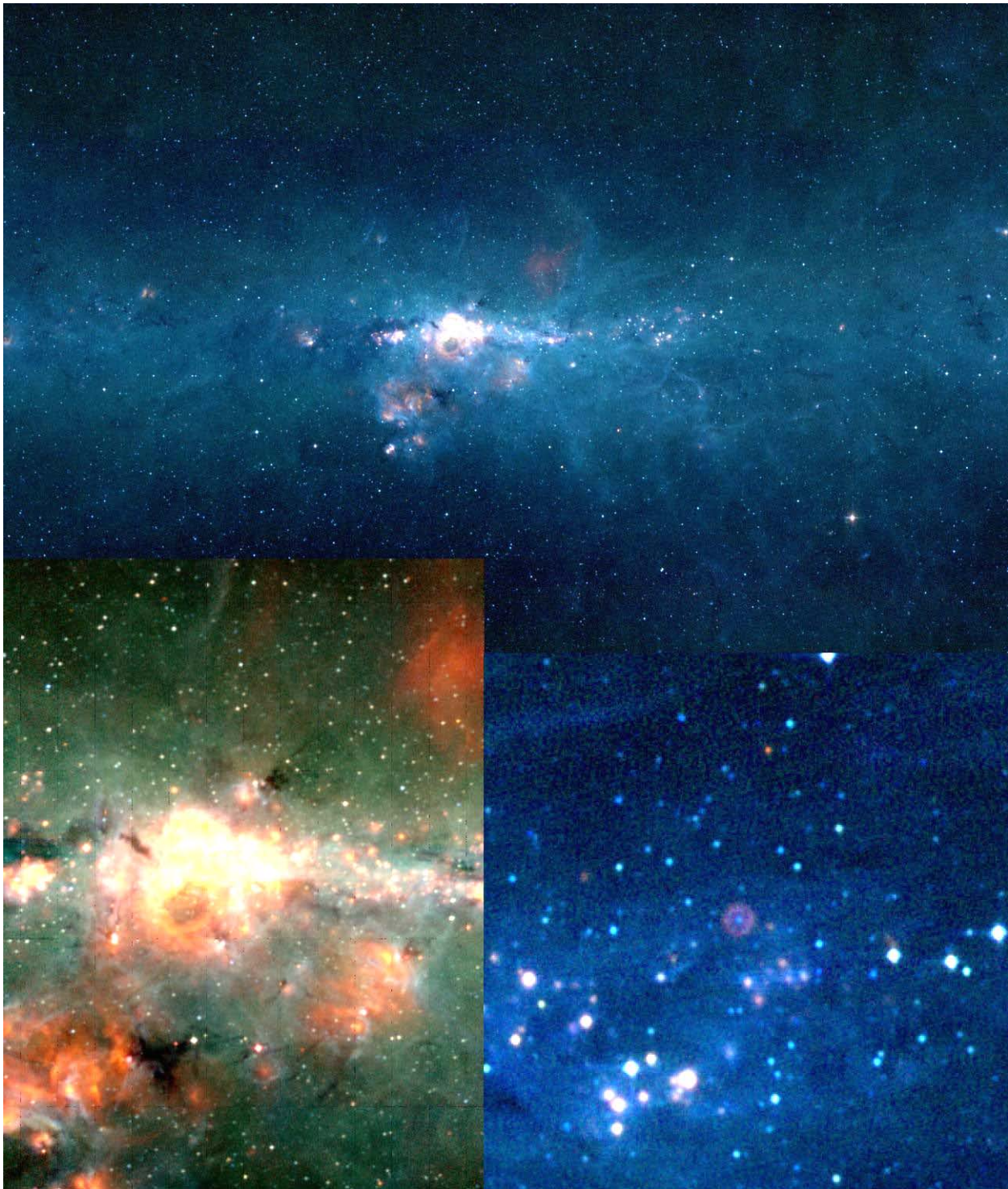


Figure 90. The MSX Galactic Center. The top image spans 6.1° in longitude and $\pm 2.25^\circ$ in latitude. The luminous blue variable (LBV) studied by Egan et al. (2002) that is almost half way from the center to the right edge in the top image is shown in more detail at the lower right. The best MSX view of the Galactic center is at the left in which two 25-leg raster scans were co-added to create this $1^\circ \times 1.5^\circ$ image. The Band A flux radiance is color coded blue and highlights emission from PAHs or relatively warm dust; Bands C + D is in green while Band E is red and limns areas of relatively cool emission.

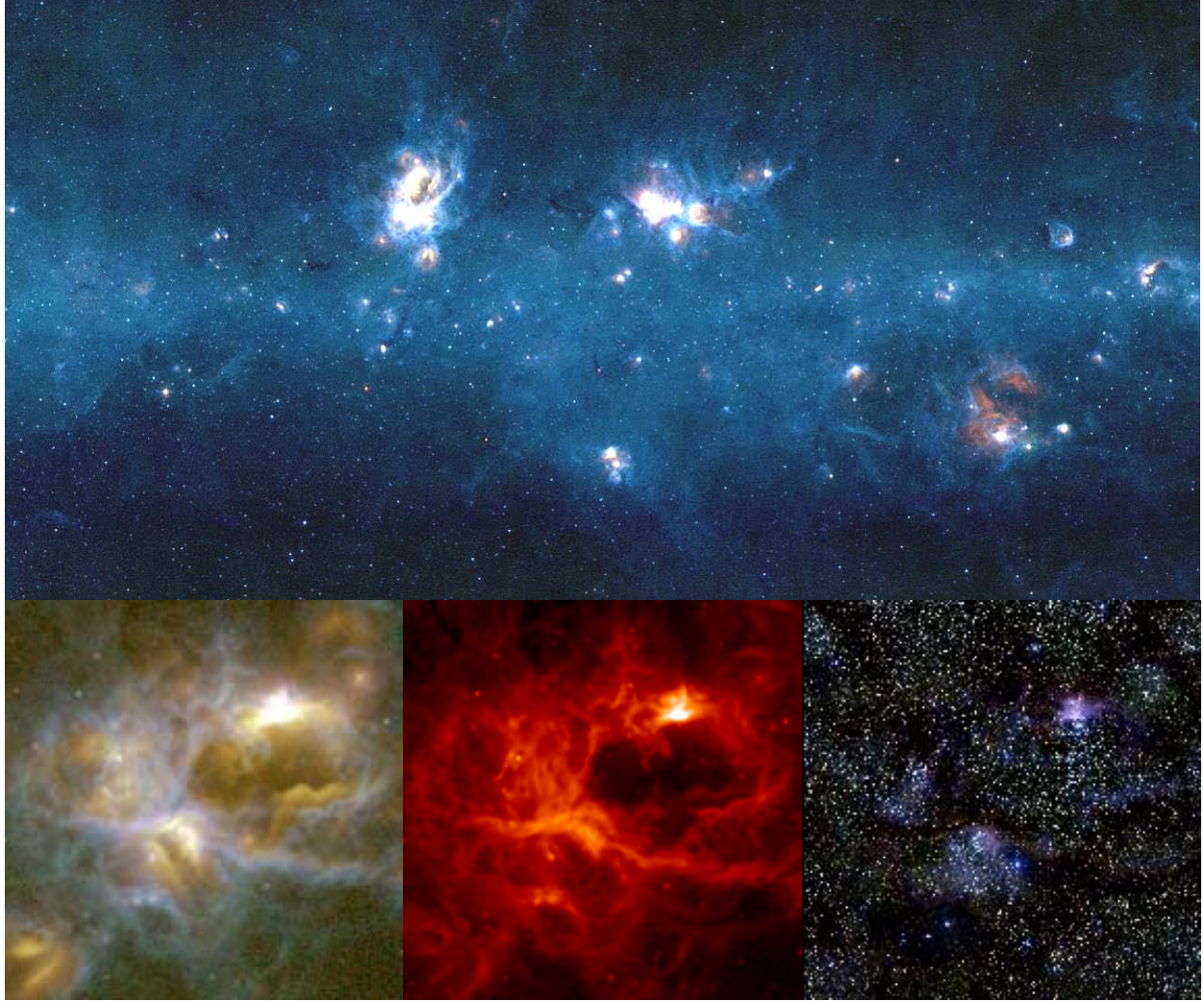


Figure 91. Infrared images of the Galactic plane between $\sim 357^\circ$ and 346° longitude. The top image abuts the right edge of Figure 90. NGC 6357 is the bright extended complex to the left while NGC 6334, another prominent H II region, is in the center. A spray of objects appear to have been ejected from the bottom of NGC 6357, one of which seems to have created a linear dark feature in the interstellar medium at the end of which is a small extended red source. Expanded views of NGC 6357 are shown rotated into equatorial coordinates at the bottom with an MSX three color image at the left, the more sensitive Band A image in the center and a 2MASS near-infrared image at right. This H II region is labeled the war and peace nebula as the bright area is shaped like a dove while the luminous outline of a skull is next to it.

A $6^\circ \times 4.5^\circ$ color image of the central region of the Galaxy is shown at the top of Figure 90. Unless otherwise noted, the color coding has the in-band flux from Band A in blue, that from Band C plus Band D in green and Band E in red. Since the major 7.7 and 8.6 μm PAH features that have been detected in the interstellar medium lie within the Band A bandpass, the bluish color in these images denote either physically warmer dust or preferentially traces PAH emission. The range of dust temperatures in the Galactic center is emphasized by the deep image in the lower left panel. Two 25 leg raster scanned observations were combined to produce this image, which is about five times more sensitive than the co-added survey scans. The spectral fluxes are color coded to enhance Band E to A ratio by about a factor of 3.5 compared to that of

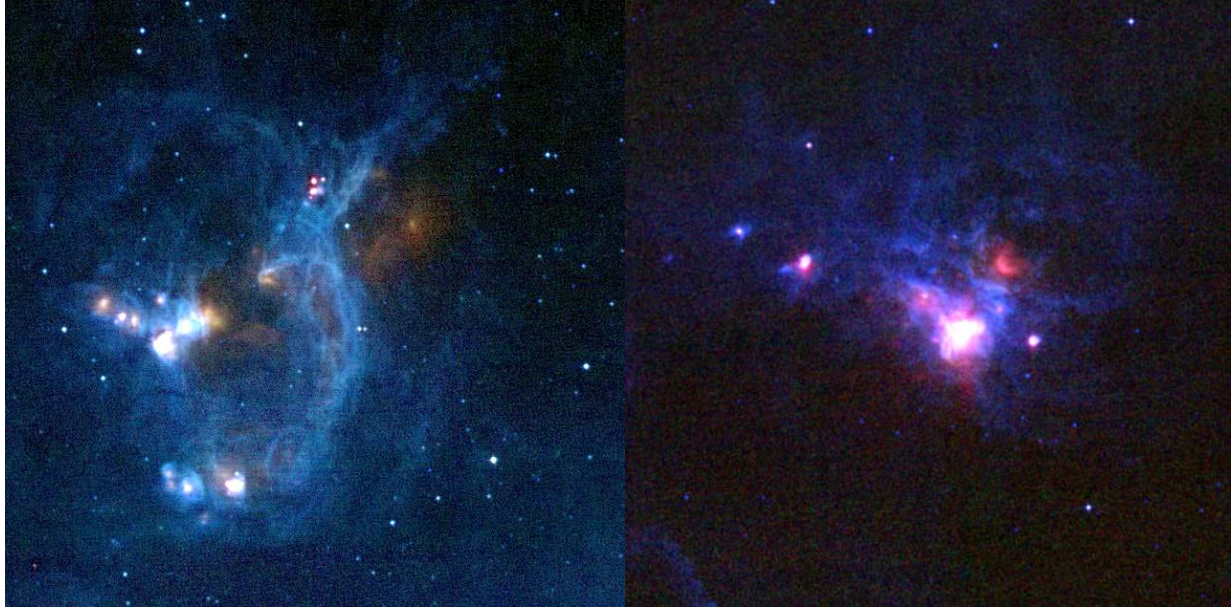


Figure 92. MSX images of two star forming region in the Galactic plane. The open Galactic cluster Trumpler 24 in Scorpius is shown on the left and the H II region RCW 38 is on the right.

the in-band flux, thus highlighting the emission from cooler dust. The linear wisp near the top center of the lower left hand plot of Figure 90 appears at the left of Figure 89.

The complex structure around the Galactic center has loops and swirls that extend 1° – 3° from the plane. Bland-Hawthorn and Cohen (2003) noted that the overall shape was indicative of a bipolar outflow from the center; the arms of this outflow are apparent in the top image in Figure 90. These images also contain a number of infrared dark clouds, the most prominent example of which is the sinuous cloud just to the left (positive longitude) of the center. Egan et al. (1998) determined that these clouds are so cold that they absorb the infrared background emission in the IRAS 60 μm and 100 μm spectral bands. Follow-up sub-millimeter observations by Carey et al. (1998, 2000) found that the clouds were dense (10^5 – 10^6 H_2 molecules cm^{-3}) and very cold, $T \sim 15\text{K}$ to $< 20\text{K}$. Simon et al. (2006) identified about 10, 000 infrared dark clouds from MSX Band A images of the first and fourth Galactic quadrants.

An expanded view of the luminous blue variable Wray 17-96 (MSX 5CG358.5391+00.1305) is shown at the bottom right in Figure 90. This suspected planetary nebula has a high temperature central star, which appears blue, that has ejected some of its atmosphere, which condensed to form a circumstellar dust shell. The shell is far enough from the star that the equilibrium temperature is low, hence the red ring. We see a ring rather than a filled disk since the optical depth of the emission is much greater at the shell edges than closer to the center since we look through more material at the edge.

The MSX panorama adjacent and south of the Galactic center is the top image in Figure 91. The bottom three panels show three images of NGC 6357, which contains the “war and peace nebula”, so called because the bright knot is shaped like a dove in flight with an adjacent outline of a skull. At bottom left image is a three color MSX image, the more sensitive MSX band A image is in the center while, for contrast, the 2MASS near-infrared image color coded J (blue), H (green) and K (red) is at the right and highlights the nebular extinction that is traced in the mid-infrared.

Some colorful objects with interesting characteristics are shown in the next several Figures. Figure 92 shows Trumpler 24 on the left, an open star cluster at $(l, b) \sim (345^\circ, +1.5)$ and RCW 38, an ionized H II region at $(l, b) \sim (268^\circ, -0.1)$, on the right. The diffuse structure in both images is emission from the dust out of which the stars are being created. The blue denotes areas

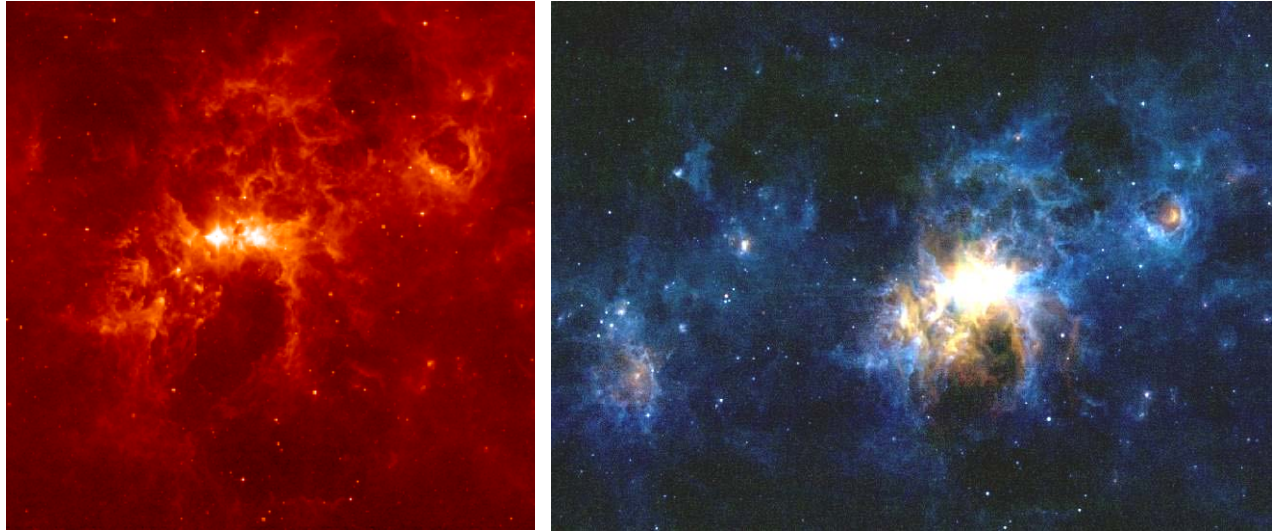


Figure 94. The η Carina complex. The more sensitive Band A image at the left shows fainter details than the larger scale false color image on the right; the latter highlights the wide range of temperatures in this object.



Figure 93. Three regions in the northern Galactic plane. The Lagoon nebula (M 8) is at lower center of the right image. This infrared image spans 4.5° in longitude and latitude and is centered at 6° longitude. In the middle is a deeper $1^\circ \times 3^\circ$ raster-scan image centered at 7° longitude just the left of M 8 while the raster scan centered on 25° longitude is shown at the left. The raster scan images are about four times more sensitive than the survey image at the right.



Figure 95. H II regions along the northern Galactic plane. M16, the Eagle nebula (NGC 6611) is the bright region well left of center in the top image. The colorful region at the top left is NGC 6604 and M17, the Omega Nebula (NGC 6618) is somewhat below the center. The bottom row compares the MSX M16 full resolution image (left) to a 7.7 μm (blue) plus 14.5 μm (red) ISO image (center) and a Spitzer image (right), which shows the improved capabilities of these latter two observatories. The Spitzer image is color coded blue, green and red for 4.5 μm , 8 μm and 24 μm , respectively. The Spitzer image is adapted from the Spitzer Science Center.

most likely dominated by PAH emission, which is excited by the short wavelength radiation from the newly formed stars. A fair amount of cool dust is also seen in red and several stars still cocooned in the natal shrouds are the red point and fuzzy sources.

MSX imaged the area surrounding the super-luminous star η Car as shown in Figure 93. Smith et al. (2000) concluded from these images that the overall morphology of the complex is that of a distorted bipolar nebula and that the knots and condensations in the nebula were likely sites of triggered star formation.

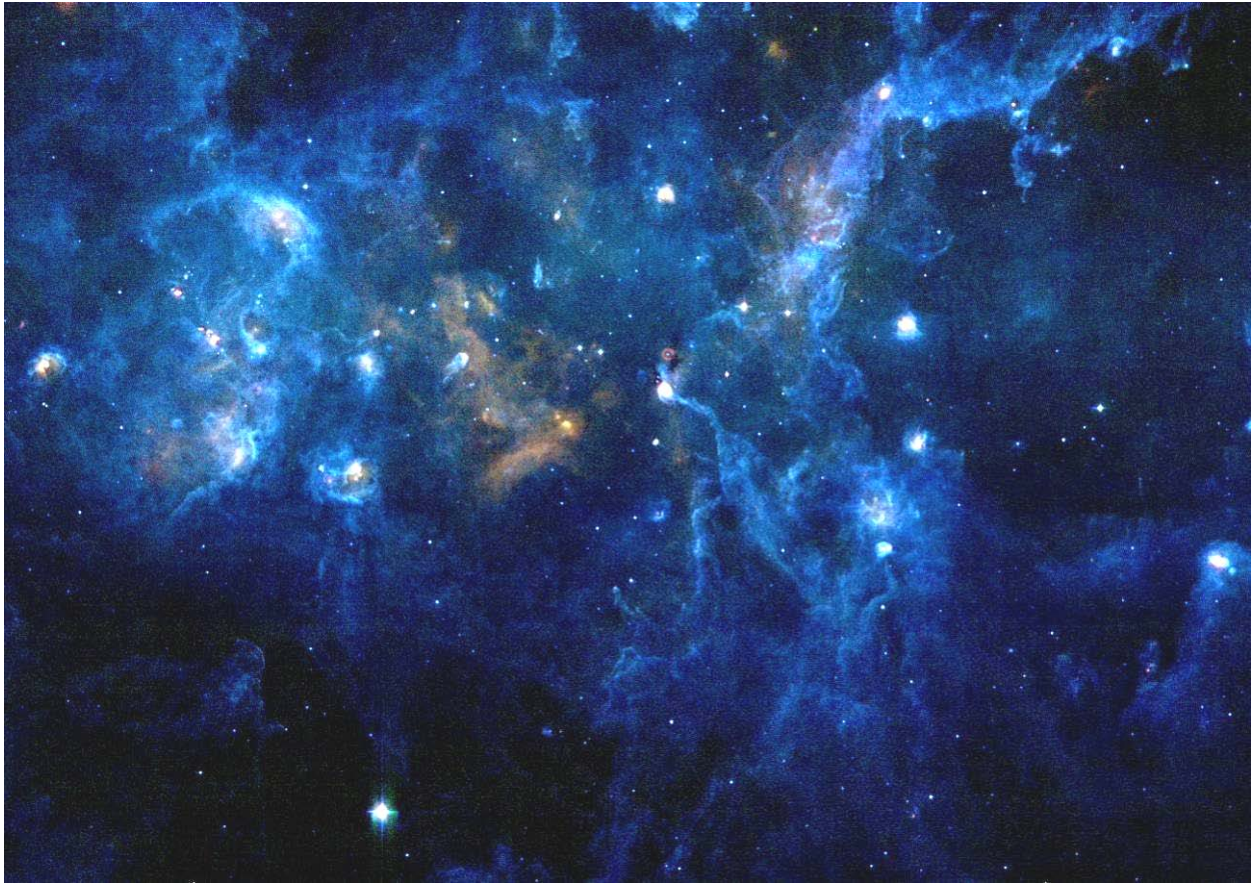


Figure 96. A $(\Delta l, \Delta b) \sim (6.5^\circ \times 4.5^\circ)$ MSX image of the Cygnus region centered at 79° longitude. This image covers about a quarter of the Band A image displayed in Figure 39. Besides the complex structure and numerous star forming regions in the images, objects of note are: The bright star near the bottom left of center is NML Cyg, one of the first very red stars published by the TMSS. The colorful area in the center that is dominated by cool dust emission. A luminous blue variable is just above the bright knot center right.

The next several Figures display region in the northern Galactic plane. The $\pm 2.25^\circ$ region centered at 6° longitude, to the left of the panorama in Figure 90, is displayed in Figure 94. The image at right contains a number of areas of concentrated cool infrared emission, the most prominent of which is the Lagoon nebula (M 8) below center; an overlapping raster-scan image is shown at the center. The $15^\circ \times 10^\circ$ panorama centered at $l \sim 15^\circ$ in the Galactic plane is shown in the top of Figure 95 with expanded views of M16 from other infrared satellites.

The Cygnus X region, shown in Figure 96, lies in the direction of a near-by spiral arm. Diffuse emission extends over the entire area with wisps that were detected beyond the limits of the larger Figure 39 image during the MSX IRAS gaps survey (the gap in the Cygnus region are shown in Figure 79). A luminous blue variable star just above the bright knot in the center of the image has the characteristic red ring surrounding the blue stellar core. The dark cloud to the lower right of the LBV takes a “bite” out of the ring indicating that the LBV may be more distant than the 1.7 – 3 Kpc of the Cygnus X complex (Kraemer et al., 2010).

Egan et al. (1999) extracted sources from the Galactic survey scans and compiled an MSX infrared Galactic plane point source catalog while Cohen, Hammersley and Egan (2000) validated the source calibration and assessed the infrared colors and radiometric properties of the

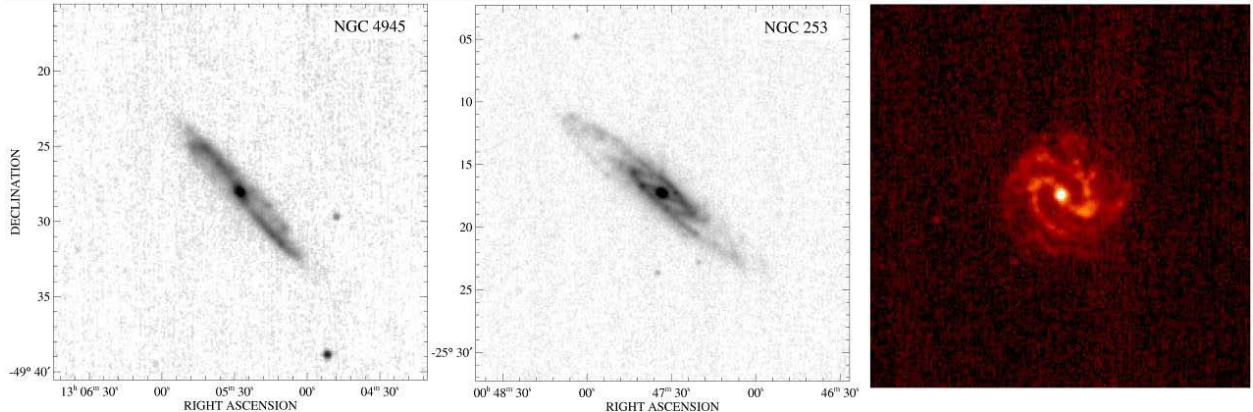


Figure 97. Well resolved galaxies in Band A. NGC 4945, NGC 253 and M83 are left to right.

different classes of stars in the catalog. Egan et al. (2003) then introduced a number of upgrades to create the final version (2.3) of the MSX catalog. These included the processing improvements that were incorporated for the images, the addition of sources extracted from all the celestial experiments rather than just the Galactic plane and photometry from the full resolution images using the a priori Band A catalogued positions. Extracting point source parameters from the images improved the signal-to-noise of the photometry by a factor of 2 to 6.

8.2.5. A Survey of the Zodiacal Background and Regions Missed by IRAS

A survey of the 4% of the sky not included in the IRAS Point Source Catalog also sampled the zodiacal background out to sun-centered longitudes of 180° with scans in ecliptic latitude at constant sun-centered longitude. Using MSX's unusual versatility, five additional ecliptic pole-to-pole scans at sun-centered longitudes between 25° and 30° were obtained by timing the scan such that the Earth obscured the Sun at the smaller elongations. The Early Midcourse team's scan along the ecliptic plane between 30° and 180° elongation and the Data Certification team's latitude scans at 90° and 180° elongation were also included in the MSX zodiacal data set, and was also published by Price et al. (2003).

8.2.6. Raster Scan Maps of Galaxies and H II Regions

Thirty regions containing extended and structured infrared emission were raster scanned, about half of which were resolved galaxies and the other half molecular clouds and H II regions where star formation is ongoing. The smaller galaxies, such as those shown in Figure 97 and the $1^\circ \times 3^\circ$ MSX map of the Andromeda galaxy in Figure 75 were covered in a single observation. On the other hand, the largest object mapped, the Large Magellanic Cloud (LMC), required six separate observations to twice cover the $10^\circ \times 10^\circ$ area surveyed with redundant scans. Kraemer, Price et al. (2002) present the MSX galaxy observations for all except for the SMC and LMC.

We gave priority to processing the MSX infrared LMC observations to provide IPAC with images and a point source catalog by fall of 1998, before the NASA Wide-field Infrared Experiment (WIRE) was scheduled to fly. The WIRE team, led by Perry Hacking, had chosen to map the LMC for the initial performance validation of the system. Since the MSX LMC images were more sensitive and had much better spatial resolution than the IRAS maps that the WIRE

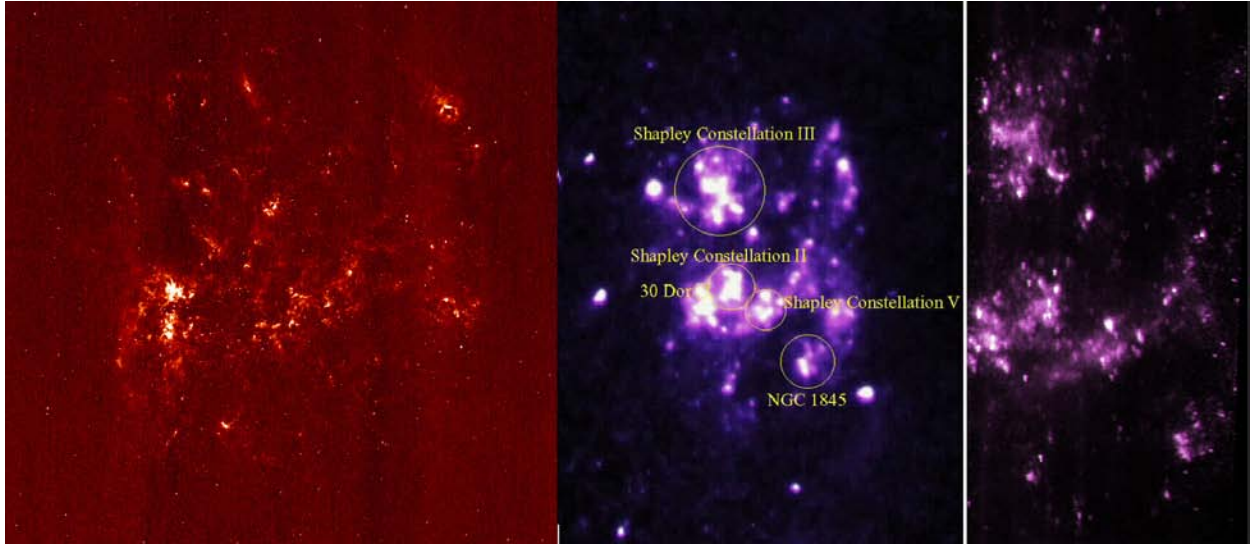


Figure 98. MSX images of the Large Magellanic Cloud. The $9^\circ \times 9^\circ$ Band A image at left was created from six raster-scan observations. Ultraviolet images simultaneously obtained with the first infrared observation in a $145 - 180$ nm band taken with the wide field imager and in a $210 - 253$ nm narrow field imager band are shown in the middle and right, respectively. The middle image covers somewhat larger area scale than the Band A image; major stellar clusters and H II regions are denoted in this image. The image at right covered the central region of the galaxy, from the 30 Dor, the small, bright extended region left of the center of the Band A image to the dark vertical streak.

team planned to use, they were much better suited to the WIRE needs, especially since WIRE had about the same resolution as MSX. WIRE failed and the LMC data languished until Egan, Van Dyck and Price (2001) did a population analysis of the brightest LMC mid-infrared sources.

Figure 98 shows MSX infrared and ultraviolet images of the LMC to highlight one of the unrealized objectives of the MSX astronomy experiments. For maximum data return, the two ultraviolet imagers and all the ultraviolet – visible spectral imagers were operated during the infrared astronomy experiments, as was the SPIRIT III interferometer whenever possible. The intent was to obtain panchromatic photometry and spectroscopy, especially of the extended sources such as the galaxies, the LMC and the eight star forming regions that were mapped (Kraemer et al. 2003). Such observations would have provided unique diagnostics with which to analyze the physical processes that govern the energy balance in star forming regions. At the nominal survey rate of $0.125^\circ \text{ sec}^{-1}$, the $13^\circ \times 9^\circ$ large field ultraviolet imager would sample a given region ~ 80 times with $3.2' \times 2.3'$ pixels but the 0.5 sec frame would have smeared the data over $9-10$ of the $21'' \times 18''$ pixels in the $1.5^\circ \times 1.2^\circ$ narrow field imager; the scan rate over the LMC was $0.1^\circ \text{ sec}^{-1}$, which resulted in somewhat less smearing in the narrow field imager. Thus, there were many more wide field imager frames to average for a specific area than for the narrow field imager and, as may be seen in Figure 98, the result was more sensitive despite having five times smaller collecting area.

Co-adding the photon counts from all the data would have improved on the single frame sensitivity by about a factor of 10 and even more for the slower scan rates. Unfortunately, pointing ambiguities and problems with the distortion map thwarted ultraviolet mapping during the cryogen phase of the mission although some results were obtained, such as the wide and narrow field ultraviolet LMC images as well as images of the SMC (Henry et al., 1996), the Pleiades (Allen et al., 1997) and Orion (Dring et al., 1997).

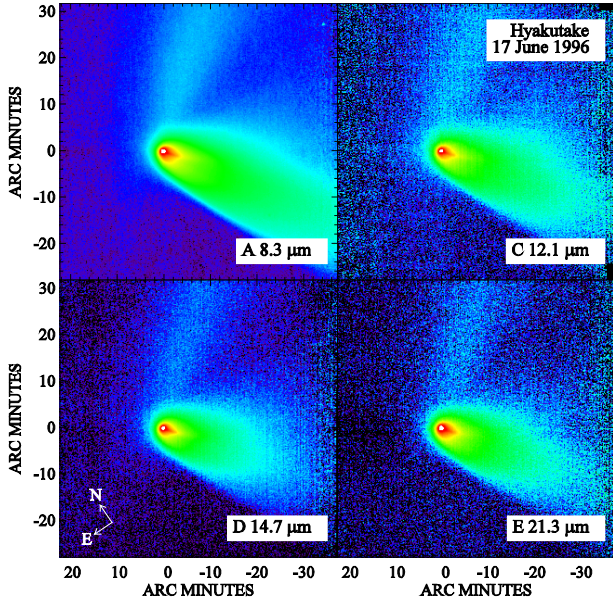


Figure 99. MSX mid-infrared images of comet Hyakutake. The comet appears to have two dust tails, an effect of optical thickness variation across a single dust distribution. The faint “tail” extending to the upper right of the coma is composed of grains that were ejected from the nucleus several months earlier than those that comprise the main dust tail, which extends downward to the right in the images. Thus, a broad fan of material is spatially separated by age. Images and preliminary analysis are courtesy of Russ Walker (Walker et al., 1997).

center were obtained during the time the interferometer returned good data. Simpson et al. (1998) analyzed the 2 cm^{-1} resolution $5 - 25 \mu\text{m}$ MSX spectra of the Orion nebula. Although the spatial resolution of the $6' \times 9'$ detectors was too coarse to trace features such as the shock front, the large spectral range allowed direct elemental abundance of neon, argon and sulphur to be determined compared to hydrogen with a single instrument. Simpson et al. concluded that the Orion nebula was relatively metal poor compared to the Sun. Simpson et al. (1999) analyzed the $2.5 - 25 \mu\text{m}$ low (20 cm^{-1}) resolution spectral maps of the Galactic center taken at 22 positions over a $15' \times 25'$ grid and found spectral similarities with low excitation active galactic nuclei. Simpson et al. also derived an extinction map due to astronomical silicates for the center.

8.2.7. Targets of Opportunity

These observations are of a mixed bag of objects. Kraemer, Lisse et al. (2005) present the SPIRIT III targeted observations for the six comets, three transition objects (asteroids that have or had comet like characteristics) and one near Earth asteroid targeted by MSX. Their analysis included the single serendipitous comet observation of Hale-Bopp obtained during the Galactic plane survey. One comet, 22P/Kopff, showed a distinctive dust trail in Band A (Walker et al., 1997). Lisse et al. (2004) conducted a more in-depth analysis of the dust coma of 126P/IRAS using the SPIRIT III and ISO photometer observations.

Infrared spectra were to be obtained at the lowest resolution, 20 cm^{-1} , concurrently with the radiometer as the 0.4 second interferometer scans would not be aliased at the survey or raster scan rate. The interferometer field-of-view is offset from that of the radiometer by $\sim 2.5^\circ$ (Figure 85) so observations of bright sources by the radiometer could be used to key the spectral extraction at the appropriate time delay. The comet and calibration experiments initially included time for the interferometer to point and stare at the targeted object while a separate experiment spectrally mapped areas with extended emission, such as H II regions.

Misalignment and noise rendered the interferometer observations unusable during the first six weeks of routine operations. The interferometer and radiometer were simultaneously operated for the next two months after which a power supply over-current led to the program decision to use either the radiometer or interferometer, but not both. Noise again rendered the interferometer useless by the end of November 1996. Spectra only of the Orion nebula and a spectral map of the Galactic

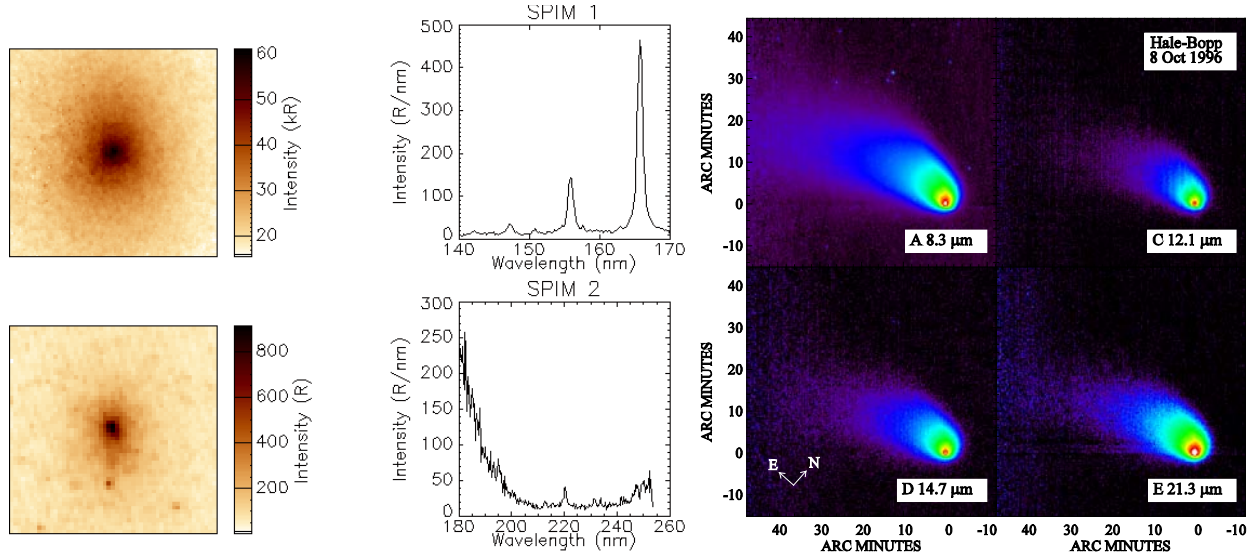


Figure 100. MSX observations of comet Hale-Bopp. The mid-infrared measurements from the targeted observations are shown on the right, courtesy of Walker et al. (1997), while results from the ultraviolet images and spectra from a post cryogen mission observation, provided by Dick Henry, are shown on the left.

Since mission planning scheduled observations several weeks in advance, observations were made of transient targets whose position could be predicted well ahead of time and those serendipitously observed on other experiments. Figure 99 shows the MSX observations for comet Hyakutake while Figure 100 shows MSX observations of comet Hale-Bopp. The rather nondescript mid-infrared Hale-Bopp results from the raster scanned measurements are on the right. Our attempt to obtain simultaneous ultraviolet measurements was thwarted by sunlight glinting from the spacecraft but several observations of the comet during the post-cryogen phase of the mission were successful; the 19 April 1997 measurements are shown. Kupperman et al. (1998) report on the visible spectral imager observations of the dust continuum, H_2O^+ emission and the sodium dust tail of the comet. The unpublished images and spectra created from ultraviolet spectral imagers from that observation are shown at the left of Figure 100.

The Galactic plane and IRAS gaps surveys also serendipitously obtained 332 infrared observations on 169 asteroids, 31 of which were not in the Tedesco et al. (2002) SIMPS compilation of IRAS asteroid measurements. Tedesco, Egan and Price (2002) derived diameters and albedos for the asteroids from the MSX radiometry.

The Data Certification team observed the 27 September 1996 eclipse of the Moon as a target of opportunity. This eclipse was observed on three consecutive orbits, at the beginning and end of totality and when half or more of the Moon was illuminated by the Sun; Figure 12 shows the middle measurement near the end of totality. Price, Mizuno and Murdock (2003) derived cooling curves for various lunar features during this eclipse.

While the three satellites teams measured about 30 or so selected resident space objects (RSOs) between 50 to several hundred times on a given observation, little was done beyond processing the highest priority events. We independently found RSOs in the astronomy survey scans, the unique signature of which are seen in the false color MSX images on the right side of Figure 101. Band C is color coded green and is offset by about 0.2° from Bands A, D and E, which are color coded blue, green and red, respectively. In the inertial coordinates of these images, the satellite motion during the observation offsets the green Band C measurement from the whitish Band A, D and E spot. This is analogous to how Dow et al. (1990) found RSOs in

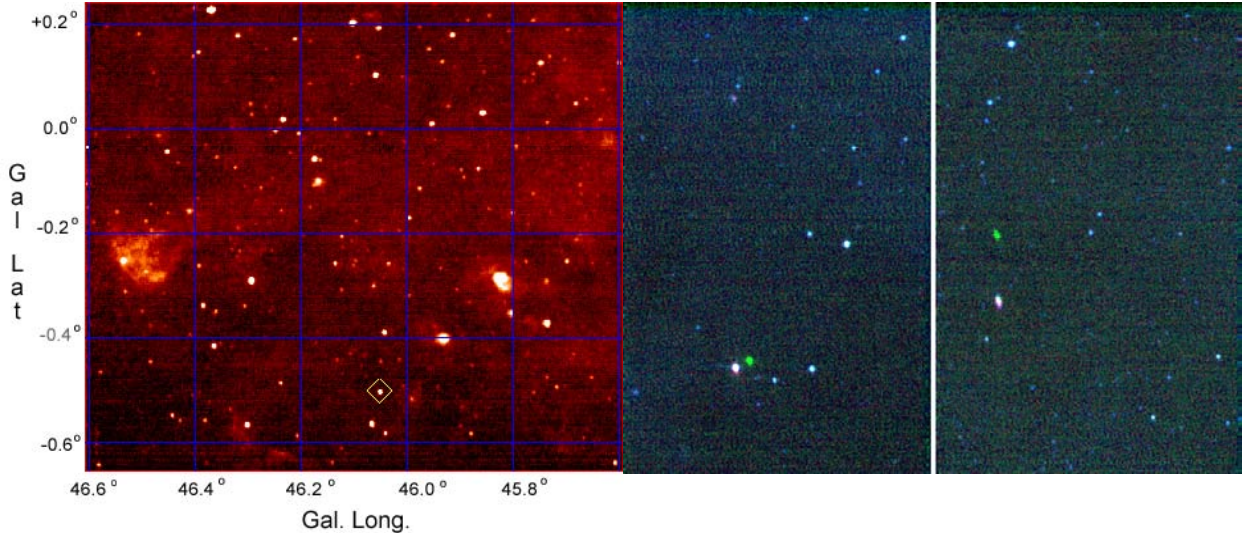


Figure 101. RSOs serendipitously observed by MSX. The left hand Band A image is of a piece of space debris, the Arianne spelda from the launch AR-V81, highlighted by the yellow box, that MSX observed against the Galactic plane. The characteristic offset false color signatures of two RSOs are shown in the right hand images. If the RSO moves fast enough, their images are elongated in inertial coordinates and the offset columns are separated.

the IRAS sky flux plates. The angular rate of the satellite is reflected in the amount of smearing in the RSO spots and the separation between the satellite images due to the focal plane offset.

We revisited the serendipitously observed RSOs a decade later in response to a rekindled interest in mining the MSX RSOs observations and analyzing the characteristics of the infrared signatures of the more than 1700 objects that were found in the Celestial and Earth Limb experiments. As with HI STAR, encounter geometries were predicted from the satellite element set for the individual experiments and matches found with sources in the data. The matching was facilitated by casting the data in object oriented coordinates that removed the offset and smearing apparent in the image to the right in Figure 101 and enhanced the signal. Characteristic temperatures for RSOs with measurements in three or four infrared bands were calculated by a non-linear least squares fit to the data. The results are more robust than color temperatures derived from two Bands.

8.2.8. MSX Astronomy in the Post Cryogen Phase

The APL ultraviolet–visual imagers and spectral imagers (UVISI) used image intensifiers with photocathodes that were selected for the wavelength regime of interest. The electrons generated by the photocathode were multiplied by a micro-channel plate and directed to a phosphor screen that reconverted them into visible photons that were relayed by a fiber optic reducer onto a CCD array (Carbary et al., 1994). The APL default data processing treated the sensors as current devices although they were supposed to be capable of photon counting at low background. Dick Henry, at Johns Hopkins Univ., was the MSX Celestial Background team Co-Investigator responsible for processing and analyzing the UVISI data.

The performance of the UVISI was nominally superior to previous ultraviolet surveys and the MSX program office supported an initial UV sky survey in the post cryogen phase with the expectation that we would be able to obtain operating funds from NASA to complete the

task. NASA did not fund the proposed survey, principally because we were unable to quantify the system performance and calibration after a year of acquiring data. However, about half the sky had been surveyed with the large field imager in spectral bands spanning 128 – 138 nm and 145 – 180 nm by the time the effort was terminated. The narrow field imagers surveyed about a tenth of the area covered by the wide field imager but in four bands: 180 – 300, 200 – 230, 230 – 260, 260 – 300 nm and a narrow filter centered at 294 nm, rather than two. The data processing for these point and stare observations was more tractable than for the scans executed for the cryogen phase experiments and Newcomer et al. (2004) subsequently averaged the data from the individual survey frames, extracted sources from the resulting images, calibrated the measurements and published the results in an MSX ultraviolet catalog.

Toward the end of this limited post cryogen survey, 32 of the ultraviolet observations targeted specific objects. The limited results from these measurements include the analysis of Murthy et al. (2002) of the diffuse ultraviolet emission from three fields in Orion. Although the 20 March 1997 Hale-Bopp measurement was compromised by solar glint, a 19 April observation by the Terrestrial Backgrounds team was more successful (Kupperman et al., 1998), as shown in Figure 100. The Terrestrial Backgrounds team executed five more Hale-Bopp observations from the middle of August to the middle of September 1998, but did not process the data from them.

AFRL also supported Peter Jenniskens in his Leonid meteor campaigns with observations from the AFRL KC-135 flying optical/infrared laboratory and with three MSX UVISI observations over a 30 hour period during the 17–18 November 1998 peak. Jenniskens et al. (2000) describe the MSX meteor images while Jenniskens et al. (2002) analyzed the spectra of one of the bright meteors. During the shower two years later, Carbary et al. (2003) obtained full range 110 to 869 nm meteor spectra, identified the emission lines and derived brightness time profiles of the atmospheric emissions associated with the meteor. In a related investigation, the Contamination team executed a large number of experiments during the mission looking for near field debris created by meteorite strikes of the spacecraft but found none.

8.3. Personal Perspective

Any experimental program has a dynamic tension between the scientific objectives of the experimenter(s) to obtain the best data possible and the engineering trades that are forced by the program funding and schedule. While almost any experimenter wish list can be met with limitless resources, the instrument and system engineers have to deliver a working instrument on a defined schedule. Ideally, good program management will strive to facilitate dialog between the experimenters and the instrument builders to obtain the best science possible within the realities of the budget and schedule. This requires that scientifically driven improvements be included as best they can into the engineering design trades. It is not unheard of for the engineers to regard engineering input from the program scientists as uninformed interference and the scientists to regard the engineers as uncooperative and too narrowly focused. Communication is essential to overcome the arrogance of expertise or the ‘not invented here’ attitude and the open interchange of ideas is often the difference between success and failure to meet the objective of a program. Conrad and Irace (1984) and Smith and Squibb (1984) provide the lessons learned for IRAS and Rieke (2006) presents a similar discussion for Spitzer while some of the MSX problems that had to be overcome for a successful mission are discussed in Section 8.1. However, it was also the case that the more serious MSX hardware problems that compromised performance could have been avoided if the SDL engineers had heeded the suggestions from the PI team.

For example, while the thermal design for SPIRIT III and the causes of the vent line rupture may be debated, questionable decisions regarding internal calibration of the sensor were made. One was locating the internal hot wire stimulators that were supposed to flood the detectors with repeatable amounts of flux to calibrate the responses as a function of time. These were placed on the cold focal planes, rather than near the field stop as is usually done, over the objections of several PIs. Exercising the stimulators in flight warmed the focal planes, as predicted by the PIs. In the end, this calibration could only be done at the end of a data collection event by specific request.

Also, the standard calibration sequences at the beginning and end of a data collection event included cycling through the gain states to measure the dark offset at each gain even though a Band could only have a single gain during a data collection event. This sequence warmed the focal planes and introduced an error into the offset measurements. As discussed by Price et al. (2001), a separate dark offset measurement was inserted after the initial calibration sequence and before the last one for the Celestial Background experiments. However, a number of observations were obtained, such as the Early Midcourse ecliptic plane scan, before it was realized that this extra dark offset measurement was necessary and corrective measures taken. Price et al. (2000) described how the necessary corrections were derived.

Despite the problems, MSX did return valid and valuable scientific information. Once good images were created from the 0° latitude scan along the Galactic plane, it was evident that MSX was producing valuable science results. As may be seen in the Figures in Section 8.1, extended emission near the Galactic plane is complex and highly structured down to the sensor resolution. We created a video of the Band A data from the 0° latitude scan for public release that highlighted the striking structure of the emission. The video was an attention grabber and elicited interest from Harley Thronson, Gunther Riegler and Ed Wieler at NASA's Office of Space Science. They liked what they saw and Harley offered to support us but at about a tenth the amount I thought was needed to produce scientific quality products. Harley requested that I present the material to the next infrared advisory meeting that was to be held at IPAC the following month and to solicit their endorsement as to the value of the MSX results. The presentation was well received; Martin Harwit commented that the video showed that the Galaxy was indeed a violent and turbulent place. NASA provided the funds requested for the MSX processing and included the analysis of our ISO experiments as part of the package under the aegis of a memorandum of agreement between BMDO and NASA. Dr. Wesley Huntress, the NASA Associate Administrator for Space Science, commented on the value of the MSX data in his 19 March 1997 letter to Lt. Gen Lester Lyles, BMDO Director, stating that "...MSX data will be very valuable to the astronomical community." Furthermore, that MSX "...will improve the efficiency of SIRTF by eliminating the need to obtain images with the SIRTF camera so that the spectrometer can be precisely pointed in complex and crowded areas of the sky."

In reality, the MSX made more extensive contributions to Spitzer's operation than those envisioned by Wes Huntress. The MSX images and catalogs became frequently used resources for Spitzer proposals and planning observations. The MSX absolute calibration that was transferred to the ISO spectra by Engelke, Price and Kraemer (2006) corrected systematic biases in the Cohen et al. spectra of the secondary standard stars, which resolved the discrepancy between the A and K stars used for calibrating the Spitzer camera (Reach et al., 2005). Cohen et al. (2006) also used the MSX Band A images to validate the $8.0\text{ }\mu\text{m}$ diffuse calibration of the Spitzer camera, while Cohen (2009) did the same for MIPS.

9. NEW NEAR-INFRARED SURVEYS

Large scale ground-based visible and near-infrared surveys were inaugurated with the new millennium when large format visible and near-infrared two-dimensional focal plane arrays became available. Visible intrinsic silicon charge coupled devices (CCDs) were developed in the late 1970s and shortly thereafter, InSb two dimensional near-infrared arrays. The first arrays came with rudimentary readouts that had to be integrated into a focal plane camera for use at the telescope. Developing such readouts as pathfinders for LAIRTS was the rationale for the AFOSR contracts to Hegyi, Thuan and Lebofsky. Around 1980, the DoD began funding a concerted effort to develop two-dimensional extrinsic silicon arrays, which was followed by a DoD program about five years later to improve the MWIR and LWIR intrinsic HgCdTe arrays. These intrinsic devices could operate with respectable sensitivity at higher temperatures compared to extrinsic arrays with comparable spectral response.

The spectral response of the intrinsic arrays could be tuned to the wavelength regime of interest by appropriately adjusting the proportions of the Hg, Cd and Te in the detector lattice, which also set the operating temperature of the arrays. Based on this technology, AFGL teamed with the Smithsonian Institution Astrophysical Observatory, among others, to propose a Near-infrared Astronomical Survey (NIRAS) to NASA in 1988, a small explorer class satellite to survey the sky in two near-infrared spectral bands. Two redundant 58×62 HgCdTe arrays in the focal plane of the FIRSSE optical bench were to survey the sky at $1.9 \mu\text{m}$ and $3.5 \mu\text{m}$. The $1.9 \mu\text{m}$ band ($\Delta\lambda \sim 1 \mu\text{m}$) was projected to be about 10,000 times more sensitive than the TMSS. Since this spectral band overlapped the 1.6 and $2.2 \mu\text{m}$ astronomical bands, survey sources could easily be verified and quantified with ground-based observations while the thermal emission from stars with circumstellar dust shells would be detected in the $3.5 \mu\text{m}$ band. As the $3.5 \mu\text{m}$ band covered a spectral region compromised from the ground by the atmosphere, a space-based survey was needed. The optical bench and focal planes were to be radiatively cooled to $\sim 100\text{K}$ by a radiator on the back of the secondary mirror structure, which meant that the duration of the experiment would have been limited only by funding for mission operation or re-entry.

The satellite motion would scan the sky at (nearly) the orbital rate while the secondary mirror moved in the opposite direction during the observation, thus freezing the motion of the sky on the focal planes while data were being acquired. The secondary was then to snap back to the start position to begin a new frame of data. This approach would efficiently acquire images using two-dimensional arrays and was adopted for the mid-infrared photometer on SIRTF (Rieke et al., 2004) and for WISE (Mainzer, et al., 2006).

The NIRAS proposal was not funded but did leave a legacy. The chair of the proposal review panel, Susan Kleinmann, thought that the basic idea of a near-infrared survey was sound but that many of the objectives could be met at a fraction of the cost with a ground-based $1.25 - 2.2 \mu\text{m}$ survey. She began promoting the idea in 1990 and assembled a study definition team that included about a third of the NIRAS co-Investigators. This survey became viable with Rockwell's development of the high quality back-illuminated 256×256 element HgCdTe arrays on a sapphire substrate in the late 1980s for the Near-infrared Camera and Multi-Object Spectrometer (NICMOS) camera on the Hubble Space Telescope. Susan Kleinmann's concept for a new two-micron sky survey also resonated strongly in Europe and a European Southern Observatory team led by Nicolas Epcstein proposed their own southern hemisphere survey shortly thereafter, the Deep Near-infrared Survey of the Southern Sky (DENIS).

9.1. The Near-infrared Camera and Multi-Object Spectrometer (NICMOS)



Roger Thompson (1994) described the NICMOS camera as *NICMOS: The Next U.S. Infrared Space Mission* as indeed it was after MSX and ISO. The near-infrared NICMOS3 camera, installed on the Hubble Space Telescope in February 1997, is actually three cameras with separate optical paths that provide different magnifications (pixel sizes). Each camera has a 20 position filter wheel with a blank for dark offset

measurements, filters to measure continuum and line emission in astrophysical sources, polarizers, and a grism (grating plus prism dispersive elements) to provide spectra of multiple objects in the fields. The instrument has a coronographic capability that can block the light from the central Airey ring of a bright source in order to examine the fainter nearby emission.

NICMOS also had an AFRL connection. The camera was originally cooled with solid nitrogen in a cryostat filled with aluminum foam. On orbit, the nitrogen expanded as it was cooled further by the vacuum pumping of space, which created a thermal short between the baffles and the vapor cooled shield that accelerated cryogen depletion, reducing the cryo lifetime to less than 1.5 year, far short of the five year goal. NASA convened an Independent Science Review panel in September 1997 chaired by Martin Harwit to consider the problem. I participated on the panel because Martin thought that that I might be familiar with the Creare reverse turbo-Brayton cycle cryocooler proposed to rejuvenate the NICMOS camera. The AFRL Space Technologies Division of the Space Vehicles Directorate at Kirtland AFB, New Mexico had funded Creare to develop this mechanical cooler and, by the time the panel met, Creare had delivered a 65K engineering demonstration model and was working on a 35/60K cooler.

The Review Panel recommended installing the cryocooler but only if it could be shown that it could function in space and not interfere with Hubble Space Telescope operations. The Goddard Space Flight Center successfully demonstrated on STS-95 that the Creare cooler could achieve the requisite 8 watts of cooling at 70K in space needed by NICMOS. The cooler was installed on Hubble in March 2002 and the cryocooler had NICMOS operating again within six weeks; it has been in service since.

9.2. The Two-Micron All Sky Survey (2MASS)



By the late 1980s the scientific merits of a much deeper near-infrared all sky survey than the mid-1960s TMSS were being demonstrated by small area mapping, while the development of sensitive larger format NICMOS near-infrared detector arrays made such a survey practicable. Consequently, the Infrared Astronomy Panel of the Astronomy and Astrophysics section of the 1990 Decadal Survey (Bahcall, 1991) gave

top ranking to the concept of such a sensitive, near-infrared all sky survey. In 1989, Susan Kleinmann requested that the objectives of her AFOSR grant be broadened to include using the Kitt Peak "SQIID" camera with four PtSi detector arrays on the 50" (1.3 m) telescope for a mini-survey to address the technical issues involved in such a survey. By the time of her AFGL 1991 follow-on contract, Susan Kleinmann had determined that the SQIID array and electronics were

not suited for an efficient sky survey and decided that Infrared Laboratories would build the prototype camera that was needed for an operational demonstration. Consequently, Nishimura and Low conducted a preliminary instrument design for the survey in 1990 that optimized the survey performance parameters for a near-infrared camera on a 1 meter telescope using the best available NICMOS 3 array. Preliminary designs for both a prototype camera and the three color camera were laid out in their 11 January 1991 Final Report.

The University of Massachusetts subsequently submitted a proposal for the 2MASS development phase of the survey in late spring 1991. The concept was called the Two Micron All Sky Survey (2MASS), a name that gives a nod to the first large scale Two Micron Sky Survey of Neugebauer and Leighton (1969a) and the 2MASS acronym provides name recognition to the University of Massachusetts, U. Mass, the institution conducting the survey. On 17 May, the proposal review committee recommended that a more extensive conceptual study be conducted before NASA gave the go-ahead for the design phase. The reviewers were particularly concerned about the data processing, which they deemed to be much more difficult, extensive and expensive than what was described in the proposal (Susan Kleinmann: 6 June 1991 letter to the 2MASS team). NASA and the proposal reviewers also required the project to be reorganized into a core team of funded individuals mainly drawn from the University of Massachusetts and IPAC, and a Science Advisory Panel who would contribute their time.

AFGL, NASA, the Naval Observatory, and the University of Massachusetts funded the ensuing proof-of-concept study. The observations were obtained by the single prototype camera that could survey in one color at a time, which Infrared Laboratories delivered in early 1992. However, the camera filter could be changed out for multi-color observations. Nearly 800 deg² of sky was surveyed mostly in the K band with the prototype camera on the Kitt Peak 50" telescope between April 1992 and May 1993. Principal questions that Kleinmann (1994) addressed with this feasibility effort were:

- 1) Would the freeze-frame strategy produce quality images? The telescope was tracked in right ascension at the sidereal rate while being scanned in declination. The secondary mirror scanned in the opposite direction compensation for the telescope motion in declination, thus freezing the frame during integration.
- 2) How would moonlight affect the background at the sensitivity of the survey?
- 3) What were the ghost imaging problems from bright stars?
- 4) What were the effects of confusion in the Galactic plane?

This study revealed no serious impediments for the survey and demonstrated the efficacy of the survey strategy. It also produced a large enough database to develop and exercise the data processing algorithms.

The University of Massachusetts resubmitted the proposal to NASA in the fall of 1994 to construct the 2MASS telescopes and cameras and to conduct the survey. Susan Kleinmann left the program not long thereafter, and Mike Skrutskie, who had joined the 2MASS project in 1990 with the initial responsibility for telescope design and construction, replaced her as the Principal Investigator. Ray Steining was brought in shortly afterward as the Program Manager.

Two matching 1.3m telescopes were built to efficiently survey the sky, one for the northern sky the other for the southern (Figure 102). Telescopes this size were commercially readily available and sufficient to meet the performance objectives, although the special survey requirements did require an individual design and construction. Each telescope had an integrated camera assembly with three 256×256 HgCdTe NICMOS arrays with a plate scale that obtained an 8.5'×8.5' image with 2"×2" pixels. The camera used the standard astronomical J, H and K_s

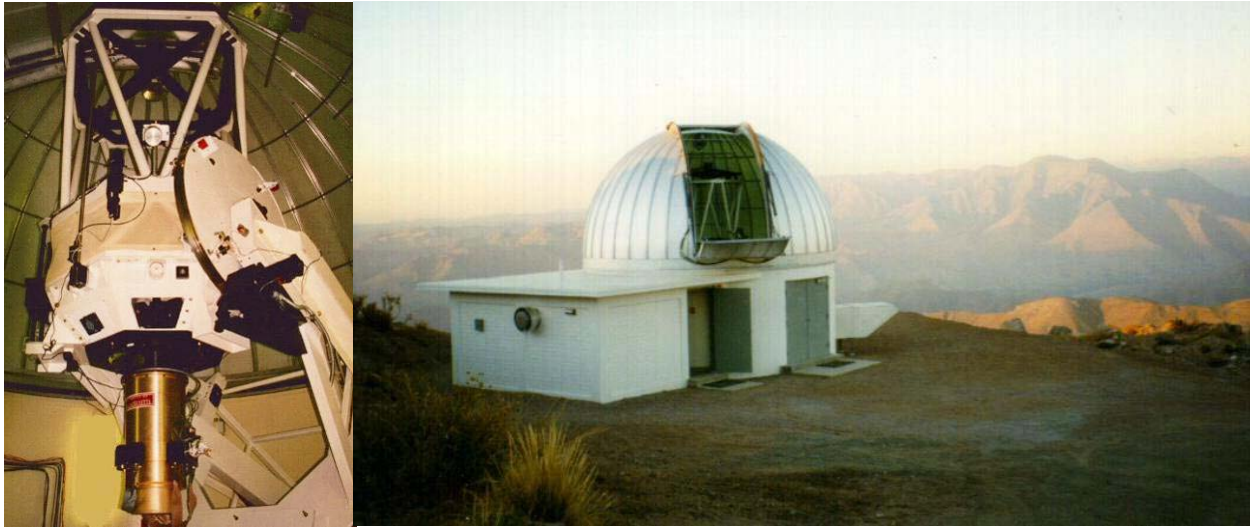


Figure 102. The 2MASS facilities. At left is the northern telescope at Mt. Hopkins in Arizona. The cylinder at the back of the telescope is the three-color near-infrared camera. The 2MASS site at the Cerro Tololo Inter-American Observatory is shown at right. These and the other images in this section are courtesy of the Two Micron All Sky Survey (2MASS), a joint project of the University of Massachusetts and the Infrared Processing and Analysis Center/California Institute of Technology, funded by the National Aeronautics and Space Administration and the National Science Foundation.

filters centered at $1.25\text{ }\mu\text{m}$, $1.65\text{ }\mu\text{m}$ and $2.17\text{ }\mu\text{m}$, respectively. Dichroic beam splitters were used to co-align the arrays to view the same region of the sky.

Routine 2MASS survey operation began in June 1997 at Mt. Hopkins, Arizona and in March 1998 at the Cerro Tololo facility. Although starting later and covering more sky, the superior observing conditions at Cerro Tololo resulted in the southern hemisphere survey being completed in February 2001 while the northern hemisphere coverage finished in November of that year. Nominal operations had the telescopes tracking the sky at the sidereal rate while scanning in declination at about 1-arc minute per sec. The secondary mirror moved in the opposite direction, freezing the sky on the focal planes for 1.3 seconds of exposure time per frame after which the secondary mirror returns to the home position to begin a new freeze frame.

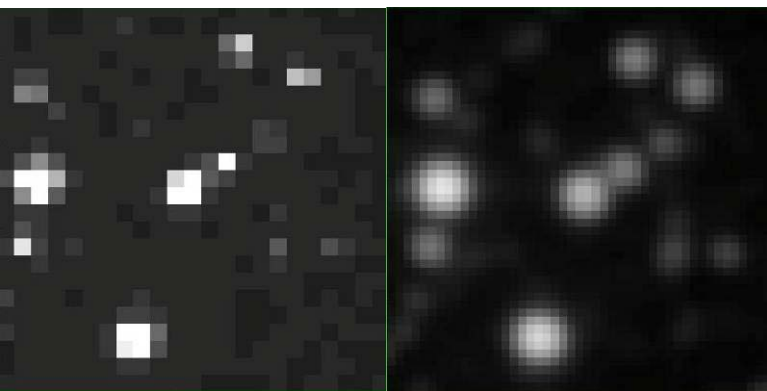


Figure 103. 2MASS imaging. A single 'raw' frame is at the left and shows the discrete nature of the single image. The survey strategy sub-sampled the pixels in the six frames that image at a given position. The image on the right is on a $1''$ grid and removes the under-sampling in the raw image. Image from http://pegasus.astro.umass.edu/mapping/map_scan.html.

A given source will appear on six such frames and, consequently, have a total integration time of 7.8 seconds. About 70 deg^2 could be mapped in this fashion on a clear night.

It was recognized early in the design that since the pixels were larger than the diffraction of the telescope plus atmospheric blur, a single data frame under-sampled point sources and the consequent aliasing would compromise both astrometric and photometric accuracy. Therefore, successive steps between frames

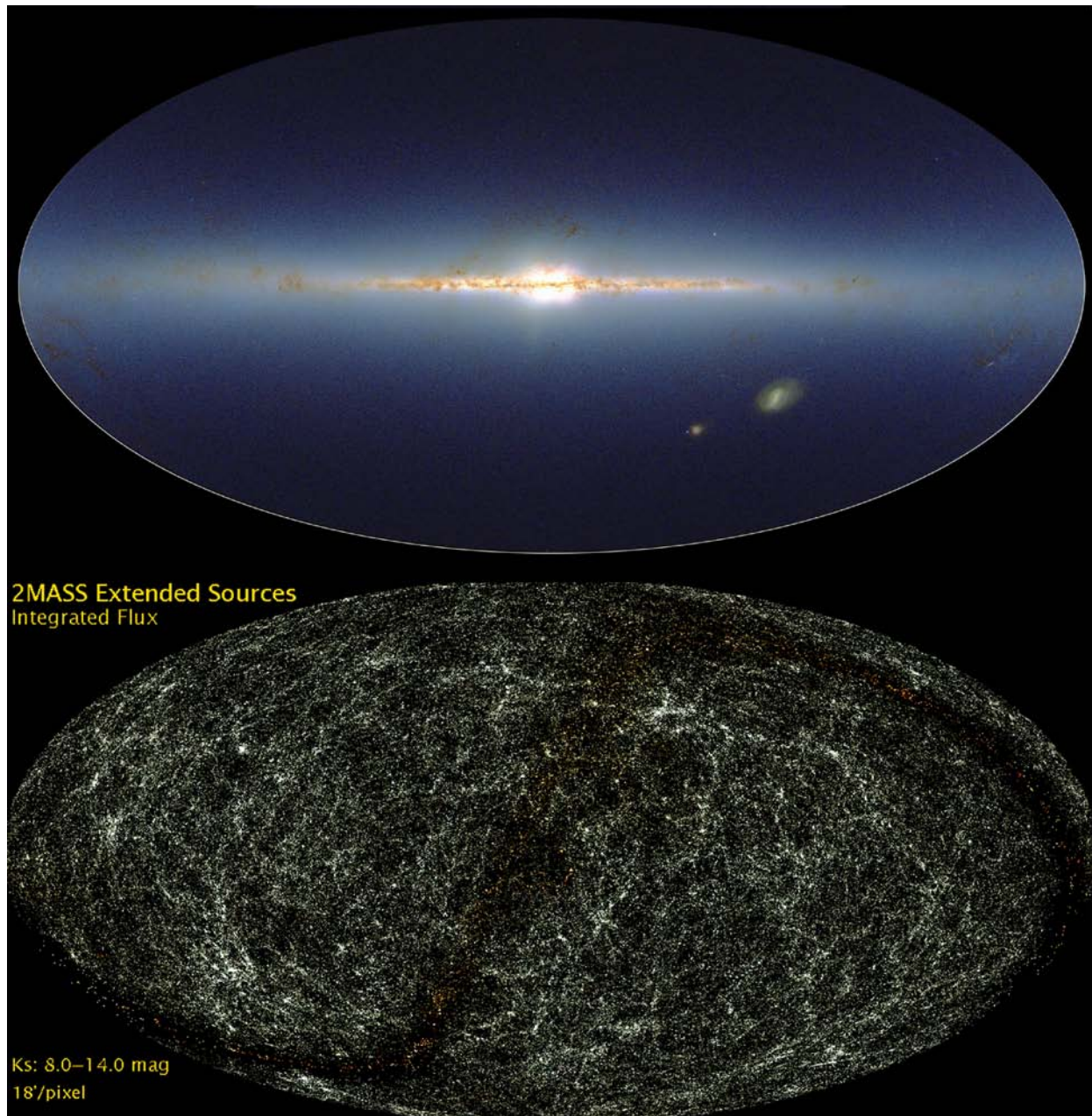


Figure 104. 2MASS all sky images. The point sources are plotted in Galactic coordinates on an Aitoff projection at the top, coded blue, green and red for 1.25, 1.6 and 2.2 μ m, respectively. The distribution of K band 2MASS extended sources, mostly galaxies, in equatorial coordinates is shown at the bottom; the dark band is due to extended sources in the Galactic plane that have been subtracted. Both images are color. The top images adapted from Skrutskie et al. (2005) <http://www.ipac.caltech.edu/2mass/gallery/index.html>.

were in non-integer increments of a pixel height and the focal plane was rotated by a small amount so the six apparitions appear at different in-scan and cross-scan positions on a pixel. Figure 103 compares the single frame image on the left with an image generated by combining the six frames that cover the area.

The entire sky was mapped at J, H and K_s to a signal-to-noise of ≥ 10 at 15.8, 15.1 and 14.3 limiting magnitude respectively, outside of confused regions such as the Galactic plane.

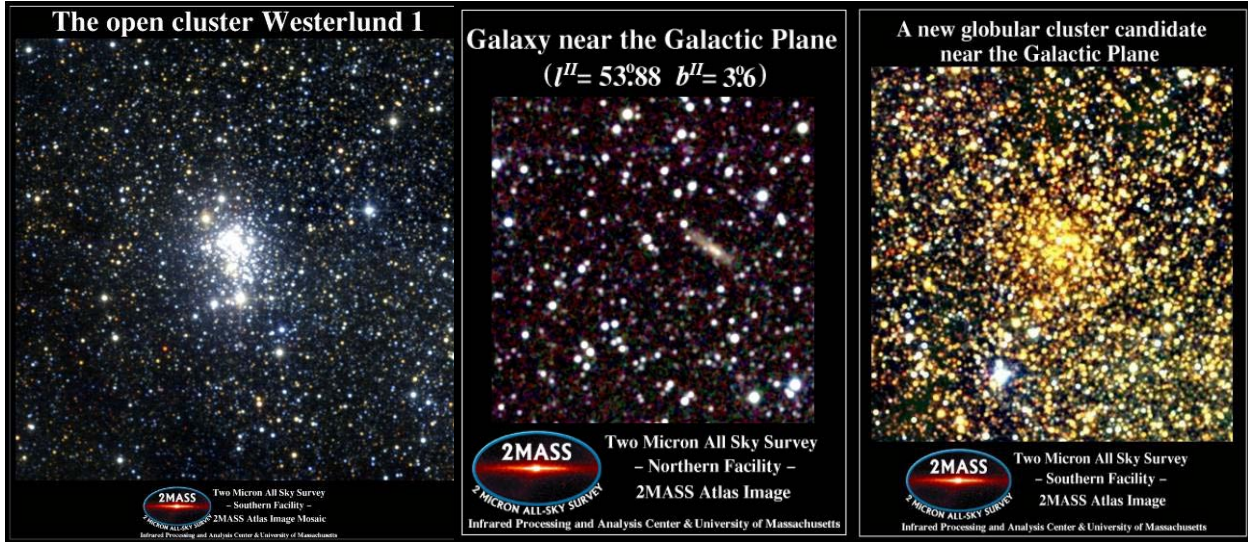


Figure 105. Objects in the Galactic plane observed by 2MASS. At left is a $13' \times 13'$ image of Westerlund 1, the near-infrared source that Price (1968a, b) found to be extended to the $1' \times 1'$ ITT survey detectors. In the center is a previously unknown galaxy found in the zone of avoidance. At right is a new globular cluster near the Galactic center. J, H and K are color coded blue, green and red, respectively. The extinction to the globular cluster is large enough that it was not detected in the J band; hence, the cluster stars are yellow. The Atlas Image mosaics are courtesy of 2MASS/UMass/IPAC-Caltech/NASA/NSF.

The principal products created from the survey are: a Point Source Catalog (PSC) with accurate positions and photometry on ~ 471 million point sources, an Extended Source Catalog with accurate positions, photometry and basic shape information for ~ 1.6 million resolved sources, most of which are galaxies, an all sky Image Atlas of 4.2 million calibrated images. Figure 104 displays the distribution of the point sources and the resolved objects. The resolved objects are galaxies for the most part; the extended sources near the Galactic plane have been removed, thus creating the sinuous shadow. Therefore, the project achieved its objective of a uniform and complete sky survey at $\sim 30,000$ times fainter than the TMSS and provides a comprehensive database to study structure of the Galaxy and the local universe. Skrutskie et al. (2005) described the survey instruments, strategy and performance. Jarrett et al. (2000a) discussed the extended sources processing and quantification of source parameters used to create the 2MASS extended source catalog while Jarrett et al. (2003) published a 2MASS Large Galaxies atlas that recovered galaxies that were lost or distorted in the small scale structure processing. Details of the data processing and the products may be found at

<http://www.ipac.caltech.edu/2mass/releases/allsky/doc/expsup.html>.

This web site also has the information on the 2MASS extended mission, which provides more sensitive data on smaller areas of the sky. Approximately 590 deg^2 of sky in 30 separate targeted regions were scanned at least once with a six times longer ($6\times$) integration time than the 7.8s exposure used for the all sky survey. Most of the area, 383 deg^2 and 127 deg^2 , was covered on deep surveys of the Large and Small Magellanic Clouds, respectively. These $6\times$ observations probe ~ 1 magnitude deeper than the main survey. There are 73,230 calibration scans that cover $8.5' \times 1^\circ$ in 35 fields that are distributed at approximately two hour intervals in right ascension near $\sim 0^\circ$ and $\pm 30^\circ$ declinations. The limiting magnitudes in these fields are between 3.5 and 4.0 magnitudes fainter than the general 2MASS survey. Thus, they sample the stellar main sequence more deeply as well as extending measurements on the local universe to the fainter galaxies. In

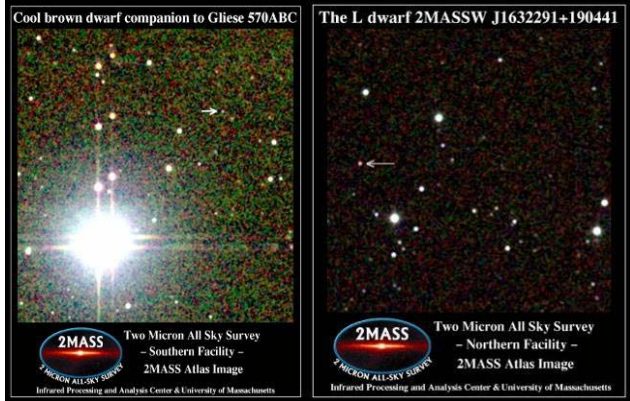


Figure 106. 2MASS Atlas images of T (left) and L (right) sub-stellar brown dwarfs. The T dwarf is a companion to Gliese 570, the bright binary star at left. Three pair of regularly spaced ghost sources along the vertical diffraction spikes are image artifacts created by the bright binary stars.

survey. This cluster lies behind ~ 13 magnitudes of visual extinction, which makes it very faint in the visual but a bright near-infrared source. Furthermore, extinction along lines of sight that are closer than 30° from the Galactic plane dim the light of distant objects and the amount of dimming increases as the plane is approached. Thus, a zone of avoidance is created in which the fainter galaxies are sufficiently dimmed that they fall below the detection limit in visible surveys. The near-infrared cuts through this extinction and, as noted by Jarrett et al (2000b), 2MASS was able to see galaxies well within the Galactic plane. The middle image of Figure 105 shows one such 2MASS galaxy. Even more heavily reddened is the globular cluster discovered by 2MASS and shown in the right panel of the Figure. This cluster is at $b = 0.1^\circ$ and only 10° from the Galactic center. Since the reddening in the 2MASS J band is about twice that in K_s , the extinction to this cluster is high enough that it was not detected in J. The combination of the H and K_s measurements results in the yellow-red colors.

2MASS proved to be most effective in achieving one of its original science goals, the discovery of brown dwarf stars (Kleinmann, 1992). These sub-stellar objects are too small to fuse hydrogen in their core, a process that defines a star. Becklin and Zuckerman (1988) found the first object, GD 165B, which had the unequivocal characteristics of a brown dwarf in their search for sub-stellar companions to white dwarf stars. Subsequent searches in the Pleiades stellar cluster were also productive (Rebolo et al., 1995, Basri and Marcy, 1995), while Nakajima et al. (1995) were successful in their search for cooler brown dwarf companions to M dwarf stars. However, it was the large scale deep digital sky surveys of the 1990s, prominently 2MASS, that were most productive, discovering hundreds of these objects. Actually, the first 2MASS brown dwarf was observed with the prototype camera but not recognized until much later (Kirkpatrick, Beichman and Skrutskie, 1997). Subsequent systematic searches through the 2MASS database turned up several hundred objects, the follow-up spectral observations of which were used by Kirkpatrick et al. (1999) to define the L spectral sequence and the cooler T classification (ultra-cool Y dwarfs are yet to be discovered). Figure 106 shows an example of a 2MASS L and a T dwarf. New dwarfs continue to be found in the 2MASS database (Looper, Kirkpatrick and Burgasser, 2007). By the time of Kirkpatrick's (2005) review of the L and T

aggregate, these fields cover about $\sim 5 \text{ deg}^2$ of sky. The calibration working database has positions, magnitudes and characteristics of about 191.5 million point sources and 404,000 extended objects extracted from these observations, while the corresponding Calibration Image Atlas has nearly 9×10^5 images in the three survey bands redundantly covering the areas.

The survey also lifted the veil of interstellar extinction near the Galactic plane. Figure 105 shows some of the objects 2MASS has seen in or through the Galactic plane: Westerlund (1961) discovered the open cluster Westerlund 1 on deep photographic plates of the region, which Price (1968a) later detected as an extended object in his near-infrared southern sky

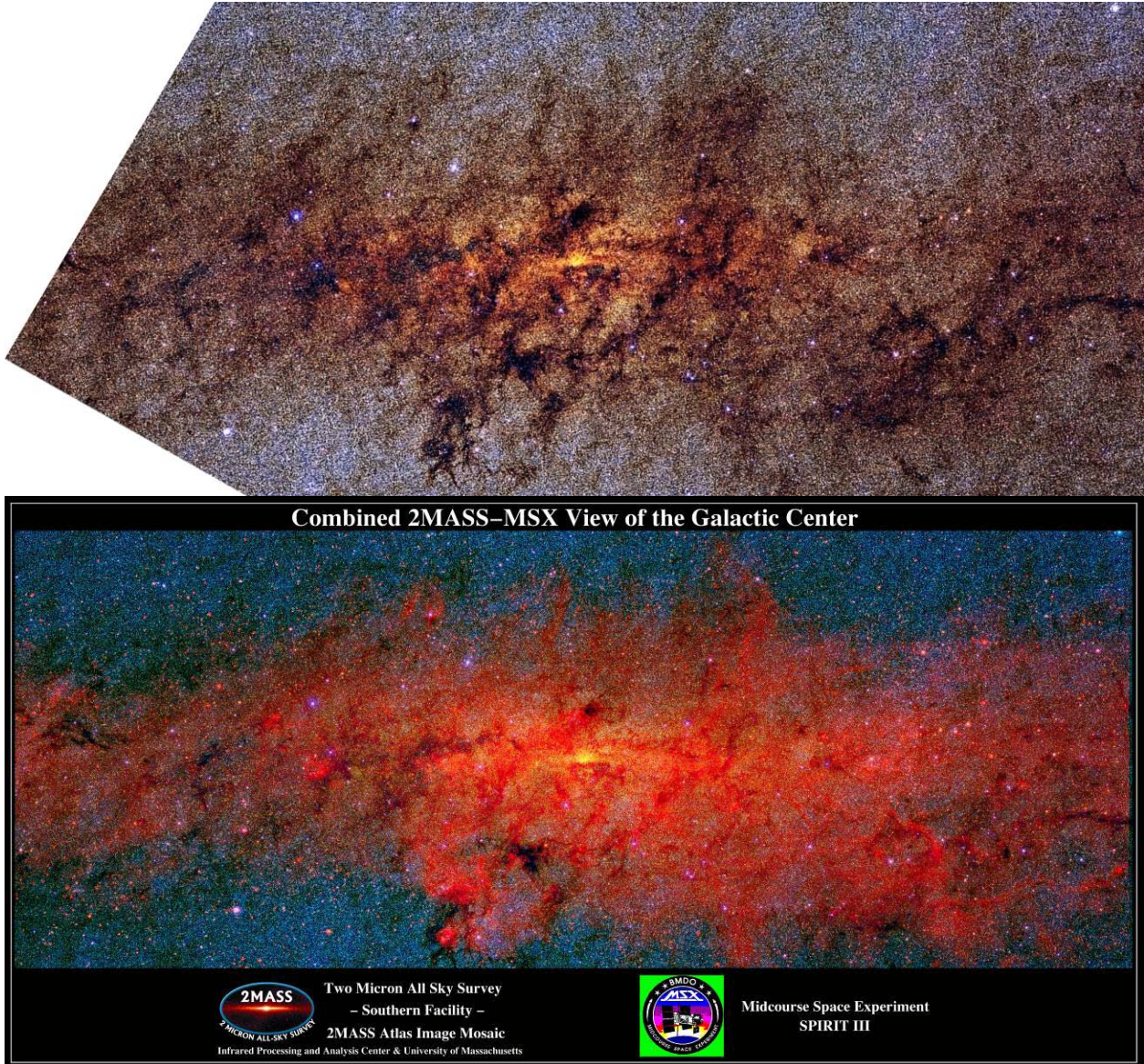


Figure 107. The Galactic center in the near-infrared and combined with mid-infrared observations. The 2MASS false color J, H and K image of the center is at the top. The image at bottom plots J (blue), K (green) and MSX 8.3 μ m (red). Much of the extinction in the 2MASS image is filled in with diffuse 8.3 μ m emission; areas that are still obscured are infrared dark clouds.

spectral classification scheme, approximately 450 of sub-stellar dwarfs were known; the number was 753 as of August 2009 (<http://spider.ipac.caltech.edu/staff/davy/ARCHIVE/index.shtml>).

Although the majority of these objects were extracted from the 2MASS database, the DENIS southern hemisphere survey did contribute several dozen sub-stellar discoveries (e.g. Delfosse et al., 1997). Because of its $\sim 23^{\text{rd}}$ limiting magnitude in the visible, the Sloan Digital Sky Survey (SDSS) has also proven to be quite productive, discovering well over a hundred objects (e.g. Chiu et al., 2006). The SDSS, a 2.5 m alt-azimuth telescope at Apache Point, New Mexico (Gunn et al., 2006), images a $\sim 3^{\circ}$ diameter field onto a matrix of $30 - 2048 \times 2048$ CCDs. Each of the five cross-scan rows of CCDs is filtered for a different spectral bandpass, ranging from 0.35 μ m to 0.92 μ m. Thus, the columns scan six multicolor swaths of sky. The columns

are separated by about half the width of a CCD and successive scans are similarly offset to provide complete five color information over a 2.5° strip. The scan and CCD transfer rate are synchronized so that the data are co-added by time delay and integration on the telescope. Nominally, the survey covered the northern Galactic cap outside the zone of avoidance and a smaller area at southern Galactic latitudes; a second pass coverage is currently underway.

The uniformity and completeness of 2MASS data makes it ideal for studying Galactic structure and a number of papers have been written on this topic. An example is that of Cabrera-Lavers et al. (2007) who derive vertical scale lengths for the Galactic thin and thick disk using 2MASS color selected red giant stars as tracers. The interesting result of this study was that the old disk stars track the Galactic warp but the thin disk does not. Also, both 2MASS and SDSS probe deeply into the Galactic halo. Rocha-Pinto (2004) detected an over density of Halo M giants selected by color criteria from the 2MASS data in a $\sim 60^\circ$ long swath in the direction of Triangulum – Andromeda that appears to be the remnants of a small nearby galaxy disrupted by the Milky Way. The SDSS also detected several of such streams (e.g. Newberg et al., 2002) as well as nine new sparse Milky Way companion dwarf galaxies (Zucker, et al., 2006).

Generally, the interstellar dust producing the extinction that obscures the stars in the visible and near-infrared re-emits the absorbed energy in the mid-infrared, a characteristic that is highlighted in Figure 107. The Galactic center 2MASS image at the top is color coded blue, green and red for the J, H and K_s observations, respectively. Away from the plane, the stars are dominated by J band emission and hence are blue. In the plane, the stars are heavily reddened and are either obscured (dark regions) or are dominated by emission in the K_s band and hence are yellow to red. The bottom image plots J, K_s and MSX Band A in blue, green and red, respectively. Much of the near-infrared extinction has been filled in with mid-infrared emission. The regions that remain obscured are infrared dark clouds, the visibility of which is strongly enhanced in the Figure.

9.3. The Deep Near-infrared Survey of the Southern Sky (DENIS)



Susan Kleinmann discussed the 2MASS project with infrared astronomers at the European Southern Observatory (ESO) in 1990, who enthusiastically embraced the concept. ESO appointed a Science team led by Thije deJong, and a Project team with Nicolas Epcstein as the principal investigator to pursue the concept of a southern hemisphere survey complementary to 2MASS. Nicholas Epcstein was a logical choice to lead the effort as previously he had laboriously surveyed the 120° swath of the southern Galactic plane within $|b| < 5^\circ$ below the -32° southern declination limit of the TMSS with a single large ($3.5'$) beam $2\ \mu\text{m}$ detector on the Valinhos (Brazil) $60''$ telescope in mid-1982. Having completed the survey in 1985, Epcstein et al. (1985) published the catalog of 338 sources with $K < 3.5$, and then followed up with more accurate multicolor infrared photometry of the sources (Epstein et al., 1987).

The ESO plans for the Deep Near-infrared Survey of the Southern Sky (DENIS) were well solidified by the time of the *ad hoc* session on the topic at the Schloss Elmau meeting in November 1990 to discuss ISO dedicated time experiments. For economy, the existing 1 m telescope at La Silla was chosen for the survey. Two NICMOS arrays were selected to observe in the J and K bands at 1.25 and $2.2\ \mu\text{m}$; the 2MASS and DENIS ultimately incorporated a K short (K_s) band, which had a shorter long wavelength cutoff to reduce the atmospheric effects at the long wavelength edge of the K band. Instead of a 2MASS H band analogue, the DENIS team

chose to use a Tektronix 1024×1024 CCD array filtered for a shorter wavelength I band centered at 0.82 μ m, ostensibly for improved position determination and to provide higher spatial resolution and better color discrimination for the observed sources. The pixel size of the infrared arrays was set at 3" while 1" was used for the CCD. Consequently, only the central 756×756 pixels of the CCD were read out to match the instantaneous field of the infrared arrays.

Initially, a collaboration between 2MASS and DENIS was contemplated in which the survey coverage might be divided (Kleinmann, 1992). However, as the survey strategy and science objectives of the two projects began to diverge, Susan Kleinmann (9 September 1990 letter to Nicolas Epcstein) declined a collaborative effort on behalf of the 2MASS team. After due consideration, Kleinmann had concluded that, because of the numerous technical differences between the two surveys, combining the DENIS and 2MASS databases would compromise the fundamental 2MASS science goal of creating a uniform and consistent database that could be used to study the large scale structure of the Galaxy and the Local Universe. At that time, 2.5" pixels were baselined for 2MASS while 2" pixels were being considered, and ultimately chosen, in order to reduce the atmospheric background and for spatial definition of the resolved galaxies. Also, interstellar extinction in the I band near the Galactic plane would seriously compromise the DENIS color analyses of galaxies and distant reddened stars. That the European proponents still hoped for a collaboration in which DENIS was a component of a single all sky survey with 2MASS as may be noted from the subsequent November 1991 Version 2.2 of the DENIS proposal that states: "*The present proposal concerns the achievement of the southern part of the survey that will be undertaken in connection with a twin project proposed by an association of American Universities and primarily aimed at surveying the Northern Sky*" (underline is in the original). Susan Kleinmann (20 December 1991 letter) again demurred, pointing out that the DENIS and 2MASS systems were not identical and, consequently, the data would be incompatible since a single set of software could not be used to reduce both datasets. She again emphasized that the surveys were optimized for different goals, making them inconsistent.

Epcstein et al. (1994) presented the DENIS concept and strategy used to survey the sky at declinations south of +2° by scanning overlapping 30° long declination strips while Epcstein et al. (1997) provided a more illustrative description of the hardware and survey operations. Three separate cameras were built, one for each color. To reduce weight on the telescope, a magnesium support structure was constructed to hold the dichotic filters and relay mirrors and to position the cameras. Since the secondary mirror of the 1 m telescope is fixed, sub-sampling of the array pixels was obtained by an internal micro-scanning mirror in the beam path to the infrared cameras that moved the field over a grid of nine positions spaced $\pm \frac{1}{3}$ pixels from the center point in declination and $\pm 2\frac{1}{3}$ pixels right ascension.

The DENIS survey began in December 1995 and ended in September 2001 after covering 97% of the planned survey area; the last data release in 2005 listed approximately 355 million point sources detected in ~80% of the southern sky. The 3 σ detection limits were 18.5, 16.5 and 13.5 magnitudes at I, J and K_s, respectively. At J, 2MASS is ~1.6 times more sensitive, which is the difference in the collecting areas of the telescopes used. 2MASS is about seven times more sensitive than DENIS in K_s with the most of the difference likely being due to background noise because, unlike 2MASS, DENIS did not cool the optical train of the K_s band. Despite the differences in telescopes and survey strategy, Carpenter (2001) and Cabrera-Lavers and Garzón (2003) found that the 2MASS and DENIS J and K_s stellar photometry were well correlated, which permits direct comparisons between the two datasets to study source variability.

A very brief summary of the significant DENIS observations include: the discovery of a number of brown dwarf stars and the ~ 2000 galaxies Vauglin et al. (2002) found at $|b| < 15^\circ$ in the DENIS J and K_s images. Although such studies were superseded by 2MASS and other more sensitive surveys, DENIS has a singular contribution for transient objects, such as asteroids. Baudrand, Bec-Bosenberger and Bosenberger (2004) extracted I, J and/or K magnitudes on approximately 2000 asteroids identified in the DENIS database. While this is far fewer than the $\sim 62,000$ asteroids measured by 2MASS (see Sykes et al., 2000; 2002; for a discussion), each of the DENIS observations is unique in that either the object was not observed by 2MASS or was measured at a different time and phase angle.

9.4. Deeper Near-Infrared Surveys

Cabrera-Lavers et al. (2006) sampled approximately 41 deg^2 of the Galactic first quadrant out to $\sim 27^\circ$ longitude with a $1''$ pixel plate scale in J, H and K_s with an infrared camera equipped with a NICMOS 3 array on the 1.5 m Tenerife telescope. With half the pixel size of 2MASS, this survey suffered less confusion along the plane, which allowed this survey to probe 1 to 1.5 magnitudes more deeply.

On a larger scale, about 7000 deg^2 of the northern sky is being surveyed in five spectral bands between 0.83 and $2.37 \mu\text{m}$ with a Wide Field Camera (WFCam) on the 3.8 m United Kingdom Infrared Telescope (UKIRT). The camera has four 2048×2048 Rockwell HgCdTe arrays with $0.4''$ pixels covering a total field of 0.207 deg^2 . The tip-tilt secondary mirror on the telescope compensates for atmospheric scintillation, which results in a nearly diffraction limited near-infrared optical performance. The stellar images for ground based telescopes are smeared out over $\sim 1''$ by optical turbulence. Adaptive optics is used to sense and compensate for the wave-front distortions introduced by turbulence, thus improving both the resolution and, for arrays with pixels smaller than the optical blur, sensitivity. The first order correction is obtained by simply correcting for the direction and angle of the incoming wave-front (tip-tilt correction), which is quite adequate for the near-infrared. Beckers (1993) and Roggemann, Welsh and Fugate (1997) describe adaptive optics techniques and review their astronomical applications.

Lawrence et al. (2007) described the UK Infrared Deep Sky Survey (UKIDSS) concept as the “...near-infrared counterpart of the Sloan Digital Sky Survey.” Routine operations started May 2005 and the surveys are expected to take seven years to complete. UKIDSS is covering 4000 deg^2 toward the north Galactic pole and the $\sim 1900 \text{ deg}^2$ within $|b| < 5^\circ$ of the Galactic plane that is available at the observing site to a 5σ detection limit of ~ 18 at K, which is ~ 30 times more sensitive than 2MASS. Lucas et al. (2008) provide details of the UKIDSS Galactic plane survey. The first UKIDSS data release was in July 2006 for which Warren et al. (2007) provides an overview of the data processing; currently there have been seven UKIDSS data releases.

Some initial science results have been obtained from the various data releases. For example, Tata et al. (2006) announced the identification of the first brown dwarfs in the survey data while Lodieu et al. (2007) extracted T dwarfs in the UKIDSS release 1 data and Hogan et al. (2009) found L dwarfs. Much more distant, Venemans et al. (2007) announced the first luminous highly red shifted quasar discovered by UKIDSS. The UKIDSS surveys are still a work in progress and most of the data mining is yet to be done.

McPherson et al. (2006) described the Visible and Infrared Survey Telescope for Astronomy (VISTA). Begun in 2000 as a UK project, the visible component in the original concept was removed when the facility became an ESO asset after the UK joined that organization. VISTA has a 4.1-m telescope, which was delivered in July 2008, with 16 focal

plane arrays that sparsely populate a 1.5 deg^2 field. Three exposures are used to fill in the gaps in the field of regard. Six filters span the wavelengths between 0.9 and $2.5 \mu\text{m}$. Various surveys are planned with this telescope; the largest will cover half the sky with $0.2''$ pixels to a limiting magnitude of 18.5 with smaller targeted areas observed to fainter levels (e.g. Lawrence, 2007). The science verification of the system began mid-October 2009.

9.5. The Search for Near-Earth Objects

Although the search for near Earth objects (NEOs) is primarily a visible ground-based effort, several space-based infrared missions are to survey for NEO as a secondary objective or do follow-up observations but none of the efficient infrared surveys proposed have been funded.

I visited Gene Shoemaker in Pasadena in March 1973. He was seeking financial support for the near Earth asteroid survey that he and Glo Helin were conducting with the Palomar 1.2 m Schmidt telescope (Helin and Shoemaker, 1979), arguing that the angular rates and brightnesses of these objects were comparable to that of Earth orbiting satellites, especially when the NEOs were near the Earth. Such objects were, therefore, a source of false detections that should be studied and characterized for space surveillance. The idea was interesting although such false detections would be relatively rare; but the bottom line was that we had no money for the effort. Subsequently, Taff (1981) used the GEODSS Experimental Test System (ETS) at the White Sands Missile Range near Socorro, New Mexico to show that asteroids did, indeed, provide optical surveillance targets but as sought after objects rather than interference. He demonstrated that, with straightforward modifications to the GEODSS surveillance hardware and software, the ETS could be used for an efficient asteroid survey, thus presaging the comprehensive Lincoln Laboratory effort in the late 1990s.

In the early 1980s, the fact that asteroids and/or comets have collided with the Earth with catastrophic results became a matter of public discussion. Alvarez et al. (1980) had proposed that the dinosaurs were killed off by the ‘nuclear’ winter created by a large impact that marked the boundary between the Cretaceous-Tertiary (K-T) eras ~65 million years ago. Hildebrand et al. (1991) found the ‘smoking gun’ for this hypothesis by associating the sought after impact site with the Chicxulub crater off the coast of the Mexican Yucatan peninsula. The public attention at the time focused on the K-T extinction as a demonstration of nuclear winter in the context of the nuclear disarmament debate rather than highlighting the issue of imminent threat from asteroid impacts. This changed with the impact of comet Shoemaker-Levy with Jupiter in July 1994 (Levy, 1996), which raised the possibility that impacts with the Earth could occur today with catastrophic results. Indeed, it has been estimated that an impact causing significant local devastation occurs on the average of once a millennium. About 175 craters or their remnants have been identified on the Earth to date and there are about 20 additional probable associations (Napier and Asher, 2009), the most recent ‘sizable’ crater was created by an impact in Siberia that occurred in the late 1940s; the oldest identified crater is 2.5 billion years old.

Analyses of impact damage have defined the size of threat objects as ranging from 50 m to 10 km in diameter. An object a few dozen meters in diameter would be locally devastating, as demonstrated by the Tunguska, Siberia impact of a stony asteroid, or comet, in 1908 that flattened trees over a \sim 100 km² area (e.g. Stone, 2008). A 10 km diameter object, the estimated size of the impactor that ended the Cretaceous era, would be globally catastrophic.

Several early to mid-1990 workshops assessed the impact hazard and what to do about it. Morrison (1992) and Shoemaker (1995) reported the workshop results that recommendation that NASA fund an effort to discover 90% of the objects larger than 1 km within 10 years. This

effort was designated, Spaceguard after the system visualized by Arthur C. Clark in his 1973 book *Rendezvous with Rama*. The Air Force also had an early interest in a Planetary Defense Initiative for detecting and monitoring potentially hazardous objects the rationale for which were laid out in a white paper by Air Force Majors Holt, Johnson and Williams (1994).

A small number of asteroid search programs using meter class optics were operating at the time. There was the long standing Palomar 1.2 m Schmidt telescope photographic survey originally named the Planet Crossing Asteroid Survey. Tom Gehrels (1984) and Robert McMillan led the Lunar and Planetary Laboratory/Kitt Peak Spacewatch effort that began in 1981 using a relatively small CCD on a 0.9 m telescope. A 1.8 m telescope was added to the effort in 2001 and several upgrades to the CCD cameras improved the étendue and sensitivity of the survey; it is now able to reach a limiting magnitude of 23. This program is still operational.

In the mid-1990s, new programs were funded under the Spaceguard initiative. The Near Earth Asteroid Tracking program (NEAT – Helin et al., 1997, Pravdo et al., 1999) began in December 1995 as a cooperative program between NASA/JPL and AFRL. Initially, NEAT used a large format 4096×4096 pixel CCD camera with a $1.2^\circ \times 1.6^\circ$ field-of-view on the AMOS Mt. Haleakala` one-meter GEODSS telescope. Air Force contractor personnel operate the telescope and the data were routed directly to the Jet Propulsion Laboratory for analyses. Paul Kervin (Kervin et al., 1996), AFRL, provided additional follow-up astrometric observations on the AMOS 1.2 m telescope (these facilities are shown in Figure 8). NEAT was assigned the 12 nights each month centered on the new moon. NEAT operations were transferred to the AMOS 1.2 m/B37 telescope in early 2000 (Talent et al., 2000) and the 1.2 m Palomar Schmidt telescope was upgraded for an NEO survey at about the same time. The NEAT survey ended in 2007 after discovering more than 400 NEOs.

Ted Bowell is the principal investigator for the Lowell Observatory Near-Earth-Object Search (LONEOS), which used two large format 2048×2048 CCD arrays on the 57 cm Schmidt telescope at Anderson Mesa that is operated by the Lowell Observatory in Flagstaff, Arizona. The arrays subtend $1.6^\circ \times 3.2^\circ$. On chip time delay and integration over the declination pixels, in which the telescope is driven in declination while tracking in right ascension increases the sensitivity (e.g. Diercks et al., 1995). LONEOS went into operation in 1993 and terminated in February 2008, having discovered 288 NEOs. LONEOS will be succeeded by the NEO survey on the Discovery Channel Telescope. This telescope has a 4.2 m primary mirror and a 2.3 deg^2 field of view at the prime focus that is covered by 40 2048×4096 CCD arrays. Bowell et al. (2007) discuss the NEO survey to $\sim 23^{\text{rd}}$ magnitude with this telescope. The Discovery Channel telescope is due to become operational in late 2010.

The singularly most productive resource for discovery and recovery of small bodies in the solar system has been the Lincoln Laboratory (LL) Near Earth Asteroid Research (LINEAR) Project funded by NASA and AFOSR (Stokes et al., 2000). Following Taff's lead, this survey is being conducted with the two GEODSS 1 m telescopes at the Experimental Test Site (ETS) but with much more sensitive, large format CCD arrays rather than the vidicon cameras that Taff used. LINEAR routinely discovers objects as faint as 18th visual magnitude, which translates to a search radius of 0.3 AU for the canonical 1 km diameter object. The best sensitivity achieved is 19th magnitude on winter nights with excellent seeing. The LINEAR program developed an efficient survey strategy that optimized discovery, with the result that this system has discovered more main belt asteroids than all the other efforts combined from the time it went into operation to the present. LINEAR also has been credited with discovering $\sim 35\%$ of the $\sim 6500+$ near Earth asteroids known as of the end of 2009. However, a collaboration between the Catalina, Siding

Springs and Mt. Lemon Observatories began routine operations in 2004 that, combined, began to outpace LINEAR's discovery rate in 2005 and individually in 2006. The Catalina Mountain facility (Spahr et al., 1996) has a ~0.8 m Schmidt telescope, while that at Siding Springs uses a 0.5 m Schmidt camera. The 1.5 m infrared telescope originally installed by Ed Ney for infrared observations on an abandoned Air Force radar site atop Mt. Lemon was refurbished for the near Earth asteroid survey after languishing for a number of years. The Catalina survey surpassed the total number of NEOs found by LINEAR in 2009.

With regard to the Safeguard objective, the predictions of several studies (e.g. Tedesco, Muinonen and Price, 2000, Jedicke et al., 2003) were borne out: namely, that less than 80 % of the expected 1000 or so 1 km or greater diameter objects were discovered by mid-2008, the end of the 10 year mandated discovery period. Indeed, Napier and Asher (2009) estimate of the current discovery status is that it is essentially complete for objects with $D > 3$ km, ~80% for >1 km diameter objects but it has found only a fraction of one percent for asteroid ~ 100 m in diameter. What does the community do in such circumstances? It moves the bar! Thus, the current Spaceguard surveys are to continue as NASA projects a budget for them through 2012. Additionally, the 2005 NASA Authorization Act directed NASA to provide Congress with recommendations as how best to detect, track, catalog and characterize all objects larger than 140 m in diameter that approach within 1.3 AU of the Sun by the end of 2020. NASA was also asked to propose methods to avoid an impact. The response was given in the *NASA Near Earth Object Survey and Deflection Analysis of Alternatives* (hereafter the 2007 NASA Report to Congress), which did the requested study but altered the objective to the more tractable census of all potentially hazardous objects (PHOs) greater than 140 m; a PHO is defined as one that passes within ~ 7.5 million km or 0.05 AU of the Earth's orbit. In 2008, Congress requested NASA to ask the Nation Research Council to consider the findings of the 2007 NASA report to Congress and to analyze the adequacy of current and proposed NEO surveys and hazard mitigation strategies. The current results of this study is in an interim report (NRC; 2009: *Near-Earth Object Surveys and Hazard Mitigation Strategies: Interim Report*; NRC Report hereafter).

The NRC Report projected that near Earth objects searches with the existing surveys and those using the large visible telescopes currently under development, the Panoramic Survey Telescope and Rapid Response System (Pan-STARRS, Hodap et al., 2004), the Large Synoptic Survey Telescope (LSST, Sweeny et al., 2006) and the Discovery Channel Telescope (DCT – Sebring, Dunham and Millis, 2004), could complete the 140 m hazardous object survey to the 90% level by ~2030. The March 2007 Report to Congress noted that the discovery rate is slowed by the fact that the NEO search is a secondary mission for all three programs.

Pan-STARRS was primarily an Air Force project that, when completed, will consist of four 1.8 m telescopes (Pan-STARRS-4), each with a ~ 7 deg² field-of-regard covered by a mosaic of 60 CCD arrays with $\sim 0.3''$ pixels that could image in a selection of eight optical spectral filters. In addition to the tip-tilt wave-front compensation, the system has a unique higher order method of correction. Rather than using a deformable mirror, the motion of a guide star is monitored and used to shift charges around the Orthogonal Transfer CCD (OTCCD) Pan-STARRS arrays during exposure to follow the motion of an object caused by turbulence and jitter (Burke et al., 2007). The system is also designed to electronically combine simultaneous exposures of the same area of sky from the four telescopes and is projected to be able to detect moving objects with a 300 m or larger diameter. Kaiser et al. (2004) describe the Pan-STARRS science goals, including the survey strategy for the near Earth objects while Kubica et al. (2007) describe the automated processing that links observations of the same object on exposures taken

on the same night and night to night that is critical for follow-up astrometry for orbit determination. The prototype telescope, Pan-STARRS-1, was installed at the AMOS site on Mt. Haleakala in June 2006, is shown in Figure 8,. The initial checkout and science observations began in September 2007 and the science mission began in 2009 (Chambers, 2009) with the first scientific results being a report of an optical transit (Narayan et al., 2009). The program has yet to contribute to the NEO discovery archives. However, a realistic date for the full Pan-STARRS-4 system at Mauna Kea has not been set.

The Large Synoptic Survey Telescope project (LSST – Sweeney et al., 2006) will survey the sky to faint levels with 0.3" pixels in a choice of five filters with a large 8.4 m telescope that has a ~ 9 deg 2 instantaneous field-of-view. The LSST has about 10 times the effective collecting area as Pan-STARRS and will be able to detect moving objects that are about a magnitude fainter when the system comes on line in \sim 2016. Ivezić et al. (2006) discussed the LSST near Earth object survey requirements and considerations. Unfortunately, the SDSS survey strategy does not have the follow-up capability to link asteroid observations to project positions for others to obtain astrometry over a long enough time to determine a good quality preliminary orbit.

Jedicke et al. (2003) analyzed various discovery scenarios and concluded that a single space-based visual survey instrument would significantly outperform the current ground-based systems, even including reasonable upgrades. This is especially the case for the smaller diameter objects. In 2003, NASA commissioned a study by a NASA Near-Earth Object Science Definition Team (<http://neo.jpl.nasa.gov/neo/neoreport030825.pdf>) of how best to complete the 1 km survey and extend the census to 300 m objects as well as all PHA. This study examined ground- and space-based options and favorably considered visible space-based sensors with apertures between 0.5 and 2 m. This report cursorily examined and rejected a space-based infrared system as being too costly and technologically demanding. The advantages of space also prompted the Canadian Ministry of Defense and the US Air Force (through the participation of then BG (now ret.) Worden) to propose a small 15 cm visual telescope closely patterned after Canada's first astronomical satellite, the microvariability and oscillation of stars (MOST) program (Walker et al., 2003), as a proof-of-concept NEO space-based survey (Wallace et al., 2006). The discovery objectives of the Canadian system recently shifted to emphasize inner Earth asteroids (Hildebrand et al., 2007), objects whose orbit lie entirely within that of the Earth. Laurin et al. (2008) described the operational strategy to survey $\pm 20^\circ$ between 45° to 55° elongations on either side of the Sun. Although the performance capabilities of this instrument are grossly exaggerated in the published material, the mission concept is designed for the optimal detection of NEOs. A larger 25 cm primary aperture system, AsteroidFinder (Mottola et al., 2008), is a wide field visible telescope that has been selected by the German Aerospace Center as a mission to be flown in 2012 (or likely later). The experiment will be inserted into a dawn-dusk 600 km altitude orbit with the primary objective of searching for inner Earth asteroids to a limiting magnitude of 18.7 within 30° to 60° elongation on either side of the Sun.

Beginning in 1995 we, at AFRL, teamed with Ed Tedesco, Alberto Cellino and others to present the advantages of an infrared system to near Earth object workshops and other forums. The information in these presentations was formalized in a 2000 COSPAR paper by Price and Egan (2001), in which it was shown that an infrared space-based survey was quite sensitive to near Earth objects. Tedesco, Muinonen and Price (2000) ran simulations that indicated that the discovery rate would significantly increase by surveying elongations between 40° and 60° from the Sun, which is closer than can be achieved by visible ground-based surveys. Although this analysis was originally performed to demonstrate the efficacy of an infrared space-based system

to detect and characterize near Earth objects at these smaller elongations using MSX as an example, it also provided the rationale for the Canadian mission and the German AsteroidFinder.

A hardware design trade analysis was incorporated into the notional system described by Cellino, et al. (2000). This concept was developed into a proposal for a two color three-quarter meter near Earth asteroid surveillance system. The satellite was to be placed in the L2 Lagrangian point about 1.5 million km from the Earth opposite the Sun. The proposal was submitted to the European Space Agency but was not funded.

The 2003 NASA Near-Earth Object Science Definition Team Report concluded that technical maturity of the infrared focal planes and mechanical cryocoolers required to cool the focal planes and optics in an infrared NEO detection system was inadequate. However, a few years later, the 2007 NASA Report to Congress conceded that the technology to field a long duration mid-infrared space-based system was rapidly maturing and included an analysis of the discovery potential of a half meter infrared telescope in Solar orbit at the heliocentric distance of Venus. This study concluded that it alone could meet the 2020 census deadline. Such an infrared system also could accelerate by three years the completion of the survey goals using the baseline system of sharing the Pan-STARRS, LSST and the DCT.

IRAS had shown that, with careful thermal design, it was possible to cool the outer shell of the telescope housing to $T < 100$ K, which reduced the thermal load that the expendable cryogen had to handle. Indeed, the SAO/AFRL NIRAS proposed to passively (radiatively) cool the optics and focal planes, thus eliminating the need for cryogen. The Spitzer program also demonstrated that it was possible to passively cool large structures, the telescope in this case, to ~ 35 K, by getting away from the thermal input from the Earth. This is cool enough to operate mid-infrared HgCdTe arrays. Extrinsic two-dimensional mid-infrared focal planes have also improved. WISE incorporates large format 1028×1028 Si:As arrays and even larger formats will soon be available. Such arrays could be used in a sensor with passively cooled optics and mechanically cooled focal planes. The Akari telescope has flight demonstrated the long term operations of a pair of 20K mechanical coolers in space, completely relying on them to cool the near-infrared focal planes in the post cryogen mission. The Webb telescope program claims that 10K coolers have been developed to the level of technical maturity necessary for a space system.

The idea of a space-based infrared search apparently resonated with some of the 2003 Definition Team as JPL submitted a proposal to NASA for an infrared discovery system, NEOCam (Mainzer, 2006), at about the time of the NASA March Report to Congress, with five members of the Science Definition Team on the JPL consortium. The size of the proposed system (0.5 m), choice of focal plane arrays and wavelength coverage ($\lambda < 11$ μ m) and the 35K cooling requirements are similar to the system AFRL presented to the 2003 Definition Team. We found these parameters to be the most conservative while still being able to do the job. NASA declined to fund the NEOCam proposal. However, the concept was discussed further at the end of January 2009 at a session held by the NRC Review Committee at which infrared strategies were favorably considered. The current infrared contributions are to use the Wide-Field Infrared Survey Experiment (WISE) for an NEO survey (NEOWISE – McMillan et al., 2009) as a no impact secondary mission to survey the entire sky and to characterize about 700 NEOs with the Spitzer telescope during the warm mission (Trilling et al., 2009).

The value of an infrared space-based discovery system is highlighted in Figure 108. The spectral energy distribution of a 1 km diameter object with a geometric albedo of 0.15, which is consistent with the NASA 2007 Report to Congress ‘best estimate’ of 0.12, located 1 AU from both the Earth and Sun is plotted on the left. This geometric albedo is the fraction of sunlight

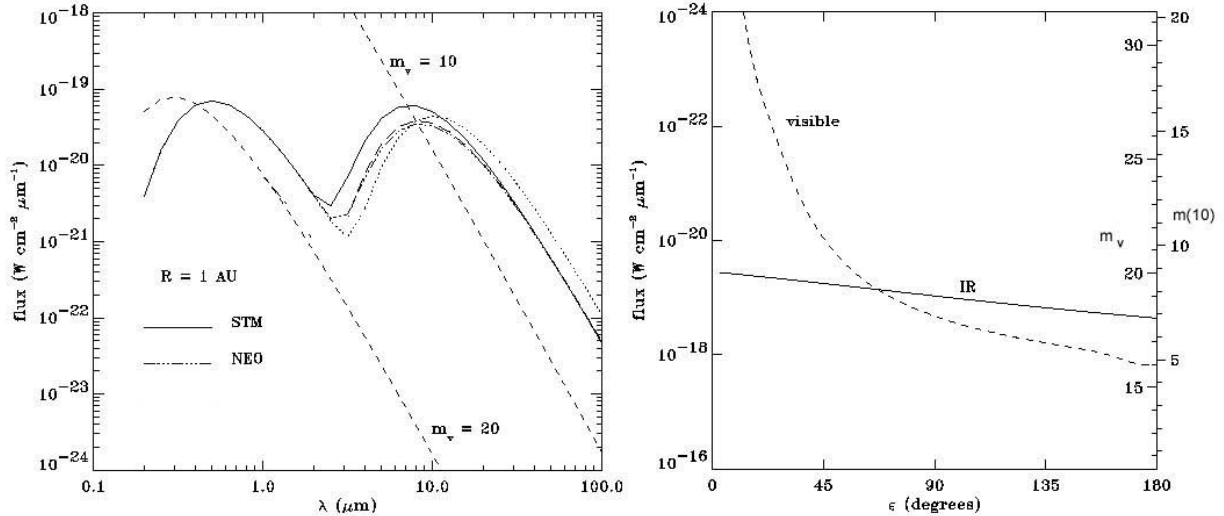


Figure 108. The modeled spectral irradiances of a near Earth object for two detection scenarios. The plot at the left shows the spectral energy distribution of a 1 km diameter S type asteroid with a geometric albedo of 0.15 that is at 1 AU from the Sun and 1 AU from the Earth. The phase angle for this geometry is 60° . The infrared curves are calculated using the Standard Thermal model of Lebofsky et al. (1986) and Lebofsky and Spencer (1989) (STM – the solid line), a more representative NEO model of Harris (1998) (NEO – dot – dashed line) and the rapidly rotating or isothermal latitude model (ILM – dashed line) that Lebofsky and Spencer noted gave better results for some near Earth asteroids are also plotted. The cooler dotted line is an isothermal model. The right hand plot shows the variation of visual and infrared irradiance from a 100 m diameter S type object that is 8.64 million kilometers from the Earth as a function of solar elongation. Note that the magnitude scale on the right increases upward, which means that the irradiance scale on the left decreases. The visual magnitude scale is on the inside of the right hand axis while the infrared values are on the outside.

reflected by a flat circular area with the same cross-section as the asteroid that would produce irradiance observed. The standard thermal model (Lebofsky et al., 1986) is shown as is the NEO model of Harris (1998) and (dashed line) the rapidly rotating model (Lebofsky and Spenser, 1989). The NEO and rapidly rotating models are more representative of the near Earth population that, in this case, gives similar results. The cooler dotted line is an isothermal model, which is often assumed in calculating RSO fluxes. The visual irradiance is about twice that predicted at $10 \mu\text{m}$ by the NEO or ILM models. However, converting the flux to photons, there are about 5 times more infrared photons in a $6 - 12 \mu\text{m}$ infrared band from this object than from an unfiltered visible CCD. Since, to first order, the visible CCDs and the IR arrays count photons, the infrared system can detect an asteroid about twice as far as a visible system. Also shown are the spectral energy curves for 10^{th} and 20^{th} magnitude sources and, as may be seen, the visible to infrared color is about $9 - 10$ magnitudes. One implication is that there are fewer infrared background sources with which the survey would have to contend, say in the Galactic plane, than in the visible. This considerably reduces the complexity of linking multiple observations of a given object (e.g. Kubicka et al., 2007).

The infrared intensity is also significantly less dependent on the phase angle than the visible. For example, the difference in visible brightness between viewing the object face on and the 60° phase angle depicted by the geometry in the left plot of Figure 108 is about a factor of six while the infrared flux changes by only $\sim 40\%$. The visible and infrared phase angle variation is compared at the right in which the flux and magnitude are modeled for a 100 m diameter object

with 0.15 geometric albedo at a distance of 8.64 million km from the Earth and is plotted as a function of solar elongation, the angle between the Sun and object as viewed from the Earth (phase angle $\sim 180^\circ$ – elongation for this geometry). Although the visible and infrared values for elongations less than 120° are highly uncertain, the plot indicates that the infrared advantage applies even for the smaller phase angles.

In addition to the contributions of AMOS for follow-up astrometry and photometry (Kervin et al., 1996), the LINEAR survey on the GEODSS ETS and Pan-STARRS, the Air Force has an additional unique capability for assessing the impact threat: space-based sensors, principally in the near-infrared, that monitor the bright flashes created by meteoroids as they enter the atmosphere. According to Tagliaferri, et al. (1994), these systems have been operating since the early 1970s, continuously observing almost the entire Earth's surface. Approximately 30 events are detected each year that have sizes estimated at between 1 and 10 m in diameter as inferred from the observed brightness. Brown et al. (2002) studied the size (energy) – frequency distribution for 8.5 years of observations and concluded that a Tunguska event occurs once a millennium. These results are entirely consistent with the size – frequency distribution of the larger NEOs detected by the various surveys (e.g. NRC Report).

9.6. Personal Perspectives

After my permissive TDY to Groningen in 1984, I returned to Europe once or twice a year for the next couple of decades. Initially, the purpose of the trips to Groningen was to monitor progress on the AFGL funded effort to remove artifacts from the IRAS data and to super-resolve the observations. This evolved into attending ISO program and SWS consortium meetings after I was given co-Investigator status on the SWS team. I also went to several topical meetings, such as the three Euroconferences on near-infrared surveys at which the scientific objectives and progress of the DENIS and 2MASS programs were discussed. Thanks to the good offices of Ed Tedesco, I also attended the September 1995 Vulcano, Italy meeting, which was one of the first to debate the European role in Spaceguard. We visited Alberto Cellino and Vincenzo Zappalá at the Turin Observatory after this conference and discussed the mutual interests we had with regard to infrared characterization of asteroids in general and detection of Near Earth Objects in particular. This led to more detailed discussions of what it would take to field such a system and a conceptual design (Cellino et al., 2000), which was fleshed out in a study funded by ESA (*Remote Observations of NEOs from Space, Final Report*, SD-RP-AI-0370, 2003). ESA declined to pursue the design beyond this report.

Critical elements of the infrared NEO search system would have benefited from the technology being pursued by the Space Vehicles Directorate's Space Technologies Division, particularly the 35K mid-infrared HgCdTe detector arrays and the mechanical coolers needed to achieve the necessary focal plane and optics temperatures. To this end Mike Egan and I reworked the proposal as a dual use space surveillance and NEO discovery system. Successful operation of this system would buff up the tarnished image of mechanical coolers left by the failure of the Vielleumier cooler on the Celestial Mapping Program satellite in 1971 and demonstrate the infrared advantage in space surveillance. However, the Space Vehicles Directorate did not pursue this opportunity.

10. SPACE-BASED INFRARED ASTRONOMICAL OBSERVATORIES

The European Space Agency (ESA) flew the first true infrared space-based astronomical observatory on 17 November 1995, the Infrared Space Observatory (ISO). Superficially, the 60 cm aperture f/15 Cassegrain ISO telescope resembled that of IRAS but the short and long wavelength spectrometers, the camera and the photometer were tailored for pointed observations, not a survey. The ISO mid-infrared camera had about 20 times better sensitivity and spatial resolution than IRAS for comparable observing parameters. ISO routine operations began on 4 February 1996 and the cryogen lasted until 8 April 1998. An additional 150 hours of near-infrared spectral observations were obtained before the satellite was turned off six weeks later. A total of about 31,000 individual observations were made with approximately equal observing time allocated to each of the four instruments. The capability and scientific versatility of this observatory was unmatched until the Spitzer telescope became operational in 2004.

The Spitzer infrared telescope facility had about twice the collecting area of ISO, was much more sensitive and had better spatial resolution. The larger format imaging arrays could map a given area much more efficiently and they included the 20 μm region that was missing on ISO due to a malfunction in the ISO photometer. On the other hand, the spectral resolution of the ISO spectrometers was superior to that of Spitzer, at least for the brightest stars, and covered the near infrared (2.4 – 6 μm) where many of the diagnostic stellar molecular bands lie. Thus, the two observatories were complementary with ISO observing the brighter sources in the sky while Spitzer obtained definitive measurements on a larger population of fainter sources. Spitzer was launched at the end of August 2003 and the super-fluid helium lasted until May 2009. The two near-infrared cameras currently obtain images during the on-going warm mission.

With the 1995 IRTS success, ISAS approved a much larger and more complex infrared astronomy mission, the Infrared Imaging Surveyor (IRIS) as the 21st ISAS science mission, ASTRO-F, in fiscal year 1997. Funding for developing and prototyping was approved at about the time ISAS successfully flew their first M-V launch vehicle. The M-V had about three times the payload capacity as the HII rocket that launched IRTS, which was necessary for the larger IRIS payload (Murakami, 1998). ASTRO-F, renamed Akari with successful on orbit operations, was launched on 21 February 2006 and carried an f/6 Ritchey-Chretien telescope with a 68.5 cm primary mirror. A near-infrared array and two mid-infrared arrays obtained nearly diffraction limited images in various filters between 1.9 and 26 μm . The far-infrared instruments extend to 200 μm . Akari also had a spectral capability that spanned the near- to far-infrared. During the first six months, mission priority was given to a mid- and far-infrared sky survey at considerably higher resolution and sensitivity than IRAS. The next 10 months of the cryogen mission were devoted to filling in the survey gaps and conducting observatory type observations. A post-cryogen mission was initiated after the super-fluid helium ran out in August 2007.

ISO and the Spitzer Space Telescope are concisely described in this chapter since they are well documented with extensive reference material posted on the internet. NASA also provided interim products so that the community doesn't wait years for the final results to become available and there are lengthy descriptions of Spitzer that do justice to the history and scale of the projects. Although the Akari instrumentation and general flight performance is documented, the data are slow to be released.

The Chapter concludes with a brief description of the WISE which is scheduled for an end of 2009 flight and SOFIA, which is soon to be on-line. Mention is also made of the next generation of observatories, Webb the telescope and SPICA.



10.1. The Infrared Space Observatory (ISO)

The Infrared Space Observatory (ISO) was initially proposed to the European Space Agency (ESA) in 1979. After a couple of years of Phase-A study (e.g. Emery, 1982), ESA funded ISO as a new start in 1983. ISO's astronomical objectives were similar to those of the shuttle-based German Infrared Laboratory to obtain 2.5 – 200 μm observations with a camera, grating spectrometer, Michelson interferometer and photopolarimeter with a 50 cm telescope (Lemke et al., 1985). However, the ISO design called for an IRAS sized optical system with a much longer cryogen lifetime. The telescope used an f/15 Ritchey-Chretien optics with a 60 cm aperture primary mirror and four

focal plane instruments: two scanning grating spectrometers that covered 2.4 to 200 μm , a near-to mid-infrared camera and a mid- to far-infrared photometer. The focal plane instrument teams were selected in 1985 from the submissions to the call for proposals a year earlier. The system was cooled by 2300 liters of super-fluid helium in a cryotank built by the same DASA team that constructed the 300 liter GIRL cryostat (Seidel and Passvogel, 1994).

The 2.3 ton, 5.3 m tall spacecraft was launched on an Arianne IV rocket on 17 November 1995 into a 24 hour, highly elliptical 70,600 km (apogee) \times 1000 km (perigee) orbit. Mission science operations began in February 1996 after a two month post-launch satellite check-out and sensor performance validation and more than 30,000 astronomical observations were made during the mission. The cryogen ran out in April 1997 but post mission operations continued for another month to obtain near-infrared spectroscopy. ISO also made another \sim 120,000 observations for calibration purposes, in the parallel mode and during the serendipitous survey. In the parallel mode, the camera and long wavelength spectrometer obtained measurements of whatever was within their fields while the primary observation was taken by another instrument; the far-infrared serendipity survey was conducted by the photometer and long wavelength spectrometer while the spacecraft was slued between primary targets.

The ISO program is extensively documented in The ISO Handbook (ESA SP-162): Volume I describes the ISO satellite, mission and operations (Kessler et al., 2003), Volume II details the camera, the operating modes and data processing (Blommaert et al., 2003), Volume III has similar information for the 43 – 197 μm long wavelength spectrometer (Gry et al., 2002), Volume IV describes the photometer (Laureijs et al., 2003) while the 2.4 – 44 μm Short Wavelength Spectrometer (SWS) is described in Volume V (Leech et al., 2003).

Given the success of IRAS, one might have expected a similar international cooperation between NASA and ESA on ISO, but such was not the case. Leverington (2000) provides the broad context with a European view: The International Solar Polar Mission (ISPM) “*...affair had a fundamental effect on ESA-NASA relations, so that when in 1983, for example, NASA tried to pressure ESA to merge ESA's proposed Infrared Space Observatory (ISO) with the similar NASA SIRTF programme, the suggestion was roundly rebuffed.*” The ISPM eventually became Ulysses but only after a number of unilateral decisions by NASA that rejected the electronic propulsion proposed by ESA, delayed the launch date from 1983 to 1985 and changed the name, among other things; all of which the Europeans found provocative. Later, the possibility of NASA providing instrument/detector upgrades to ISO was discussed at the ISO dedicated time meeting at Schloss Elmau in November 1990, but the US export control restrictions was too

onerous for ESA to accept. Such a discussion would have occurred in a rather strained context as ESA and NASA had previously explored cooperation with regard to the focal plane instruments. The ISO instruments had been selected in March 1985, about 10 months after the SIRTF instruments. However, as George Rieke (2006) noted: “*The ISO detectors were a couple of generations behind SIRTF*” and further observed that: “*NASA felt that ISO would be inferior to SIRTF, and the Europeans resented the condescension.* Consequently, “*(n)egotiations between ESA and NASA became increasingly rancorous ...*” in the mid-1980s.

Eventually, NASA and ESA did cooperate to increase the observational duty cycle. Despite having a 24 hour period, the ISO orbit was not geostationary because of its high eccentricity. Initially, ESA selected a semi-synchronous (12 hour) orbit and provided for two ground stations but the orbit was changed in 1987 to minimize exposure to the Earth’s radiation belts; the second ground station was sacrificed to the cost of the dedicated Arianne rocket required to achieve the chosen orbit (Davies, 1997). Thus, a second ground station was needed for operations while the satellite was below the horizon of the VILSPA receiving station in Spain and funds were needed for an additional VILSPA shift to handle the relayed data. In a typical orbital duty cycle, ISO was turned off for perigee passage when the detectors would have been rendered useless due to the Earth’s particle radiation environment. Then the satellite and instruments were reactivated to begin observations about four hours after perigee. Data acquisition continued for approximately 16 hours before everything was shut down for next perigee pass. NASA provided the Goldstone facilities but the Japanese space agency (ISAS) provided the funds. In return NASA and ISAS were given about 10% of the observing time on the satellite. The US objectives for ISO were announced at the end of a March 1991 meeting at Caltech to support the broad science goals in favor at NASA at the time: namely to observe young stellar objects and ultraluminous and active galactic nuclei.

10.1.1. Phillips Laboratory Connection

The Phillips Lab contributed to the ISO mission in several ways. We played a small but key role in recovering the performance in the 15 – 29 μm detector module of the spectrometer, contributed several observing programs and participated in others. Our ISO participation was an outgrowth of our SRON collaboration to improve and extract information from the IRAS data, which led to my appointment to the Dutch-German Short Wavelength Spectrometer (SWS) team in 1988 by Thijs deGraauw, the consortium leader. Although my participation was limited by distance, AFGL was able to make valuable contributions.

We submitted two dedicated time proposals to the SWS principal investigator. One, the Selected Area Galactic Plane Survey or GPSurvey, imaged fields at various positions in the Galactic plane. The ISO camera operated as a secondary instrument in a parallel mode when measurements with other instruments were primary. In the original proposal these ‘free’ images would be taken as a matter of course when another instrument observed in or near the Galactic plane and the proposed allocated time would be for re-imaging these fields in another infrared spectral band. The parallel mode images proved difficult to calibrate but, fortunately, enough time, ~ 14 hours, was given to this proposal that six areas could be imaged and analyzed without recourse to the parallel mode observations. Burgdorf et al. (2000) processed the data on the 11.5’ \times 11.5’ images and extracted source counts from which they noted differences between the observed source density distribution and SKY 5 model predictions for the field that probed the Galactic bulge. Figure 109 shows an MSX Band A image on the left from the raster scan

MSX CB03 (A)

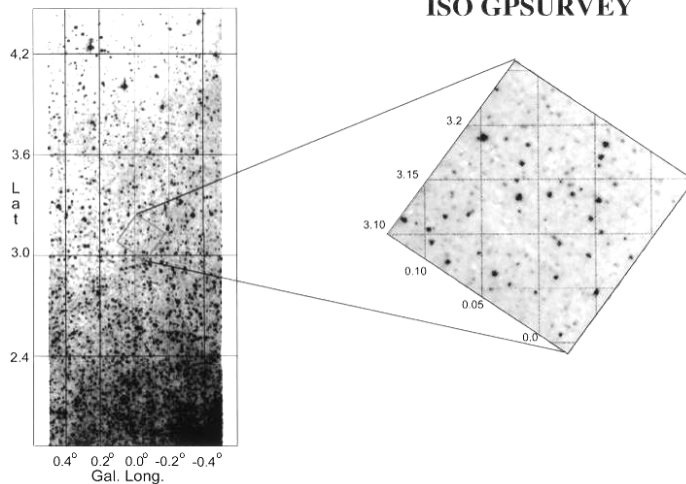


Figure 109. MSX raster scanned observations in the Galactic bulge (left) and an ISOCam image within the MSX field. The stars in the two fields do not map one for one because the MSX 6.8 – 10.8 μm Band A preferentially detects redder sources than the ISOCam LW2 (5.0–8.5 μm) Band.

($\sim 3500 \text{ deg}^2$) to a Band A completeness level of $\sim 150 \text{ mJy}$ compared to 250 hours for ISOCam to map approximately 16 deg^2 to about 10 mJy . A graphical example of this contrast is shown in Figure 110 in which the top image co-adds the results from five Band A Galactic plane scans of the $(\Delta l \times \Delta b) \sim 0.2^\circ \times 1^\circ$ field at $(l \times b) \sim (315^\circ, 0^\circ)$ that was observed at $6.7 \mu\text{m}$ by the ISO camera during the checkout phase of the mission (bottom image). Although the ISO image obviously has better spatial resolution and sensitivity, it took over an hour to acquire in one spectral band with a single pointing integration time of 21 seconds. The five MSX scans over the area took a total of 8 seconds to acquire with a consequent 1.6 second integration time per image point in each of four spectral bands. Perhaps a more appropriate comparison would be with the MSX raster scans, e.g. Figures 89, 94, 109 and 118, that covered $\sim 30 \text{ deg}^2$ along the Galactic plane with an effective integration time of 20 seconds per pixel. The $8.3 \mu\text{m}$ flux limit of these raster scanned images was $\sim 30 \text{ mJy}$, about three that of ISOGal, albeit confusion degraded the limit to $\sim 200 \text{ mJy}$ in the inner plane. Price and Omont (2004) highlighted the scientific results from ISOGal and the MSX Galactic plane surveys and how in their respective area covered, sensitivity and dynamic range complement each other.

As a consequence of the impact IRAS has had on infrared astronomy, most infrared space experiments compare their performance against the IRAS baseline. Thus, a word on these comparisons is in order. Although the chapter introduction states that ISO had about 20 times better sensitivity and resolution than IRAS, Kessler et al. (2003) claimed in *The ISO Handbook* that ISO was 1000 times more sensitive and had 100 times higher resolution than IRAS. The difference is that the first estimate is for comparable system measurement conditions, such as integration time, while the second uses parameters that maximize the contrast in sensitivity and resolution with very long integration times and using the smallest camera pixels at wavelengths shorter than used by IRAS. The performance differences could be expressed in terms of inherent system capabilities. Since the IRAS and ISO telescopes were of comparable size, normalizing to

observation above the Galactic center which contains the ISO LW2 ($6.7 \mu\text{m}$) GPSURVEY field on the right.

We also participated on Alain Omont's ISOCam survey of the Inner Galaxy, ISOGal for short, that he proposed for the spring of 1994 call for open time proposals; I had decided not intend to bid for open time to expand upon the GPSurvey observations because I felt that the ISO and camera observing limitations made such a survey rather inefficient. I thought it better to cover the entire Galactic plane with MSX, which was tailor-made for surveying, then use the ISOCAM point and stare observations to extend the statistical results from MSX to fainter levels. To put this in perspective, it took MSX 35 hours to cover the entire Galactic plane within $\pm 5^\circ$ latitude

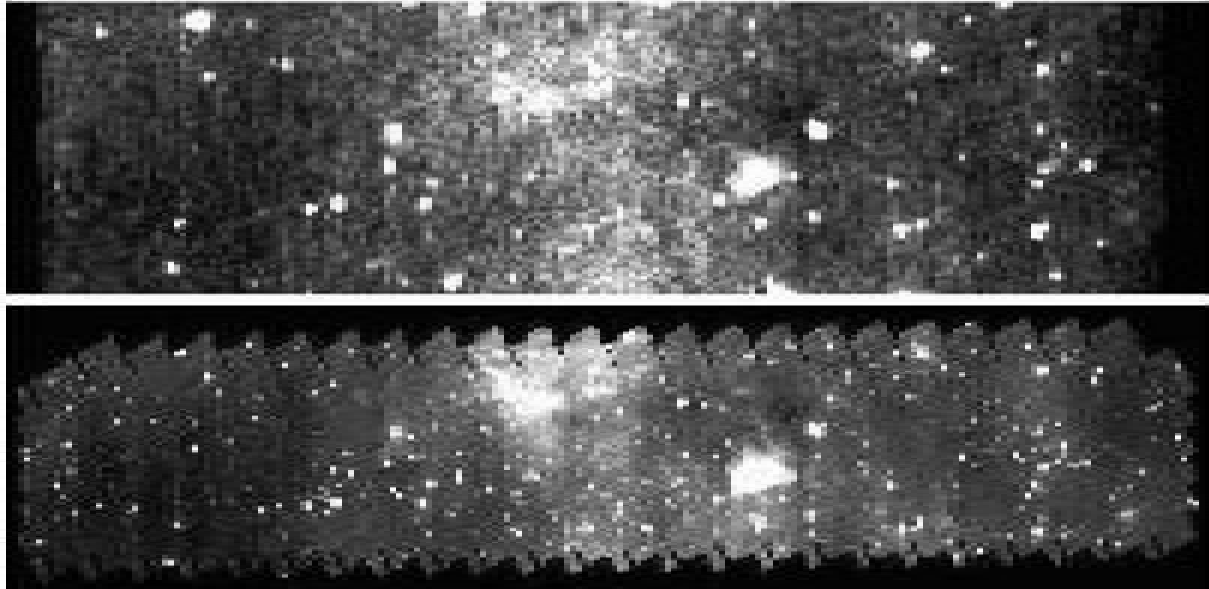


Figure 110. MSX and ISOGAL ($\Delta l, \Delta b$) $\sim 0.2^\circ \times 1^\circ$ infrared images centered at $(l, b) \sim (315^\circ, 0.0^\circ)$. The MSX $8.3 \mu\text{m}$ full resolution image at $6''$ grid spacing is shown at top, the ISO Camera $6.7 \mu\text{m}$ image with $6''$ pixels, three times smaller than those on MSX, is below.

unit integration time would result in the major sensitivity difference being due to the inherent sensitivity of the detectors, which is only about a factor of five. Rather than comparing the ISO performance with the IRAS all sky survey, which had a 0.2 second integration time, a more appropriate performance comparison would be based on comparable observing conditions such as the IRAS Additional Observation macro H mode would be more apt. This macro, which had a total integration time of about 12 seconds and covered $\sim 140 \text{ deg}^2$ of sky, comes closer to the 21 seconds effective integration time used for the ISOGal survey and the $\sim 16 \text{ deg}^2$ surveyed.

Kleinmann et al (1986) estimated that the $12 \mu\text{m}$ flux limit at 50 mJy for this macro, which is ~ 20 times brighter than the ISO camera operating in the analogous IRAS band. However, it is legitimate to compare sensors where other factors limit their system performance such as confusion as long as that restriction is specified. Thus, ISOGal is, indeed, 1000 times more sensitive than IRAS in the inner Galactic plane where confusion dominates. On the other hand, the ISOGal $6.7 \mu\text{m}$ band is ~ 10 times more sensitive than the Egan et al. (2003) MSX Band A survey catalog. The flux limit of the catalog and, as noted above, that of the more sensitive raster scans is set by confusion in the inner Galaxy.

How does one compare the resolution of the rectangular IRAS or HI STAR detectors with the MSX square pixels or those in the ISO and Spitzer cameras? Resolution is usually defined as the ability to separate two closely spaced point sources, so the resolution of systems with rectangular detectors would be aspect dependent. An appropriate measure might be the ratio of the square root of the solid angles of the system response functions. The resolution for a diffraction limited system or one with a quasi-Gaussian response profile, such as MSX, scales as the square root of the solid angle of the beam with a proportionality factor of about 0.6. The beam size for a diffraction limited system is $(\lambda/D)^2$, where λ is the wavelength and D is the diameter of the primary mirror. The diffraction value is added to the solid angle subtended by the detector and the resolution is proportional to the square root of this sum. Thus, the best LW2 ISO Cam resolution using the smallest $1.5''$ pixels results in a factor of 40 improvement over

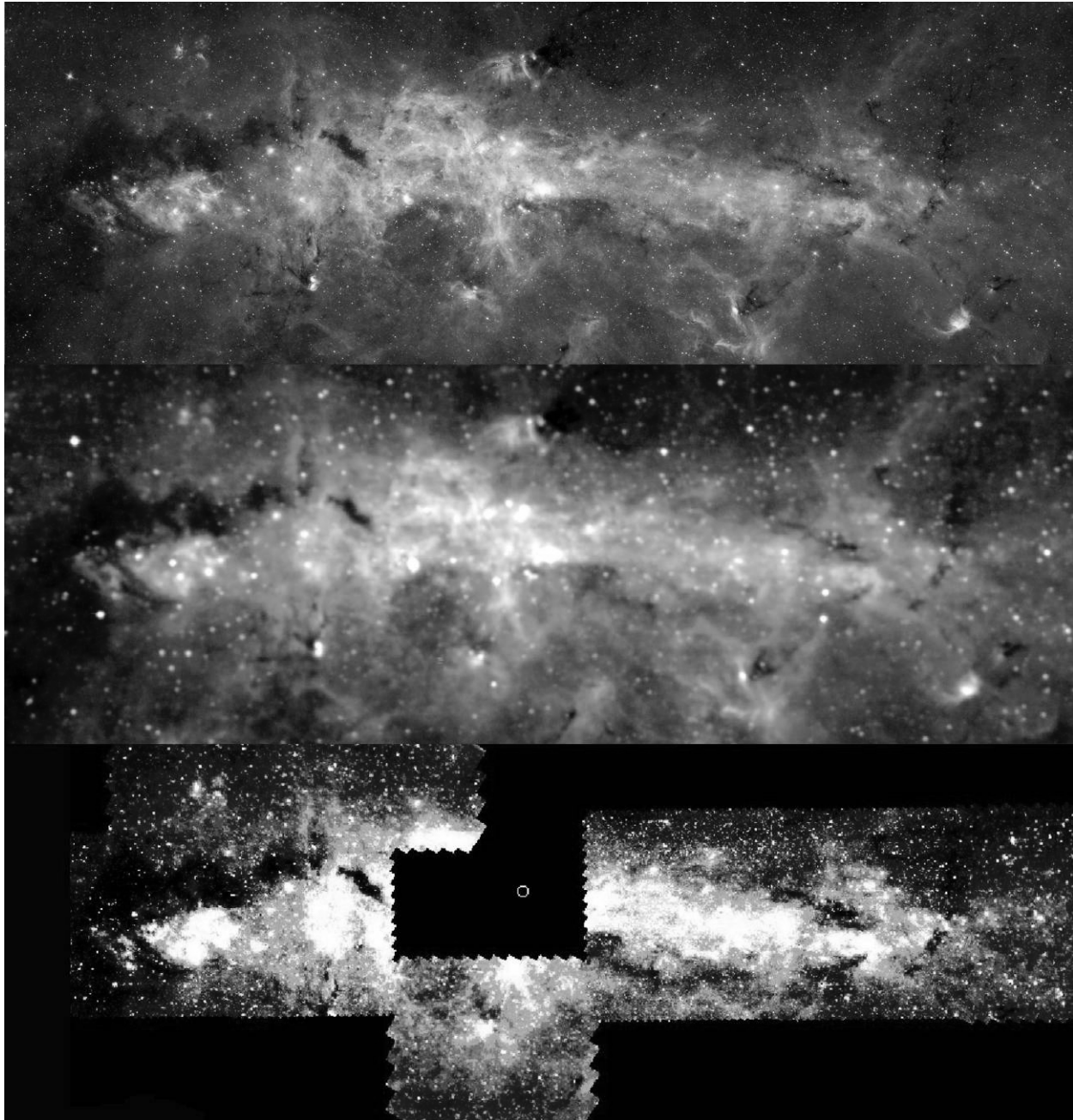


Figure 111. The Galactic center at $\sim 8 \mu\text{m}$ from Spitzer (top), MSX (middle) and ISO (bottom). These images highlight the spatial resolutions of the different instruments. The Spitzer image is courtesy of NASA/JPL-Caltech, the ISO image courtesy of ESA/ISO and the ISOGal team.

IRAS. The improvement is reduced to a factor of 20 with the $6''$ pixels that were used to cover the maximum area in a given time. With $6''$ pixels, ISO had 3.5 times better resolution than MSX, which is graphically illustrated in Figures 110 and 111; Figure 111 compares images of the Galactic center from Spitzer, MSX and ISO.

The Air Force supported our participation in ISO and, thus, there had to be a demonstrable return for the participation (as specified in the Mansfield amendment!). In this light, the GPSurvey and ISOGal experiments provided validation at fainter infrared fluxes for the SKY model used for background characterization. However, Paul Wesselius pointed out that it

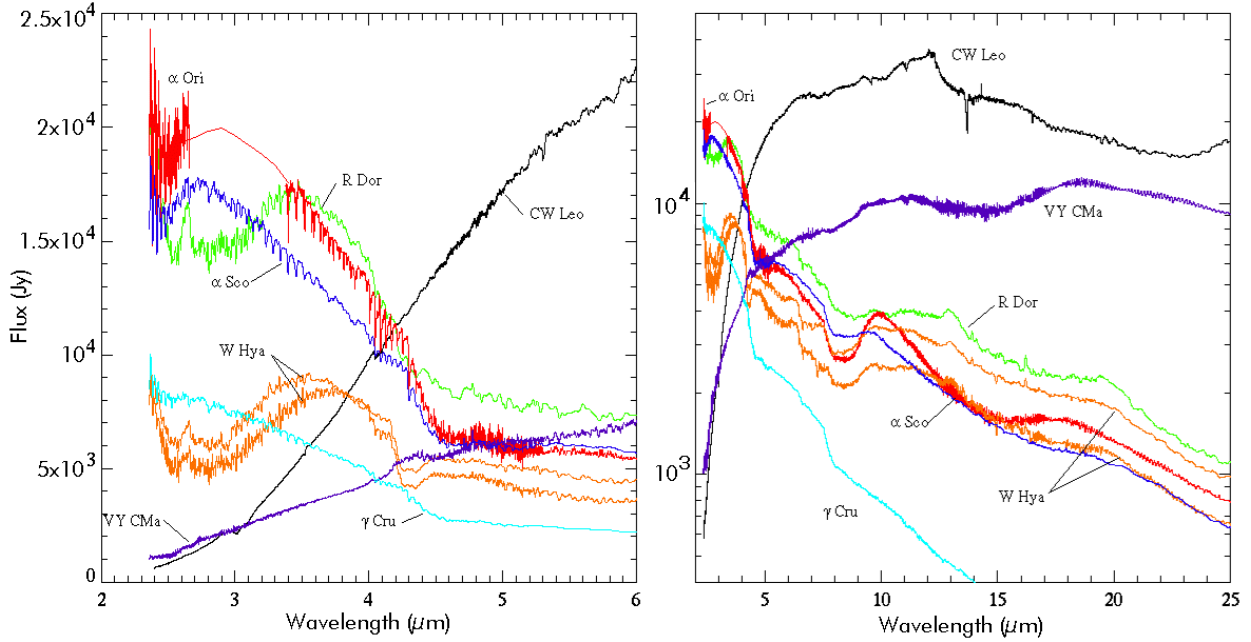


Figure 112. A sample of ISO SWS spectra of the brightest infrared sources. The plot at left highlights the near-infrared molecular absorption in the stars while sources with mid-infrared circumstellar shell emission are shown on the right. A low resolution spectral template has been substituted for the saturated ISO near infrared spectrum of α Ori.

would be appropriate for an SWS co-Investigator to come up with a dedicated time proposal that observed with the team's instrument. The result was the Spectral Characterization of Bright Celestial Sources, or StarType proposal, to improve upon the AFGL analysis of the IRAS LRS spectra (Little-Marenin, 1988; Little-Marenin and Little, 1988, 1990; Sloan and Price, 1995). The idea was accepted and I assembled a team to flesh out the details at the November 1989 and 1990 Schloss Elmau meetings held to discuss the dedicated time experiments. Agreement on the observing list was somewhat contentious as some on the team consistently wandered away from the main objective of observing a large enough variety of objects to be able to classify them. Helen Walker, from Rutherford-Appleton Lab, was of immense help in keeping attention focused on the objectives and creating the observing list.

This proposal was given 23 hours of dedicated observing time and an additional 9½ hours of open time. This wasn't nearly enough to sample the full range of known objects with different spectral characteristics. Consequently, we allocated the majority of the observations to measuring spectra of the mundane or ordinary sources and rather sparsely sampled the more exotic objects with the anticipation that the latter would be observed by other experimenters for astrophysical reasons and we would incorporate their results in due course. Figure 112 samples the variety of bright stars with SWS infrared spectra. Except for γ Cru, our brightest infrared calibration standard, and the carbon star CW Leo, the stars show excesses at ~ 10 μ m and 18 μ m indicative of silicate emission from circumstellar dust. The carbon rich circumstellar shell of CW Leo is revealed by its infrared spectral features, α Ori and α Sco are oxygen rich supergiant stars, while W Hya and R Dor are giant variable stars; spectra for W Hya are shown at different times in its light curve.

Our ISO dedicated time experiment used the SWS to extend the wavelength coverage on a subset of ~ 400 stars observed by the IRAS LRS with much higher spectral resolution. Sloan et

al. (2003) uniformly reduced the 1271 SWS spectra that were ultimately considered in the analyses for the objectives of this experiment while Kraemer, Sloan, et al. (2002) classified the 840 or so individual objects by the overall shapes of their infrared spectral energy distributions. Heras et al. (2002) and Engelke, Price and Kraemer (2006) did a more conventional analysis by correlating the infrared molecular features in the stellar photosphere with the optically based MK spectral sequence. Hodge et al. (2004) and Engelke, Kraemer and Price (2004) did a similar reduction and classification for the ISO spectrophotometer and circular variable filter observations, respectively. Once a classification scheme was established it was planned, but not realized, to use the results to refine the population analysis in the SKY model. Instead, Engelke, Price and Kraemer (2006) used the Sloan et al. spectra to improve the spectral resolution of the Cohen et al. (1999) secondary and tertiary calibration standards.

Early in the process of rationalizing the SWS spectra, we discovered that the hot stars, Sirius and Vega in particular, displayed 4.5 and 8 μm excesses, the latter wavelength regime being complicated by rather low signal-to-noise for these stars. We concluded that this had to be a reflex of an overcorrection of the CO and SiO bands in the modeled spectra for the cooler and much brighter stars that were used for calibrating the SWS. We sent a draft of a paper (Price, Kraemer and Sloan, 2002) to Thijs deGraauw, the SWS PI, for comment. Thijs directed that the SWS processing be modified to correct for these artifacts but requested that we not submit the paper. The draft had been written in late summer of 2001 and was held up when AFRL suspended the public affairs approval process for two months after 9/11. This gave us plenty of time to ponder what to do: to publish and let those who had analyzed flawed SWS spectra know of the problem or consider the corrections as an AFRL internal contribution to the SWS data processing. In the end, we decided to inform the user community that there were problems with early versions of the SWS calibration because of earlier analogous misinterpretations of the IRAS LRS data. The original IRAS LRS calibration assumed that the K5 giant α Tau ($T_{\text{eff}} \sim 3900$ K) radiated as a 10,000 K blackbody. Consequently, an excess of emission was calibrated into the LRS spectra. Volk and Cohen (1989) noticed this excess in the 8 μm SiO fundamental band in hot stars and derived a calibration correction. However, Vardya, de Jong and Willems (1986) assumed that what they observed for very cool Mira variable stars real and speculated as to why such emission should exist.

The ISO spectral analysis was the culmination of the AFGL infrared stellar calibration effort sponsored by SDIO that began in the mid-1980s to determine the absolute flux of the astronomical zero infrared magnitude scale, to create absolute calibration spectra for primary and secondary stars that may be used to derive the absolute stellar fluxes in any defined spectral band and to transfer the calibration to a large set of tertiary standards that then may be used for ‘calibration-on-the-fly’. The density of the tertiary stars is large enough that it is likely that the field-of-regard of a surveillance sensor would cross one of them as the system scanned across the sky (hence, calibration-on-the-fly) or the sensor would require only a few degrees of pointing displacement to measure a calibration star. AFGL funded Martin Cohen and his colleagues to establish the network. Cohen et al. (1992) used a modeled spectral energy distribution for α Lyr to tie the measured absolute visual flux recommended by Hayes (1985) to the absolute infrared flux of this primary standard star. They then derived the absolute spectrum of their second primary standard, α CMa, by scaling this calibration to a modeled energy distribution through accurate photometric reference to α Lyr. As the next step, Cohen, Walker and Witteborn (1992) created a calibrated infrared spectrum of the infrared standard, α Tau, by photometric scaling the spectral measurements on α Tau referenced to photometry between α Tau and the primary

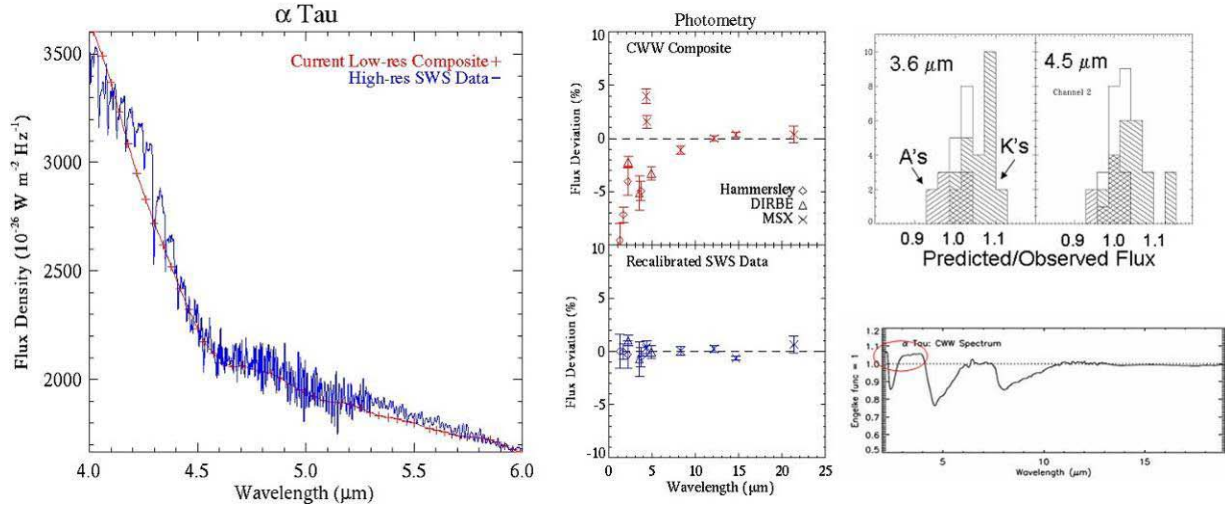


Figure 113. Calibration results. The Cohen et al. calibrated spectrum of α Tau is compared to the much higher resolution SWS spectrum in the region of the CO fundamental and SiO overtone absorption. The center plots show the improvement of the current α Tau calibration over that of Cohen et al., which is widely used. The errors in the top plot are due to an overestimate in the near-infrared portion of the Cohen et al. calibrated spectrum, which is also seen in the plot at the lower right. The Spitzer camera team found a systematic separation of the warm calibration A stars from the cooler K stars, shown by the cross hatched areas in the figure at the upper right, which is corrected by the current calibration (lines without cross hatching).

standards. Cohen et al. (1995) added six secondary standard stars with 1.2 to 35 μ m calibrated spectra to the list and Cohen et al. (1996) did the same for three secondary standards in the southern hemisphere. For calibration-on-the-fly, Cohen et al. (1999) created a network of 422 uniformly distributed fainter tertiary calibration stars. The representative spectrum for each spectral type was created from the secondary standards and the appropriate spectral template was assigned to the network star according to its spectral type after accounting for interstellar extinction, if needed. The number of stars in the network was subsequently increased to 617 (Walker and Cohen, 2003).

Cohen et al. (2001) then transferred the accurate calibration of the SPIRIT III radiometer to \sim 35 stellar secondary standards. These observations were subsequently reprocessed and combined with the results of 192 averaged stellar irradiances from the 89 Data Certification stellar calibration experiments from which Price et al. (2004a, b) derived accurate photometric differences between the primary and secondary standard stars in the MSX spectral bands. Price et al. then established a direct absolute calibration by referencing this photometric system to the absolute fluxes measured from five well quantified reference spheres episodically released during the mission. This was the first direct stellar infrared calibration in 20 years and the most accurate. Price (2005) places the Cohen et al. analysis and the MSX calibration in the context of other efforts and discusses the physical consequences of the results. Rieke et al. (2008) incorporated the MSX results in their calibration of the absolute spectral flux scale.

Engelke, Price and Kraemer (2006) then created calibrated spectra at higher spectral resolution and absolute accuracy by scaling the ISO SWS spectral segments to the MSX absolute radiometry of standard stars and the corrected DIRBE photometry (Smith, Price and Baker, 2004). The left hand plot in Figure 113 demonstrates the very large improvement in the SWS resolution for α Tau with respect to the Cohen et al. calibrated spectrum. The SWS 4 – 6 μ m spectrum of α Tau, that encompass the CO fundamental and SiO overtone absorption features,

compared to the much lower resolution absolute spectrum of Cohen, Walker and Witteborn (1992) that was widely used as an absolute calibration reference. The middle panels show the improvement for α Tau photometry. The top image compares selected infrared photometry referenced to that predicted from the Cohen, Walker and Witteborn normalized absolute spectrum (dashed horizontal line). The photometry compared to AFGL higher resolution recalibrated α Tau spectrum is a much better fit. That the Cohen et al. near-infrared calibration is too high may be seen in the spectrum in the bottom right, a fact that was reflected in the Spitzer camera calibration (Reach et al., 2005). The cooler K calibration stars used by Reach et al. deviated from prediction as seen in the top of this image, while the new AFRL calibrations eliminates the errors.

Very bright celestial reference sources were required to calibrate the upper dynamic range of sensors that observe against the Earth. Although most of the brightest stars are known variables, AFGL had Walker et al. (2004) create ‘calibrated’ spectra for the best of them as a resource of last resort. Walker and Cohen adopted the appropriate Sloan et al. (2003) rationalized SWS spectra for the spectral content of these bright stars and estimated the uncertainty in using them for calibration when the variability is included in the calibration. This variability estimate will be significantly improved with the DIRBE warm era light curves.

10.1.2. ISO Zodiacal Measurements

ISO improved upon the very small zodiacal spectral database that previously existed. Briotta (1976; Briotta, Pipher and Houck, 1976) flew a mid-infrared spectrophotometric experiment in 1975 and a Japanese team flew three rocket experiments in the late 1980 to early 1990s that obtained near-infrared 1 – 5 μm zodiacal spectra (Matsuura et al., 1994). The Japanese observations are particularly interesting as they spanned the spectral transition in the zodiacal brightness from reflected sunlight to thermal emission. Unfortunately, these observations were rendered uncertain to some degree by effluvia from the rocket/payload and/or residual atmosphere above the payload. Contamination-free observations from space were reported by Matsumoto et al. (1996) who derived a 1.4 – 4 μm spectrum by averaging \sim 1100 observations taken over five days. Ootsubo et al. (1998, 2000) similarly averaged the 4.5 – 11.7 μm data but only over two days. In combination, these data provide a nice snapshot of large scale spatially averaged zodiacal spectra.

Reach et al. (1996, 2003) published 7 – 16 μm zodiacal spectra, obtained with the ISOCam circular variable filter over a wide range of latitudes and Sun centered longitudes with which they probed the chemical composition of the dust and the particle size distribution while Leinert et al (2002) analyzed the 6 – 11.7 μm ISOPhot spectrophotometry. The Reach et al. observations show a 5 – 7% excess between 9 – 12 μm that they attribute to a combination of silicates. These published zodiacal spectra are a minority of those in the ISO database that are available for study; Hodge et al. (2004) estimated that there are several hundred additional ISOPhot spectra while Engelke, Kraemer and Price (2004) place the number of additional CVF spectra at \sim 50.

Far fewer ISO photometric observations have been analyzed. Ábrahám, Leinert and Lemke (1997) looked for but did not find fluctuation in the 25 μm photometry in five fields in a search for granularity in the zodiacal cloud while Holmes and Dermott (2000) monitored the infrared variation in the brightness at the ecliptic poles during a 50 day period. Tedesco and Désert (2000) derived the zodiacal brightness for several fields as a by-product to their principal

effort of extracting asteroid observations. The ISO archive contains many more such photometric observations (e.g. Holmes and Dermott, 2000).

10.1.3. Brief Summary of Other ISO Results

ISO results have been the topic of fifteen workshops, conferences and meetings between 1996 and 2007 (<http://www.iso.esac.esa.int/meetings/>). Volume 119 of Space Science Reviews (2005) has a number of articles written mainly by younger scientists participating in the ISO project that summarily review the major ISO scientific achievements. I note the two most significant results: the spectroscopic discoveries and a deep probe of the universe.

The good sensitivity, the wide 2.4 – 200 μm wavelength range and high ($\lambda/\Delta\lambda \sim 1000$) spectral resolution of the ISO spectrometers produced a number of discoveries and much improved definitions of previous observed spectral features. ISO spectroscopy permitted, for the first time, unambiguous identification of crystalline silicates outside the solar system. Crystalline silicates had been tentatively identified in the IRAS LRS spectra of circumstellar dust around of oxygen rich Mira variable stars (e.g. Little-Marenin and Little, 1990) but ISO spectroscopy at wavelengths longer than the 23 μm cutoff of the LRS was required to secure the identification. According to Molster and Kemper (2005), ISO found crystalline silicate in AGB outflows, young stellar objects and some circumstellar discs but not in the interstellar medium because of radiation damage in that environment. Water was also found in a large variety of environments (Chernicharo and Crovisier, 2006) and Dartois (2005) provide a line list of various ices observed by ISO in dust shells, molecular clouds and the interstellar medium.

The European Large Area ISO Survey (ELIAS) deserves mention if for no other reason than the fact that the 375 hours of observing time assigned to this project was more than any other experiment. ELIAS conducted a very deep survey of approximately 6 deg^2 of the sky at 6.7, 15, 90, and 170 μm . Oliver and Pozzi (2005) review the principal results, namely that strong star formation in the early galaxies is needed to account for the excess infrared emission over predictions from visible observations and that significant galactic evolution was necessary to reconcile the observations at the two wavelength regimes.

10.2. SPITZER Space Telescope



Arthur Code (1960) gave an early passing reference to a satellite based infrared observatory to conduct systematic infrared spectral and photometric measurements of known objects in his presentation at a conference on astronomy outside the atmosphere that was chaired by Lyman Spitzer. However, as Augason and Spinrad (1965) noted a few years later, a considerable amount of improvement in ground-based infrared astronomy was needed before space applications could be attempted. The technology rapidly matured and the 1970s National Academy of Science's decadal study advanced the idea for a space-based infrared observatory while the June 1973 National Academy of Sciences (1974) conference chaired by Bill Hoffman at Woods Hole, Massachusetts considered Shuttle based experiments that included an infrared observatory. Werner (2006) cites an unpublished manuscript by Witteborn and Manning in which they described the initial plans for a far-infrared telescope for a shuttle sortie configuration that were drawn up and submitted to NASA by the Ames Research Center (ARC) in 1971. NASA Ames was the lead center for infrared astronomy in the 1970s although Mike Hauser's group at Goddard Space Flight Center (GFSC) did have an active program of far-infrared and

sub-millimeter balloon borne measurements (e.g. Silverberg et al.; 1979). The Kuiper Airborne Infrared Observatory (Bader and Witteborn, 1972) was based at Moffett Field and Ames Research Center was given the program management responsibility for the IRAS instrument development. It was natural that ARC also be the lead center to develop an infrared space observatory.

Ames contracted with Hughes Aircraft Co. in the mid-1970s to develop the conceptual design for the telescope system. The Hughes study was concluded in 1975 (McCarthy, Young and Witteborn, 1975) and was followed by a more complete exposition of the preliminary design (Witteborn and Young, 1976). Simpson and Witteborn (1977) then discussed the effects that shuttle induced contamination might have on observations with an infrared telescope. In 1978 ARC subsequently began a technology development program for infrared detectors headed by Craig McCreight while Ramsey Melugin led the cryogenic telescope component program.

A major milestone in the SIRTF program was the selection of the three instrument teams in 1984 and the formation of a science working group as the steering committee. Five years later, in 1989, program management was transferred to JPL. Werner (2006) gives a brief, personal history of SIRTF while Rieke (2006) provides more details on the technical development of the instrument as well as on the management and program politics. During the more than 30 years from inception to flight, SIRTF evolved from a shuttle sortie mission to an Earth orbiting free-flyer to the final configuration in which the sensor was launched warm into a heliocentric Earth trailing orbit to be subsequently radiatively cooled to operating temperatures.

The Spitzer f/16 Ritchey-Chretien Cassegrain beryllium telescope has an 85 cm primary mirror. Three focal plane instruments collectively span 3.6 to 160 μm with a spectrometer, a four band near- to mid-infrared array camera, and a longer wavelength imaging photometer that can obtain images with three arrays and provides low resolution far-infrared spectra. Notable is that each of the camera and imaging photometer bands has its own array and that the only moving part in the focal plane instruments is the internal scan mirror in the imaging photometer. The infrared array camera (IRAC), described by Fazio et al. (2004), has two InSb 256 \times 256 arrays with \sim 1.22" pixels filtered for effective wavelengths of 3.6 and 4.5 μm and two similar sized Si:As BIB arrays to image at 5.8 and 8 μm . The 3.6 and 5.8 μm arrays share a common field, which is adjacent to the 4.5 and 8 μm field. Thus, the camera obtained data simultaneously in all four bands to efficiently maps large areas. The 128 \times 128 Si:As BIB array in the multi-band imaging photometer for Spitzer (MIPS – Rieke et al., 2004) has 2.5" pixels that cover a 5.4' \times 5.4' instantaneous field, which is nearly the same as the shorter wavelength array camera. A 32 \times 32 Ge:Ga array obtains images at 70 μm while a 2 \times 20 array of stressed Ge:Ga detectors provides information at 160 μm (this mode was carefully used as it increased the expenditure of helium). Of the four MIPS operating modes, the scan map configuration is used to efficiently scan the sky. In this mode, the spacecraft scans the sky at a constant rate while an internal scan mirror is used to freeze frame the image for the integration time. Four separate grating spectrographs were folded into the InfraRed Spectrograph (IRS – Houck et al., 2004). Two spectrographs have 128 \times 128 pixel Si:As BIB arrays, one for 5 – 14.5 μm spectra at a resolution ($\Delta\lambda/\lambda$) of 65 – 128 and the other for 10 – 19.6 μm spectra at $\Delta\lambda/\lambda \sim$ 600. Comparably sized Si:Sb BIB arrays, the first astronomical space application of Si:Sb BIBs, spanned 14 to 38 μm at a resolution of 65 – 128 and 19 – 37 μm at a $\Delta\lambda/\lambda \sim$ 600. Only one of these modules can be read out at a time.

The 861 kg, 4.5 m tall by 2.1 m diameter Spitzer payload was launched warm on 25 August 2003 on a Titan II rocket into a heliocentric Earth trailing orbit. A 337 liter superfluid helium dewar kept the focal plane instruments cold at launch and while the telescope reached

operating temperature after several weeks of radiative cooling. The combination of careful thermal control, radiative cooling and elimination of the thermal input from the Earth translated into a five plus year cryogen lifetime.

The SIRTF mission and instrumentation have been well documented (e.g. *SPIE Proceedings*, Volume 4850, 2003 and references therein) and summaries are given in articles published in the SIRTF announcement issue of the *Astrophysical Journal Supplement*, Volume 154, September 2004, in which Werner et al. (2004) described the telescope and mission profile. A sample of initial Spitzer results was also published in this *Astrophysical Journal Supplement* volume. Subsequently, Burgdorf et al. (2005) summarized the results from the *First Look Survey*, one of the first set of scientific observations obtained by Spitzer that included a small scale survey of the outer Galaxy, zodiacal emission and extragalactic sources. The 2006 Astronomical Society of the Pacific Conference *The Spitzer Space Telescope: New View of the Cosmos* contains later results on a broader range of research. Werner et al. (2006) reviewed the contributions Spitzer has made to our understanding of two of the defining Spitzer scientific programs: stellar evolution and the formation and evolution of planetary debris disks. The other two defining programs are the formation of galaxies in the early universe and ultra-luminous galaxies and active galactic nuclei.

Spitzer observing time was divided into three blocks: time allocated to the instrument teams and others associated with the Spitzer program, time assigned to large legacy projects while the largest amount of time was given to guest observers. The legacy projects were designed to obtain a sufficiently large database to address various specified astrophysical problems. The AFRL infrared astronomers teamed with European colleagues to propose two legacy programs: one to obtain infrared spectroscopy and imagery of a large variety of environments to study the life cycle of dust, the other to survey the inner Galactic plane. While others were given legacy programs for these topics, AFRL did obtain early guest observer time and association with a legacy program as a result of the second round of legacy proposals.

A collaboration led by Ed Churchwell, Univ. Wisconsin, won the legacy proposal to survey the region within 1° in latitude of the Galactic plane out to $\pm 65^\circ$ longitude in the four IRAC bands (Benjamin et al., 2003). GLIMPSE had about 50 times the MSX sensitivity and 5 – 7 times that of ISOGL and Akari while the spatial resolution is better by factors of about 10, 3 and 4, respectively. Approximately 30 million stars were extracted with fluxes > 2 mJy from the $10^\circ < |l| < 65^\circ$ region initially surveyed in the four bands (Benjamin et al., 2005). This survey was matched by the Spitzer MIPSGL legacy program led by Sean Carey at the Spitzer Science Center (SSC). MIPSGL surveyed roughly the same area as GLIMPSE but at 24 and 70 μm ; Shenoy et al. (2008) extracted about 3 million sources above 3 mJy flux from the MIPSGL survey. AFRL (Mizuno et al. 2008) created the 24 μm images of the inner Galactic plane and of the Galactic center observations taken by Yusef-Zadeh et al. (2009). These were delivered to the SSC in early in 2008 (Carey et al., 2009). After creating the MIPSGL 24 μm images, AFRL moved on to process the 24 μm survey measurements from the Cygnus X region legacy program (Hora et al., 2009) and selected areas in the outer Galaxy.

MIPSGL data is combined with GLIMPSE in Figures 114 and 115. The difference in sensitivity and resolution between MSX and Spitzer may be seen in Figures 111 and 114, the latter compares images of a 10° longitude strip along the Galactic plane from MSX at the top left with a Spitzer GLIMPSE plus MIPSGL mosaic in the bottom pane; both images are centered at 333° longitude. The MSX full resolution image at top right highlights a string of H II regions and provides the best comparison with Spitzer. The better spatial resolution and sensitivity of

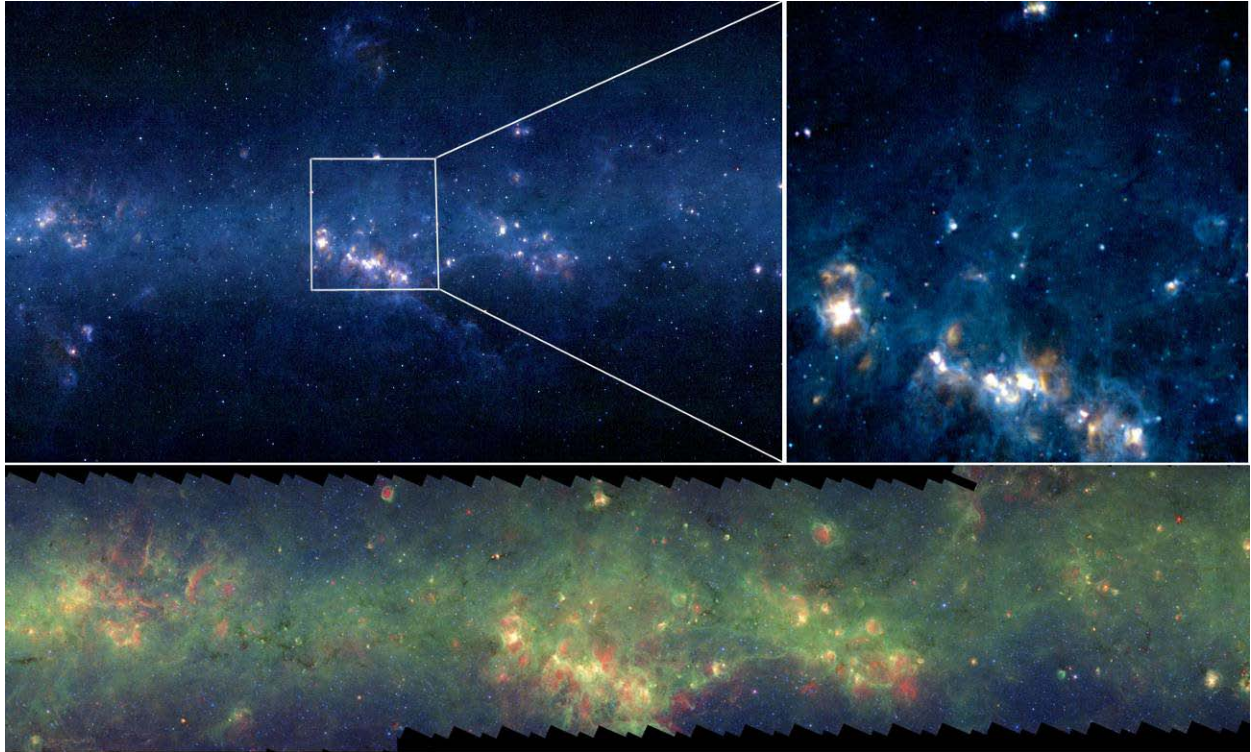


Figure 114. A section of the southern infrared Galactic plane. At top left is a $6^\circ \times 10^\circ$ MSX panorama with a $1.5^\circ \times 1.5^\circ$ full resolution image at right centered on the cluster of H II regions at $\sim 333^\circ$ longitude. The overlapping Spitzer GLIMPSE plus MIPSgal survey image at bottom is color coded: 3.6 μm (blue), 8.0 μm (green), and 24 μm (red). The Spitzer camera is much more sensitive than the MSX arrays and the spatial resolution is ten times better ($\sim 100 \times$ smaller detectors). The bright H II regions in the center of the Spitzer image are saturated at 24 μm and the 21 μm data from the MSX full resolution images were used by the Spitzer processing team to fill in the gaps. The Spitzer image is courtesy of the Spitzer Science Center.

Spitzer is apparent and the shorter wavelength 3.6 μm band detected stars to much fainter magnitudes. On the other hand, the $\pm 2.25^\circ$ latitude extent of the MSX image traces diffuse emission to higher latitudes than the $\pm 1^\circ$ GLIMPSE/MIPSgal limit. The MSX observations also provides photometry of sources well above the 1 – 2 Jy saturation levels of the Spitzer cameras that are used to ‘fill in’ for the missing Spitzer measurements (e.g. Povich et al., 2007; Yusef-Zadeh et al., 2009). Indeed, such is the case for the string of H II regions highlighted in Figure 114 that were saturated in the 24 μm images. Although Reach et al. (2005 and Rieke et al. (2008) calibrated the irradiance responses of the IRAC and the MIPS 24 μm camera, respectively, against a stellar standards, Cohen et al. (2007) and Cohen (2009) obtained absolute diffuse calibrations against MSX measurements of HII regions for the IRAC 8 μm band and the MIPS 24 μm camera, respectively. Also, since MSX observations were taken at a different epoch, they provide information on the variability of the sources (Robitaille et al., 2007).

A summary of results from the Galactic plane surveys include: Yusef-Zadeh et al. (2009) provide a nice description of the infrared morphological features in the central region of the Galactic center in their study of massive young stellar objects; Marleau et al. (2008) discovered 25 highly reddened galaxies in the GLIMPSE/MIPSgal surveys between 36° and 64° longitude; Churchwell et al. (2006) visually surveyed the GLIMPSE images and found a large number of rings and arcs between 1' and 4' in diameter that they believe are thermal bubbles in projection. They derived a density of about 1.5 objects deg^{-2} , at longitudes away from the Galactic center but

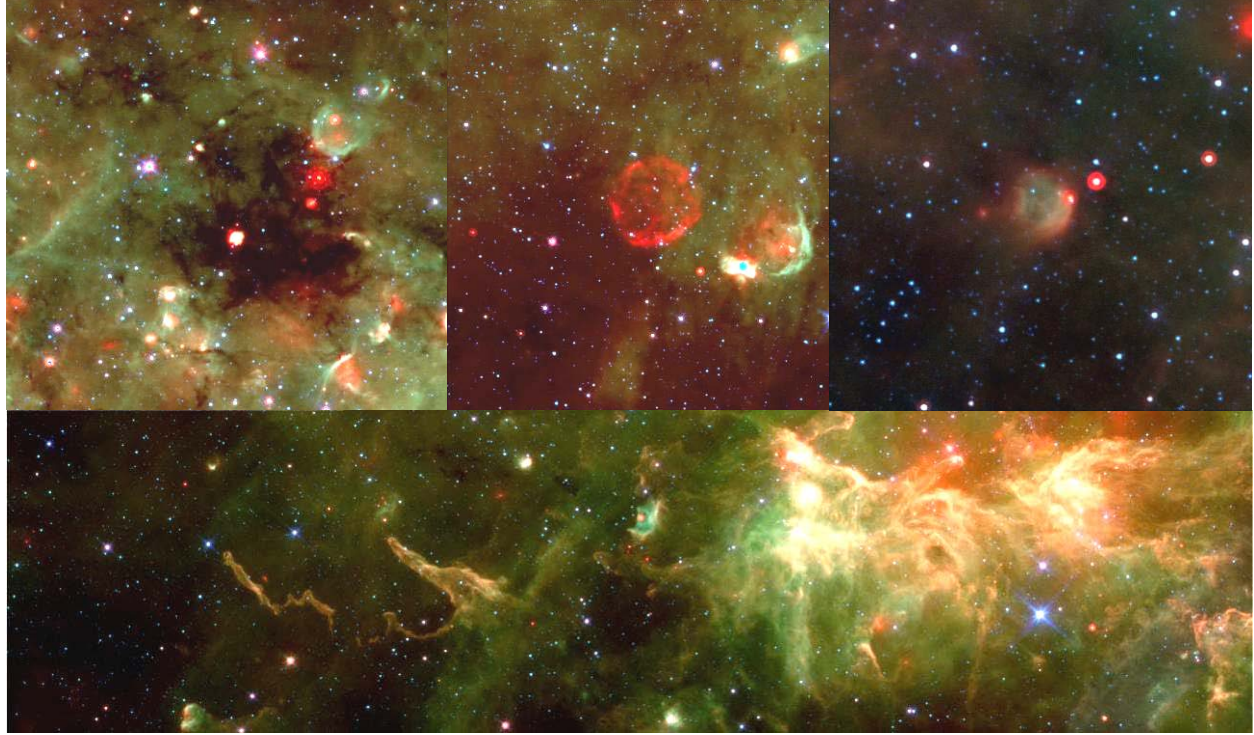


Figure 115. Selected images from the Spitzer Galactic plane surveys. The $5.8\text{ }\mu\text{m}$ (blue) and the $8\text{ }\mu\text{m}$ (green) GLIMPSE observations are combined with the $24\text{ }\mu\text{m}$ (red) MIPS Gal data in these images. At top left is an $18'\times18'$ field at $(l, b) = (28.4^\circ, +0.1^\circ)$ centered on an infrared dark cloud. The star at right of center in this image shows the diffraction pattern of the system, which is three times larger at $24\text{ }\mu\text{m}$ than at $8\text{ }\mu\text{m}$. Thus, moderate to bright sources in these images will have a white core surrounded by a red ring and, if the source is bright enough, the second Airey ring of dots created by diffraction from the three cantilever spider vanes that support the secondary mirror. At top center is a $20'\times20'$ field at $(l, b) = (11.18^\circ, -0.34^\circ)$ centered on a large supernova shell remnant that is dominated by $24\text{ }\mu\text{m}$ emission; an H II region is to the lower right. The $10'\times10'$ field, centered at $(l, b) = (47.86, -0.85)$, in the upper right contains a filled ring of emission. The bottom panel is a $1.25^\circ\times0.33^\circ$ image at $(l, b) \sim (60^\circ, -0.3^\circ)$. Images adapted from Kuchar et al. (2006).

a higher density, $\sim 5\text{ deg.}^{-2}$, within the central $\pm 10^\circ$ longitude region) and a smaller mean size of $\sim 2'$ (Churchwell et al., 2007); part of the difference is a selection effect as Churchwell et al. noted that searched the inner region more carefully for the smaller bubbles. The larger bubbles were seen by MSX (Price et al., 2001; Cohen and Green, 2001). Indeed, a number of them are visible in Figure 115. The bubbles that Churchwell et al. (2006) label as S44 and S57 in the upper left and upper middle, respectively, of the Spitzer image are visible in the large area MSX image, but are rather small at this scale. Better defined is S52 at the left edge of the MSX insert. Churchwell et al. (2006) found that the bubbles were narrowly confined to the Galactic plane with a scale height of $\sim 0.6^\circ$ and that relatively few of them were associated with objects catalogued at other wavelengths. At $24\text{ }\mu\text{m}$, the MIPS Gal survey revealed approximately 400 small ($\sim 1'$) compact sources that appear as bubbles, rings, disks or shells. These bubbles are uniformly distributed along the Plane at an average areal density of about 1.5 deg^{-2} (Mizuno et al., 2010). There is little correspondence between these disks and the GLIMPSE bubbles.

AFGL astronomers were also given observing time to image infrared dark clouds, to obtain spectroscopy on bright infrared sources in the SMC and very red objects. The material in the SMC is less processed than that in either the Galaxy or the LMC, so we hoped to study evolution of stars and dust by comparing our results with similar observations of analogous

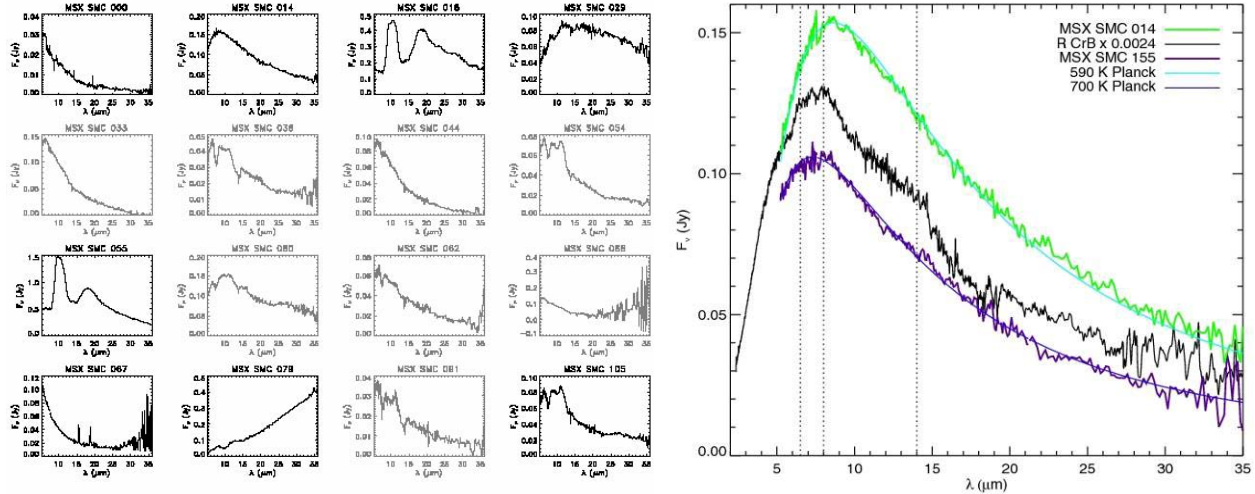


Figure 116. Spitzer spectra of SMC objects. Thumbnail spectra for a third of the objects selected are shown in the upper left. A similar variety of infrared spectral energy distributions are evident in the other two-thirds. Almost two-thirds of the objects are carbon rich; the eight carbon stars in this panel are highlighted by being plotted in grey. The oxygen rich objects with thick circumstellar dust shells are distinguished by their silicate emission features at 10 and 18 μm . The plot at right compares the two candidate SMC R CrB stars with the arch-typical spectrum of R CrB itself and the best fitting black body curves.

Galactic and LMC objects. The MSX – 2MASS color classification criteria of Egan, Van Dyck and Price (2001) for LMC sources was used to select what we thought to be a roughly equal number of oxygen and carbon stars from among the brighter SMC sources for IRS spectral measurements. Somewhat surprisingly, Sloan et al. (2006) found that nearly two-thirds of their sample of 36 color selected stars turned out to be carbon rich. A selection of spectra from a third of the SMC samples studied is shown in the upper left spectral plots in Figure 116 with the 9 (of 19) carbon stars in this subsample highlighted in grey. Some rare, carbon rich objects were also observed. These include a couple of R CrB stars (Kraemer et al., 2005), the spectra of which are shown in the right hand plot of Figure 117 and, for comparison with other stars in the sample, the postage stamp spectrum of MSX SMC 014 is the second one in the top row of the left hand plot. R CrB stars are relatively rare carbon rich and hydrogen deficient stars that have large visual variations and dust shells with (almost) featureless infrared spectral energy distributions. Kraemer et al (2006) also observed a post AGB/pre-planetary nebula star (MSX SMC 029, the postage stamp spectrum of which is in the last panel of the top row of spectra). This stage of stellar evolution is relatively short.

Sloan et al. (2008) compared AGB stars in the LMC, SMC and the Galaxy and found that the amount of dust produced by these stars depended on metallicity (the relative proportion of elements heavier than helium in the star). The more metals an oxygen-rich star has the more dust it produces but no such variation was found for the carbon-rich stars. The chemistry in oxygen rich circumstellar dust shells also depends on metallicity. According to Sloan et al. (2010), the same trends hold for globular clusters.

Spitzer ran out of helium on 15 May 2009 after which a post-cryogen phase was begun during which images are taken with the 3.6 μm and 4.5 μm arrays. The remaining Galactic plane not covered during the cryogen phase of the mission will be surveyed in these two bands by the GLIMPSE360 program (Whitney, 2009). The results from which will be used to determine the edge of the Galactic stellar disk, analyze star formation in the outer Galaxy and how interstellar reddening varies as a function of Galactic longitude.



10.3. Akari – ASTRO-F

Even with the more capable M-V rocket, weight was a premium for the ASTRO-F payload. The 68.5 cm Akari primary mirror and the secondary mirror of the f/6 Ritchey-Chretien optical system was made by chemical vapor depositing silicate carbide on a porous SiC core while beryllium was used for the support structure. The entire optical system weighed only \sim 31 kg. The optical surfaces

of the SiC elements were gold coated for good reflectivity and then overcoated with ZnS. The optics and the near and mid-infrared arrays were cooled to 5.8 K while the long wavelength detectors were directly connected to the 170 liter super-fluid helium dewar and cooled to \sim 1.8 K. To minimize weight, maximum use was made of radiative cooling of the outer shell to reduce parasitic loads and two 2-stage Sterling-cycle coolers provided additional cooling for the inner vapor cooled shield of the telescope, thus doubling the lifetime of the cryogen. The total weight of the spacecraft was about 952 kg.

The focal plane had a near- to mid-infrared and a far-infrared module. The 512×412 element InSb array in the near-infrared camera had 1.5" pixels while the two 512×512 Si:As mid-infrared arrays had \sim 2.4" pixels. Each of the arrays used a filter wheel with three spectral bands that, combined, covered the spectral range from 1.9 to 26 μ m. The camera also had a slitless spectrometer with a resolution of approximately $\lambda/\Delta\lambda \sim 30$, roughly comparable to the IRAS LRS, and a second 2.5 – 5 μ m spectrometer with 10 times better resolution (Wada et al., 2002). The Far-infrared Surveyor had four far-infrared arrays for the 50 – 180 μ m spectral region, two arrays each with 30" and 50" detectors. Eight of the 13 Infrared Camera (IRC) filters were analogous to COBE/DIRBE bands 2 through 9 (see Table 1 in Matsuhara et al., 2005) while the spectral response of the shortest survey band is a reasonable match to the MSX Band A.

Akari was launched into a sun-synchronous 745 km altitude orbit on 21 February 2006 and began mission operations the following May. The priority in the first six months of the mission was to conduct an all sky survey in all four far-infrared bands and in two of the mid-infrared bands. During the following year, before the cryogen ran out on 26 August 2007, observatory style observations were obtained and the gaps in the survey due to the South Atlantic Anomaly and the Moon were filled in. Ishihara et al. (2006) discussed the particulars for the 9 and 18 μ m mid-infrared portion of this survey in which four cross-scan pixels were binned creating a single column of \sim 10" tall elements. The integration time per read resulted in an effective pixel width also of about 10". A second column of binned detectors provides 5" offset in cross-scan from the first column and was used to reject energetic particle interactions, improve positions and for source confirmation. At 50 mJy, the 9 μ m survey band sensitivity was about three times than MSX Band A while the resolution was two times better; the differences may be seen by comparing the Akari map of the LMC in Figure 7 of Murakami and Matsuhara (2008) to the Band A image in Figure 97. The survey was conducted by having the telescope scan a great circle at 90° solar elongation at the orbital angular rate. The sky moved \sim 4' at the ecliptic plane during the 100 minute orbit, which is slightly less than half the width of the focal plane arrays. Thus, continuous scanning produces redundant coverage of the sky in six months (May – November 2006), except for outages caused by the Moon and the radiation environment of the South Atlantic Anomaly. Ninety eight percent of the sky was covered, 60% 4 or more times

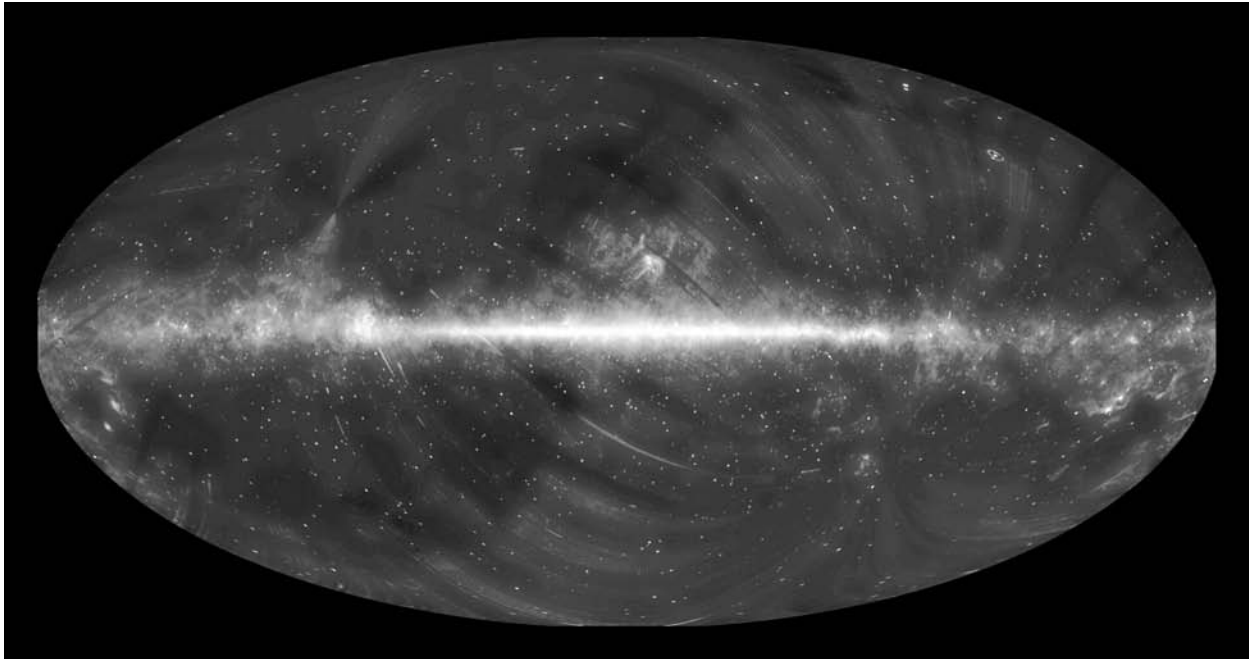


Figure 117. The 9 μm sky observed by Akari. The sensitivity and resolution are about four times that of MSX. The telescope has a modest intermediate field rejection as demonstrated by the off-axis ring from Saturn in the upper right of the image and the semi-monthly artifacts that are the streaks created by incomplete subtraction of the off-axis contamination from the Moon. An estimate of the zodiacal light has been subtracted from the image. This image was obtained from http://www.ir.isas.jaxa.jp/ASTRO-F/Outreach/results/IRC_AllSky_big.jpg

while lunar interference resulted in 8% of the sky being covered only once (Murakami and Matsuhara, 2008). The 9 μm results of the all-sky survey are imaged in Figure 117, which highlights the extended infrared structure.

Approximately, 700,000 9 μm point sources were extracted from the survey. Since scans converge toward the ecliptic poles, increasing the redundancy at the higher ecliptic latitudes, pointed observations were combined with the highly redundant survey scans at the Ecliptic Poles to create a deep 2.4 to 34 μm survey of those regions (e.g. Lee et al., 2009); the LMC was similarly mapped (Onaka et al., 2009). The images of the Ecliptic Poles and the LMC in the non-survey bands were a small percentage of the 5380 pointed observations were obtained during the mission. These pointed observations used the full 2.4" resolution of the mid-infrared arrays as well as the spectrometers.

The Akari cryogenic mission, instruments and in-orbit performance assessment are described in the Akari section of the *Proc. SPIE*, Vol. 7010 (2008). Onaka and Salama (2009) present an excellent concise description of the telescope and focal plane instruments, observation modes and timing during the cryogenic mission as well as a brief summary of initial results. They also comment that some of the Akari data will be made available by the end of calendar 2009. The December 2008 special issue of the *Publications of the Astronomical Society of Japan* (SP2, Vol. 60) presents more detailed initial result from the mission.

Phase 3 of the mission began after the helium was exhausted on 26 August 2007, after which cooling by the Sterling-cycle mechanical refrigerators allows the InSb array camera and spectrometers to be used. In the first three-year cycle of Phase 3 commenced on 15 October 2008, during which 20 – 25 pointed observations are executed each day. Since the Spitzer 3.6

and 4.9 μm post-cryogen observations are more sensitive and have better spatial resolution than the equivalent Akari bands, the Akari post cryogen mission will emphasize observations with the spectrometer, a capability Spitzer doesn't have.

10.4. Submillimeter Experiments

Three space-based submillimeter missions were operating in the first decade of the millennium: the Submillimeter Wave Astronomy Satellite (SWAS), Odin and Herschel. These missions are briefly outlined as they cover the submillimeter, which is beyond our mid-infrared focus. However, they have made some notable observations and Herschel deserves mention if for no other reason than it is the largest telescope ever flown into space.

SWAS was a NASA Small Explorer (SMEX) mission that flew a 55×67 cm off-axis Cassegrain telescope into a 650 km altitude, 70° inclination circular orbit on 5 December 1998 to obtained 1°×1° maps of giant molecular clouds, dark cloud cores and the interstellar medium at the wavelengths of five submillimeter atomic and molecular lines (water, carbon and oxygen). The satellite was active through July 2004 and reactivated for three months in the summer of 2005 to observe the effects of the Deep Impact probe's intercept of comet P/Temple I. Tolls et al. (2004) provide the details of the instrument and performance, while Melnick et al. (2000) described the mission objectives and hardware. The 20 August 2000 issue of the *Astrophysical Journal Letters* presents the initial results from this experiment while Melnick (2004) updates this overview.

Odin, a 1.1 m off-axis Gregorian telescope for aeronomy and astronomy between 0.5 and 2.5 mm, is a Swedish satellite built and operated in collaboration with Canada, France and Finland. Odin was launched into a 900 km altitude Sun-synchronous orbit in February 2001 and is still operational. The instrument has a 1.1 m aperture, twice the diameter of SWAS with twice the spatial resolution and better sensitivity. Nordh et al. (2003) describe the observatory and mission operations while the preliminary astronomical results may be found in the Letters section of the May 2003 No.2 issue of *Astronomy and Astrophysics*. Hjalmarson (2005) gives a more recent update.

The Herschel submillimeter space observatory, formerly the Far-infrared Space Telescope (FIRST) is the most versatile of the submillimeter instruments flown. Herschel is the final the ESA cornerstone missions, which were flagship experiments to be flown between ~2000 and 2010. Besides Herschel, the other cornerstone missions were ISO, Newton – an x-ray observatory originally named the x-ray multi-mirror (XMM) satellite and the Integral γ -ray observatory.

Herschel was launched on an Arianne rocket along with the Planck cosmic background survey experiment in mid-May 2009 and inserted into an L2 orbit ~1.5 million km beyond the Earth. Harwit (2004) and Pilbratt (2004) describe the Herschel system, a 3.5 m passively cooled Cassegrain telescope with the three focal plane instruments that are designed to obtain 60 – 650 μm photometry, mapping and spectroscopy on selected objects. The cryogen to cool the focal planes is projected to last for three years. As with previous infrared astronomy missions, the inner Galactic plane is an attractive target for a survey because of the large variety of densely packed sources and the bright diffuse emission from extended objects as well as the interstellar medium and Herschel will conduct such a survey. The Herschel Key-Project HI-Gal survey, led by Sergio Molinari, will cover the same $|l| < 60^\circ$ and $|b| < 1^\circ$ area of the inner Galaxy surveyed by GLIMPSE/MIPSGal in five bands between 60 and 600 μm .

10.5. In the Queue



With SPIRIT III well into hardware development, JPL and USU Space Dynamics Laboratory responded to the 1992 NASA call for proposals for a small explorer (SMEX) class experiment with a concept to build a small, lightweight on-axis infrared instrument that leveraged the MSX optical and solid hydrogen cryogenic cooling developments. On 14 September 1994, NASA announced approval of the Wide Field Infrared Experiment (WIRE), to study the evolution of starburst galaxies and luminous

protogalaxies at 12 and 25 μm . WIRE was an MSX sized Cassegrain telescope (30 cm diameter primary mirror) cooled with solid hydrogen. Hacking et al. (1999) summarized the WIRE hardware and mission objectives. Briefly, a dichroic filter diverted the beam from the two mirror telescope to two 128×128 element Si:As BIB arrays. The 12 μm array had a spatial resolution of 15" while the 24 μm array resolution was comparable to MSX.

WIRE was launched from a Pegasus rocket carried by an L-1011 aircraft on 4 March 1999 into a 400 km altitude nearly polar orbit for a nominal four month mission during which the experiment was to survey 1000 deg^2 of sky with one minute exposures on $\sim 1/2^\circ \times 1/2^\circ$ fields. This exposure time was some 2000 times longer than MSX and that, combined with cooler operating temperatures and better arrays meant that WIRE was expected to be about 1000 times more sensitive. The cryogen reservoir was sized for a longer mission than four months and the Cornell/JPL/Caltech/GSFC/Ball Bros. science team anticipated approval to operate for the duration of the cryogen if the results from the first four months proved worthwhile.

After successful orbital insertion and initial functional checks, the spacecraft went into an uncontrolled tumble after the signal was sent to open the cryogen vent line; see <http://klabs.org/richcontent/Reports/wiremishap.htm>. The unofficial speculation was that the signal to open the cryostat vent line also triggered the cover release; coincidentally, the power regulator used in the cover circuit was the same type that was suspected of allowing the MSX overcurrent events. The thermal input into the cryotank when the sensor looked at the Earth markedly increased cryogen venting. Like MSX, WIRE had positioned the vent line outlet to use the small thrust from the vented gas for orbital station keeping. The rapid venting produced a spacecraft torque that was too high to be controlled by the magnetic reaction wheels and the cryogen was quickly expended, thus ending the mission. Spacecraft control was established after the hydrogen was gone but all was not lost, however. The star tracker has been used as the first spaced-based astroseismology instrument; see Brunt and Buzasi (2006) for a brief overview

Three years after the WIRE failure, NASA issued a Phase A study for a much more capable Wide-field Infrared Survey Explorer (WISE) in the spring of 2002. WIRE is slated for a December 2009 launch.

The Stratospheric Observatory for Infrared Astronomy (SOFIA) has a 100" telescope installed on a Boeing 747. It is in its final check-out phase and will go into operation early in 2010, roughly concurrent with WISE. A 15 to 20 year lifetime is expected.

Five years or so in the future is the James Webb telescope, the next large funded space facility for infrared astronomy. This facility will obtain high spatial and spectral resolution measurements primarily in the 5 – 29 μm spectral region with a telescope that has a 6.6 m diameter mirror. The telescope is currently being constructed and the instruments are being

developed. The critical design review for the program will be held in spring of 2010 while the current anticipated launch date is 2014.

10.5.1. The Wide-Field Infrared Survey Explorer (WISE)

The initial attempt to resurrect WIRE proposed to use the engineering optics for an inexpensive duplicate. However, the WISE Phase A study led to a number of design improvements. The 40 cm primary mirror almost doubles the WIRE collecting area and four 1024×1024 element focal plane arrays, rather than two, are to be used: two HgCdTe arrays for 3.3 and 4.7 μm bands and two Si:As arrays to duplicate the original WIRE 12 and 23 μm bands. The 2.75" detectors provide diffraction limited resolution in all bands (10" at 12 μm) and the 47' instantaneous field of view is almost three times the size of the WIRE focal planes. The four focal plane arrays are co-aligned with dichroic filters.

As with SPIRIT III, WISE has an internal scan mirror. However, the WISE mirror scans to compensate for the spacecraft motion, freezing the sky for an 8.8 second integration after which the scan mirror returns in 1.1 seconds to begin the next integration while the focal planes are read out. The satellite will be in a sun-synchronous orbit and the efficiency of the survey, which scans at $\sim 90^\circ$ elongation, is noted by the fact that WIRE will cover all the sky at least four times during the nominal ten month mission following the projected launch of December 2009. Mainzer, Eisenhardt et al (2006) presented an overview of the satellite and scientific objectives of the mission while Larsen et al. (2008) provides an update of the satellite and hardware.

10.5.2. Stratospheric Observatory for Infrared Astronomy (SOFIA)

The Stratospheric Observatory for Infrared Astronomy (SOFIA) observatory is a German (Deutsches Zentrum Für Raumfahrt – DLR) built 2.5 m (100") effective aperture, gyrostabilized telescope on a Boeing 747 AP aircraft (named the Clipper Lindberg) that NASA reconfigured to carry the telescope. The telescope has two f/19.6 Nasmyth foci: the visible focus is used for guiding while the other hosts a variety of infrared instruments that, in total, spans the wavelength regime from the visible to 1 mm. The projected 1000 hours of observing each year will be obtained on 80 – 100 flights anticipated annually. At altitude of 45,000", the atmospheric transmission averages $\sim 80\%$ over the 0.3 μm to 1.3 mm wavelength range covered by SOFIA (see Figure 13). SOFIA is the successor to the Kuiper Airborne Observatory (KAO), which was taken out of service in the 1995 to free up funds to develop SOFIA. The SOFIA Science Center is located at NASA Ames Research Center while the Dryden Flight Research Center in Palmdale, CA will conduct flight operations. The first generation of nine different instruments will obtain a wide variety of observations; the instruments can be changed out for each flight. Primary science objectives are: stellar and planetary formation, understanding the interstellar medium, obtaining detailed measurements on galaxies and the Galactic center, and solar system science. A major SOFIA resource is the very high spatial and spectral resolution measurement capability in the infrared that can extract kinematics from the observed source.

The initial study for SOFIA was conducted in 1986 and first SOFIA test flight occurred 20 years later in April 2007. Routine astronomical operations are scheduled to begin in 2010 with a projected lifetime of 20 years. Gehrz et al. (2009) describe the telescope, instruments and the science anticipated from SOFIA. SOFIA is a significant resource for infrared astronomy and the reader is referred to the SOFIA web site <http://www.sofia.usra.edu/Sofia/sofia.html>, which posts a regular newsletter that provides current information on the program.

10.5.3 The Webb Telescope

With the launch of the Hubble telescope in 1990, consideration turned to a successor. Bély, Burrows and Illingworth (1990) laid out the considerations for a 8 – 16 m successor system to the Hubble Space Telescope in the 1989 *The Next Generation Telescope* conference proceedings. Over the following decade, the concept evolved from emphasizing the ultraviolet-visible wavelengths with near-infrared capability to an infrared observatory as the telescope diameter decreased to 6.6 m as outlined by Mather et al. (1997) for the 1996 NASA concept of a Next Generation Space Telescope. The system was renamed James Webb Space Telescope in 2002. Gardner et al. (2006) provides an extensive preview of NASA's James Webb Space Telescope in an article that defines the scientific objectives (updated by Gardner, 2008), discusses the performance requirements necessary to meet those objectives and encompasses previous descriptions of the instrumentation. The primary mirror or the telescope is composed of 18 hexagonal 1.32 m beryllium mirrors, each with wavefront control, for a total collecting area of $\sim 25 \text{ m}^2$. The telescope is to be diffraction limited at $2 \mu\text{m}$ at an effective aperture of 6.6 m. Four focal plane instruments collectively cover the wavelength range from 0.6 to $29 \mu\text{m}$. There is a near-infrared camera, a near-infrared spectrometer with addressable slits to obtain simultaneous spectra of a number of discrete sources within the field-of-view, a tunable filter imager for narrow spectral band ($\lambda/\Delta\lambda \sim 100$) imaging in the near-infrared and a mid-infrared instrument for imaging and spectra. Three sections in the *Proc. SPIE*, Vol. 7010 (2008) are devoted to description of the Webb telescope, on-ground testing and instruments. The Webb telescope will be stationed in the L2 region. Current optimistic estimates are for a 2014 launch.

10.6. Space Infrared Telescope for Cosmology and Astrophysics (SPICA)

The Space Infrared Telescope for Cosmology and Astrophysics (SPICA) is currently in the concept development stage and not all the commitments have been made for the proposed program.

With the Akari success, the Japan Aerospace Exploration Agency (JAXA) is developing the technology for SPICA. The concept was originally proposed by Nakagawa et al. (1998) as the HII/L2 mission, a placeholder name that combined the proposed HII launch vehicle with the (Lissajous) L2 orbit. The concept evolved into SPICA, an infrared 5 to $200 \mu\text{m}$ observatory with a 3.5 m Ritchey-Chretien telescope cooled to 4.5 K. The original 2010 proposed launch of the estimated 2600 kg experiment has slipped to 2017.

Like Spitzer, SPICA will be launched warm doing away with the heavy cryostat needed for a cold launch. The SPICA structure is to be radiatively cooled while at least four mechanical cryocoolers will cool the silicon carbide composite primary mirror to $<20 \text{ K}$, the Si:As focal planes to 4.5K, the Ge:Ga arrays to 2.5 K and the stressed Ge:Ga detectors to 1.7K (Sugita et al., 2006). Two of the 20K two stage Sterling cycle coolers are to be coupled to Joule-Thompson (JT) coolers to achieve the 4K focal plane temperature requirement of the mid-infrared arrays; a Sterling cycle cooler will be coupled to a He^3 JT cooler for the Ge:Ga arrays.

ESA is conducting an assessment study to determine whether to collaborate with JAXA on SPICA for it to serve as one of their Cosmic Vision 2015 – 2025 missions. Under the proposed collaboration, ESA would provide the telescope and a European based ground station to increase the data volume received. ESA is also considering building a far-infrared (30 – $200 \mu\text{m}$) Mach-Zehnder Fourier Transform Spectrometer called SAFARI for SPICA that is capable of a 10 – 10000 spectral resolution within a 4 arcmin 2 field.

The scientific objectives over the nominal 5 year mission include observations that address issues with regard to the formation of galaxies, stars and planets, to study the evolution of gas and dust in the interstellar medium, the solar system and the origin of the universe. SPICA will be capable of wide field, high sensitivity photometric mapping at high spatial resolution, spectral analysis as well as using a coronagraph to observe planets and planetary disks. Onaka and Nakagawa (2005) provide a general overview of the SPICA mission while Swinyard and Nakagawa (2009) discuss the latest considerations for the mission profile and scientific objectives. An update on the mission and hardware is given in the three papers in the Akari-WISE section of the *Proc. SPIE*, Vol. 7010 (2008). .

10.7. Personal Perspective

During the long history of infrared survey experiments, a number of ‘discoveries’ have been claimed. It is the nature and hoped for objective of a survey to find new things, either previously unknown objects or unusual aspects of known sources. What is labeled a ‘discovery’ is based upon perceptions. The community can assign a discovery to the person or program that obtains the very first observation, to the first individual(s) who recognize the importance of the observations or to the program that has the best publicity machine. For the Air Force surveys, we highlighted objects that had no previously known counterparts and those with interesting morphological or spectral characteristics. Thus, Price (1968a, b) pointed to the extended nature of the source in Ara. I was unaware of the previous association of the object with an open star cluster by Westerlund (1961), having very little undergraduate experience in an unguided literature search. Indeed, it was only in graduate school that I became aware of and learned to use the *Astronomischer Jahresbericht*, later the *Astronomy and Astrophysics Abstracts*, to track down previously published articles on a given topic. However, identifying the object did not detract from the initial assessment that one of Freeman Hall’s objectives had been realized, the observation of an extended near-infrared source.

A number of objects in the AFCRL/AFGL catalogs were deemed interesting if they were bright in the infrared, faint in the visible and had no prominent association. Hence, UoA 01 (Low et al., 1976) is designated RAFGL 490 because of the relatively large number of such sources found the Air Force survey, even though Low (1973) detected this object seven months before the rocket survey found it. Analogously, although the unusual morphology and spectral properties of the red rectangle were known before HI STAR, the classification was uncertain until the mid-infrared observations were available (e.g. Cohen et al., 1975). On the other hand, that AFCRL 2688 and 618 were previously unidentified objects that were bright in the infrared prompted Ney et al. (1975) and Westbrook et al. (1975) to spectroscopically examine them to ascertain their nature.

Also, prior publication often trumps the first observation. For example, Gautier et al. (1984) published a low resolution map of the Galactic center in the March 1984 IRAS announcement issue of the *Astrophysics Journal Letters*. This article appeared before AFGL published the BMP astronomy results, specifically the Little and Price, (1985) AFCRL/AFGL Galactic center maps. Although obtained before IRAS, the SPICE map was published 1½ years after the Gautier et al. map; which is the basis for the claim that IRAS “...*(r)evealed for the first time the core of our Galaxy*” (http://www.ipac.caltech.edu/Outreach/Edu/iras_discoveries.html). George Aumann sent an overlay of the SPICE cover illustration on the September 1985 *Astronomical Journal* that featured the SPICE 11 μm map and the IRAS 12 μm contour plot of the Galactic center, which is reproduced in the insert to Figure 46. Although it may be said that



Figure 118: MSX raster image of the Galactic plane at 28° longitude. Several dark clouds are apparent, particularly the one toward the center right edge.

the IRAS observations (heavy lines) confirm the SPICE results (light lines), the fact is that IRAS published their map before we did. On the other hand, the AFGL catalog was published a year before the IRAS catalog and a paper trail exists for prior detection of AFGL 5376, the very red blob in the upper right of the Galactic center image in Figure 90. Then there was the curious consistent early referencing to the Willems and de Jong (1986) “discovery” of carbon stars with silicates in their circumstellar shells, especially in Europe, even though Irene Marenin had published this finding two months before in the same journal.

More ambiguous is the credit for one of the most notable MSX observations: that of well over a thousand infrared dark clouds (IRDCs) in the Galactic plane (Egan et al., 1998). These are clouds that are so cold as to be seen silhouetted against the general background emission from the Galactic plane and cold enough to have little or no 60 or 100 μm flux in the IRAS maps. The most conspicuous dark clouds in the Figures in Chapter 8 are the ones surrounding the Galactic center, especially the sinuous cloud to the left of the center in Figures 46 and 90. Michel Péault emphatically pointed out in an e-mail to us that he and the ISO Gal team had a prior discovery announcement (Péault et al., 1996). Egan et al. responded by acknowledging the Péault et al. article in an addendum to their announcement paper. However, some pretty strong feelings regarding the priority of discovery were expressed to me during several trips to European conferences. Péault et al. noted in their paper that the dark cloud they found corresponded to a deficit of DENIS K band survey sources, a not unanticipated result as a dark cloud at 15 μm should show up at 2 μm if it is a foreground object. Egan et al., on the other hand, found that that the clouds were very cold because they were dark even in the IRAS 60 and 100 μm images, something that was not expected. Carey et al. (1998, 2000) also soon obtained sub-millimeter observations that defined the unusually cold and dense nature of these objects. Furthermore, the MSX survey encompassed the entire inner Galaxy and, therefore, observed thousands of these objects. Consequently, the only published census of the dark clouds to date (Simon et al., 2006) was based on the

MSX data. However, neither MSX nor ISO were the first to observe the dark clouds as the larger ones clearly appeared in the MMSE full resolution IRAS images, although the sharp edged nature of the clouds that is evident at the higher MSX and ISOCam resolution made them much more easily identifiable. Although the dark clouds in the IRAS image in Figure 72 are rather subtle the one at $\sim 28^\circ$ longitude, shown in the MSX raster image of the region in Figure 118 and, with even better definition, in the Spitzer image at the top left of Figure 115, is large and strikingly evident even at much lower resolution in the IRAS MMSE image of the region.

Michel Péroult also expressed his opinion I had to have known about the ISO Gal priority because I was an author, one of 24, on the paper. This touches on an issue I have long had as to what constitutes appropriate credit and co-authorship on publications. The article was published without soliciting my input or, indeed informing me that it was being submitted. Thus, I only became aware of its existence until it appeared in *Astronomy and Astrophysics*. Not only did I not have an opportunity to contribute to the paper or review its contents prior to publication, the procedure violated the Air Force's public affairs requirement that the contents of papers on which AFGL employees appears as (co-)authors have to be approved before they are published. I cursorily read the article and neither the brief paragraph about the dark cloud nor the accompanying Figure made much of an impression.

As previously mentioned, we played a small but key role in recovering the performance of band 3 of the SWS. Lt. Col. Dan Wilhelm paid me a courtesy call shortly before I returned to the Netherlands to attend the November 1992 ESA meeting on detectors at Noordwijk. Dan was Chief of the Phillips Lab branch responsible for executing much of the BMDO focal plane development. I mentioned to him that the SWS Si:P detectors had severe non-linearities, which made them virtually uncalibratable, and that they had no better luck with the Si:Sb detectors built by Frank Low's Infrared Laboratories company. Dan Wilhelm thought it possible to obtain an export license for discrete Si:As BiBs to replace these faulty devices and recommended that I contact Irv Myrick, the science, engineering and technical advisory contractor supporting Col Swenson, the BMDO program manager for focal plane development. Acting on this advice, I provided Mr. Myrick with a position paper detailing why the required small linear array of large detectors would not be a transfer of critical technology. I subsequently discussed the issue with Dutch Stablebroek, a senior Rockwell detector engineer, at the Noordwijk SPIE meeting on detectors. The only problem he saw was in obtaining export license. Thijs deGraauw had arranged an *ad hoc* meeting with Michel Anderegg (ESA Payload and Operations Manager), Martin Kessler (ESA Project Scientist) and Dietrich Lemke (ISOPhot lead) to discuss the possibility of replacing the problematic 15 – 30 μm array with BIB Si:As detectors and asked me to sit in. When asked to comment on the export license, I said that I had been in contact with the appropriate people in Washington and that they seem to be favorably disposed, but could make no promises. Thijs deGraauw was given extra time to try to replace the array as long as he met the final delivery date for sensor integration. Although the ISOPhot 20 μm array was non-functional, Dieter Lemke declined to consider the option of replacing the inoperative detector with a Si:As BIB because his instrument was buttoned up to be delivered on schedule. I talked to Paul LeVan, who was then in Lt. Col Wilhelm's branch, about the situation. Under the aegis of the Dutch/Air Force MOU covering the ISO collaboration, I provided Paul \$50K to put on the Rockwell contract to design the appropriate detector mask and to manufacture several engineering arrays for test and evaluation by Rockwell and the Air Force. During this time Rockwell applied for and was granted an export license for the Dutch to purchase the SWS detectors. The detectors were installed and worked well during the mission; the only drawback

was that their shorter wavelength cutoff reduced the sensitivity to the 28 μm molecular hydrogen line.

Despite the various reorganizations and redirection of research objectives, the infrared astronomy program had survived for forty-five years by adapting to the changing Air Force research objectives and responding to timely opportunities, thanks to entrepreneurial efforts of the infrared astronomers who used their solid scientific reputation built upon delivering quality products to sponsors and to leverage access to civilian and DoD assets. Fortunately, as one major program was completed, a new opportunity arose: the Background Measurements Program was funded just as the HI STAR experiments were completed in the mid-1970s. After the BMP was over in the mid-1980s, SDIO supported AFGL celestial background modeling and analysis for synthetic scene generation and funded processing and analysis of the AFGL astronomy experiments on the 1996 Midcourse Space Experiment. AFGL astronomers also participated on the Dutch/German SWS consortium on ISO. We obtained NASA support for our MSX and ISO experiments in the late 1990s for turning the MSX observations into research quality products for the civilian community as well and analyzing the ISO observations. NASA then funded us to conduct the MIPGAL legacy program on the Spitzer Space Telescope and the reduction and analysis of data.

Perhaps more importantly, the program has lasted because it addressed the more practical Air Force space research needs and clearly demonstrated the value of the applied aspects of the astronomy, such as calibration, thus providing Air Force program rationale. Improving and extending the stellar calibration network is still a funded effort within the DoD. Also, the techniques used to reduce our astronomical survey observations naturally apply to artificial satellites as the observing procedures and data reduction techniques are the same and there is a great deal of similarity in the analysis of the physical properties of asteroids and Earth orbiting objects.

REFERENCES

Abbott, C.G. (1929) Energy Spectra of the Stars, *Astrophys. J.*, **69**, 293 – 311.

Abbott, C.G. (1930) Solar Variation and Temperature Changes, *Pub. Astron. Soc. Pac.*, **38**, 593.

Ábrahám, P., Ch. Leinert & D. Lemke (1997) Search for Brightness Fluctuations in the Zodiacal Light at 25 μ m with ISO, *Astron. Astrophys.*, **328**, 702 – 705.

Adel, A. (1942) The Extension of the Prismatic Solar Spectrum from 14 μ to 24 μ through a New Atmospheric Window in the Infrared, *Astrophys. J.*, **96**, 239 – 241.

Adel, A. (1946) The Infrared Spectrum of the Moon, *Astrophys. J.*, **103**, 19 – 46.

Adler-Golden, S.M., M.W. Matthew & D.R. Smith (1991) Upper Atmospheric Infrared Radiance from CO₂ and NO Observed During the SPIRIT 1 Rocket Experiment, *J. Geophys. Res.*, **96**(A7), 11,319–11,329.

Ahmadjian, M., D.E. Jennings, M.J. Mumma, F. Espenak, C.J. Rice, R.W. Russell & B.D. Green (1992) Infrared Spectral Measurements of Space Shuttle Glow, *Geophys. Research Lett.*, **19**, 989 – 992.

Ahmadjian, M., D.R. Smith, A.T. Stair & K. Baker (1981) CIRRIS – A Cryogenic Infrared (IR) Radiance Instrument for Shuttle, *Proc. SPIE.*, **280**, 45 – 53,

Air Force Cambridge Research Laboratories Report on Research for the Period Jul 1963 – Jun 1965, AFCRL-65-595, AD0631411.

Air Force Cambridge Research Laboratories Report on Research for the Period Jul 1967 – Jun 1970, AFCRL-71-0022, AD0720277.

Air Force Cambridge Research Laboratories Report on Research for the Period Jul 1970 – Jun 1972, AFCRL-73-0384, AD0774743.

Air Force Cambridge Research Laboratories Report on Research for the Period Jul 1972 – Jun 1974, AFCRL-75-0288. ADA027358.

Allamandola, L.J., A.G.G.M. Tielens & J.R. Barker (1985) Polycyclic Aromatic Hydrocarbons and the Unidentified Infrared Emission Bands – Auto Exhaust along the Milky Way. *Astrophys. J.*, **290**, L25 – L28.

Allen, D.A. (1970) Infrared Diameter of Vesta, *Nature*, **227**, 158 – 159.

Allen, D.A. (1971a) Infrared Studies of the Lunar Terrain I. The Background Moon, *The Moon*, **2**, 320 – 337.

Allen, D.A. (1971b) Infrared Studies of the Lunar Terrain II. Thermal Anomalies, *The Moon*, **2**, 435 – 462.

Allen, D.A. (1975) *INFRARED, The New Astronomy*, John Wiley, New York.

Allen, D.A. (1977) Infrared Astronomy - An Assessment, *Quart. J. Roy. Astron. Soc.*, **188**, 188 – 198.

Allen, D.A., A.R. Hyland & A.J. Longmore (1976) A First Look at the AFCRL Infrared Sky Survey Catalog, *Mon. Not. Roy. Astron. Soc.*, **175**, 61P – 64P.

Allen, D.A., A.R. Hyland, A.J. Longmore, J.L. Caswell, W.M. Croos & R.F. Haynes (1977) Optical, Infrared, and Radio Studies of AFCRL Sources, *Astrophys. J.*, **217**, 108 – 126.

Allen, L.E., S.G. Kleimann & M.D. Weinberg (1993) IRAS Variables as Galactic Structure Tracers: Classification of the Bright Variables, *Astrophys. J.*, **411**, 188 – 199.

Allen, M.M., J. Murthy, J. Daniels, A.R. Dring, R.E. Newcomer, R.C. Henry, L. Paxton, E. Tedesco & S.D. Price (1997) UVISI Observations of the Pleiades, *Bull. Amer. Astron. Soc.*, **29**, 805.

Alvarez, L.W., W. Alvarez, F. Asaro & H.V. Michel (1980) Extraterrestrial Cause for the Cretaceous Tertiary Extinction, *Science*, **208**, 1095 – 1108.

Amato, I. (2001) *Pushing the Horizon. Seventy-Five Years of High Stakes Science and Technology at the Naval Research Laboratory*, ADA387688.

Ames, H.O. & D.A. Burt (1993) Development of the SPIRIT III Sensor, *Proc. SPIE*, **1765**, 10 – 40.

Ames, H.O. & D.A. Burt (1994) Development of the SPIRIT III Sensor, *Proc. SPIE*, **2227**, 74 – 86.

Anderson, R.C., W.H. Brune, R.C. Henry, P.D. Feldman & W.G. Fastie (1979a) The Spectrum of the Diffuse Cosmic Ultraviolet Background, *Astrophys. J.*, **233**, L39 – L42.

Anderson, R.C., W.H. Brune, R.C. Henry, P.D. Feldman & W.G. Fastie (1979b) Far-Ultraviolet Studies. V – Rocket Observations of the Diffuse Cosmic Background, *Astrophys. J.*, **234**, 415 – 426.

Anon. (1958) *Contributions of Balloon Operations to Research and Development at the Air Force Missile Development Center Holloman Air Force Base, N. Mex 1947 – 1958*, Air Force Missile Development Center Holloman AFB NM, ADA323109.

Anz-Meador, P.D., D.M. Oró, D.J. Kessler & D.E. Pitts (1986) Analysis of IRAS Data for Orbital Debris, *Adv. Space Res.*, **6** (7), 139 – 144.

Arendt, R.G., G.B. Berriman, N. Boggess, E. Dwek, M.G. Hauser, T. Kelsall, S.H. Moseley, T.L. Murdock, N. Odegard, R.F. Silverberg, T.J. Sodroski & J.L. Weiland (1994) COBE Diffuse Infrared Background Experiment: Observations of Galactic Reddening and Stellar Populations, *Astrophys. J.*, **425**, L85 – L88.

Arquist, W.N. (1959) A Survey of Early Infrared Development, *Proc. Inst. Radio Eng.*, **47**, 1420 – 1430.

Arrington, D.C., R.L. Bates, W.L. Eisenman & M.H. Sweet, (1976) *Properties of Photodetectors (Photodetector Series, 97th Report). Spatial Sensitivity of LWIR Detectors*, NELC/TR-2014. ADA033795.

Arrington, D.C. & W.L. Eisenman (1977) Detector Behavior at Low Frequencies, *Proc. SPIE*, **124**, 57 – 68.

Augason, G.C. & H. Spinrad (1965) *Infrared Astronomy Review for the Astronomy Subcommittee of the National Aeronautics and Space Administration*, NASA TM X-1074

Aumann, H.H., C.A. Beichman, F.C. Gillett, T. de Jong, J.R. Houck, F.J. Low, G. Neugebauer, R.G. Walker & P.R. Wesselius, (1984) Discovery of a Shell Around Alpha Lyrae. *Astrophys. J.*, **278**, L23 – L27.

Aumann, H.H., J.W. Fowler & M. Melnyk (1990) A Maximum Correlation Method for Image Construction for IRAS Survey Data, *Astron. J.*, **99**, 1674 – 1681.

Aumann, H.H. & F.J. Low (1970) Far-Infrared Observations of the Galactic Center, *Astrophys. J.*, **159**, L159 – L164.

Aviation Week, (1958) **67**, 31.

Aviation Week (1975) **103**, 15 – 17.

Bader, M. & F.C. Witteborn (1972) The NASA 91.5 cm Aperture Airbornbe Telescope *Astrophys. & Space Sci. Lib.*, **60**, 29 – 40.

Bahcall, J.N. (1991) *The Decade of Discovery in Astronomy and Astrophysics*, National Academy Press.

Bahcall, J.N. & R.M. Soneira (1980a) The Universe at Faint Magnitudes I. Models for the Galaxy and the Predicted Star Counts, *Astrophys. J. Supp.* **44**, 73 – 110.

Bahcall, J.N. & R.M. Soneira (1980b) Star Counts as an Indicator Of Galactic Structure and Quasar Evolution, *Astrophys. J.*, **8**, L17 – L20.

Bahcall, J.N. & R.M. Soneira (1981) Predicted Star Counts in Selected Fields and Photometric Bands: Applications to Galactic Structure, the Disk Luminosity Function and the Detection of a Massive Halo, *Astrophys. J. Supp.*, **47**, 401 – 403.

Bahcall, J.N. & R.M. Soneira (1984) Comparision of a Standard Galaxy Model with Stellar Observations in Five Fields, *Astrophys. J. Supp.*, **55**, 67 – 99.

Bahcall, J.N., K.U. Ratnatunga, R. Buser, R.P. Fendart & A. Spaenhauer (1985) An Analysis of the Basel Catalog, *Astrophys. J.*, **299**, 616 – 632.

Baker, D., A. Steed & A.T. Stair, Jr. (1981) Development of Infrared Interferometry for Upper Atmosphere Emission Studies, *App. Opt.*, **20**, 1734 – 1746.

Bakos, G.A. & L. Campbell, Jr. (1960) Moonwatch Progress Report and Research, *Astron. J.*, **65**, 482.

Baldran, A., A. Bec-Borsenberger & J. Borsenberger (2004) Asteroidal I, J, K Magnitudes Recovered in the DENIS Survey: Second Release, *Astron. Astrophys.*, **423**, 381 – 383.

Baldwin, J.R., J.A. Frogel & S.E. Persson (1973) The Strengths of Infrared CO and H₂O Bands in Late-Type Stars, *Astrophys. J.*, **184**, 427 – 434.

Balsamo, S.B. & J.W. Salisbury (1973), Slope Angle and Frost Formation on Mars, *Icarus*, **18**, 156 – 163.

Barnaby, D. & H.A. Thronson, Jr. (1992) The Distribution of Light in Galaxies: The Edge-on Spiral NGC 5907, *Astron. J.*, **103**, 41 – 53.

Barnhart, P.E. & W.H. Haynie (1964) A Program of Stellar Narrow Band Infrared Photometry, *Mem. Roy. Soc. Liege*, **IX**, 425 – 431.

Banhart, P.E. & W.E. Mitchell, Jr. (1966), Stellar Background Measurement Program, *Cont. Perkins Obs. Series II*, No. 16.

Banhart, P.E. W.E. Mitchell, Jr., R. Roll & W.H. Haynie (1961), A Program of Stellar Photometry at 3 to 4 μ m, *Astron. J.*, **66**, 37.

Barr, E.S. (1960) Historical Survey of the Early Developments of the Infrared Spectral Region, *Amer. J. Phys.*, **28**, 42 – 54.

Barr, E.S. (1963) The Infrared Pioneers III: Samuel Pierpont Langley, *Infrared Phys.*, **3**, 195 – 296.

Bartschi, B.Y., D.E. Morse & T.L. Woolston (1996) The Spatial Imaging Infrared Telescope III, *JHU APL Tech. Digest*, **17**, 215 – 225.

Basri, G. & G.W. Marcy (1995) A Surprise at the Bottom of the Main Sequence: Rapid Rotation and No H-Alpha Emission, *Astron. J.*, **109**, 339 – 356.

Bateson, F.M. (1962) Site Testing in New Zealand, *Sky & Tel.*, **24**, 4 – 9.

Baum, W.A., F.S. Johnson, J.J. Oberly, C.C. Rockwood, C.V. Strain, & R. Tousey, (1946) Solar Ultraviolet Spectrum to 88 Kilometers, *Phys. Rev.*, **70**, 781 – 782.

Becker, B.J. (1993) *Eclecticism, Opportunism, and the Evolution of a New Research Agenda: William and Margaret Huggins and the Origins of Astrophysics*, PhD Thesis, Johns Hopkins University, <http://eee.uci.edu/clients/bjbecker/huggins/>.

Beckers, J.M., (1993) Adaptive Optics for Astronomy: Principles, Performance, and Applications, *Ann. Rev. Astron. Astrophys.*, **31**, 13 – 62.

Becklin, E.E. & G. Neugebauer (1968) Infrared Observations of the Galactic Center, *Astrophys. J.*, **145**, 145 – 161.

Becklin, E.E. & B. Zuckerman (1988) A Low-Temperature Companion to a White Dwarf Star, *Nature*, **336**, 656 – 658.

Beckman, J.E. & A.F.M. Moorwood (1979) Infrared Astronomy, *Rep. Prog. Phys.*, **42**, 87 – 157.

Beichman, C.A. (1987) The IRAS View of the Galaxy and the Solar System, *Ann. Rev. Astron. Astrophys.*, **25**, 521 – 563.

Beichman, C.A. (1988) The Infrared Universe Revealed by IRAS, *Astrophys. Lett. & Comm.*, **27**, 67 – 88.

Beintema, D.A. (1979) Spline Approximation as a Data Processing Tool, in *Workshop on Image Processing in Astronomy: Proc. of the 5th Colloquium on Astrophysics*, G. Sedmak, M. Capaccioli & R.J. Allen (eds.), Pub. Osservatorio Astronomico di Trieste, 339 – 346.

Bély, P.-Y., C.J. Burrows & G.D. Illingworth (eds) (1990) *The Next Generation Space Telescope(NGST)* Proc. Workshop at the Space Telescope Science Institute.

Benjamin, R.A., E. Churchwell, B.I. Babler, T.M. Bania, D.P. Clemens, M. Cohen, J.M. Dickey, R. Indebetouw, J.M. Jackson, H.A. Kobulnicky, A. Lazarian, A.P. Marston, J.S. Mathis, M.R. Meade, S. Seager, S.R. Stolovy, C. Whatson, B.A. Whitney, M.J. Wolff & M.G. Wolfire (2003) GLIMPSE. I. An SIRTF Legacy Project to Map the Inner Galaxy, *Pub. Astron. Soc. Pac.*, **115**, 953 – 964.

Benjamin, R.A., E. Churchwell, B.L. Babler, R. Indebetouw, M.R. Meade, B.A. Whitney, C. Watson, M.G. Wolfire, M.J. Wolff, R. Ignace, T.M. Bania, S. Bracker, D.P. Clemens, L. Chomiuk, M. Cohen, J.M. Dickey, J.M. Jackson, H.A. Kobulnicky, E.P. Mercer, J.S. Mathis, S.R. Stolovy, & B. Uzpen (2005) First GLIMPSE Results on the Stellar Structure of the Galaxy, *Astrophys. J.*, **630**, L149 – L152.

Benson, J.A., N.H. Turner & H.M. Dyck (1989) 10 μ m Speckle Interferometry Observations of Evolved Stars, *Astron. J.*, **97**, 1763 – 1765.

Bentley, A.F. (1989) *Study of the Infrared Celestial Background*, AFOSR-TR-89-0318, ADA205649.

Bernstein, R.A., W.L. Freeman & B.F. Madore(2002) The First Detection of Extragalactic Light at 3000, 5500 and 800 \AA , *Astronphys. J.* **571**, 56 – 84

Binney, J., O. Gerhard & D. Spergel (1997) The Photometric Structure of the Inner Galaxy, *Mon. Not. Roy. Astron. Soc.*, **288**, 365 – 374.

Blanchard M.B. & N.H. Farlow (1966) Contamination Control During the Design, Fabrication, Test and Launch of an Upper Atmosphere Rocket Payload, *J. Contam. Control*, **5**, 22 – 30.

Blanchard, M.B., N.H. Farlow & G.V. Ferry (1967) Contamination vs. Micrometeorites from the 1965 Leonid Meteor Shower, *J. Contam. Control*, **6**, 135 – 145.

Blanchard, M.B., G.V. Ferry & N.H. Farlow (1968) Analyses of Particles on Surfaces Exposed to the 1965 Leonid Meteor Shower by the Luster Sounding Rocket, *J. Geophys. Res.*, **73**, 6347 – 6360.

Bland-Hawthorn, J. & M. Cohen (2003) A Large-Scale Bipolar Wind in the Galactic Center, *Astrophys. J.*, **582**, 246 – 256.

Blommaert, J., R. Siebenmorgen, A. Coulais, L. Metcalfe, M.-A. Miville-Deschénes, K. Okumura, S. Ott, A. Pollock, M. Sauvage & J-L. Starck (2003) *The ISO Handbook Volume II: CAM – The ISO Camera*, ESA SP-1262

Blouke, M.M., E.E. Harp, G.R. Jeffus & R.L. Williams (1972) Gain Saturation in Extrinsic Germanium Photoconductors Operating at Low Temperatures, *J. App. Phys.*, **43**, 188 – 194.

Bock, J.J., V.V. Hristov, M. Kawada, H. Matsuhara, T. Matsumoto, S. Matsuura, P.D. Mauskoff, P.L. Richards, M. Tanaka & A.E. Lange (1993) Observations of the [C II] 158 Micron Emission From the Diffuse Interstellar Medium at High Galactic Latitude, *Astrophys. J.*, **410**, L15 – L18.

Bock, J.J., M. Kawada, A.E. Lange, T. Matsumoto, K. Uemizu, T. Watabe, S.A. Yost, G.G. Fazio, W.J. Forrest, J.L. Pipher & S.D. Price (1998) Rocket-borne Instrument to Search for Infrared Emission from Baryonic Dark Matter in Galactic Halos, *Proc. SPIE*, **3354**, 1139 – 1149.

Bock, J.J., A.E. Lange, T. Matsumoto, P.B. Eisenhardt, P.B. Hacking & H.R. Schember (1994) NIFTE: The Near Infrared Faint-Object Telescope Experiment, *Exper. Astronomy*, **3**, 1 – 4.

Boggess, N.W., J.C. Mather, R. Weiss, C.L. Bennett, E.S. Cheng, E. Dwek, S. Gulkis, M.G. Hauser, M.A. Janssen, T. Kelsall, S.S. Meyer, S.H. Moseley, T.L. Murdock, R.A. Shafer, R.F. Silverberg, G.F. Smoot, D.T. Wldinson & E.L. Wright (1992) The COBE Mission: Its Design and Performance Two Years After Launch, *Astrophys. J.*, **397**, 420 – 429.

Boisvert, J.C., J.D. Merriam, D.L. Stierwalt, R.K. Bentley & M.H. Sweet (1992) Spectral Effect on Bulk Photoconductors Operated at Cryogenic Temperatures, *Proc. SPIE*, **1686**, 204 – 215.

Bontekoe, Tj.R., D.J.M. Kester, A.R.W. de Jonge, P.R. Wesselius & S.D. Price (1991) Image Construction from the IRAS Survey, *Astron. Astrophys.*, **248**, 328 – 336.

Bontekoe, Tj.R., E. Koper, D.J.M. Kester (1994) Pyramid Maximum Entropy Images of IRAS Survey Data, *Astron. Astrophys.*, **284**, 1037 – 1053.

Borgman, J., J. Koornneef & J. Slingerland (1970) Infra-Red Photometry of a Heavily Reddened Cluster in Ara, *Astron. Astrophys.*, **4**, 248 – 252.

Bottema, M., W. Plummer & J. Strong (1964) Water Vapor in the Atmosphere of Venus, *Astrophys. J.*, **139**, 1021 – 1022.

Boulanger, F., A. Abergel, D. Cesarsky, J.P. Bernard, M.-A. Miville-Deschénes, E. Verstraete & W.T. Reach (2000) Small Dust Particles Seen by ISO, *ISO beyond Point Sources: Studies of Extended Infrared Emission*, L.J. Laureijs, K. Leech & M.F. Kessler (eds), ESA **SP-455**, 91 – 98.

Boulanger, F. & M. Péault (1987) Diffuse Infrared Emission from the Galaxy. I. Solar Neighborhood *Astrophys. J.*, **330**, 964 – 985.

Bowell, E., R.L. Millis, E.W. Dunham, B.W. Koehn & B.W. Smith (2007) Searching for NEOs using Lowell Observatory's Discovery Channel Telescope (DCT), *IAU Symp.*, **236**, 363 – 370.

Boys, C.V. (1890) On the Heat Radiation of the Moon and Stars. *Proc. Roy. Soc.*, **47**, 480 – 499.

Boys, C.V. (1895) On the Newtonian Constant of Gravitation, *Phil. Trans. Roy. Soc of London*, **186**, 1 – 72.

Brancazio, P.J. & A.G.W. Cameron (1968) *Infrared Astronomy*, Gordon and Breach, NY.

Brashear, R. (1990) A Trustworthy Instrument: Langley and the Bolometer, *Bull. Amer. Astron. Soc.*, **22**, 1224.

Brashear, R. (1991) Feeling the Heat: The Early Years of Infrared Astronomy, *Pub. Astron. Soc. Pac.*, **103**, 1117.

Brashear, R. (1992) Physicists and Radiometers: The Early History of Infrared Astronomy (1860 – 1960), *Bull. Amer. Astron. Soc.*, **23**, 871.

Briggs, R.E. (1962) Steady-State Space Distribution of Meteoric Particles under the Operation of the Poynting-Roberson Effect, *Astron. J.*, **67**, 710 – 723.

Briotta, Jr., D.A. (1976) *Rocket Infrared Spectroscopy of the Zodiacal Dust Cloud*, Ph.D. Thesis, Cornell Univ.

Briotta, Jr., D.A., J.L. Pipher & J.R. Houck (1976) *Rocket Infrared Spectroscopy of the Zodiacal Dust Cloud*, AFGL-TR-76-0236. ADA034054

Brown, C.W. & D.R. Smith (1990) High-Resolution Spectral Reflection Measurements on Selected Optical-Black Coatings in the 5 – 20 μm Region, *Proc. SPIE*, **1331**, 210 – 240.

Brown, L. (1960) *The Threshold of Space 1945 – 1959*, USAF History Division Liaison Office

Brown, P., R.E. Spalding, D.O. ReVelle, E. Tagliaferri & S.P. Worden (2002) The Flux of Small Near-Earth Objects Colliding with the Earth, *Nature*, **420**, 294 – 296.

Bruntt, H. & D.L. Buzasi (2006) High Precision Photometry with the WIRE Satellite, *Mem. Soc. Astron. Italiana*, **77**, 278 – 281.

Buffington, A., M.M. Bisi, J.M. Clover, P.P. Hick, B.V. Jackson, T.A. Kuchar & S.D. Price (2009) Measurements of the Gegenschein Brightness from the Solar Mass Ejection Imager (SMEI), *Icarus*, **203**, 124 – 133.

Burdick, S.V., J. Chalupa, W.K. Cobb, C.L. Hamilton & T.L. Murdock (1994) *Zodiacal Light Data Investigation*, PL-TR-94-2275, ADA310084.

Burgdorf, M.J., M. Cohen, J.G. Ingalls, S. Ramirez, J. Rho, S.R. Stolovy, S.J. Carey, S.B. Fajardo-Acosta, W.J. Glaccum, G. Helou, D.W. Hoard, J. Karr, P.J. Lowrance, J. O'Linger, D.L. Padgett, W.T. Reach, L.M. Rebull, J.R. Stauffer & S. Wachter (2005) The Galactic First-Look Survey with the Spitzer Space Telescope, *Adv. Space Res.*, **26**, 1050 – 1056.

Burgdorf, M.J., M. Cohen, S.D. Price, S. Ott, M.P. Egan, T. deGraauw, R.F. Shipman, S. Ganesh, C. Alard & E. Schuller (2000) A Survey of Selected Areas in the Galactic Plane with ISOCAM, *Astron. Astrophys.*, **360**, 111 – 119.

Burke, B.E., J.L. Tonry, M.J. Cooper, P.E. Doherty, A.H. Loomis, D.J. Young, T.A. Lind, P. Onaka, D.J. Landers, P.J. Daniels & J.I. Daneu (2007) Orthogonal Transfer Arrays for the Pan-STARRS Gigapixel Camera, *Proc. SPIE*, **6501**, 6501-1 – 9.

Burnup, J. & R. Canterna (1991) A Comparison of the Major IRAS Populations in the Galactic Plane, *Bull. Amer. Astron. Soc.*, **23**, 1331.

Byard, P.L. & R.E. Roll (1965) Temperature Measurements in Shock Heated Gasses, *J. Quant. Spec. Rad. Transfer.*, **5**, 715 – 722.

Byard, P.L., R.W. Roll & A. Slettebak, (1963) *The Design and Construction of a Luminous Shock Tube for Spectroscopic Investigations of High temperature Gasses: Preliminary Results for some Elements of Astrophysical Interest*, AFCRL-63-252. AD0602077.

Cabrera-Lavers, A., S. Bilir, S. Ak, E. Yas & M. Lopez-Corredoira (2007) Estimation of Galactic Model Parameters in High Latitudes with 2MASS, *Astron. Astrophys.*, **464**, 565 – 571.

Cabrera-Lavers, A. & F. Garzón (2003) Correlation between 2MASS and DENIS Data, *Astron. Astrophys.*, **403**, 383 – 387.

Cabrera-Lavers, A., F. Garzón, P.L. Hammersley, B. Vicente & C. González-Fernández (2006) A Deep Multi-Colour NIR Survey of the Galactic Plane, *Astron. Astrophys.*, **458**, 371 – 385.

Caledonia, G.F., R.E. Murphy, R.M. Nadile & A.J. Ratkowski (1995) Analysis of Auroral Infrared Emission Observed During the ELIAS Experiment, *Ann. Geophysicae*, **13**, 247 – 252.

Cambrésy, L., W.T. Reach, C.A. Beichman & T.H. Jarrett (2001) The Cosmic Diffuse Infrared Background at 1.25 and 2.2 Microns Using DIRBE and 2MASS: A Contribution not due to Galaxies, *Astrophys. J.*, **555**, 563 – 571.

Cameron, R.M., M. Bader & R.W. Mobley (1971) Design and Operation of the NASA 91.5-cm Airborne Telescope, *App. Opt.*, **10**, 2011 – 2015.

Campbell, Jr., L. & J.A. Hynek (1957) Visual Observations of Alpha One made by Moonwatch Stations During the Lifetime of the Object, *SAO Special Report*, **6**.

Campens, Jr., C.F., A.E. Cole, T.P. Condron, W.S. Ripley & N. Sissenwine (1957) *Handbook of Geophysics for Air Force Designers. First Edition*. ADA955708.

Cao, Y., S. Terebey, T.A. Prince & C. Beichman (1997) The High Resolution IRAS Galaxy Atlas, *Astrophys. J. Supp.*, **111**, 387 – 408

Carbary, J.F., E.H. Darlington, T.J. Harris, P.J. McEvaddy, M.J. Mayr, K. Peacock, C.-I. Meng (1994) Ultraviolet and Visible Imaging and Spectrographic Imaging Instruments, *App. Opt.*, **33**, 4201 – 4213.

Carbary, J.F., D. Morrison, G.J. Romick & J.-H. Yee (2003) Leonid Meteor Spectrum from 110 to 860 nm, *Icarus*, **131**, 223 – 234.

Carey, S.J., F.O. Clark, M.P. Egan, S.D. Price, R.F. Shipman & T.A. Kuchar (1998) The Physical Properties of the *Midcourse Space Experiment* Galactic Infrared-Dark Clouds, *Astrophys. J.*, **508**, 721 – 728.

Carey, S.J., P.A. Feldman, R.O. Redman, M.P. Egan, J.M. MacLeod & S.D. Price (2000) Submillimeter Observations of MSX Galactic Infrared Dark Clouds, *Astrophys. J.*, **543**, L157 – L161.

Carey, S.J., A. Noriega-Crespo, D.R. Mizuno, S. Shenoy, R. Paladini, K.E. Kraemer, S.D. Price, N. Flagey, E. Ryan, G. Ingalls, T.A. Kuchar, D. Gonçalves, R. Indebetouw, N. Billot, F.R. Marleau, D.L. Padgett, M. Bebull, E. Bressert, B. Ali, S. Molinari, P.G. Martin, G.B. Berriman, F. Boulanger, W.B. Latter, M.-A. Miville-Deschénes, L. R. Shipman & L. Testi (2009) MIPS GAL: A Survey of the Inner Galactic Plane at 24 and 70 Microns, *Pub. Astron. Soc. Pac.*, **121**, 76 – 97.

Carnevalle, R.G., S.A. Chrest, R.D. Sarkesian & R.A. Skrivanik (1970) Rocket Sampling of a 1968 Noctilucent Cloud Display over Fort Churchill, Canada, *Space Research*, **X**, 337 – 344.

Carpenter, J.M. (2000) Color Transformations for the 2MASS Second Incremental Data Release, *Astron. J.*, **121**, 2851 – 2871.

Case, T.W. (1917) Notes on the Change of Resistance of Certain Substances by Light, *Phys. Rev.*, **9**, 289 – 292.

Cecil, T.E., J.W. Salisbury, L.M. Logan & G.R. Hunt (1973) *Celestial Infrared Calibration in the 8 – 14 μ m Region: Venus and Jupiter*, AFCRL-TR-73-0559. AD0772660.

Cellino, A., M. Di Martino, E. Dotto, P. Tanga, V. Zappalá, S.D. Price, M.P. Egan, E.F. Tedesco, A. Carusi, I. Boattini, P. Persi, K. Muinonen, A.W. Harris, M.M. Castronuovo, M. Baley, J. Lagerros, L. Bussolino, A. Ferri, P. Merlina, A. Mariani, S. Brogi, & T.L. Murdock (2000) Spaceguard-1: A Space-based Observatory for NEO Physical Characterisation & Discovery, *Proc. SPIE*, **4013**, 433 – 443.

Cellino, A., V. Zappalá & P. Farinella (1991) The Size Distribution of Main-Belt Asteroids from the IRAS Data. *Mon. Not. Roy. Astron. Soc.* **253**, 561 – 574.

Chambers, K.C. (2009) Pan-STARRS Telescope #1 Status and Science Mission, *Bull. Amer. Astron. Soc.*, **41**, 270.

Champetier, R.J. & R.P. Giguere (1982) Deterioration of Superpolished Metal Mirrors by Blue Haze, *Opt. Eng.*, **41**, 743 – 750.

Champion, K. (1995) *Early Years of Air Force Geophysics Research Contributing to Internationally Recognized Standard and Reference Atmospheres*, PL-TR-95-2164. ADA314770

Chan, K.-W., T.L. Roellig, T. Onaka, M. Mizutani, K. Okumura, I. Yamamura, T. Tanabé, H. Shibai, T. Nakagawa & H. Okuda (2001) Unidentified Infrared Emission Bands in the Diffuse Interstellar Medium, *Astrophys. J.*, **546**, 273 – 278.

Chan, K.-W., T.L. Roellig, T. Onaka, I. Yamamura & T. Tanabé (1998) The Nature of the Mid-Infrared Radiation in the Galactic Bulge from the Infrared Telescope in Space Observations, *Astrophys. J.*, **505**, L31 – L 34.

Chang, H. & S. Leonelli (2005a) Infrared Metaphysics: The Elusive Ontology of Radiation. Part 1, *Studies in History and Philosophy of Science*, **36**, 477 – 508.

Chang, H. & S. Leonelli (2005b) Infrared Metaphysics: Radiation and Theory Choice, Part 2. *Studies in History and Philosophy of Science*, **36**, 686 – 705.

Chapman, C.R. & J.W. Salisbury (1972) Comparison of Meteorite and Asteroid Spectral Reflectivities, *Icarus*, **19**, 507 – 522.

Chapman, J.C. (1981) Groundbased Infrared Measurements using the AMOS/MOTIF Facility, *Proc. SPIE*, **280**, 196 – 193.

Chernicharo, J. & J. Crovisier (2006) Water in Space: The Water World of ISO, *Space Sci. Rev.*, **119**, 29 – 69.

Chester, T. (1986) A Statistical Analysis and Overview of the IRAS Point Source Catalog, *Light on Dark Matter*, F.P. Israel (ed.) D.Reidel Pub., 3 – 22.

Chiu, K., X. Fan, S.K. Leggett, D.A. Golimowski, W. Zheng, T.R. Geballe, D.P. Schneider & J. Brinkmann (2006) Seventy-One New L and T Dwarfs from the Sloan Digital Sky Survey, *Astron. J.*, **131**, 2722 – 2736.

Churchwell, W., M.S. Povich, D. Allen, M.G. Taylor, M.R. Meade, B.L. Babler, R. Indebetouw, C. Watson, B.A. Whitney, M.G. Wolfire, T.M. Bania, R.A. Benjamin, D.P. Clemens, M. Cohen, C.J. Cyganowski, J.M. Jackson, H.A. Kobulnicky, J.S. Mathis, E.P. Mercer, S.R. Stolovy, B. Uzpen, D.F. Watson & M.J. Wolff (2006) The Bubbling Galactic Disk, *Astrophys. J.*, **649**, 759 – 778.

Churchwell, E. D.F. Watson, M.S. Povich, M.G. Taylor, B.L. Babler, M.R. Meade, R.A. Benjamin, R. Indebetouw & B.A Whitney (2007) The Bubbling Galactic Disk. II. The Inner 20°, *Astrophys. J.*, **679**, 428 – 441.

Clark, F.O., M.V. Torbett, A.A. Jackson, S.D. Price, J.P. Kennealy, P.V. Noah, G.A. Glaudell & M. Cobb (1993) The Out-of-Plane Distribution of Zodiacal Dust Near the Earth, *Astron. J.*, **105**, 976 – 979.

Cobb, W.K., S.V. Burdick & T.L. Murdock (1993) *Zodiacal Light Data Investigation. Interim Results for the Earthlimb Clutter Experiment*, PL-TR-93-2179. ADA274461

Coblentz, W.W. (1915) Radiometric Measurements on 110 Stars with the Crossley Reflector, *Lick Obs. Bull.*, **266**, 104 – 123.

Coblentz, W.W. (1922) The Effective Temperatures of Stars as Estimated from the Energy Distributions in the Complete Spectrum, *Proc. Natl. Acad. Sci.*, **8**, 49 – 53.

Code, A.D., (1960) Stellar Astronomy from a Space Vehicle, *Astron. J.*, **65**, 278 – 284.

Cohen, M. (1973) An Unusual Infrared Source near the Rosette Nebula, *Astrophys. J.*, **185**, L75 – L78.

Cohen, M. (1975) Optical Identifications of AFCRL Rocket Infrared Sources, *Astron. J.*, **80**, 125 – 174.

Cohen, M. (1993) A Model of the 2 – 35 μ m Point Source Infrared Sky, *Astron. J.*, **105**, 1860 – 1879.

Cohen, M. (1994) Powerful Model for the Point Source Sky: Far-Ultraviolet and Enhanced Mid-Infrared Performance, *Astron. J.*, **107**, 582 – 593.

Cohen, M. (1995) The Displacement of the Sun from the Galactic Plane using IRAS and Faust Source Counts, *Astrophys. J.*, **444**, 874 – 878.

Cohen, M (2009) Absolute Diffuse Calibration of MIPS24 from a Mid-Infrared Study of H II Regions, *Astron. J.*, **137**, 3449 – 3454.

Cohen, M. C.M. Anderson, A. Cowley, G.V. Coyne, W. Fawley, T.R. Gull, E.A. Harlan, G.H. Herbig, F. Holden, H.S. Hudson, R.O. Jakoubek, H.M. Johnson, K.M. Merrill, F.H. Schiffer, B.T. Soifer & B.Zuckerman (1975) The Peculiar Object HD 44179 (“The Red Rectangle”), *Astrophys. J.*, **196**, 179 – 189.

Cohen, M. & M.J. Barlow (1973) Infrared Observations of Two Symmetric Nebulae, *Astrophys. J.*, **185**, L37 – L40.

Cohen, M. & A.J. Green (2001) Extended Galactic Emission at $l = 312^\circ$: A Comparison of Mid-Infrared and Radio Continuum (843 MHz) Images, *Mon. Not. Roy. Astron. Soc.*, **325**, 331 – 344.

Cohen, M., A.J. Green, M.R. Meade, B. Babler, R. Indebetouw, B.A. Whitney, C. Watson, M. Wolfire, M.J. Wolff, J.S. Mathis & E.B. Churchwell (2007) Absolute Diffuse Calibration of IRAC Through Mid-Infrared and Radio Study of HII Regions, *Mon. Not. Roy. Astron. Soc.*, **374**, 979 – 998.

Cohen, M., P.L. Hammersley & M.P. Egan (2000) Radiometric Validation of the Midcourse Space Experiment’s (MSX) Point Source Catalogs and the MSX Properties of Normal Stars, *Astron. J.*, **120**, 3362 – 3370.

Cohen, M., D.E. Schwartz, A. Chokshi & R.G. Walker (1987) IRAS colors of normal stars *Astron. J.*, **93**, 1199 – 1219.

Cohen, M. & R.G. Walker (2002) *IRAS Low Resolution Spectra of Asteroids*, Tech Report VRISV-1140-001.

Cohen, M., R.G. Walker, M.J. Barlow & J.R. Deacon (1992) Spectral Irradiance Calibration in the Infrared. I. Ground Based and IRAS Broadband Calibration, *Astron. J.*, **104**, 1650 – 1657.

Cohen, M., R.G. Walker, B. Carter, P. Hammersley & M. Kidger (1999) Spectral Irradiance Calibration in the Infrared. X. A Self-Consistent Radiometric All-Sky Network of Absolutely Calibrated Stellar Spectra, *Astron. J.*, **117**, 1864 – 1889.

Cohen, M., R.G. Walker, S. Jayaraman, E. Barker & S.D. Price (2001) Spectral Irradiance Calibration in the Infrared. XII. Radiometric Measurements from the Midcourse Space Experiment (MSX), *Astron. J.*, **121**, 1180 – 1191.

Cohen, M., R.G. Walker & F.C. Witteborn (1992) Spectral Irradiance Calibration in the Infrared. II. α Tau and the Recalibration of the IRAS Low Resolution Spectrometer, *Astron. J.*, **104**, 2030 – 2044.

Cohen, M., F.C. Witteborn, J.D. Bregman, D.H. Wooden, A. Salama & L. Metcalfe (1996) Spectral Irradiance Calibration in the Infrared. VI. 3 – 35 μ m Spectra of Three Southern Standard Stars, *Astron. J.*, **112**, 241 – 251.

Cohen, M., F.C. Witteborn, R.G. Walker, J. Bregman & D.H. Wooden (1995) Spectral Irradiance Calibration in the Infrared. IV. 1.2 – 35 μ m Spectra of Six Standard Stars, *Astron. J.*, **110**, 275 – 289.

Cole, A.A. & M.D. Weinberg (2002) An Upper Limit to the Age of the Galactic Bar, *Astrophys. J.*, **574**, L43 – L46.

Conrad, A.G. & W.R. Irace (1984) The First Orbiting Astronomical Infrared Telescope System – Its Development and Performance, *Proc SPIE*, **445**, 232 – 243.

Cornell, J. (1975) The Moonwatch Era Ends, *Sky and Tel.*, **50**, 160.

Coulais, A. & A. Abergel (2000) Transient Correction of the LW-ISOCAM data for Low Contrasted Radiation, *Astron. Astrophys. Supp.*, **141**, 533 – 544.

Cox, P., E. Krugel & P.G. Mezger (1986) Principal Heating Sources of Dust in the Galactic Disk, *Astron. Astrophys.* **155**, 380 – 396.

Crawford, M.K., A.G.G. Tielens & L.A. Allamandola (1985) Ionized Polycyclic Aromatic Hydrocarbons and the Diffuse Interstellar Bands, *Astrophys. J.*, **293**, L45 – L48.

Cunniff, C.V. (1978), AFGL Infrared Survey Experiments Cleaning Procedures, *Proc. USAF/NASA International Spacecraft Contamination Conference*, AFM-TR-78-190/NASA-CP-2039, 880 – 898. ADA070386

Danielson, R.E., J.E. Gaustad, M. Schwarzschild, H.F. Weaver & N.J. Woolf (1964) Mars Observations from Stratoscope II, *Astron. J.*, **69**, 344 – 352.

Dartois, E. (2005) The Ice Survey Opportunity of ISO, *Space Sci. Rev.*, **119**, 293 – 310.

Davies, J.K. (1997) *Astronomy from Space: The Design and Operation of Orbiting Observatories*, Wiley & Sons in associated with Praxis Pub.

Day, D.A. (2000) *Lightning Rod – A History of the Air Force Chief Scientist's Office*, Chief Scientist's Office, US Air Force, Wash. DC.

Dean, D.A., E.R. Huppi, D.R. Smith, R.M. Nadile & D.K. Zhou (1994) Space Shuttle Observations of Collisionally Excited Outgassed Water Vapor, *Geophys. Res. Lett.*, **29**, 609 – 612.

Delfosse, X., C.G. Tinney, T. Forveille, N. Epcstein, E. Bertin, J. Borsenberger, E. Copet, B. de Batz, P. Fouqué, S. Kimswenger, T. Le Bertre, F. Lacombe, D. Rouan & D. Tiphène (1997) Field Brown Dwarfs found by DENIS, *Astron. Astrophys.*, **327**, L25 – L28.

De Jonge, A.R.W., P.R. Wesselius, R.M. van Hees & B. Viersen (1992), Detecting Orbital Debris with the IRAS Satellite, *ESA Journal*, **16**, 13 – 21.

Dermott, S.F., R.S. Gomes, D.D. Durda, B.Å.S. Gustafson, S. Jayaraman, Y.L. Xu & P.D. Nicholson (1992) Dynamics of Zodiacal Light, *IAU Symp* **152**, 333 – 347.

Dermott, S.F., S. Jayaraman, Y.L. Xu & J.C. Liou (1994) IRAS Observations of a Ring around the Sun: Astreroidal Particles in Resonant Lock with the Earth, *Nature*, **369**, 719 – 723.

Dermott, S.F. & P.D. Nicholson (1989) IRAS Dust Bands and the Origin of the Zodiacal Cloud, *Highlights of Astron.*, **8**, 259 – 266.

Desért, F. X., F. Boulanger & S.N Shore (1986) Grain Temperature Fluctuations - A Key to Infrared Spectra, *Astron. Astrophys.*, **160**, 295 – 300.

Deul, E.R. & H.J. Walker (1989) Responsivity Variations in the IRAS Survey, *Astron. Astrophys. Supp.*, **81**, 207 – 214.

Deul, E.R. & R.D. Wolstencroft (1988) A Physical Model for Thermal Emission from the Zodiacal Dust Cloud, *Astron. Astrophys.*, **286**, 277 – 286.

deVaucouleurs, G. (1960) *Planetary Astronomy from Satellite Substitute Vehicles II, A Survey of Physical Problems of the Near Planets and a Review of Observational Techniques Applicable to Balloon-Borne Telescopes*, AF Missile Development Center Tech. Note AFMDC-59-37, 25 – 148. AD0233561

deVaucouleurs, G. & W.P. Pence (1978) An Outsider's View Of The Galaxy: Photometric Parameters, Scale Lengths, and Absolute Magnitudes of the Spheroidal And Disk Components of Our Galaxy, *Astron. J.*, **83**, 1163 – 1173.

DeVorkin, D.H. (1986) *Race to the Stratosphere: Manned Scientific Ballooning in America*, Springer-Verlag, NY.

DeVorkin, D.H. (1992) *Science with a Vengeance How the Military Created the US Space Science after World War II*, Springer-Verlag, NY.

DeVorkin, D.H. (1999) The Post War Society: Responding to New Patterns of Patronage, in *The American Astronomical Society's First Century*, D.H. DeVorkin (ed), 107 – 121, Amer. Inst. Phys.

deVries, C.P. & R.S. LePoole (1985) Comparison of the Optical Appearance and Infrared Emission of Some High Latitude Dust Clouds, *Astron. Astrophys.*, **145**, L7 – L9.

Diercks, A.H., J. Angione, C.W. Stubbs, K.H. Cook, E. Bowell, B.W. Koehn, W. Bruce, R.A. Nye & D. Dodgen (1995) 8-Megapixel Thermoelectrically Cooled CCD Imaging System, *Proc. SPIE.*, **2416**, 58 – 64.

Djorgovski, S. & C. Sosin (1989) The Warp of the Galactic Stellar Disk Detected in IRAS Source Counts, *Astrophys. J. Lett.*, **341**, L13 – L16.

Doel, R.W. (1996) *Solar System Astronomy in America: Communities, Patronage, and Interdisciplinary Science, 1920–1960*, Cambridge Univ. Press, NY.

Dollfus, A. (1964) Mesure de la Vapeur D'Eau dans les Atmosphères de Mars et de Venus, *Mem. Roy. Soc. Liege*, **IX**, 392 – 395.

Dow, K.L. (1992) *Earth Orbiting Objects Observed by the Infrared Astronomical Satellite*, M.Sci. Thesis, University of Arizona.

Dow, K.L., M.V. Sykes, F.J. Low & F. Vilas (1990) The Detection of Earth Orbiting Objects by IRAS, *Adv. Space Res.*, **10**, 381 – 384.

Draine, B.T. & N. Anderson (1985) Temperature Fluctuation and Infrared Emission from Interstellar Grains, *Astrophys. J.*, **292**, 494 – 499.

Dring, A.R., J. Murthy, M.M. Allen, J. Daniels, R.E. Newcomer, RC. Henry, L. Paxton, E. Tedesco & S.D. Price (1997) UVISI Observations of Orion Dust, *Bull Amer. Astron. Soc.*, **29**, 785.

Dubin, M. (1960) Meteorite Dust Measured from Explorer I, *Planet. Space Sci.*, **2**, 121 – 129.

Duffner, R.W. (2000) *Science and Technology The Making of the Air Force Research Laboratory*, Air Univ. Press, Maxwell AFB, Ala. ADA421978

Duley, W.W. & D. A. Williams (1986) PAH Molecules And Carbon Dust In Interstellar Clouds, *Mon. Not. Roy. Astron. Soc.*, **219**, 859 – 864.

Dumont, R. & F. Sanchez (1975) Zodiacial light photopolarimetry II. Gradients along the Ecliptic and the Phase Function of Interplanetary Matter, *Astron. Astrophys.*, **38**, 405 – 412.

Dwek, E., R.G. Arendt & F. Kennrich (2005) The Near-Infrared Background: Interplanetary Dust or Primordial Stars?, *Astrophys. J.*, **635**, 784 – 794.

Eaton, N., D.J. Adams & A.B. Giles (1984) The 2.2 μm Stellar Distribution in the Galactic Plane, *Mon. Not. Roy. Astron. Soc.*, **208**, 241 – 251.

Eddy, J.A. (1972) Thomas A. Edison and Infrared Astronomy, *J. History Astron.*, **3**, 165 – 187.

Edison, T.A. (1878) On the Use of the Tasimeter for Measuring the Heat of Stars and the Sun's Corona, *Amer. J. Sci.*, **117**, 52 – 54.

Egan, M.P., J.S. Clark, D.R. Mizuno, S.J. Carey, I.A. Steele & S.D. Price (2002) An Infrared Ring Nebula Around MSX 5CG358.5391+00.1305: The True Nature of Suspected Planetary Nebula Wray 17-96 Determined via Direct Imaging and Spectroscopy, *Astrophys. J.*, **572**, 288 – 299.

Egan, M.P., S.D. Price, M.M. Moshir, M. Cohen, E.F. Tedesco, T.L. Murdock, A. Zweil, S. Burdick, N. Bonito, G.M. Gugliotti & J. Duszlak (1999) *MSX Point Source Catalog Explanatory Guide*, AFRL-VS-TR-1999-1522. ADA381933

Egan, M.P., S.D. Price, D.R. Mizuno, S.J. Carey, C.O. Wright, C.W. Engelke, M. Cohen, G.M. Gugliotti, (2003) *The Midcourse space Experiment Point Source Catalog Version 2.3 Explanatory Guide*, AFRL-VS-TR-2003-1589. ADA418993

Egan, M.P., R.F. Shipman, S.D. Price, S.J. Carey, F.O. Clark & M. Cohen (1998) A Population of Cold Cores in the Galactic Plane, *Astrophys. J.*, **494**, L199 – L202.

Egan, M.P., S.D. Van Dyk & S. D. Price (2001) MSX, 2MASS and the LMC: A Combined Near- & Mid-Infrared View, *Astron. J.*, **122**, 1844 – 1860.

Elias, J.H. (1978a) 2.2-micron Field Stars at the North Galactic Pole, *Astron. J.*, **83**, 791 – 794.

Elias, J.H. (1978b) A Study of the IC 5746 Dark Cloud Complex, *Astrophys. J.*, **223**, 859 – 861.

Emberson, R.M. (1941) Radiometric Magnitudes of Some of the Brighter Stars, *Astrophys. J.*, **94**, 427 – 435.

Emery, R. (1982) Infrared Space Observatory (ISO): An ESA Study of a Cryogenically-Cooled Telescope in Space for Infrared Astronomy, in *The Scientific Importance of Submillimetre Observations*, T. de Graauw & G.T. Duc (eds.), Proc. May, 1982 Workshop, 81 – 88.

Engelke, C.W., K.E. Kraemer & S.D. Price (2004) A Uniform Database of 2.2 – 16.5 μm Spectra from the ISOCAM CVF Spectrometer, *Astrophys. J. Supp.*, **150**, 343 – 365.

Engelke, C. W., S. D. Price & K. E. Kraemer (2006) Spectral Irradiance Calibration in the Infrared. XVI. Improved Accuracy in the Infrared Spectra of Secondary and Tertiary Standard Calibration Stars, *Astron. J.*, **132**, 1445 – 1463.

Engelke, C. W., S. D. Price & K. E. Kraemer (2010) Spectral Irradiance Calibration in the Infrared. XVII. Zero Magnitude Broadband Flux Reference for Visible to Infrared Photometry, *Astron. J.*, (submitted).

Epcstein, N., B. de Batz, L. Capoani, L. Chevallier, E. Copet, P. Fouqué, F. Lacombe, T. Le Bertre, S. Pau, D. Rouan, S. Ruphy, G. Simon, D. Tiphéne, W. B. Burton, E; Bertin, E. Deul, H. Habing, J. Borsenberger, M. Dennefeld, F. Guglielmo, C. Loup, G. Mamon, Y. Ng, A. Omont, L. Provost, J.-C. Renault, F. Tanguy, S. Kimeswenger, C. Kienel, F. Garzón, P. Persi, M. Ferrari-Toniolo, A. Robin, G. Paturel, I. Vauglin, T. Forveille, X. Delfosse, J. Hron, M. Schultheis, I. Appenzeller, S. Wagner, L. Balazs, A. Holl, J. Lepine, P. Boscolo, E.

Picazzio, P.-A. Duc & M.-O. Mennessier (1997) The Deep Near-Infrared southern Sky Survey (DENIS), *Messenger*, **87**, 27 – 34.

Epchtein, N., B. de Batz, E. Copet, P. Fouqué, F. Lacombe, T. Le Bertre, G. Mamon, D. Rouan, D. Tiphéne, W.B. Burton, E. Deul, H. Habing, J. Borsenberger, M. Dennefeld, A. Omont, J.C. Renault, B. Rocca Volmerange, S. Kimeswenger, I. Appenzeller, R. Bender, T. Forveille, F. Garzón, J. Hron, P. Persi, M. Ferrari-Toniolo & I. Vauglin (1994) DENIS: A Deep Near-Infrared Survey of the Southern Sky, *Astrophys. & Space Sci.*, **217**, 3 – 9.

Epchtein, N., T. LeBerte, J.R.D. Lepine, P. Marques Dos Santos, O.T. Matsuura & E. Picazzio (1987) Valinhos 2.2 μ m Survey of the Southern Galactic Plane. II Near-IR Photometry, IRAS Identifications and Nature of the Sources, *Astron. Astrophys. Supp.*, **71**, 39 – 55.

Epchtein, N., O.T. Matsuura, M.A. Braz, J.R.D. Lepine, E. Picazzio, P. Marques Dos Santos, P. Boscolo, T. Le Bertre, A. Roussel & P. Turon (1985) Valinhos 2.2 Micron Survey of the Southern Galactic Plane Positions and Infrared Photometry of 338 Sources, *Astron. Astrophys.*, **61**, 203 – 210.

Epstein, P.S. (1929) What is the Moon Made of?, *Phys. Rev. Ser 2*, **33**, 269.

Evans, A., R. Hermann, R. Canterna & J.A. Hackwell (1989) The Infrared Source Counts in the Galactic Thin Disk Population from High-Spatial Resolution IRAS Images. *Bull. Amer. Astron. Soc.*, **21**, 1126.

Evans, D.C. & L. Dunkelman (1969) Airglow and Star Photographs in the Daytime from a Rocket, *Science*, **164**, 191 – 193.

Farlow, N.H. (1968) Electron Microscope Studies of Particles on Sampling Surfaces Recovered from Space with Sounding Rockets, *J. Geophys. Res.*, **73**, 4363 – 4361.

Farlow, N.H., M.B. Blanchard & G.V. Ferry (1966) Sampling with a Luster Sounding Rocket during a Leonid Meteor Shower, *J. Geophys. Res.*, **71**, 5689 – 5693.

Farlow, N.H., M.B. Blanchard & G.V. Ferry (1970) Microparticle Collection Experiments during the '66 Orionid and Leonid Meteor Showers, *J. Geophys. Res.*, **75**, 859 – 870.

Fazio, G.G., J.L. Hora, L.E. Allen, M.L.N. Ashby, P. Barmby, L.K. Deutsch, J.-S. Huang, S. Kleiner, M. Marengo, S.T. Megeath, G.J. Melnick, M.A. Pahre, B.M. Patten, J. Polizotti, H.A. Smith, R.S. Taylor, Z. Wang, S.P. Willner, W.F. Hoffmann, J.L. Pipher, W.J. Forrest, C.W. McMurtry, C.R. McCreight, M.E. McKelvey, R.E. McMurray, D.G. Koch, S.H. Moseley, R.G. Arendt, J.E. Mentzell, C.T. Marx, P. Losch, P. Mayman, W. Eichhorn, D. Krebs, M. Jhabvala, D.Y. Gezari, D.J. Fixsen, J. Flores, K. Shakoorzadeh, R. Jungo, C. Hakun, L. Workman, G. Karpati, R. Kichak, R. Whitley, S. Mann, E.V. Tollestrup, P. Eisenhardt, D. Stern, V. Gorjian, B. Bhattacharya, S. Carey, B.O. Nelson, W.J. Glaccum, M. Lacy, P.J. Lowrance, S. Laine, W.T. Reach, J.A. Stauffer, J.A. Surace, G. Wilson, E.L. Wright, A. Hoffman, G. Domingo & M. Cohen (2004) The Infrared Array Camera (IRAC) for the Spitzer Space Telescope *Astrophys. J. Supp.*, **154**, 10 – 17.

Fazio, G.G., D.E. Kleinmann, R.W. Noyes, F.J. Low & M. Zelik, II (1975) A High Resolution Map of the W3 Region at Far Infrared Wavelengths, *Astrophys. J.*, **199**, L177 – L179.

Fechtig, H. (2001), Historical Perspectives, in *Interplanetary Dust*, E. Grün, B.Å.S. Gustofson & S. Dermott (eds), Springer-Verlag, NY, 1 – 56.

Feldman, P.D., D.P. McNutt & K. Shivanandan (1968) Rocket Observations of Bright Celestial Infrared Sources in Ursa Major, *Astrophys. J.*, **154**, L131 – L136.

Fellgett, P. B. (1951) An Exploration of Infra-Red Stellar Magnitudes Using the Photo-Conductivity of Lead Sulphide, *Mon. Not. Roy. Astron. Soc.*, **111**, 537 – 559.

Ferdman, S.C. & S.G. McCarthy (1981) SIRE – Transition from Free Flyer to Shuttle Sortie, *Proc. SPIE.*, **280**, 157 – 168.

Fixsen, D.J. E.S. Cheng, J.M. Gales, J.C. Mather, R.A. Shafer & E.L. Wright (1996) The Cosmic Microwave Background Spectrum from the Full COBE FIRAS Data Set, *Astrophys. J.*, **473**, 576 – 587.

Flagey, N., F. Boulanger, L. Verstraete, M.-A. Miville-Deschénes, A. Noriega Crespo & W.T. Reach (2006) Spitzer/IRAC and ISOCAM/CVF Insights on the Origin of the Near to Mid-IR Galactic Diffuse Emission, *Astron. Astrophys.*, **453**, 969 – 978.

Forrest, W.J., F.C. Gillett & W.A. Stein (1975) Circumstellar Grains and Intrinsic Polarization of Starlight, *Astrophys. J.*, **195**, 423 – 440.

Fossett, Jr., M.R. (1976) *Demise of the Air Force In-House Basic Research Laboratories*, Air War College Air University Report No. 5911. ADB010343

Fouks, B. (1993) Nonstationary Processes in Extrinsic Photoconductors, *Proc. SPIE.*, **1762**, 519 – 530.

Fraser, E.F., B.D. Green & R.R. O’Neil (1991) Infrared Emission from Electron Irradiated Upper Atmosphere Produced by the Excede: Spectral Experiment, *J. Geophys. Res.*, **96**, 19,491 – 19,497.

Frazier, E.N. (1977a) Infrared Radiation of the Zodiacal Light, *Proc. SPIE*, **124**, 139 – 146.

Frazier, E.N. (1977b) *Infrared Radiation of the Zodiacal Light*, Aerospace report TOR-0076(2288-01)-1.

Frazier, E.N., D.J. Boucher & G.F. Mueller (1987) A Self Consistent Model of the Zodiacal Light Radiance, *Proc. SPIE*, **819**, 2 – 6.

Freudenreich, H. (1996) The Shape and Color of the Galactic Disk, *Astrophys. J.*, **492**, 495 – 510.

Freudenreich, H.T., G.B. Berriman, E. Dwek, M.G. Hauser, T. Kelsall, S.H. Moseley, R.F. Silverberg, T.J. Sodroski, G.N. Toller & J.L. Weiland (1994) DIRBE Evidence for a Warp in the Interstellar Dust Layer and Stellar Disk of the Galaxy, *Astrophys. J.*, **429**, L69 – L72.

Friedlander, M.W., J.H. Goebel & R.D. Joseph (1974) Detection of New Celestial Objects at Far-Infrared Wavelengths, *Astrophys. J.*, **194**, L5 – L8.

Friedlander, M.W. & T.D. Joseph (1970) Detection of Celestial Sources at Far-Infrared Wavelengths, *Astrophys. J.*, **162**, L87 – L91.

Furniss, I., R.E. Jennings & A.F.M. Moorwood (1972) Detection of Far-Infrared Astronomical Sources, *Astrophys. J.*, **176**, L105 – L108.

Futrell, R.G. (1971) *Ideas, Concepts, Doctrine: A History of Basic Thinking in the United States Air Force 1907 – 1964, Volume I*. ADA006418

Gaposchkin, E.M. & R.J. Bergemann (1995) *Infrared Detections of Satellites by IRAS*, LL Tech. Report 1018, ESC-TR-94-116.

Gardner, J.P. (2008) The Scientific Capabilities of the James Webb Telescope, *Proc. SPIE*, **7010**, 70100K.

Gardner, J.P., J.C. Mather, M. Champin, R. Doyon, M.A. Breenhouse, H.B. Hammel, J.B. Hutchings, P. Jakobsen, S.J. Lilly, K.S. Long, J.I. Lunine, M.J. McCaughrean, M. Mountain, J. Nela, G.H. Rieke, M.J. Rieke, H.-W. Rix, E.P. Smith, G. Sonneborn, M. Stiavelli, H.S.

Stockman, R.A. Windhorst & G.S. Wright (2006) The James Webb Space Telescope, *Space Sci. Rev.*, **123**, 485 – 606.

Garwood, R. & T.J. Jones (1987) Modeling the Milky Way in the Infrared, *Pub. Astron. Soc Pac.*, **99**, 453 – 460.

Garzón, F., P.L. Hammersley, T. Mahoney & X. Calbet (1993) A Two-micron Galactic Survey, *Mon. Not. Roy. Astron. Soc.*, **264**, 773 – 784.

Gautier, III, T.N., F. Boulanger, M. Péault & J.L. Puget (1992) A Calculation of Confusion Noise Due to Infrared Cirrus, *Astron. J.*, **103**, 1313 – 1324.

Gautier, III, T.N., M.G. Hauser, C.A. Beichman, F.J. Low, G. Neugebauer, M. Rowan-Robinson, H.H. Aumann, N. Boggess, J.P. Emerson, S. Harris, J.R. Houck, R.E. Jennings & P.L. Marsden (1984) IRAS Images of the Galactic Center. *Astrophys. J.*, **278**, L57 – L58.

Gehrels, T. (1984) Fundamental Studies of Asteroids. *Bull. Astron. Soc. India.*, **12**, 16 – 39.

Gehrz, R.D., E.E. Becklin, I. de Pater, D.F. Lester, T.L. Rollig & C.E Woodward (2009) A New Window on the Cosmos: The Stratospheric Observatory for Infrared Astronomy (SOFIA), *Adv. Space Res.*, **44**, 413 – 432.

Gehrz, R.D. & J.A. Hackwell (1976) A Search for Anonymous AFCRL Infrared Sources, *Astrophys. J.*, **206**, L161 – L154.

Georjian, V., E.L. Wright & R. Chary (2000) Tentative Detection of the Cosmic Infrared Background at 2.2 and 3.5 μm using Ground-Based and Space-Based Observations, *Astrophys. J.*, **536**, 550 – 560.

Giacconi, R. (2005) An Education in Astronomy, *Ann. Rev. Astron. Astrophys.*, **43**, 1 – 30.

Giacconi, R., H. Gursky, F.R. Paolini & B.B. Rossi (1962) Evidence for X-Rays from Sources Outside the Solar System, *Phys. Rev. Lett.*, **9**, 439 – 443.

Giard, M., F. Pajot, J.M. Lamarre, G. Serra & E. Caux (1989) The Galactic Emission in the 3.3 μm Aromatic Feature I - Observations, *Astron. Astrophys.*, **215**, 92 – 100.

Giese, R.H., B. Kneissel & U. Rittich (1986) The 3-Dimensional Models of the Zodiacal Dust Cloud: A Comparative Study, *Icarus*, **68**, 395 – 411.

Gifford, Jr., F. (1956) The Surface-Temperature Climate of Mars, *Astrophys. J.*, **123**, 154 – 161.

Gillespie, Jr., C.M. (1981) Kuiper Airborne Observatory – Space Science Platform, *Proc. SPIE.*, **265**, 1-7.

Gillett, F.C. (1986) IRAS Observations of Cool Excess Around Main Sequence Stars, in *Light on Dark Matter; Proc. First Infra-Red Astronomical Satellite Conf.*, F.P. Israel (ed.), D. Reidel Publishing., 61 – 69

Gillett, F.C., J.W. Forrest & K.M. Merrill (1973) 8-13 Micron Spectra of NGC 7027, BD +30 3639 and NGC 6572, *Astrophys. J.*, **183**, 87 – 93.

Gold, T. (1956) The Lunar Surface, *Mon. Not. Roy. Astron. Soc.*, **115**, 585 – 604.

Gold, T. (1965) The Moon's Surface, in *The Nature of the Lunar Surface*. W.N. Hess, D.H. Menzel & J.A. O'Keefe (eds) John Hopkins Press, Baltimore, MD, Section 5: 107 – 124.

Gonsalves, R.A. & H.M. Kao (1986) Maximum Entropy Image Restoration: Formulated as a Correction Term to the Inverse Filter Solution, *Proc. SPIE*, **697**, 357 – 363.

Gonsalves, R.A. & H.M. Kao (1987) An Entropy-Based Algorithm for Reducing Artifacts in Image Restoration, *Opt. Eng.*, **26**, 617 – 622.

Gonsalvas, R.A., J.P. Kennealy, R.M. Korte & S.D. Price (1990) FIER: A Filtered Entropy Approach to Maximum Entropy Image Restoration, in *Maximum Entropy and Bayesian Methods*, P.F Fougere (ed.), Kluwer Academic Press (Neth), 369 – 382.

Gonsalves, R.A., R.M. Korte & J.P. Kennealy (1987) Entropy-Based Image Restoration: Modifications and Additional Results, *Proc. SPIE*, **804**, 36 – 43.

Gonsalves, R.A., T.D. Lyons, S.D. Price, P.D. Levan & H.H. Aumann (1987) IRAS Image Reconstruction and Restoration, *Proc. SPIE*, **804**, 16 – 27.

Gonsalves, R.A. & P. Nisenson (1991) HST Image Processing: An Overview of Algorithms for Image Restoration, *Proc. SPIE*, **1567**, 294 – 307.

Good, J. (1994) Zodiacal Dust Cloud Modeling Using IRAS Data, *IRAS Sky Survey Atlas Explanatory Supp., Appen. G.*, S. Wheelock et al. (eds), JPL Pub. **94-11**.

Gorn, M.H. (ed), *Prophecy Fulfilled: (1994) "Toward New Horizons" and its Legacy*, Air Force History and Museums Program, Wash. DC. ADA 305 537

Gosnell, T.R., H. Hudson & R.C. Puetter (1979) Ground-Based Observations of Sources in the AFGL Infrared Sky Survey, *Astron. J.*, **84**, 538 – 547.

Grasdalen, G.L., R.D. Gehrz, J.A. Hackwell, M. Castelaz & C. Gullixson (1983) The Stellar Component of the Galaxy as Seen by the AFGL Infrared Sky Survey, *Astrophys. J. Supp.*, **53**, 413 – 457.

Greeb, M.E. & G.A. True (1973) Balloon Infrared Astronomy Platform (BIRAP) in *NASA Ames Res. Center Telescope Systems for Balloon-Borne Research*, 268 – 283. N7512735

Green, S.F., J.K. Davies, N. Eaton, B.C. Steward & A.J. Meadows (1985) The Detection of Fast-Moving Asteroids and Comets by IRAS, *Icarus*, **64**, 517 – 527.

Grün, E., H.A. Zook, H. Fechtig & R.H. Giese (1985) Collisional Balance of the Meteoritic Complex, *Icarus*, **62**, 244 – 272.

Gry, C., B. Swinyard, A. Harwood, N. Trams, S. Leeks, T. Lim, S. Sidher, C. Lloyd, S. Pezzuto, S. Molinari, R. Lorente, E. Caux, E. Polehampton, J. Chan, G. Hutchinson, T. Müller, M. Burgdorf & T. Grundy (2003) *The ISO Handbook Volume III: LWS – The Long Wavelength Spectrometer*, ESA SP – 1262.

Gunn, J.E., A. Walter, E.J. Mannery, J. Edward, R.E. Owen, C.L. Hull, R.F. Léger, L.N. Carey, G.R. Knapp, D.G. York, W.N. Boroski, S.M. Kent, R.H. Lupton, C.M. Rockosi, M.L. Evans, P. Waddell, J.E. Anderson, J. Annis, J.C. Barentine, L.M. Bartoszek, S. Bastian, S.B. Bracker, H.J. Brewington, C.I. Briegel, J. Brinkmann, Y.J. Brown, M.A. Carr, P.C. Czarapata, C.C. Drennan, T. Dombeck, G.R. Federwitz, B.A. Gillespie, C. Gonzales, S.U. Hansen, M. Harvanek, J. Hayes, W. Jordan, E. Kinney, M. Klaene, S.J. Kleinmann, R.G. Kron, J. Kresinski, G. Lee, S. Limmongkol, C.W. Lindenmeyer, D.C Long, C.L. Loomis, P.M. McGehee, P.M. Mantsch, E.H. Neilsen, Jr., R.M. Neswold, P.R. Newman, A. Nitta, J. Peoples, Jr., J.R. Pier, P.S. Prieto, A. Prosapio, C. Rivetta, D.P. Schneider, S. Snedden & S. Wang (2006) The 2.5 m Telescope of the Sloan Digital Sky Survey, *Astron. J.*, **131**, 2333 – 2359.

Gursky, H., R. Giacconi, F.R. Paolini & B.B. Rossi (1963) Further Evidence for the Existence of Galactic X-Rays, *Phys. Rev. Lett.*, **12**, 530 – 535.

Gush, H.P. (1981) Rocket Measurements of the Cosmic Background Submillimeter Spectrum, *Phys. Rev. Lett.*, **47**, 745 – 748.

Gwinn, C.M. (1985) *LAIRTS Pixel Formatter*, AFGL-TR-85-0192. ADA164512

Habing, H.J. (1986) The IRAS Two-Colour Diagram as a Tool for Studying Late Stages of Stellar Evolution, *Astron. Astrophys.*, **194**, 125 – 134.

Habing, H. J. (1988) IRAS Edge-On View Of Our Galaxy - The Disk, *Astron. Astrophys.*, **200**, 40 – 50.

Habing, H.J., F.M. Olnon, T. Chester, F.C. Gillett, M. Rowan-Robinson & G. Neugebauer (1985) Stars in the Bulge of our Galaxy Detected by IRAS, *Astron. Astrophys.*, **152**, L1 – L4.

Hacking, P., C. Lonsdale, T. Gautier, T. Herter, D. Shupe, G. Stacey, F. Fang, C. Xu, P. Grap, M. Werner, B. Soifer, H. Moseley & J. Houck (1999) The Wide-Field Infrared Explorer (WIRE) Mission, *Astron. Soc. Pac. Conf. Ser.*, **177**, 409 – 420.

Hahn, J.M., H.A. Zook, B. Cooper & B. Sunkara (2002) Clementine Observations of the Zodiacal Light and the Dust Content of the Inner Solar System, *Icarus*, **158**, 360 – 378.

Hall, Jr., F.F. (1961) Measurements of Stellar and Planetary Magnitudes in the Lead Sulfide Spectral Region, *Proc. Infrared Inf. Symp.*, **6**, 137 – 143.

Hall, Jr., F.F. (1964) An Infrared Stellar Mapping Program, *Mem. Roy. Soc. Liege*, **IX**, 432 – 459.

Hall, Jr., F.F. (1966) A Preliminary Report on Absolute Sky Radiance Measurements in the 1.2 – 3.2 μ Region, *Astron. J.*, **71**, 386.

Hall, Jr., F.F. (1967) *The Effects of Cirrus Clouds on Infrared Sky Radiance*, PhD Thesis, UCLA.

Hall, Jr., F.F. (1968a) The Effect of Cirrus Clouds on 8-13 Micrometer Infrared Sky Radiance, *App. Opt.*, **7**, 891 – 898.

Hall, Jr., F.F. (1968b) A Physical Mode of Cirrus 8-13-Micrometer Infrared Radiance, *App. Opt.*, **7**, 2264 – 2269.

Hall, Jr., F.F. & C.V. Stanley (1962) Infrared Satellite Radiometry, *App. Opt.*, **1**, 97 – 102.

Hammersley, P.L., F. Garzón, T. Mahoney & X. Calbet (1995) The Tilted Disc and Corrugations, *Mon. Not. Roy. Astron. Soc.*, **273**, 206 – 214.

Hapke, B. (2002) Bidirectional Reflectance Spectroscopy 5. The Coherent Backscatter Opposition Effect and Anisotropic Scattering, *Icarus*, **157**, 523 – 534.

Hapke, B. & A.S. Hale (2000) Theoretical Modeling of Radiation Transfer in Planetary Regoliths, *Astron. Soc. Pac. Conf. Series*, **106**, 213 – 219.

Harper, D.A. & F.J. Low (1971) Far-Infrared Emission from H II Regions, *Astrophys. J.*, **165**, L9 – L13.

Harris, A.S. (1998) A Thermal Model for Near-Earth Asteroids, *Icarus*, **131**, 291 – 301.

Harris, S. & M. Rowan-Robinson (1977) The Brightest Sources in the AFCRL Survey, *Astron. Astrophys.*, **60**, 405 – 412.

Harrison, D.C. & J.C. Chow (1996) The Space-Based Visible Sensor, *JHU APL Tech. Digest*, **17**, 226 – 235.

Harwit, M. (1981) *Cosmic Discoveries*, Basic Books.

Harwit, M. (2000) Instrumentation and Astrophysics: How Did We Get to be so Lucky?, *Astron. Soc. Pac. Conf. Ser.*, **195**, 3 – 10.

Harwit, M. (2001) Infrared/Submillimeter Astronomy: Are We Prepared for Success, in *The Promise of the Herschel Observatory*, ESA SP-460, 341 – 345.

Harwit, M. (2003) The Early Days of Infrared Space Astronomy, Ch. 14 in *The Century of Space Science*, Vol. I, J. Bleeker, J. Geiss & M.C.E. Huber (eds) Kluwer Academic Pub. (Neth.), 301 – 330.

Harwit, M. (2004) The Herschel Mission, *Adv. Space Res.*, **34**, 568 – 572.

Harwit, M., D.P. McNutt, K. Shivanandan & B.J. Zajac (1966) Results of the First Infrared Astronomical Rocket Flight, *Astron. J.*, **71**, 1026 – 1029.

Hauser, M.G. (1988) Models for Infrared Emission from Zodical Dust, *Lect. Notes in Phys.*, **297**, 27 – 38.

Hauser, M.G., R.G. Arendt, T. Kelsall, E. Dwek, N. Odegard, J.L. Weiland, H.T. Freudenreich, W.T. Reach, R.F. Silverberg, S.H. Moseley, Y.C. Pei, P. Lubin, J.C. Mather, R.A. Shafer, G.F. Smoot, R. Weiss, D.T. Wilkinson & E.L. Wright (1998) The COBE Diffuse Infrared Background Experiment Search for the Cosmic Infrared Background. I. Limits and Detections, *Astrophys. J.*, **508**, 25 – 43.

Hauser, M.G., F.J. Low, G.H. Rieke & S.D. Price (1976) *The AFCRL Sky Survey: Supplementary Report to the Joint Scientific Mission Definition Team for the Infrared Astronomical Satellite (IRAS)*, Internal Goddard Space Flight Center report.

Hayakawa, S. (1982) Infrared Telescope in Space – IRTS, *Adv. Space Res.*, **2**, 107 – 111.

Hayakawa, S., K. Ito, T. Matsumoto, H. Murakami & K. Uyama (1978) Near-Infrared Observations of the Galaxy in the Galactic Anticenter Direction, *Pub. Astron. Soc. Jap.*, **30**, 369 – 376.

Hayakawa, S., T. Matsumoto, H. Murakami, K. Uyama, T. Yamagami & J.A. Thomas (1979) Near IR Brightness of the Southern Galactic Plane, *Nature*, **279**, 510 – 512.

Hayakawa, S., T. Matsumoto, H. Murakami, K. Uyama, J.A. Thompson & T. Yamagami (1981) Distribution of Near-infrared Sources in the Galactic Disk, *Astron. Astrophys.*, **100**, 116 – 123.

Hayes, D.L. (1985) Stellar Absolute Fluxes and Energy Distributions from 0.32 to 4.0 Microns, *Proc. IAU Symp.*, **111**, 225 – 252.

Hearnshaw, J. (1994) Astronomy at the University of Canterbury Department of Physics and Astronomy and Mt John University Observatory—Annual Report 1992, *Quart. J. Roy. Astron. Soc.*, **35**, 123 – 128.

Hearnshaw, J. (1996) *The Measurements of Starlight: Two Centuries of Astronomical Photometry*, Cambridge Univ. Press.

Hearnshaw, J. (2005) A Brief History of Mt John – and a Tribute to Frank Bateson’s Involvement in Mt John’s Development, *Southern Stars, J. Roy. Astron. Soc. New Zealand*, **44**, 7 – 11.

Hegy, D (1985) *The Detection of Faint Space Objects with Solid State Image Detectors*, AFOSR-85-0095. ADA158594

Hegyi, D.J. (1989) *Observing Primeval Galaxies and Dark Matter with LAIRTS*, AFOSR-TR-89-0575. ADA208286

Helin, E.F., S.H. Pravdo, D.L. Rabinowitz & K.J. Lawrence (1997) Near-Earth Asteroid Tracking (NEAT) Program, *Ann. NY Acad. Sciences*, **822**, 6 – 25.

Helin, E.F. & E.M. Shoemaker (1979) The Palomar Planet-Crossing Asteroid Survey, 1973 – 1978, *Icarus*, **40**, 321 – 328.

Heinsheimer, T.F., L.H. Sweeney, F.F. Yates, S.P. Maran, J.R. Lesh & T.A. Nagy (1978) Development of the Equatorial Infrared Catalog from Satellite Data, *Proc. SPIE*, **156**, 87 – 92.

Heintz, J.F. (1972) CMP Flight Results and Sky Map, *Infrared Inf. Symp.*, **17**, 637 – 656.

Hemenway, C.L. & R.K. Soberman (1962), Studies of Micrometeorites Obtained from a Recoverable Sounding Rocket, *Astron. J.*, **67**, 256 – 266.

Henry, R.C. (1991) Ultraviolet Background Radiation, *Ann. Rev. Astron. Astrophys.*, **29**, 89 – 127.

Henry, R.C., J. Murthy, M. Allen, J. Daniels A.R. Dring, L.J. Paxton, E.F. Tedesco & S.D. Price (1996) UVISI Observations of the Small Magellanic Cloud, *Bull Amer. Astron. Soc.*, **28**, 1397.

Heras, A.M., R.F. Shipman, S.D. Price, Th. DeGraauw, H.J. Walker, M. Jourdain de Muizon, M.F. Kessler, T. Prusti, R. Waters, L. Decin & F. Vandenbussche (2002) Infrared Spectral Classification of Normal Stars, *Astron. Astrophys.*, **394**, 539 – 552.

Herschel, W. (1800a) Investigations of the Powers of the Prismatic Colours to Heat and Illuminate Objects; with Remarks, that Prove the Different Refrangibility of Radiant Heat. To which is added, an Inquiry into the Method of Viewing the Sun Advantageously, with Telescopes of Large Apertures and Magnifying Powers. *Phil. Trans. Roy. Soc. London*, **90**, 255 – 283.

Herschel, W. (1800b) Experiments on the Refrangibility of the Invisible Rays of the Sun, *Phil. Tran. Roy. Soc. London*, **90**, 284 – 292.

Herschel, W. (1800c) Experiments on the Solar, and Terrestrial Rays that Occasion Heat; with a Comparative View of the Laws of Light and Heat, or Rather the Rays that Occasion Them, are Subject, in Order to Determine Whether they are the Same, or Different [Part I]. *Phil. Trans. Roy. Soc. London*, **90**, 293 – 326

Herschel, W. (1800d) Experiments on the Solar, and Terrestrial Rays that Occasion Heat; with a Comparative View of the Laws of Light and Heat, or Rather the Rays that Occasion Them, are Subject, in Order to Determine Whether they are the Same, or Different [Part II]. *Phil. Trans. Roy. Soc. London*, **90**, 437 – 538.

Hildebrand, A.R., G.T. Penfield, D.A. Kring, M. Pilkington, A.Z. Camargo, S.B. Jacobsen & W.V. Boynton (1991) Chicxulub Crater: A possible Cretaceous-Tertiary Boundary Impact Crater on the Yucatan Peninsula, *Geology*, **19**, 867 – 871.

Hildebrand, A.R., E.F. Tedesco, K.A. Carroll, R.D. Cardinal, J.M. Matthews, R. Kuschnig, G.A.H. Walker, B. Gladman, N.R. Kaiser, P.G. Brown, S.M. Larson, S.P. Worden, B.J. Wallace, P.W. Chodas, K. Muimonen, A. Cheng & P. Gural (2007) The Near Earth Object Surveillance Satellite (NEOSSat) Mission Enables an Efficient Space-Based Survey (NESS) Project of Interior-to-Earth-Orbit (IEO) Asteroids, *Lunar and Planet. Sci.*, **38**, 2372 – 2373.

Hillier, J., B. Buratti & K. Hill (1999) Multispectral Photometry of the Moon and Absolute Calibration of the Clementine UV/Vis Camera, *Icarus*, **141**, 205 – 225.

Hjalmarson, Å., P. Bergman, N. Biver, H.-G. Forén, U. Frisk, T. Hasagawa, K. Justtanont, B. Larsson, S. Lundin, M. Olberg, H. Olofsson, G. Persson, G. Rydbeck, A. Sandqvist & the Odin Team (2005) Recent Astronomy Highlights from the Odin Satellite, *Adv. Space Res.*, **36**, 1031 – 1047.

Hodapp, K.W., W.A. Siegmund, N. Kaiser, K.C. Chambers, U. Laux, J. Morgan & E. Mannery (2004) Optical Design of the Pan-STARRS Telescopes, *Proc. SPIE*, **5489**, 667 – 678.

Hodge, P.W. (1981) *Interplanetary Dust*, Gordon and Breach Science Pub., NY.

Hodge, T.M., K.E. Kraemer, S.D. Price & H.J. Walker, (2004) Classification of Spectra from the Infrared Space Observatory PHT-S Database, *Astrophys. J. Supp.*, **151**, 299 – 312.

Hoffman, W.F. (1977) Balloon-Borne Telescopes for Far-Infrared Astronomy, *Astrophys. Space Sci. Lib.*, **63**, 155 – 168.

Hoffman, W.F., C.L. Frederick & R.J. Emery (1969) 100-Micron Map of the Galactic Center, *Astrophys. J.*, **164**, L23 – L28.

Hoffman, W.F., C.L. Frederick & R.J. Emery (1971a) 100-Micron Map of the Galactic-Center Region, *Astrophys. J.*, **164**, L23 – L28.

Hoffman, W.F., C.L. Frederick & R.J. Emery (1971b) 100-Micron Survey of the Galactic Plane, *Astrophys. J.*, **170**, L89 – L97.

Hoffman, W.F., N.J. Woolf, C.L. Frederick & F.J. Low (1967) A Far-Infrared Sky Survey, *Astron. J.*, **72**, 804.

Hogan, E. R.F. Jameson, S.L. Casewell, S.L. Osbourne & N.C. Hambly (2008) L dwarfs in the Hyades, *Mon. Not. Roy. Astron. Soc.*, **388**, 495 – 499.

Holbrow, C. (2006) Scientists, Security, and Lessons from The Cold War, *Physics Today*, **59** (7), 39 – 44.

Holdale, G.B. & S.M. Smith (1969) Analysis of the Giant Particle Component of the Atmosphere of an Interior Desert Basin, *Tellus*, **20**, 251 – 268.

Holman, A.B., E.C. Smith & G.W. Autio (1976) Verificaiton of Radiation Background Rates in an IR Sensor System, *IEEE Trans. Nuc. Sci.*, **NS-23**, 1775 – 1780.

Holmes, E.K. & S.F. Dermott (2000) Comparison of ISO and COBE Observations of the Zodiacial Cloud, *ISO Beyond Point Sources: Studies of Extended Infrared Emission*, R.J. Laureijs, K. Leech & M.F. Kessler (eds.), ESA-SP-**455**, 67 – 70.

Holt, J.L., L.N. Johnson & G. Williams (1994) *Preparing for Planetary Defense: Detection and Interception of Asteroids on Collision Course with Earth*, Submission to the Air Command and Staff College.

Hong, S.S. (1985) Henyey-Greenstein Representation of the Mean Scattering Phase Function for Zodiacial Dust, *Astron. Astrophys.*, **146**, 67 – 75.

Hora, J.L., S. Bontemps, S.T. Megeath, N. Schneider, F. Motte, S. Carey, R. Simon, E. Keto, H.A. Smith, L.E. Allen, R. Gutermuth, G.G. Fazio, J.D. Adams & the Cygnus-X 24 μ m Data Processing Team (2009) The Spitzer Survey of Cygnus-X and Infrared Dark Clouds, *Bull. Amer. Astron. Soc.*, **41**, 498.

Houck, J.R. & M. Harwit (1969) Far-Infrared Nightsky Emission above 120 Kilometers, *Astrophys. J.*, **157**, L45 – L48.

Houck, J.R., T.L. Roellig, J. van Cleve, W.J. Forrest, T. Herter, C.R. Lawrence, K. Matthews, H.J. Reitsema, B.T. Soifer, D.M. Watson, D. Weedman, M. Huisjen, J. Troeltzsch, D.J. Barry, J. Bernard-Salas, C.E. Blacken, B.R. Brandl, V. Charmandaris, D. Devost, G.E. Gull, P. Hall, C.P. Henderson, S.J.U. Higdon, B.E. Pirger, J. Schoenwald, G.C. Sloan, K.I. Uchida, P.N. Appleton, L. Armus, M.J. Burgdorf, S.B. Fajardo-Acosta, C.J. Grillmair, J.G. Ingalls, P.W. Morris & H.I. Teplitz (2004) The Infrared Spectrograph (IRS) on the Spitzer Space Telescope, *Astrophys. J. Supp.*, **154**, 18 – 24.

Houck, J.R., B.T. Soifer, M. Harwit & J.L. Pipher (1974) *The Far Infrared and Submillimeter Background*, AFCRL-TR-74-0202. ADA002374

Houck, J.R., B.T. Soifer, J.L. Pipher & M. Harwit (1971) Rocket-Infrared Four-Color Photometry of the Galaxy's Central Regions, *Astrophys. J.*, **169**, L31 – L34.

Houck, J.R., B.T. Soifer, M. Harwit & J.L. Pipher (1972) The Far-Infrared and Sumillilmeter Background, *Astrophys. J.*, **178**, L29 – 33.

Hovenier, J.W. & P.B. Bosma (1991) Light Scattering of Dust Particles in the Outer Solar System, in *Origin and Evolution of Interplanetary Dust*, A.C. Levasseur-Regourd & H. Hasegawa (eds.), Kluwer Academic Press (Neth.), 155 – 158.

Howell, A.H. (1973) *Experiences with Balloon-Borne Telescopes* Tech. Report AFCRL-TR-73-0051. AD757895

Hudson, Jr., R.D. (1969) *Infrared System Engineering*, 3 – 8, John Wiley & Sons.

Huggins, W. (1869) Note on the Heat of Stars, *Proc. Roy. Soc.* **17**, 309 – 312.

Humphreys, R.M., D.O. Strecker, T.L. Murdock & F.J. Low (1973) IRC+10420 – Another Eta Carinae?, *Astrophys. J.*, **179**, L49 – L52.

Hunt, G.R. & L.M. Logan (1972) Variation of Single Particle Mid-Infrared Emission Spectrum with Particle Size, *App. Opt.*, **11**, 142 – 147.

Hunt, G.R., L.M. Logan & J.W. Salisbury (1973) Mars: Components of Infrared Spectra and the Composition of the Dust Cloud, *Icarus*, **18**, 459 – 469.

Hunt, G.R. & J.W. Salisbury (1964) Lunar Surface Features; Mid-Infrared Spectral Observations, *Science*, **146**, 461 – 462.

Hunt, G.R. & J.W. Salisbury (1967) Infrared Images of Tycho on Dark Moon, *Science*, **155**, 1098 – 1100.

Hunt, G.R. & J.W. Salisbury (1969) Mid-Infrared Spectroscopic Observations of the Moon, *Philosophical Trans.*, **264**, 109 – 139.

Hunt, G.R., J.W. Salisbury & R.K. Vincent (1968) Lunar Eclipse: Infrared Images and an Anomaly of Possible Internal Origin, *Science*, **162**, 223 – 225.

Hynek, J.A., K.G. Henize & F.L. Whipple (1959) Report on the Precision Optical Tracking Program for Artificial Satellites, *Astron. J.*, **64**, 52.

Hynek, J.A. W.C. & White (1963) Report on Project Star Gazer, *Astron. J.*, **68**, 282.

Infrared Astronomical Satellite (IRAS) Catalogs and Atlases (1988) NASA Ref. Pub. 1190, Wash. DC. Gov. Printing Office. N8518898

Volume I Explanatory Supplement, C. Beichman, G. Neugebauer, H.J. Habing, P.E. Clegg & T.J. Chester (eds.). N8914194

Volumes 2 through 6 The Point Source Catalog. N8914195 through 8, N8914201

Volume 7 The Small Scale Structure Catalog, G. Helou & D.W. Walker (eds.). N8914199

Infrared Astronomical Satellite Asteroid and Comet Survey, Preprint No. 1 (1986) JPL D3698.

Ingalls, J.G., M.-A. Miville-Deschénes, W.T. Reach, A. Noriega-Crespo, S.J. Carey, F. Boulanger, S.R. Stolovy, D.L. Padgett, M.J. Burgdorf, S.B. Fajardo-Acosta, W.J. Glaccum, G. Helou, D.W. Hoard, J. Karr, J. O'Linger, L.M. Rebull, J. Rho, J.R. Stauffer & S. Wachter (2004) Structure and Colors of Diffuse Emission in the Spitzer Galactic First Look Survey, *Astrophys. J. Supp.*, **154**, 281 – 285.

Ingalls, J.G. & et al. (2006) Erratum: “Structure and Colors of Diffuse Emission in the Spitzer Galactic First Look Survey” (ApJS, 154, 281 [2004]), *Astrophys. J. Supp.*, **164**, 306.

Ipatov, S.E., A.S. Kutyrev, G.J. Madsen, J.C. Mather, S. Harvey Moseley and R.J. Reynolds (2008) Dynamical Zodiacal Cloud Models Constrained by High Resolution spectroscopy of the Zodiacal Light, *Icarus*, **194**, 769 – 788.

Ishiguro, M., R. Nakamura, Y. Fujii, K. Morishige, H. Yano, S. Tokogawa & T. Mukai (1999) First Detection of Visible Zodiacal Dust Bands from Ground-Based Observations, *Astrophys. J.*, **511**, 432 – 435.

Ishihara, D.T. Wada, T. Onaka, H. Matsuhara, H. Kataza, M. Ueno, N. Fujihiro, W. Kim. H. Watarai, K. Uemizu, H. Murakami, T. Matsumoto & I. Yamamura (2006) Mid-Infrared All –

Sky Survey with the Infrared Camera (IRC) on Board the ASTRO-F Satellite, *Pub. Astron. Soc. Pac.*, **118**, 324 – 343.

Israel, F.P. (1986) Light on Dark Matter; Proceedings of the First Infra-Red Astronomical Satellite Conference, D. Reidel Pub.: *Astrophys. Space Sci. Library*, **124**.

Ivezić, Z., J.A. Tyson, M. Jurić, J. Kubica, A. Connolly, F. Pierfederici, A.W. Harris, E. Bowell & the LSST Collaboration (2007) LSST: Comprehensive NEO Detection, Characterization, and Orbits, *Proc. IAU Symp.*, **236**, 353 – 362.

Jackson, B.V., A. Buffington, P.P. Hick, R.C. Altrock, P.E. Holladay, J.C. Johnston, S.W. Kahler, J.B. Mozer, S.D. Price, R.R. Radick, R. Sagalyn, D. Sinclair, G.M. Simnett, C.J. Eyles, M.P. Cooke, S.J. Tappin, T. Kuchar, D. Mizuno, D.F. Webb, P.A. Anderson, R.E. Gold & N.R. Waltham (2004) The Solar Mass Ejection Imager (SMEI) Mission, *Sol. Phys.* **225**, 177 – 204.

Jackson, A.A. & H.A. Zook (1989) A Solar System Dust Ring with the Earth as Its Shepherd, *Nature*, **337**, 629 – 631.

James, J.F., T. Mukai, T. Watanabe, M. Ishiguro & R. Nakamura (1997) The Morphology and Brightness of the Zodiacal Light and Gegenschein, *Mon. Not. Roy Astron. Soc.*, **288**, 1022 – 1026.

Jamieson, J.A., (1984) Infrared Technology: Advances 1975 – 1984 and Challenges 1985 – 1994. *Proc. SPIE*, **510**, 56 – 68.

Jamieson, J.A. (1995) Ballistic Missile Defense and Infrared Technology – The Influence of Infrared Technology on the Russian Revolution and the Soviet Empire, *Proc. Infrared Inf. Symp.*, **40**, 13 – 40.

Jarrett, T.H., T. Chester, R. Cutri, S. Schneider & J.P. Huchra (2003) The 2MASS Large Galaxy Atlas, *Astron. J.*, **125**, 515 – 554.

Jarrett, T.H., T. Chester, R. Cutri, S. Schneider, M. Skrutskie & J.P. Huchra (2000a) 2MASS Extended Sourc Catalog: Overview and Algorithms, *Astron. J.*, **119**, 2498 – 2531.

Jarrett, T.H., T. Chester, R. Cutri, S. Schneider, J. Rosenberg, J.P. Huchra & J. Mader (2000b) 2MASS Extended Sources in the Zone of Avoidance, *Astron. J.*, **120**, 298 – 313.

Jedicke, R., A. Morbidelli, T. Spahr, J.-M. Petit & W.F. Bottke, Jr. (2003) Earth and Space Based NEO Survey Simulations: Prospects for Achieving the Spaceguard Goal, *Icarus*, **161**, 17 – 33.

Jenniskens, P. (2008) Mostly Dormant Comets and their Disintegration into Meteoroid Streams: A Review, *Earth, Moon & Planet.*, **102**, 505 – 520.

Jenniskens, P., D. Nugent, E. Tedesco & J. Murthy (2000) 1997 Leonid Shower from Space, *Earth, Moon and Planets*, **82**, 305 – 312.

Jenniskens, P., E. Tedesco, J. Murthy, C.O. Laux & S.D. Price (2002) Spaceborne Ultraviolet 251–384 nm Spectroscopy of a Meteor During the 1997 Leonid Shower, *Meteoritics & Planet. Science*, **37**, 1071 – 1078.

Jensen, E.B. & T.X. Thuan (1982) Stellar Populations in the Edge-on Spiral Galaxy NGC4565, *Astophys. J. Supp.*, **50**, 421 – 450.

Jerzykiewicz, M. & K. Serkowski (1966) *The Sun as a Variable Star III*, AFCRL–66–792. AD0646446

Johnson, H.L. (1962) Infrared Stellar Photometry, *Astrophys. J.*, **135**, 69 – 79.

Johnson, H.L. (1965) Interstellar Extinction in the Galaxy, *Astrophys. J.*, **141**, 923 – 952.

Johnson, H.L. (1966) Astronomical Measurements in the Infrared, *Ann. Rev. Astron. Astrophys.*, **4**, 193 – 206.

Johnson, H.L., F.J. Low & D. Steinmetz (1965) Infrared Observations of the Neugebauer-Martz “Infrared Star” in Cygnus, *Astrophys. J.*, **142**, 808 – 810.

Johnson, H. L. & R. I. Mitchell (1963) Stellar Photometry at 5 Microns, *Astrophys. J.*, **138**, 302 – 303.

Johnson, P.E., K.J. Vogler & J.P. Gardner (1993) The Effect of Surface Roughness on Lunar Thermal Emission Spectra, *J. Geophys. Res.* **98 No. E11**, 20,825 – 20,829.

Johnson, S.B. (2002) *The United States Air Force and the Culture of Innovation 1945 – 1965*, Air Force History and Museums Program. ADA440395

Jones, B. & J.M. Rodriguez-Espinosa (1984) *Further Ground-Based Studies of Sources from the AFGL Infrared Sky Survey*, AFGL-TR-84-0114. ADA156189

Jones, A.W., M.J. Selby, M. Prieto Muños & C. Sánchez Magro (1984) A Survey of Faint, Near-Infrared Sources toward the Center of the Galaxy, *Astron. Astrophys.*, **138**, 297 – 302.

Jones, T.J. & D. Morrison (1974) Recalibration of the Photometric/Radiometric Method of Determining Asteroid Sizes, *Astron. J.*, **79**, 892 – 895.

Jursa, A.S. (1985) *Handbook of Geophysics and the Space Environment*, AFGL-TR-85-0315, ADA167000.

Kaiser, N. & the Pan-STARRS Team (2004) Pan-STARRS — A Wide-Field Optical Survey Telescope Array, *Proc. SPIE*. **5489**, 11 – 22.

Kao, Huei-Mei (1986) *Maximum Entropy Image Restoration Formulated a Correction Term to the Inverse Filer Solution*, PhD Thesis, Northeastern University.

Kawara, K., T. Kozara, S. Sato, Y. Kobiashi & H. Okuda (1982) Near-Infrared Source Counts in the Galactic Plane, *Pub. Astron. Soc. Jap.*, **34**, 389 – 405.

Kelsall, T., J.L. Weiland, B.A. Franz, W.T. Reach, R.G. Arendt, E. Dwek, H.T. Freudenreich, M.G. Hauser, S.H. Moseley, N.P. Odegard, R.F. Silverberg & E.L. Wright (1998) The COBE Diffuse Infrared Background Experiment Search for the Cosmic Infrared Background. II. Model of the Interplanetary Dust Cloud. *Astrophys. J.*, **508**, 44 – 73.

Kemp, J.C., K.D. Larsen & E.R. Huppi (1994) Rocketborne Spatial Radiometer – SPIRIT II, *Opt. Eng.*, **33**, 37 – 43.

Kennealy, J.P., P.V. Noah, E.F. Tedesco, R.M. Cutri, & S.F. Dermott (1993) *CBSD: The Celestial Background Scene Descriptor*, PL-TR-93-2215. ADA275521.\

Kennealy, R.M., R.S. Sample, J.P. Kennealy, R.A. Gonsalves, R. Canterna, R. Hermann & L. Townsley (1994) *High Resolution Descriptions of IRAS 12 and 25 Microns Confused Regions*, PL-TR-94-2197. ADA285487

Kennelly, E.J., S.D. Price, K.E. Kraemer & R. Aschbrenner (2010) Calibration against the Moon. I. A Disk-Resolved Lunar Model for Absolute Reflectance Calibration, *Icarus*, (submitted)

Kent, S.M., T.M. Dame & G.G. Fazio (1991) Galactic Structure from the Spacelab Infrared Telescope II – Luminosity Models Of The Milky Way, *Astrophys. J.*, **378**, 131 – 138.

Kent, S. M., D. Mink, G. Fazio, D. Koch, G. Melnick, A. Tardiff & C. Maxson (1992) Galactic Structure from the Spacelab Infrared Telescope I – 2.4 micron Map, *Astrophys. J. Supp.*, **78**, 403 – 408.

Kerton, C.R. & P.G. Martin (2000) A Mid-Infrared Galaxy Atlas (MIGA), *Astrophys. J.*, **126**, 85 – 103.

Kervin, P., D. O'Connell, P. Sydney, R. Medrano, D. Nishimoto, J. Africano, E. Tedesco & J. Lambert (1996) Near-Earth Object (NEO) Characterization at the Air Force Maui Optical Station (AMOS), *Proc. SPIE*, **2813**, 32 – 43.

Kessler, M.F., T.G. Müller, K. Leech, C. Arviset, P. Garcia-Lario, A.M.T. Pollock, T. Prusti & A. Salama (2003) *The ISO Handbook Volume I: ISO – Mission & Satellite Overview*, ESA SP-1262.

Kieffer, H.H. & J.M. Anderson (1998) Use of the Moon for Spacecraft Calibration over 350 – 2500 nm, *Proc SPIE*, **3948**, 325 – 336.

Kieffer, H.H. & T.C. Stone (2005) The Spectral Irradiance of the Moon, *Astron. J.*, **129**, 2887 – 2901.

Kim, Y., G.H. Rieke, K. Misselt, R. Indebetouw & K.E. Johnson (2008) Structure of the Interstellar Medium around Cas A, *Astrophys. J.*, **678**, 287 – 296.

King, Jr., J. (1959) *History of Air Force Cambridge Research Center: 20 September 1945 – 30 June 1959*, United Stars Air Force: Air Development Center.

Kirkpatrick, J.D. (2005) New Spectral Types L and T, *Ann. Rev. Astron. Astrophys.*, **43**, 195 – 245.

Kirkpatrick, J.D., C.A. Beichman & M.F. Skrutskie (1997) The Coolest Isolated M Dwarf and Other 2MASS Surprises, *Astrophys. J.*, **476**, 311 – 318.

Kirkpatrick, J.D., I.N. Reid, J. Liebert, R.M. Cutri, B. Nelson, C.A. Beichman, D.D. Kahn, D.G. Monet, J.E. Gizis & M.F. Skrutskie (1999) Dwarfs Cooler than “M” The Definition of Spectral Type “L” Using Discoveries from the 2-Micron All-Sky Survey (2MASS), *Astrophys. J.*, **519**, 802 – 833.

Kissell, K. (1969) *Application of an Infrared Image Tube to Astronomical Spectroscopy*, PhD. Thesis, The Ohio State University.

Kleinmann, S.G. (1988) *Analysis of Deep Sky Sources Found by the Infrared Astronomy Satellite*, AFOSR-TR-92-0194. ADA248416

Kleinmann, S.G. (1992) 2MASS - The 2 Micron All Sky Survey, *Astron. Soc. Pac. Conf. Series*, **34**, 203 – 212.

Kleinmann, S.G. (1994) *Final Report for Near-Infrared Imaging of Selected Areas*. ADA283519

Kleinmann, S.G., R.M. Cutri, E.T. Young, F.J. Low & F.C. Gillett (1986) *Explanatory Supplement to the IRAS Serendipitous Survey Catalog*, JPL/IPAC internal report.

Kleinmann, S.G., F.C. Gillett & R.R. Joyce (1981) Preliminary Results of the Air Force Infrared Sky Survey, *Ann. Rev. Astron. Astrophys.*, **19**, 411 – 456.

Kleinmann, S.G., R.R. Joyce, D.G. Sargent, F.C. Gillett & C.M Telesco (1979) An Observational Study of the AFGL Infrared Sky Survey. IV. Further Results from the Revised Catalog, *Astrophys. J.*, **227**, 126 – 130.

Kleimann, S.G., M.J. Lebofsky (1975) Accurate Positions for Some New Sources in the AFCRL Catalog, *Bull. Amer. Astron. Soc.*, **7**, 433.

Kleinmann, S.G., M.G. Lysaght, W.L. Pughe, S.E. Schneider, M.F. Skrutskie, M.D. Weinberg, S.D. Price, K.Y. Mathews, B.T. Soifer, C.A. Beichman, T.J. Chester, T. Jarrett, G.L. Kopan, C.J. Lonsdale, J. Elias, J.W. Liebert & P. Seitzer (1994) The Two Micron All Sky Survey – Survey Strategy and Prototyping, in *Infrared Astronomy with Arrays*, I. McLean (ed.), Kluwer Academic Press (Neth.), 219 – 226. ADA283519

Koch, D. G.G. Fazio, W.A. Traub, G.H. Rieke, T.N. Gautier, W.F. Hoffman, F.J. Low, E.T. Young, E.W. Urban & L. Katz (1982) Infrared Telescope in Space, *Opt. Eng.*, **21**, 141 – 147,

Koch, D.G., G.G. Fazio, W. Hoffman, G. Melnick, G. Rieke, J. Simpson, F. Witteborn & E. Young (1987) Infrared Observations of Contaminants from Shuttle Flight 51-F, *Adv. Space Res.*, **7**, 211 – 221.

Koch, D.G., G.J. Melnick, G.G. Fazio, G.H. Rieke, F.J. Low, W. Hoffman, E.T. Young, E.W. Urban, J.P. Simpson & F.C. Witteborn (1988) Overview of Measurements from the Infrared Telescope on Spacelab 2, *Astrophys. Lett. & Comm.*, **27**, 211 – 222.

Kolb, C.E., R.B. Lyons, J.B. Elgin, R.E. Huffman, D.E. Paulson & A. McIntyre (1983) Scattered Visible and Ultraviolet Solar Radiation from Condensed Attitude Control Jet Plumes, *J. Spacecraft & Rockets*, **20**, 383 – 389.

Kolb, C.E., R.B. Lyons, J.B. Elgin, R.E. Huffman, D.E. Paulson & A. McIntyre (1985) Mitigation of Scattered Solar Radiation from Condensed Attitude Control Jet Plumes, *J. Spacecraft & Rockets*, **22**, 215 – 216.

Korte, R.M., J.P. Kennealy, R.A. Gonsalves & C. Wong (1989) *Analysis of IR Celestial Survey Experiment*, GL-TR-89-0265, 46–54. ADA235997

Kraemer, K.E., C.M. Lisse, S.D. Price, D. Mizuno, R.G. Walker, T.L. Farnham & T. Mäkinen, (2005) Midcourse Space Experiment Observations of Small Solar System Bodies, *Astron. J.*, **130**, 2363 – 2382.

Kraemer, K.E., J.L. Hora, M.P. Egan, J. Adams, L.E. Allen, S. Bontemps, S. Carey, G.G. Fazio, R. Gutermuth, E. Keto, S.T. Megeath, D.R. Mizuno, F. Motte, S.D. Price, N. Schneider, R. Simon & H. Smith (2010) Circumstellar Structure around Evolved Stars in the Cygnus-X Star Formation Region, *Astrophys. J.*, (in press).

Kraemer, K.E., S.D. Price, D.R. Mizuno & S.J. Carey (2002) Observations of Galaxies with the Midcourse Space Experiment, *Astron. J.*, **124**, 2990 – 3008.

Kraemer, K.E., R.F. Shipman, S.D. Price, T. Kuchar & D.R. Mizuno (2003) Observations of Star-Forming Regions with the Midcourse Space Experiment, *Astron. J.*, **126**, 1423 – 1450.

Kraemer, K.E., G.C. Sloan, J. Bernard-Salas, S.D. Price, M.P. Egan & P.R. Wood (2006) A Post-AGB Star in the Small Magellanic Cloud Observed with the *Spitzer* Infrared Spectrograph, *Astrophys. J.*, **652**, L25 – L28.

Kraemer, K.E., G.C. Sloan, S.D. Price & H.J. Walker (2002) Classification of 2.4 – 45.2 Micron Spectra from the Infrared Space Observatory Short Wavelength Spectrometer, *Astrophys. J. Supp.*, **140**, 389 – 406.

Kraemer, K.E., G.C. Sloan, P.R. Wood, S.D. Price, & M.P. Egan (2005) R CrB Candidates in the Small Magellanic Cloud: Observations of Cold, Featureless Dust with the Spitzer Infrared Spectrograph, *Astrophys. J.*, **631**, L47 – L50.

Krassner, J.P. (1979) Predicted 2.2 Microns Celestial Backgrounds for Infrared Telescopes, *Proc. SPIE*, **172**, 340 – 357.

Krassner, J.P. (1981) Prediction of Infrared (IR) Celestial Source Counts, *Proc. SPIE*, **280**, 194 – 201.

Kresak, L. (1980) Source of Inteplanetary Dust, *Proc. IAU Symp.*, **90**, 211 – 222.

Kubica, J., L. Denneau, T. Grav, J. Heasley, R. Jedicke, J. Masiero, A. Milani, A. Morre, D. Tholen & R.J. Wainscoat (2007) Efficient Intra- and Inter-Night Linking of Asteroid Detections Using kd-Trees, *Icarus*, **189**, 151 – 168.

Kuchar, T.A., D. Mizuno, S. Shenoy, R. Paladini, K. Kraemer, S. Price, F. Marleau, D. Padgett, R. Indebetouw, J. Ingalls, B. Ali, B. Berriman, F. Boulanger, R. Cutri, W. Latter, M. Miville-Deschénes, S. Molinari, L. Rebull, L. Testi, R. Shipman, P. Martin, S. Carey & A. Noriega-

Crespo (2006) The Astronomical Zoo in MIPSGAL I and II, *Bull. Amer. Astron. Soc.*, **38**, 1024.

Kuiper, G.P. (1938) The Magnitude of the Sun, the Stellar Temperature Scale, and Bolometric Corrections, *Astrophys. J.*, **88**, 429 – 471.

Kuiper, G.P. (1964) Infrared Spectra of Planets and Cool Stars; Introductory Report, *Mem. Roy. Soc. Liege*, **IX**, 365 – 391.

Kuiper, G.P., W. Wilson, & R.J. Cashman (1947) An Infrared Stellar Radiometer, *Astrophys. J.*, **106**, 43 – 251.

Kupperman, D.G., L.J. Paxton, J. Carbary, G.J. Romick, D.E. Anderson, C.-I. Meng & P.D. Feldman (1998, On the Sodium Tail of Comet Hale-Bopp (C/1995 O1), *Geophys. Res. Lett.*, **25**, 3261 – 3264.

Kurtz, R.F., F.J. Low, G.H. Rieke & F.J. Vrba (1973) Study of Unidentified Infrared AFCRL Sky Survey Sources, *Bull. Amer. Astron. Soc.*, **5**, 414.

Kwok, S.M. (2008) Organic Matter in Space: from Star Dust to the Solar System, *Astrophys. Space Sci.*, **319**, 5 – 21.

Kwok, S., K. Volk & W.P. Bidelman (1997) Classification and Identification of IRAS Sources with Low-Resolution Spectra, *Astrophys. J. Supp.*, **112**, 557 – 584.

Kwon, S.M., S.S. Hong & J.L. Weinberg (1991) Temporal and Spatial Variation of the Atmospheric Diffuse Light, in *Origins and Evolution of Interplanetary Dust*, A.C. Levasseur-Regourd & H. Hasegawa (eds), *Astrophys. Space Sci. Lib.*, Kluwer Academic Press (Neth,) 179 – 182.

Kwon, S.M., S.S. Hong, J.L. Weinberg & N.Y. Misconi (1991) Fine Resolution Brightness Distribution of the Visible Zodiacal Light, in *Origins and Evolution of Interplanetary Dust*, A.C. Levasseur-Regourd & H. Hasegawa (eds), *Astrophys. Space Sci. Lib.*, Kluwer Academic Press (Neth,) 183 – 186.

Labs, D. & H. Neckel (1968) The Radiation of the Solar Photosphere from 2000 Å to 100 μ, *Zeit. Astrophys.*, **69**, 1 – 79.

Lacy, J.H. (1997) *High Resolution Mid-Infrared Spectroscopy of Celestial Sources*, PL-TR-97-2076. ADA330688

Lambert, J.V. (1999) Maui Space Surveillance System (MSSS) Sensors, *1999 AMOS Tech. Conf.*, Maui Economic Development Board, Kihei, Maui, 75 – 84.

Lambert, J.V. & K. Kissell (2000), Historical Overview of Optical Space Object Identification, *Proc. SPIE*, **4091**, 159 – 163.

Lamy, P., J.R. Kuhn, H. Lin, S. Koutchmy & R.N. Smart (1992) No Evidence of A Circumsolar Dust Ring From Infrared Observations of the 1991 Solar Eclipse, *Science*, **257**, 1377 – 1380.

Lamy, P.L. & J.-M. Perrin (1986) Volume Scattering Function and the Space Distribution of the Interplanetary Dust Cloud, *Astron. Astrophys.*, **163**, 269 – 286.

Lane, M.T., J.F. Baldassini & E.M. Gaposchkin, (1995) *A Metric Analysis of IRAS Resident Space Object Detections*, LL Tech. Report 1022, ESC-TR-95-21. ADA302289

Lange, G., E. Weichs, U. Schmidt & D. Sodeikat (1990) Spectrometer/Radiometer Measurements of Infrared Signatures from Space, *Proc. SPIE*, **1340**, 203 – 216.

Langley, S.P. (1904) On a Possible Variation of the Solar Radiation and its Probable Effect on Terrestrial Temperature, *Astrophys. J.*, **19**, 305 – 321.

Langley, S.P. & F.W. Very (1889) The Temperature of the Moon. From Studies at the Allegheny Observatory, *Mem. Nat. Acad. Sciences*, **4**, Part 2, 107.

Larmour, L. (1952) *Infrared Radiation from Celestial Bodies*, Rand Research Memo. RM-793-1. AD0098443

Laureijs, R.J., U. Klaas, P.J. Richards, B. Schulz & P. Abrahám (2003) *The ISO Handbook Volume IV: PHT – The Imaging Photo-Polarimeter*, ESA SP-**1262**.

Larsen, M.G., H. Latvakoski, A.K. Mainzer, S. Schick & J. Drake (2008) Wide-Field Infrared Survey Explorer Science Payload, *Proc. SPIE*, **7010**, 70100G.

Laurin, D., A. Hildebrand, R. Cardinal, W. Harvey & S. Tafazoli (2008) NEOSSat – A Canadian Small Space Telescope for Near Earth Asteroid Detection, *Proc. SPIE*, **7010**, 701013.

Lawrence, A. (1988) Comets to Cosmology: Proceedings of the Third IRAS Conference, Springer-Verlag: *Lecture Notes in Physics*, **297**.

Lawrence, A. (2007) Wide-Field Surveys and Astronomical Discovery Space, *Astron. Geophys.*., **48**, 3.27 – 3.33.

Lawrence, A., S.J. Warren, O. Almani, A.C. Edge, N.C. Hambly, R.F. Jameson, P. Lucas, M. Casali, A. Adamson, S. Dye, J.P. Emerson, S. Foucaud, P. Hewett, P. Hirst, S.T. Hodgkin, M.J. Irwin, N. Lodieu, R. G. McMahon, C. Simpson, I. Smail, D. Mortlock & M. Folger (2007) The UKIRT Infrared Deep Sky Survey (UKIDSS), *Mon. Not. Roy. Astron. Soc.*, **379**, 1599 – 1617.

Lawson, S.L., B.M. Jakosky, H.S. Park & M.T. Mellon (2000) Brightness Temperatures of the Lunar Surface: Calibration and Global Analysis of the Clementine Long-Wave Camera Data, *J. Geophys. Res.*, **105 E**, 4273 – 4290.

Le Bertre, M. Matsuura, J.M. Winters, H. Murakami, I. Yamamura, M. Freund & M. Tanaka (2001) Galactic Mass-Losing AGB Stars Probed with the IRTS. I., *Astron. Astrophys.*, **376**, 997 – 1010.

Le Bertre, M. Tanaka, I. Yamamura & H. Murakami (2003) Galactic Mass-Losing AGB Stars Probed with the IRTS. II., *Astron. Astrophys.*, **403**, 943 – 954.

Lebofsky, L.A. & J.A. Spencer (1989) Radiometry and Thermal Modeling of Asteroids, in *Asteroids II*, R.P. Binzel, T. Gehrels & M.S. Matthews (eds), Univ. Ariz. Press, 128 – 147.

Lebofsky, L.A., M.A. Sykes, E.F. Tedesco, G.J. Vevera, D.L. Matson, R.H. Brown, J.C. Gladie, M.A. Feierberg & R.J. Rudy (1986) A Refined “Standard” Thermal Model for Asteroids Based on Observations of 1 Ceres and 2 Pallas, *Icarus*, **68**, 239 – 251.

Lebofsky, M.J. (1989) *A Deep Optical Infrared Survey*, AFOSR-TR-89-0435. ADA207930

Lebofsky, M.J., S.G. Kleinmann & G.H. Rieke (1975) New AFCRL IR Sources, *Bull. Amer. Astron. Soc.*, **7**, 410.

Lebofsky, M.J., S.G. Kleinmann, G.H. Rieke & F.J. Low (1976) An Observational Study of the AFCRL Infrared Sky Survey. II. Present Results of a New Program to Study the Final Catalog, *Astrophys. J.*, **206**, L157 – L160.

Lebofsky, M.J., D.G. Sargent, S.G. Kleinmann & G.H. Rieke (1978) An Observational Study of AFGL Infrared Sky Survey. III. Further Searches for AFCRL/AFGL Sources and an Evaluation of the Contents of the Mid-Infrared Sky, *Astrophys. J.*, **219**, 487 – 493.

Lee, H.M., S.J. Kim, M. Im, H. Matsuura, S. Oyabu, T. Wada, T. Nakagawa, J. Ko, H.J. Shim, M.G. Lee, N. Hwang, T. Takagi, & C. Pearson (2009) North Ecliptic Pole Wide Field Survey of AKARI: Survey Strategy and Data Characteristics, *Pub. Astron. Soc. Jap.*, **61**, 375 – 385.

Leech, K., D. Kester, R. Shipman, D. Beintema, H. Feuchtgruber, A. Heras, B. Huygen, F. Lahuis, D. Lutz, P. Morris, P. Roelfsema, A. Salama, S. Schaeidt, E. Valentijn, B. Vandenbussche, E. Weprecht & T. de Graauw (2003) *The ISO Handbook Volume V: SWS – The Short Wavelength Spectrometer*, ESA SP-1262

Léger, A. & L. d'Hendecourt (1985) Are Aromatic Hydrocarbons the Carriers of the Diffuse Bands in the Visible, *Astron. Astrophys.*, **146**, 81 – 85.

Léger, A. & J.L. Puget, (1984) Identification of the ‘Unidentified’ IR Emission Features of Interstellar Dust? *Astron. Astrophys.*, **137**, L5 – L8.

Leighton, R.B. (1998) Other Octaves – Oral History, *Eng. & Science*, **61**, No. 2, 18 – 27.

Leinert, C. (1975) Zodiacal Light - A Measure of the Interplanetary Environment, *Space Sci. Rev.*, **18**, 281 – 339.

Leinert, Ch., P. Ábrahám, J. Acosta-Pulido, D. Lemke & R. Siebenmorgen (2002) Mid-Infrared Spectrum of the Zodiacal Light Observed with ISOPHOT, *Astron. Astrophys.*, **393**, 1073 – 1079.

Leinert, Ch., S. Bowyer, L.K. Haidala, M.S. Hanner, M.G. Hauser, A.-Ch. Levasseur-Regourd, I. Mann, K. Mattila, W.T. Reach, W. Schlosser, H.J. Staude, G.N. Toller, J.L. Weiland, J.L. Weinberg & A.N. Witt (1998) The 1997 Reference of Diffuse Night Sky Brightness, *Astron. Astrophys. Supp.* **127**, 1 – 99.

Leinert, C., I. Richter, E. Pitz & M. Hanner (1980) The Plane of Symmetry of Interplanetary Dust in the Inner Solar System, *Astron. Astrophys.*, **82**, 328 – 336.

Leinert, C., I. Richter, E. Pitz & B. Planck (1981) The Zodiacal Light from 1.0 to 0.3 A.U. as Observed by the Helios Space Probes, *Astron. Astrophys.*, **103**, 177 – 188.

Lemke, D., W. Martin, M. Grewing, P. Preussner & D. Offerman (1985) The German Infrared Laboratory (GIRL) – A Progress Report, *Adv. Space Sci.*, **3**, 11 – 17.

Lena, P., Y. Viala, D. Hall & A. Soufflat (1974) The Thermal Emission of the Dust Corona During the Eclipse of June 30, 1973. II: Photometric and Spectral Observations, *Astron. Astrophys.*, **37**, 81 – 86.

Levan, P.D. (1985) *An Application of Maximum Entropy Techniques for Increased Spatial Resolution of Infrared Celestial Sources*, AFGL-TR-85-005. ADB092357

LeVan, P.D. (1990) Capabilities of the AFGL Mosaic Array Spectrometer - Ten-Micron Spectra of Bright Infrared Stars, *Pub. Astron. Soc. Pac.*, **102**, 190 – 199.

LeVan, P.D. & S.D. Price (1984) 85-micron fluxes from asteroids - 2 Pallas, 7 Iris, 15 Eunomia, and 45 Eugenia, *Icarus*, **57**, 35 – 41.

Levasseur-Regourd, A.C. & R. Dumont (1980) Absolute Photometry of Zodiacal Light, *Astron. Astrophys.*, **84**, 277 – 279.

Levasseur-Regourd, A.-C. & R. Dumont (1988) Properties of Interplanetary Dust from Optical Observations I – Temperature, Global Volume Intensity and Their Heliocentric Gradients, *Astron. Astrophys.*, **191**, 154 – 160.

Leverington, D. (2000) *New Cosmic Horizons – Space Astronomy from the V2 to the Hubble Space Telescope*, Cambridge University Press.

Levenson, L.R., E.L. Wright & D. Johnson (2007) DIRBE Minus 2MASS: Confirming the CIRB in 40 New Regions at 2.2 and 3.5 μ m, *Astrophys. J.*, **666**, 34 – 44.

Levy, D.H. (1996) Comet Shoemaker-Levy 9 and Jupiter: The Collision of the Century, *J. Roy. Astron. Soc. Canada*, **90**, 42 – 56.

Liebowitz, R.P. (1985) *CHRONOLOGY From the Cambridge Field Station to the Air Force Geophysics Laboratory 1945 – 1995*, AFGL-TR-85-0201. ADA164501

Liebowitz, R.P. (1987) *Air Force Geophysics 1945 – 1985 Contributions to Defense and the Nation*, PL-TR-97-2034. ADA327360

Liebowitz, R.P. (1990) *Historical Brief GL Atmospheric Propagation Codes for DoD Systems*. ADA332703

Liebowitz, R.P. (1995) *Satellite and Space-Shuttle Experiments Flown by the Geophysics Directorate and other Units of Phillips Laboratory at Hansoms AFB, MA and by Their Predecessor Organizations, 1958 – 1994*, PL-TR-95-2010. ADA299290

Liebowitz, R. P. (2002) Donald Menzel and the Creation of Sacramento Peak Observatory, *J. History of Astronomy*, **33**, 193 – 211

Liebowitz, R.P. & E.M. Kindler (1995), *Chronology: From the Air Force Geophysics Laboratory to the Geophysics Directorate, Phillips Laboratory, 1985 –1995*, PL-TR-2134. ADA301134

Lien, J.R., R.J. Marou, J.C. Ulwick, D.R. McMorrow, D.B. Linsford & O.C. Haycock (1953) Bifurcation of the E Region, *Phys. Rev. Letters*, **92**, 508 – 509.

Lisse, C.M., Y.R. Fernández, M.F. A'Hearn, E. Grün, H.U. Käufl, D.J. Osip, D.J. Lien, T. Kostiuk, S.B. Peschke & R.G. Walker (2004) A tale of two very different comets: ISO and MSX measurements of dust emission from 126P/IRAS (1996) and 2P/Encke (1997), *Icarus*, **171**, 444 -462.

Little, S.J., G. Gulixson, R.D. Dietz, J.A. Hacwell, R.D. Gehrz & G.L. Grasdalen (1989) High-Resolution H and K Mapping of W51, *Astron. J.*, **97**, 1716 – 1720.

Little, S.J. & S.D. Price (1985) Infrared Mapping of the Galactic Plane IV. The Galactic Center, *Astron. J.*, **90**, 1812 – 1819.

Little-Marenin, I.R. (1986) Carbon Stars with Silicate Dust in their Circumstellar Shells, *Astrophys. J.*, **307**, L15 – L19.

Little-Marenin, I.R. (1988) *Analysis of the IRAS Low Resolution Spectra*, GL-TR-88-0811. ADA234482

Little-Marenin, I.R. & S. Little (1988) Emission Features in IRAS Low-Resolution Spectra of MS, S and SC Stars, *Astrophys. J.*, **333**, 305 – 315.

Little-Marenin, I.R. & S. Little (1990) Emission Features in IRAS LRS Spectra of M Mira Variables, *Astron. J.*, **99**, 1173 – 1186.

Lodieu, N., N.C. Hambly, R.F. Jameson, S.T. Hodgkin, G. Carraro & T.R Kendall (2006) New Brown Dwarfs in Upper Sco Using UKIDSS Galactic Cluster Survey Science Verification Data, *Mon. Not. Roy. Astron. Soc.*, **374**, 372 – 284.

Lodieu, N., D.J. Pinfield, S.K. Leggett, R.E. Jameson, D.J. Mortlock, S.J. Warren, B. Burningham, P.W. Lucas, K. Chiu, M.C. Liu, B.P. Venemans, R.G. McMahon, F. Allard, I. Baraffe, D. Barrado y Navascués, G. Carraro, S.J. Casewell, G. Chabrier, R.J. Cappelle, F. Clarke, A.C. Day-Jones, N.R. Deacon, P.D. Dobbie, S.L. Folkes, N.C. Hambly, P.C. Hewett, S.T. Hodgkin, R.A. Jones, T.R. Kendall, A. Magazzù, E.L. Martín, M.J. McCaughrean, T. Nakajima, Y. Pavlenko, M. Tamura, C.G. Tinney & M.R. Zapatero Osorio (2007) Eight New T4.5 – T7.5 Dwarfs Discovered in the UKIDSS Large Area Survey Data Release 1, *Mon. Not. Roy. Astron. Soc.*, **379**, 1423 – 1430.

Logan, L.L., S.B. Balsamo & G.R. Hunt (1973) Absolute Measurements and Computed Values for Martian Irradiance between 10.5 and 12.5 μm , *Icarus*, **18**, 451 – 458.

Logan, L.L., G.R. Hunt, S.B. Balsamo & J.W. Salisbury (1972) Midinfrared Emission Spectra of Apollo 14 and 15 Soils and Remote Compositional Mapping of the Moon, *Geochemica et Cosmochimica Acta*, **3**, 3069 – 3076.

Logan, L.M., G.R. Hunt, A.L. Long & J.P. Dybwad (1974) *Absolute Infrared Radiance Measurements of Venus and Jupiter*. AFCR-TR-74-0573. ADA003662

Longmore, A.J., A.R. Hyland & D.A. Allen (1976) The AFCRL Catalog: Some Southern Sources Studied. *Proc. Astron. Soc. Australia*, **3**, 47 – 48.

Lonsdale, C.J., G. Helou, J.C. Good & W. Rice (1985) *Cataloged Galaxies and Quasars Observed in the IRAS Survey*, JPL publication D – 1932.

Looper, D.L., J.D. Kirkpatrick & A.J. Burgasser (2007) Discovery of 11 New T Dwarfs in the Two Micron All sky Survey Including a Possible L/T Transition Binary, *Astrophys. J.*, **134**, 1162 – 1182.

López-Corredoira, M., F. Garzón, P. Hammersley, T. Mahoney & X. Calbet (1997) The Morphology and Luminosity Function of the Galactic Bulge, *Mon. Not. Roy. Astron. Soc.*, **292**, L15 – L19.

Lovell, D.J. (1968) The Development of Lead Salt Detectors, *Amer. J. Phys.*, **37**, 467 – 478.

Lovell, D.J. (1969) *Some Early Lead Salt Detector Developments*, AFOSR-TR-68-0264. AD0666031

Lovell, D.J. (1971) Cashman Thallous Sulfide Cell, *Appl. Opt.*, **10**, 1003 – 1008.

Low, F.J. (1961) Low-Temperature Germanium Bolometer, *J. Opt. Soc. Amer.*, **51**, 1300 – 1304.

Low, F.J. (1965) Lunar Nighttime Temperature Measured at 20 Microns, *Astrophys. J.*, **142**, 806 – 808.

Low, F.J. (1966) The Infrared Brightness Temperature of Uranus, *Astrophys. J.*, **146**, 136 – 137.

Low, F.J., (1973) *Groundbased Infrared Measurements FINAL REPORT*, AFCRL-73-0371. AD0768620

Low, F.J. & H.H. Aumann (1970) Observation of Galactic and Extragalactic Sources between 50 and 300 Microns, *Astrophys. J.*, **162**, L79 – L85.

Low, F.J., H.H. Aumann & C.M. Gillespie, Jr. (1970) Closing Astronomy's Last Frontier – Far Infrared, *Astronautics and Aeronautics*, **8**, 26 – 30 (AFCRL-71-0332).

Low, F.J. & H.L. Johnson (1964) Stellar Photometry at 10 μ , *Astrophys. J.*, **139**, 1130 – 1134.

Low, F.J., R.F. Kurtz, F.J. Vrba & G.H. Rieke (1976) An Observational Study of the AFCRL Infrared Sky Survey. I. Limited Groundbased Survey and Results from Preliminary Catalog, *Astrophys. J.*, **206**, L153 – L155.

Low, F.J., G.H. Rieke & R.E. Gehrz (2007) The Beginning of Modern Infrared Astronomy, *Ann. Rev. Astron. Astrophys.*, **45**, 43 – 75.

Low, F.J., G.H. Rieke & K.R. Armstrong (1973) Ground-Based Observations at 34 Microns, *Astrophys. J.*, **183**, L105 – L109.

Low, F., M. Sykes & R. Cutri (1991) *A Characterization of the Hot Infrared Background: The Infrared Cirrus, Zodiacial Dust Bands, and Solar System Dust Trails*, PL-TR-91-2065. ADA239132

Low, F.J., E. Young, D.A. Beintema, T.N. Gautier, C.A. Beichman, H.H. Aumann, F.C. Gillett, G. Neugebauer, N. Boggess & J.P. Emerson (1984) Infrared Cirrus - New Components of the Extended Infrared Emission, *Astrophys. J.*, **278**, L19 – L22.

Lucas, P.W., M.G. Hoare, A. Longmore, A.C. Schröder, C.J. Davis, A. Adamson, R.M. Bandyophyay, R. de Grijs, M. Smith, A. Gosling, S. Mitchison, A. Gáspár, M. Coe, M.

Tamura, Q. Parker, M. Irwin, N. Hambly, J. Bryant, R.S. Collins, N. Cross, D.W. Evans, E. Gonzalez-Solares, S. Hodgkin, J. Lweis, M. Read. M. Riello. E.T. Sutorius, A. Lawrence, J.E. Drew, S. Dye & M.A. Thompson (2008) The UKIDSS Galactic Plane Survey, *Mon. Not. Roy. Astron. Soc.*, **301**, 136 – 63.

Lunel, M. (1960) Recherches de Photométrie Stellaire dans L'infra-Rouge au Moyen d'une Cellule au Sulfure De Plomb, *Ann. d'Astrophys.*, **23**, 1 – 61.

Maas, R.W., E.P. Ney & N.J. Woolf (1970) The 10-Micron Emission Peak of Comet Bennett 1969, *Astrophys. J.*, **160**, L101 – L104.

MacQueen, R.M. (1968) Infrared Observcations of the Outer Chromosphere, *Astrophys. J.*, **154**, 1059 – 1068.

Maihara, T., K. Mizutani, H. Hiromoto, H. Takami & H. Hasegawa (1985) A Balloon Observation of the Thermal Radiation from the Circumsolar Dust Cloud in the 1983 Total Eclipse, *Proc. IAU Symp.*, **85**, 55 – 58.

Maihara, T., N. Oda, T. Sugiyama & H. Okuda (1978) 2.4-micron Observations of the Galactic Plane and Galactic Structure, *Pub. Astron. Soc. Japan*, **30**, 1 – 20.

Mainzer, A.K., (2006) NEOCam: The Near-Earth Object Camera, *Bull. Amer. Astron Soc*, **38**, 568.

Mainzer, A.K., P. Eisenhardt, E.L. Wright, F.-C. Liu, W. Irace, I. Heinrichsen, R. Cutri & V. Duval (2006) Update on the Wide-Field Infrared Survey Explorer (WISE), *Proc. SPIE*, **6265**, 21-1 – 12.

Makiuti, S., H. Shibai, T. Nakagawa, H. Okuda, K. Okumura, H. Matsuhara, N. Hiromoto & Y. Doi (2002) Diffuse Far-Infrared [C II] Line Emission From High Galactic Latitude, *Astron. Astrophys.*, **383**, 600 – 609.

Mamon, G.A. & R.M. Soneira (1982) Stellar Luminosity Function on R, I, J, K Bands Obtained by Transformations from the Visual Band, *Astrophys. J.*, **255**, 181 – 190.

Mankin, W.G., R.M. MacQueen & R.H. Lee (1974), The Coronal Radiance in the Intermediate Infrared, *Astron. Astrophys.*, **31**, 17 – 21.

Maran, S.P., T.F. Heinsheimer, T.L. Stocker, R.D. Chapman, R.W. Hobbs & A.G. Michalitsanos (1976) Characteristics of IR Variable Stars as Observed from Orbit, *Proc. SPIE*, **95**, 23 – 29.

Marcuse, M.L. (1988) *A Statistical Approach to Linear Minimum Mean Squared Error Interpolation of InfraRed Astronomical Survey Data*, MSci. Thesis, Tufts Univ.

Marleau, F.R., A. Noriega-Crespo, R. Paladini, D. Clancy, S. Carey, S. Shenoy, K.E. Kraemer, T. Kuchar, D.R. Mizuno & S. Price (2008) Discovery of Highly Obscured Galaxies in the Zone of Avoidance, *Astron. J.*, **136**, 662 – 675.

Mastandrea, A.A., R.T. Benoit & R.R. Glasheen (1989) Cryogenic Testing of Reflective Optical Components and Telescope Systems, *Proc. SPIE*, **1113**, 249 – 256.

Mather, J.C. & J. Boslough (1996) *The Very First Light – The True Inside Story of the Scientific Journey Back to the Dawn of the Universe*, Basic Books (Harper-Collier Publ).

Mather, J.C., P.Y. Bély, P. Stockman & H. Thronson (1997) The Next Generation Space Telescope, NGST, *Astron. Soc. Pac. Conf. Ser.*, **124**, 441 – 448.

Matsumoto, T., M. Akiba & H. Murakami (1984) Rocket Oservation of the Near-Infrared Extragalactic Background Radiation, *Adv. Space Res.*, **3**, 469 – 472

Matsumoto, T., M. Akiba & H. Murakami (1988) A Search for the Near-Infrared Extragalactic Background Light, *Astrophys. J.*, **332**, 572 – 595.

Matsumoto, T., S. Hayakawa, H. Matsuo, H. Murakami, S. Sato, A.E. Lange & P.L. Richards (1988) The Submillimeter Spectrum of the Cosmic Background Radiation, *Astrophys. J.*, **329**, 567 – 571.

Matsumoto, T., M. Kawada, M. Mitsunobu, H. Murakami, M. Noda, S. Matsuura, M. Tanaka & K. Narita (1996) IRTS Observation of the Near-Infrared Spectrum of the Zodiacal Light, *Pub. Astron. Soc. Jap.*, **48**, L47 – L51.

Matsumoto, T., S. Matsuura, H. Murakami, M. Tanaka, M. Freund, M. Lim, M. Cohen, M. Kawada & M. Noda (2005) Infrared Telescope in Space Observations of the Near-Infrared Extragalactic Background Light, *Astrophys. J.*, **626**, 31 – 43.

Matsuura, S., M. Kawada, H. Matsuhara, T. Matsumoto, M. Noda & M. Tanaka (1994) A Rocket-Borne Observation of the Near-Infrared Sky Brightness, *Pub. Astron. Soc. Pac.*, **106**, 770 – 779.

Matsuura, S., T. Matsumoto, H. Matsuhara & M. Noda (1995) Rocket-Borne Observations of the Zodiacal Light in the Near-Infrared Wavelengths, *Icarus*, **115**, 199 – 208.

Matsuura, S., I. Yamamura, H. Murakami, M.M. Freund & M. Tanaka (1999) Water Vapor Absorption in Early M-Type Stars, *Astron. Astrophys.*, **348**, 579 – 583.

Mattila, K., D. Lemke, L.K. Haikala, R.J. Laureijs, A. Léger, K. Lehtinen, Ch. Leinert & P.G. Mezger (1996) Spectrophotometry of UIR Bands in the Diffuse Emission of the Galactic Disk, *Astron. Astrophys.*, **315**, L353 – L356.

Matty, J.J., R. Dawbarn, & R. Menzel, (1991) Test Facilities for Calibration and Evaluation of LWIR Sensors at AEDC. *Proceedings of the 13th Aerospace Testing Seminar*, 363 – 369.

Maucherat, A., A. Llebaria & J.C. Gonin (1985) Zodiacal Light, Gegenschein and Sky Background, *Proc. IAU Symp.*, **85**, 27 – 30.

Mayo, J. (1999) AEOS 3.67 Meter Telescope Optics: Design, Fabrication and Performance, *1999 AMOS Tech. Conf.*, Maui Economic Development Board, Kihei, Maui, 21 – 32.

McAndrew, J. (1995) *The Roswell Report: Fact versus Fiction in the New Mexico Desert*, Gov. Printing Office. ADA326148

McAndrew, J. (1997) *The Roswell Report: Case Closed*, Gov. Printing Office. ADA326147

McCarthy, S.G. & G.W. Autio (1978) Infrared Detector Performance in the Shuttle Infrared Telescope Facility (SIRTF), *Proc SPIE*, **132**, 81 – 89.

McCarthy, S.G., L.S. Young & F.C. Witteborne (1975) A Large Cooled Infrared Telescope Facility for Spacelab, *Proc. Meeting on Space Shuttle Missions of the 1980s*, 39.

McCrosky, R.E. & R.K. Soberman (1962) *Results from an Artificial Iron Meteroid at 10 km/sec*, AFCRL 62-803. AD0291929

McEwen, A.S. (1996) A Precise Lunar Photometric Function, *Lunar. Planet. Sci.*, **XXVII**, 841.

McEwen, A.S., E. Eliason, P. Lucey, et al. (1998) Summary of Radiometric Calibration and Photometric Normalization Steps for the Clementine UVSIS Imager, *Lunar. Planet. Sci.*, **XXIX**, 1466.

McKenna, E.F. (1981) *Post Burnout Thrust Measurements*, AFGL-TR-81-0006. ADA100267

McMillan, R.S., A.K. Mainzer, R.G. Walker, E.L. Wright, P.R. Eisenhardt, R.M. Cutri, T. Gray & WISE Science Team (2009) NEOWISE: Proposed Discovery of Near-Earth Objects in the Infrared by the WISE Mission, *Bull. Amer. Astron. Soc.*, **41**, 364.

McPherson, A.M., A. Born, W. Sutherland, J. Emerson, B. Little, P. Jeffers, M. Stewart, J. Murray & K. Ward (2006) VISTA: Project Status, *Proc SPIE*, **6267**, 626707: 1 – 12.

Melnick, G.J. (2004) Submillimeter Wave Astronomy Satellite Science Highlights, *Adv. Space Res.*, **34**, 511 – 518.

Melnick, G.J., J.R. Stauffer, M.L.N. Ashby, E.A. Bergin, G. Chin, N.R. Erickson, P.F. Goldsmith, M. Harwit, J.E. Howe, S.C. Kleiner, D.G. Koch, D.A. Neufeld, B.M. Patten, R. Plume. R. Schieder, R.L. Snell, Z. Wang, G. Winnewisser & Y.F. Zhang (2000) The Submillimeter Wave Astronomyc Satellite: Science Objectives and Instrument Description, *Astrophys. J.*, **539**, L77 – L85.

Merrill, K.M. & B.T. Soifer (1974) Spectrophotometric Observations of a Highly Absorbed Object in Cygnus, *Astrophys. J.*, **189**, L27 – L30.

Merrill, K.M. (1975) Infrared Spectrophotometry of Compact Sources from the AFCRL Survey, *Bull. Amer. Astron. Soc.*, **7**, 433 – 434.

Merrill, P.W. & M.L. Humason (1927) Note on Very Cool Stars, *Pub. Astron. Soc. Pac.*, **39**, 198 – 203.

Mertz, L. (1973) *Investigations of Infrared Stellar Spectra with High-Resolution Instrumentation*, AFCRL-TR-73-0253. AD0763107

Mikami, T. & K. Ishida (1981) Space Density Distribution of Late-Type Giants and Supergiants in the Solar Neighborhood, *Pub. Astron. Soc. Jap.*, **33**, 135 – 147.

Mill, J.D., R.R. O’Neil, S. Price, G.J. Romick, O.M. Uy, E.M. Gaposchkin, G.C. Light, W.W. Moore Jr., T.L. Murdock & A.T. Stair Jr. (1994) Midcourse Space Experiment: Introduction to the Spacecraft, Instruments and Scientific Objectives, *J. Spacecraft and Rockets*, **31**, 900 – 907.

Milne, D.K. & L.H. Aller (1980) An Average Model for the Galactic Absorption, *Astron. J.*, **85**, 17 – 21.

Minchin, G.M (1895) The Electrical Measurements of Starlight, *Proc. Roy. Soc. London*, **59**, 231 – 233.

Misconi, N.Y., E.T. Rusk, J.L. Weinberg & S. Yu (1990) Small Scale Structure in the Brightness of the Zodiacal Light: Ground-Based Observations, *Planet. Space Sci.*, **38**, 517 – 527.

Misconi, N.V. & J.L. Weinberg (1978), Is Venus Concentrating Interplanetary Dust Toward Its Orbital Plane?, *Science*, **200**, 1484 – 1485.

Mizuno, D.R., S.J. Cary, A. Noriega-Crespo, R. Paladini, D. Padgett, S. Shenoy, T.A. Kuchar, K.E. Kraemer & S.D. Price (2008) Processing for the MIPSGAL 24 μ m Survey of the Innner Galactic Plane, *Pub. Astron. Soc. Pac.*, **120**, 1028 – 1042.

Mizuno, D.R., K.E. Kraemer, N. Flagey, N. Billot, S. Shenoy, R. Paladini, E. Ryan, A. Noriega-Crespo & S.J. Carey (2010) A Catalog of MIPSGAL Disk and Ring Sources, *Astron. J.*, (submitted).

Molster, F. & C. Kemper (2005) Crystalline Silicates, *Space Sci. Rev.*, **19**, 3 – 28.

Moroz, V.I. (1964) Recent Observations of Infrared Spectra of Planets (Venus 1-4 μ , Mars 1-4 μ , Jupiter 1-1.6 μ), *Mem. Roy. Soc. Liege*, **IX**, 406 – 419.

Moroz, V.I. (1965a) New Observations of the Infrared Spectrum of Venus ($\lambda = 1.2 – 3.8 \mu$), *Sov. Astron.*, **8**, 566 – 572.

Moroz, V.I. (1965b) Infrared Spectrum of Mercury ($\lambda = 1.2 – 3.9 \mu$), *Sov. Astron.*, **8**, 882 – 889.

Moroz, V.I. (1966) Infrared Spectra of Stars ($\lambda = 1.2 – 2.5 \mu$), *Sov. Astron.*, **10**, 47 – 55.

Moroz, V.I., V.D. Davydov & B.S. Zhegulëv (1969) Photometric and Spectroscopic Observations of Planets in the 8 – 14 μ Range, *Sov. Astron.*, **13**, 101 – 109.

Moroz, V.I., N.V. Vasil'chenko, L.B. Danilyants & S.A. Kaufman (1968) Experimental Observations at 8 – 14 μ with a Photoconductive Cell Cooled by Liquid Helium, *Sov. Astron.*, **12**, 150 – 154.

Morrison, D. (1977) Asteroid Sizes and Albedos, *Icarus*, **31**, 185 – 220.

Morrison, D. (ed.) (1992) *The Spaceguard Survey –Protecting the Earth from Cosmic Impact. Report of the NASA International Near-Earth-Object Detection Workshop*, Wash., DC. N9234245

Moshir, M., G. Kopan, T. Conrow, H. McCallon, P. Hacking, D. Gregorich, G. Rohrbach, M. Melnyk, W. Rice, L. Fullmer, J. White & T. Chester (1992) *IRAS Faint Source Survey Explanatory Supplement Version 2*, JPL D-10015

Moss, T.S. & D.R. Brown (1958), Tech. Note RAD. 720, Royal Aircraft Establishment, Farnsborough.

Mottola, S., A. Börner, J.T. Grundmann, G.J. Hahn, B. Kazeninejad, E. Kührt, H. Michaelis, S. Montenegro, N. Schmitz & P. Spietz (2008) AsteroidFinder: A Space-Based Search for IEOs, *Lunar and Planet. Inst.*, Contribution No. 1405.

Mukai, T., M. Fujino, M. Ishiguro, R. Nakamura, M. Ueno, F. Usui & S.K. Kwon (2003) The Influence of the Brightness of the Asteroidal Dust Bands on the Gegenschein, *Icarus*, **162**, 337 – 343.

Müller, T.G. & J.S.V. Lagerros (2002) Asteroids as Calibration Standards in the Thermal Infrared for Space Observatories, *Astron. Astrophys.*, **381**, 324 – 339.

Murakami, H. (1998) Japanese Infrared Survey Mission IRIS (ASTRO-F), *Proc SPIE*, **3356**, 471 – 477.

Murakami, H., J. Bock, M.M. Freund, H. Guo, T. Hirao, A.E. Lange, H. Matsuhara, T. Matsumoto, S. Matsuura, T.J. McMahon, M. Murakami, T. Nakagawa, M. Noda, K. Noguchi, H. Okuda, K. Okumura, T. Onaka, T.L. Roellig, S. Sato, H. Shibai, T. Tanabé, T. Watabe, T. Yagi, N. Yajima & M. Yui (1994) The Infrared Telescope in Space (IRTS), *Astrophys. J.*, **428**, 354 – 362.

Murakami, H., M.M. Freund, K. Ganga, H. Guo, T. Hirao, N. Hiromoto, M. Kawada, A.E. Lange, S. Makiuti, H. Matsuhara, T. Matsumoto, S. Matsuura, M. Murakami, T. Nakagawa, M. Narita, M. Noda, K.H. Okuda, K. Okumura, T. Onaka, T.L. Roellig, S. Sato, H. Shibai, B.J. Smith, T. Tanabé, M. Tanaka, T. Watabe, I. Yamamura & L. Yuen (1996) The IRTS (Infrared Telescope in Space) Mission, *Pub. Astron. Soc. Jap.*, **48**, L41 – L46.

Murakami, H. & H. Matsuhara (2008) The Infrared Astronomical Satellite Akari: Overview, Highlights of the Mission, *Proc. SPIE*, **7010**, 70100A.

Murcray, F.H. (1965) The Spectral Dependence of Lunar Emissivity, *J. Geophys. Res.*, **70**, 4959 – 4962.

Murcray, F.H., D.G. Murcray & W.J. Williams (1964) The Spectral Radiance of the Sun from 4 μ to 5 μ , *App. Opt.*, **3**, 1373 – 1377.

Murcray, F.H., D.G. Murcray & W.J. Williams (1970), Infrared Emissivities of Lunar Surface Features. Balloon Observations, *J. Geophys. Res.*, **75**, 2662 – 2669.

Murdock, T.L. (1972) *Measurements of Infrared-Radiation from Mercury and the Moon*, PhD Thesis, Univ. Minn.

Murdock, T.L. (1973) *The Contributions of Asteroids to the Infrared Astronomical Sky Survey*, AFCRL-TR-73-0154.

Murdock, T.L. (1974) Mercury's Infrared Phase Effect, *Astron. J.*, **79**, 1457 – 1464.

Murdock, T.L., (1977) *Infrared Emission from the Interplanetary Dust Cloud at Small Solar Elongation Angles*, AFGL-TR-77-0280. ADC013735

Murdock, T.L. & S.D. Price (1985) Infrared Measurements of Zodiacal Light, *Astron. J.*, **90**, 375 – 386.

Murdock, T.L., P. Tandy, R. Walters & D. Wang (1980) An Infrared Sensor Designed to Measure the Diffuse Zodiacal Light, *Proc. SPIE*, **245**, 9 – 13.

Murphy, J.P., M.I. Kiya, M. Werner, P.N. Swanson, R.B.H. Kuiper & P.D. Batelaan (1980) A Large Aperture Space Telescope for Infrared and Submillimeter Astronomy, *Proc SPIE*, **228**, 117 – 127.

Murray, B.C. & R.L. Wildey (1964) Surface Temperature Variations during the Lunar Nighttime, *Astrophys. J.*, **139**, 734 – 750.

Murthy, J., R.C. Henry, L.J. Paxton & S.D. Price (2002) MSX Observations of Diffuse UV Emission in Orion, *Bull. Astron. Soc. India*, **29**, 563 – 575.

Nagy, T.A., S.P. Maran, J.M. Mead, J.R. Lesh, T.F. Heinsheimer, L.H. Seeney & F.F. Yates (1979) Stellar Contents of the Equatorial Infrared Catalog No. 2, *Bull. Amer. Astron. Soc.*, **11**, 396.

Nagy, T.A., L.H. Sweeney, J.R. Lesh, H.M. Mead, S.P. Maran, T.F. Heinsheimer & F.F. Yates (1979) Distribution of Astronomical Sources in the Second Equatorial Infrared Catalog, *Proc. SPIE*, **197**, 217 – 224.

Nakagawa, T., M. Hayashi, M. Kawada, H. Matsuhara, T. Matsumoto, H. Murakami, H. Okuda, T. Onaka, H. Shibai & M. Ueno (1998) HII/L2 Mission: Future Japanese Infrared Astronomical Mission, *Proc. SPIE*, **3356**, 462 – 470.

Nakajima, T., B.R. Oppenheimer, S.R. Kulkarni, D.A. Golimowski, K. Mathews & S.T. Durrance (1995) Discovery of a Cool Brown Dwarf, *Nature*, **378**, 463 – 465.

Nakamura, N., Y. Fujii, M. Ishiguro, K. Morishige, S. Yokogawa, P. Jenniskens & T. Mukai (2000) The Discovery of A Faint Glow of Scattered Sunlight from the Dust Trail of the Leonid Parent Comet 55P/Temple-Tuttle, *Astrophys. J.*, **540**, 1172 – 1176.

Napier, W. & D. Asher (2009) The Tunguska Impact Event and Beyond, *Astron. & Geophys.*, **50**, 1.18 – 1.26

Narayan, G., E. Berger, A. Rest, R. Foley & M. Huber (2009) Discovery and Classification of Pan-STARRS Transient PS10909006, *Astron. Telegram*, #2214.

National Academy of Sciences (1973) *Astronomy and Astrophysics for the 1970's VOLUME 2 Report of Panels*, National Academy Press, Wash. DC, 50 – 150.

National Academy of Sciences (1974) *Scientific Uses of the Space Shuttle*, National Academy Press, Wash. DC.

National Academy of Sciences (1975) *Opportunities and Choices in Space Sciences*, National Academy Press, Wash. DC, 18 – 19.

National Research Council (2009) *Near-Earth Object Surveys and Hazard Mitigation Strategies : Interim Report*, National Academy Press.

Neant, M. & M.J. Bigay (1952) Déterminations de Magnitudes InfraRouges avec une Cellule au Sulfure de Plomb, *J. Observateurs*, **6**, 61 – 67.

Nesvorný, D., W.F. Bottke, H.F. Levison & L. Dones (2003) Recent Origin of the Solar System Dust Bands, *Astrophys. J.*, **591**, 486 – 497.

Nesvorný, D., W.F. Bottke, D. Vokrouhlický, M. Sykes, D.J. Lien & J. Stansberry (2008) Origin of the Near Ecliptic Circumstellar Dust Band, *Astrophys. J.*, **679**, L443 – L446.

Nesvorný, D., D. Vokrouhlický & W.E. Bottke (2006) The Breakup of a Main-Belt Asteroid 450 Thousand Years Ago, *Science*, **312**, 1490.

Nesvorný, D., D. Vokrouhlický, W.E. Bottke & M. Sykes (2006) Physical Properties of Asteroid Dust Bands and Their Sources, *Icarus*, **181**, 107 – 144.

Neugebauer, G. (1972) *Infrared Photometry of Bright Celestial Sources*, AFCRL-TR-73-0114. AD0764686

Neugebauer, G., E. Becklin & A.R. Hyland (1971) Infrared Sources of Radiation, *Ann. Rev. Astron. Astrophys.*, **9**, 67 – 102.

Neugebauer, G., C.A. Beichman, B.T. Soifer, H.H. Aumann, T.J. Chester, T.N. Gautier, F.C. Gillett, M.G. Hauser, J.R. Houck, C.J. Lonsdale, F.L. Low & E.T. Young (1984) Early Results from the Infrared Astronomical Satellite, *Science*, **224**, 14 – 21.

Neugebauer, G. & R.B. Leighton (1968a), *Two Micron Sky Survey A Preliminary Catalog*, NASA SP-3047. N6937993

Neugebauer, G. & R.B. Leighton (1968b) The Infrared Sky, *Scientific American*, **219**, 50 – 65.

Neugebauer, G., D.E. Martz & R.B. Leighton (1965) Observations of Extremely Red Stars, *Astrophys. J.*, **142**, 399 – 401.

Newberg, H.J., B. Yanny, C. Rockosi, E.K. Grebel, H.-W. Rix, J. Brinkmann, I. Csabai, G. Hennessy, R.B. Hindsley, R. Ibata, Z. Ivezić, D. Lamb, E.T. Nash, M. Odenkirchen, H.A. Rave, D.P. Schneider, J.A. Smith, A. Stolte & D.G. York (2002) The Ghost of Sagittarius and Lumps in the Halo of the Milky Way, *Astrophys. J.*, **569**, 245 – 274.

Newcomer, R.E., J. Murthy, R.C. Henry, S.D. Price & L. Paxton (2004) *UVISI Stellar Calibration and Catalog*, AFRL-VS-HA-TR-2004-1056. ADM001987

Ney, E.P. & K.M. Merrill (1980) *Study of Sources in AFGL Rocket Infrared Study*, AFGL-TR-80-0050.

Ney, E.P., K.M. Merrill, E.E. Becklin, G. Neugebauer & C.G. Wynn-Williams (1975) Studies of the Infrared Source CRL 2688, *Astrophys. J.*, **198**, L129 – L134.

Nichols, E.F. (1901) On the Heat Radiation of Arcturus, Vega, Jupiter, and Saturn, *Astrophys. J.*, **13**, 101 – 141.

Nikolsky, G., S. Koutchmy, P.L. Lamy & I.A. Nesmjanovich (1985) Photographic Observations of the Inner Zodiacal Light aboard Saliout 7, *Proc. IAU Symp.* **85**, 7 – 10.

Noah, P.V. & M.A. Noah (2001a) *Validation Report for the Celestial Background Scene Descriptor (CBSD) Zodiacal Emission Model CBZODY6*, AFRL-VS-TR-2001-1578. ADA418442

Noah, P.V. & M.A. Noah (2001b) *Celestial Background Scene Descriptor: Final Report*, AFRL-VS-TR-2001-1584. ADA413194

Noda, M., V.V. Christov, H. Matsuhara, T. Matsumoto, S. Matsuura, K. Noguchi, S. Sato & H. Murakami (1992) Rocket Observations of the Near-Infrared Spectrum of the Sky, *Astrophys. J.*, **391**, 456 – 465.

Noguchi, K., S. Hayakawa, T. Masumoto & K. Uyama (1981) Near-Infrared Multicolor Observation of the Diffuse Galactic Emission, *Pub. Astron. Soc. Jap.*, **33**, 583 – 590.

Nordh, H.L., F. von Schéele, U. Frisk, K. Ahola, R.S. Booth, P.J. Encrenaz, Å. Hjalmarson, D. Kendall, E. Kyrölä, S. Kwok, A. Lecacheux, G. Leppelmeier, E.J. Llewellyn, K. Mattila, G.

Mégie, D. Murtagh, M. Rougeron, & G. Witt (2003) The Odin Orbital Observatory, *Astron. & Astrophys.*, **402**, L21 – L25.

Nozette, S., P. Rustan, L.P. Pleasance, J.F. Kordas, I.T. Lewis, H.S. Park, R. E. Priest, D.M. Horan, P. Regeon, C.L. Lichtenberg, E.M.; Shoemaker, E.M. Eliason, A.S. McEwen, M.S. Robinson, P.D. Spudis, C.H. Acton, B.J. Buratti, T.C. Duxbury, D.N. Baker, B.M. Jakosky, J.E. Blamont, M.P. Corson, J.H. Resnick, C.J. Rollins, M.E. Davies, P.G. Lucey, E. Malaret, M.A. Massie, C.M. Pieters, R.A. Reisse, R.A. Simpson, D.E. Smith, T.C. Sorenson, R.W. Vorder Breugge & M. T. Zuber (1994) The Clementine Mission to the Moon: Scientific Overview, *Science*, 266. 1835 – 1839.

Okuda, H. (1981) The Large Scale Infrared Emission in the Galactic Plane – Observations, *Proc. IAU Symp.*, **96**, 247 – 259.

Oliver, S. & F. Pozzi (2005) The European Large Area ISO Survey, *Adv. Space Sci.*, **119**, 411 – 423.

Olon, F.M., E. Raimond, G. Neugebauer, R.J. van Duinen, H.J. Habing, H.H. Aumann, D.A. Beintema, N. Boggess, J. Borgman, P.E. Clegg, F.C. Gillett, M.G. Hauser, J.R. Houck, R.E. Jennings, T. de Jong, F.J. Low, P.L. Marsden, S.R. Pottasch, B.T. Soifer, R.G. Walker, J.P. Emerson, M. Rowan-Robinson, P.R. Wesselius, B. Baud, C.A. Beichman, T.N. Gautier, S. Harris, G.K. Miley & E. Young (1986) IRAS Catalogues and Atlases - Atlas of Low-Resolution Spectra, *Astron. Astrophys. Supp.*, **65**, 607 – 1065.

Olthof, H. & R.J. van Duinen (1973) Two Colour Far Infrared Photometry of Some Galactic H II Regions, *Astron. Astrophys.*, **29**, 315 – 320.

Omont, A., G.F. Gilmore, C. Alard, B. Aracil, T. August, K. Balliyan, S. Beaulieu, S. Bégon, X. Bertou, J.A.D.L. Blommaert, J. Borsenberger, M. Burgdorf, B. Cailand, C. Cesarsky, A. Chitre, E. Copet, B. de Batz, M.P. Egan, D. Egret, N. Epchtein, M. Felli, P. Fouqué, S. Ganesh, R. Genzel, I.S. Glass, R. Grendel, M.A.T. Groenewegen, F. Guglielmo, H.J. Habing, P. Hennebelle, B. Jiang, U.C. Joshi, S. Kimeswenger, M. Messineo, M.-A. Miville-Deschénes, A. Monetti, M. Morris, D.K. Ojha, R. Ortiz, S. Ott, M. Parthasarathy, M. Péault, S.D. Price, A.C. Robing, M. Schultheis, F. Schuller, G. Simon, A. Soive, L. Testi, D. Teyssuerm, D. Tiphène, M. Unavane, J.T. van Loon & R. Wyse (2003) ISOGAL: A Deep Survey of the Obscured Inner Milky Way with ISO at 7 μ m and 15 μ m and with DENIS in the Near-Infrared, *Astron. Astrophys.*, **403**, 975 – 992.

Onaka, T., Y. Ita, D. Kato, T. Shimonishi, I. Sakon, Y. Nakada, T. Tanabé, H. Kaneda, T. Wada, A. Kawamura, B.C. Koo, H. Takahashi, M. Tamura & T. Hasegawa (2008) AKARI Large Area Survey of the Large Magellanic Cloud, *Proc. Fourth Spitzer Science Center Conference*, <http://ssc.spitzer.caltech.edu/mtgs/ismevo/>.

Onaka, T. & T. Nakagawa (2005) SPICA: A 3.5 m Space Infrared Telescope for Mid- and Far-Infrared Astronomy, *Adv. Space Res.*, **36**, 1123 – 1127.

Onaka, T. & A. Salama (2009) AKARI: Space Infrared Cooled Telescope, *Exp. Astron.*, (on-line article) <http://www.springerlink.com/content/b65pr511115083xv/>.

O'Neil, R.R., J. Gibson & E. Richards (2006) Midcourse Space Experiment: Off-Axis Rejection Performance of the Infrared Sensor, *J. Spacecraft & Rockets*, **43**, 1347 – 1358.

O'Neil, R. R., E. Richards, C. H. Humphrey, & A. T. Stair (2008) Polar Mesospheric Clouds: Infrared Measurements from the Midcourse Space Experiment, *J. Geophys. Res.*, **113**, A07303: 1- 10.

Ootsubo, T., T. Onaka, I. Yamamura, T. Tanabé, T.L. Roellig, K.-W. Chan & T. Matsumoto (2000) IRTS Observations of the Mid-Infrared Spectrum of the Zodiacal Emission, *Adv. Space Res.*, **25**, 2162 – 2166.

Ootsubo, T., J. Yamamura, T. Tanabé, T.L. Roellig, K.-W. Chan & T. Matsumoto (1998) IRTS Observations of the Mid-Infrared Spectrum of the Zodiacal Emission, *Earth Planets Space*, **50**, 507 – 511.

Page, L., C. Jackson, C. Barnes, C. Bennett, M. Halpern, G. Hinshaw, N. Jarosik, A. Kogut, M. Limon, S.S. Meyer, D.N. Spergel, G.S. Tucker, D.T. Wilkinson, E. Wollack & E.L. Wright (2003) The Optical Design and Characterization of the Microwave Anisotropic Probe, *Astrophys. J.*, **585**, 566 – 586.

Pajot, F., P. Boisse, R. Gispert, J. M. Lamarre, J. L. Puget & G. Serra (1986) Temperature Distribution of Interstellar Dust, *Astron. Astrophys.* **157**, 393 – 399.

Paley, E.S. F.J. Low, J.T. McGraw, R. Cutri & H-W Rix (1992) An Infrared/Optical Investigation of 100 Micron “Cirrus”, *Astrophys. J.*, **376**, 335 – 341.

Papoulias, R., J. Conard, M. Giuliano, J. Kister & G. Mille (1989) A Coal Model for the Carriers of the Unidentified IR Bands, *Astron. Astrophys.*, **217**, 204 – 208.

Peeples, P.J.P., L.A. Page, Jr. & R.B. Partidge (2009) *Finding the Big Bang*, Princeton Univ. Press.

Pelzmann, Jr., R.W. (1976) *Efficient Computer Algorithms for Infrared Astronomy Data Processing*, NASA CR-151943. N7716780

Pelzmann, Jr., R.W., (1977) *Point Source Detection in Infrared Astronomical Surveys*, NASA CR-152004. N7734061

Pelzmann, Jr., R.W. (1978a) *Final Report: SUPER HI STAR*, AFGL-TR-78-0047. ADA054964

Pelzmann, R.F (1978b) Data Processing in Infrared Astronomy, *Proc. SPIE*, **156**, 36 – 42.

Pelzmann, R.F. (1978c) Data Processing Tests on the Celestial Mapping Program Data, NASA CR-2-9847. N7716780

Péroult, M., A. Omont, G. Simon, P. Séguin, D. Ojha, J. Blommaert, M. Felli, G. Gilmore, F. Guglielmo, H. Habing, S.D. Price, A. Robin, B. de Batz, C. Cesarsky, D. Elbaz, N. Epschtein, P. Fouqué, S. Guest, D. Levine, A. Pollock, T. Prusti, R. Siebenmorgen, L. Testi & D. Tiphène (1996) First ISOCAM Images of the Milky Way, *Astron. Astrophys.*, **315**, L165 – L168.

Persi, P. & M. Ferrari-Toniolo (1984) Infrared Studies of Southern Hemisphere AFGL Sources. I. Limited Ground-Based Survey, *Astron. Astrophys. Suppl.*, **55**, 165 – 170.

Peterson, A.W. (1967) Experimental Detection of Thermal Radiation from Interplanetary Dust, *Astrophys. J.*, **148**, L37 – L39.

Peterson, A.W. (1969) The coronal brightness at 2.23 Microns, *Astrophys. J.*, **155**, 1009 – 1015.

Pettit, E. (1935) Lunar Radiation as Related to Phase, *Astrophys. J.*, **81**, 17 – 37.

Pettit, E. (1940) Radiation Measurements on the Eclipsed Moon, *Astrophys. J.*, **91**, 408 – 420.

Pettit, E. (1961) Planetary Temperature Measurements, in *Planets and Satellites*, G.P. Kuiper & B.M. Middlehurst (eds) Chicago: The University of Chicago Press, pp. 40.

Pettit, E. & S.B. Nicholson (1927) Radiometric Magnitudes of Certain Faint Red Stars, *Pub. Astron. Soc. Pac.*, **39**, 241 – 242.

Pettit, E. & S.B. Nicholson (1928) Stellar Radiation Measurements, *Astrophys. J.*, **68**, 279 – 308.

Pettit, E. & S.B. Nicholson (1930) Lunar Radiation and Temperatures, *Astrophys. J.*, **71**, 102 – 135.

Pettit, E. & S.B. Nicholson (1933) Measurements of the Radiation from Variable Stars, *Astrophys. J.*, **78**, 320 – 353.

Pettit, E. & S.B. Nicholson (1936) Radiation from the Planet Mercury, *Astrophys. J.*, **83**, 84 – 102.

Pettit, E. & S.B. Nicholson (1955) Temperature on the Bright and Dark sides of Venus, *Pub. Astron. Soc. Pac.*, **67**, 293 – 303.

Pfund, A.H. (1904) A Study of the Selenium Cell, *Philosophical Mag. 6th Ser.*, **7**, 25 – 39.

Pfund, A.H. (1916) Thermo-Electric Measurements of Stellar Radiation, *Pub. Allegheny Obs.*, **3**, 42 – 48.

Pijpers, F.P. (1999) Unbiased Image Reconstruction as an Inverse Problem, *Mon. Not. Roy. Astron. Soc.*, **307**, 659 – 668.

Pilbratt, G.L. (2004) Herschel Mission: Status and Observing Opportunities, *Proc. SPIE*, **5487**, 401 – 412.

Pipher, J.L., (1971) *The Submillimeter Observations of the Galaxy and Background*, PhD Thesis, Cornell Univ.

Povich, M.S. J.M. Stone, E. Churchwell, E.G. Zweibel, M.G. Wolfire, B.L. Babler, R. Indebetouw, M.R. Meade & B.A. Whitney (2007) A Multiwavelength Study of M17: The Spectral Energy Distribution and PAH Emission Morphology of A Massive Star Forming Region, *Astrophys. J.*, **660**, 346 – 362.

Pravdo S.H., D.L. Rabinowitz, E.E. Helin, K.J. Lawrence, R.J. Bambery, C.C. Clark, S.L. Groom, S. Levin, J. Lorre, S.B. Shaklan, P. Kervin, J.A. Africano, P. Sydney & V. Soohoo (1999) The Near-Earth Asteroid Tracking (NEAT) Program: an Automated System for Telescope Control, Wide-Field Imaging, and Object Detection. *Astron. J.*, **117**, 1616 – 1633.

Prete Martinez, A. (ed.) (1987) Planetary and Proto-Planetary Nebulae: from IRAS to ISO, D. Reidel: *Astrophys. & Space Sci. Lib.*, **135**.

Press, W.H., S.A. Teukolsky, W.T. Vetterling & B.R. Flannery (2007) *Numerical Recipes*, Univ. Cambridge Press

Price, S.D. (1968a) *Research on Infrared Celestial Backgrounds*, AFCRL-TR-68-004. AD671576

Price, S.D. (1968b) Results of an Infrared Stellar Survey, *Astron. J.*, **73**, 431 – 441.

Price, S.D (1970) *Quantitative Interpretation of the Infrared Spectra of Late-Type Stars*, PhD Thesis, The Ohio State University.

Price, S.D. (1977) *The AFGL Four Color Infrared Sky Survey: Supplemental Catalog*, AFGL-TR-77-0160. ADA048048

Price, S.D. (1978a) Extended Source Extraction from the AFGL Infrared Sky Survey Data, *Proc. SPIE*, **156**, 108–113.

Price, S.D. (1978b) Calibration of Infrared Celestial Sensors in Space, *Proc. SPIE*, **132**, 89 – 96.

Price, S.D. (1981) Infrared Mapping of the Galactic Plane I. Low-Resolution Maps of the Galactic Plane Between 0° and 320° Longitude, *Astron. J.*, **86**, 193 – 205.

Price, S.D. (1988a) The Infrared Sky: A Survey of Surveys, *Pub. Astron. Soc. Pac.*, **100**, 171 – 186.

Price, S.D. (1988b) Extraneous Radiation on Space Borne Infrared Experiments, *Proc. SPIE*, **972**, 169–187.

Price, S.D. (2004) The Surface Properties of Asteroids, *Adv. Space Res.*, **33**, 1548 – 1557.

Price, S.D. (2005) Infrared Irradiance Calibration, *Space Sci. Rev.*, **113**, 409 – 456.

Price, S.D. (2009) Infrared Sky Surveys, *Space Sci. Rev.*, **142**, 233 – 321.

Price, S.D., D.S. Akerstrom, C.V. Cunniff, L.P. Marcotte, P.C. Tandy & R.G. Walker (1978) *Aspect Determination for the AFGL Sky Survey Experiments*, AFGL-TR-78-0255. ADA067017

Price, S.D., C.V. Cunniff & R.G. Walker (1978), *Cleanliness Considerations for the AFGL Sky Survey Experiments*, AFGL-TR-78-0171. ADA060116

Price, S.D. & M.P. Egan (2001) Space-Based Infrared Characterization of Near Earth Objects, *Adv. Space Sci.*, **28**, 1117 – 1127.

Price, S.D., M.P. Egan, S.J. Carey, D. Mizuno & T.A. Kuchar (2001) MSX Survey of the Galactic Plane, *Astron. J.*, **121**, 2819 – 2842.

Price, S.D., R. Korte, R. Sample, J.P. Kennealy & R. Gonsalvas (1994) A High Resolution Atlas of the Galactic Plane at 12 and 25 μ m, in *Science with High Spatial Resolution Far-Infrared Data*, S. Terebey & J. Mazzarella (eds), JPL Publication 94-5. N9521749

Price, S.D. & L.P. Marcotte (1980) *An Infrared Survey of the Diffuse Emission Within 5° of the Galactic Plane*, AFGL-TR-80-0182. ADA100289

Price, S.D., L.P. Marcotte & T.L. Murdock (1982) Infrared Mapping of the Galactic Plane II. Medium-Resolution Maps of the Cygnus X Region, *Astron. J.*, **87**, 131 – 140.

Price, S.D., D.R. Mizuno & T.L. Murdock (2003), Thermal Profiles of the Eclipsed Moon, *Adv. Space Res.*, **31**, 2299 – 2304.

Price, S.D. & T.L. Murdock (1983) *The Revised AFGL Infrared Sky Survey Catalog*, AFGL-TR-83-0161. ADA134007

Price, S.D. T.L. Murdock & L.P. Marcotte (1980) Infrared Observations of the Zodiacal Dust Cloud, *Astron. J.*, **85**, 765 – 771.

Price, S.D., T.L. Murdock, A. McIntyre, R.E. Huffman & D.E. Paulsen (1980) On the Diffuse Cosmic Ultraviolet Background Measured from ARIES A-8, *Astrophys. J.*, **240**, L1 – L2.

Price, S.D., T.L. Murdock & K. Shivanandan (1981) The Air Force Geophysics Laboratory, AFGL, Infrared Sky Survey Experiments, *Proc. SPIE*, **280**, 33 – 44.

Price, S.D., P.V. Noah, D. Mizuno, R.G. Walker & S. Jayaraman, (2003) Midcourse Space Experiment Mid-Infrared Measurements of the Thermal Emission from the Zodiacal Dust Cloud, *Astron. J.*, **125**, 962 – 983.

Price, S.D. & A. Omont (2004) Mid-Infrared Surveys of the Galactic Plane, *Astron. Soc. Pac. Conf. Ser.*, **317**, 123 – 132.

Price, S.D., C. Paxson, C. Engelke & T.L. Murdock (2004a) Spectral Irradiance Calibration in the Infrared. XV. Absolute Calibration of Standard Stars by Experiments on the Midcourse Space Experiment, *Astron. J.*, **128**, 889 – 910.

Price, S.D., C. Paxson, E. Engelke, T.L. Murdock & K.E. Kraemer (2004b) *Absolute Infrared Calibration of Standard Stars by the Midcourse Space Experiment*, AFRL-VS-HA-TR-2004-1109. ADA458662

Price, S.D., K. Shivanandan & T.L. Murdock (1983) *The Far-Infrared Sky Survey Experiment Final Report*, AFGL-TR-83-0055. ADA131966

Price, S.D., K. Shivanandan, T.L. Murdock & P.F. Bowers (1983) The Brighter 94 Micron Sources Observed by the Far-Infrared Sky Survey Experiment, *Astrophys. J.*, **275**, L25 – L29.

Price, S.D., G.C. Sloan & K.E. Kraemer (2002) Artifacts at 4.5 and 8.0 Microns in Short-Wavelength Spectra from the Infrared Space Observatory, *Astrophys. J.*, **565**, L55 – L58.

Price S.D. & R.G. Walker (1976) *The AFGL Four Color Infrared Sky Survey: Catalog of Observations at 4.2, 11.0, 19.8 and 27.4 μ m*, AFGL-TR-76-0208. ADA034448

Price S.D. & R.G. Walker (1978) *Calibration of the HI STAR Sensors*, AFGL-TR-78-0172. ADA061020

Puetter, R.C., T.R. Gosnell & A. Yahil (2005) Digital Image Reconstruction: Deblurring and Denoising, *Ann. Rev. Astron. Astrophys.*, **43**, 139 – 194.

Pugascheva, S.G. & V.V. Shevchenko (2001) The Spatial Angular Function of Thermal Emission of the Moon, *Solar Sys. Res.*, **35**, 181 – 189.

Pugascheva, S.G., V.V. Shevchenko, S.G. Yakovlev & V.M. Kibardin (1999) Calibration of the Moon's Infrared Images from Geostationary Satellite GOMS, *Lun. Planet Sci.*, **XXX**, Abst #1247.

Puget, J.L., A. Léger & F. Boulanger (1985) Contribution of Large Polycyclic Aromatic Molecules to the Infra-Red Emission of the Interstellar Medium, *Astron. Astrophys.* **142**, L19 – L22.

Racca, G. (1995) Moon Surface Thermal Characteristics for Moon Orbiting Spacecraft Thermal Analysis, *Planet. Space Sci.*, **43**, 835 – 842.

Ramsey, R.C. (1961) Spectral Irradiances from Stars and Planets, above the Atmosphere, from 0.1 to 100.0 Microns, *App. Opt.*, **1**, 465 – 471.

Rappaport, S.A., R.J. Rieder, W.P. Reidy, R.L. McNutt Jr., J.J. Atkinson, and D.E. Paulsen (1993) Remote X Ray Measurements of the Electron Beam From the EXCEDE III Experiment, *J. Geophys. Res.*, **98**(A11), 19,093–19,098.

Reach, W.T. (1988) Zodiacal Emission I. Dust near the Earth's Orbit, *Astrophys. J.*, **335**, 468 – 485.

Reach, W.T. (1991) Zodiacal Emission. II. Dust near the Ecliptic, *Astrophys. J.*, **369**, 529 – 543.

Reach, W.T., A. Abergel, F. Boulanger, F.-X. Désert, M. Pérault, J.-P. Bernard, J. Blommaert, C. Cesarsky, D. Cesarsky, L. Metcalfe, J.-L. Puget, F. Sibille & L. Vigroux (1996) Mid-Infrared Spectrum of the Zodiacal Light, *Astron. Astrophys.*, **315**, L381 – L384.

Reach, W.T., B.A. Franz & J.L. Weiland (1997) The Three-Dimensional Structure of the Zodiacal Dust Bands, *Icarus*, **127**, 461 – 484

Reach, W.T., B.A. Franz, J.L. Weiland, M.G. Hauser, T.N. Kelsall, E.L. Wright, G. Rawley, S.W. Stemwedel & W.J. Spiesman (1995) COBE Diffuse Infrared Background Experiment Confirms Near-Earth Dust Ring Around Sun, *Nature*, 521 – 523.

Reach, W.T., M.S. Kelley & M.V. Sykes (2007) A Survey of Debris Trails from Short Period Comets, *Icarus*, **191**, 298 – 322.

Reach, W.T., S.T. Megeath, M. Cohen, J. Hora, S. Carey, J. Surace, S.P. Willner, P. Barmby, G. Wilson, W. Glaccum, P. Lowrance, M. Marengo & G. Fazio (2005) Absolute Calibration of the Infrared Array Camera on the Spitzer Space Telescope, *Pub. Astron. Soc. Pac.*, **117**, 978 – 990.

Reach, W.T., P. Morris, F. Boulanger & K. Okumura (2003) The Mid-Infrared Spectrum of the Zodiacal and Exozodiacal Light, *Icarus*, **164**, 384 – 403.

Rebolo, R., M.R. Zapatero Osorio & E.L. Martín (1995) Discovery of a Brown Dwarf in The Pleiades Star Cluster, *Nature*, **377**, 129 – 131.

Regan, F. (1988) *LAIRTS Documentation Executive Summary*, AFGL-TR-88-0242.
 ADA204075

Renes, J.J. (1979) B-Spline Approximation - Background and Algorithms, in *Workshop on Image Processing in Astronomy: Proc. of the 5th Colloq. Astrophys.*, G. Sedmak, M. Capaccioli, R.J. Allen (eds.), Pub. Osservatorio Astronomico di Trieste, 329 – 338.

Renes, J.J. & D.A. Beintema (1981) The Use of B-Spline Approximation and an Array Processor in the IRAS Ground Operations and Preliminary Analysis Facility, *J. British Interplanetary Soc.*, **34**, 123 – 128.

Rense, W.A. (1953) Intensity of Lyman-Alpha Line in the Solar Spectrum, *Phys. Rev.*, **91**, 299 – 302.

Reynolds, R.J., G.J. Madsen & S.H. Moseley (2004) New Measurements of the Motion of the Zodiacial Dust, *Astrophys. J.*, **612**, 1206 – 1213.

Rice, W., C.J. Lonsdale, B.T. Soifer, G. Neugebauer, E.L. Kopan, L.A. Lloyd, T. de Jong & H.J. Habing (1988) A Catalog of IRAS Observations of Large Optical Galaxies, *Astrophys. J. Supp.*, **68**, 91 – 127.

Rice, W. (1993) An Atlas of High-Resolution IRAS Maps of Nearby Galaxies, *Astron. J.*, **105**, 67 – 96.

Rickard, L.J., S.W. Stemwedel & S.D. Price (1990) Observations of the Galactic Plane by the Zodiacial Infrared Project, *Astron. Soc. Pac. Conf. Ser.*, **12**, 323 – 324.

Rickard, L.J., S.W. Stemwedel & S.D. Price (1991) Reconciling ZIP and IRAS Observations of the Zodiacial Background, *Amer. Inst. Phys. Conf. Proc.*, **222**, 183 – 186.

Rieke, G.H. (2006) *The Last of the Great Observatories, Spitzer and the Era of Faster, Better, Cheaper at NASA*, Univ. Ariz. Press. Tucson.

Rieke, G.H. (2007) Infrared Detector Arrays for Astronomy, *Ann. Rev. Astron. Astrophys.*, **45**, 77 – 115.

Rieke, G.H., M. Blaylock, L. Decin, C. Engelbracht, P. Ogle, E. Avrett, J. Carpenter, R.M. Cutri, L. Armus, K. Gordon, R.O. Gray, J. Hinz, K. Su & C.N.A. Willmer (2008) Absolute Calibration in the Infrared, *Astron. J.*, **135**, 2245 – 2263.

Rieke, G.H., M.J. Lebofsky, & F.J. Low (1985) An Absolute Photometric System at 10 and 20 μ m, *Astron. J.*, **90**, 900 – 906.

Rieke, G.H. & F.J. Low (1972a) Infrared Photometry of Extragalactic Sources, *Astrophys. J.*, **176**, L95 – L100.

Rieke, G.H., & F.J. Low (1972b) Variability of Extragalactic Sources, *Astrophys. J.*, **176**, L115 – L119.

Rieke, G.H. E.T. Young, C.W. Engelbracht, D.M. Kelly, F.J. Low, E.E. Haller, J.W. Beeman, K.D. Gordon, J.A. Stansberry, K.A. Misselt, J. Cadien, J.E. Morrison, G. Rivlis, W.B. Latter, A. Noriega-Crespo, D.L. Padgett, K.R. Stapelfeldt, D.C. Hines, E. Egami, J. Muzerolle, A. Alonso-Herrero, M. Blaylock, H. Dole, J.L. Hinz, E. Le Floch, C. Papovich, P.G. Pérez-González, P.S. Smith, K.Y.L. Su, L. Bennett, D.T. Frayer, D. Henderson, N. Lu, F. Masci, M. Pesenson, L. Rebull, J. Rho, J. Keene, S. Stolovy, S. Wachter, W. Wheaton, M.W. Werner, & P.L. Richards (2004) The Multiband Imaging Photometer for *Spitzer* (MIPS), *Astrophys. J. Supp.*, **154**, 25 – 29.

Rigden, J.S. (2007) Eisenhower, Scientests, and Sputnik, *Phys. Today.*, **60** (6), 47 – 52.

Ristorcelli, I., M. Giard, C. Meny, G. Serra, J.M. Lamarre, C. Le Naour, J. Leotin, & F. Pajot (1994) The Diffuse Galactic Emission at 6.2 Micrometer, *Astron. Astrophys.*, **286**, L23 – L26.

Robitaille, T.P., M. Cohen, B.A. Whitney, M. Meade, B. Babler, R. Indebetouw & E. Churchwell (2007) Infrared Point-Source Variability between Spitzer and Midcourse Space Experiemnt Suirveys of the Galactic Plane, *Astron. J.*, **134**, 2099 – 2112.

Rocha-Pinto, H.J., S.R. Majewski, M.F. Skrutskie, J.D. Crane & R.J. Patterson (2004) Exploring Halo Substructure with Giant Stars: A Diffuse Star Cloud or Tidal Debris around the Milky Way in Triangulum-Andromeda, *Astrophys. J.*, **615**, 732 – 737.

Roggemann, M.C., B.M. Welsh & R.Q. Fugate (1997) Improvine the Resolution of Ground-Based Telescopes, *Rev. Modern Phys.*, **69**, 437 -503.

Röser, S. & H.J. Staude (1978) The Zodiacial Light from 1500 Å to 60 Micron, *Astron. Astrophys.* **67**, 381 – 394.

Rosse, 4th Earl (1869) On the Radiation of Heat from the Moon, *Proc. Roy. Soc. London*, **17**, 436 – 443.

Rosse, 4th Earl (1870) On the Radiation of Heat from the Moon, no II *Proc. Roy. Soc. London*, **19**, 9 – 14.

Rosse, 4th Earl (1873) On the Radiation of Heat from the Moon, *Phil. Trans. Roy. Soc. London*, **163**, 597 – 627.

Rowan-Robinson, M. (1993) *Ripples in the Cosmos. A View behind the Scene of the New Cosmology*, W.H. Friedman/Spektrum.

Rudy, R.J., T.R. Gosnell & S.P. Willner (1979) *Ground-Based Measurements of Sources in the AFGL Infrared Sky Survey*, AFGL-TR-79-0172. ADA081381

Ruelas-Mayorga, R.A. (1991a) Distribution and Studies of the Infrared Stellar Population in the Galaxy. II. The Data Base, *Rev. Mex. Astron. Astrofis.*, **22**, 43 – 97.

Ruelas-Mayorga, R.A. (1991b) Distribution and Studies of the Infrared Stellar Population in the Galaxy. I. The Model, *Rev. Mex. Astron. Astrofis.*, **22**, 27 – 41.

Rust, C.F. (1938) Spectral Types and Radiometric Observations of Stars of Large Infrared Index, *Astrophys. J.*, **88**, 525 – 527.

Ryadov, V. Ya., N.I. Furashov & G.A. Sharonov (1964) Measurements of the Moon's Natural Infrared Thermal Radiation, *Soviet Astron.*, **8**, 82 – 85.

Ryan, C., (1995) *The Pre-Astronauts: Manned Ballooning on the Threshold of Space*, US Naval Inst. Press.

Saari, J.M & R.W. Shorthill (1963) Isotherms of Crater Regions on the Illuminated and Eclipsed Moon, *Icarus*, **2**, 115 – 136.

Saari, J.M. & R.W. Shorthill (1966) *Isotherms in the Equatorial Region of the Totally Eclipsed Moon*, Boeing Sci. Research Doc. D1-82-0530. AD0633033

Saari, J.M. & R.W. Shorthill (1967a) *Isothermal and Isophotic Atlas of the Moon*, NASA CR- 855. N6737303

Saari, J.M. & R.W. Shorthill (1967b) Review of Lunar Infrared Observations, in *Physics of the Moon: Science and Tech Ser.*, **13**, Amer. Astronaut. Soc. Pub. (Tarzana CA).

Saari, J.M., R.W. Shorthill & T.K. Deaton (1966) Infrared and Visible Images of the Eclipsed Moon of December 19, 1964, *Icarus*, **5**, 635 – 659

Salisbury, J.W. (1968) *Bibliography of Lunar and Planetary Research, Supplement No. 3-1967*, AFCRL-TR-68-05331. AD0700051

Salisbury, J.W. & C.F. Campens (1961) *Location of a Lunar Base*, Geophysics Research Directorate Tech Note **71**.

Salisbury, J.W., P.E. Glaser, B.A. Stein & B. Vonnegut (1963) Adhesive Behavior of Silicate Powders in Ultra-high Vacuum, *J. Geophys. Res.*, **69**, 235 – 242.

Salisbury, J.W., D.G. Murcray, W.J. Williams & R.D. Blatherwick (1995) Thermal Infrared Spectra of the Moon, *Icarus*, **115**, 181 – 190.

Salisbury, J.W. & R.A. Van Tassel (1962) State of Lunar Dust, *Pub. Astron Soc. Pac.*, **74**, 245 – 248.

Salisbury, J.W., R.A. Van Tassel & J.E.M. Adler (1962) *Bibliography of Lunar and Planetary Research, 1961*, AFCRL-TR-62-676. AD0428471

Salisbury, J.W., R.K. Vincent, L.M. Logan & G.R. Hunt (1970) Infrared Emissivity of Lunar Surface Features 2. Interpretation, *J. Geophys. Res.*, **75**, 2671 – 2682.

Sargent, S.D. (1997) Temperature-dependent Responsivity Correction for the SPIRIT III Radiometer, *Opt. Eng.*, **36**, 2948 – 2955.

Sayre, G., D. Arrington, W. Eisenman & J. Merriam, (1976) Characteristics of Detectors Having Partially Illuminated Sensitive Areas In *Minutes of the IRIS Specialty Group on IR Detectors Meeting*, Environ. Res. Inst. Mich.

Scheer, D.J. & J.D. Kraus (1967) A High-Sensitivity Survey of the North Polar Galactic Region at 1415 MHz, *Astron. J.*, **72**, 536 – 543.

Schick, S. & G. Bell (1997) Performance of the SPIRIT III Cryogenic System, *Proc SPIE*, **3122**, 69 – 77.

Schuerman, D.W. (1980) Evidence that the Properties of Interstellar Dust beyond 1 AU are not Homogeneous, *Proc. IAU Symp.* **90**, 71 – 74.

Schurin, R. & R.E. Ellis (1966) First- and Second-Overtone Intensity Measurements for CO and NO, *J. Chem. Phys.*, **45**, 2528 – 2532.

Scilar, N. (1983) Development Status of Silicon Extrinsic Detectors, *Proc. SPIE*, **443**, 11 – 41.

Scientific American (1878) **39**, 52.

Sebring, T.A., E. Dunham & R.L. Millis (2004) The Discovery Channel Telescope: A Wide Field Telescope in Northern Arizona, *Proc. SPIE*, **5489**, 658 – 666.

Seidel, A. & T. Passvogel (1994) The Cryosystems for Infrared Missions GIRL, IBSS and ISO, *Proc. SPIE*, **2268**, 318330.

Seiden, P.E., L.S., Schulman & B.G. Elmegreen (1984) A Galactic Disk is not a True Exponential, *Astrophys. J.*, **282**, 95 – 100.

Sellgren, K. (1984) The Near-Infrared Continuum Emission of Visual Reflection Nebulae, *Astrophys. J.*, **227**, 623 – 633.

Shanks, J.L. (1967) Recursion Filters for Digital Processing, *Geophys.*, **32**, 33 – 51.

Shenoy, S.S., S.J. Carey, A. Noriega-Crispo & MIPSGAL Data Processing Group (2008) 24 μ m Point Source Catalog along the Galactic Plane: MIPSGAL PSC v1.0, *Bull. Amer. Astron. Soc.*, **40**, 213.

Shivanandan, K. (1988) *Far Infrared Imaging Spectrometer for Large Aperture Infrared Telescope Sytem*, AFGL-TR-88-0244. ADA201652

Shivanandan, K., D.P. McNutt, S. Price & T. Murdock (1978) Far Infrared Sky Survey Experiment, *Proc. SPIE*, **132**, 75 – 80.

Shoemaker, E.M. (chair.) (1995) *Asteroid and Comet Impact Hazards. Report of the Near-Earth Object Survey Working Group*, NASA, Wash. DC.

Shorthill, R.W. (1973) Infrared Atlas Charts of the Eclipsed Moon, *Moon*, **7**, 22 – 45.

Shorthill, R.W. (1990) *Infrared Observations of the Solar System in Support of Large Aperture Infrared Telescope (LARITS): Calibration*, AFOSR-TR-90-0645. ADA222222

Shorthill, R.W., H.C. Borough & J.M. Conley (1960), Enhanced Lunar Thermal Radiation During a Lunar Eclipse, *Pub. Astron. Soc. Pac.*, **72**, 481 – 485.

Shorthill, R.W. & J.M. Saari (1965a), Nonuniform Cooling of the Eclipsed Moon: A Listing of Thirty Prominent Anomalies, *Science*, **150**, 210 – 212.

Shorthill, R.W. & J.M. Saari (1965b), Recent Results of Lunar Eclipse Measurements Showing Hot Spots, in *Post Apollo Space Exploration, Advances in Astronautical Sciences*, **20**, 545 – 556.

Sigethy, R. 1980, *The Air Force Organization for Basic Research 1945 – 1970: A Study in Change*, PhD Dissertation, the American University (Univ Microfilms)

Silbermann, N.A. (1989) *An Investigation of the IRAS Point Response Functions*, MSci. Thesis, Univ. Wyoming.

Silverberg, R.F., M.G. Hauser, J.C. Mather, D.Y. Gezari, T. Kelsall & L.H. Cheung (1979) A 1.2 Meter Balloon-Borne Telescope for a Submillimeter Wave Sky Survey, *Proc. SPIE*, **172**, 149 – 154.

Simon, R., J.M. Jackson, J.M. Rathborne & E.T. Chambers (2006) A Catalog of Midcourse Space Experiment Infrared Dark Cloud Candidates, *Astrophys. J.*, **639**, 227 – 236.

Simon, T. & H.M. Dyck (1975) Silicate absorption at 18 μm in two peculiar infrared sources, *Nature*, **253**, 101 – 102.

Simons, D. (1958) Manned Balloon Capabilities for Astronomical Observations, *Pub. Astron. Soc. Pac*, **70**, 69 – 74.

Simonson, S.C., III & G.L. Mader (1977) Motions Near the Galactic Center and the “3-kpc Arm”, *Astron. Astrophys.*, **27**, 337 – 350.

Simpson, J.P. & F.C. Witteborn (1977) Effects of the Shuttle Contamination Environment on a Sensitive Infrared Telescope, *App. Opt.*, **16**, 2051 – 2073.

Simpson, J.P., F.C. Witteborn, M. Cohen & S.D. Price (1999) The Mid-Infrared Spectrum of the Galactic Center, a Starburst Nucleus, *Astron. Soc. Pac. Conf. Ser.*, **186**, 527 – 535.

Simpson, J.P., F.C. Witteborn & S. D. Price (1998) MSX Spectra of the Orion Nebula, *Astrophys. J.*, **508**, 268 – 274.

Sinton, W.M. (1959) A Pyrometer for Planetary Temperature Measurements, *Lowell Obs. Bull.* No. 104, **4**, 260 – 263.

Sinton, W.M. (1960) Eclipse Temperature of the Lunar Crater Tycho, *Lowell Obs. Bull.* No. 108, **5**, 25 – 26.

Sinton, W.M. (1962a) Temperatures on the Lunar Surface, Ch. 11 in *Physics and Astronomy of the Moon, 1st Ed.*, Z. Kopal (ed), Academic Press, NY, 407 – 428.

Sinton, W.M. (1962b) Eclipse Temperatures of the Lunar Crater Tycho, *Proc. IAU Symp.*, **14**, 469 – 474.

Sinton, W.M. (1986) Through the Infrared with Logbook and Lantern Slides A History of Infrared Astronomy from 1868 to 1960, *Pub. Astron. Soc. Pac.*, **98**, 246 – 251.

Sinton, W.M., H.L. Johnson & B. Iriarte (1959) *The Albedos and Phase Variations of Uranus and Neptune (and) the Sun as a Variable Star*, AFCRC-TN-59-271. AD0213854

Sinton, W.M. & J. Strong (1960a) Radiometric Observations of Mars, *Astrophys. J.*, **131**, 449 – 459.

Sinton, W.M. & J. Strong (1960b) Radiometric Observations of Venus, *Astrophys. J.*, **131**, 470 – 490.

Skrivanek, R.A., S.A. Chrest & R.G. Carnevalle (1969) Particle Collection Results from Recent Rocket and Satellite Experiments, *Space Research*, **IX**, 129 – 130.

Skrivanek, R.A., R.F. Carnevalle & R.D. Sarkesian (1970) Results of in-flight Shadowing Performed on an ESRO Rocket Flight of 7 June 1968, *Space Research*, **X**, 281 – 286.

Skrutskie, M.F., R.M. Cutri, R. Stiening, M.D. Weinberg, S. Schneider, J.M. Carpenter, C. Beichman, R. Capps, T. Chester, J. Elias, J. Huchra, J. Liebert, C. Lonsdale, D.G. Monet, S. Price, P. Seitzer, T. Jarrett, J.D. Kirkpatrick, J.E. Gizis, E. Howard, T. Evans, J. Fowler, L. Fullmer, R. Hurt, R. Light, E.L. Kopan, K.A. Marsh, H.L. McCallon, R. Tam, S. Van Dyk & S. Wheelock (2005) The Two Micron All Sky Survey (2MASS), *Astron. J.*, **131**, 1163 – 1183.

Sloan, G.C., K.E. Kraemer, M. Matsuura, P.R. Wood, S.D. Price & M.P. Egan (2006) Mid-Infrared Spectroscopy of Carbon Stars in the Small Magellanic Cloud, *Astrophys. J.*, **645**, 1118 – 1130.

Sloan, G.C., K.E. Kraemer, S.D. Price & R.F. Shipman (2003) A Uniform Database of 2.4 – 45.4 Micron Spectra from the Infrared Space Observatory Short Wavelength Spectrometer, *Astrophys. J. Supp.*, **147**, 379 – 401.

Sloan, G.C., K.E. Kraemer, P.R. Wood, A.A. Zijlstra, J. Bernard-Salas, D. Devost & J.R. Houck (2008) The Magellanic Zoo: Mid-Infrared Spitzer Spectroscopy of Evolved Stars and Circumstellar Dust in the Magellanic Clouds, *Astrophys. J.*, **686**, 1056 – 1081.

Sloan, G.C., P.D. LeVan & P.C. Tandy (1993) *Report on Operations of the Air Force Geophysics Laboratory Infrared Array Spectrometer*, PL-TR-93-2012. ADA273800

Sloan, G.C., N. Matunaga, M. Matsuura, A.A. Zijlstra, K.E. Kraemer, P.R. Wood, J. Nieusma, J. Bernard-Salas, D. Devost & J.R. Houck (2010) Spitzer Spectroscopy of Mass Loss and Dust Production by Evolved Stars in Globular clusters, *Astrophys. J.*, (submitted)

Sloan, G. C. & S.D. Price (1995) Silicate Emission at 10 Microns in Variables on the Asymptotic Giant Branch, *Astrophys. J.*, **451**, 758 – 767.

Smith, B.A. & J.W. Salisbury (1962) Evaluation of Cloud Croft, New Mexico Site for a United States Air Force Planetary Telescope, AFCRL Tech. Rep. 1064. AD274987

Smith, B.J. (2003) Infrared Colors and Variability of Evolved Stars from COBE DIRBE Data, *Astron. J.*, **126**, 935 – 963.

Smith, B.J., D. Leisawitz, M.W. Castelaz & D. Luttermoser (2002) Infrared Light Curves of Mira Variable Stars from COBE DIRBE Data, *Astron. J.*, **123**, 948 – 965.

Smith, B.J. & S.D. Price (2009) Warm Era COBE DIRBE Infrared Light Curves of Dusty Evolved Stars, *Astron. Soc. Pac. Conf. Ser.*, **413**, 247 – 351.

Smith, B.J., S.D. Price & R.I. Baker (2004) The COBE DIRBE Point Source Catalog, *Astrophys. J. Supp.*, **154**, 673 – 704.

Smith, B.J., S.D. Price & A.J. Moffet (2006) Phase Lags in the Optical-Infrared Light Curves of Asymptotic Giant Branch Star, *Astron. J.*, **131**, 612 – 620.

Smith, C.P. (1858) *Tenerife, an Astronomer's Experiment*, Lovell Reeve (London).

Smith, D.R. (1989) Evidence for Off-Axis Leakage Radiance in High-Altitude IR Rocketborne Measurements. *Proc. SPIE*, **967**, 30 – 36.

Smith, D.R., A.J. Ratkowski, S.M. Adler-Golden, M.W. Matthew & W.F. Grieder (1991) *SPIRIT I Final Flight Report*, PL-TR-91-2226. ADA257088

Smith, G.M. & G.F. Squibb (1984) Development of the First Infrared Satellite Observatory, AIAA-84-0079, AIAA 22nd Aerospace Sciences Mtg in Reno, Nevada.

Smith, N., M.P. Egan, S. Carey, S.D. Price, J.A. Morse & P.A. Price (2000) Large Scale Structure of the Carina Nebula, *Astrophys. J.*, **532**, L145 – L148.

Smoot, G.F. (1990) *Cosmic Background Radiation Study Sunyaev-Zel'dovich Effect and Small Angular Scale Anisotropy*, AFOSR-TR-90-0826. ADA224782

Smoot, G. & K. Davidson (1994) *Wrinkles in Time*, William Morrow Pub.

Soberman, R. & L. Della Lucca (1961) *Micrometeorite Measurements from the MIDAS II Satellite*, Geophysics Research Directorate Notes, No. **72**, AFCRL-1053. AD 0268556 & *Smithsonian Contributions to Astrophys.sics*, **7**, 1063

Soberman, R.K. & C.L. Hemenway (1965) Meteoritic Dust in the Upper Atmosphere, *J. Geophys. Res.*, **70**, 4943 – 4949.

Sodickson, L., S. Orr, J. Tadelli & J. Youngstrom (1968) *Pointed Lunar Experiment*, AFCRL-TR-68-0411. AD0675144

Soifer, B.T. (1972) *Rocket Infrared Multicolor Observations of the Interplanetary Medium, Hydrogen-II Regions, and the Galactic Center Region*, PhD Thesis, Cornell University.

Soifer, B.T., J.R. Houck & M. Harwit (1971) Rocket-Infrared Observations of the Interplanetary Medium, *Astrophys. J.*, **168**, L73 – L78.

Soifer, B.T., J.R. Houck & G. Neugebauer (1987) The IRAS View of the Extragalactic Sky, *Ann. Rev. Astron. Astrophys.*, **25**, 187 – 230.

Soifer, B.T. & J.L. Pipher (1978) Infrared Astronomy, *Ann Rev. Astron. Astrophys.*, **16**, 335 – 369.

Soifer, B.T., J.L. Pipher & J. Houck (1972) Rocket Infrared Observations of H II Regions, *Astrophys. J.*, **177**, 315 – 323.

Soref, R.A., (1967) Extrinsic IR Photoconductivity of Si Doped with B, Al, Ga, P, As or Sb, *J. App. Phys.*, **38**, 5201 – 5209.

Spahr, T.B., C.W. Hergenrother, S.M. Larson & H. Campins (1996) High Ecliptic Latitude Asteroid and Comet Surveying with the Catalina Schmidt, *Astron. Soc. Pac. Conf. Ser.*, **107**, 115 – 122.

Spitzer, Jr., L. (1960) Space Telescopes and Components, *Astron. J.*, **65**, 242 – 263.

Stair, Jr., A.T. (1970) Fourier Spectroscopy at the Air Force Cambridge Research Laboratories, *Aspen International Conf. Fourier Spectroscopy*, 127 – 138, AFCRL-71-0019. AD0724100

Stair, Jr., A.T. (1996) MSX Design Parameters Driven by Targets and Backgrounds, *Johns Hopkins APL Tech Digest*, **17**, 11 – 18.

Stair, Jr., A.T., J. Prichard, I. Coleman, C. Bohne, W. Williamson, J. Rodgers & W.T. Rawlins (1983) Rocketborne Cryogenic (10K) High-Resolution Interferometer, Spectrometer Flight HIRIS: Auroral and Atmospheric IR Emission Spectra, *App. Opt.*, **22**, 1056 – 1088.

Stair, Jr. A.T., R.D. Sharma, R.M. Nadile, D.J. Baker & W.F. Grieder (1985) Observations of Limb Radiance with Cryogenic Spectral Infrared Rocket Experiment, *J. Geophys. Res.*, **90**, 9763 – 9775.

Stebbins, J. (1908) The Color Sensibility of Selenium Cells, *Astrophys. J.*, **27**, 183 – 187.

Stein, W.A. (1975) Recent Revelations in Infrared Astronomy, *Pub. Astron. Soc. Pac.*, **87**, 5 – 16.

Stetson, S.K., D.B. Reynolds, M.G. Stapelbroek & R.L. Sterner (1986) Design and Performance of Blocked-Impurity-Band Detector FPAs, *Proc. SPIE*, **686**, 48 – 65.

Stokes, G.H., J.B. Evans, H. Viggh, F.C. Shelly & E.C. Pearce, (2000) Lincoln Near Earth Asteroid Research (LINEAR), *Icarus*, **148**, 21 – 28.

Stokes, G.H., C. von Braun, R. Sridharan, D. Harrison & J. Sharma (1998) The Space-Base Visible Program, *Lincoln Lab. J.*, **11**, 205 – 238. (*AIAA Space Conf. 2000*, 2000-5334)

Stone, E.J. (1870a) Approximate Determinations of the Heating-Powers of Arcturus and α Lyrae, *Proc. Roy. Soc.*, **18**, 159 – 165.

Stone, E.J. (1870b) Heating Powers of Stars, *Mon. Not. Roy. Astron. Soc.*, **30**, 107 – 109.

Stone, R. (2008) Preparing for Doomsday, *Science*, **319**, 1326 – 1329.

Stone, T.C., H.H. Kieffer & J.M. Anderson (2002) Status and Use of Lunar Irradiance for On-Orbit Calibration, *Proc. SPEI*, **4483**, 165 – 175.

Strom, S.E., K.M. Strom, G.L. Grasdalen & R.W. Capps (1974) Infrared Observations of H II Regions in External Galaxies, *Astrophys. J.*, **193**, L7 – L10.

Strong, J. (1959), *Planetary Astronomy from Satellite Substitute Vehicles I, A Review of Meteorological and Astrophysical Programs for Observatories Carried Effectively into Space by Satellite Substitute Vehicles* AF Missile Development Center Tech. Note AFMDC-TR-59-22. AD0226070

Sugita, H., T. Nakagawa, H. Murakami, A. Okamoto, H. Nagai, M. Murakami, K. Narasaki, M. Hirabayashi & the SPICA Working Group (2006) Cryogenic Infrared Mission “JAXA/SPICA” with Advanced Cryocoolers, *Cryogenics*, **46**, 149 – 157.

Swanson, P.N., S. Gulkis, T.B.H. Kuiper & M. Kiya (1983) Large Deployable Reflector (LDR) A Concept for an Orbiting Submillimeter-Infrared Telescope for the 1990s, *Opt. Eng.*, **22**, 725 – 731.

Sweeney, D.W. & the LSST Collaboration (2006) Overview of the Large Synoptic Survey Telescope Project, *Proc. SPIE*, **6267**, 676706: 1 – 9.

Sweeney, L.H., T.F. Heinsheimer, F.F. Yates, S.P. Maran, J.R. Lesh & T.A. Nagy (1977) High-Precision Infrared Sky Survey at Wavelength $2.7 \mu\text{m}$, *Proc. SPIE*, **124**, 125 – 131.

Sweeney, L.H., T.F. Heinsheimer, F.F. Yates, S.P. Maran, J.R. Lesh & T.A. Nagy (1978) *Interim Equatorial Infrared Catalogue, Number 1*, Aerospace Report TR-0078(3409-20)-1. ADA074640

Sweeney, L.H. & T. Richardson (1995) *Equatorial Infrared Catalog*, VizieR On-line Catalog: ii/161. Originally published as a Space Applications Corp. internal report (1990).

Swenson, G., R. Raideren, D. Jennings & M. Ahmadjian (1994) Vehicle Glow Measurements on STS-62, *AIAA Presentation 95-0492 at the 33rd Aerospace Sciences Meeting*.

Swift, I.H. (1962) Performance of Background Limited Systems for Space, *Infrared Phys.*, **2**, 19 – 30.

Swinyard, B. & T. Nakagawa (2009) The Space Infrared Telescope for Cosmology and Astrophysics: SPICA A Joint Mission Between JAXA and ESA (2009), *Exp. Astron.*, **23** 193 – 209.

Sykes, M.V. (1988) IRAS Observations of Extended Zodiacal Sources, *Astrophys. J.*, **224**, L56 – L58.

Sykes, M.V. (1990) Zodiacal Dust Bands: Their Relationship to Asteroid Families, *Icarus*, **85**, 267 – 289.

Sykes, M.V., R.M. Cutri, J.W. Fowler, D.J. Tholen, M. Skrutskie, S. Price & E.F. Tedesco, (2000) The 2MASS Asteroid and Comet Survey, *Icarus*, **146**, 161 – 175.

Sykes, M.V., R.M. Cutri, J.W. Fowler, B. Nelson, D.J. Tholen, M. Skrutskie & S. Price (2002) 2MASS Observations of the Solar System, *Proc. Asteroids, Comets, Meteors - ACM 2002 ESA SP-500*, 481 – 484.

Sykes, M.V. & R. Greenberg (1986) The Formation and Origin of the IRAS Zodiacial Dust Bands as a Consequence of Single Collisions Between Asteroids, *Icarus*, **65**, 51 – 69.

Sykes, M.V., R. Greenberg, S.F. Dermott, P.D. Nicholson, J.A. Burns & T.N. Gautier (1989) Dust Bands in the Asteroid Belt, in *Asteroids II*, R.P. Binzel, T. Gehrels & M.S. Maththews (eds.) Tucson: Univ. Ariz., 336 – 367.

Sykes, M.V., L.A. Lebofsky, D.M. Hunten & F. Low (1986) The Discovery of Dust Trails in the Orbits of Periodic Comets, *Science*, **282**, 1115 – 1117.

Sykes, M.V. & R.G. Walker (1992) Cometary Dust Trails. I – Survey, *Icarus*, **95**, 180 – 210.

Szczerba, R. & S.K. Górný (2000) *Post-AGB Objects as a Phase of Stellar Evolution*, Proc. Toruń Workshop R., Szczerba and S.K. Górný (eds), Kluwer Academic Press (Neth,), xi – xii.

Taff, L.C. (1981) A New Asteroid Observation and Search Technique, *Pub. Astron. Soc. Pac.*, **93**, 658 – 660.

Tagliaferri, E., R. Spalding, C. Jacobs, S.P. Worden & A. Erlich (1994) Detection of Meteoroid Impacts by Optical Sensors in Earth Orbit, in *Hazards due to Comets and Asteroids*, T. Gehrels, (ed), Univ. Arizona Press, Tucson.

Talent, D.L., R. Maeda, S. Walton, P. Sydney, Y. Hsu, B. Cameron, P. Kervin, E. Helin, S. Pravdo, K. Lawrence & D. Rabinowitz (2000) A New Home for Neat on the 1.2-m/B37 at AMOS, *Proc. SPIE*, **4091**, 225 – 236.

Tata, R., E.L. Martin, T. Kendall, R. Jameson, A. Magazzu & D. Barrado y Navascués (2006) First Brown Dwarfs from the UKIRT Infrared Deep Sky Survey (UKIDSS), *Mem. Soc. Astron. Ital.*, **77**, 1167.

Tedesco, E.F., A. Cellino & V. Zappalá (2005) The Statistical Asteroid Model. I. The Main-Belt Population for Diameters Greater than 1 Kilometer, *Astron. J.*, **129**, 2869 – 2886.

Tedesco, E.F. & F.-X. Désert (2002) The Infrared Space Observatory Deep Asteroid Survey, *Astron. J.*, **123**, 2070 – 2082.

Tedesco, E.F., M.P. Egan & S.D. Price (2002) The MSX Infrared Minor Planet Survey (MIMPS), *Astron. J.*, **124**, 583 – 591.

Tedesco, E.F., K. Muinonen, & S.D. Price (2000) Space-Based Infrared Near-Earth Asteroid Survey Simulation, *Planet & Space Sci.*, **48**, 801 – 816.

Tedesco, E.F., P.V. Noah, M. Noah, & S.D. Price (2002) The Supplemental IRAS Minor Planet Survey (SIMPS), *Astron J.*, **123**, 1056 – 1085.

Tedesco, E.F., G.J. Veeder, J.W. Fowler & J. Chillemi (1992) *The IRAS Minor Planet Survey*, PL-TR-92-2049. ADA276726

Thomson, J.L. & J.W. Salisbury (1993) The Mid-Infrared Reflectance of Mineral Mixtures (7-14 Microns), *Remote Sensing of the Environment*, **45**, 1 – 13.

Thompson, R. (1994) NICMOS: The Next U.S. Infrared Space Mission, *Proc. SPIE*, **2198**, 1202 – 1213.

Thompson, R. (2008) The Near Infrared Background: Resolved and Identified, *Amer. Inst. Phys. Conf. Proc.*, **990**, 132 – 135.

Thronson, Jr., H.A. & S.D. Price (1982) Infrared Mapping of the Galactic Plane III. Large-Scale Mid-Infrared Structure of W3, W4 and W5, *Astron. J.*, **87**, 1288 – 1294.

Thuan, T.X. (1988) *Infrared Astronomy at Extremely Faint Light Levels in Support of the LAIRTS Program*, AFOSR-TR-88-0040. ADA191497

Thuan, T.X. (1995) *The 12 μ m Contribution of Nearby Galaxies to the Infrared Background*, AFOSR-95-0103. ADA 291 185

Toller, G.N. & J.L. Weinberg (1985) The Change in Near-Ecliptic Zodiacal Light with Heliocentric Distance, *IAU Colloq.*, **85**, 21 – 25.

Tolls, V., G.J. Melnick, M.L.N. Ashby, E.A. Bergin, M.A. Gurwell, S.C. Kleiner, B.M. Patten, R. Plume, J.R. Stauffer, Z. Wang, Y.F. Zhang, G. Chin, N.R. Erickson, R.L. Snell, P.F. Goldsmith, D.A. Neufeld, R. Scheder & G. Winnewisser (2004) Submillimeter Wave Astronomical Satellite Performance on the Ground and in Orbit, *Astrophys. J. Supp.*, **152**, 137 – 162.

Tousey, R. & M.J. Koomen (1967) Particles of Unknown Origin Photographed at Rocket Altitudes, in *The Zodiacal Light and Interplanetary Medium*, J.L. Weinberg (ed) NASA SP-**150**, 109 – 113.

Treffers, R. & M. Cohen (1974) High Resolution Spectra of Cool Stars in the 10 and 20 Micron Regions, *Astrophys. J.*, **188**, 545 – 552.

Trilling, D.E., B. Bhattacharya, W. Bottke, S. Chesley, M. Delbo, J. Emery, G. Fazio, A. Harris, J. Hora, A. Mainzer, M. Mueller, B. Penprase, H. Smith, T. Spahr & J. Stansberry (2009) The Warm Spitzer NEO Survey: Exploring the History of the Inner Solar System and Near Earth Space, *Bull. Amer. Astron. Soc.*, **41**, 716.

Trulsen, J. & A. Wiken (1980) Numerical Simulation of Poynting-Roberson and Collisional Effects in the Interplanetary Dust Cloud, *Astron. Astrophys.* **91**, 155 – 160.

Uemizu, K., J.J. Bock, M. Kawada, A.E. Lange, T. Matsumoto, T. Watabe & S.A. Yost (1998) A Search for a Near-Infrared Halo around NGC 4565, *Astrophys. J.*, **506**, L15 – L18.

Ulrich, B.T., G. Neugebauer, D. McCammon, R.B. Leighton, R.D. Hughes & E.E. Becklin (1966) Further Observations of Extremely Cool Stars, *Astrophys. J.*, **146**, 285 – 289.

Ulrich, B.T., G. Neugebauer, D. McCammon, R.B. Leighton, R.D. Hughes & E.E. Becklin (1967) Erratum: Further Observations of Extremely Cool Stars, *Astrophys. J.*, **147**, 858.

Unavane, M., G. Gilmore, N. Epcstein, G. Simon, D. Tiphéne & B. de Batz (1998) The Inner Galaxy Resolved at IJK Using DENIS Data, *Mon. Not. Roy. Astron. Soc.*, **295**, 119 – 144.

Uy, O.M., R.P. Cain, J.C. Lesho, B.D. Green, G.E. Galica, M.T. Boies, R.E. Wood, D.F. Hall, J.S. Dyer, E.G. Layon & M.C. Osborne (2000) Outgassing of Optical Baffles and Primary Mirror During Cryogen Depletion of a Space-Based Infrared Sensor. *Proc, SPIE*, **4096**, 11 – 21.

van Dijk, M.H.H., P.B. Bosma, & J.W. Hovenier (1988) Interpretation of the Zodiacal Light on Terms of a Finite Dust Cloud, *Astron. Astrophys.*, **211**, 373 – 378.

van Driel, W., Th. de Graauw, T. de Jong & P.R. Wesselius (1993) IRAS CPC Observations of Galaxies. I. Catalog and Atlas, *Astron. Astrophys. Supp.*, **101**, 207 – 252.

Van Tassel, R.A. (1968) A Lunar Infrared Spectrum from a Balloon-Borne System, *Icarus*, **8**, 486 – 491.

Van Tassel, R.A. & J.W. Salisbury (1964) The Composition of the Martian Surface, *Icarus*, **3**, 264 – 269.

Van Tassel, R.A. & I. Simon (1964) Thermal Emission Characteristics of Mineral Dusts, in *The Lunar Surface Layer*, J.W. Salisbury and P.E. Glaser (eds.), Academic Press, New York, 445 – 468.

Vardya, M.S., T. de Jong & F.J. Willems (1986) IRAS Low-Resolution Spectrograph Observations of Silicate and Molecular SiO Emission in Mira Variables, *Astrophys. J. Lett.*, **304**, L29 – L32.

Vauglin, I., J. Rousseau, G. Paturel, J. Borsenberger, N. Epchtein, P. Fouqué, S. Kimeswenger, T. Le Bertre & G.A. Mamon (2002) Serendipitous Detection of Galaxies Behind the Milky Way from the DENIS Survey, *Astron. Astrophys.*, **387**, 1 – 7

Venemans, B.P., R.G. McMahon, S.J. Warren, E.A. Gonzalez-Solares, P.C. Hewett, D.J. Mortlock, S. Dye & R.G. Sharp (2007) The Discovery of the First Luminous $z \sim 6$ Quasar in the UKIDSS Large Area Survey, *Mon. Not. Roy. Astron. Soc.*, **376**, L76 – L80.

Viehmann, W. & A.G. Eubanks (1972), *Effects of Surface Contamination on the Infrared Emissivity and Visible-Light Scattering of Highly Reflective Surfaces at Cryogenic Temperatures*, NASA TN C-6585. N7215623

Vogler, K.J., P.E. Johnson & R.W. Shorthill (1991) Modeling the Non-Grey-Body Thermal Emission from the Full Moon, *Icarus*, **92**, 80 – 93.

Volk, K. & M. Cohen (1989) On the Calibration of the IRAS Low-Resolution Spectra, *Astron. J.*, **98**, 1918 – 1934.

Voss, L. (1997) Military Satellite Brings Civilian Benefits, *Aerospace America*, **35**, 26 – 31.

Wada, T. S. Fujita, H. Kataza, W. Kim, I. Maeda, H. Matsuhara, T. Matsumoto, H. Murakami, K. Uemizu, H. Watara, D. Ishihara, T. Hegishi, T. Onala, T. Ootsubo, H. Takeyama & M. Ueno (2002) Infrared Camera Onboard ASTRO-F, *Adv. Spac. Sci.*, **30**, 2111 – 2116.

Wainscoat, R.J., M. Cohen, K. Volk, H.J. Walker & D.E. Schwartz (1992) A Model of the 8-25 Micron Point Source Infrared Sky, *Astrophys. J. Supp.*, **83**, 111 – 146.

Walker, G., J. Matthews, R. Kuschling, R. Jonson, S. Rucinsky, J. Pazder, G. Burley, A. Walker, K. Skaret, R. Zee, S. Grocott, K. Carroll, P. Sinclair, D. Sturgeon & J. Harron (2003) The MOST Astroseismology Mission: Ultraprecise Photometry from Space, *Pub. Astron. Soc. Pac.*, **115**, 1023 – 1035.

Walker, H.J. & M. Cohen (1988) The Classification of Stars from IRAS Colors, *Astron. J.*, **95**, 1801 – 1816.

Walker, H.J. M. Cohen, K.V. Volk, R.J. Wainscoat & D.E. Schwartz (1989), A Practical Approach to the Classification of IRAS Sources using Infrared Colors Alone, *Astron. J.*, **98**, 2163 – 2181.

Walker, R.G. (1962) *Infrared Celestial Backgrounds*, AFCRL-TR-62-807.

Walker, R.G. (1964) *Infrared Celestial Background Radiation 1. Revised Scale of Bolometric Corrections*, AFCRL-64-169.

Walker, R.G. (1969) Near Infrared Photometry of Late-Type Stars, *Philosophical Trans.*, **264**, 209 – 225.

Walker, R.G. (1971) Observations of the 12 μ m Background Flux, *Bull. Amer. Astron. Soc.*, **3**, 26.

Walker, R.G. (1978) The Celestial Background in the Spectral Range from 4.0 to 30.0 μ m, *The Infrared Handbook*, W.L. Wolfe & G.J. Zissis (eds.) Environmental Research Institute, Mich., IR Info. Anal. Center (IRIA), Section 3.3, 3-27 – 3-34.

Walker, R.G. & A. D'Agati (1964), Infrared Stellar Radiance, *App. Opt.*, **3**, 1289 – 1292.

Walker, R.G., & M. Cohen (2003) *Irradiance Calibration of Space-Based Infrared Sensors Ann. Report No. 4*, AFRL-TR-2003-1551. ADA418 543

Walker, R.G., C.V. Cunniff & A.P. D'Agati (1966) *Measurements of the Infrared Horizon of the Earth*, AFCRL-66-631. AD0642928

Walker, R.G., S. Jayaraman, M. Cohen & E. Barker (2004) *Infrared Calibration of Space-Based Sensors, Final Report*, AFRL-VS-HA-2004-1161. ADA435636

Walker, R.G., D.J. Lein, S. Jayaraman, E.A. Barker & S.D. Price (1997) MSX Observations of Comets, *Bull. Amer. Astron. Soc.*, **29**, 1015.

Walker, R.G. & S.D. Price (1970), Rocket Borne Celestial Background Measurements at 12 Microns, *Bull. Amer. Astron. Soc.*, **2**, 362.

Walker, R.G. & S.D. Price (1973) Infrared Celestial Backgrounds, *20th Midcourse Measurements Meeting*, ARPA-TIO- 73-10, 339 – 354.

Walker, R.G. & S.D. Price (1975) *The AFCRL Infrared Sky Survey Volume I. Catalog of Observations at 4, 11 and 20 Microns*, AFCRL-TR-75-0373. ADA016397

Wallace, B., R. Scott, D. Bedard, J. Matthews & S. Grocott (2006) The Near-Earth Orbit Surveillance Satellite, *Proc. SPIE*, **6265**, 626526: 1 – 9.

Walsh, L., P.R. Wesselius & H. Olthof (1989) Detecting Space Debris above 900 km using IRAS, in *Space Safety and Rescue, 1988 - 1989*, IAA Science and Technology Series 89-629, **77**, 345 – 354.

Warren, S.J., N.C. Hambly, S. Dye, O. Almaini, N.J.G. Cross, A.C. Edge, S. Foucaud, P.C. Hewett, S.T. Hodgkin, M.J. Irwin, R.F. Jameson, A. Lawrence, P.W. Lucas, A.J. Adamson, R.M. Bandyopadhyay, J. Bryant, R.S. Collins, C.J. Davis, J.S. Dunlop, J.P. Emerson, D.W. Evans, E.A. Gonzales-Solares, P. Hirst, M.J. Jarvis, T.R. Kendall, T.H. Kerr, S.K. Leggett, J.R. Lewis, R.G. Mann, R.J. McLure, R.G. McMahon, D.J. Mortlock, M.G. Rawlings, M.A. Read, M. Riello, C. Simpson, D.J.B. Smith, E.T.W. Sutorius, T.A. Targett & W.P. Varricatt (2007) The United Kingdom Infrared Telescope Infrared Deep Sky Survey First Data Release, *Mon. Not. Roy. Astron. Soc.*, **375**, 215 – 226.

Waters, L.B.F.M., J. Coté & J.J. Aumann (1987) IRAS Far-Infrared Colours of Normal Stars, *Astron. Astrophys.*, **172**, 225 – 235,

Watson, S.K. & J.G. Jones (1992) *Fractal-Based Signal Processing Applied to Infrared Celestial Backgrounds*, Final Report of Task 10 US SDIO Contract No. SDIO 84-89-C-0033.

Webbink, R.F. & W.Q. Jeffers (1969) Infrared Astronomy, *Space Sci. Rev.*, **10**, 191 – 216.

Weiland, J.L., R.G. Arendt, G.B. Berrimanc, E. Dwek, H.T. Freudenreich, M.G. Hauser, T. Kelsall, C.M. Lisse, M. Mitra, S.H. Moseley, N.P. Odegard, R.F. Silverberg, T.J. Sodroski, W.J. Spiesman & S.W. Stemwedel (1994) COBE Diffuse Infrared Background Experiment Observations of the Galactic Bulge, *Astrophys. J.*, **425**, L81 – 84.

Weinberg, J.L. & H.M. Mann (1967) A Program of Ground-Based Studies of the Zodiacal Light, In *The Zodical Light and the Interplanetary Medium*, J.L. Weinberg (ed) NASA SP-150, 3 – 8.

Weinberg, J.L. & D.W. Schuerman (1981) *Background Sky Brightness Measurements for Application to Space Surveillance Systems*, AFOSR-80-0043. ADA214692

Weinberg, M. (1992a). Detection of a Large-Scale Stellar Bar in the Milky Way, *Astrophys. J.*, **384**, 81 – 92.

Weinberg, M. (1992b) Constraints on the Galactic Bulge using IRAS Variable Point Sources, *Astrophys. J.*, **392**, L67 – L69.

Werner, M. (2006) A Short and Personal History of the Spitzer Space Telescope, *Astron. Soc. Pac. Conf. Ser.* **357**, 7 – 22.

Werner, M., G. Fazio, G. Rieke, T.L. Roellig & D.M. Watson (2006) First Fruits of the Spitzer Space Telescope: Galactic and Solar System Studies, *Ann. Rev. Astron. Astrophys.*, **44**, 269 – 321.

Werner, M.W., T.L. Roellig, F.J. Low, G.H. Rieke, M. Rieke, W.F. Hoffmann, E. Young, J.R. Houck, B. Brandl, G.G. Fazio, J.L. Hora, R.D. Gehrz, G. Helou, B.T. Soifer, J. Stauffer, J. Keene, P. Eisenhardt, D. Gallagher, T.N. Gautier, W. Irace, C.R. Lawrence, L. Simmons, J.E. Van Cleve, M. Jura, E.L. Wright & D.P. Cruikshank (2004) The Spitzer Space Telescope Mission, *Astrophys. J. Supp.*, **154**, 1 – 9.

Wesselink (1948) Heat Conduction and Nature of the Lunar Surface Material, *Bull. Astron. Neth.*, **X**, 351 – 363.

Wesselius, P.R., D.A. Beintema, A.R.W. de Jonge J. de Vries & M. Pérault (1985), *IRAS-DAX Chopped Photometric Channel, Explanatory Supplement*, Lab. for Space Research, Groningen, Netherlands. N8620771

Wesselius. P.R., A.R.W. de Jonge, R.M. van Hees & B. Viersen (1990) Detecting Transtage 66-53J with IRAS, *IRAS (UK) newsletter*, **3**, 10 – 12.

Wesselius, P.R., D.J. Kester & P.R. Roelfsema (1993) *Nature of Cirrus*, PL-TR-93-2007. ADA262942

Wesselius, P.R., R. van Hees, A.R.W. De Jonge, P.R. Roelfsema & B. Viersen, (1992) Space Debris Observed by IRAS, *Adv. Space Research*, **13**, 49 – 57.

Westbrook, W.E., E.E. Becklin, K.M. Merrill, G. Neugevauer, M. Schmidt, S.P. Willner & C.G. Wynn-Williams (1975) Obsevation of an Isolated Compact Infrared Source in Perseus, *Astrophys. J.*, **202**, 407 – 414.

Westerlund, B.E. (1961) A Heavily Reddened Cluster in Ara, *Pub. Astron. Soc. Pac.*, **73**, 51 – 55.

Westerlund, B.E. (1968) On the Extended Infrared Source in Ara, *Astrophys. J.*, **154**, L67 – L68.

Westrum, R. (1999) *Sidewinder Creative Missile Development at China Lake*, Naval Institute Press, Annapolis, Md:

Wheeler, N.B., D. Smith, D. Dean, H. Gardiner, J. Gibson, J. Griffin, S. Price, R. Nadile, L. Bates & G. Bingham (1992) An Assessment of the Near-Field Contamination and Off-Axis Leakage Effects on Earthlimb Background Measurements from CIRRIS 1A,, *Proc. SPIE*, **1754**, 156 – 168.

Wheelock, S.L., T.N. Gautier, J. Chillemi, D. Kester, H. Mc Callon, C. Oben. J. White, F. Boulanger, J. Good & T. Chester (1994) *IRAS Sky Survey Atlas Explanatory Supplement*, JPL Pub **94-11**. N9522539

Whipple, F.L. (1943) Meteors and the Earth's Upper Atmosphere, *Rev. Modern Phys.*, **15**, 246 – 264.

Whipple, F. & J.A. Hynek (1956) The Optical Tracking Program for IGY Satellites, *Astron. J.*, **61**, 92 – 93.

Whitford, A.E. (1948a) An Extension of the Interstellar Absorption-Curve, *Astrophys. J.*, **107**, 102–105.

Whitford, A.E. (1948b) An Infra-red Survey of the Sagittarius Region at Wave Length 2 μ , *Astron. J.*, **53**, 206 – 207.

Whitford, A.E. (1958) The Law of Interstellar Reddening, *Astron. J.*, **63**, 201 – 207.

Whitney, B. & GLIMPSE360 team (2009) GLIMPSE360: Completing the Spitzer Galactic Plane Survey, *Bull. Amer. Astron. Soc.*, **41**, 715.

Wildey, R.L., B.C. Murray & J.A. Westphal (1967) Reconnaissance of Infrared Emission from the Lunar Nighttime Surface, *J. Geophys. Res.*, **72**, 3743 – 3749.

Wildey, R.L. & B.C. Murray (1964) 10 - μ Photometry of 25 Stars from B8 to M7, *Astrophys. J.*, **139**, 435 – 441.

Willems, F.J. & T. de Jong (1986) Carbon Stars with Oxygen-Rich Circumstellar Dust Shells; Observational Evidence for the Onset of the Carbon Star Phase, *Astrophys. J.*, **309**, L39 – L42.

Winter, D.F. (1971) Infrared Emission from the Surface of the Moon, *Adv. Astron. Astrophys.*, **9**, 203 – 242.

Winter, E.M & M.C. Smith (1977) Processing Techniques for Infared Astronomical Surveys, *Proc. SPIE*, **124**, 147 – 155.

Wise, J.O., D.R. Smith, N.B. Wheeler, M. Ahmadjian & R.M. Nadile (2001) Overview and Summary of Results and Significant Findings from the CIRRIS 1A Experiment, *J. Spacecraft and Rockets*, **38**, 297 – 322.

Witte, D.J., R.A. Landee & C.J. Musial (1999) The AEOS LWIR Imager: A Tool for Space Object Thermometry, *1999 AMOS Tech. Conf.*, Maui Economic Development Board, Kihei, Maui, 33 – 46.

Witteborn, F.C. & L.S. Young (1976) Spacelab Infrared Telescope Facility (SIRTF), *J. Spacecraft & Rockets*, **13**, 667 – 674.

Wolnik, S.J., R.O. Berthel, E.H. Carnevalle & G.W. Wares (1969), Additional Shock-Tube Measurements of Absolute Cr I gf-Values, *Astrophys. J.*, **157**, 983 – 997.

Wong, W.W., D. Wang & T.L. Murdock (1980) Out of Field of View Rejection Measurements of the ZIP Telescope No. 2, *Proc SPIE*, **384**, 118 – 122.

Wood, B.E., W.T. Bertrand, D.F. Hall, J.C. Lesho, O.M. Uy & J.S. Dyer (1998) Midcourse Space Experiment Satellite Flight Measurement of Contamination on Quartz Crystal Microbalances, *J. Spacecraft & Rockets*, **35**, 533 – 538.

Woolf, N.J. (1965) Infra-Red Spectra of Stars, Planets and the Moon from Stratoscope II, *Ann. D'Astrophys.*, **28**, 218 – 224.

Woolf, N.J. & E.P. Ney (1969) Circumstellar Infrared Emission from Cool Stars, *Astrophys. J.*, **155**, L181 – L184.

Woolf, N.J., M. Schwarzschild & W.K. Rose (1964) Infrared Spectra of Red-Giant Stars, *Astrophys. J.*, **140**, 833 – 852.

Wright, E.L. (1976) Recalibration of the Far-Infrared Brightness Temperatures of the Planets, *Astrophys. J.*, **210**, 250 – 253.

Wright, E.L. (1998) Angular Power Spectra of the COBE/DIRBE Maps, *Astrophys. J.* **496**, 1 – 8.

Wright, E.L. & E.D. Reese (2000) Detection of the Cosmic Infrared Background at 2.2 and 3.5 Microns Using DIRBE Observations, *Astrophys. J.*, **545**, 43 – 55.

Wyatt, C.P. & F.L. Whipple (1950) The Poynting-Robertson Effect on Meteor Orbits, *Astrophys. J.*, **111**, 134 – 141.

Wynn-Williams, C.G. & E.E. Becklin (1974) Infrared Emission from H II Regions, *Pub. Astron. Soc. Pac.*, **86**, 5 – 25.

Xu, J., J.J. Bock, K.M. Ganga, V. Gorjian, K. Uemizu, M. Kawada, A.E. Lange, T. Matsumoto & T. Watabe (2002) Measurements of Sky Surface Brightness Fluctuations at $\lambda = 4$ Microns, *Astrophys. J.*, **580**, 653 – 662.

Yost, S.A., J.J. Bock, M. Kawada, A.E. Lange, T. Matsumoto, K. Uemizu, T. Watabe & T. Wada (2000) A Search for Near-Infrared Emission from the Halo of NGC 5907 at Radii of 10 – 30 Kiloparsecs, *Astrophys. J.*, **535**, 644 – 649.

Yusef-Zadeh, F., J.W. Hewitt, R.G. Arendt, B. Whitney, G. Rieke, M. Wardle, J.L. Hinz, S. Stolovy, C.C. Land, M.B. Burton & S. Ramirez (2009) Star Formation in the Central 400 pc of the Milky Way: Evidence for a Population of Massive Young Stellar Objects, *Astrophys. J.*, **702**, 178 – 225.

Zachor, A.S. & E.R. Huppi (1981) Nonlinear Response of Low-Background Extrinsic Silicon Detectors, *App. Opt.*, **20**, 1000 – 1004.

Zachor, A.S., E.R. Huppi, I. Coleman & D.G. Grodsham (1982) Nonlinear Response of Low-Background Extrinsic Silicon Detectors. 2. A revised Model, *App. Opt.*, **21**, 2027 – 2035.

Zucker, D.B., V. Belokurov, N.W. Evans, J.T. Kleyna, M.J. Irwin, M.I. Wilkinson, M. Fellhauer, D.M. Bramich, G. Gilmore, H.J. Newberg, B. Yanny, J.A. Smith, P.C. Hewett, E.F. Bell, H.-W. Rix, O.Y. Gnedin, S. Vidrih, R.F.G. Wyse, B. Willman, E.K. Grebel, D.P. Schneider, T.C. Beers, A.Y. Kniazev, J.C. Barentine, H. Brewington, J. Brinkmann, M. Harvanek, S.J. Kleinmann, J. Krzesinski, D. Long, A. Nitta & S.A. Snedden (2006) A Curious Milky Way Satellite in Ursa Major, *Astrophys. J.*, **650**, L41 – L44.

ACRONYMS AND ABBREVIATIONS

2MASS	Two Micron All Sky Survey
AAF	Army Air Force
ABMDA	Army Ballistic Missile Defense Agency
ACS	Attitude Control System
AEDC	Arnold Engineering and Development Center
AEOS	Advanced Electro-Optical System
AF	United States Air Force
AFB	Air Force Base
AFCRS	Air Force Cambridge Field Station
AFCRC	Air Force Cambridge Research Center
AFCRL	Air Force Cambridge Research Laboratories
AFGL	Air Force Geophysics Laboratory
AFIRST	Advanced Far InfraRed Search/Track sensor
AFOSR	Air Force Office of Scientific Research
AFRDC	Air Force Research and Development Command
AFRL	Air Force Research Laboratory
AGB	Asymptotic Giant Branch star
AI	Aerospace Instrumentation Laboratory (AFCRL)
Akari	Japanese Infrared Survey Satellite flown in 2005
AMOS	ARPA (later Air Force) Maui Optical Station
ANS	Astronomical Netherlands Satellite
ARC	Ames Research Center (NASA)
ARPA	Advanced Research Projects Agency
BEAM	Background Equatorial Astronomical Measurements
BIB	Blocked Impurity Band detector technology
BMDO	Ballistic Missile Defense Organization
BMP	Background Measurement Program
BMS	Background Measurement Satellite
BRDF	Bidirectional Reflectance Distribution Function
Caltech	California Institute of Technology
CB	Celestial Backgrounds
CBSD	Celestial Background Scene Descriptor
CCD	Charge Coupled Device focal plane
CIRM	Celestial Infrared Mapper built by Autonetics
CIRRIS 1	Cryogenic Infrared Radiance Instrumentation for the Shuttle (1981 flight)
CIRRIS 1A	Cryogenic Infrared Radiance Instrumentation for the Shuttle (1991 flight)
CME	Coronal Mass Ejection
CMP	Celestial Mapping Program built by Hughes Aircraft Co.
COBE	Cosmic Background Explorer
COSPAR	International Committee on Space Research

D*	D-Star – A measure of detector performance
DARPA	Defense Advanced Research Projects Agency
DASA	Deutsche Aerospace AF
DCT	Discovery Channel Telescope
DENIS	Deep Near Infrared Survey of the Southern Sky
DIGBE	Diffuse Infrared Galactic Background Experiment
DIRBE	Diffuse Infrared Background Experiment on COBE
DoD	Department of Defense
DOT	Designated Optical Tracker
DSP	Defense Support Satellite
DSSS	Deep Space Surveillance System
ELC	Earth Limb Clutter experiment
ELE	Earth Limb Experiment
ELIAS	European Large Area ISO Survey
ELIAS	Earth Limb Infrared Atmospheric Structure Experiment
ELMS	Earth Limb Measurement Satellite
ELS	Earth Limb Sensor
ESA	European Space Agency
ESO	European Southern Observatory on Cerro Tololo
ESTEC	European Space Research and Technology Centre
ETS	Experimental Test Site for GEODSS
FAIR	Fly Along Infrared sensor
FEA	Future Engineers of America
FIER	Filtered Image Entropy Reconstruction
FIRAS	Far-Infrared Absolute Spectrometer on COBE
FIRST	Far Infrared Search and Track
FIRST	Far-Infrared and Submillimetre Telescope – the original name of Herschel
FIRSSE	Far-Infrared Sky Survey Experiment
FLIR	Forward Looking Infrared technology
GEODSS	Ground-based Electro-Optical Deep Space Surveillance system
GLIMPSE	Galactic Legacy Infrared Mid-Plane Survey Extraordinaire (Spitzer Obs)
GIRL	German Infrared Laboratory
GSFC	Goddard Space Flight Center (NASA)
HAC	Hughes Aircraft Company
HCON	Hours Confirmation strategy used by IRAS
Herschel	ESA's far-infrared and submillimeter satellite
HI HI STAR	Rockwell sensor flown by AFCRL 1974
HI STAR	Hughes sensor flown by AFCRL 1971 – 1974
HISTAR South	Modified HI STAR sensor flown by AFCRL
HYSAT	Hybrid Satellite – Follow-on to the BMS/ELMS concepts
IAU	International Astronomical Union

IBC	Impurity Band Conduction in extrinsic silicon detectors
IBSS	Infrared Background Signature Survey
ILM	Isothermal Latitude Model
IMPS	IRAS Minor Planet Survey
IPAC	Infrared Processing and Analysis Center at JPL funded by NASA
IRAC	Infrared Array Camera on the Spitzer Observatory
IRAS	Infrared Astronomical Observatory
IRB	Infrared Backgrounds – The initial label for the BMP
IRBS	Infrared Background Satellite
IRBS	Infrared Backgrounds Sensor on the Infrared Backgrounds Experiment
IRCD	Infrared dark clouds
IR&D	Industrial Research and Development
IRIS	Infrared imaging Survey – the original name for Akari
IRS	Infrared Spectrometer on the Spitzer Observatory
IRTF	Infrared Telescope Facility on Mauna Kea, Hawaii
IRTS	Infrared Telescope in Space flown by the Japanese Space Agency
ISAS	Institute of Space and Aeronautical Science in Japan
ISO	Infrared Space Observatory
ISOCam	ISO Camera
ISOGal	ISO Galactic Plane survey
ISOPhot	ISO photometer
ISPM	International Solar Polar Mission
ISSA	IRAS Sky Survey Atlas
ITTFL	International Telephone and Telegraph Federal Laboratory
JAXA	Japan Aerospace Exploration Agency
JFET	Junction Field Effect Transistor
JPL	Jet Propulsion Laboratory
JT	Joule Thompson (mechanical cooler)
LAAFS	Los Angeles Air Force Station
LAIRTS	Large Aperture Infrared Telescope System
LINEAR	Lincoln Near Earth Asteroid Research
LL	Lincoln Laboratory
LLWIR	Long-Long Wavelength Infrared
LMC	Large Magellanic Cloud
LONEOS	Lowell Observatory Near Earth Object Search
LO STAR	Experiments with the Autonetics SRS sensor 1970
LBV	Long Period Variable star
LRS	Low Resolution Spectrometer on IRAS
LSST	Large Synoptic Survey Telescope
LWIR	Long Wavelength Infrared
MAP	Minute of Arc Probe – AFGL atmospheric experiments
MBB	Messerschmitt-Boelkow-Blohm
Mbps	Mega-bits per second

Mda	Missile Defense Agency
MIPS	Multi-band Imaging Photometer on the Spitzer Observatory
MIPSGal	MIPS Galactic plane survey
MLI	Multi-Layer Insulation
MLWIR	Mid-Long Wavelength Infrared
MMSE	Maximum Mean Square Error Estimation
MOSFET	Metal Oxide Semiconductor Field Effect Transistor
MOST	Microvariability and Oscillation of Stars satellite flown by Canada
MRC	Mission Research Corporation
MSMP	Muli-Spectral Measurement Program
MSX	Midcourse Space Experiment
MWIR	Mid-Wave Infrared
NASA	National Aeronautics and Space Administration
NEAT	Near Earth Asteroid Telescope survey
NEO	Near Earth Object
NEP	Noise Equivalent Power
NGST	New Generation Space Telescope
NIRV	Nederlands Instituut voor Vliegtuigontwikkeling en Ruimtevaart
NMSU	New Mexico State University
NORAD	North American Defense Command
NOSC	Naval Oceans System Center
NRER	Non-Rejected Earth Radiation
NRL	Naval Research Laboratory
OAR	Air Force Office of Aerospace Research
OAR	Off-Axis Rejection
ONR	Office of Naval Research
OP	Optical Physics Laboratory within AFCRL and division within AFGL
OPI	Infrared physics branch within OP
OSU	Ohio State University
OSU	Oklahoma State University
OUSDR&E	Office of the Under Secretary of Defense for Research and Engineering
PAH	Polycyclic Aromatic Hydrocarbon
Pan-STARRS	Panoramic Survey Telescope and Rapid Response System
PbS	Lead Sulphide detectors
PCM	Pulse Code Modulation
PDR	Preliminary Design Review
PI	Principal Investigator
PSC	Point Source Catalog
PSF	Point Source Response Function
PSL	Physical Sciences Laboratory of NMSU
PSRR	Point Source Rejection Ratio
RCC	Range Control Center at White Sands Missile Range

RIF	Reduction in Force
RSO	Resident Space Object - an Earth orbiting satellite
SAMSO	Air Force Space and Missile System Center at LAAFS
SAO	Smithsonian Astrophysical Observatory
SBSS	Space Based Surveillance System
SBV	Space Based Visible sensor on MSX
SCOOP	Hughes IR target measuring sensor – late 1970s
SD	Space Division – SAMSO component at LAAFS
SDIO	Strategic Defense Initiative Organization
SDL	Space Dynamics Laboratory of Utah State University
SDSS	Sloan Digital Sky Survey
SERB	Space Experiment Review Board
SEST	MSX System and Engineering Support Team
SIMPS	Supplemental IRAS Minor Plane Survey
SIRE	Space (later Shuttle) Infrared Experiment
SIRTF	Shuttle (later Space) Infrared Telescope Facility – now Spitzer
SOFT	Signature of Targets – Hughes sensor circa 1970s
SMC	Small Magellanic Clouds
SMEI	Solar Mass Ejection Instruments
SMEX	NASA's Small Explorer Class experiments
SNR	Signal to Noise Ratio
SOFIA	Stratospheric Observatory for Infrared Astronomy
SPAS II	Shuttle-Pallet Satellite II
SPICA	Space Infrared Telescope for Cosmology
SPICE	Survey Program of Infrared Celestial Experiments
SPIE	Society of Photo-Optical Instrumentation Engineers
SPIRIT I	Spectrl Infrared Interferometric Telescope
SPIRIT II	Spatial Spectral Rocketborne Interferometric Telescope
SPIRIT III	Spatial Infrared Imaging Telescope on MSX
SRON	Space Research of the Netherlands
SRS	Stellar Radiation Sensor built by Autonetics
SSC	Spitzer Science Center
SSG	Sensor Systems Group
SSPM	Infrared Solid Stat Photomultiplier
SSTS	Space Surveillance and Tracking System
STC	Space Technologies Center
STM	Standard asteroid Thermal Model
SVC	Space Vector Corporation
SWAS	Submillimeter Wave Astronomy Satellite
SWIR	Short Wavelength Infrared
SWS	Short Wavelength Spectrometer on ISO
TEM	Target Engine Module on MSMP
TMGS	Two Micron Galactic Survey
TMS	Target Measurement Satellite

TMSS	Two Micron Sky Survey
UKIDSS	UKIRT Infrared Deep Sky Survey
UKIRT	United Kingdom Infrared Telescope
USU	Utah State University
UVISI	Ultraviolet – Visible Imagers and Spectral Imagers on MSX
VIPER	Visible Photometric ExpeRiment
VISTA	Visible and Infrared Survey Telescope for Astronomy
VLWIR	Very Long Wavelength Infrared
VS	Space Vehicles Directorate of AFRL
VSB	Battlespace Environment Division of VS
VSE	Integrated Experiment Division of VS
VSS	Spacecraft Technology Division in VS
WFCam	Wide Field Camer an UKIRT
WIRE	Wide-field Infrared Experiment
WISE	Wide-field Infrared Survey Explorer
WIT	Wentworth Institute of Technology
ZIP	Zodiacal Infrared Project